# JOINT TACTICAL ELECTRIC VEHICLE

## ACTIVE RIDE HEIGHT

## AND

## DAMPING CONTROL

## FINAL REPORT FOR FY '95

---

CALSTART SYSTEM

DEVELOPMENT PROJECT FOR ADVANCED

HYBRID RECONNAISSANCE VEHICLES

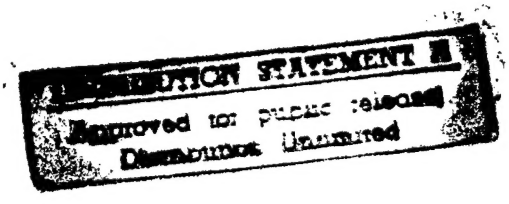

Rod Millen

Special Vehicles

April 8, 1997

RE: Final report for the Active Ride Height and Damping Control Project

Enclosed is the above mentioned report for CALSTART Agreement #MDA972-95-2-0011 from Rod Millen Special Vehicles, Inc. If you have any questions, please contact Dr. Eric Anderfaas at (714) 847-2111

Sincerely,

Cindy Smith
Controller



Copies sent to:

2 copies
Defense Technical Information Center
Attn.: DTIC-DTAC
Cameron Station
Alexandria, VA 22304-6145

1 copy
DARPA/OASB Library
DARPA/TTO
3701 North Fairfax Drive
Arlington, VA 22203-1714

2 copies
John Gully
DARPA/TTO
3701 North Fairfax Drive
Arlington, VA 22203-1714

1 copy
Elaine Ely
DARPA/TTO
3701 North Fairfax Drive
Arlington, VA 22203-1714

1 copy
Dr. Robert Rosenfeld
DARPA/TTO
3701 North Fairfax Drive
Arlington, VA 22203-1714



Rod Millen Special Vehicles
7575 Reynolds Circle, Huntington Beach, CA 92647 Tel (714) 847-2111 Fax (714) 841-6839

# DISCLAIMER NOTICE

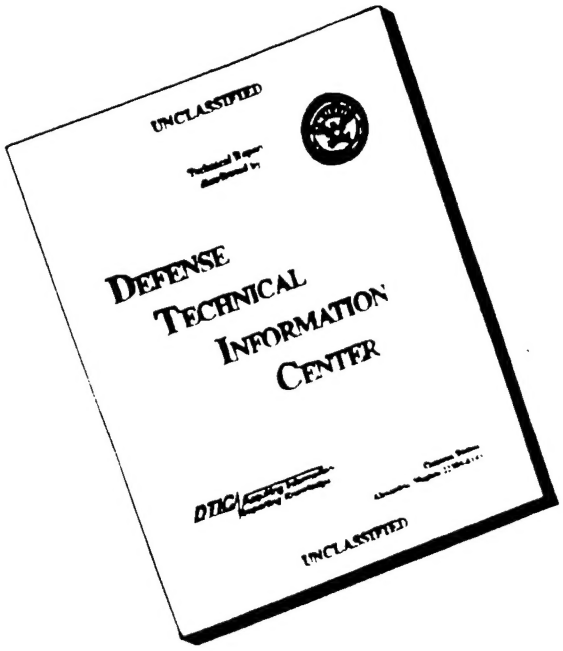


**THIS DOCUMENT IS BEST QUALITY AVAILABLE. THE COPY FURNISHED TO DTIC CONTAINED A SIGNIFICANT NUMBER OF PAGES WHICH DO NOT REPRODUCE LEGIBLY.**

Table of Contents


Executive Summary ..... 1

1. Introduction ..... 4

1.1 Background ..... 4

1.2 Program Overview and Goals ..... 6

2. Concept of the Suspension System ..... 8

2.1 Active Damper ..... 12

2.2 Active Ride Height ..... 17

2.3 Control Schemes ..... 18

2.4 Summary of the Design Solution ..... 20

3. Design Method and Approach ..... 21

4. Results ..... 22

4.1 Range of operating conditions ..... 22

4.2 Measurement and Analysis of Vehicle Parameters of JTEV ..... 23

4.3 Tire Models and tire parameters ..... 24

4.4 Damper models ..... 27

4.5 Quarter Car Model ..... 34

4.6 Half Car Models ..... 51

4.7 Full Car Model ..... 55

4.8 Requirements and Design of Active Damper ..... 57

4.9 Requirements and Design of Active Ride Height ..... 62

5. Continuation of work ..... 63

5.1 Summary of work performed to date ..... 63

5.2 Required work to complete system ..... 65

6. Conclusions ..... 66

7. References ..... 67

Appendices ..... 72

## Executive Summary

The active suspension system developed for this project is based on an active damper for controlling the medium and high speed dynamics involved with vehicle body and wheel motions, and an active ride height system for controlling the low speed body motions. This type of system makes improvements over a passive system by allowing the optimal damping required for differing terrain and vehicle control requirements to be automatically set by the suspension system while the active ride height system controls the vehicle attitude without sacrificing either passenger isolation or handling. This type of system has been shown to be very competitive with fully active systems over a wide range of running conditions with lower cost, lower energy usage and improved failure modes.

The vehicle properties of the Joint Tactical Electric Vehicle, which this suspension system will be implemented on, have been determined and are listed in the main body of this report. Parameters for a selection of tires which are used on this and similar vehicles have been determined for a range of tire pressures and other test conditions, some of this data is given in the appendix. Testing was also performed to determine the possibility of determining the tire deflection from tire pressure measurements. It was found that there was a correlation between the tire pressure and tire deflection although the pressure raise was small, on the order of 5 psi. Because of this relatively small pressure raise, there would be difficulties involved in filtering out other changes in pressure from temperature changes and acoustic effects which are of the same order of magnitude as the pressure raise from tire deflection.

A wide range of mathematical models for use in design and development of the active damper and active ride height systems have been created. These models, ranging from a nonlinear tire model to a nonlinear full car model, have been shown to be very useful in designing both the suspension systems actuators and control systems. The simplest of these models are two tire models which are based on the tire deflection data taken. These

tire models are used in the more complex vehicle models used for designing and analyzing the suspension system.

A nonlinear model of a hydraulic damper has been developed and validated through testing with the RMSV in-house shock dynamometer to allow the dynamic behavior to be determined and allow a complete analysis for the design of the active damper actuator. Based on this damper model and with performance requirements based on past vehicle testing and computer simulations, a prototype hydraulic active damper based on a suitable high performance servo valve has been built. Preliminary testing has shown that this prototype active damper has the controllable range required for good suspension control. Further testing for measuring the speed of response and hardware in the loop testing need to be carried out to determine if this active damper has the frequency bandwidth required for this application.

A quarter car model has been constructed and used for determining the usefulness of different types of suspension control methods and control variables. Analysis with this model has shown that the most effective suspension actuator is an active damper which was found to be very useful for improving both the isolation properties and handling properties of a vehicle suspension. Controlling the suspension spring rate was found to have less of an effect on the isolation properties of a suspension than the active damper and have very small effects on the tire grip based on the dynamic tire contact force. It was also found that the most important control variables are the suspension deflection, the suspension deflection rate and the absolute vertical velocity of the sprung mass. Feedback of the tire deflection did not significantly improve the overall suspension performance. From his analysis it was determined that the main improvement in isolation achieved by an active suspension system was on the order of 20% compared to an optimal passive suspension exhibiting the same level of suspension travel and wheel control. This improvement was gained from improved damping of the vehicle body resonance motions.

Two half car models have been constructed, one to analyze the pitch motions of a vehicle and the second to analyze the roll motions of a vehicle. The pitch model is used for designing the active damper suspension system, the spring rates, damper forces and active damper control system. The roll model is used for designing the active ride height actuators and control system along with integration between the active ride height and active damper systems. The roll model has been used to evaluate the power requirements of three active ride height systems. The power required was found to be between ½ to 1¾ kW to control the body roll to within 1° for a ½ g lateral acceleration cornering maneuver.

The most complex model developed for this project is a full car model. Once the active damper and active ride height systems have been designed through the progression of models from the damper model to the quarter car model to the half car models, the full car model will be used to check the results and to fine tune the complete suspension system.

The control system being developed for the active damper system is based on a two dimensional look up table based on suspension deflection and suspension deflection rate. This is similar in nature to an engine control unit fuel injection map. Based on this easily changed table, the force of the damper is determined by the combination of these two parameters allowing the damper to be quickly tailored to an optimal configuration for a wide range of operating conditions. The control system used for controlling the active ride height system is based on linear feedback with the addition of some simple nonlinear control methods for improving the energy efficiency and performance at the extreme limits of the operational envelop.

# 1. Introduction

## 1.1 Background

A vehicle's suspension system is a critical element in passenger comfort and safety. The advanced passive suspensions developed by Rod Millen for the Helo-Transportable Multi Mission Platform (HTMMP) and the Joint Tactical Electric Vehicle (JTEV) vehicles greatly improves the ride quality, handling, stability and speed over rough terrain by integrating a position sensing mechanism into a high performance passive damper capable of the high force and velocities required to control an off-road vehicle. Although passive suspensions such as these have evolved to a very high level, there are some inherent restrictions on their performance since only suspension velocity and position can be sensed and acted on with mechanical elements. Computer controlled suspensions have the potential for improved performance over passive suspensions since a higher number of critical vehicle variables, such as body vertical velocity and lateral acceleration, can be incorporated into a computer based algorithm and the force constitutive relations are not solely based on mechanical elements. Literature and testing have shown that this increased information and flexibility allow a computer controlled suspension to have improved isolation, improved traction of a suspended tire, improved vehicle load rejection from both static and dynamic loads and be adaptable for optimal performance under a wider range of conditions as compared to a passive suspension. The improvement in isolation occurs from improved control of vehicle body motions and resonance behavior such as 'freeway hop' shown by both passenger vehicles as well as trucks. The improvement in tire traction stems from reductions in changes in tire contact force. This improvement increases the stability and control of a vehicle and also reduces damage to the road surface. A computer controlled suspension has the capability for the system parameters to be easily and automatically changed depending on the driving conditions such as speed and driver steering behavior or road conditions such as roughness. This allows the computer controlled suspension to be optimized for a wider range of operating conditions compared to a passive suspension which requires difficult and time consuming hardware changes for optimization. Computer controlled

suspensions can also adjust to changes in vehicle loading from static loads such as increases of payload or fuel state and dynamic loads imposed by vehicle maneuvering. By compensating for these changes in loading, a vehicle can have consistent behavior improving driver control and safety. All of these improvements are useful in both commercial and military applications.

Because of the improvements offered by computer controlled suspension, there has been a great interest in developing these systems for automotive applications. Computer controlled suspension systems can be broken down into two main categories, active and semi-active (which is also known as active damper). An active system uses a power source, such as a hydraulic pump, and high bandwidth control valves to determine the suspension forces based on sensor readings. This type of system has shown improved suspension performance as compared to a comparable passive system, most notably in reducing motions and resonance behavior of the vehicle body and providing the ability to adapt between optimal passenger isolation and optimal vehicle handling. Active suspension systems have also shown many problems. One major problem is the high initial costs from expensive and complex hardware, increased maintenance requirements and increased fuel consumption. Another problem is safety, since energy is always available to control the suspension an error or sensor failure may cause the system to become unstable. To reduce the chances of this happening redundancy is required further increasing cost and complexity. This type of system has also shown to have other poor failure modes besides instability. When the vehicle encounters bumps with frequencies higher than that of the control valves, this type of system transmits the jolts directly into the vehicle body as ride harshness. These jolts and the system hardware also tend to create a lot of acoustic noise. Because of these problems there has been no commercially viable active suspension system that is clearly superior to a good passive suspension in all aspects of performance, let alone when factors such as cost and reliability are accounted for.

A semi-active or active damper suspension is based on the idea of modulating the dissipation in basically a passive damper as a function of sensed variables. This type of

system has been shown to be lighter, smaller and less expensive than an active system while still giving most of the performance advantages. With the addition of a low power, low bandwidth load leveling system the combined suspension system can have improved performance compared to an active system without the disadvantages of high power use, poor failure modes, ride harshness, high costs and acoustic noise associated with an active suspension system.

To date, almost all of the past computer controlled suspension systems have been developed for on-road use. The off-road environment requires an improved computer controlled suspension system to handle the increased performance requirements demanded by the rough terrain, increased loads and long travel suspension systems of off-road vehicles. A successful active damper off-road suspension system will require a very wide range of operating characteristics with a low damping force to provide an excellent ride quality during normal conditions but requiring a very high damping force to prevent extreme suspension bottoming and the loss of vehicle stability or control if the vehicle lands from a jump or hits a large bump at high speeds.

## 1.2 Program Overview and Goals

The goals of this program are to develop a computer controlled suspension system implemented on JTEV offering improvements in performance, adaptability, reliability with the knowledge and practical experience to quickly and cost effectively apply the system to a wide range of both commercial and military vehicles. The suspension system developed will be based on active damping and active ride height control. This type of computer controlled suspension system which integrates a soft passive suspension with an active damper and low bandwidth ride height control should offer improved performance over a passive suspension system without the limitations of high energy consumption, high frequency harshness, poor failure modes and high costs associated with a fully active suspension system. The priority of vehicle responses to be improved with this suspension system are:

i) improved stability over single event bumps to eliminate catastrophic forward rollovers.

ii) reduce peak loading over half round bumps using a limiting speed criterion for improved driver control.

iii) reduce pitch sensitivity over sinusoidal terrain inputs for improved driver comfort and control.

iv) reduce absorbed power at the drivers seat for improved driver comfort and reduced driver and vehicle fatigue

v) reduce body motion from handling loads such as cornering and braking for improved control and use of the suspension.

To reach this goal the program has been broken down into the following tasks:

1) **Task 1: Design and Fabrication.** RMSV will design and fabricate an actively-controlled damper as well as design and fabricate an active ride height actuator and control system

2) **Task 2: Integration and Testing.** RMSV will test the actively-controlled damper and ride height actuators on its shock absorber test dynamometer. RMSV will use the dynamometer testing to develop the suspension actuators and control algorithms in a rapid manner using the actual components for hardware in the loop simulations. It will then integrate the components into the JTEV test platform for evaluation and testing. RMSV will refine the suspension algorithms for these components and prepare a final report.

3) **Task 3: Test Platform Support.** RMSV will prepare or modify the JTEV as needed to test the various components developed under this program and the companion program by AeroVironment. Appropriate instrumentation packages will be installed to evaluate and quantify the performance of the components. Modifications to the chassis or drive train will be performed to integrate the components or change the drive configuration to allow testing of different drive and steering schemes.

4) **Task 4: Analysis and Reporting.** RMSV will provide quarterly progress reports, proof of expenditures and a final report including the final results.

## 2. Concept of the Suspension System

A passive suspension system can be simplified down to a quarter car model, as shown in Figure 2.1A, for analysis of many suspension performance factors [Sharp, 87]. In this model the vehicle body is represented by the sprung mass, $M_s$, being held up by a spring, $K_s$, and a damper, $B_s$. The tire is represented by the unsprung mass, $M_u$, and a tire spring, $K_u$. In an ideal computer controlled suspension the passive springs and dampers can be thought to be replaced by an ideal force actuator that can both supply and dissipate energy, shown in Figure 2.1B. One example of this type of system is shown by Figure 2.1C in which a controlled hydraulic strut is used to generate a desired force [Karnopp, 91]. This type of actuator configuration works well for low frequency control, but it has significant limitations at high frequencies since the hydraulic strut becomes very stiff. In essence the control system attempts to soften a stiff system. To do this properly requires very accurate sensors and fast powerful actuators. Today's technology is pushed to meet these exacting requirements in a cost effective manner. Any system that does met them is very expensive and any system that does not fully meet them is significantly harsher than a conventional passive suspension [Beard, 95].

A system of the type shown in Figure 2.1C would also have high energy consumption since the hydraulic strut is used to support the weight of the entire vehicle and is required to supply large forces at high speeds. Such a system would use considerable power in the suspension just to drive on a level road. The power consumption can be reduced by including a spring in parallel with the hydraulic strut, as shown in Figure 2.1D. This system still requires just as fast a hydraulic system as the system of Figure 2.1C to avoid harshness.

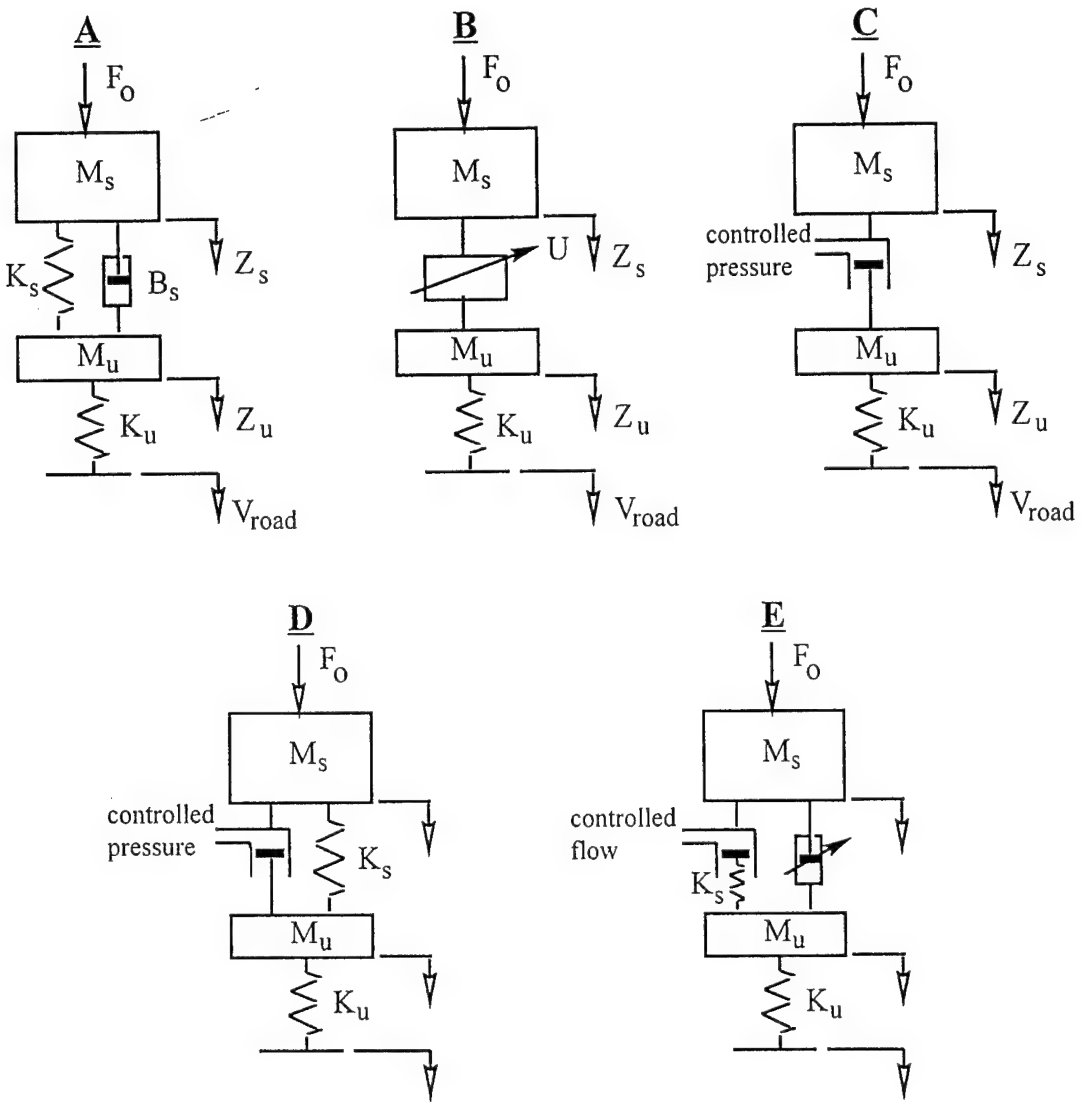


Figure 2.1 Suspension system representations

While a passive suspension system can perform well in providing road isolation especially in the high frequency range, it has three major shortcomings for off-road vehicles. The first of these is the difference in damping stiffness for optimal performance on varying road surfaces, especially when the terrain is extremely rough or large single event bumps are encountered where bottoming of the suspension is an issue. The second is the compromise between damping vehicle body resonances and road isolation inherent in a passive suspension. The third is the compromise between vehicle body attitude control and road isolation. The suspension system shown in Figure 2.1E focuses on

improving these three weak points in the passive suspension system with the use of an active damper and an active ride height system without replacing it entirely as with the active systems of Figure 2.1 B, C and D.

In the suspension system of Figure 2.1E the passive damper is replaced with an active damper which effectively controls the damper valve so that the damping force tracks a desired force for optimal performance based on a wide range of sensor inputs. This damping force does not require power to be developed as with the active system. One difference between this system and the active system is that the active damper can only create forces in the opposite direction of the relative velocity across the damper. At times it may be desirable for forces in the same direction which would require power to be supplied by the damper. In such a case, the active damper valve is controlled to produce the minimum force possible, ideally zero. Fortunately, because suspensions essentially dissipate energy the active damper can supply the desired suspension forces most of the time [Karnopp, 91]. The active damper part of this computer controlled suspension solves the first two problems involved in the use of a passive suspension with adaptable damping for varying road surfaces and improvement in the compromise in damping body motions versus high frequency isolation.

To solve the third problem with a passive suspension by improving the compromise between vehicle attitude control and road isolation, the suspension system of Figure 2.1E uses a flow source in series with the suspension spring similar to a load leveler or the ride height control on JTEV. Although this active ride height control requires a power source, it only is required to control body motions around 2 to 4 Hz. since the spring isolates it from the road and tire motions. The effect of this system is to actively stiffen an innately soft system. Since this active ride height system leaves the passive suspension in place, this system only requires power under cornering or braking conditions and is turned off during normal driving conditions. This is in contrast to an active system which is required to control the much higher frequency motions of the tire and always consumes energy.

It is interesting to note that all of the suspension systems shown in Figure 2.1 have certain limitations since the suspension forces are being applied between the tire and the body of the vehicle. Hedrick and Butsuen point out [Hedrick, 88] that in this type of dynamic system there are some invariant points in the frequency spectrum of a suspension system which cannot be changed by altering the suspension force dynamics. To show these invariant points, they used Bode plots and transfer functions. A Bode plot, named in honor of H. W. Bode, is a graph of the steady state magnitude of a given performance criteria as a function of input frequency. While a transfer function is the dynamic frequency ratio between the output of a system (or a performance criteria) and the input of a system such as road roughness. Hedrick and Butsuen showed that:

> *...only one of the three transfer functions (acceleration, rattle space*{suspension deflection}*and tire deflection) can be independently specified and that the first two contain "invariant points" at frequencies within the frequency range of interest. ... It was shown that when considering ride quality and road holding trade-offs that both can be improved at low frequencies and at the sprung natural frequency. If we try to improve road holding at frequencies near and above the unsprung natural frequency, there must be a corresponding large increase in the acceleration Bode plot. Similarly if we reduce the acceleration magnitude near the unsprung natural frequency, there is a corresponding large increase in the tire deflection Bode plot.*

This implies that the benefits from a computer controlled suspension, both active and semi-active, occur in the low frequency spectrum controlled by the active ride height and active damper suspension concept. The expensive high frequency performance required in an active suspension system to eliminate harshness has very little potential for increased performance of the suspension in regards to isolation or vehicle control.

## 2.1 Active Damper

A damper can produce forces in tension and compression. But it can only do so when the instantaneous relative velocity is in the proper direction. When the relative velocity is in the incorrect direction most control system designs reduce the force as much as possible. In an actual system this switching can be performed either mechanically by the damper mechanism or electronically by the control system. This choice is dependent on the speed of the actuator, the speed of the control system and the sensors involved in the control system. Figure 2.2 shows four configurations for a hydraulic implementation of an active damper. In each case energy is dissipated as oil is forced through a controllable valve.

In Figure 2.2A a fast valve which allows the flow to be controlled in both directions is required. This valve could be a controllable orifice or a magneto-rheological fluid/valve combination. To control this valve the direction of the relative velocity across the damper is sensed and the control system performs all of the switching and control of the valve.

In Figure 2.2B a valve which allows flow in only one direction can be used, although it is still required to be as fast as required by the valve in Figure 2.2A. By allowing flow in one direction by a set of mechanical check valves, a wider range of valve designs can be used which may lead to simpler implementation and improved performance.

In Figure 2.2C two valves which allow flow in one direction are used, one for compression of the damper and one for extension of the damper. This configuration allows much slower valves to be used since these valves only need to be controlled as a function of the much slower sprung mass motions as compared to the valves shown in Figure 2.2A & B which require control signals as a function of wheel motions [Emura, 94].

The final active damper valve configuration shown by figure 2.2D uses four single directional flow valves controlled by two actuators. The symmetric actuator controls the damping force in both tension and compression. The anti-symmetric actuator increases the damping force in one direction while decreasing the damping force in the other direction. This configuration would be especially useful in implementing "sky-hook" damping for controlling vehicle body motions and slow actuators could be used [Karnopp, 90]. Although this Figure 2.2 shows a hydraulic implementation of these valve arrangements, the same ideas could be used for electromechanical or coulomb friction types of computer controlled dampers.

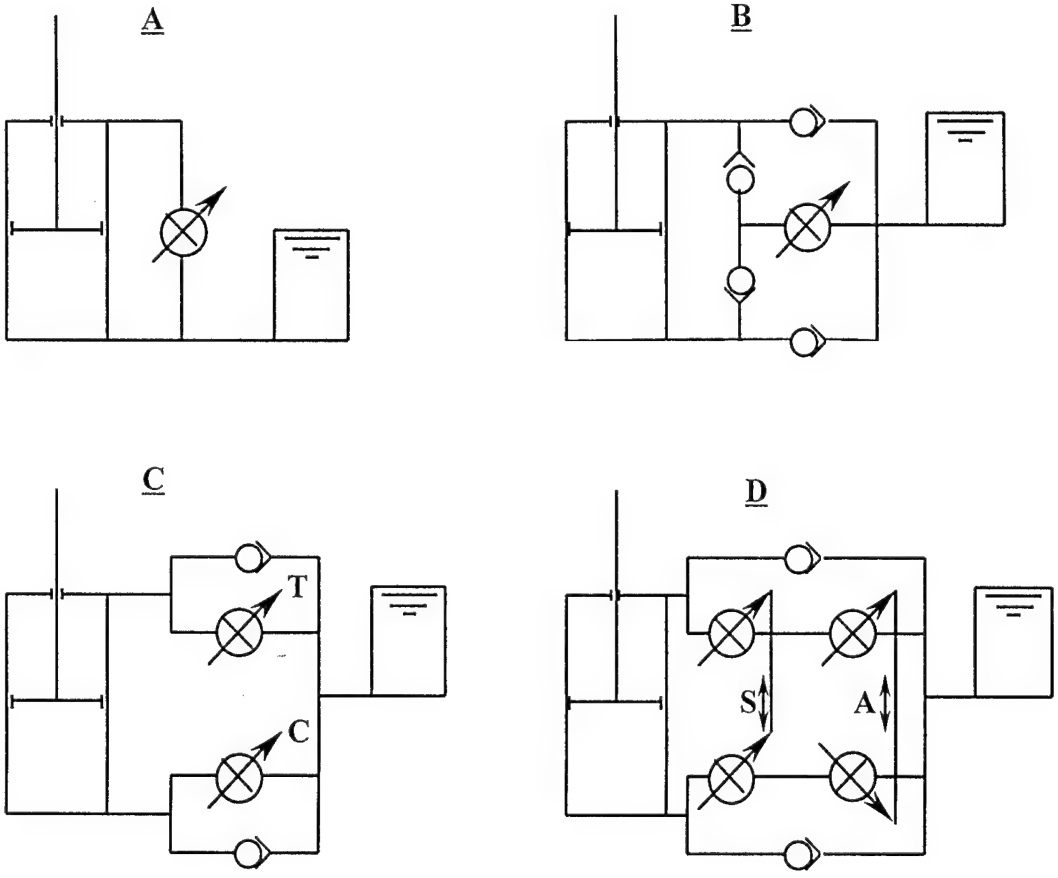


Figure 2.2 Some hydraulic active damper configurations

### Hydraulic dampers

All modern vehicle passive dampers are hydraulic units because the constitutive relationships between fluid flow and fluid pressure are a relatively good match to the velocity/force requirements of a suspension damper. At least two types of hydraulic valves are used in a high performance passive damper, fixed orifice and pressure control valves. For low speed motions of a damper an adjustable orifice is used to adjust the force/velocity relationship. As the velocities across the damper are increased, the pressure across the valve increases greatly and the damper would become too stiff. A pressure control type valve is therefore used to control the medium to high speed damper forces. Figure 2.3 shows the different force/velocity relationships for a orifice type valve and for a pressure control type valve. Between the increasing curve of an orifice and the decreasing curve of a pressure control valve, the desired damping characteristics of a passive damper can be approximated relatively well. The types of valves used in a high performance passive damper have also been optimized to have very low mass. This allows them to have very fast response and excellent high frequency behavior.

Either type of valve, orifice or pressure control, can be used in a hydraulic active damper. A controlled orifice valve could be used to vary the resistance across the damper making the damper force have a strong dependence on the velocity. For a damper of this type the velocity must be measured very accurately and the orifice size must be controlled accurately. A controlled orifice could also be used as a force control with the addition of either a pressure or force sensor and feedback control loop. In this case a very fast and accurate feedback control loop is required to control the orifice so that a given force is developed by the damper independent of velocity.

An electromagnetically loaded pressure control valve can be used to control the force produced by an active damper. This type of valve does not require a very fast control system for pressure control, but there are problems in producing a large enough control force with an electromagnet actuator. This type of valve may also have relatively large inertias as compared to a passive pressure control valve so will not have as good high frequency response.

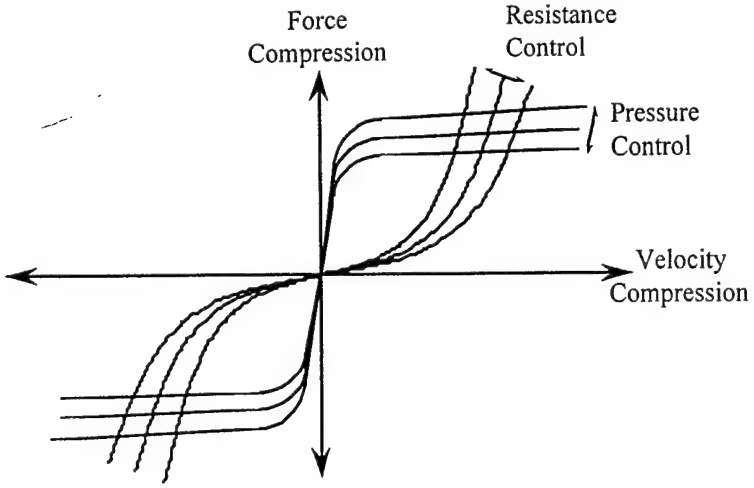


Figure 2.3 Resistance and pressure control valve force/velocity relationships

Another method for controlling a fluid damper is with magneto-rheological fluids. These fluids are oil based with micron-sized magnet particles suspended in them. An electromagnetic field can be used to control the force velocity relationship of this type of damper as shown in Figure 2.4. Active dampers of this type can have very fast response, on the order of one millisecond, but have had problems such as the magnetic particles falling out of suspension, very high component wear and reduced performance over time. It is being investigated if this technology can be applied to high performance off-road vehicle suspensions at this time.

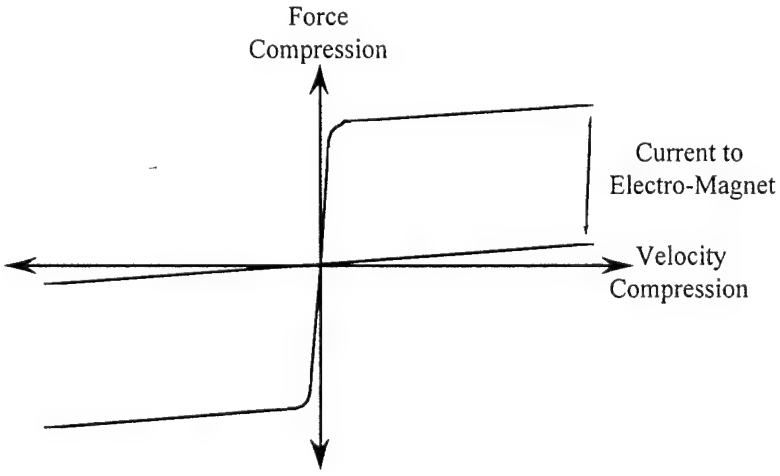


Figure 2.4 Magneto-rheological fluid force/velocity relationships

Some of the first dampers used on vehicles were based on coulomb or dry friction. This type of damper was discarded once suitable passive hydraulic dampers were able to be manufactured. The problem with this type of passive damper can be seen in the force/velocity relationship shown in Figure 2.5. At zero velocity, the damper tends to stick and therefore transmit forces directly into the vehicle body. Once a velocity occurs across the damper, the damping force is constant and does not increase with velocity as desired with a passive damper. At low velocities this constant force is too high and at high velocities the damping force is too low. With the benefit of computer control, the coulomb friction damper may be very useful. For a desired damping force a controller would adjust the pressure on the friction pads. Accurate measurement of the relative velocity would not be required, since the force may be relatively independent of velocity. Issues which are being addressed to determine the performance of this type of active damper system are the speed of response, the switching dynamics between velocities of different directions, system configuration, temperature effects, heat build up, wear and noise.

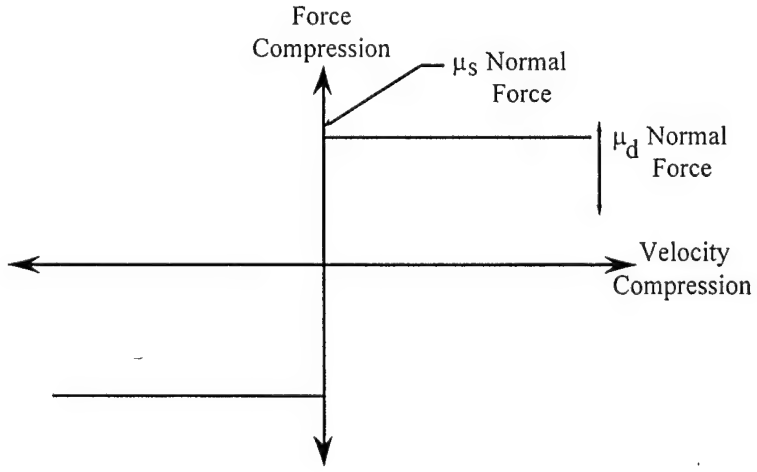


Figure 2.5 Coulomb friction force/velocity relationship

## 2.2 Active Ride Height

There are numerous methods to implement an actively stiffened soft system such as the active ride height system used in this suspension. The energy and power requirements required to correct for a given vehicle body disturbance strongly depends on the system configuration. Three different configurations where considered and are shown in Figure 2.6. System A connects the left and right sides of the vehicle with a pump, or other type of flow source, which pumps oil from the low pressure side of the vehicle (towards the inside of the corner) to the high pressure side of the vehicle (the outside of the corner). The advantage to this system is that the pump only needs to supply a pressure equal to the pressure difference between the left and right sides of the vehicle. This type of system could also be used for controlling pitch motions. This should be the most energy efficient of the three systems shown.

System B uses a separate pump for each suspension strut of the vehicle. Oil is pumped from a sump at atmospheric pressure to the pressure required at each strut. Higher power is required with this system as compared to system A since the pressure across each pump in this system is the full pressure required and not the difference in pressure between the left and right suspensions (or fore and aft for pitch control).

System C uses valves to control the oil flowing to each suspension strut from a central accumulator. The central accumulator is charged to a pressure high enough for controlling each strut with oil from a sump by a pump which could be engine driven or electrical. If oil is required to be released from a strut, the control valve releases it back to the sump. This type of system would be similar to a slow acting active suspensions system. This system is also the least energy efficient since all of the oil used in controlling the suspension must be pumped up to the high pressure in the central accumulator. Once the oil is at the system pressure, energy is lost as the excess pressure is bleed down to the pressure required at each strut by a valve.

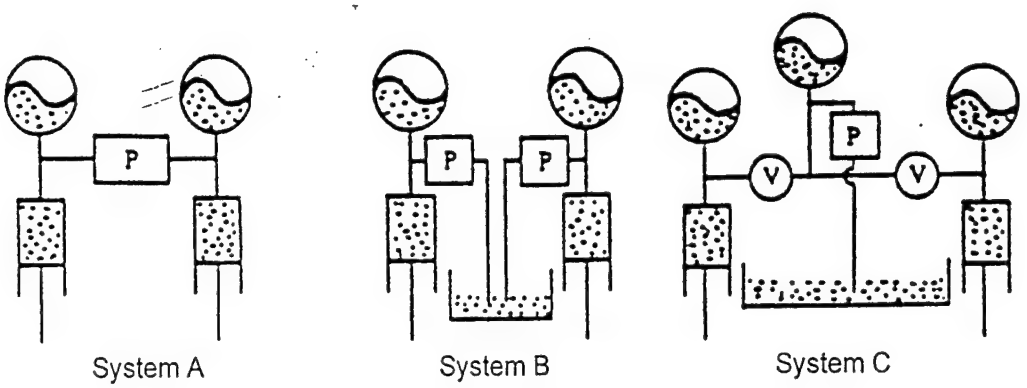


Figure 2.6 Some hydraulic active ride height configurations

## 2.3 Control Schemes

### Control scheme for Active damper

The control scheme to be implemented will be based on a two dimensional look-up table with the active damper force as a function of suspension displacement on one axis on the look-up table and suspension velocity on the other. This type of control scheme allows for a practical implementation which relies on the past experience with passive suspension developed at Rod Millen Special Vehicles. The use of this type of practical control method allows for changes to be made to the control system as quickly and easily as possible. Once the active damper suspension has been developed to a high performance level with this two dimensional look-up table implementation, a three dimensional look-up table based on suspension displacement, suspension velocity and sprung mass velocity will be implemented. This three dimensional look-up table will allow a wider range of both linear and nonlinear control schemes to be tested with a minimal amount of programming and set up time. An overview of the control system for both the active damper and active ride height is shown in Figure 2.7. In this Figure, the table look-up for the active damper control is in the active damper system controller. From measurements of the vehicle outputs the system controller determines the desired force for the active damper at each wheel based on the table look-up values. The active damper actuator controller, which is required to be faster than the system controller, sets

the active damper force to the desired level based on the relative velocity across the damper. All of the switch and actuator feedback as discussed in section 2.1 occurs in the active damper actuator controller.

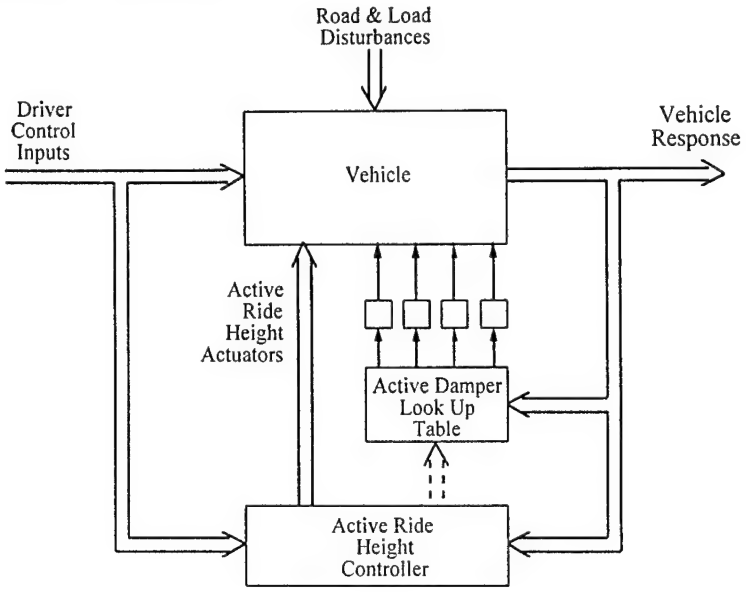


Figure 2.7 Overview of suspension control system

### Control scheme for active ride height

The control system used for controlling the active ride height system is based on linear feedback with the addition of some simple nonlinear control methods for improving the energy efficiency and performance of the system at the extreme limits of the operational envelope. The linear feedback will use the suspension deflection with inputs of vehicle speed and driver control of the steering, brake and throttle control to determine the amount of suspension displacement to occur at each wheel station.

The active ride height system will have a large effect on the handling of the vehicle. In essence the active ride height control with a feedback control system for controlling roll motions acts like a set of very stiff anti-sway bars. In a vehicle with passive suspension it is well known that the stiffness distribution between the front suspension and rear suspension can change a vehicle's handling between understeer to oversteer. The

controller for the active ride height system will take this into account and have the roll stiffness distribution between the front and rear axles easily adjustable.

## 2.4 Summary of the Design Solution

This suspension system design is based on two types of actuators: an active damper actuator which allows computer control of the damping force in the suspension and an active ride height control which allows computer control of the suspension spring deflection. The active dampers are used for controlling the higher frequency body and wheel motions. A table look-up type of supervisory control system will be used for controlling the active dampers in which linear and nonlinear control methods can easily be applied. The active ride height system will be used for controlling body motions induced by static and dynamic loads to the vehicle sprung mass which occur in the low frequencies around 2 to 4 Hz. This system will reduce the effects of handling loads on the suspension and allow for better utilization of the suspension travel for isolation. The control system used for the active ride height system will allow for the weight distribution during maneuvering to be adjusted for optimal vehicle handling.

This combination of suspension actuators, an active damper and an active ride height, will yield a suspension with the good high frequency isolation properties of a passive suspension and control the low frequency body motions as well as a fully active suspension without the cost, complexity, inefficiency and other problems of the fully active system. The high frequency control of the active dampers will also increase the range of the suspension system to allow for improvements in suspension performance for improved vehicle stability over extremely rough terrain and single event bumps where bottoming of the suspension is an issue.

## 3. Design Method and Approach

Simultaneously satisfying the design goals of improvements in road isolation, vehicle attitude control, tire contact and energy efficiency over the wide range of conditions encountered by a high performance off-road vehicle is not a simple task. To make the suspension design task more manageable the problem is broken down into the following tasks:

1) Determine the range of operating conditions for the vehicle and desired performance.
2) Determine the vehicle parameters and the range of the parameters for the operating conditions.
3) Model the system.
4) Based on vehicle modeling and testing, determine the performance requirements for the suspension system actuators.
5) Design and fabricate the actuators based on the performance requirements.
6) Test and optimize the actuators to meet the performance requirements.
7) Design the control system based on operating conditions, vehicle parameters and actuator performance.
8) Test control system using system components.
9) Implement system on vehicle.
10) Test and optimize components, controls and vehicle to meet or exceed performance requirements.

The results and continuation of work sections are organized according to this listing of tasks. The use of mathematical models is emphasized through out this project. With the use of accurate mathematical models it is usually much easier to evaluate changes in a dynamic system by changing the mathematical model than by modifying a prototype system. Also, it is virtually impossible to design a high performance control system without knowing something about the dynamic response of the system to be controlled. Mathematical modeling gives this knowledge in a relatively quick and efficient manner. This is not to say that testing is of lesser importance. The goal of this project is to design and fabricate a working suspension which requires a thoroughly tested system. When

accurate mathematical models can be constructed and validated with testing, systems can be designed for optimum performance with a greatly reduced need for cut-and-try experimentation and its associated costs in terms of time and capital.

## 4. Results

### 4.1 Range of operating conditions

The operating conditions and performance criteria to be evaluated will be based on:

1) Maximum speeds over half round bumps with radii of 5, 10 and 15 inches. The suspension will be optimized for the highest speed possible while meeting the peak loading of 2.5 G. Vehicle pitch sensitivity will also be improved since it is felt that this and the peak loading are the most important factors in improving vehicle stability and driver control.
2) Pitch sensitivity of the vehicle at different speeds over sinusoidal terrain inputs. Two sinusoidal terrain inputs will be considered, one with a wavelength of 5 ft with an amplitude of 1 ft and the second will have a wavelength of 60 ft with an amplitude of 10 ft. These two cases are felt from past vehicle testing at RMSV to represent the roughest medium and low frequency conditions that a high performance off-road vehicle would be operated on. It is felt that pitch sensitivity over this type of terrain input is important in maintaining vehicle stability and driver control and is also important in vehicle fatigue loading considerations.
3) Vehicle response to random road inputs. This is based on stochastic response methods in which the road velocity disturbance is treated as a white noise input into the suspension system. From this type operating condition, absorbed power into the driver or vehicle body or other performance criteria can be used for determining the effectiveness of a suspension design or a particular control strategy.
4) Vehicle roll response to a lane change maneuver and to a J-turn maneuver with a steady state lateral acceleration of 0.5 G. The performance criteria use to determine the effectiveness of the active roll control is the roll angle and general behavior of the

roll response. The steady state roll angle should be less than one degree of roll for this type of maneuver and the general response should not have any major discontinuities in the roll response which tend to reduce the driver's perception of ride quality.

## 4.2 Measurement and Analysis of Vehicle Parameters of JTEV

The test vehicle that this computer controlled active damper active ride height suspension system will be fitted to is the Joint Tactical Electric Vehicle (JTEV). JTEV is a hybrid diesel electric drive tactical military type vehicle for rough terrain testing and technology demonstrator. The suspension on JTEV is based on off-road vehicle racing technology and has 18" of suspension travel and uses high performance passive dampers which have been tuned for optimal suspension performance. JTEV has an adjustable ride height system which can vary the ride height up to 5" giving JTEV a ground clearance between 10 to 15".

The critical vehicle parameters which are required for vehicle modeling and analysis where determined and are shown below in Table 4.1, other vehicle parameters are given in the appendix.

All of these parameters were measured directly on the vehicle except for the moment of inertias and the roll axis height. The moment of inertias were calculated based on the mass and location of the vehicle's parts as designed. A correction factor based on [Garrott, 88][Riede, 84] was used to account for the errors associated with this method. The roll axis height was determined from the suspension geometry using the suspension analysis program TLS 100 by T.L. Satchell.

Table 4.1 JTEV Parameters

| | |
|---|---|
| Overall length: | 174" |
| Overall width: | 65.0" |
| Overall height: | 66.0" |
| Wheelbase: | 119" |
| Track width: | 52.5" |
| Vehicle weight, empty (with all fluids): | 4370 lb. |
| Weight percent on the front axle: | 51.1% |
| Distance from C.G to front axle: | 58.22" |
| Distance from C.G. to rear axle: | 60.78" |
| Weight percent on the left side: | 51.6% |
| Distance from C.G. to left side: | 25.4" |
| Distance from C.G. to right side: | 27.1" |
| C.G. height at lowest ride height setting: | 24.2" |
| Unsprung weight (same for each wheel): | 140 lb. |
| Approx. Pitch moment of Inertia: | 12,000,000 lb. $in^2$ |
| Approx. Roll moment of Inertia: | 1,700,000 lb. $in^2$ |
| Approx. Yaw moment of Inertia: | 12,500,000 lb. $in^2$ |
| Roll axis height at nominal ride height: | 4.15" |
| Front spring rate: | 700 lb./in (500 & 600 lb./in available) |
| Front suspension motion ratio: | 1.6 |
| Rear spring rate: | 300 lb./in (400 & 500 lb./in available) |
| Rear suspension motion ratio: | 1.55 |

## 4.3 Tire Models and tire parameters

In suspension analysis for on-road vehicles the tire is typically modeled as a simple vertical spring between the road and the unsprung mass which is allowed to lift off the road so that the tire spring can only be compressed. For off-road vehicles, since the road surfaces are usually much rougher, a more sophisticated tire model is sometimes used [Jones, 92][Ingram, 73][Sharp, 87]. One of these tire models is the radial spring tire model in which the tire is represented not by one vertical spring but by many radial springs spanning out from the hub to the tire circumference separated by a given angle as shown in Figure 4.1. This model accounts for the tire's finite length contact area with the ground and its ability to envelope short wavelength irregularities.

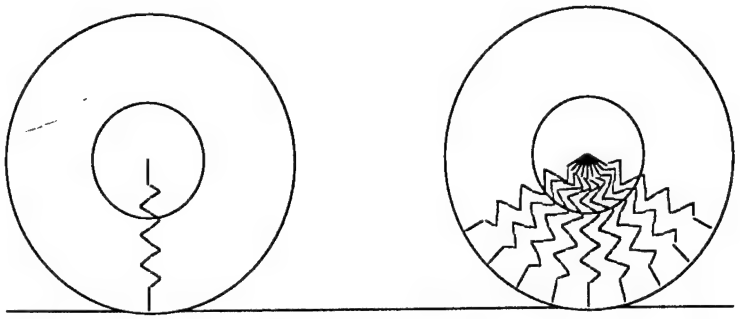

Figure 4.1 Single spring and radial spring tire models

For lower speed conditions and small tire deflections the radial spring tire model can improve the accuracy of a vehicle model since under these conditions tire enveloping can provide significant filtering of the road profile input. At higher speeds, over 25 mph, the filtered frequencies are generally above the suspension frequencies of interest [Sharp, 87], and do not significantly effect the accuracy. Also, at high tire deflections the radial spring tire model tends to break down as shown by Figure 4.2. The shape of the force deflection curve for the radial spring tire model tends to be parabolic due to the geometry of the springs. An actual tire tends to be linear until the tire tread starts to contact the tire bead and rim.

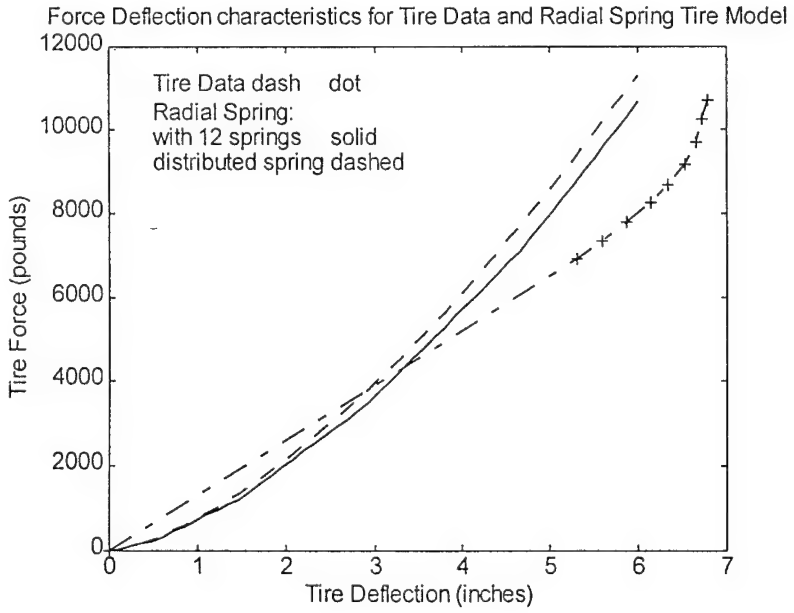


Figure 4.2 Force deflection curves for Radial spring tire model and actual tire data

For this project, a single spring tire model will be used for the operating conditions involving sinusoidal terrain inputs, random stochastic road inputs and for the vehicle handling analysis. Under these conditions the speeds are relatively high, the tire deflections can be large and the road profile frequencies are below the conditions where tire contact patch enveloping could have a significant effect on the suspension dynamics. For the single event half round bump operating conditions, where tire enveloping can have a significant effect on the suspension dynamics and where the tire deflections are very large, a two spring tire model will be used. This model is similar to the radial spring tire model except that only two springs are used, one vertical spring between the unsprung mass and the road surface and a second spring between the half round bump and the unsprung mass. The second spring is not fixed as with the radial spring tire model, but is allowed to rotate so that the spring axis is always between the wheel centerline and the half round bump centerline. This model accounts for the tire enveloping around the bump while allowing nonlinear tire force deflection data to be used.

To determine the nonlinear tire force deflection curves a test fixture was made which allowed this data to be experimentally measured along with changes in tire pressure as the tire was compressed. Data was taken for three types of tires designed for high performance off-road use, at five different pressures on a flat surface and on three half round bumps with radii of 5, 10 and 15". This data has been found to be very useful in modeling tires and for comparing the different tire models used in vehicle analysis. The data taken is presented in the appendix of this report.

The tire pressure data taken during the test was used to evaluate the feasibility of measuring the tire deflection as a function of change in tire pressure. The changes in tire pressure as the tire was deflected from zero to maximum deflection with the bead contacting the rim tended to be on the order of 5 psi. Test conditions with higher initial pressures and on larger radii surfaces had larger increases in pressure while test

conditions with lower initial pressures on smaller radii test surfaces had the lowest increases in pressure. From this data it is conceivable that the tire deflection could be measured by monitoring the dynamic changes in tire pressure. The difficulties involved in filtering out changes in pressure from temperature changes and acoustic effects on the tire pressure plus the problems of accurately measuring and monitoring the pressure on a rotating tire would all have to be overcome. Further analysis into the benefits of using this information in the suspension control system was carried out in section 4.4 of this report.

## 4.4 Damper models

In designing an active damper, a good mathematical model can be very valuable and allow a wide range of designs to be tried in a relatively fast and efficient manner. There are many papers in the literature which discuss modeling both passive as well as active dampers [Emura, 94][LaJoie, 96][Reybrouck, 94][Warner, 96b] and there are also papers presenting experimental data on different damper designs [Haney, 96][Warner, 96a]. Bond Graph modeling, which is a dynamic system modeling technique based on power and energy conservation [Karnopp, 83], has a number of advantages which make them well suited to the design and simulation of active dampers as well as complete suspension systems and vehicles. One advantage with bond graphs is that since they are based on power conservation they can be applied to mechanical, hydraulic, electrical and thermodynamic systems as well as systems involving all of these types of elements such as an active damper system. Another advantage is that bond graphs are modular. From this property, a simple dynamic model can be created and validated and then used in increasingly more complex systems with a minimal amount of additional modeling or validation.

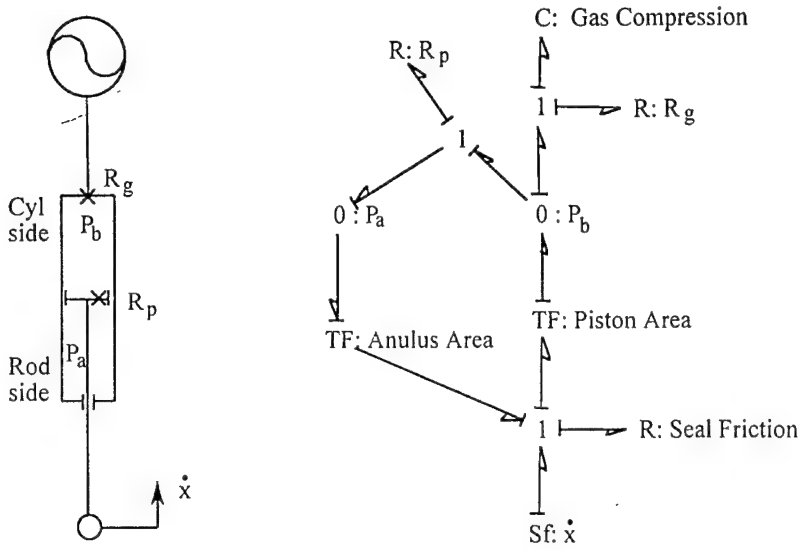


Figure 4.3 Basic damper model and bond graph

The basic damper model and bond graph are shown in Figure 4.3 and consists of a high pressure hydraulic damper. The most complex part of the model is the fluid resistance across the piston. This fluid resistance is a combination of nonlinear fluid resistance laws based on fixed orifices and force controlled blow-off valves for both passive and active dampers. In an active damper model, the orifice area can be controlled or the force on the controlled blow-off valve can be varied but the same nonlinear fluid resistance laws are used. These fluid resistance laws are based on turbulent flow and that the fluid velocity is constant across the orifice. Temperature effects are accounted for by varying the fluid density and viscosity. The resistance between the gas reservoir and hydraulic cylinder is assumed to be a fixed orifice, although in later designs a more complex valve system may be included. The fluid resistance laws and a complete damper model are given in the appendix. For the active damper system the valves and actuators are modeled as mechanical and electrical elements to allow the complete dynamic response of the active damper system to be analyzed

Figures 4.4 and 4.5 present a comparison between the damper model and actual test data taken with the RMSV in-house shock dynamometer. The damper model for these cases had a 2.5" diameter bore and a passive damper piston assembly which incorporated both

orifice and blow-off type valves and was set up to approximate the damping of a high performance off-road vehicle. A controllable orifice valve was connected across the piston assembly which could be opened or closed to determine the range of control of this type of system. Two cases are presented here, one with the damper reservoir on the cylinder side of the damper and the other had the reservoir on the rod side of the damper. By locating the reservoir on either side of the damper piston, the effective area of the piston is changed. When the reservoir is on the cylinder side, the effective area is the annulus area between the piston and rod. When the reservoir is on the rod side, the piston area is the effective area of the damper.

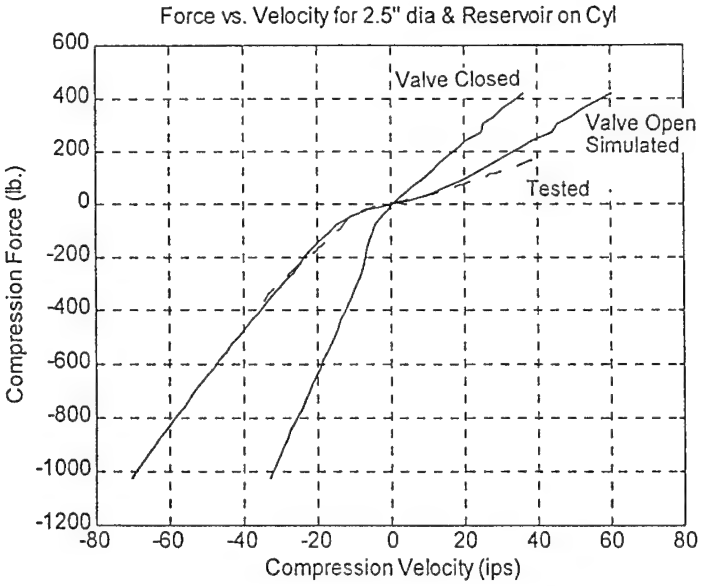


Figure 4.4 Comparison between damper model and damper test data for test damper A

To model the damper, the test case with the controllable orifice closed was used to determine the fluid resistance of the orifice and blow-off valves in the passive damper. This data was then used to predict the behavior of the damper throughout the range of the controllable orifice at various damper speeds. Figure 4.4 presents the comparison between the test data and the model for the case with the reservoir on the cylinder side of the damper. Since the effective area is smallest for this case, the damping forces are also the smallest of the two cases. The damper model matches the test data reasonably well

and the greatest error, about 20%, occurs at the highest compression speed tested while the highest rebound speed has an error of about 15%. The error is from the damper model underestimating the effect of the controllable orifice on the damping force. With further testing, the controllable orifice will be better quantified and the model will provide higher accuracy. Figure 4.5 presents the comparison of the test data to model prediction for the case with the reservoir connected to the rod side of the damper. This case has a larger effective area and therefore develops larger forces. The range of damping force provided by the control valve is smaller for this case than for the first case since the valve has less effect on the higher flows arising from the larger effective damper piston area. Similar errors are shown for this case as for the first case with a maximum error of 20% at the highest compression velocity and about 15% error at the highest rebound velocity.

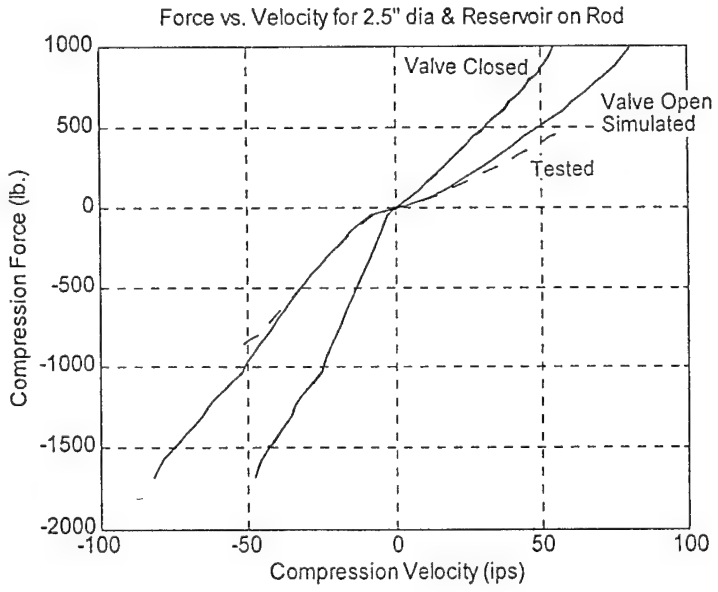


Figure 4.5 Comparison between damper model and damper test data for test damper B

Testing was also performed to determine the best method for modeling the gas pressure in the damper reservoir. It was felt that for very slow or steady state conditions, the gas should be treated as an isotropic expansion or compression where the gas temperature is assumed to be constant and heat is allowed to transfer between the gas and surroundings.

Figure 4.6 presents the data and model prediction for this condition for the 2.5" bore damper with the reservoir connected to the cylinder side of the damper. The gray dots are the data points and the black line is the model prediction based on the isotropic compression. As the Figure shows there is excellent agreement between the data and model.

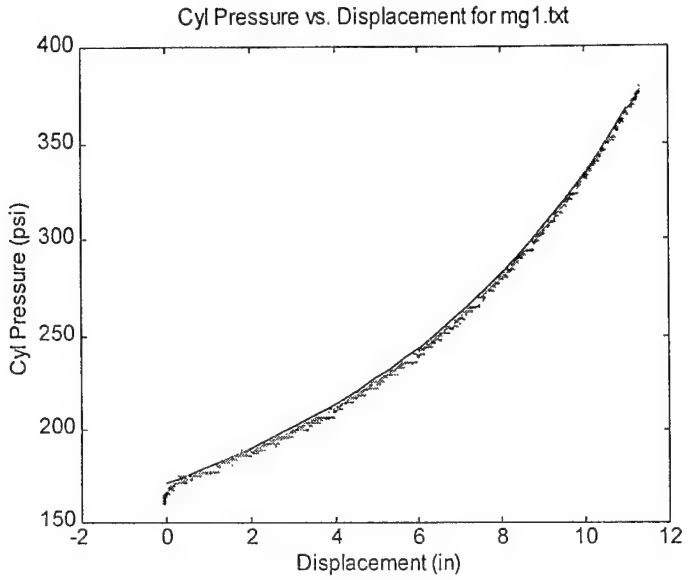


Figure 4.6 Damper gas pressure at slow speed (0.05 ips)

For faster motions, the gas compression is treated as an adiabatic process in which no heat is assumed to be lost or gained between the gas and the surroundings and the gas temperature is allowed to change. Figure 4.7 presents the test data and model prediction for a medium speed test (5 ips). For this test, the first compression (the curve with the highest pressure) has excellent agreement between the test data and model prediction. As the testing is carried out further, the gas tends to lose heat to the surroundings and the pressure is reduced. For higher test speeds of the damper, the heat loss has less of an effect. Figure 4.8 presents data for a test velocity of 38 ips. Under these conditions, the time is too short for the gas to lose heat, also other important effects are shown in this graph which will be discussed below. It is felt that for the purposes of this project, the accuracy of the adiabatic assumption is satisfactory for modeling the gas compression for

damper speeds greater than 1ips. For slower speeds the isotropic assumption should be satisfactory.

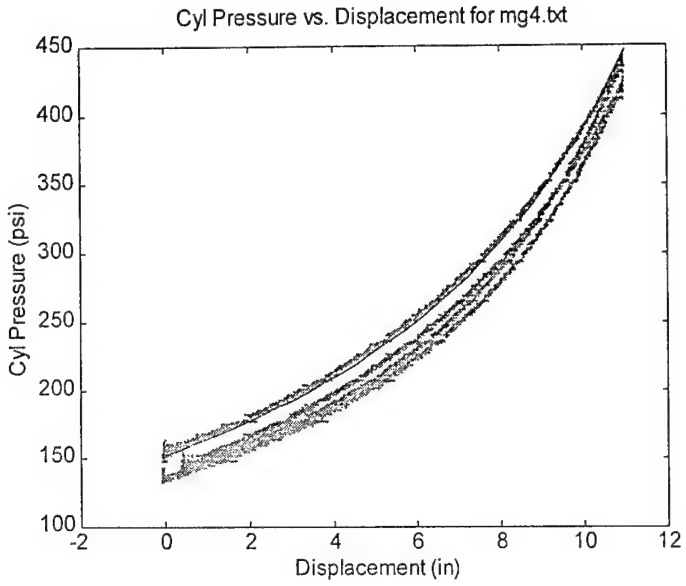


Figure 4.7 Damper gas pressure at medium speed (5 ips)

Figure 4.8 shows other interesting effects which occur at higher velocities and forces. The bounces in the pressure are caused by cavitation of the oil on the rod side of the cylinder. Under these high speed/ high force conditions, the pressure drop across the piston is so large that a vacuum occurs on the rod side of the piston causing the oil to boil at ambient temperatures. Once the oil on the rod side cavitates, the piston pushes oil into the reservoir increasing the gas pressure. The bouncing in the pressure occurs from oscillations between the reservoir gas compliance and the reservoir fluid line inertia as the oil is quickly pushed into the reservoir. The problem of cavitation is of great concern with high performance off-road vehicle dampers since it is this effect which limits the maximum compression damping force. There are three basic methods for reducing cavitation in dampers. The first is to increase the gas pressure in the reservoir so that high pressures across the piston do not create a vacuum on the rod side of the damper. The second method to reduce cavitation, is to increase the piston area so that higher forces can be achieved for a given pressure drop across the piston. Increasing the damper

diameter or increasing the number of dampers for each wheel are two ways of reducing cavitation effects based on this method. The third method for reducing cavitation is to connect the reservoir to the rod side of the damper. This eliminates cavitation when the damper is being compressed, but cavitation will then occur during the rebound stroke. Based on this method, some high performance off-road vehicle use two dampers per wheel. One of these dampers has the reservoir on the rod side and is used for compression damping. The second damper has the reservoir on the cylinder side and is used for rebound damping.

The damper model created for this project allows the onset of cavitation to be determined so that this important effect can be accounted for in the damper design. Although the damper model could be enhanced to model the effects of cavitation it is felt that the increased complexity and reduction in computational speed of such a model would not lead to much further insight into the design of a successful computer controlled hydraulic damper than the simpler model already developed for this project.

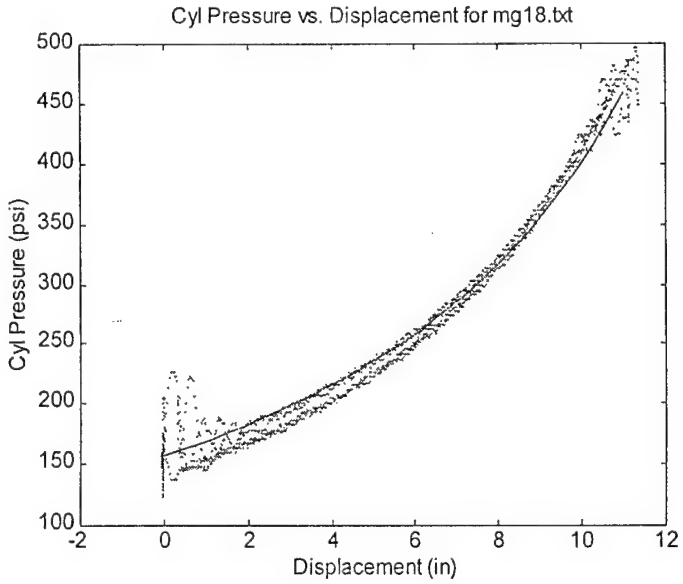


Figure 4.8 Damper gas pressure at high speed (38 ips)

Further testing using these hydraulic test dampers with different bores and damping arrangements is being performed to determine the optimal damper size and the dynamic performance of a high performance off-the-shelf electromechanical servo valve. These test units will provide valuable data into the range of velocities, forces and speed of response available from a system based on available servo valve technology.

Besides hydraulic dampers, a unit for testing the concept of a coulomb friction active damper has been designed and fabricated. The test unit is based on an automotive disc brake caliper, but instead of pressing brake pads onto a rotating brake rotor the caliper will press the brake pads onto a sliding member. With computer control of the pressure to the caliper, such as used in anti-lock braking systems and some types of traction control systems, a controllable damping force is achieved. One drawback with this system is that low flows from an external pump are required to control the caliper. This test unit will be used to determine the feasibility of the coulomb friction concept. The problems involved with the speed of response, the switching dynamics between velocities of different directions, heat build up, wear and acoustic noise will be addressed.

## 4.5 Quarter Car Model

In order to successfully design and develop a computer controlled suspension, simple models of the crucial dynamics are needed which can lead to a clear understanding of the system. To paraphrase Einstein, "The models should be as simple as possible, but no simpler." [Beard, 95]. The quarter car model, shown in Figure 4.9 (and was shown in Figure 2.1 to shown the different suspension systems) has proven to be very useful in modeling vehicle suspension systems because of its simplicity. A vehicle can be broken down into a quarter car model because typical body motions, even for high performance off-road vehicles are relatively small and there is little coupling between the wheel stations. This model is the simplest one which includes the essential features of independent wheel motion and the coupling of the suspension force between the unsprung mass and the sprung mass and can be used for analysis of a suspension design for

isolation, traction and static attitude control [Sharp, 87][Chalasani, 88a and b]. For modeling vehicle body motions in pitch and roll and dynamic weight transfer more complex models are more useful, such as half car roll or pitch models. For modeling dynamic weigh transfer and the effects of a suspension design on vehicle handling a full car model is required. These models will be discussed in the next sections.

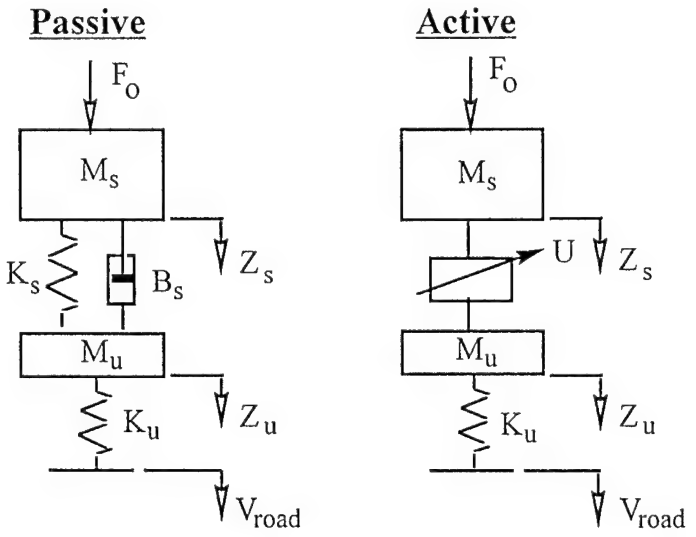


Figure 4.9 Quarter car suspension model, passive and active

Most of the parameters of the quarter car model are self explanatory and are given in Table 4.2. Typically in a suspension design the sprung mass, $M_s$, the unsprung mass, $M_u$, and the tire spring constant, $K_u$, are fixed. The suspension spring constant, $K_s$, and the suspension damping characteristics ($B_s$ is the passive damping coefficient while $B_a$ is an active "sky-hook" damping coefficient) are optimized to suit the operating conditions of the vehicle. In evaluating a given suspension system, the suspension deflection is an important variable and all the suspension designs should all be evaluated with equal suspension deflections or working space [Sharp, 87].

Table 4.2 Parameters for quarter car model

| | |
|---|---|
| $M_s$ | Sprung Mass |
| $M_u$ | Unsprung Mass |
| $K_s$ | Suspension spring Constant |
| $K_u$ | Tire Vertical Spring Constant |
| $B_s$ | Suspension Passive Damping Coefficient |
| $B_a$ | Active Damping Coefficient |
| $(Z_s - Z_u) / V_{road}$ | Suspension Deflection |
| $r_m$ | Mass Ratio ($M_u / M_s$) |
| $r_k$ | Stiffness Ratio ($K_u / K_s$)) |
| $r_d$ | Active Damping Ratio ($B_a / B_s$) |
| $\omega_u$ | Natural Frequency of the Unsprung Mass ( $\sqrt{K_u/M_u}$ ) |
| $\zeta_s$ | Damping Ratio of Sprung Mass ( $\frac{(B_s+B_a)}{2\sqrt{K_s M_s}}$ ) |
| $\zeta_u$ | Damping Ratio of Unsprung Mass * ( $\frac{B_s}{2\sqrt{K_u M_u}}$ ) |
| $g_4$ | Control gain relating suspension control force to tire deflection |

* This has a minimum practical value of 0.2 for wheel control [Chalasani, 86].

The inputs to the quarter car model, listed in Table 4.3, are the static vehicle load ($F_o$), the road vertical velocity ($V_{road}$), and the forces for the active suspension actuators. The road vertical velocity represents the road irregularities as the vertical spring tire model rolls over it. For general studies a good approximation is that the vertical velocity is white noise with a spectral density, $S_o$, which is proportional to road roughness and forward velocity [Yue, 88][Chalasani, 86].

Table 4.3 Inputs for quarter car model

| | |
|---|---|
| $F_o$ | Static Vehicle Load |
| $V_{road}$ | Road Vertical Velocity |
| $S_o$ | Spectral Density of White Noise Vertical Velocity Input * |
| U | Actuator Force for Active Suspension |

* proportional to road roughness and forward velocity

The performance criteria for the quarter car model are listed in Table 4.4. These are the sprung mass acceleration which has been shown to give a good correlation to the isolation qualities of a suspension system. The tire deflection which represents the load variation in the tire contact force has been shown to correlate well to the traction properties of a suspension design [Sharp, 87]. Root mean square (rms) values of these performance criteria and frequency response plots (Bode plots) of the performance criteria which show the frequencies where a given suspension design has been improved or degraded give important understanding and insight into the dynamics of a given suspension design. The low frequency asymptote of the load deflection behavior of a suspension design can provide some information on the static attitude control, while the frequency response plot can give some insight into the dynamic attitude control.

Table 4.3 Performance criteria for quarter car model

| | |
|---|---|
| $\ddot{Z}_s / V_{road}$ | Sprung Mass Acceleration (isolation qualities) |
| $(Z_u - Z_r) / V_{road}$ | Tire Deflection (traction qualities) |
| $(Z_s - Z_u) / F_o$ | Load Deflection |

### Suspension system performance based on Quarter Car Model

The quarter car model was used to determine the critical variables to be used in the active damper suspension system. Optimal control theory using full state variable feedback was used and compared to a passive suspension system. Two optimal suspensions were considered, one which was optimized for suspension isolation and the second which was optimized for traction. Both of the optimal systems and the passive systems were analyzed assuming a white noise road velocity input. To determine the effectiveness of a given state variable, perturbations in the optimal gain where used to determine the range of effectiveness for that state variable as compared to the optimal full state system to that of the passive system. Before analyzing the active systems the passive suspension system will be considered.

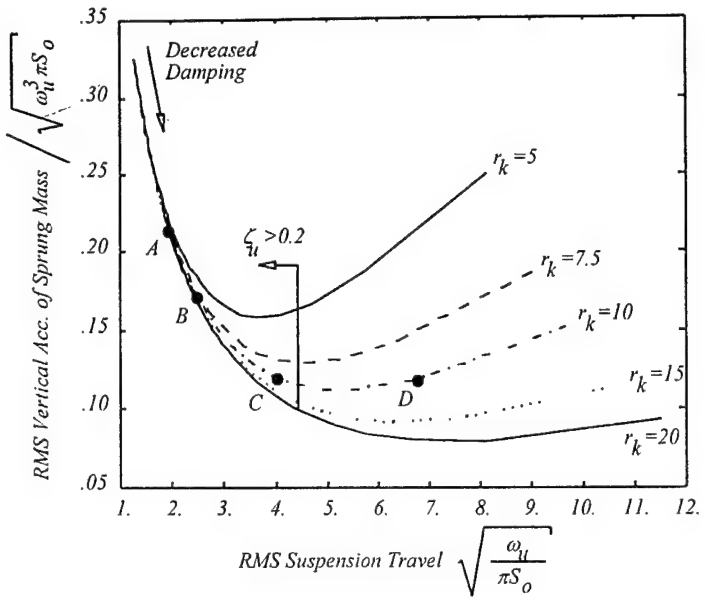


Figure 4.10 rms isolation response of a passive suspension

A passive suspension only has two design variables, suspension spring stiffness and damping coefficient. Figures 4.10 and 4.11 illustrates the relationship between rms sprung mass acceleration, and rms tire deflection, to rms suspension travel, for changes in sprung mass damping and suspension spring stiffness. In the top left of the graph, point A, the suspension has high damping, high sprung mass acceleration, high tire deflection, with low suspension travel. The large amount of damping makes the suspension practically rigid, carried to the extreme the suspension would act like a 1 degree of freedom system with no damping. With this suspension design the vehicle would act like a rigid unsuspended vehicle like a tractor. As the damping is decreased, the suspension follows the path corresponding to its stiffness ratio. Both the rms sprung mass acceleration and the rms tire deflection are reduced, while the rms suspension travel increases. This is the first compromise in a suspension system design, suspension travel versus sprung mass acceleration and tire deflection With further decreases in damping the tire deflection reaches a minimum, point B, then starts increasing. This would be the damping which would result in the best handling vehicle and would be used for a high performance sports car where vehicle ride or passenger isolation is of less importance than handling. Even less damping is required for the minimum of sprung mass

acceleration, point C. This is the second compromise, the difference in damping between the two minimums of tire deflection and sprung mass acceleration. The damping at point C would be chosen for a smooth riding luxury vehicle where passenger isolation is more important than vehicle handling. In general almost all vehicles would have damping between the points of B and C. Even less damping leads to worse performance in all of the criteria, this is due to resonance problems with both the sprung mass and the unsprung mass, point D. This would be representative of a vehicle with worn out dampers which provided very little damping. For practical purposes the unsprung damping ratio should not be less than 0.2 of critical damping [Chalasani, 88a]. This amount of damping is required to keep the wheel from vibrating excessively from tire unbalances or road disturbances and with less damping the tire traction is severely reduced. The frequency response curves, Figures 4.12, 4.13 and 4.14, for the points A, B, C and D on Figures 4.10 and 4.11 illustrate the system properties quite well.

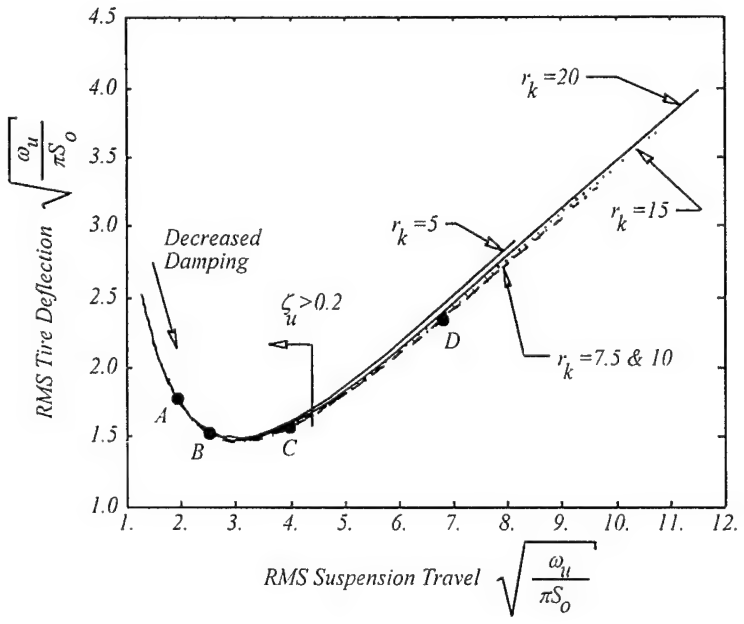


Figure 4.11 rms traction response of a passive suspension

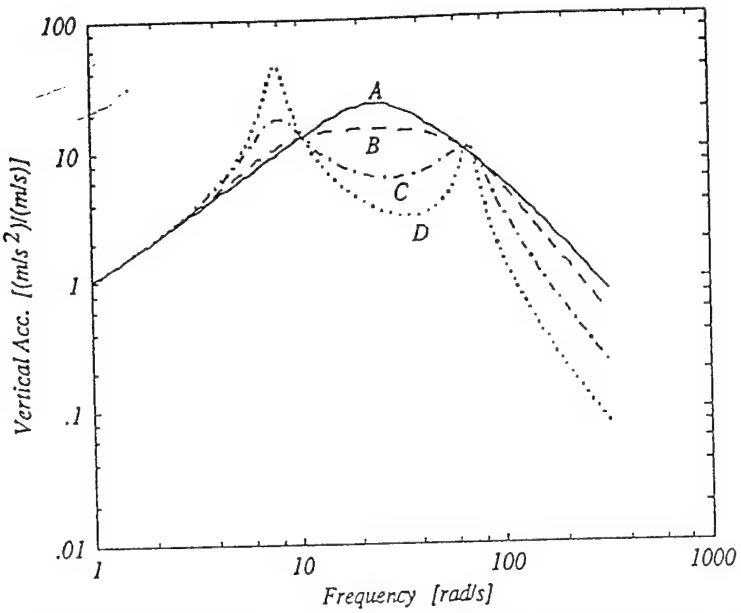


Figure 4.12 Bode isolation magnitude diagram for passive suspension

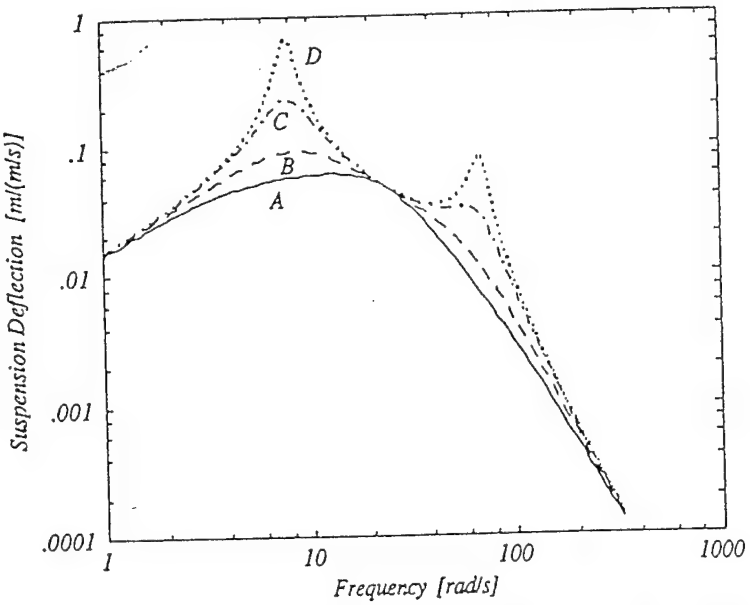


Figure 4.13 Bode suspension deflection magnitude diagram for passive suspension

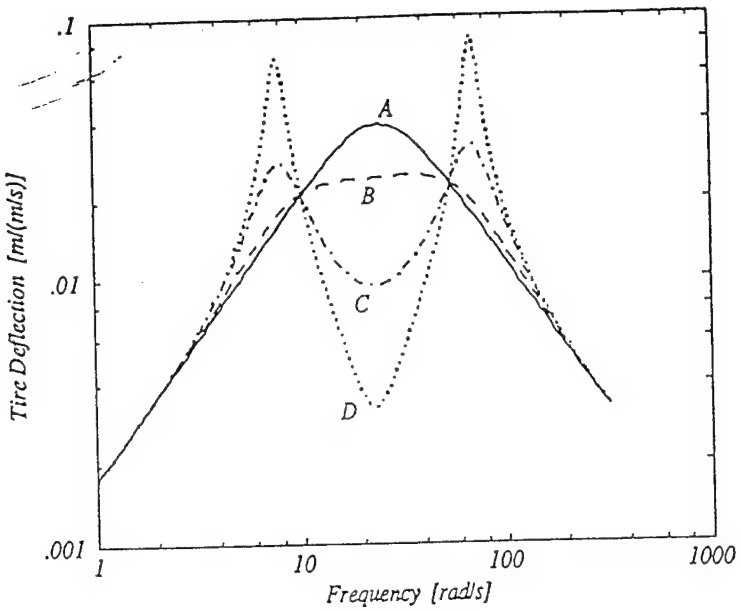


Figure 4.14 Bode traction magnitude diagram for passive suspension

Changing the suspension stiffness, $r_k$ ( $r_k$ =10 is a typical value) , improves both the tire deflection, and the sprung mass acceleration, for the same suspension travel. The major problem with a soft suspension is with attitude control, as can be seen from the low frequency asymptote of the load deflection transfer function:

$$\frac{(Z_s - Z_u)}{F_o} = \frac{1}{K_s}$$

Which shows that the lower the suspension stiffness the more sensitive the vehicle is to load changes.

Another idea would be to use a stiffer tire to increase $r_k$ . Although a stiffer tire does increase $r_k$ without effecting the attitude control, the isolation and traction of the suspension are reduced. This can be seen on the dimensionless rms plots, Figures 4.10 and 4.11, remembering to change $\omega_u$ since it is one of the factors used to remove the dimensions, and is effected by $K_u$ .

These Figures, 4.10 and 4.11, can also be used to provide some insight into the potential benefits of having an adaptable spring rate which would allow $r_k$ in these Figures to be varied. Figure 4.10 shows that for a given suspension deflection, the suspension isolation can be changed with a change in spring rate, especially for the cases with very low damping. Figure 4.11 shows that the tire deflection and tractive properties of a suspension are almost completely independent of spring rate since the curves for the different $r_k$ are grouped so close together. This implies that while suspension spring rate is a useful design parameter, the suspension damping plays a much larger role in determining the suspension performance in terms of both isolation and traction. This has been born out in suspension testing performed by RMSV. In setting up a high performance vehicle suspension system, typically the springs are chosen to be as soft as possible for satisfactory attitude control of the vehicle. The dampers are then adjusted to optimize the suspension for a given set of operating conditions. For relatively large changes in operating conditions, the damping would be adjusted while changes in spring rates are not usually required once a satisfactory spring rate has been found.

Although there have been devices for varying suspension stiffness produced, there does seem to be a fundamental problem with this type of system. For any system in which the spring rate is adjusted, the effective spring length and spring preload is also varied. This gives the undesirable result that as the spring rate is varied, the force on the suspension is also varied and the load distribution between the wheels of the vehicle may vary widely and unpredictably which would have very large effects on the vehicle's dynamic behavior and handling. It is felt that the problems involved with this secondary effect may be difficult to solve [Sharp, 87]. Changing the damping coefficient or using the damper as a controllable force element in the suspension does not have this undesirable secondary effect.

When compared to a passive suspension, an active suspension has additional design variables besides the suspension spring rate and damping coefficient. The first additional feature is the ability to have different damping for each of the two masses involved in the

quarter car model which is made possible with the measurement of the sprung mass velocity. In the literature this damping applied to the sprung mass is termed "Sky-hook" damping. A fourth design variable which is based on measuring the tire deflection relates the suspension force to the tire deflection.

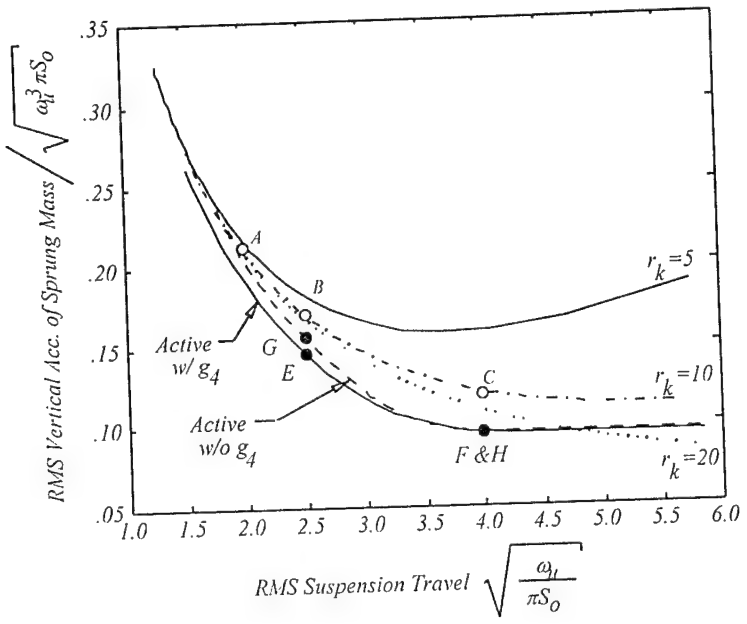


Figure 4.15 rms isolation response of a active suspension

To take advantage of these additional design variables the active suspension was optimized for isolation using optimal control. To determine the usefulness of the forth design variable of tire deflection an active suspension system was optimized with this gain set to zero. Figures 4.15 and 4.16 illustrate the relationship between rms sprung mass acceleration, and rms tire deflection, to rms suspension travel for the optimized active suspension with and with out the forth design variable (we will call it $g_4$ ). For reference, the passive suspension with three different suspension spring rates is also shown.

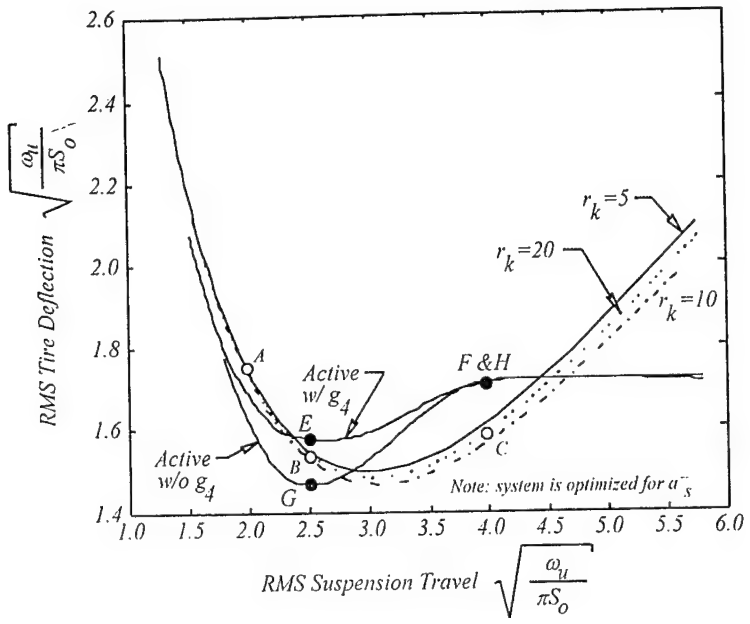


Figure 4.16 rms traction response of an active suspension

As the figures show active suspensions can improve isolation up to about 20%. There are drawbacks though. While isolation is improved, the traction is reduced. Considering the points for best traction, B (passive), E (active w/ $g_4$ ), and G (active w/o $g_4$ ), the isolation was improved by 14% for the active w/ $g_4$ suspension and 8% for the active w/o $g_4$ suspension, while the traction was reduced for the active w/ $g_4$ suspension by 3.5% and improved 4% for the active w/o $g_4$ suspension. For the points of best isolation, C (passive), F (active), and H (active damper), the isolation was improved by 20% for both the active w/ $g_4$ and active w/o $g_4$ suspensions, while the traction was reduced for both by 10%. From this it would seem that active w/o $g_4$ suspension supplies the best compromise, and that the added design flexibility of the fourth design variable does not significantly improve the overall design.

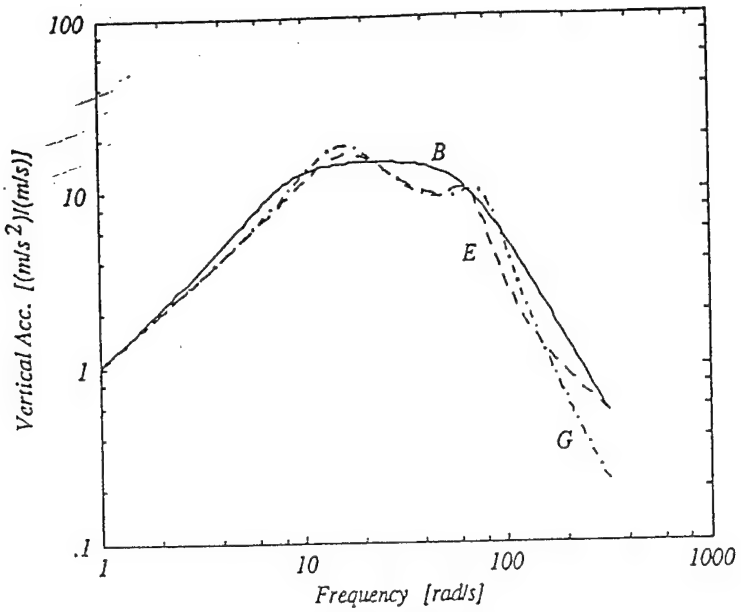


Figure 4.17 Bode isolation magnitude diagram for active suspension for best traction points

The frequency response curves of isolation in Figure 4.17 show another problem with the fourth design variable, $g_4$ , namely high frequency harshness. The high frequency asymptote of curve E does not roll off as steeply as the other two. This can be seen from the high frequency asymptote of the transfer functions for these curves. For both the passive and active w/o $g_4$ suspensions this asymptote is:

$$\frac{\ddot{Z}_s}{\dot{Z}_r}(\omega \to \infty) \propto \frac{B_s K_u}{M_s M_u \omega^2}$$

while the high frequency asymptote for the active suspension is:

$$\frac{\ddot{Z}_s}{\dot{Z}_r}(\omega \to \infty) \propto \frac{g_4}{M_u \omega}$$

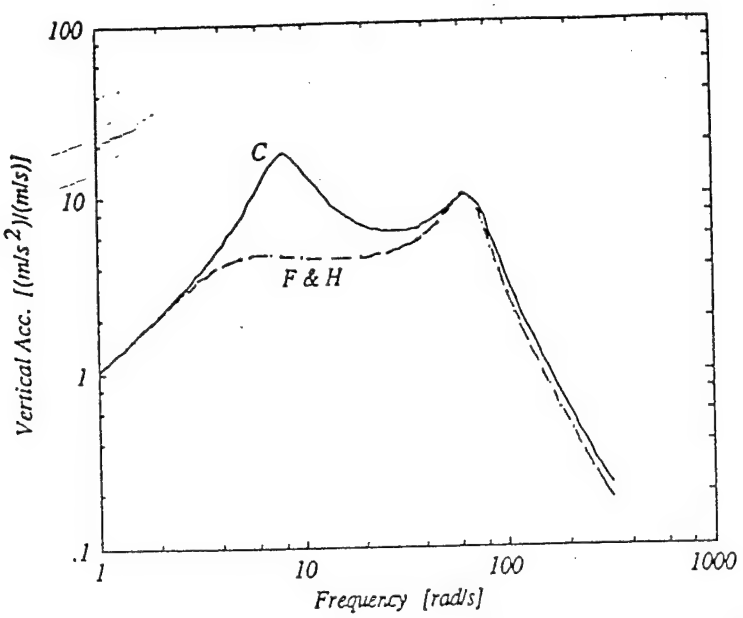


Figure 4.18 Bode isolation magnitude diagram of active suspension for best isolation points

The frequency response curves of suspension deflection in Figure 4.19 and 4.20 show another problem with both the active w/ $g_4$ and active w/o $g_4$ suspensions, namely excessive travel at low frequencies, even though each set of curves all have the same rms suspension travel. This is shown by the low frequency asymptotes for the suspension travel. For the passive suspension this asymptote is:

$$\frac{(Z_u - Z_r)}{\dot{Z}_r}(\omega \to 0) \propto \frac{-M_s \omega}{K_s}$$

For the active w/ $g_4$ and active w/o $g_4$ suspensions respectively these asymptotes are:

$$\frac{(Z_u - Z_r)}{\dot{Z}_r}(\omega \to 0) \propto \frac{-B_a}{K_s}$$

Note that these are both constants and do not drop off as with the passive suspension. This is a direct consequence of the "sky-hook" damper supplying a force proportional to the absolute velocity of the sprung mass. For an actual system, these low frequencies would be filtered out since any actual sensor would have a low frequency cut-off. With the low frequency deflection reduced by a filter, the rms suspension travel would then be lower for both active systems than for the corresponding passive suspension, leading to improved performance.

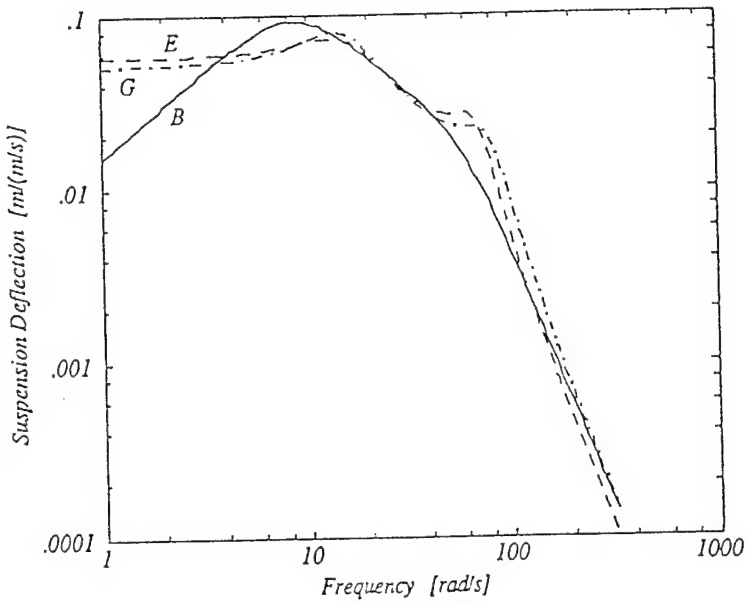


Figure 4.19 Bode suspension deflection magnitude diagram for active suspension for best traction points

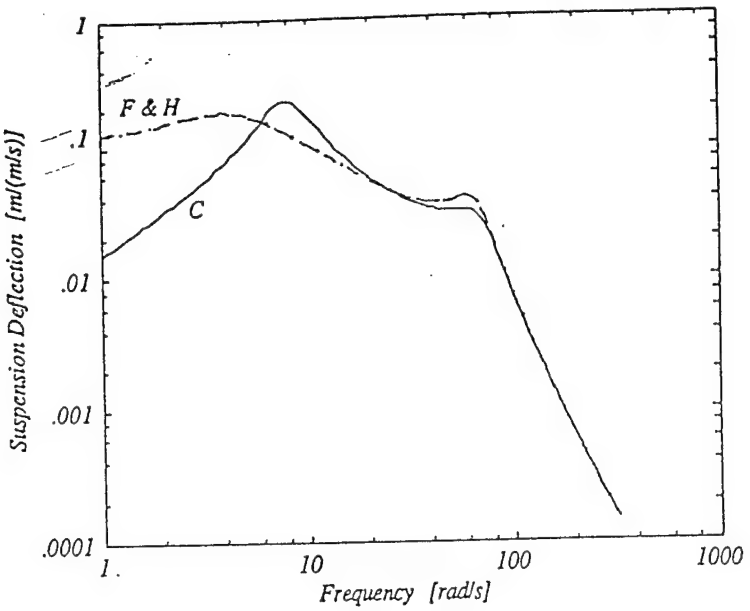


Figure 4.20 Bode suspension deflection magnitude diagram for active suspension for best isolation points

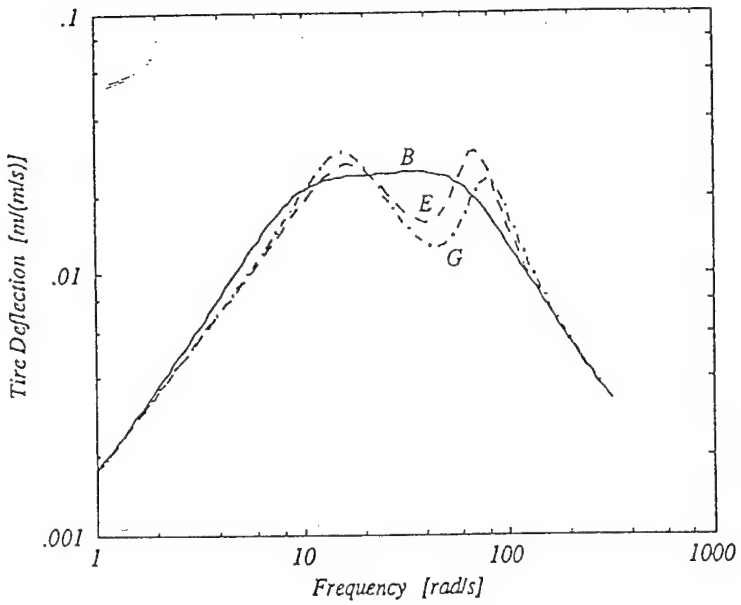


Figure 4.21 Bode traction magnitude diagram for active suspension for best traction points

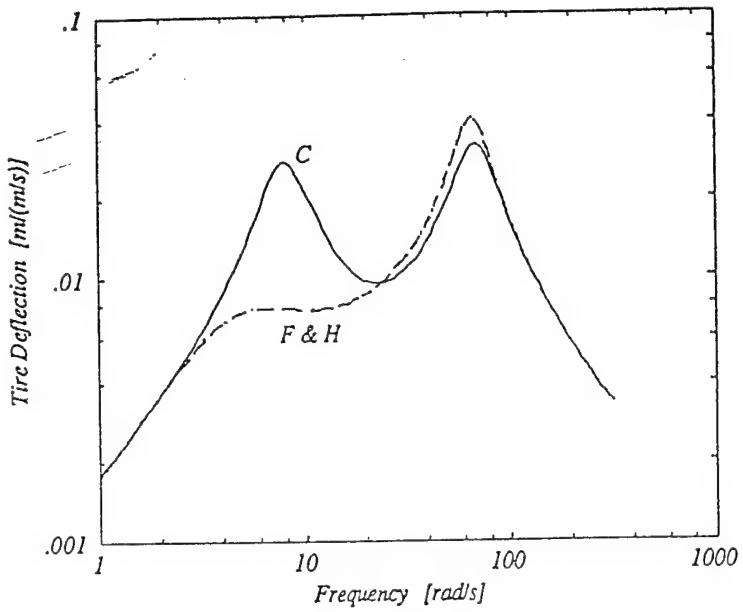


Figure 4.22 Bode traction magnitude diagram for active suspension for best isolation points

A general idea of the active systems attitude control can be seen from the low frequency asymptote of the load deflection transfer function, as with the passive system. In fact the passive and active w/o $g_4$ suspensions have the same asymptote, except that each would have a different $K_S$ :

$$\frac{(Z_s - Z_u)}{F_o} = \frac{1}{K_s}$$

The active w/ $g_4$ suspension has the factor, $g_4$ , involved:

$$\frac{(Z_s - Z_u)}{F_o} = \frac{K_u - g_4}{K_s K_u}$$

The suspensions with the best traction (B, E and G) the active systems are about 5 times stiffer than the passive system, improving the attitude control. For the suspensions with the best isolation the active systems are about 3 times softer than the passive system, reducing the attitude control.

This also points out the inadequacies of optimal control, which only has proportional control and does not have any integral terms in the control law. An integral term in the control law for the active suspensions, would force the low frequency asymptote for load deflection to zero, allowing the active suspension to load level. This is where an active suspension would have major improvements over both the passive and active damper suspensions. Optimal control will give the best suspension in regard to isolation, and other linear control laws would have the same or worse performance for isolation. The improvements from using a optimal active suspension occur mainly by controlling the components of the sprung mass motion in the vicinity of the undamped natural frequency (about 1 Hz. typically). Not much improvement is made in controlling the higher frequency wheel motions. Since this is the case, it does seem to be overkill to use a high bandwidth computer controlled suspension which requires fast components because of the wheel motions. The additional term in the fully active system relating tire deflection to suspension force does not improve the isolation of the suspension and in fact increases the high frequency harshness.

In this section an active suspension system using a relatively simple optimal linear control scheme was used to compare the performance potential of a computer controlled suspension system against a passive suspension system. This analysis showed that for this simple control scheme, a vehicle could have a reduction in passenger acceleration of up to 20% as compared to a passive suspension exhibiting approximately the same level of suspension travel and wheel hop control. Most of this improvement in vibration isolation of the computer controlled suspension occurs from improved damping of the body resonance motions. This improvement in isolation performance was achieved with the use of the sprung mass velocity as a feedback variable in the control scheme. Using the tire deflection as a variable in the control scheme did not add to the system performance substantially and in fact increased the high frequency harshness from road disturbances. Control based on an active damper type of system allowed both the isolation and tractive properties of the computer controlled suspension to be changed over a wide range. Control over the spring rate was found to only effect the isolation

properties and not the tractive properties of a suspension. From this it would seem that a computer controlled suspension based on an active damper would have a wider range of effectiveness in controlling a suspension system. It should be noted that this information was based on a simple linear control scheme and that with a more complex control scheme an active spring based system may have some very valuable traits.

## 4.6 Half Car Models

For modeling vehicle motions in pitch and roll a more complex vehicle model than the quarter car model is required. The simplest model which can describe this type of behavior is a half car model. Two different half car models are required for these types of motions, one model for pitch motions and a second for modeling vehicle roll motions. These two models are also used for different types of analysis, the pitch model is used for designing the active damper suspension system, the spring rates, damper forces and active damper control system. The roll model is used for designing the active ride height actuators and control system although the design of the active damper system must be taken into account since it will also effect the roll dynamics of the vehicle.

Initially the quarter car, half car models and data from past vehicle testing where used to determine the performance requirements for the active damper and active ride height systems actuators. These performance requirements are the range of forces the actuators must be able to produce, the speed of response of the actuators and the range of motion of the actuators. These performance requirements will then be used to design the active damper, active ride height actuators and control systems for them. Once a good preliminary design has been made for these systems, a complete full car model will be used to finalize, integrate and test the designs. A full car model is required to model the complete suspension system and to determine the dynamic weight transfer between the four wheels which can have a large effect on a vehicles handling and dynamic response.

## Pitch model

The half car pitch model used is based on symmetry between the left and right sides of the vehicle. The coordinate system used to describe the motion of the vehicle will be assumed to translate with the vehicle sprung mass and will not rotate. The x axis is in the forward direction of the vehicle and the z axis is in the vertical direction with positive pointing down. It is assumed that the vehicle body is rigid and that the mass and mass distribution does not change. It is also assumed that the vehicle will remain in the vertical plane so that lateral motions, roll motions and yaw motions are zero and do not effect the vertical plane motions.

The pitch model has basically five degrees of freedom. The model is allowed to move vertically up and down in heave, the model is also allowed to rotate in pitch with nose up motions as positive and the forward velocity is allowed to vary under braking and accelerating test conditions. Each suspension system, in the front and rear, is allowed to move and this movement is restricted so that the wheels move in the vertical direction relative to the vehicle body. Many of the model parameters are the same as for the quarter car model although there would be two sets, one for the front and one for the rear suspensions. Other additional parameters required for the half car pitch model are the wheelbase, pitch moment of inertia (half of the total value is used) and the nominal center of gravity height. For these half car pitch models, suspension linkage effects such as anti-dive and anti-squat are ignored since the JTEV suspension system has minimal amounts of these effects built into it. With this assumption, the pitch axis for the vehicle is at ground level. The motion ratios (M.R.) for the front and rear suspension systems are assumed to be constant over the suspension travel. This is close to the actual case since the front suspension motion ratio of JTEV ranges between 1.58 and 1.6 and the rear suspension motion ratio ranges between 1.52 to 1.56 for 90% of the travel (the last two inches in droop the M.R. is between 1.52 and 1.44). Additional degrees of freedom depending on the actuator modeling used for the active damper and active ride height systems may be added to the pitch model.

Two types of tire models are used for the half car pitch model depending on the type of test and terrain input used. As discussed in the tire model section, a two spring tire model is used when a half round bump is the terrain input. This model uses a single vertical tire spring to model the tire ground interaction and a second tire spring to model the tire bump interaction where both of the tire spring data has been empirically measured. For random road inputs and sinusoidal road inputs a single tire spring model is used. Under these conditions tire enveloping does not significantly effect the dynamics since the speeds are relatively high and the frequencies of interest are low. With these tire models it is also assumed that the tire forces from hitting bumps occur at the wheel center and that wheel torque effects from these bumps are ignored. Braking and accelerating forces on the tires are assumed to act on the ground surface under each tire.

Depending on the use of the half car pitch model either a nonlinear large angle model, or a small angle linear model can be used. The nonlinear model is used for determining the pitch and heave responses, suspension forces and peak accelerations of the vehicle to the different terrain inputs and for designing the active damper suspension actuators and other components. The linear model is used for designing the active damper control system where the use of linear modeling and control techniques are very useful. Once the control system has been designed based on the linear model then the control system is checked and improved using the nonlinear model. This design method, using a combination of linear and nonlinear models and design methods, has been shown to be both efficient and effective [Karnopp,83a][Beard, 95].

Block diagrams of both the nonlinear and linear half car pitch models for the computer analysis and design program Simulink® from The Math Works Inc. and some simulation results are given in the appendix.

## Roll model

The half car roll model is used for designing the active ride height actuators and control system. The coordinate system used to describe the motion of the vehicle will be assumed to translate with the vehicle sprung mass but will not rotate with it and is similar to the coordinate system used in the half car pitch model. In this coordinate system, the forward axis is the positive x axis, the vertical axis is the z axis with positive down and the lateral axis is the y axis with positive to the right when looking along the positive x axis. It is also assumed that the vehicle body is rigid and that the mass and the mass distribution does not change. A last assumption is that the vehicle will remain in the vertical plane defined by the z and y axes so that lateral motions, yaw and pitch motions are zero.

The roll model has basically four degrees of freedom, heave motion, roll motion and two suspension motions, one for the right suspension and one for the left suspension. A simplified roll model without the unsprung suspension masses was also created to help design the active ride height control system which is only required to control the vehicle body motions and not the higher frequency wheel motions. There also may be additional degrees of freedom incorporated into the model depending on the actuator modeling used for the active damper and active ride height systems. As with the pitch model, many of the parameters are the same as those for the quarter car model. In this case the right and left side would have the same parameters as either the front or rear quarter car models depending if the half car roll model was for the front or rear half of the car. Additional parameters are the additional roll stiffness added with an anti-sway bar, the vehicle track width, the nominal center of gravity height, the roll axis moment of inertia (half the total value is used) and the suspension roll axis height.

The roll model uses only the vertical spring tire model with a random road input. The main input into the model is a roll moment applied to the sprung mass center of gravity to model the effects of lateral acceleration from cornering. The magnitude of the roll

moment is equal to the distance between the roll axis height and the center of gravity multiplied by the sprung weight and the lateral acceleration assumed. As with the half car pitch model both nonlinear and linear models will be used for designing the active ride height system with the half car roll model. Block diagrams of the models developed of the half car roll model are given in the appendix.

## 4.7 Full Car Model

The full car model is the most complex vehicle model used for this project. Once the active damper and active ride height systems have been designed through the progression of models from the damper model to the quarter car model to the half car models the design should be complete. The full car model is used to check the results and to fine tune the complete suspension system. All of the previous vehicle models, the quarter car and half car models, are based on the assumption that the motions of a vehicle can be decoupled for simplicity. In general this is a very good assumption for vehicle modeling [Beard, 95][Sharp,87][Karnopp,76]. The full car model does not depend on this assumption and allows complete modeling of all the vehicle motions with coupling between them. It is always a good idea to double check a vehicle suspension design with a full car model because for some vehicle parameters and some suspension controller designs there is the possibility that there is some form of undesirable coupling between the vehicle motions which may lead to poor performance or even instability in the control system.

The full car model uses a vehicle centered coordinate frame with the origin fixed to the vehicle center of gravity which translates and rotates with the vehicle body. The x axis is in the forward direction of the vehicle, the y axis is in the lateral direction with positive to the right when looking along the x axis. The z axis is in the vertical direction with positive pointing down. This is a typical coordinate system used for both ground vehicles [Karnopp, 76] as well as aircraft [McRuer, 73]. It is assumed that the vehicle body is rigid and that the vehicle mass and mass distribution does not change. It is also assume

that the angles involved with the pitch and roll motions are relatively small on the order of ±15°, and that the forward speed is greater than the motions in the vertical and lateral directions.

The full car model has ten degrees of freedom. The model is allow to translate in the heave, lateral and longitudinal directions, and to rotate in pitch, roll and yaw. Four additional degrees of freedom arise from the separate suspension motions for each wheel. As with the half car motions the suspension is allowed to move only in the vertical direction relative to the horizontal plane of the vehicle body.

Most of the parameters used in the full car model have been used in the quarter and half car models. There are some additional parameters required thought. The yaw moment of inertia is required to describe the transient cornering behavior of the vehicle and tire forces in the lateral and longitudinal directions need to be determined. To determine these tire forces, the quasi steady state tire model developed by H. Pacejka [Pacejka, 87] will be used. This tire model is based on a nonlinear set of equations used to describe the lateral and longitudinal tire forces as a function of slip angle, longitudinal slip ratio and tire contact force. To keep the model at least relatively simple it will be assumed that the effects of camber angle are negligible, and that the slip ratios and longitudinal slip ratios are the system inputs. This assumption reduces the complexity since the vehicle steering and braking systems are not required to be modeled. As with the roll model only the vertical spring tire model will be used. Both random road inputs and a simplified version of the half round bump will be used to model road disturbances into the suspension system.

At the present time the full car model is under development, although a simplified model has been constructed. This simplified model does not have the nonlinear lateral / longitudinal Pacejka tire model incorporated and does not have the yaw or lateral degrees of freedom included. This simplified full car model does allow the roll, pitch and heave behavior of the vehicle with either passive or computer controlled suspension systems to

be simulated. The Block diagram of this simplified model as represented in the program Simulink® is given in the appendix. This simplified model also serves as the basis of the more complex full car model and with the addition of the Pacejka tire model and lateral dynamics the complex full car model will be complete.

## 4.8 Requirements and Design of Active Damper

Based on past vehicle testing and computer simulations a design envelope for a high performance off-road damper has been determined and is shown in Figure 4.23. For reference, the requirements for an on-road computer controlled damper are also shown in this Figure by the black regions in the first and third quadrants. For this on-road system forces on the order of 1,000 lb. with maximum velocities on the order of 40 ips (1 m/s) are required. The requirements for a high performance off-road system are much higher with forces on the order of 10,000 lb. and velocities up to 150 ips (4/m/s) are required for best performance. The optimal passive off-road suspension force velocity relation would be located between the Upper Bound Active Damper curve and the Lower Bound A curve. These two curves represent the required force velocity relationship for a computer controlled damper to show improved performance over a high performance passive damper. An active damper fitting this envelope would not be able to implement some of the more advanced computer controlled suspension algorithms such as sky-hook damping for controlling vehicle body motions and resonances. To implement this type of control algorithm, an off-road active damper would be required to envelope the region enclosed by the Upper Bound Active Damper and the Lower Bound B. For a hydraulic active damper to have the force velocity curve of Lower Bound B, a large controllable orifice is required to reduce the pressure drop created by the large flow rates at the high damper velocities.

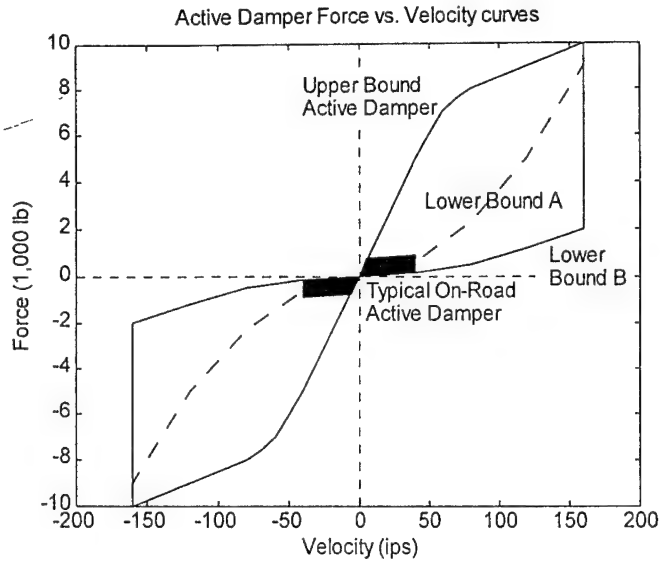


Fig. 4.23 Active Damper Performance Envelope for On-Road and Off-Road Conditions

The active damper designed for this project is based on a high performance hydraulic passive damper which incorporates a controllable orifice which bypasses flow around the passive damper assembly. This design concept allows the best properties of a passive damper to be included into the computer controlled damper such as the excellent high frequency response and good failure modes while also extending the flow and force range of the controllable components in the damper. Figure 4.24 shows the force velocity behavior and controllable range provide by an available high performance servo valve based on shock dyno test results with a 2.5" bore damper. With the controllable valve closed, the force velocity relationship is defined by the passive damper. As the control valve is opened the force of the damper is reduced to that shown by the lowest curve where the valve is completely open. The controllable range of this size damper and the largest available servo valve best suited to this application is approximately equal to that represented by the Upper bound Active damper curve and the Lower Bound A curve of Figure 4.23. To increase the controllable range of this damper assembly, either a larger valve or a smaller bore damper are required.

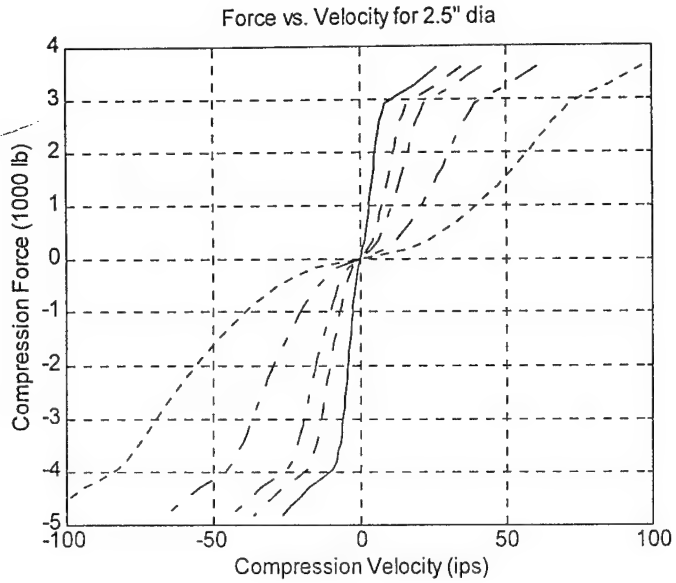


Figure 4.24 Force velocity range of 2.5" bore active damper

Figure 4.25 presents data for a smaller bore damper (46mm) with the same controllable valve used in Figure 4.24. This combination of damper size and controllable valve has a wider range of control as compared to the larger bore damper. The range provide by this active damper design matches the requirements outlined by the desired active damper performance envelope shown by Figure 4.23. To better illustrate this, the extreme curves of Figures 4.24 for the 2.5" bore active damper and of Figure 4.25 for the 46 mm damper have been shown with the curves representing the desired performance envelope are shown in Figure 4.46.

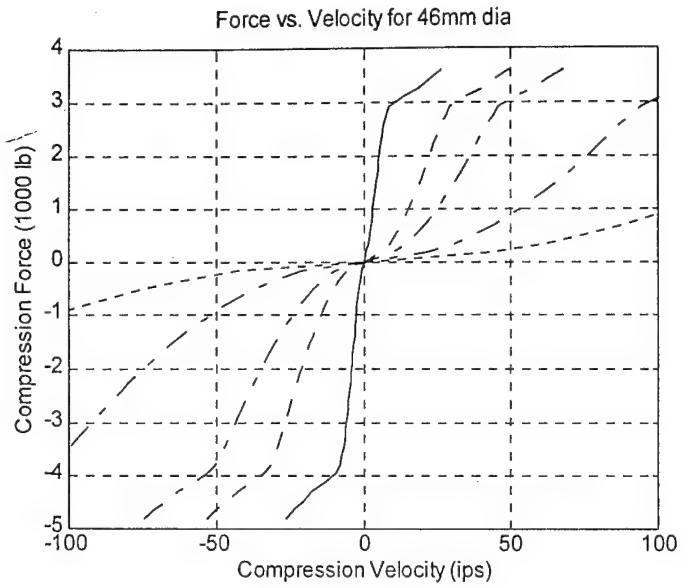


Figure 4.25 Force velocity range of 46 mm bore active damper

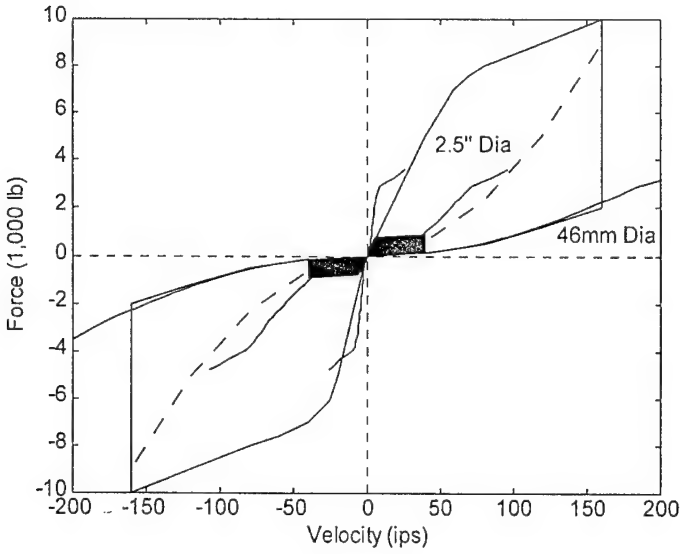


Figure 4.26 Desired performance envelope with force velocity ranges of 2.5" and 46 mm bore active dampers

As discussed in the damper modeling section of this report, one major problem which must be addressed with any high performance off-road hydraulic damper is that of cavitation. With the smaller 46 mm bore of the wide range active damper design, cavitation would typically occur at forces on the order of 1,000 lb. Obviously, some

better method of dealing with cavitation is required if this active damper design is to meet the design requirements as shown by the active damper performance envelope. Since the active damper design provides access to both sides, the cylinder side and the rod side, of the damper assembly with the controllable bypass valve. Based on this access, an innovative passive valve has been designed which allows the reservoir to be switched to the low pressure side of the cylinder and away from the high pressure side which will eliminate cavitation problems.

Besides the controllable range of the active damper, the speed of response is also very important. At 150 ips damper velocity, a delay time of 100 ms would represent a suspension travel of 15" which is almost all of the suspension travel of JTEV. For a delay time of 10 ms, 1.5 " or about 10% of the suspension travel would be used, while a very short delay time of 1 ms would represent only 0.15" or 1% of the suspension travel. From this discussion, it would seem that a control speed of less than 10 to 15 ms is required for adequate suspension control while a delay time under 5 ms would be ideal. Past testing and simulations have shown this to be true, and some on-road systems have used systems with delay times greater than 30 ms and have shown improved performance over passive systems for controlling body and wheel motions [Emura, 94]. It should also be noted that although the power required to drive a valve is relatively small, it can become large as the frequency of the valve is required to be very high since the power required to drive a high frequency valve increases as a function of the frequency cubed. Although a faster system will have benefits in control of single event bumps, impacts and suspension bottoming.

The largest available high performance servo valve best suited for this application has a step response time of 13 ms which is relatively slow for the active damper application. Additional testing on the shock dynamometer using this valve and the active damper test units will be used to determine if this valve has the speed of response and controllability required for this application. We have been working with the valve manufacture to determine if improvements can be made to reduce the step response time and increase the

valve's frequency bandwidth. Once this testing has been performed, hardware in the loop simulations in which the active damper design based on this valve will be used to determine the performance of this active damper in conditions very close to actual test conditions. Using some form of preview and adaptable control scheme may allow the requirements on active damper actuator speed to be relaxed, the effects of this will be determined using the half car pitch model. Past designs and testing have shown that most problems in dealing with stability over single event bumps arise from the rear suspension bottoming and not from the front suspension bottoming. Under these circumstances using preview from the front suspension may lead to improvements in vehicle performance while allowing a slower actuator.

## 4.9 Requirements and Design of Active Ride Height

A typical design goal for an active roll control system is for a maximum roll angle of 1° for a ½ g cornering maneuver [Beard, 95]. It was decided that this would be a satisfactory performance requirement for the active ride height control system being developed for JTEV. Two types of cornering maneuvers were considered, the first is a J-turn in which the lateral acceleration is increased in a linear ramp from zero to ½ g over ½ sec. The second maneuver is a slalom maneuver which consists of two ramp inputs, the first ramp input lasts for ½ sec and the lateral acceleration changes from zero to ½ g, the second ramp input lasts for ½ sec and the lateral acceleration changes from ½ g and is decreased to zero. It is felt that these maneuvers represent typical driving behaviors that JTEV and similar type vehicles are subjected to. For the active ride height system to have good dynamic behavior a bandwidth of 3 to 4 Hz is required to control body motions. This allows the system to be fast enough for good control of the vehicle body motions and systems of this type and bandwidth have been shown to be very competitive with fully active systems over a wide range of running conditions [Sharp, 87][Beard, 95].

To meet these performance requirements the three active ride height configurations discussed in section 2.2 and shown in Figure 2.6 where analyzed. To determine the

relative efficiencies of the three systems, the required power was calculated for the ½ g J-turn maneuver while holding the steady state roll angle to 1°. Since this power calculated does not take into account inefficiencies from friction and pump loses the actual power required to control the body motions should be slightly greater than the powers presented here. Between the three systems it was found that to control the roll angle to 1° during the ½ g J-turn cornering maneuver that system A, which pumps fluid from one corner of the vehicle across to the other side, required the least amount of power, 0.5 kW per axle. System B, which uses separate pumps for each suspension strut of the vehicle required 1.2 kW of power for each axle for the J-turn maneuver, which is about two and a half times the power required for system A. System C, which uses a single pump and accumulator with four control valves, was the least efficient and required 1.6 kW of power per axle for the same maneuver which is three times the power required for system A. Based on this analysis the design, selection of components and packing of the system into JTEV of system A is being carried out.

## 5. Continuation of work

The work for this project has been broken down into tasks as listed in section 3, Design and Approach, of this report and will be discussed following that context.

### 5.1 Summary of work performed to date

1) Determine the range of operating conditions for the vehicle and the desired performance.

The range of operating conditions and the desired performance have been determined and are discussed in section 4.1 of this report.

2) Determine the vehicle parameters and the range of the parameters for the operating conditions

The parameters of JTEV have been determined and are listed in section 4.2 of this report, also additional vehicle parameters and tire parameters are given in the appendix.

3) Model the system

Mathematical models have been developed for all of the critical vehicle systems and are discussed in sections 4.3 (tires), 4.4 (damper), 4.5 (quarter car), 4.6 (half car for pitch and roll) and 4.7 (full car). As discussed in this report, a somewhat simplified full car model has been completed and a more complex model with nonlinear lateral tire dynamics and including a yaw degree of freedom is still under development.

4) Based on vehicle modeling and testing, determine the performance requirements for the suspension system actuators.

The requirements of the suspension system actuators have been determined and are discussed in sections 4.8 for the active dampers and section 4.9 for the active ride height actuators.

5) Design the actuators based on the performance requirements (incomplete).

As discussed in section 4.8 and section 4.9 of this report, a prototype hydraulic active damper has been designed, fabricated and tested. Further testing is required to determine if the present servo valve has the speed necessary to meet the performance requirements. A prototype damper based on the coulomb friction concept has been designed and fabricated. Three designs for the active ride height system have been evaluated and a prototype of the most energy efficient one is being designed.

6) Test and optimize the actuators based on the performance requirements for the suspension system actuators (incomplete).

The prototype hydraulic active damper has undergone some testing, and it has been found to meet the required controllable range for at least speeds up to 50 ips. Further testing is needed to determine if the hydraulic servo valve has the required speed for good suspension control. We have been working with the valve manufacture to determine what improvements can be made to reduce the step response time and increase the valve's

frequency bandwidth. Testing is still required to determine the feasibility of the coulomb friction damper.

## 5.2 Required work to complete system

5) Design the actuators based on the performance requirements (continued).

The ride height actuator design needs to be completed.

6) Test and optimize the actuators based on the performance requirements for the suspension system actuators (continued).

The prototype active damper design needs to be tested at higher speeds and test to determine if the speed of response is fast enough to meet the active damper performance requirements. If it does not meet them either modification of a redesign will be performed. Once the active ride height actuators are designed a prototype actuator will be fabricated and tested.

7) Design the control system based on operating conditions, vehicle parameters and actuator performance.

8) Test control system using system components.

9) Implement system on vehicle.

10) Test and optimize components, controls and vehicle to meet or exceed performance requirements.

## 6. Conclusions

The computer controlled suspension system developed for this project is based on integrating an active damper and active ride height system into a soft passive suspension system. The active damper is used for controlling the medium and high speed dynamics involved with vehicle body and wheel motions. The active ride height system is used for controlling the low speed body motions. This type of system makes improvements over a passive system by allowing the optimal damping required for differing terrain and vehicle control requirements to be automatically set by the suspension system while the active ride height system controls the vehicle attitude without sacrificing either passenger isolation or handling. It has been determined that the critical control feedback variables are the suspension deflection, suspension deflection rate and the absolute vertical velocity of the sprung mass. Feedback with these variables could improve the isolation of this computer controlled suspension system on the order of 20% compared to an optimal passive suspension exhibiting the same level of suspension travel and wheel control. This improvement would be gained from improved damping of the vehicle body resonance motions. This type of system has been shown to be very competitive with fully active systems over a wide range of running conditions with lower cost, lower energy usage and improved failure modes.

## 7. References


Asgari, J., "Integrated Brake and Suspension Control During Braking and Maneuvering," Ph.D. Thesis, U. C. Davis, 1989.

Beard, D. C., "Design of a High Performance, Energy Efficient, Active Vehicle Suspension," Ph.D. Thesis, U. C. Davis, 1995.

Bundorf, R.T., "The Influence of Vehicle Design Parameters on Characteristic Speed and Understeer," *SAE TRANS* (670078), 1967.

Chalasani, R.M., "Ride Performance Potential of Active Suspension Systems - Part I: Simplified Analysis Based on a Quarter-Car Model," *ASME Monograph,* AMD - vol. 2, 1986.

Chalasani, R.M., "Ride Performance Potential of Active Suspension Systems - Part II: Comprehensive Analysis Based on a Full-Car Model," *ASME Monograph,* AMD - vol. 2, 1986.

Crandall, S.H., and Mark, W.O., Random Vibration in Mechanical Systems, Academic Press, 1963.

Emura, J and Kakizaki, S., "Development of the Semi-Active Suspension System Based on the Sky-Hook Damper Theory," *SAE , SP-1031* (940863), 1994.

Garrott, W. R., and Monk, M. W. , "Vehicle Inertial Parameters—Measured Values and Approximations," ,*SAE TRANS* (881767), 1988.

Haney, P. "A Comparison of Modern Racing Dampers," *SAE TRANS* (962545), 1996.

Hedrick, J.K. and Butsuen, T., "Invariant Properties of Automotive Suspensions," *IMechE Conf. On Advanced Suspensions, London,* Oct. 24-25, 1988 (Mech. Eng. Publ., London), pp35-42.

Ingram, W. F., "A Numerical Model of the Ride Dynamics of a Vehicle Using a Segmented Tire Concept," Technical Report M-73-5, US Army Engineer Waterways Experiment Station, Vicksburg, MS,1973.

Jones, R. J., "Validation Study of Two Rigid Body Dynamic Computer Models," Technical Report GL-92-17, US Army Engineer Waterways Experiment Station, Vicksburg, MS,1992.

Kailath, T., "Linear Systems," Prentice-Hall, Englewood Cliffs, N.J., 1980.

Karnopp, D.C., "Bond Graphs for Vehicle Dynamics," *Vehicle System Dynamics*, vol.5, 1976, pp171-184.

Karnopp, D.C. and Rosenberg, R.C., "Introduction to Physical System Dynamics," McGraw-Hill Book Company, New York, NY., 1983.

Karnopp, D.C., "Active Damping in Road Vehicle Suspension Systems," *Vehicle System Dynamics,* 12(1983), pp291-316.

Karnopp, D.C., "Force Generation in Semi-Active Suspensions Using Modulated Dissipative Elements," *Vehicle System Dynamics* 16(1987), pp. 333-343.

Karnopp, D.C., "Active Suspensions Based on Fast Load Levelers," *Vehicle System Dynamics* 16(1987), pp. 355-380.

Karnopp, D., and Wuh, D., "Handling Enhancement of Ground Vehicles using Feedback Steering Control," *Advanced Automotive Technologies, ASME*, Vol. 13, 1989, pp. 99-106.

Karnopp, D.C., "Design Principles for Vibration Control Systems using Semi-Active Dampers," *Trans. ASME J. Dyn. Sys. Meas. and Control*, Vol. 112, 1990, pp. 448-455.

Karnopp, D.C. and Heess, G., "Electronically Controllable Vehicle Suspensions," *Vehicle System Dynamics* 20(1991), pp. 207-217.

Karnopp, D.C., "Active and Semi-Active Vehicle Suspensions," Kia Academic Seminar, *The Automotive Technology for Safety and Environment*, Vol. 1, pp 123-147.

Karnopp, D.C., "Active and Semi-Active Vibration Isolation," *Trans. ASME Special 50$^{th}$ Anniversary Design issue*, Vol. 117(B), 1995, pp. 177-185.

LaJoie, J. C., "Damper Performance Development," *SAE TRANS* (962551), 1996.

Margolis, D.L., "The Response of Active and Semi-Active Suspensions to Realistic Feedback Signals," *Vehicle System Dynamics*, vol. 11, pp. 267-282, 1982.

Margolis, D.L., "Semi-Active Control of Wheel Hop in Ground Vehicles," *Vehicle System Dynamics*, vol. 12, pp. 317-330, 1983.

Margolis, D.L., "Bond graphs for vehicle stability analysis," *Int. J. of Vehicle Design*, vol.5, no. 4, 1984.

McRuer, D., Ashkenas, I. and Graham, D. "Aircraft Dynamics and Automatic Control," Princeton University Press, Princeton, New jersey, 1973.

Nalecz, Andrzej, G., "Investigation into the effects of Suspension Design on Stability of Light Vehicles," *SAE TRANS* (870497), 1987.

Nordeen, D.L., "Analysis of Tire Lateral Forces and Interpretation of Experimental Tire Data," *SAE TRANS* (670173), 1967.

Pacejka, Hans, B., Bakker, Egbert, and Nyborg, Lars, "Tyre Modelling for Use in Vehicle Dynamics Studies," *SAE TRANS* (870421), 1987.

Puhn, F., "How To Make Your Car Handle", HP Books, Los Angeles, CA, 1981.

Reybrouck K., "A Non Linear Parametric Model of an Automotive Shock Absorber," *SAE , SP-1031* (940864), 1994.

Riede, Peter, M., Jr., Leffert, Ronald, L., and Cobb, William, A., "Typical Vehicle Parameters for Dynamics Studies Revised for the 1980's," ,*SAE TRANS* (840561), 1984.

Sharp, R.S., and Crolla, D.A., "Road Vehicle Suspension System Design: A Review," *Vehicle System Dynamics,* 16(1987),pp.167-192.

Bakker, Egbert, Pacejka, H. B., and Lidner, L. , "A New Tire Model with an Application in Vehicle Dynamics Studies," *SAE TRANS* (890087), 1989.

Smith, S., "Advanced Race Car Suspension Development," Steve Smith Autosports Publications, Santa Ana, CA, 1974.

Warner, B., "An Analytical and Experimental Investigation of Friction and Gas Spring Characteristics of Racing Car Suspension Dampers," *SAE TRANS* (962548), 1996.

Warner, B., "An Investigation of the Influence of High Performance Dampers on the Suspension Performance of a Quarter Vehicle," *SAE TRANS* (962552), 1996.

Yue, C., Butsen, T, and Hendrick, J.K., "Alternative Control Laws for Automotive Active Suspensions," 1988 American Control Conf., Atlanta, GA, June 15-17, 1988.

## Appendices

I) JTEV Parameters

II) Tire Force/Deflection/Pressure change Data

III) Shock Dynamometer Data

IV) Hydraulic Damper Model

V) Quarter Car Model

VI) Half Car Models - Pitch Model

- Roll Model

VII) Full Car Model

# Appendix I

# JTEV Parameters

```
% jtevWD.m
% weight distribution and CG heigh of JTEV
% from measurements on 12-3-96
% loaded with 3 80 lb plates over rear axle
% at lowest ride height
wheelbase=119;
track=52.5;
rfFlate=1129;
lfFlate=1225;
rrFlate=1100;
lrFlate=1155;
total=rfFlate+lfFlate+rrFlate+lrFlate

total =

        4609

weightPfront=100*(rfFlate+lfFlate)/total

weightPfront =

   51.0740

a=(100-weightPfront)*wheelbase/100

a =

   58.2220

b=(weightPfront)*wheelbase/100

b =

   60.7780

weightPleft=100*(lrFlate+lfFlate)/total

weightPleft =

   51.6381

d=(100-weightPleft)*track/100

d =

   25.3900

c=(weightPleft)*track/100

c =

   27.1100

e=c;f=d;
% for CG height
% rear end raised up
rfangle=1171;
lfangle=1256;
rrangle=1064;
lrangle=1129;
totala=rfangle+lfangle+lrangle+rrangle;
deltarear=(67.5-47.5+67.75-46)/2;
deltafront=(44.75-45+44.75-45)/2;
angleR=asin((deltarear-deltafront)/114)

angleR =

    0.1864

angleD=180*angleR/pi

angleD =

   10.6790

ap=119*(rrangle+lrangle)/totala;
deltap=a-ap;
hcgp=deltap/tan(angleR)
```

```
hcgp =

    9.2038

tireR=16-1;
Hcg=hcgp+tireR

Hcg =

   24.2038
```

| | ride height | wheel travel | shock length | motion ratio | spring rate | wheel rate | corner wgt |
|---|---|---|---|---|---|---|---|
| | | | j | | | | 1200.00 |
| | | | 33.84 | | | | wheel freq |
| | | | | | | | |
| full bump | 1.00 | 11.00 | 22.53 | 1.60 | 700.00 | 273.52 | 89.66 |
| | 2.00 | 10.00 | 23.16 | 1.59 | 700.00 | 276.42 | 90.13 |
| | 3.00 | 9.00 | 23.79 | 1.59 | 700.00 | 278.19 | 90.42 |
| | 4.00 | 8.00 | 24.42 | 1.58 | 700.00 | 279.06 | 90.56 |
| | 5.00 | 7.00 | 25.05 | 1.58 | 700.00 | 279.25 | 90.59 |
| | 6.00 | 6.00 | 25.68 | 1.58 | 700.00 | 278.92 | 90.54 |
| | 7.00 | 5.00 | 26.31 | 1.59 | 700.00 | 278.24 | 90.43 |
| | 8.00 | 4.00 | 26.94 | 1.59 | 700.00 | 277.32 | 90.28 |
| | 9.00 | 3.00 | 27.57 | 1.59 | 700.00 | 276.28 | 90.11 |
| low adjust | 10.00 | 2.00 | 28.20 | 1.59 | 700.00 | 275.23 | 89.94 |
| | 11.00 | 1.00 | 28.83 | 1.60 | 700.00 | 274.26 | 89.78 |
| ride height | 12.00 | 0.00 | 29.45 | 1.60 | 700.00 | 273.47 | 89.65 |
| | 13.00 | -1.00 | 30.08 | 1.60 | 700.00 | 272.94 | 89.57 |
| | 14.00 | -2.00 | 30.70 | 1.60 | 700.00 | 272.80 | 89.54 |
| high adjust | 15.00 | -3.00 | 31.32 | 1.60 | 700.00 | 273.18 | 89.60 |
| | 16.00 | -4.00 | 31.95 | 1.60 | 700.00 | 274.27 | 89.78 |
| | 17.00 | -5.00 | 32.58 | 1.59 | 700.00 | 276.37 | 90.13 |
| | 18.00 | -6.00 | 33.20 | 1.58 | 700.00 | 279.95 | 90.71 |
| full droop | 19.00 | -7.00 | 33.84 | -0.03 | 700.00 | | |

JTEV FRONT SUSPENSION
UPRIGHT SHOCKOFF
LOWER A-ARM

wheel frequency in CPM

$187.8 * \sqrt{\frac{Kw}{GM}}$

adjustable height

alternate rates
600 lb/in
500 lb/in

— about 1400 lb/corner
— nominal corner weight, sprung mass

| | ground clearance | travel | rear shock length | motion ratio | spring rate | wheel rate | corner wgt | JTEV REAR SUSPENSION |
|---|---|---|---|---|---|---|---|---|
| | | | z | | | | 1300.00 | ROCKER AND PUSHROD |
| | | | 31.13 | | | | wheel freq | |
| full bump | 1.00 | 11.00 | 22.03955 | 1.54 | 300.00 | 125.81 | 58.42 | |
| | 2.00 | 10.00 | 22.68715 | 1.53 | 300.00 | 127.96 | 58.92 | |
| | 3.00 | 9.00 | 23.34023 | 1.52 | 300.00 | 129.14 | 59.19 | |
| | 4.00 | 8.00 | 23.99632 | 1.52 | 300.00 | 129.54 | 59.28 | |
| | 5.00 | 7.00 | 24.65343 | 1.52 | 300.00 | 129.33 | 59.24 | |
| | 6.00 | 6.00 | 25.31002 | 1.53 | 300.00 | 128.70 | 59.09 | |
| | 7.00 | 5.00 | 25.96499 | 1.53 | 300.00 | 127.79 | 58.88 | |
| | 8.00 | 4.00 | 26.62 | 1.54 | 300.00 | 126.75 | 58.64 | |
| | 9.00 | 3.00 | 27.26764 | 1.54 | 300.00 | 125.71 | 58.40 | |
| low adjust | 10.00 | 2.00 | 27.91496 | 1.55 | 300.00 | 124.79 | 58.19 | |
| | 11.00 | 1.00 | 28.55992 | 1.55 | 300.00 | 124.13 | 58.03 | |
| ride height | 12.00 | 0.00 | 29.20316 | 1.56 | 300.00 | 123.84 | 57.96 | |
| | 13.00 | -1.00 | 29.84565 | 1.55 | 300.00 | 124.08 | 58.02 | |
| | 14.00 | -2.00 | 30.48878 | 1.55 | 300.00 | 125.05 | 58.25 | |
| high adjust | 15.00 | -3.00 | 31.1344 | 1.54 | 300.00 | 126.99 | 58.70 | |
| | 16.00 | -4.00 | 31.78501 | 1.52 | 300.00 | 130.31 | 59.46 | |
| | 17.00 | -5.00 | 32.44407 | 1.49 | 300.00 | 135.62 | 60.66 | |
| | 18.00 | -6.00 | 33.11644 | 1.44 | 300.00 | 144.08 | 62.52 | |
| full droop | 19.00 | -7.00 | 33.80944 | -0.03 | 300.00 | | | |

400 lb/in
500 lb/in
available

JTROLL.XLS

calculated @ 1G side acceleration

ROLL ANGLE SUMMARY

| | FRONT | REAR | | |
|---|---|---|---|---|
| SPRING RATE | 700 | 400 | FREQUENCY | [redacted] CPM |
| LEVER LENGTH | 8.000 | 14.000 | VELOCITY | [redacted] MPH |
| SWAY BAR OD | 1.250 | 1.250 | FREQ @ VEL | [redacted] CPM |
| CORNER WEIGHT | 1125 | 1375 | | |

| WALL | | RESISTANCE in-lb/deg | | ROLL BAR in-lb/deg | | WT TRANSFER lb | | STIFFNESS % | | ROLL ANGLE | |
|---|---|---|---|---|---|---|---|---|---|---|---|
| FRONT | REAR | SPRING FRONT | SPRING REAR | FRONT | REAR | FRONT | REAR | FRONT | REAR | | |
| 0.188 | 0.25 | 6576.943 | 4004.616 | 8252.891 | 7231.544 | 1490.844 | 1224.87 | 0.568934 | 0.431066 | 4.462884 | |
| 0.188 | 0.188 | 6576.943 | 4004.616 | 8252.891 | 6322.58 | 1536.393 | 1179.321 | 0.589491 | 0.410509 | 4.624135 | |
| 0.188 | 0.125 | 6576.943 | 4004.616 | 8252.891 | 4905.22 | 1614.379 | 1101.336 | 0.624686 | 0.375314 | 4.900216 | |
| 0.188 | 0.095 | 6576.943 | 4004.616 | 8252.891 | 4011.99 | 1668.496 | 1047.218 | 0.649109 | 0.350891 | 5.0918 | |
| 0.188 | 0.065 | 6576.943 | 4004.616 | 8252.891 | 2953.488 | 1738.371 | 977.3428 | 0.680644 | 0.319356 | 5.33917 | |
| 0.125 | 0.25 | 6576.943 | 4004.616 | 6402.805 | 7231.544 | 1417.871 | 1297.844 | 0.536001 | 0.463999 | 4.803847 | |
| 0.125 | 0.188 | 6576.943 | 4004.616 | 6402.805 | 6322.58 | 1464.19 | 1251.525 | 0.556905 | 0.443095 | 4.991195 | |
| 0.125 | 0.125 | 6576.943 | 4004.616 | 6402.805 | 4905.22 | 1544.091 | 1171.623 | 0.592965 | 0.407035 | 5.314377 | |
| 0.125 | 0.095 | 6576.943 | 4004.616 | 6402.805 | 4011.99 | 1599.987 | 1115.728 | 0.618191 | 0.381809 | 5.540462 | |
| 0.125 | 0.065 | 6576.943 | 4004.616 | 6402.805 | 2953.488 | 1672.709 | 1043.006 | 0.65101 | 0.34899 | 5.834606 | |
| 0.095 | 0.25 | 6576.943 | 4004.616 | 5236.868 | 7231.544 | 1365.865 | 1349.849 | 0.51253 | 0.48747 | 5.04684 | |
| 0.095 | 0.188 | 6576.943 | 4004.616 | 5236.868 | 6322.58 | 1412.488 | 1303.227 | 0.533572 | 0.466428 | 5.25403 | |
| 0.095 | 0.125 | 6576.943 | 4004.616 | 5236.868 | 4905.22 | 1493.348 | 1222.366 | 0.570064 | 0.429936 | 5.61337 | |
| 0.095 | 0.095 | 6576.943 | 4004.616 | 5236.868 | 4011.99 | 1550.245 | 1165.469 | 0.595742 | 0.404258 | 5.866216 | |
| 0.095 | 0.065 | 6576.943 | 4004.616 | 5236.868 | 2953.488 | 1624.679 | 1091.035 | 0.629334 | 0.370666 | 6.196997 | |
| 0.065 | 0.25 | 6576.943 | 4004.616 | 3855.2 | 7231.544 | 1296.991 | 1418.724 | 0.481447 | 0.518553 | 5.368649 | |
| 0.065 | 0.188 | 6576.943 | 4004.616 | 3855.2 | 6322.58 | 1343.701 | 1372.013 | 0.502528 | 0.497472 | 5.603719 | |
| 0.065 | 0.125 | 6576.943 | 4004.616 | 3855.2 | 4905.22 | 1425.297 | 1290.417 | 0.539352 | 0.460648 | 6.014354 | |
| 0.065 | 0.095 | 6576.943 | 4004.616 | 3855.2 | 4011.99 | 1483.16 | 1232.554 | 0.565466 | 0.434534 | 6.30555 | |
| 0.065 | 0.065 | 6576.943 | 4004.616 | 3855.2 | 2953.488 | 1559.425 | 1156.29 | 0.599885 | 0.400115 | 6.689353 | |
| 0.001 | 0.25 | 6576.943 | 4004.616 | 69.2407 | 7231.544 | ######## | 1661.986 | 0.371662 | 0.628338 | 6.505272 | 1053.7282 |
| 0.001 | 0.188 | 6576.943 | 4004.616 | 69.2407 | 6322.58 | ######## | 1617.884 | 0.391565 | 0.608435 | 6.853644 | 1097.830 |
| 0.001 | 0.125 | 6576.943 | 4004.616 | 69.2407 | 4905.22 | ######## | 1538.832 | 0.427242 | 0.572758 | 7.478102 | 1176.8826 |
| 0.001 | 0.095 | 6576.943 | 4004.616 | 69.2407 | 4011.99 | ######## | 1481.161 | 0.453269 | 0.546731 | 7.933654 | 1234.5528 |
| 0.001 | 0.065 | 6576.943 | 4004.616 | 69.2407 | 2953.488 | ######## | 1403.016 | 0.488536 | 0.511464 | 8.550944 | 1312.6980 |

stupused 90 & 27196

MAKE .180 .125 .095 .065 F & R

## JTEV SUSPENSION CHARACTERISTICS

| LOWER PICKUPS | | UPPER PICKUPS | | | | | | | | | | | |
|---|---|---|---|---|---|---|---|---|---|---|---|---|---|
| X | Y | X | Y | LENG UA | LENG LA | LENG AX | | | | | | | |
| 1.25 | 13.00 | 6.00 | 21.75 | 17.19 | 23.53 | 22.31 | h | | | | | | |
| ride height | travel | plunge | camber angle | out cv angle | corr. angle | inner cv angle | upper ball joint angle | lower ball joint angle | shock length | motion ratio | spring rate | wheel rate | corner wgt |
| a | | b | c | d | | e | f | g | j | | | | 1000.00 |
| 3.00 | | 1.27 | 1.02 | 156.75 | | 22.24 | 128.69 | 56.23 | 33.84 | | | | wheel freq |
| | | | | | | | | | | | | | |
| 21.00 | 11.00 | 1.73 | 6.96 | 197.43 | 17.43 | -24.39 | 74.04 | 94.79 | 22.53 | 1.60 | 800.00 | 312.60 | 105.00 |
| 20.00 | 10.00 | 1.76 | 5.85 | 195.96 | 15.96 | -21.81 | 76.38 | 93.46 | 23.16 | 1.59 | 800.00 | 315.90 | 105.55 |
| 19.00 | 9.00 | 1.77 | 4.86 | 194.38 | 14.38 | -19.24 | 78.79 | 92.02 | 23.79 | 1.59 | 800.00 | 317.93 | 105.89 |
| 18.00 | 8.00 | 1.78 | 3.97 | 192.71 | 12.71 | -16.68 | 81.27 | 90.48 | 24.42 | 1.58 | 800.00 | 318.93 | 106.06 |
| 17.00 | 7.00 | 1.78 | 3.19 | 190.94 | 10.94 | -14.14 | 83.82 | 88.85 | 25.05 | 1.58 | 800.00 | 319.14 | 106.09 |
| 16.00 | 6.00 | 1.78 | 2.51 | 189.09 | 9.09 | -11.60 | 86.43 | 87.13 | 25.68 | 1.58 | 800.00 | 318.77 | 106.03 |
| 15.00 | 5.00 | 1.77 | 1.91 | 187.16 | 7.16 | -9.07 | 89.12 | 85.32 | 26.31 | 1.59 | 800.00 | 317.98 | 105.90 |
| 14.00 | 4.00 | 1.76 | 1.40 | 185.13 | 5.13 | -6.54 | 91.89 | 83.43 | 26.94 | 1.59 | 800.00 | 316.93 | 105.73 |
| 13.00 | 3.00 | 1.74 | 0.98 | 183.03 | 3.03 | -4.01 | 94.73 | 81.45 | 27.56996 | 1.59 | 800.00 | 315.75 | 105.53 |
| 12.00 | 2.00 | 1.72 | 0.64 | 180.83 | 0.83 | -1.47 | 97.66 | 79.38 | 28.20 | 1.59 | 800.00 | 314.55 | 105.33 |
| 11.00 | 1.00 | 1.69 | 0.38 | 178.55 | -1.45 | 1.07 | 100.69 | 77.22 | 28.83 | 1.60 | 800.00 | 313.44 | 105.14 |
| 10.00 | 0.00 | 1.65 | 0.21 | 176.17 | -3.83 | 3.62 | 103.83 | 74.95 | 29.45 | 1.60 | 800.00 | 312.53 | 104.99 |
| 9.00 | -1.00 | 1.62 | 0.13 | 173.68 | -6.32 | 6.19 | 107.09 | 72.58 | 30.08 | 1.60 | 800.00 | 311.93 | 104.89 |
| 8.00 | -2.00 | 1.57 | 0.15 | 171.07 | -8.93 | 8.78 | 110.50 | 70.10 | 30.70 | 1.60 | 800.00 | 311.77 | 104.86 |
| 7.00 | -3.00 | 1.52 | 0.27 | 168.33 | -11.67 | 11.40 | 114.07 | 67.47 | 31.32 | 1.60 | 800.00 | 312.20 | 104.93 |
| 6.00 | -4.00 | 1.46 | 0.50 | 165.43 | -14.57 | 14.06 | 117.84 | 64.70 | 31.95 | 1.60 | 800.00 | 313.45 | 105.14 |
| 5.00 | -5.00 | 1.39 | 0.88 | 162.35 | -17.65 | 16.77 | 121.85 | 61.74 | 32.57558 | 1.59 | 800.00 | 315.85 | 105.54 |
| 4.00 | -6.00 | 1.31 | 1.43 | 159.03 | -20.97 | 19.54 | 126.18 | 58.55 | 33.20 | 1.58 | 800.00 | 319.94 | 106.23 |
| 3.00 | -7.00 | 1.21 | 2.20 | 155.41 | -24.59 | 22.39 | 130.91 | 55.08 | 33.84 | -0.03 | 800.00 | | |

Bump

G.C.

10"

12"

15"

Droop

-11.28 max travel

+19° + =

-24° +

33.81 max Kustom

start with 700 lb/in Front

also have 600 lb/in

JTEVSUS2.XLS

9/8/94

| design view ride height | travel | rear shock length | motion ratio | spring rate | wheel rate | corner wgt | JTEV REAR SUSPEN | |
|---|---|---|---|---|---|---|---|---|
| a | | z | | | | 1250.00 | ROCKER AND PUSH | |
| 21.00 | | 22.04 | | | | wheel freq | | |
| | | 11.8 11+0+1+0 | | | | | | |
| 21.00 | 11.00 | 22.03955 | 1.54 | 800.00 | 335.50 | 97.29 | | |
| 20.00 | 10.00 | 22.68715 | 1.53 | 800.00 | 341.21 | 98.12 | | |
| 19.00 | 9.00 | 23.34023 | 1.52 | 800.00 | 344.36 | 98.57 | | |
| 18.00 | 8.00 | 23.99632 | 1.52 | 800.00 | 345.43 | 98.72 | | |
| 17.00 | 7.00 | 24.65343 | 1.52 | 800.00 | 344.89 | 98.65 | | |
| 16.00 | 6.00 | 25.31002 | 1.53 | 800.00 | 343.20 | 98.40 | | |
| 15.00 | 5.00 | 25.96499 | 1.53 | 800.00 | 340.77 | 98.06 | | |
| 14.00 | 4.00 | 26.62 | 1.54 | 800.00 | 337.99 | 97.65 | | |
| 13.00 | 3.00 | 27.26764 | 1.54 | 800.00 | 335.22 | 97.25 | | |
| 12.00 | 2.00 | 27.91496 | - 1.55 | 800.00 | 332.78 | 96.90 | | |
| 11.00 | 1.00 | 28.55992 | - 1.55 | 800.00 | 331.00 | 96.64 | | |
| 10.00 | 0.00 | 29.20316 | 1.56 | 800.00 | 330.24 | 96.53 | | |
| 9.00 | -1.00 | 29.84565 | 1.55 | 800.00 | 330.89 | 96.62 | | |
| 8.00 | -2.00 | 30.48878 | 1.55 | 700.00 | 291.78 | 90.73 | | |
| 7.00 | -3.00 | 31.1344 | - 1.54 | 600.00 | 253.98 | 84.65 | | |
| 6.00 | -4.00 | 31.78501 | 1.52 | 500.00 | 217.18 | 78.28 | | |
| 5.00 | -5.00 | 32.44407 | 1.49 | 800.00 | 361.67 | 101.02 | | |
| 4.00 | -6.00 | 33.11644 | 1.44 | 800.00 | 384.21 | 104.12 | | |
| 3.00 | -7.00 | 33.80944 | -0.03 | 800.00 | ######## | 5079.53 | | |

L.R.H. —

N.R.H

H.R.H. —

14in pushrod ℓ

RH 10–15

$\Delta\ell = 3.2$

RH 11–15

$\Delta\ell$ 2.57

3.11

−2.57

.54 less x 2 = ¾ longer

300 ~~lbs~~ starting spring

500 alternate

# JTEV SUSPENSION CHARACTERISTICS

| LOWER PICKUPS | | UPPER PICKUPS | | | | | | | | |
|---|---|---|---|---|---|---|---|---|---|---|
| X | Y | X | Y | LENG UA | LENG LA | LENG AX | | | | |
| 1.25 | 13.00 | 6.00 | 21.75 | 17.19 | 23.53 | 22.31 | h | | | |
| ride height | travel | plunge | camber angle | out cv angle | corr. angle | inner cv angle | joint angle | joint angle | half track width | grnd clrnc |
| a | | b | c | d | | e | f | g | h | i |
| 21.00 | | 1.73 | 6.96 | 197.43 | | -24.39 | 74.04 | 94.79 | 26.16 | 2.00 |
| | | | | | | | | 29.4 | | |
| 21.00 | 11.00 | 1.73 | 6.96 | 197.43 | 17.43 | -24.39 | 74.04 | 94.79 | 26.16 | 2.00 |
| 20.00 | 10.00 | 1.76 | 5.85 | 195.96 | 15.96 | -21.81 | 76.38 | 93.46 | 26.29 | 3.00 |
| 19.00 | 9.00 | 1.77 | 4.86 | 194.38 | 14.38 | -19.24 | 78.79 | 92.02 | 26.40 | 4.00 |
| 18.00 | 8.00 | 1.78 | 3.97 | 192.71 | 12.71 | -16.68 | 81.27 | 90.48 | 26.48 | 5.00 |
| 17.00 | 7.00 | 1.78 | 3.19 | 190.94 | 10.94 | -14.14 | 83.82 | 88.85 | 26.54 | 6.00 |
| 16.00 | 6.00 | 1.78 | 2.51 | 189.09 | 9.09 | -11.60 | 86.43 | 87.13 | 26.58 | 7.00 |
| 15.00 | 5.00 | 1.77 | 1.91 | 187.16 | 7.16 | -9.07 | 89.12 | 85.32 | 26.59 | 8.00 |
| 14.00 | 4.00 | 1.76 | 1.40 | 185.13 | 5.13 | -6.54 | 91.89 | 83.43 | 26.58 | 9.00 |
| 13.00 | 3.00 | 1.74 | 0.98 | 183.03 | 3.03 | -4.01 | 94.73 | 81.45 | 26.54 | 10.00 |
| 12.00 | 2.00 | 1.72 | 0.64 | 180.83 | 0.83 | -1.47 | 97.66 | 79.38 | 26.48 | 11.00 |
| 11.00 | 1.00 | 1.69 | 0.38 | 178.55 | -1.45 | 1.07 | 100.69 | 77.22 | 26.38 | 12.00 |
| 10.00 | 0.00 | 1.65 | 0.21 | 176.17 | -3.83 | 3.62 | 103.83 | 74.95 | 26.27 | 13.00 |
| 9.00 | -1.00 | 1.62 | 0.13 | 173.68 | -6.32 | 6.19 | 107.09 | 72.58 | 26.12 | 14.00 |
| 8.00 | -2.00 | 1.57 | 0.15 | 171.07 | -8.93 | 8.78 | 110.50 | 70.10 | 25.95 | 15.00 |
| 7.00 | -3.00 | 1.52 | 0.27 | 168.33 | -11.67 | 11.40 | 114.07 | 67.47 | 25.75 | 16.00 |
| 6.00 | -4.00 | 1.46 | 0.50 | 165.43 | -14.57 | 14.06 | 117.84 | 64.70 | 25.52 | 17.00 |
| 5.00 | -5.00 | 1.39 | 0.88 | 162.35 | -17.65 | 16.77 | 121.85 | 61.74 | 25.27 | 18.00 |
| 4.00 | -6.00 | 1.31 | 1.43 | 159.03 | -20.97 | 19.54 | 126.18 | 58.55 | 25.00 | 19.00 |
| 3.00 | -7.00 | 1.21 | 2.20 | 155.41 | -24.59 | 22.39 | 130.91 | 55.08 | 24.71 | 20.00 |

## CAMBER VS TRAVEL

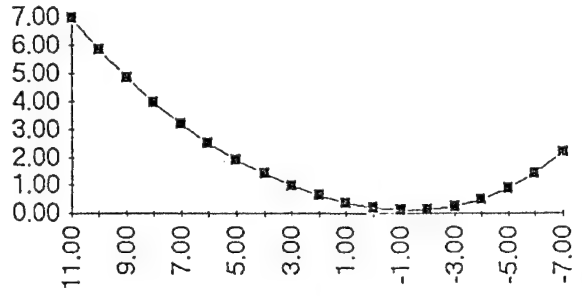


## TRACK CHANGE VS TRAVEL

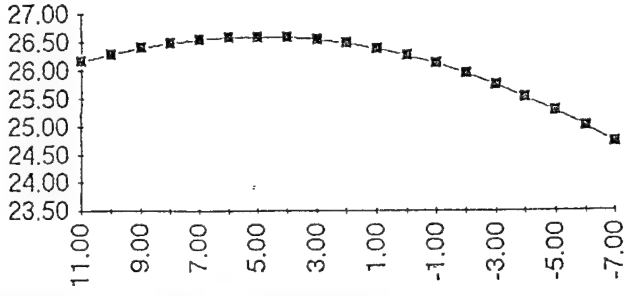


## PLUNGE VS TRAVEL

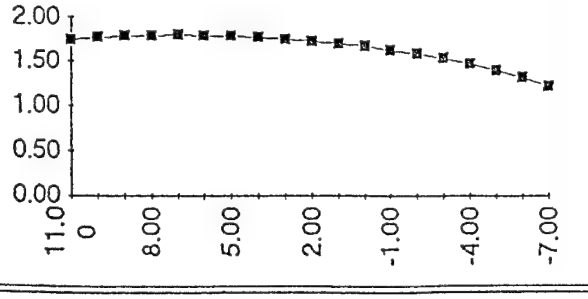

| JTEV SUSPENSION CHARACTERISTICS | | | | | | | | | | | |
|---|---|---|---|---|---|---|---|---|---|---|---|
| UPPER PICKUPS | | | | | | | | | | | |
| X | Y | LENG UA | LENG LA | LENG AX | | | | | | | |
| 6.00 | 21.75 | 17.19 | 23.53 | 22.31 | h | | | | | | |
| plunge | camber angle | out cv angle | corr. angle | inner cv angle | upper ball joint angle | lower ball joint angle | shock length | motion ratio | spring rate | wheel rate | corner wgt |
| b | c | d | | e | f | g | j | | | | 1200.00 |
| 1.27 | 1.02 | 156.75 | | 22.24 | 128.69 | 56.23 | 33.84 | | | | wheel freq |
| | | | | | | | | | | | |
| 1.73 | 6.96 | 197.43 | 17.43 | -24.39 | 74.04 | 94.79 | 22.53 | 1.60 | 700.00 | 273.52 | 89.66 |
| 1.76 | 5.85 | 195.96 | 15.96 | -21.81 | 76.38 | 93.46 | 23.16 | 1.59 | 700.00 | 276.42 | 90.13 |
| 1.77 | 4.86 | 194.38 | 14.38 | -19.24 | 78.79 | 92.02 | 23.79 | 1.59 | 700.00 | 278.19 | 90.42 |
| 1.78 | 3.97 | 192.71 | 12.71 | -16.68 | 81.27 | 90.48 | 24.42 | 1.58 | 700.00 | 279.06 | 90.56 |
| 1.78 | 3.19 | 190.94 | 10.94 | -14.14 | 83.82 | 88.85 | 25.05 | 1.58 | 700.00 | 279.25 | 90.59 |
| 1.78 | 2.51 | 189.09 | 9.09 | -11.60 | 86.43 | 87.13 | 25.68 | 1.58 | 700.00 | 278.92 | 90.54 |
| 1.77 | 1.91 | 187.16 | 7.16 | -9.07 | 89.12 | 85.32 | 26.31 | 1.59 | 700.00 | 278.24 | 90.43 |
| 1.76 | 1.40 | 185.13 | 5.13 | -6.54 | 91.89 | 83.43 | 26.94 | 1.59 | 700.00 | 277.32 | 90.28 |
| 1.74 | 0.98 | 183.03 | 3.03 | -4.01 | 94.73 | 81.45 | 27.56996 | 1.59 | 700.00 | 276.28 | 90.11 |
| 1.72 | 0.64 | 180.83 | 0.83 | -1.47 | 97.66 | 79.38 | 28.20 | 1.59 | 700.00 | 275.23 | 89.94 |
| 1.69 | 0.38 | 178.55 | -1.45 | 1.07 | 100.69 | 77.22 | 28.83 | 1.60 | 700.00 | 274.26 | 89.78 |
| 1.65 | 0.21 | 176.17 | -3.83 | 3.62 | 103.83 | 74.95 | 29.45 | 1.60 | 700.00 | 273.47 | 89.65 |
| 1.62 | 0.13 | 173.68 | -6.32 | 6.19 | 107.09 | 72.58 | 30.08 | 1.60 | 700.00 | 272.94 | 89.57 |
| 1.57 | 0.15 | 171.07 | -8.93 | 8.78 | 110.50 | 70.10 | 30.70 | 1.60 | 700.00 | 272.80 | 89.54 |
| 1.52 | 0.27 | 168.33 | -11.67 | 11.40 | 114.07 | 67.47 | 31.32 | 1.60 | 700.00 | 273.18 | 89.60 |
| 1.46 | 0.50 | 165.43 | -14.57 | 14.06 | 117.84 | 64.70 | 31.95 | 1.60 | 700.00 | 274.27 | 89.78 |
| 1.39 | 0.88 | 162.35 | -17.65 | 16.77 | 121.85 | 61.74 | 32.57558 | 1.59 | 700.00 | 276.37 | 90.13 |
| 1.31 | 1.43 | 159.03 | -20.97 | 19.54 | 126.18 | 58.55 | 33.20 | 1.58 | 700.00 | 279.95 | 90.71 |
| 1.21 | 2.20 | 155.41 | -24.59 | 22.39 | 130.91 | 55.08 | 33.84 | -0.03 | 700.00 | | |

| travel | rear shock length | motion ratio | spring rate | wheel rate | corner wgt | JTEV REAR SUSPENSION |
|---|---|---|---|---|---|---|
| | z | | | | 1300.00 | ROCKER AND PUSHROD |
| | 31.13 | | | | wheel freq | |
| | | | | | | |
| 11.00 | 22.03955 | 1.54 | 300.00 | 125.81 | 58.42 | |
| 10.00 | 22.68715 | 1.53 | 300.00 | 127.96 | 58.92 | |
| 9.00 | 23.34023 | 1.52 | 300.00 | 129.14 | 59.19 | |
| 8.00 | 23.99632 | 1.52 | 300.00 | 129.54 | 59.28 | |
| 7.00 | 24.65343 | 1.52 | 300.00 | 129.33 | 59.24 | |
| 6.00 | 25.31002 | 1.53 | 300.00 | 128.70 | 59.09 | |
| 5.00 | 25.96499 | 1.53 | 300.00 | 127.79 | 58.88 | |
| 4.00 | 26.62 | 1.54 | 300.00 | 126.75 | 58.64 | |
| 3.00 | 27.26764 | 1.54 | 300.00 | 125.71 | 58.40 | |
| 2.00 | 27.91496 | 1.55 | 300.00 | 124.79 | 58.19 | |
| 1.00 | 28.55992 | 1.55 | 300.00 | 124.13 | 58.03 | |
| 0.00 | 29.20316 | 1.56 | 300.00 | 123.84 | 57.96 | |
| -1.00 | 29.84565 | 1.55 | 300.00 | 124.08 | 58.02 | |
| -2.00 | 30.48878 | 1.55 | 300.00 | 125.05 | 58.25 | |
| -3.00 | 31.1344 | 1.54 | 300.00 | 126.99 | 58.70 | |
| -4.00 | 31.78501 | 1.52 | 300.00 | 130.31 | 59.46 | |
| -5.00 | 32.44407 | 1.49 | 300.00 | 135.62 | 60.66 | |
| -6.00 | 33.11644 | 1.44 | 300.00 | 144.08 | 62.52 | |
| -7.00 | 33.80944 | -0.03 | 300.00 | | | |

Coordinate System is X=Left, Y=Rearward, Z=Up

| Lower Arm | X | Y | Z | Upper Arm | X | Y | Z |
|---|---|---|---|---|---|---|---|
| Front Pivot | 1.250 | -6.000 | 12.875 | Front Pivot | 6.000 | -10.000 | 21.87 |
| Rear Pivot | 1.250 | 6.000 | 13.250 | Rear Pivot | 6.000 | 6.000 | 21.50 |
| Ball Joint | 24.670 | -.425 | 10.440 | Ball Joint | 23.160 | .425 | 20.50 |
| Tie Rod | | | | | | | |
| Inner Pivot | 5.575 | 6.000 | 19.325 | Outer Pivot | 23.250 | 4.500 | 17.9 |
| Wheel Center | 26.250 | .000 | 15.150 | | | | |

Other Input Parameters:

| | | | | | |
|---|---|---|---|---|---|
| Camber @ Design = | .00 | Wheelbase..... = | 119.00 | % Front Braking. = | 60.00 |
| Toe-In @ Design = | .00 | Tire Radius... = | 15.15 | C. G. Height.... = | 32.00 |
| Jounce Travel.. = | 11.00 | Rebound Travel = | -6.00 | Travel Increment = | 1.00 |
| Rack Travel Left= | 2.50 | Rack Travel Rt = | -2.50 | Rack Travel Step = | .50 |

Calculated Parameters:

| | | | |
|---|---|---|---|
| Lower Arm True Length = | 23.565 | Scrub Radius..... = | .013 |
| Upper Arm True Length = | 17.197 | Track @ Wheel Center. = | 52.500 |
| Tie Rod Length..... = | 17.792 | Track @ Ground..... = | 52.500 |
| Kingpin Length..... = | 10.208 | Kingpin Inclination.. = | 8.536 |

PgUp PgDn Home End

| Wheel Travel | Caster Angle | Camber Angle | Toe-In Angle | Percent Roll Steer | FVSA Length | SVSA Length |
|---|---|---|---|---|---|---|
| 11.000 | 8.429 | -8.030 | -.002 | -.386 | -45.50 | 226.47 |
| 10.000 | 8.071 | -6.783 | -.012 | -.302 | -50.20 | 218.12 |
| 9.000 | 7.724 | -5.668 | -.020 | -.229 | -55.52 | 211.38 |
| 8.000 | 7.385 | -4.670 | -.025 | -.161 | -61.61 | 205.89 |
| 7.000 | 7.054 | -3.780 | -.029 | -.095 | -68.68 | 201.35 |
| 6.000 | 6.727 | -2.988 | -.030 | -.026 | -77.02 | 197.56 |
| 5.000 | 6.405 | -2.286 | -.030 | .048 | -87.11 | 194.37 |
| 4.000 | 6.086 | -1.670 | -.028 | .128 | -99.65 | 191.63 |
| 3.000 | 5.770 | -1.135 | -.024 | .217 | -115.86 | 189.25 |
| 2.000 | 5.455 | -.679 | -.018 | .313 | -137.92 | 187.13 |
| 1.000 | 5.142 | -.301 | -.010 | .417 | -170.21 | 185.20 |
| .000 | 4.830 | .000 | .000 | .528 | -223.05 | 183.39 |
| -1.000 | 4.518 | .221 | .013 | .643 | -327.93 | 181.61 |
| -2.000 | 4.207 | .358 | .028 | .761 | -648.24 | 179.79 |
| -3.000 | 3.896 | .406 | .047 | .880 | 12755.01 | 177.84 |
| -4.000 | 3.585 | .353 | .069 | 1.001 | 534.64 | 175.62 |
| -5.000 | 3.274 | .188 | .095 | 1.126 | 255.34 | 172.99 |
| -6.000 | 2.962 | -.112 | .126 | 1.261 | 157.61 | 169.72 |

PgUp PgDn Home End

| Travel | Height | Scrub | Trail | Anti-Dive | Anti-Lift |
|---|---|---|---|---|---|
| 11.000 | -3.252 | .10 | .20 | 27.79 | 8.14 |
| 10.000 | -2.665 | .22 | .33 | 26.85 | 7.00 |
| 9.000 | -2.056 | .32 | .44 | 25.94 | 6.03 |
| 8.000 | -1.426 | .39 | .54 | 25.07 | 5.22 |
| 7.000 | -.778 | .43 | .63 | 24.24 | 4.54 |
| 6.000 | -.114 | .45 | .71 | 23.45 | 3.95 |
| 5.000 | .565 | .44 | .77 | 22.69 | 3.45 |
| 4.000 | 1.257 | .41 | .82 | 21.98 | 3.02 |
| 3.000 | 1.963 | .35 | .87 | 21.30 | 2.65 |
| 2.000 | 2.681 | .26 | .90 | 20.66 | 2.32 |
| 1.000 | 3.410 | .14 | .92 | 20.05 | 2.02 |
| .000 | 4.149 | .00 | .93 | 19.48 | 1.74 |
| -1.000 | 4.897 | -.17 | .93 | 18.93 | 1.48 |
| -2.000 | 5.652 | -.37 | .92 | 18.42 | 1.21 |
| -3.000 | 6.409 | -.61 | .90 | 17.95 | .94 |
| -4.000 | 7.163 | -.86 | .86 | 17.50 | .65 |
| -5.000 | 7.904 | -1.15 | .82 | 17.09 | .32 |
| -6.000 | 8.611 | -1.47 | .77 | 16.73 | -.08 |

PgUp PgDn Home End

TIE ROD LENGTH= 17.792 IN.

Steering Output Data

Wheel Travel = .000

| Rack Travel (in) | Spindle Angles Left (deg) | Spindle Angles Right (deg) | Total Toe (deg) | Camber Left (deg) | Camber Right (deg) |
|---|---|---|---|---|---|
| 2.500 | -34.564 | -39.342 | -4.777 | -1.489 | 6.503 |
| 2.000 | -27.316 | -29.718 | -2.401 | -1.418 | 4.078 |
| 1.500 | -20.328 | -21.477 | -1.149 | -1.220 | 2.553 |
| 1.000 | -13.504 | -13.963 | -.459 | -.917 | 1.468 |
| .500 | -6.757 | -6.865 | -.108 | -.513 | .645 |
| .000 | .000 | .000 | .000 | .000 | .000 |
| -.500 | 6.865 | 6.757 | -.108 | .645 | -.513 |
| -1.000 | 13.963 | 13.504 | -.459 | 1.468 | -.917 |
| -1.500 | 21.477 | 20.328 | -1.149 | 2.553 | -1.220 |
| -2.000 | 29.718 | 27.316 | -2.401 | 4.078 | -1.418 |
| -2.500 | 39.342 | 34.564 | -4.777 | 6.503 | -1.489 |

PgUp PgDn Home End

| REVISIONS | | |
|---|---|---|
| DESCRIPTION | DATE | APPROVED |

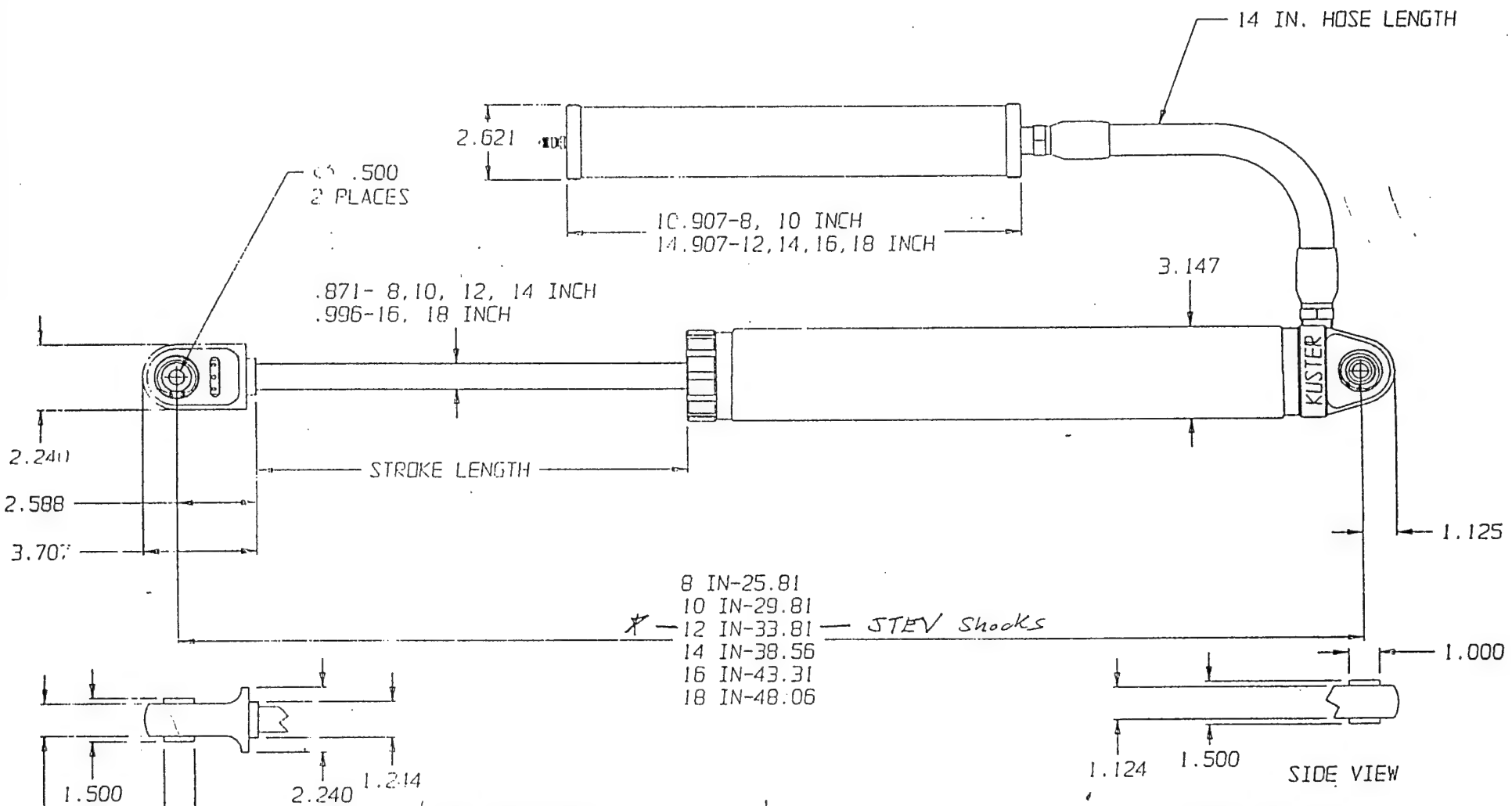


| | | | |
|---|---|---|---|
| DRAWN LMK | APPROVED | DATE | |
| DIMENSIONS PER ANSI Y14-5M | | SCALE NTS | |

PART DESCRIPTION

# SERIES C SHOCK DIMENSIONS

TOLERANCES-UNLESS OTHERWISE NOTED

| | | | |
|---|---|---|---|
| LINEAL DIM. | XXX +-.001 | CORNER FILLET | .005 |
| | XX +-.005 | EDGE BREAK | .005 MAX. |
| | FRAC. +-.010 | CHAMFERS | 45 +-5 DEG. |
| ANGLES | +-1 DEG. | | |
| SURFACE FINISH | 64 RMS | | |
| CONCENTRIC DIA. | ✓ | | |

ASSEMBLY WHERE USED

KUSTER COMPANY
2900 E. 29TH ST. LONG BEACH, CA.

| SHEET | REV | FILE NAME |
|---|---|---|
| 1 OF 1 | | SHKDIMEN |
| | | DWG NO. |

# Appendix II

# Tire Force/Deflection/Pressure change Data

Tires tested

Manufacture: BF Goodrich

Model: Baja T/A

Size: 33x10.5 R15 LT

Construction: Radial

Tread Width: 9”

Section Width: 10.5”

Section Height: 8.5”

Aspect Ratio: 80%

Manufacture: BF Goodrich

Model: Radial Mud-Terrain T/A

Size: 33x9.5 R15 LT

Construction: Radial

Tread Width: 8”

Section Width: 9.5”

Section Height: 8.5”

Aspect Ratio: 90%

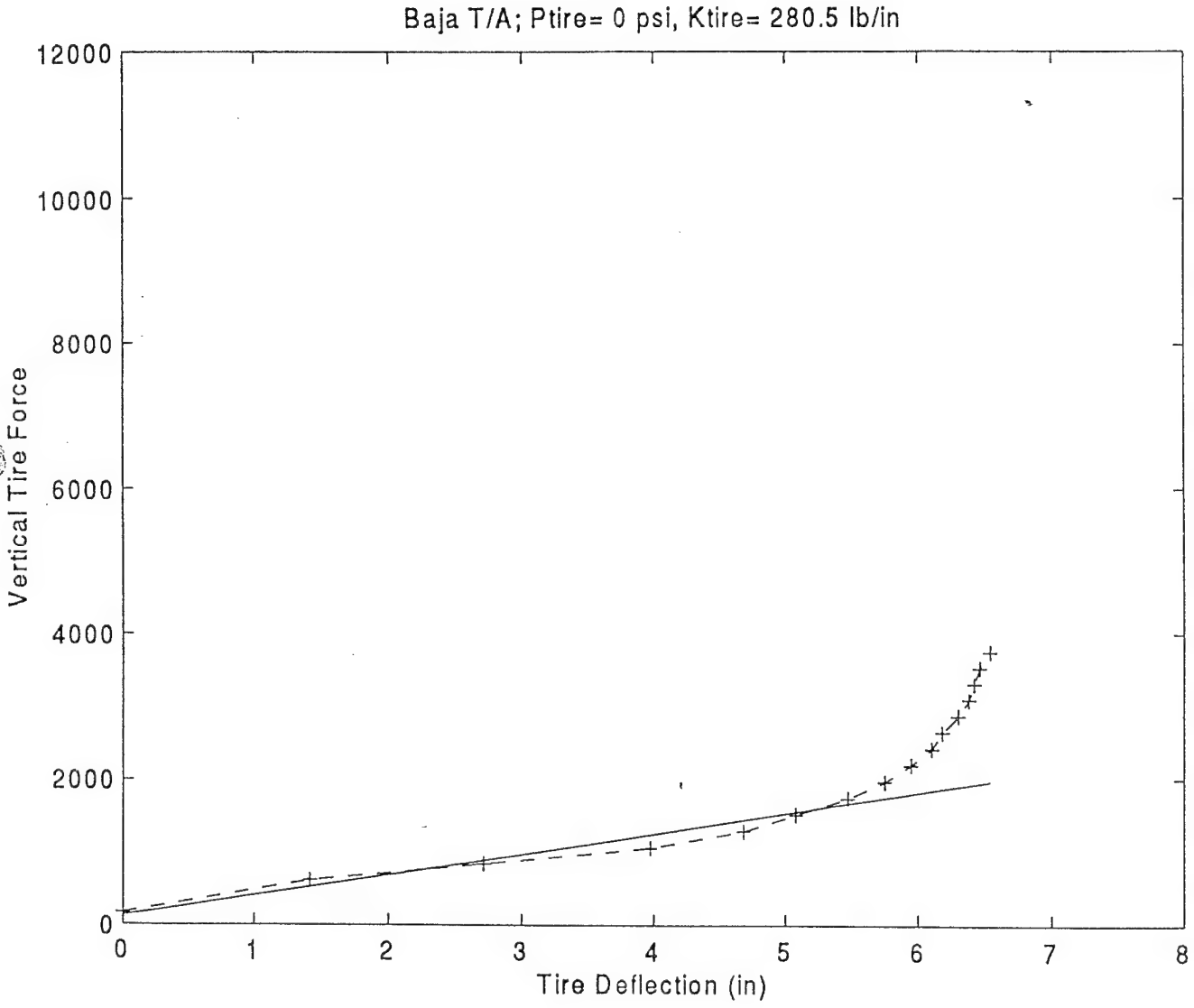
Baja T/A; Ptire= 0 psi, Ktire= 280.5 lb/in
Vertical Tire Force
Tire Deflection (in)
12000
10000
8000
6000
4000
2000
0
0
1
2
3
4
5
6
7
8

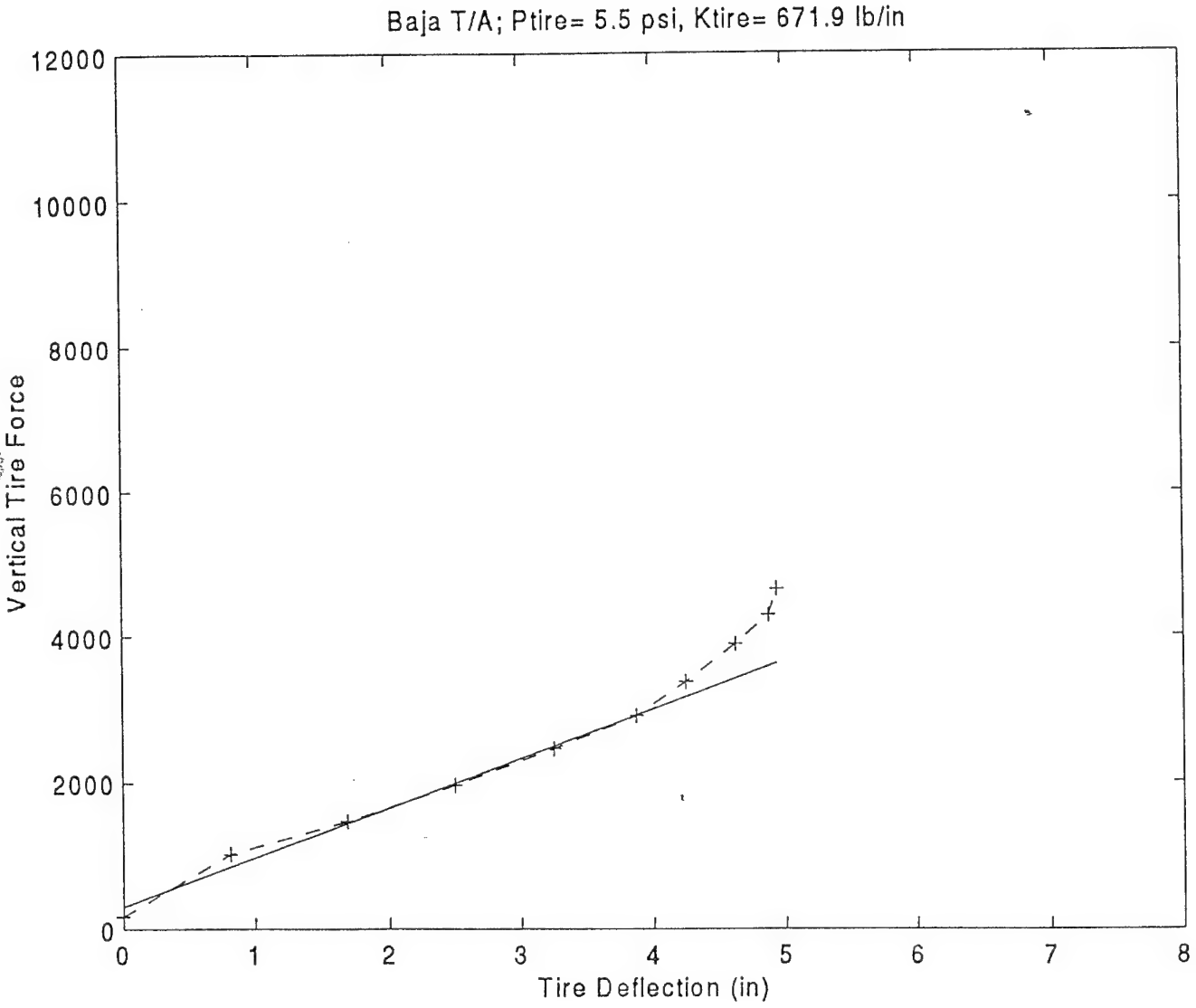
Baja T/A; Ptire= 5.5 psi, Ktire= 671.9 lb/in
Vertical Tire Force
Tire Deflection (in)
12000
10000
8000
6000
4000
2000
0
0
1
2
3
4
5
6
7
8

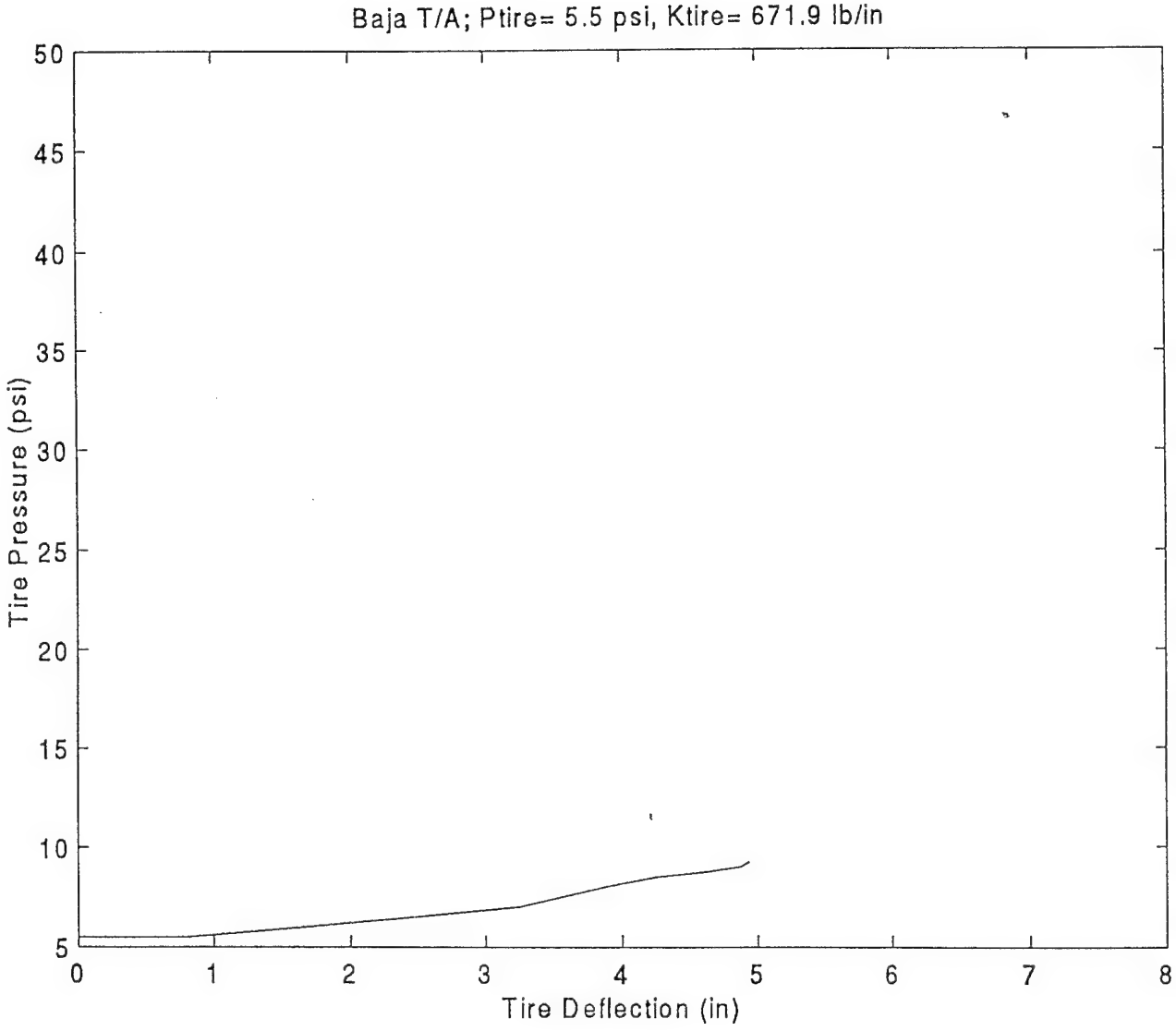
Baja T/A; Ptire= 5.5 psi, Ktire= 671.9 lb/in
Tire Pressure (psi)
Tire Deflection (in)
50
45
40
35
30
25
20
15
10
5
0
1
2
3
4
5
6
7
8

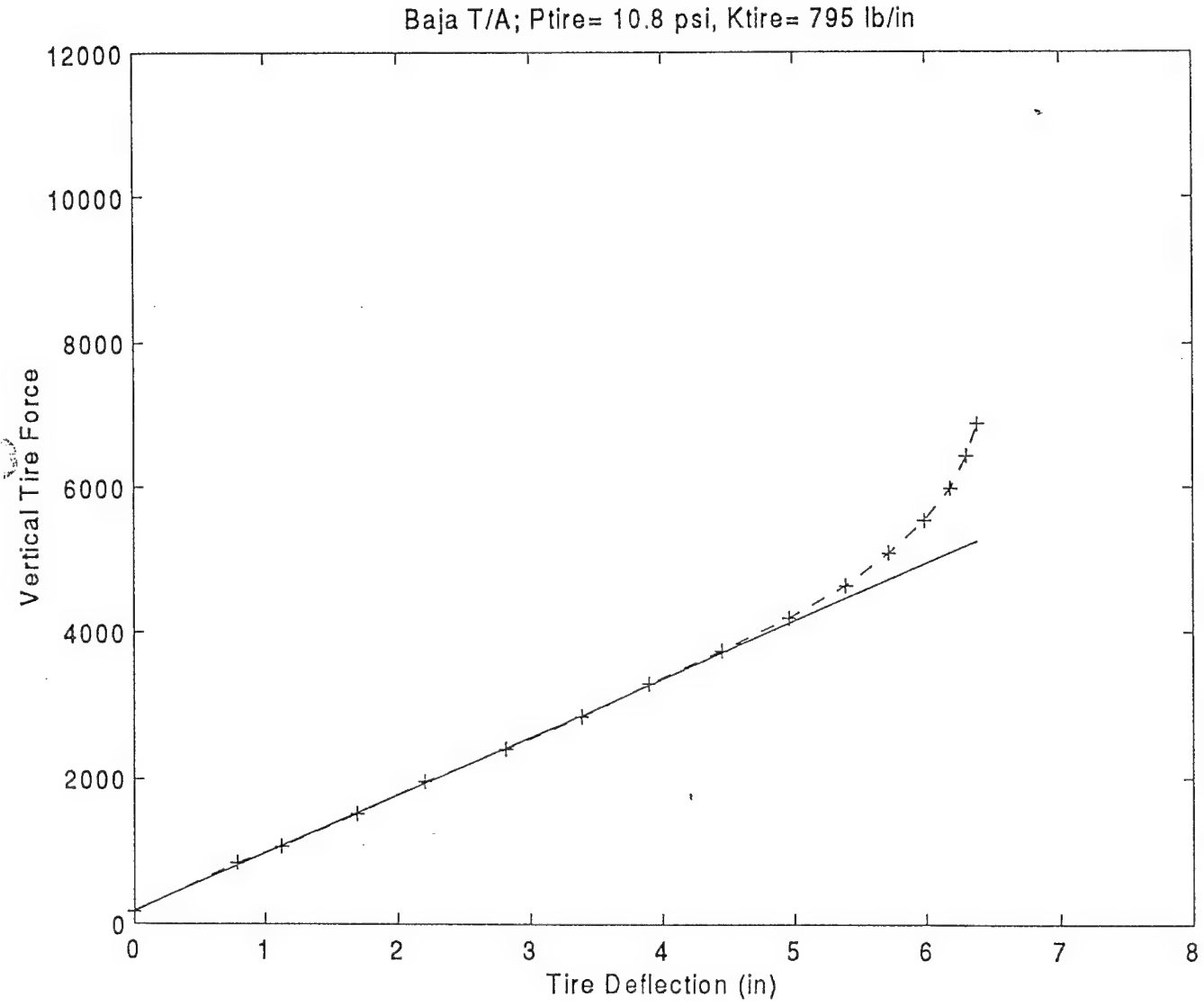
Baja T/A; Ptire= 10.8 psi, Ktire= 795 lb/in
Vertical Tire Force
Tire Deflection (in)
12000
10000
8000
6000
4000
2000
0
0
1
2
3
4
5
6
7
8

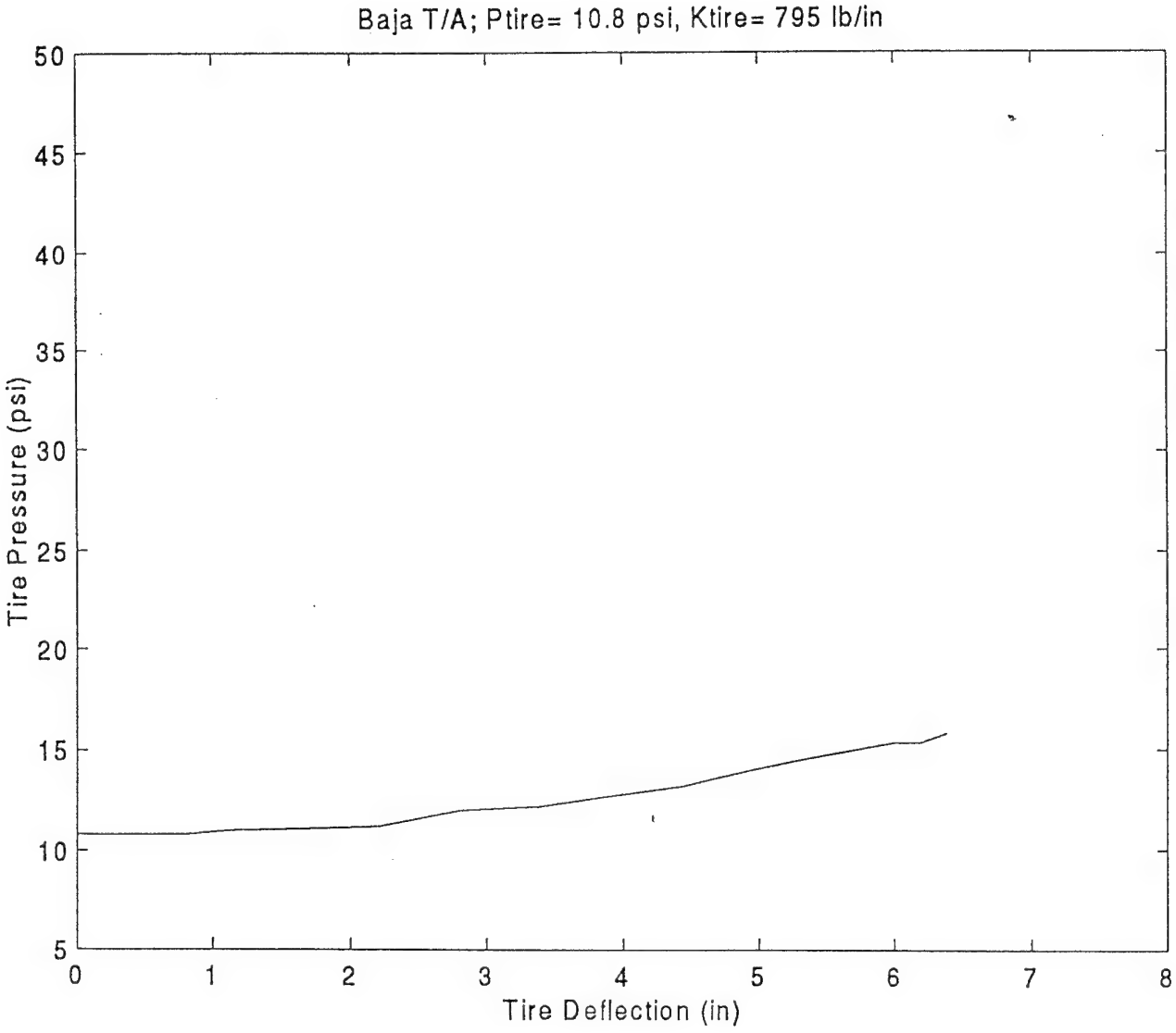
Baja T/A; Ptire= 10.8 psi, Ktire= 795 lb/in
Tire Pressure (psi)
Tire Deflection (in)
50
45
40
35
30
25
20
15
10
5
0
1
2
3
4
5
6
7
8

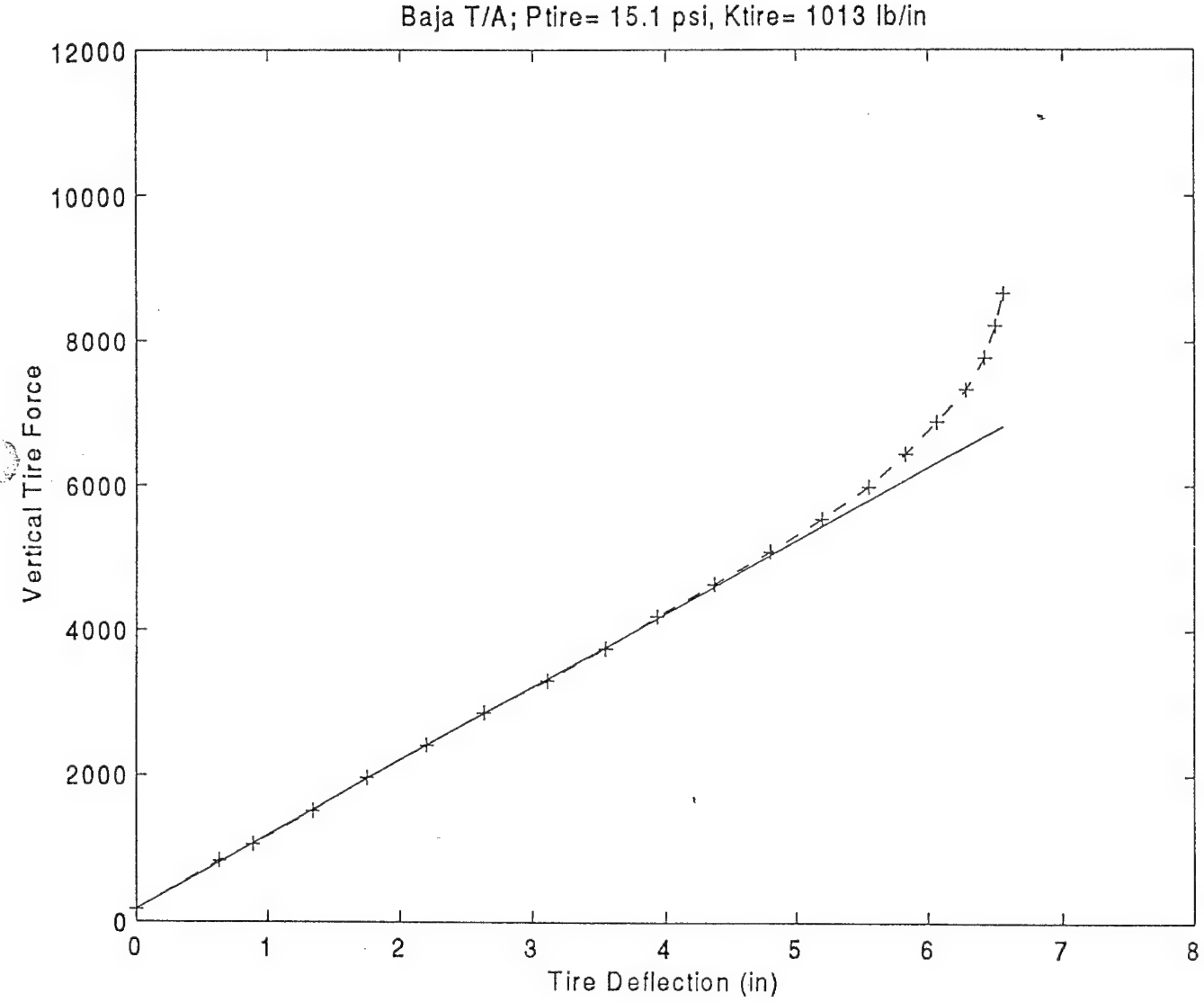
Baja T/A; Ptire= 15.1 psi, Ktire= 1013 lb/in
Vertical Tire Force
Tire Deflection (in)
12000
10000
8000
6000
4000
2000
0
0
1
2
3
4
5
6
7
8

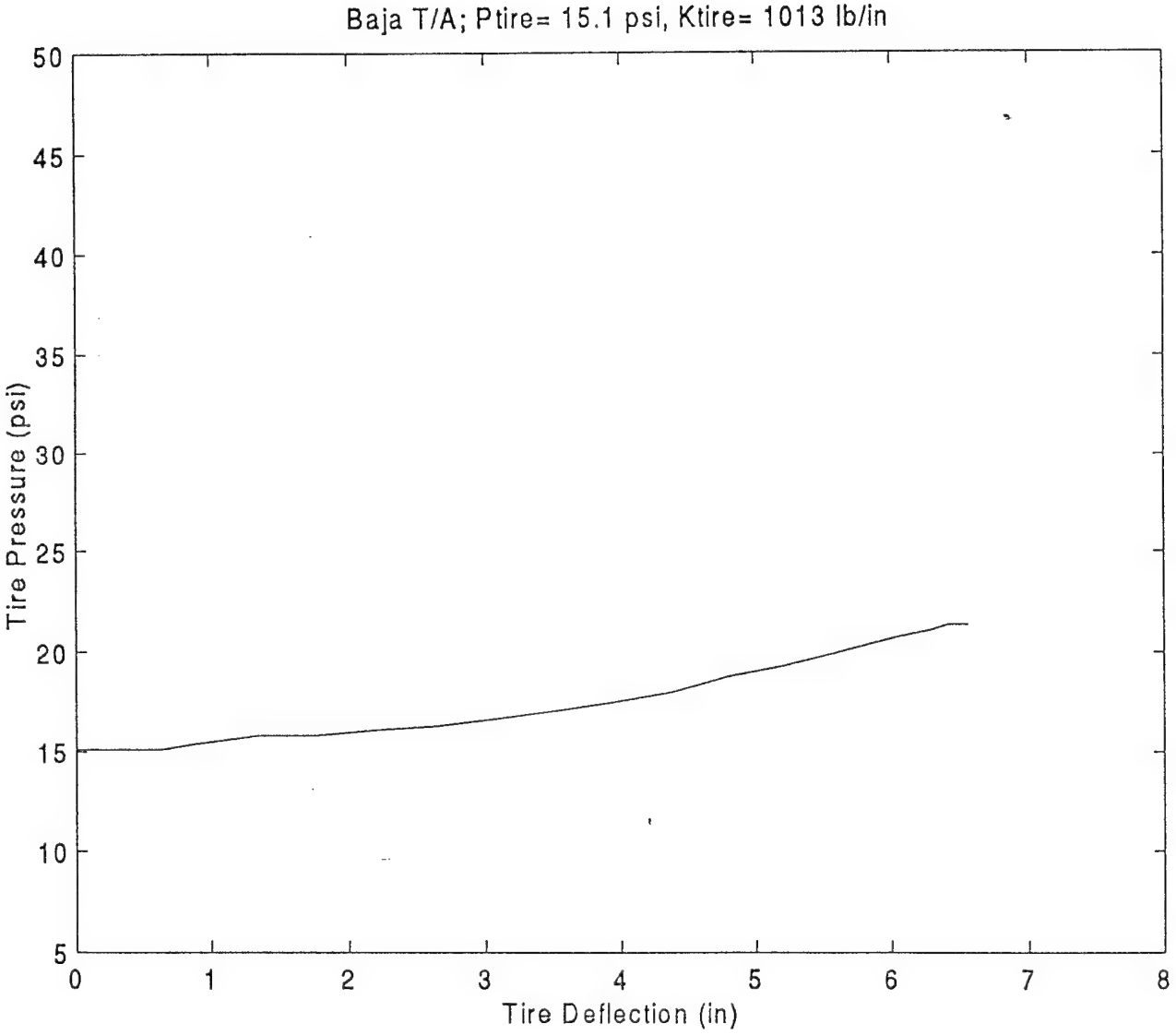
Baja T/A; Ptire= 15.1 psi, Ktire= 1013 lb/in
Tire Pressure (psi)
Tire Deflection (in)
50
45
40
35
30
25
20
15
10
5
0
1
2
3
4
5
6
7
8

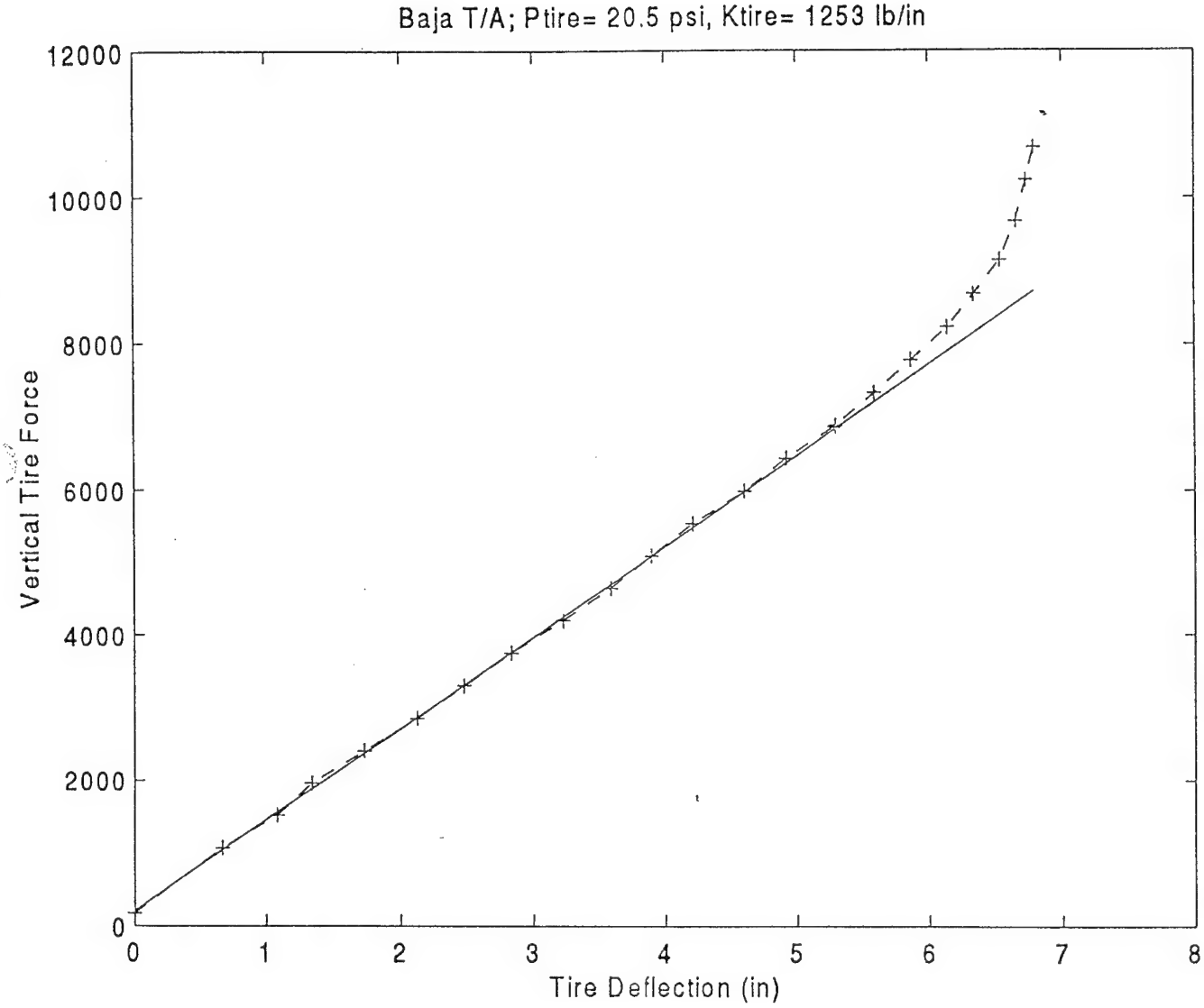
Baja T/A; Ptire= 20.5 psi, Ktire= 1253 lb/in
Vertical Tire Force
Tire Deflection (in)
12000
10000
8000
6000
4000
2000
0
0
1
2
3
4
5
6
7
8

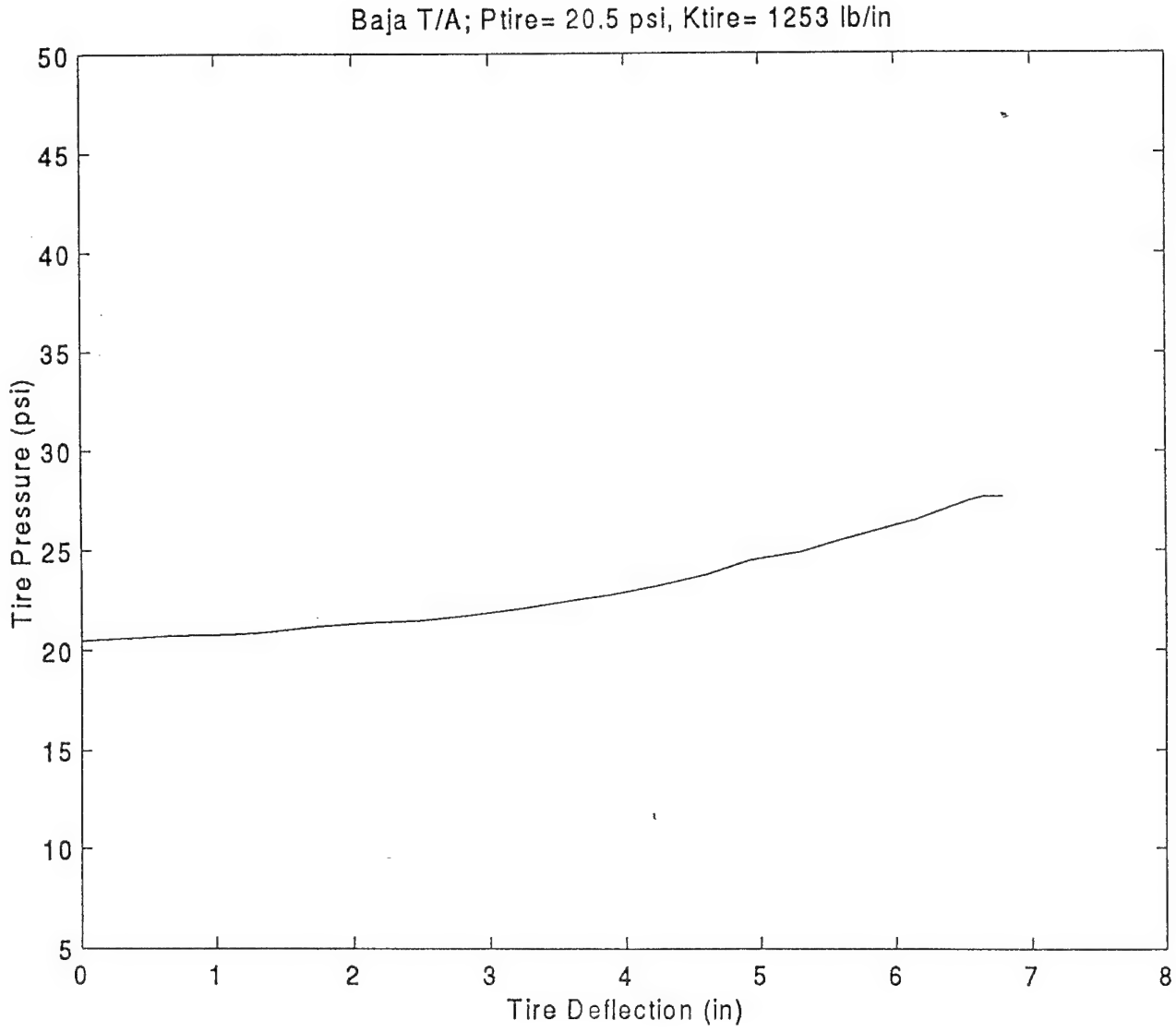
Baja T/A; Ptire= 20.5 psi, Ktire= 1253 lb/in
Tire Pressure (psi)
Tire Deflection (in)
50
45
40
35
30
25
20
15
10
5
0
1
2
3
4
5
6
7
8

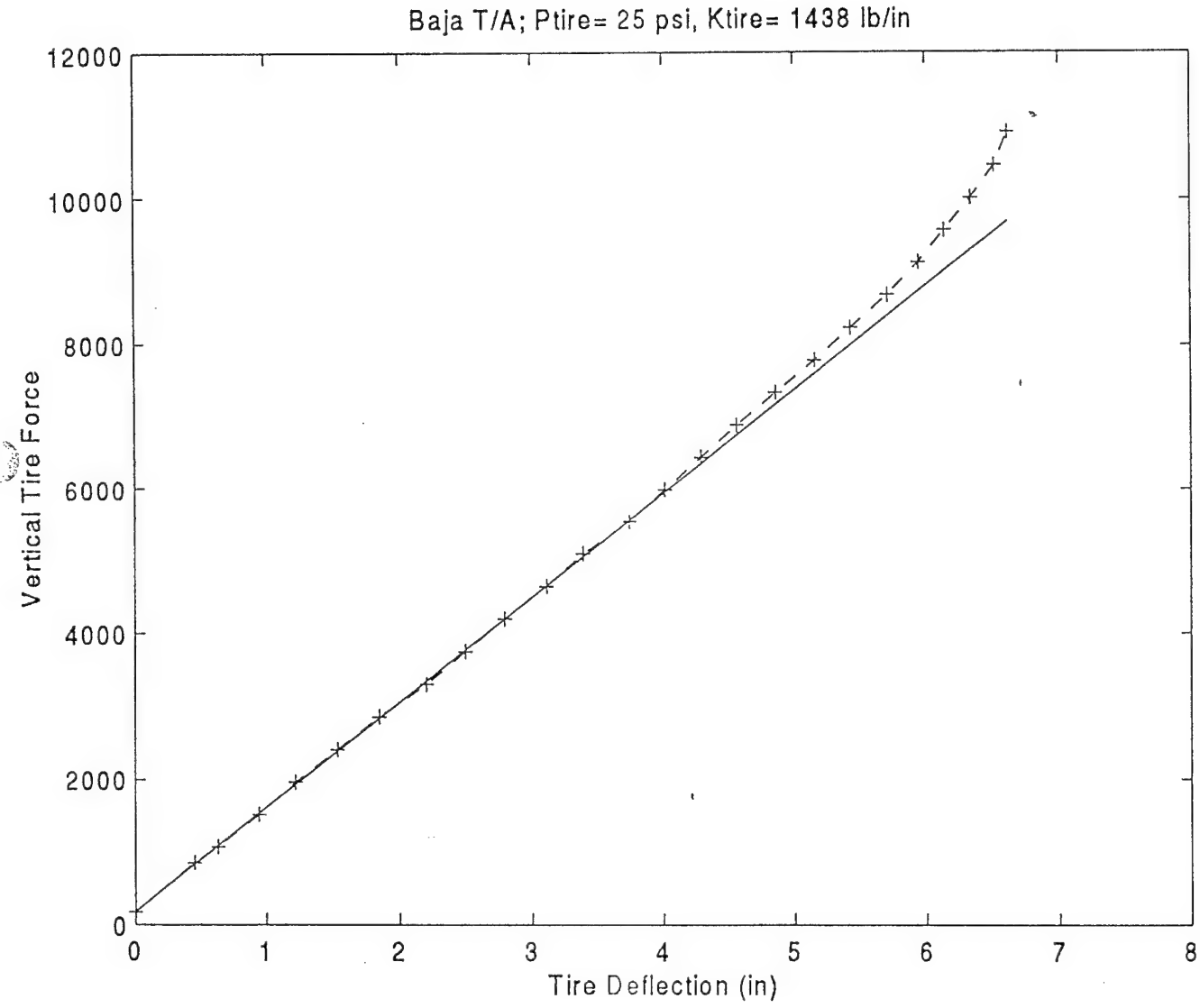
Baja T/A; Ptire= 25 psi, Ktire= 1438 lb/in
Vertical Tire Force
Tire Deflection (in)
12000
10000
8000
6000
4000
2000
0
0
1
2
3
4
5
6
7
8

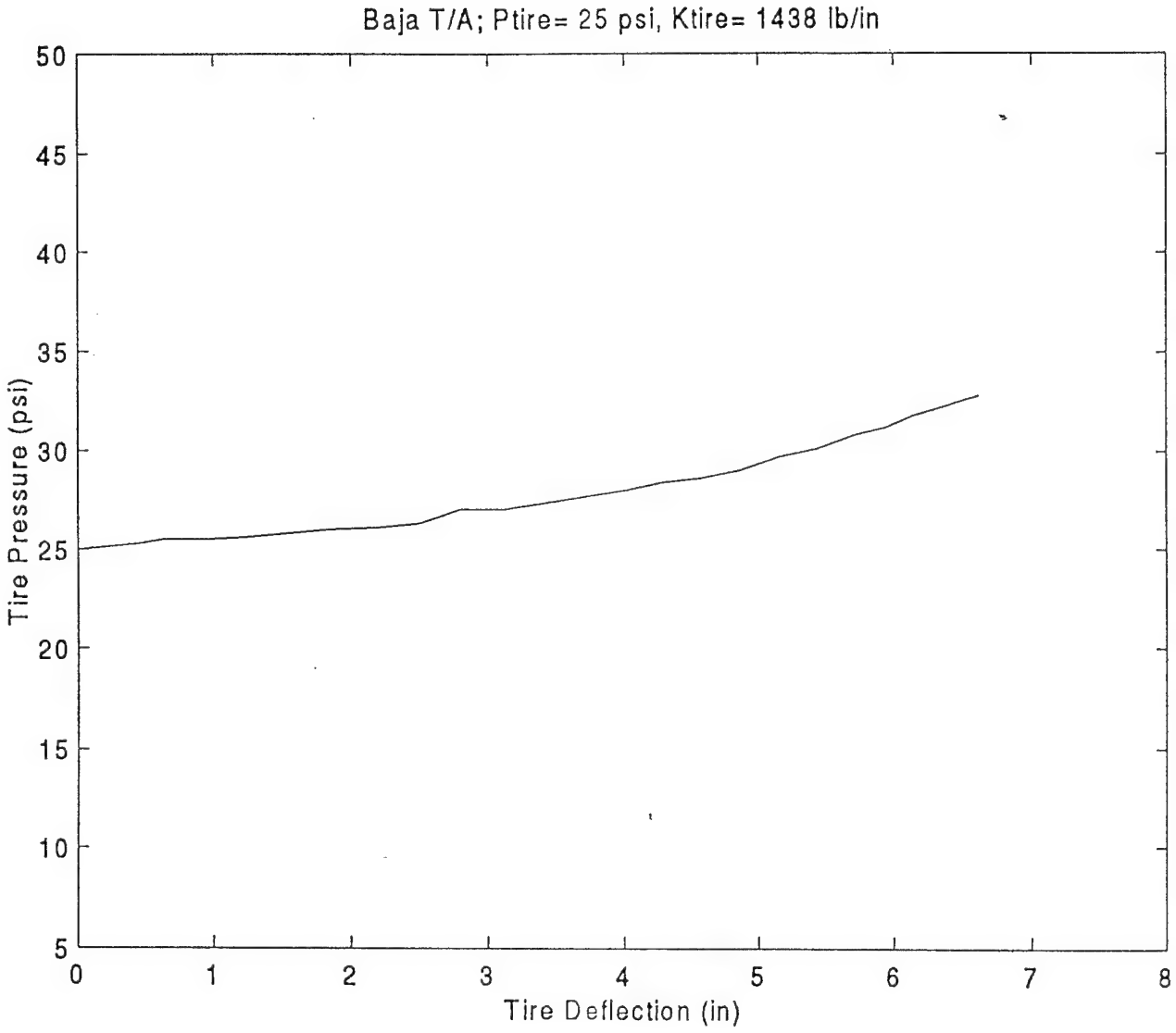
Baja T/A; Ptire= 25 psi, Ktire= 1438 lb/in
Tire Pressure (psi)
Tire Deflection (in)
50
45
40
35
30
25
20
15
10
5
0
1
2
3
4
5
6
7
8

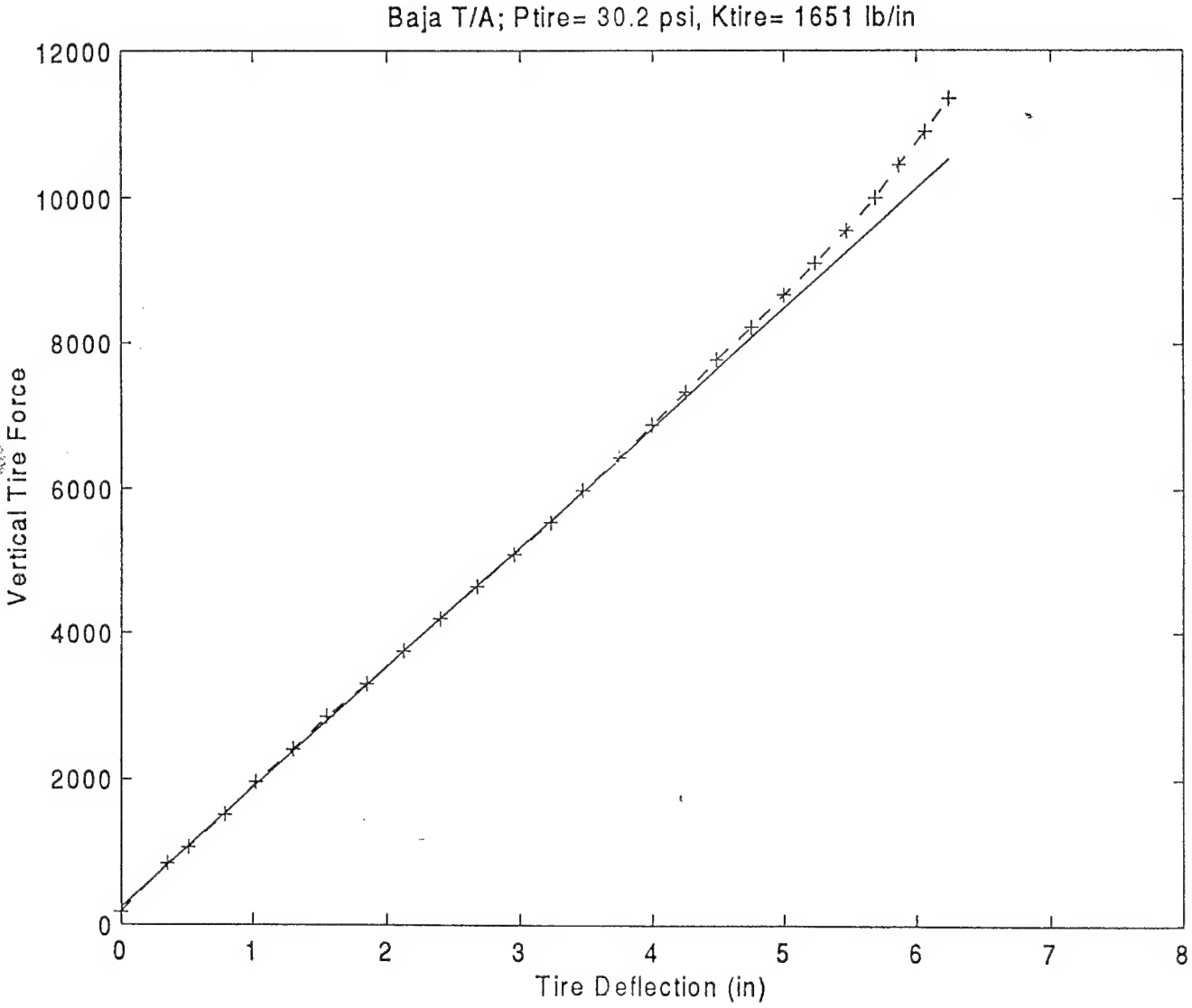
Baja T/A; Ptire= 30.2 psi, Ktire= 1651 lb/in
Vertical Tire Force
Tire Deflection (in)
12000
10000
8000
6000
4000
2000
0
0
1
2
3
4
5
6
7
8

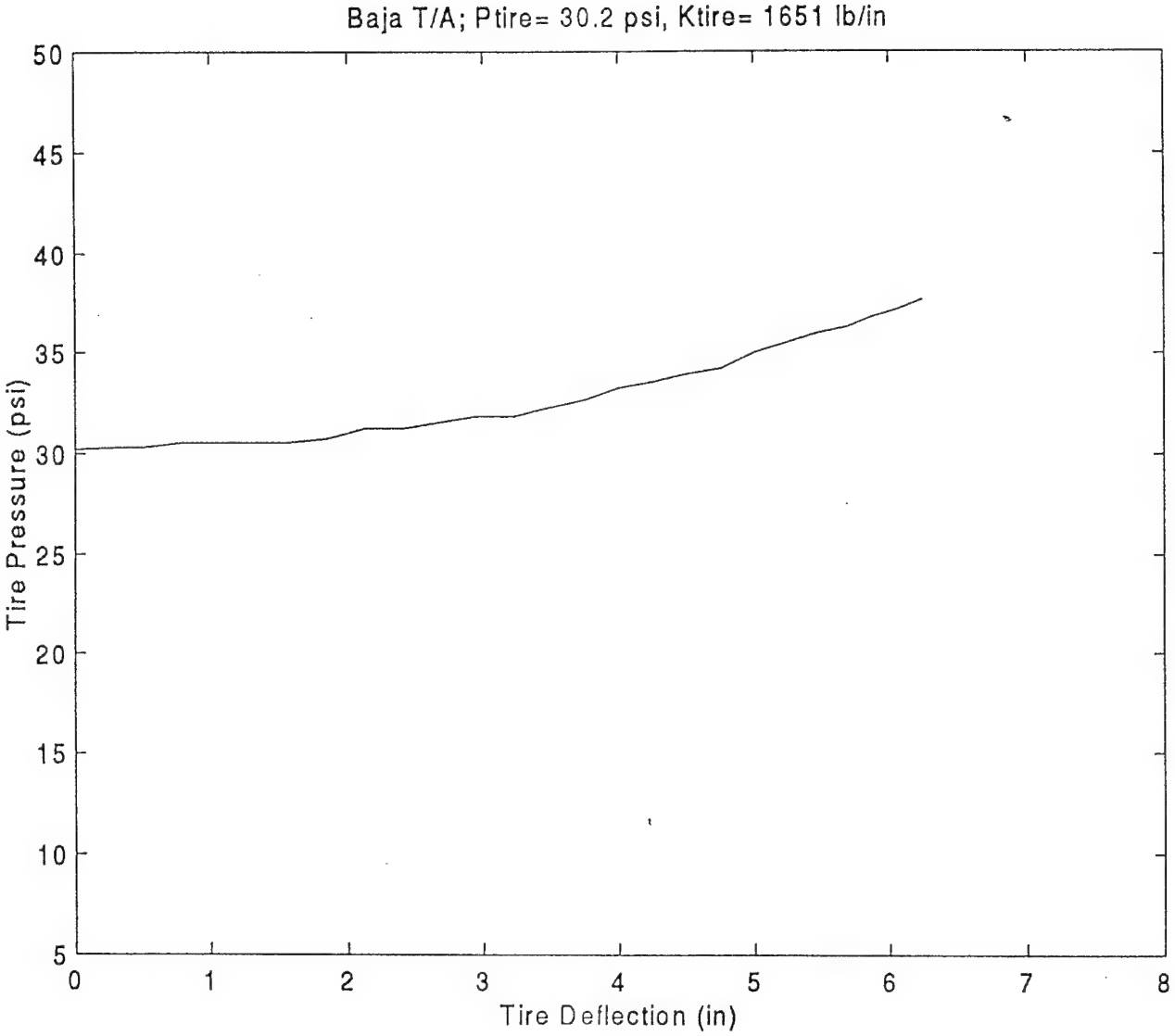
Baja T/A; Ptire= 30.2 psi, Ktire= 1651 lb/in
Tire Pressure (psi)
Tire Deflection (in)
50
45
40
35
30
25
20
15
10
5
0
1
2
3
4
5
6
7
8

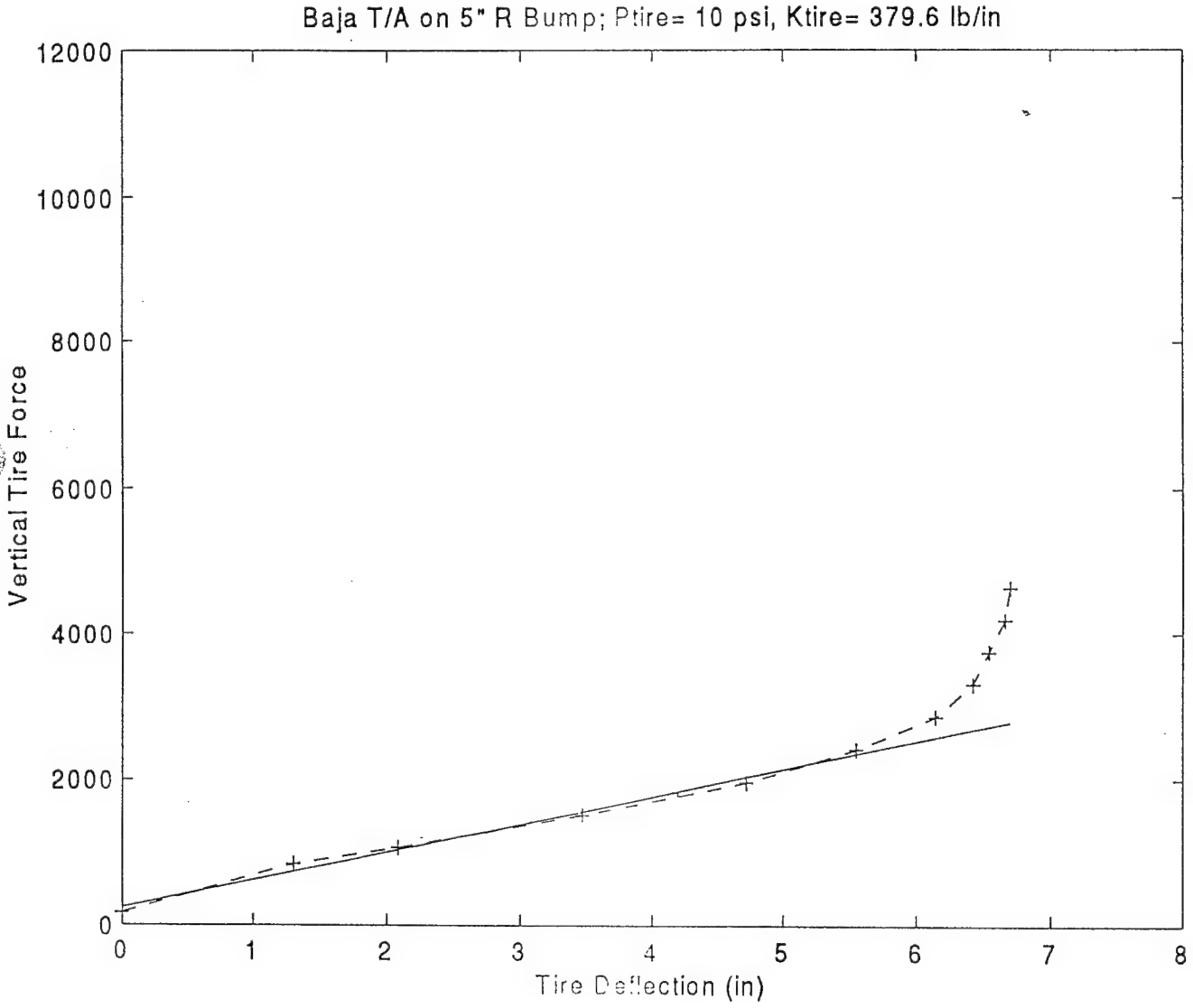
Baja T/A on 5" R Bump; Ptire= 10 psi, Ktire= 379.6 lb/in
Vertical Tire Force
Tire Deflection (in)
12000
10000
8000
6000
4000
2000
0
0
1
2
3
4
5
6
7
8

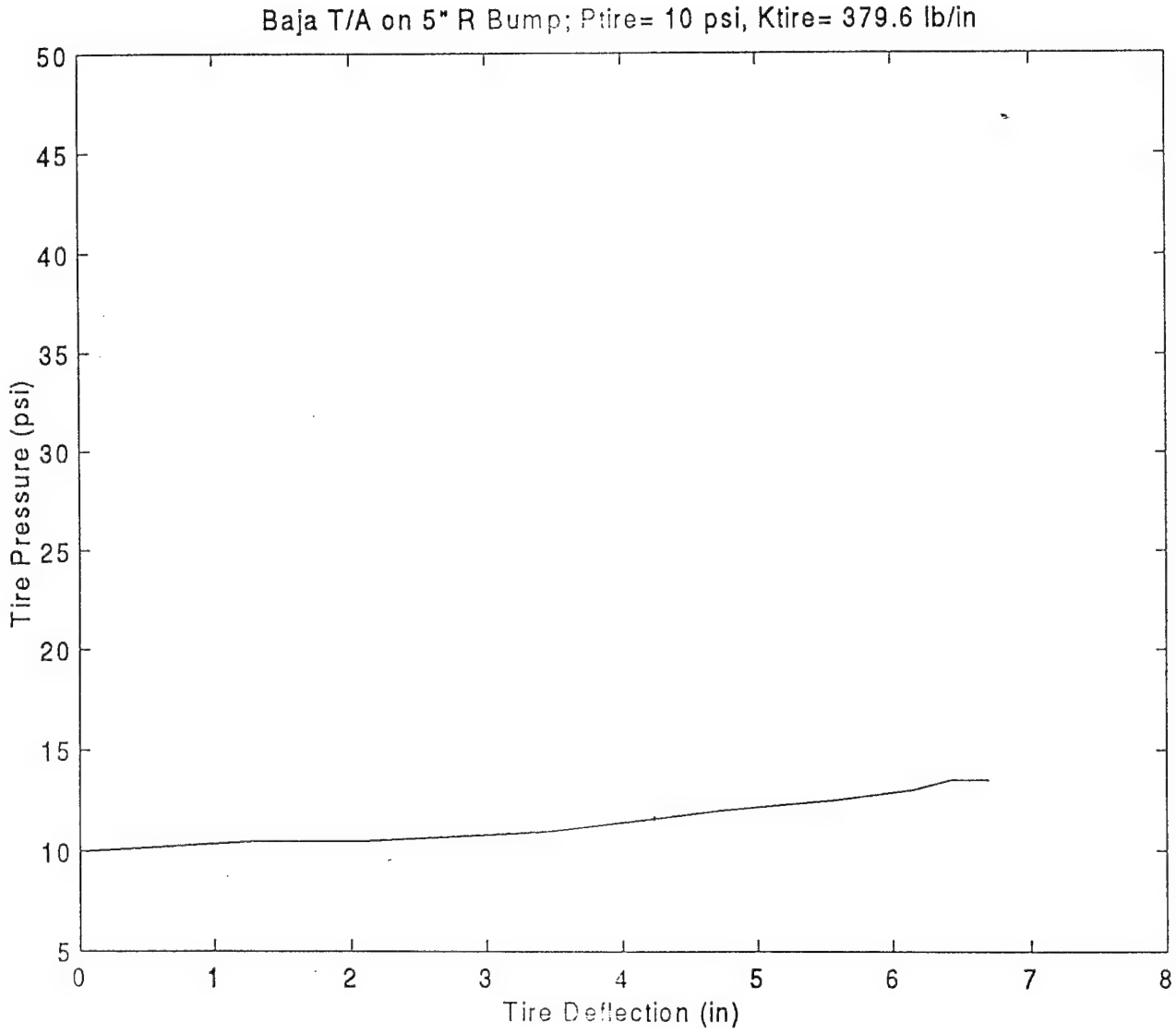
Baja T/A on 5" R Bump; Ptire= 10 psi, Ktire= 379.6 lb/in
Tire Pressure (psi)
Tire Deflection (in)
50
45
40
35
30
25
20
15
10
5
0
1
2
3
4
5
6
7
8

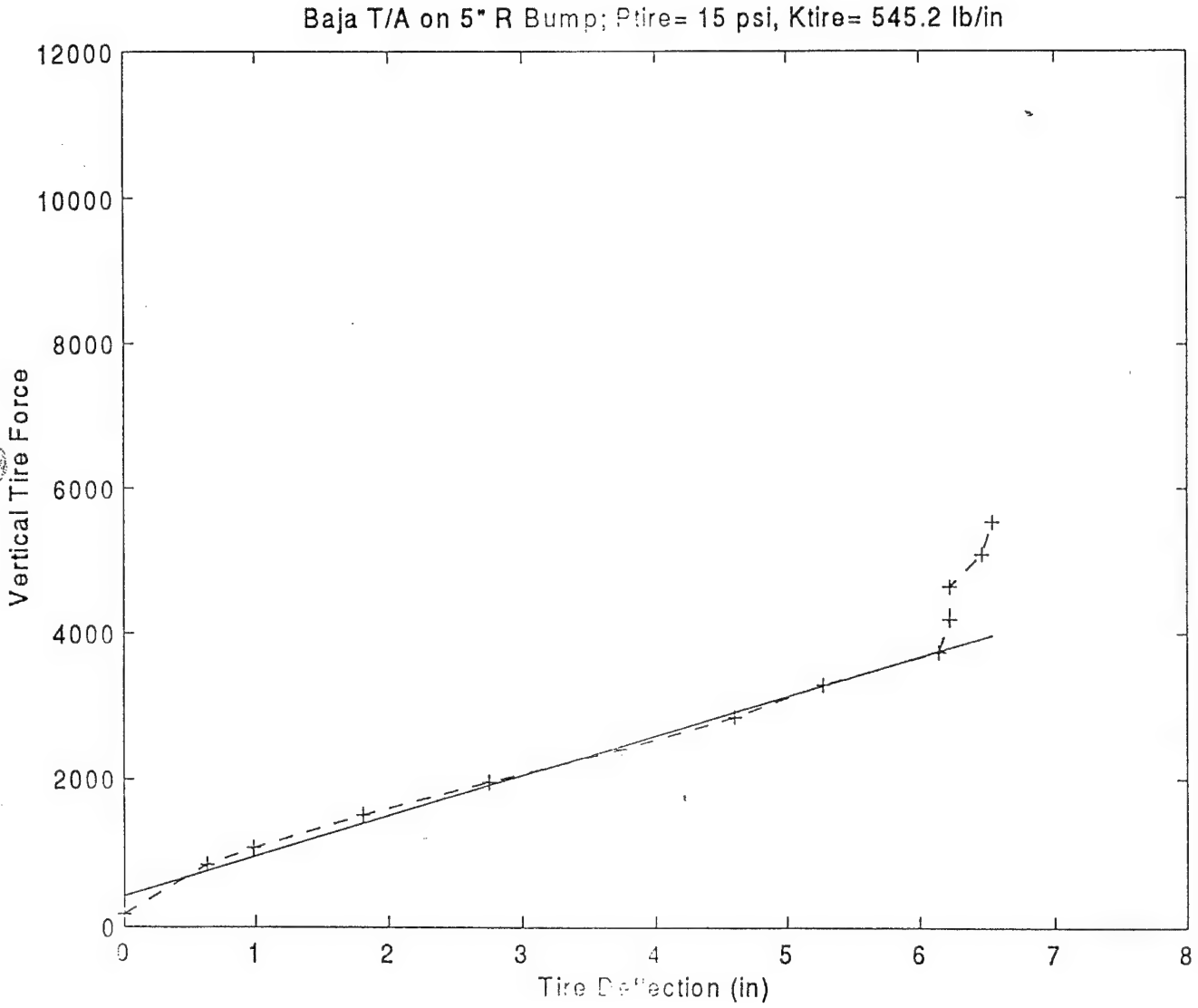
Baja T/A on 5" R Bump; Ptire= 15 psi, Ktire= 545.2 lb/in
Vertical Tire Force
12000
10000
8000
6000
4000
2000
0
0
1
2
3
4
5
6
7
8
Tire Deflection (in)

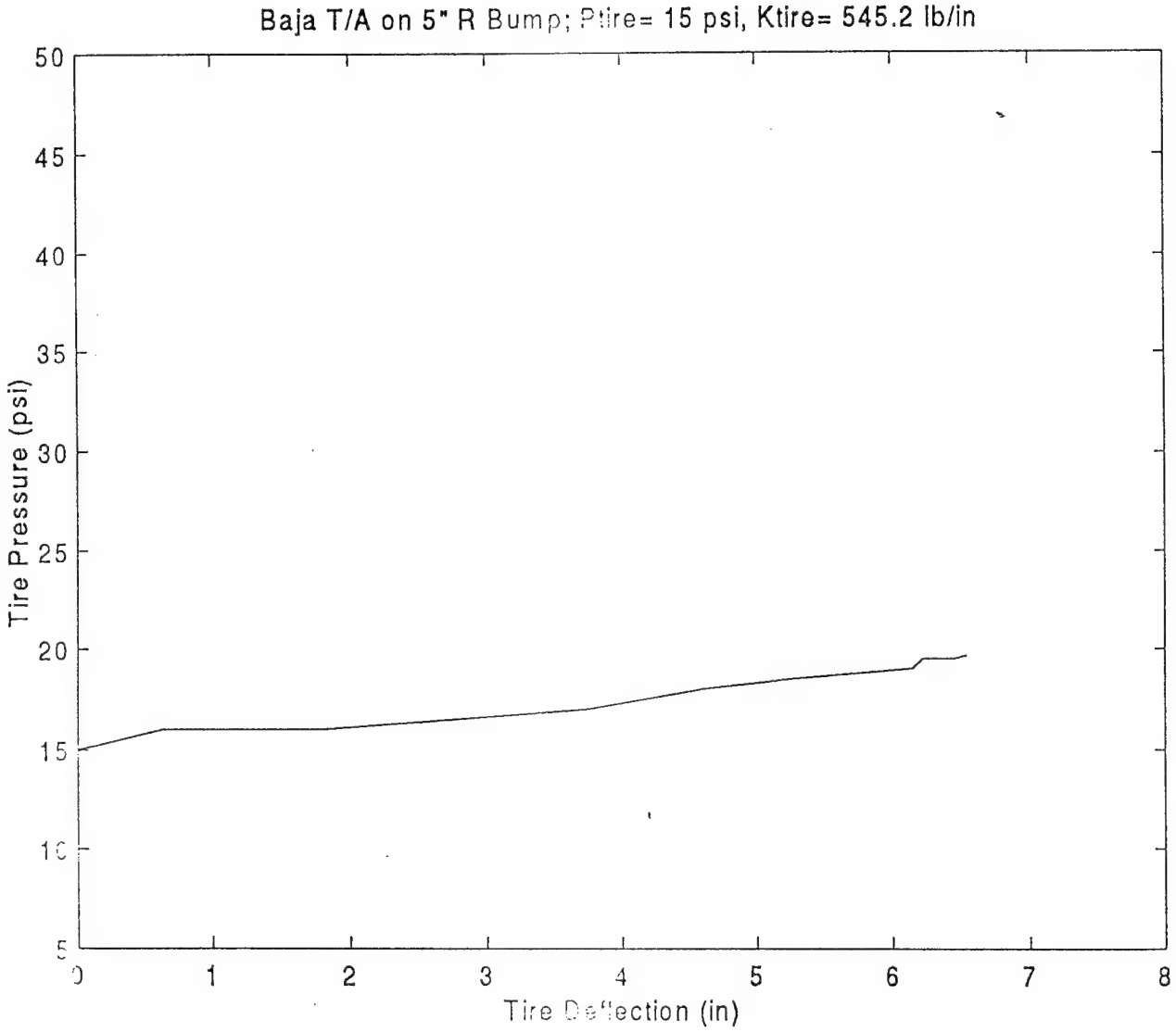
Baja T/A on 5" R Bump; Ptire= 15 psi, Ktire= 545.2 lb/in
Tire Pressure (psi)
50
45
40
35
30
25
20
15
10
5
0
1
2
3
4
5
6
7
8
Tire Deflection (in)

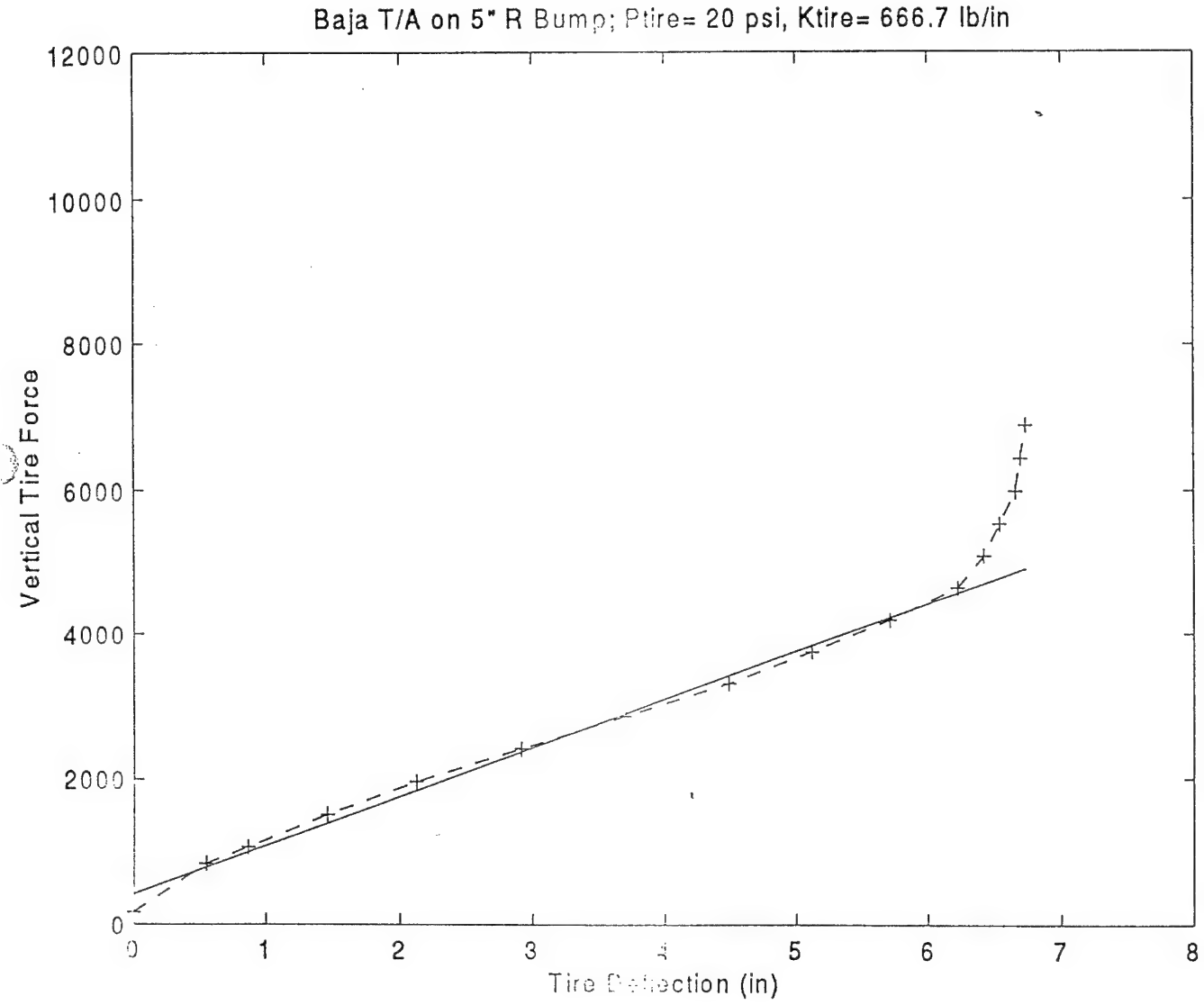
Baja T/A on 5" R Bump; Ptire= 20 psi, Ktire= 666.7 lb/in
Vertical Tire Force
12000
10000
8000
6000
4000
2000
0
0
1
2
3
4
5
6
7
8
Tire Deflection (in)

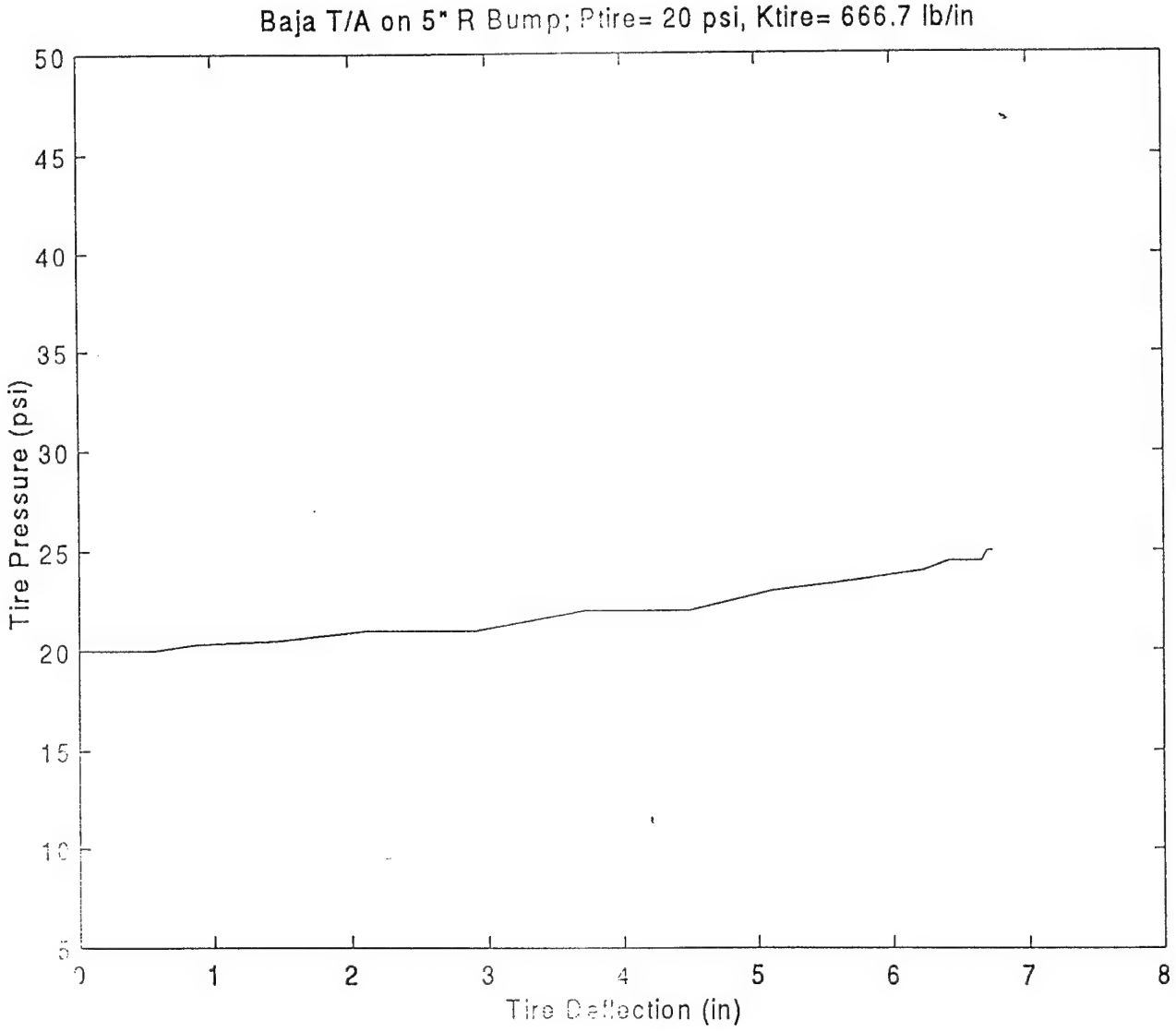
Baja T/A on 5" R Bump; Ptire= 20 psi, Ktire= 666.7 lb/in
Tire Pressure (psi)
50
45
40
35
30
25
20
15
10
5
0
1
2
3
4
5
6
7
8
Tire Deflection (in)

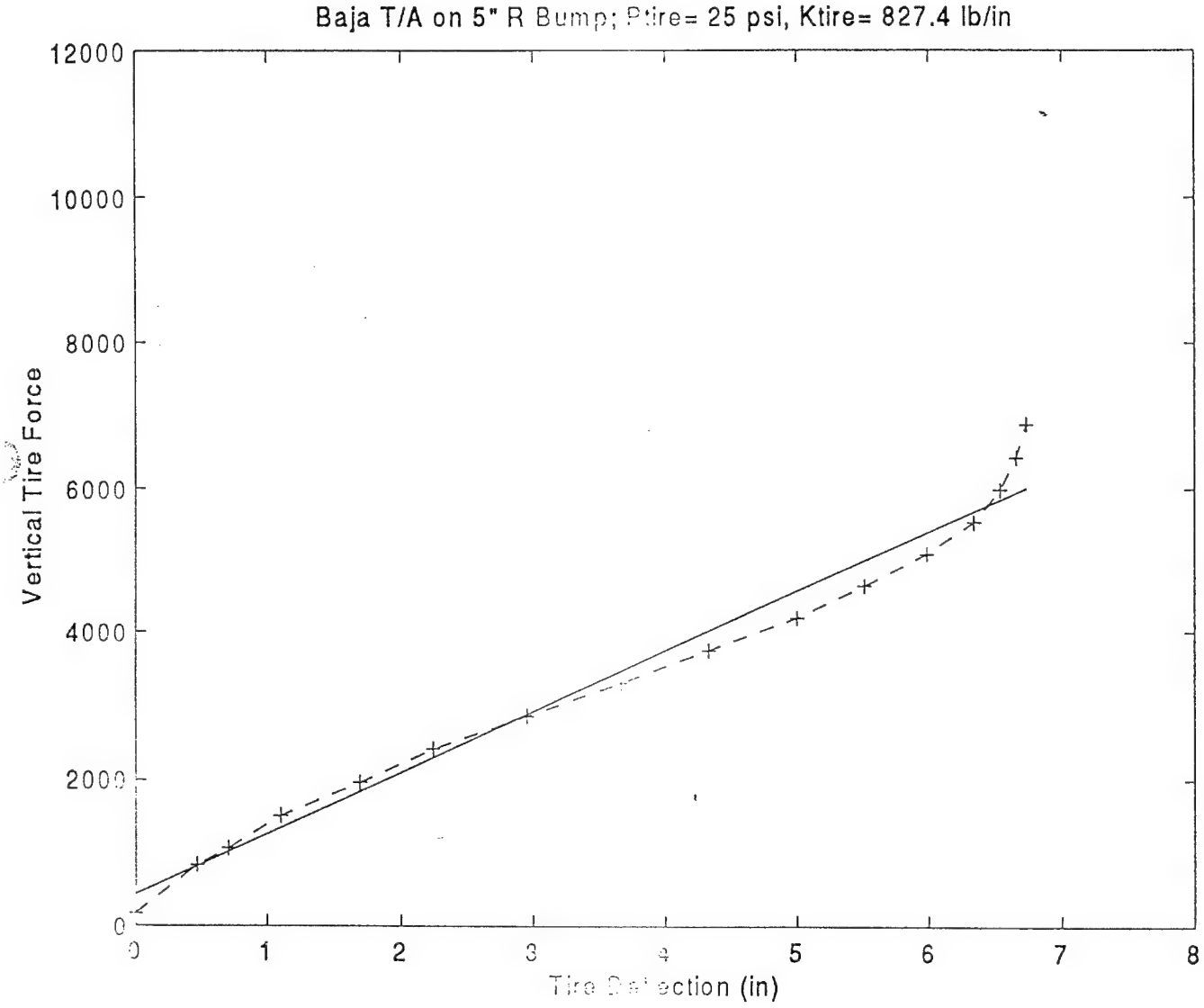
Baja T/A on 5" R Bump; Ptire= 25 psi, Ktire= 827.4 lb/in
12000
10000
8000
6000
4000
2000
0
Vertical Tire Force
0
1
2
3
4
5
6
7
8
Tire Deflection (in)

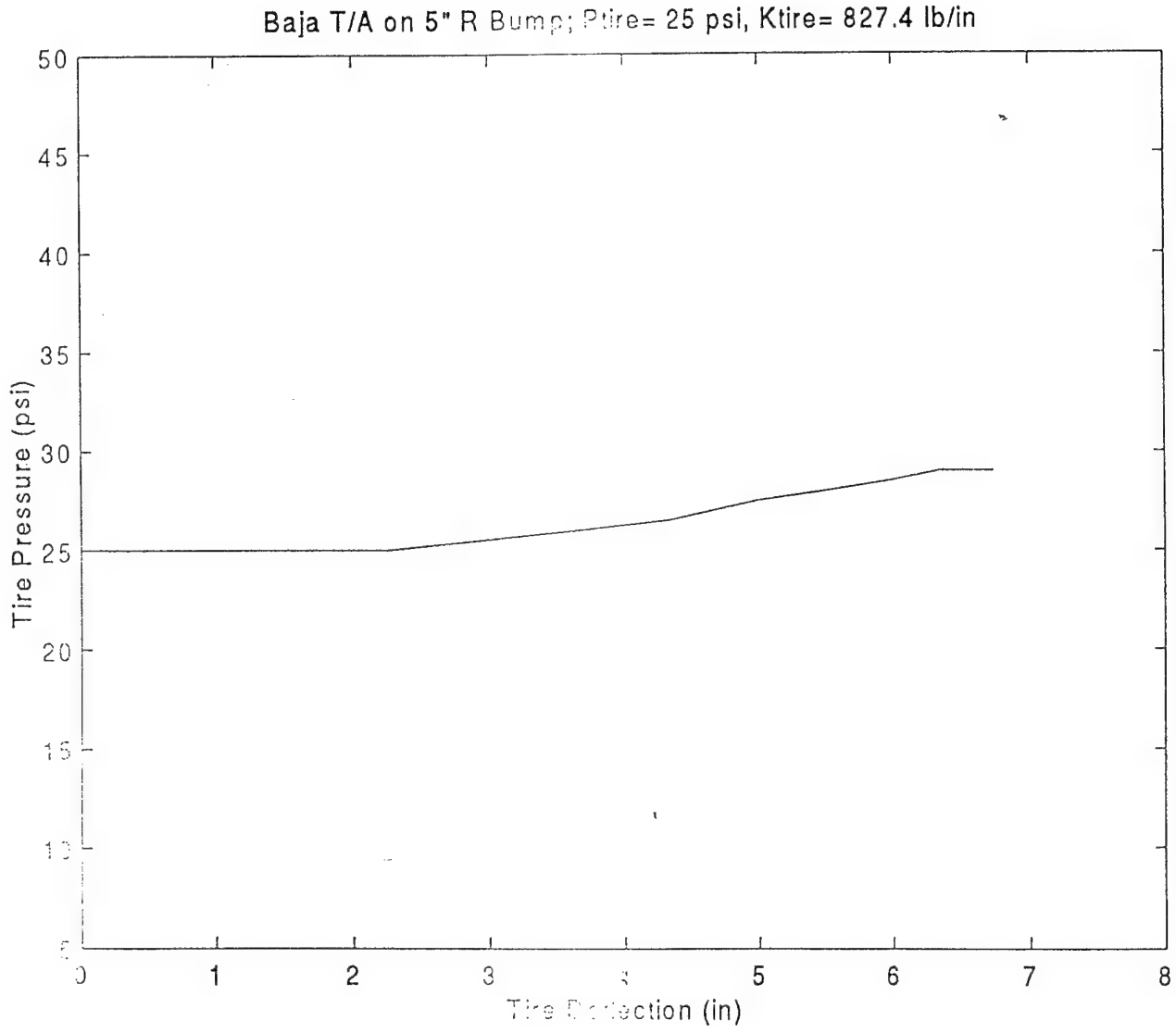
Baja T/A on 5" R Bump; Ptire= 25 psi, Ktire= 827.4 lb/in
Tire Pressure (psi)
50
45
40
35
30
25
20
0
1
2
3
5
6
7
8

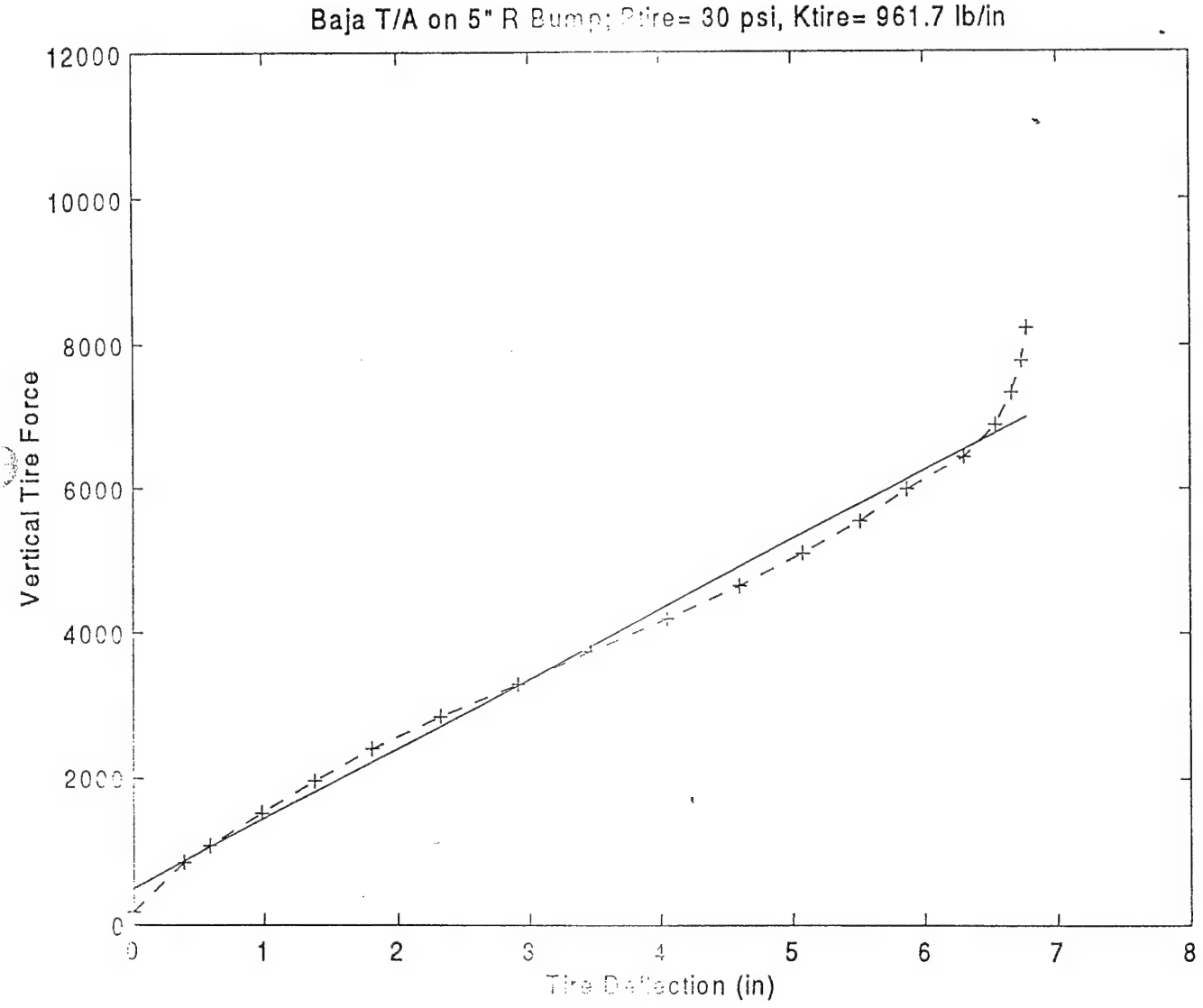
Baja T/A on 5" R Bump; Ptire= 30 psi, Ktire= 961.7 lb/in
Vertical Tire Force
Tire Deflection (in)
12000
10000
8000
6000
4000
2000
0
0
1
2
3
4
5
6
7
8

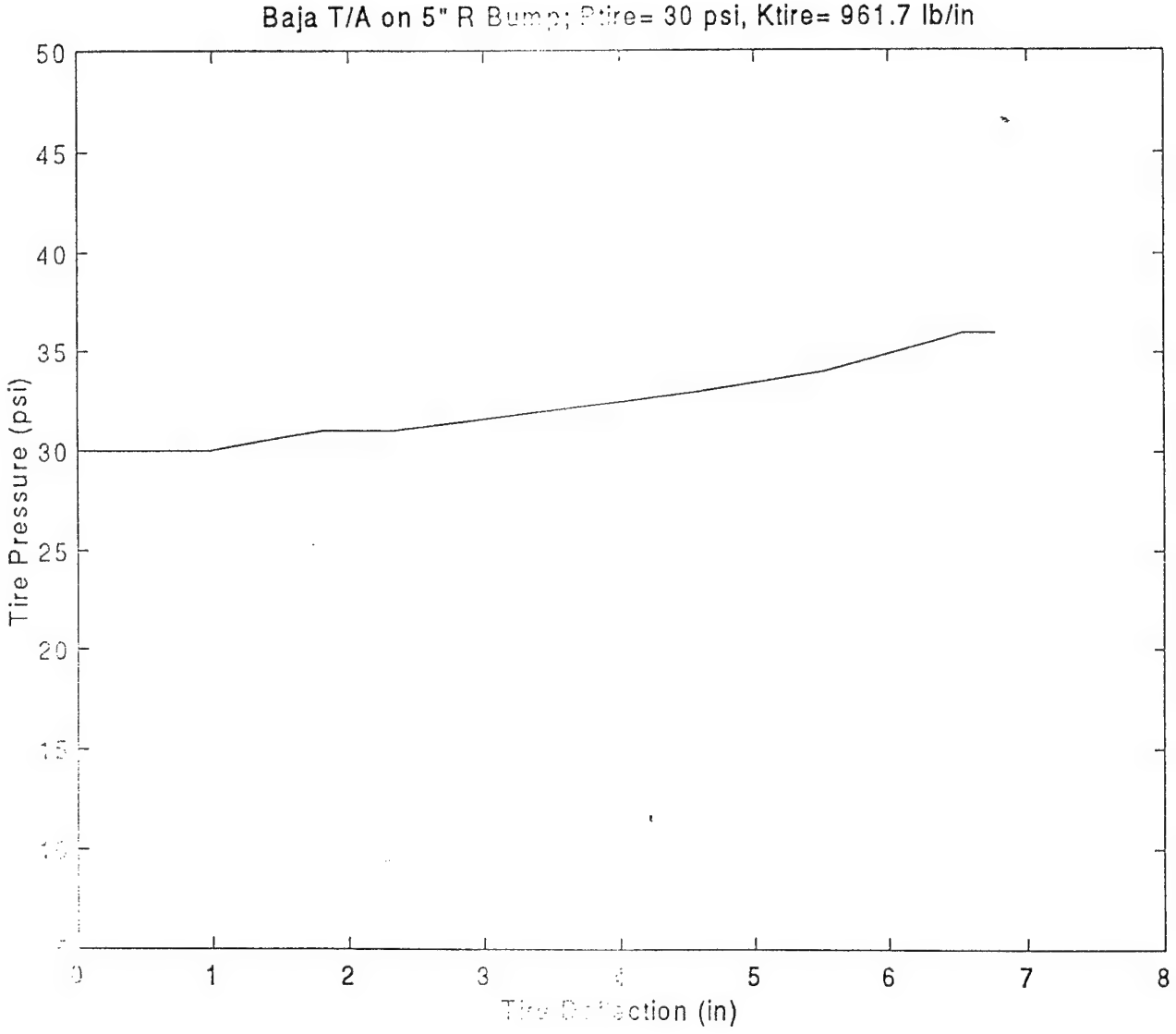
Baja T/A on 5" R Bump; Ptire= 30 psi, Ktire= 961.7 lb/in
Tire Pressure (psi)
50
45
40
35
30
25
20
1
2
3
5
6
7
8

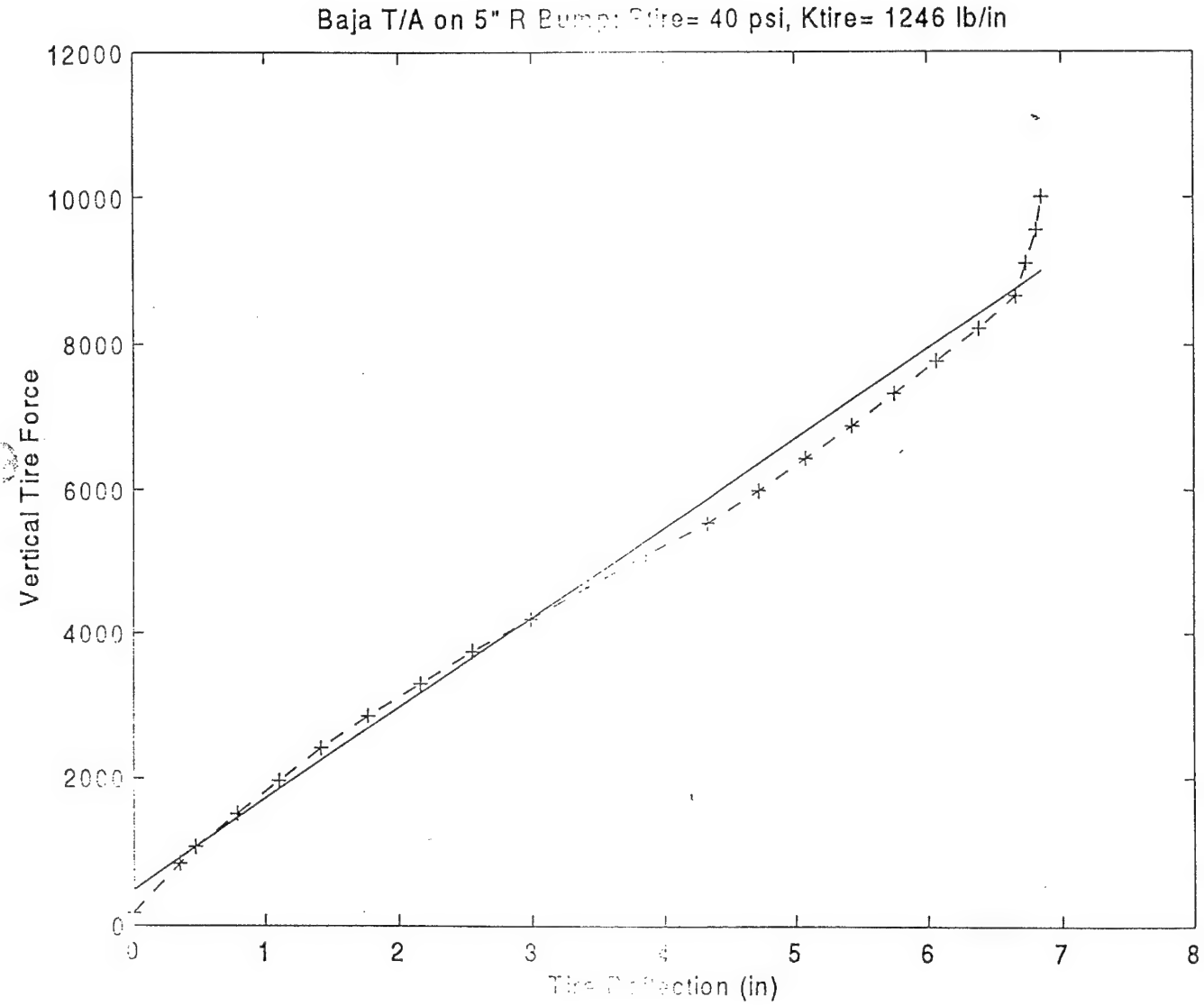
Baja T/A on 5" R Bump: Ptire= 40 psi, Ktire= 1246 lb/in
Vertical Tire Force
12000
10000
8000
6000
4000
2000
0
0
1
2
3
4
5
6
7
8
Tire Deflection (in)

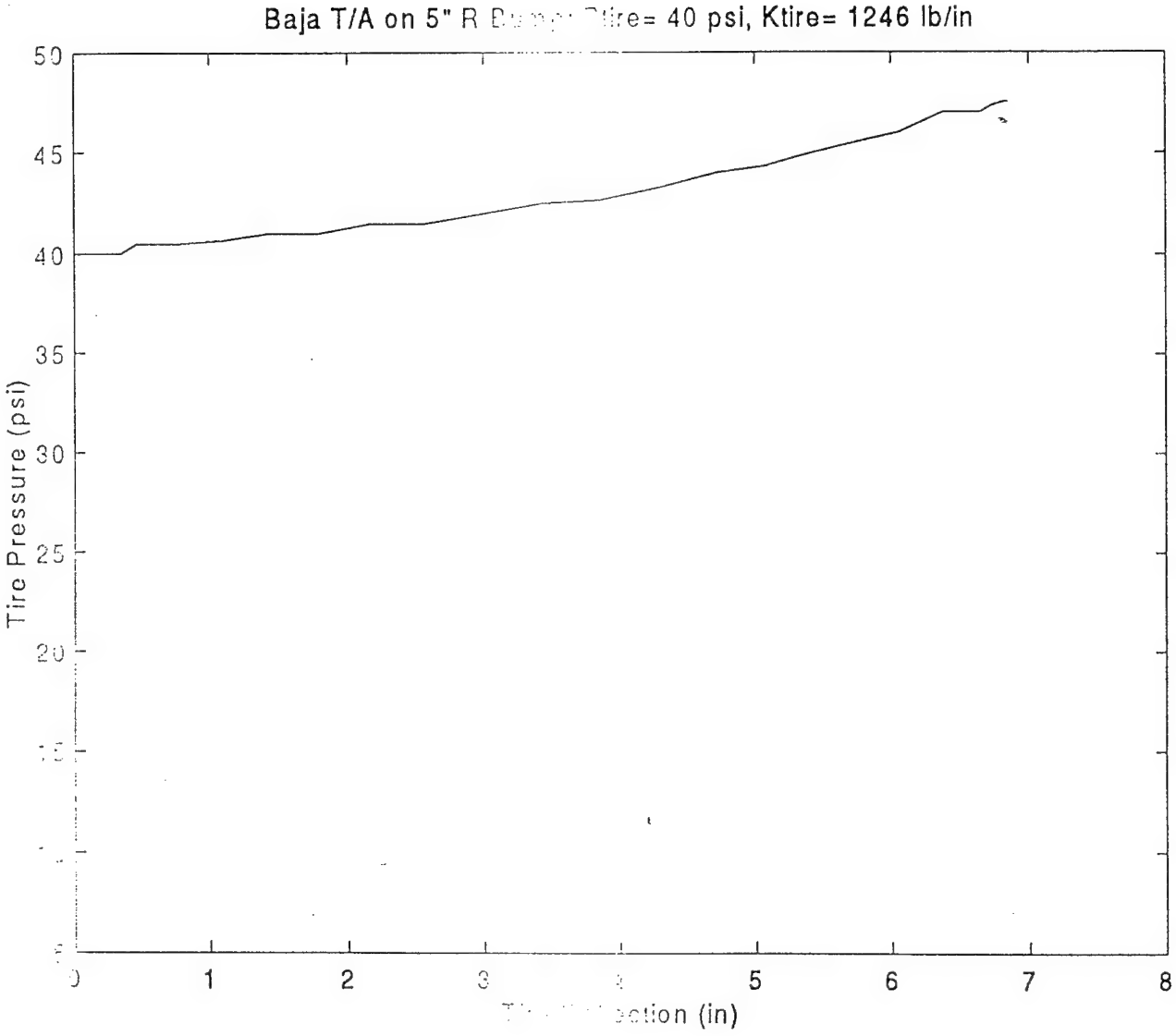
Baja T/A on 5" R
Tire= 40 psi, Ktire= 1246 lb/in
Tire Pressure (psi)
50
45
40
35
30
25
20
0
1
2
3
5
6
7
8
ection (in)

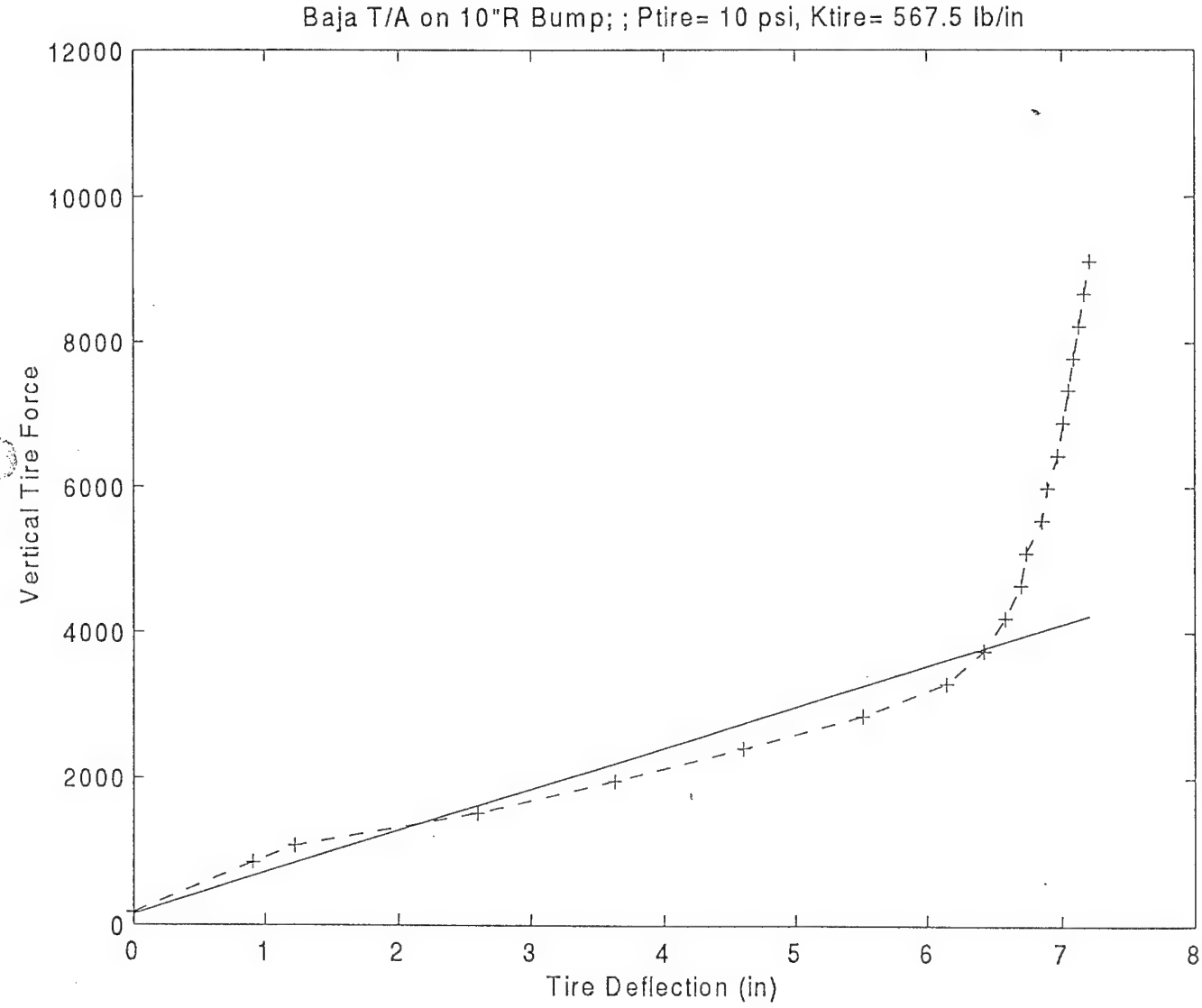
Baja T/A on 10"R Bump; ; Ptire= 10 psi, Ktire= 567.5 lb/in
Vertical Tire Force
Tire Deflection (in)
12000
10000
8000
6000
4000
2000
0
0
1
2
3
4
5
6
7
8

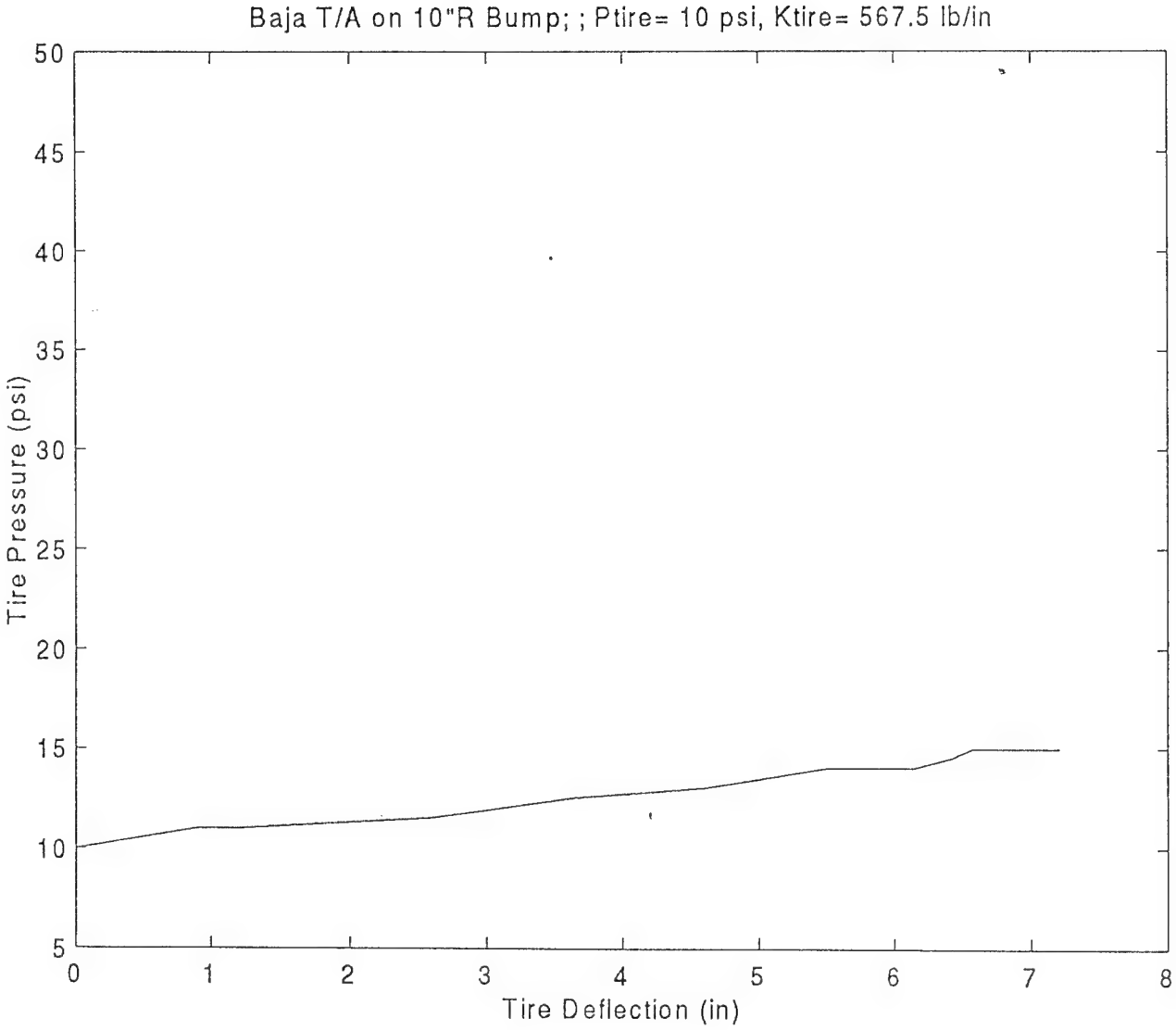
Baja T/A on 10"R Bump; ; Ptire= 10 psi, Ktire= 567.5 lb/in
Tire Pressure (psi)
Tire Deflection (in)
50
45
40
35
30
25
20
15
10
5
0
1
2
3
4
5
6
7
8

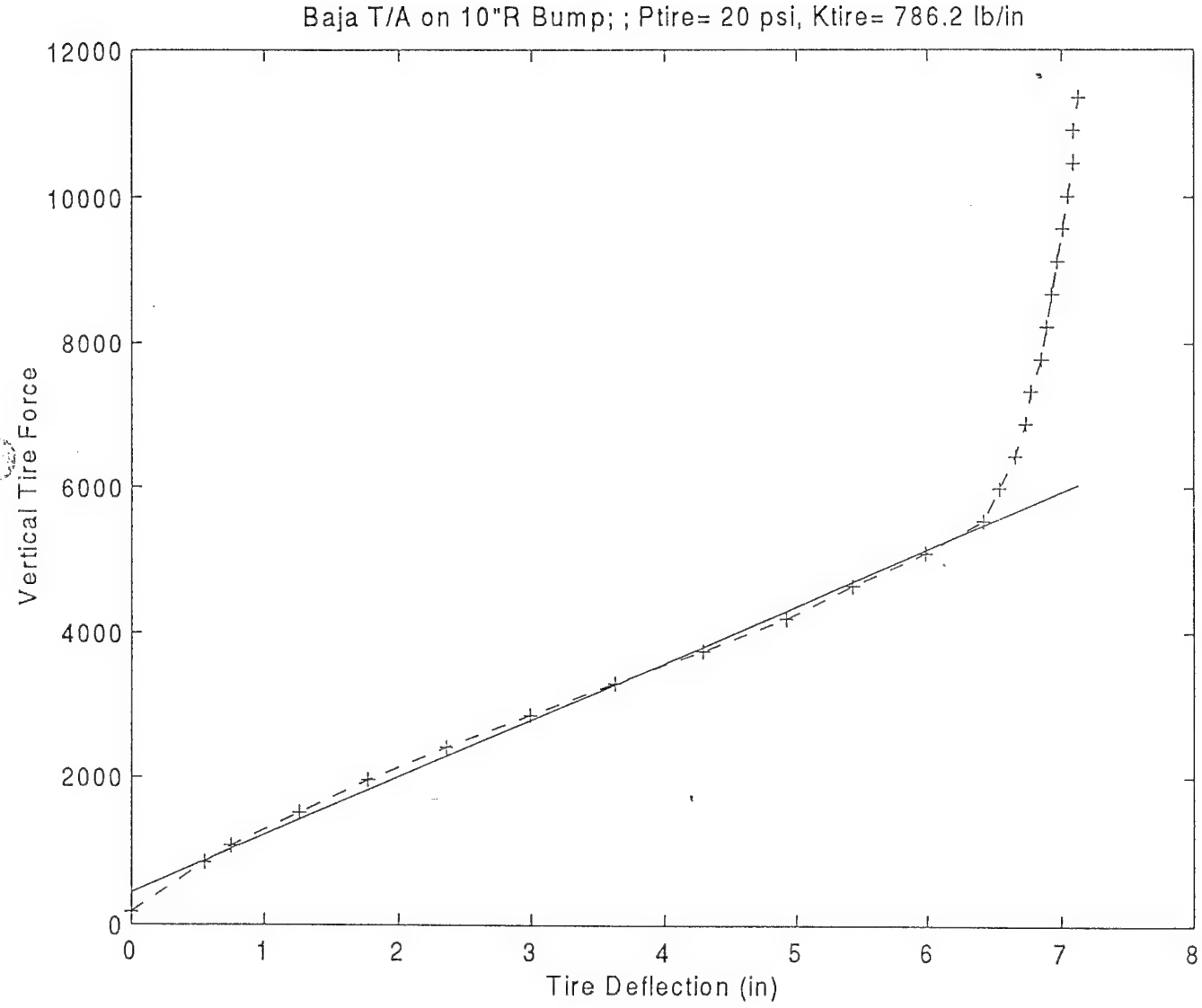
Baja T/A on 10"R Bump; ; Ptire= 20 psi, Ktire= 786.2 lb/in
Vertical Tire Force
Tire Deflection (in)
0
2000
4000
6000
8000
10000
12000
0
1
2
3
4
5
6
7
8

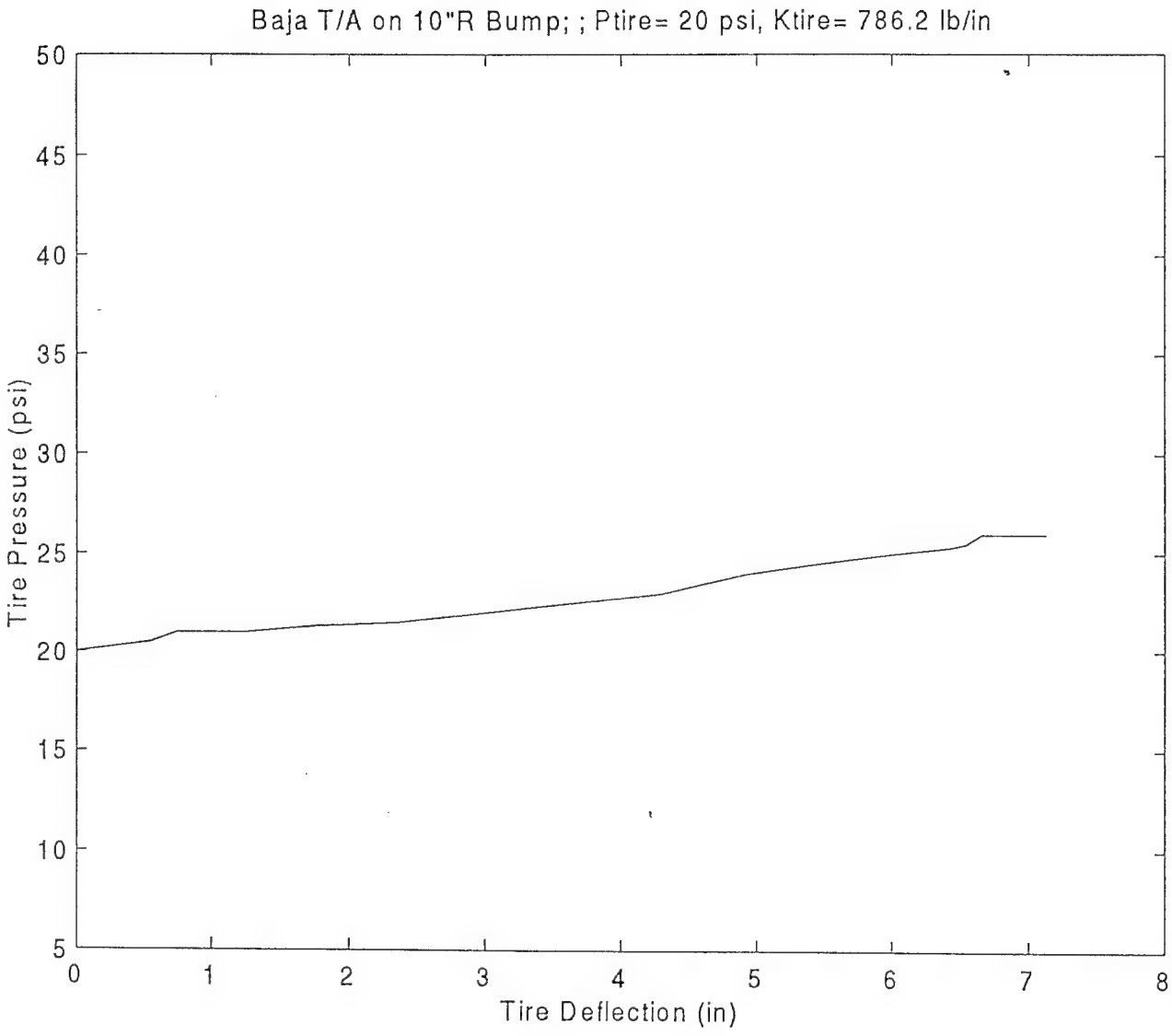
Baja T/A on 10"R Bump; ; Ptire= 20 psi, Ktire= 786.2 lb/in
Tire Pressure (psi)
Tire Deflection (in)
50
45
40
35
30
25
20
15
10
5
0
1
2
3
4
5
6
7
8

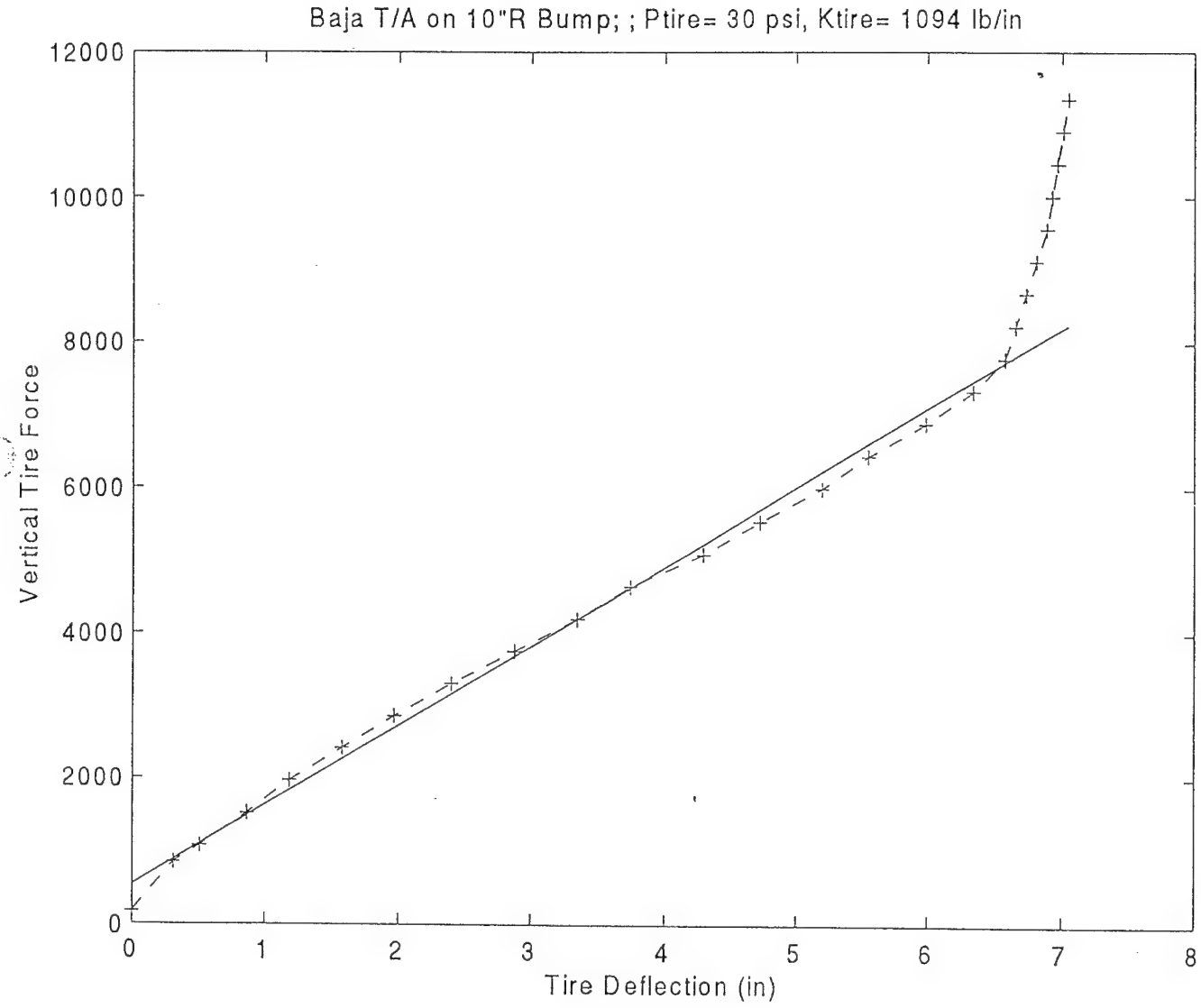
Baja T/A on 10"R Bump; ; Ptire= 30 psi, Ktire= 1094 lb/in
Vertical Tire Force
Tire Deflection (in)
0
2000
4000
6000
8000
10000
12000
0
1
2
3
4
5
6
7
8

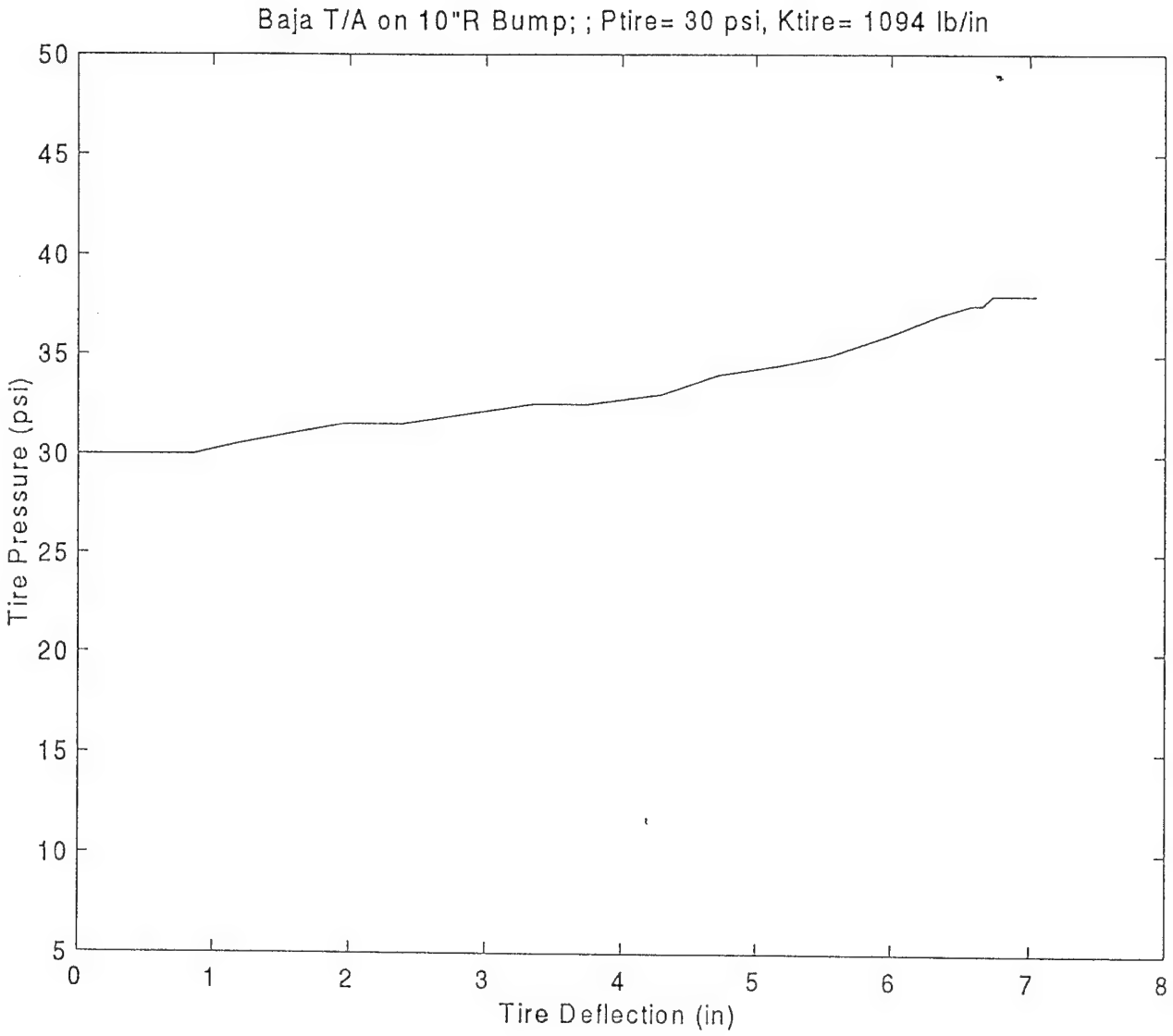
Baja T/A on 10"R Bump; ; Ptire= 30 psi, Ktire= 1094 lb/in
Tire Pressure (psi)
50
45
40
35
30
25
20
15
10
5
0
1
2
3
4
5
6
7
8
Tire Deflection (in)

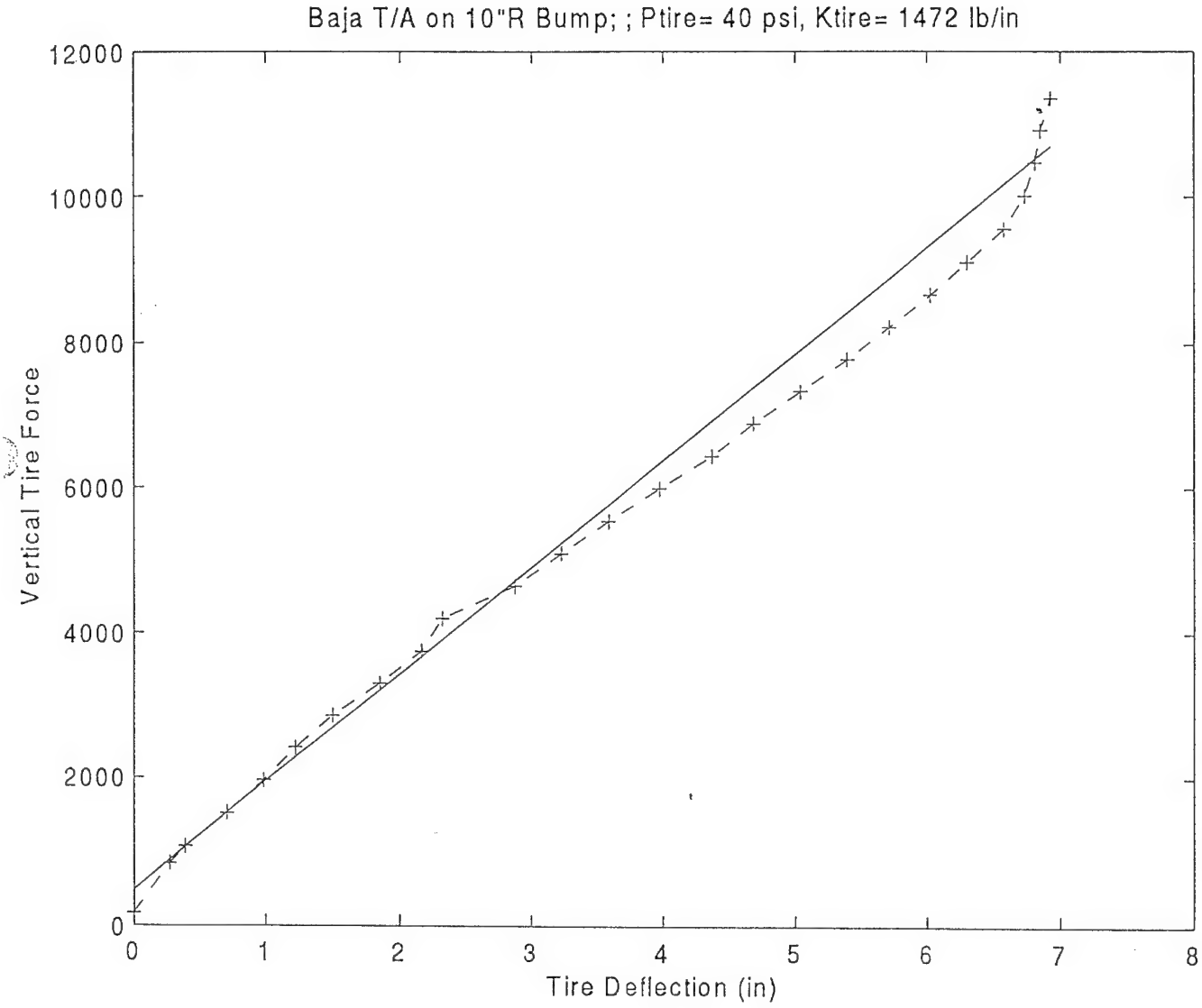
Baja T/A on 10"R Bump; ; Ptire= 40 psi, Ktire= 1472 lb/in
Vertical Tire Force
Tire Deflection (in)
12000
10000
8000
6000
4000
2000
0
0
1
2
3
4
5
6
7
8

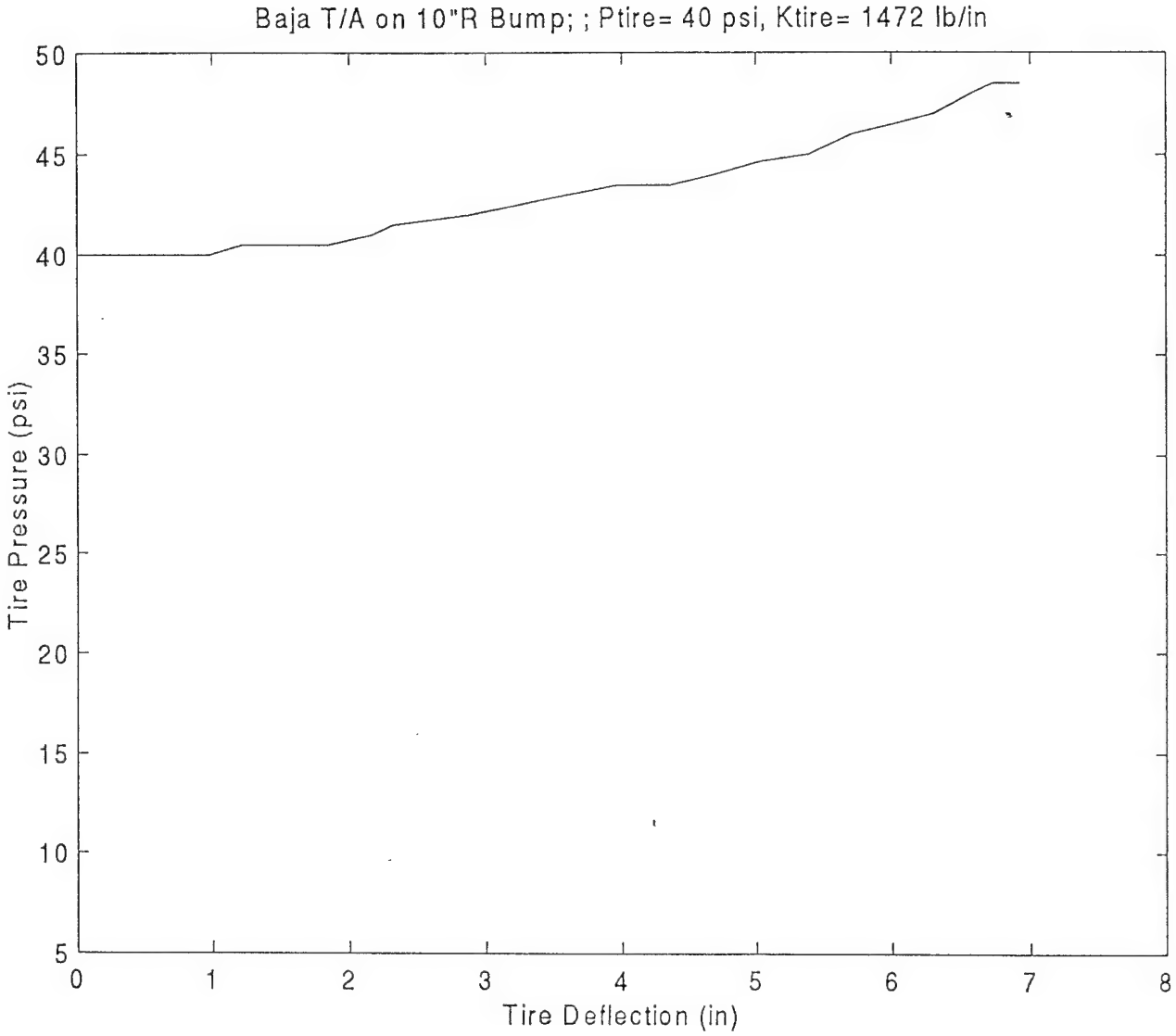
Baja T/A on 10"R Bump; ; Ptire= 40 psi, Ktire= 1472 lb/in
Tire Pressure (psi)
Tire Deflection (in)
50
45
40
35
30
25
20
15
10
5
0
1
2
3
4
5
6
7
8

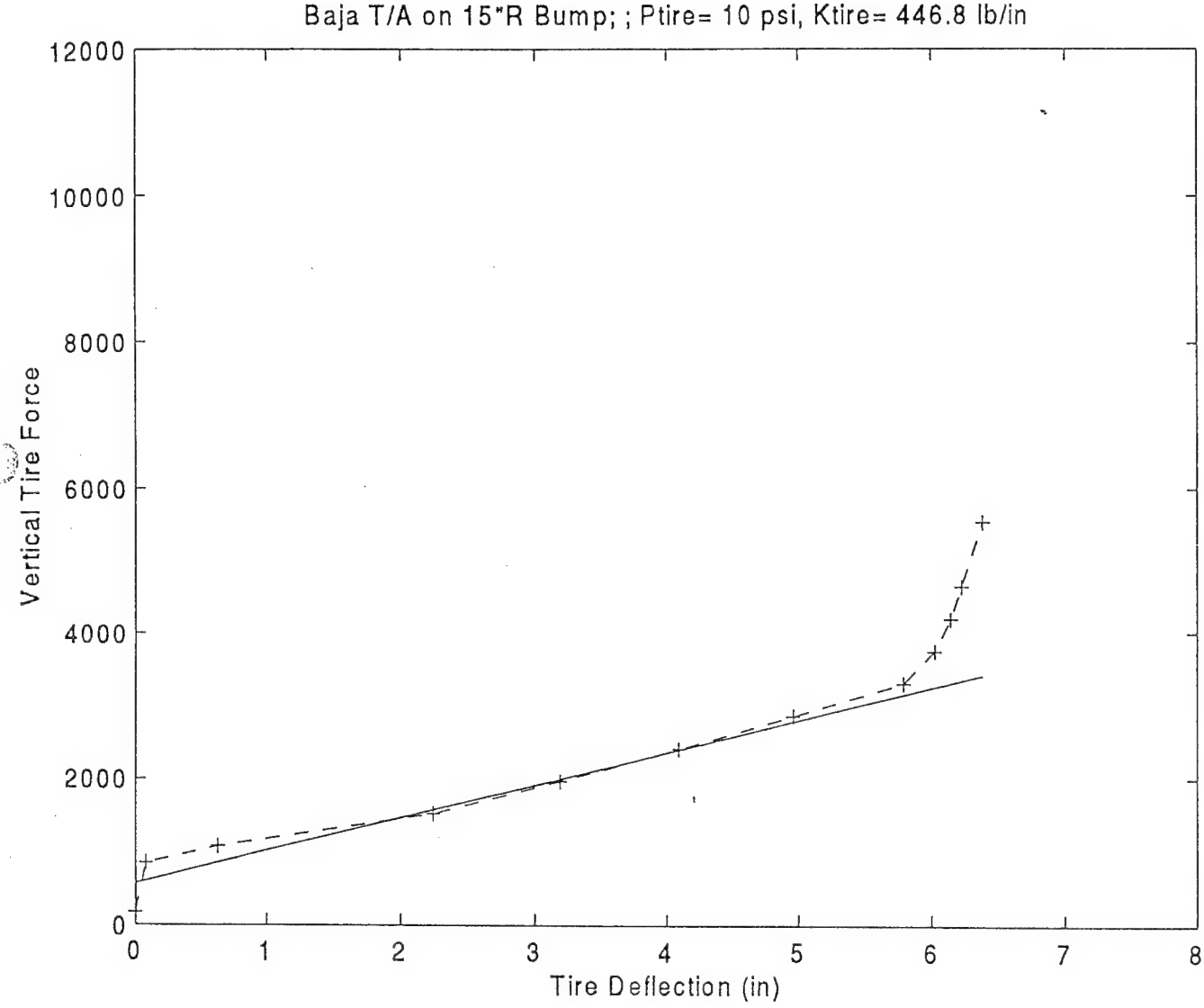
Baja T/A on 15"R Bump; ; Ptire= 10 psi, Ktire= 446.8 lb/in
Vertical Tire Force
Tire Deflection (in)
12000
10000
8000
6000
4000
2000
0
0
1
2
3
4
5
6
7
8

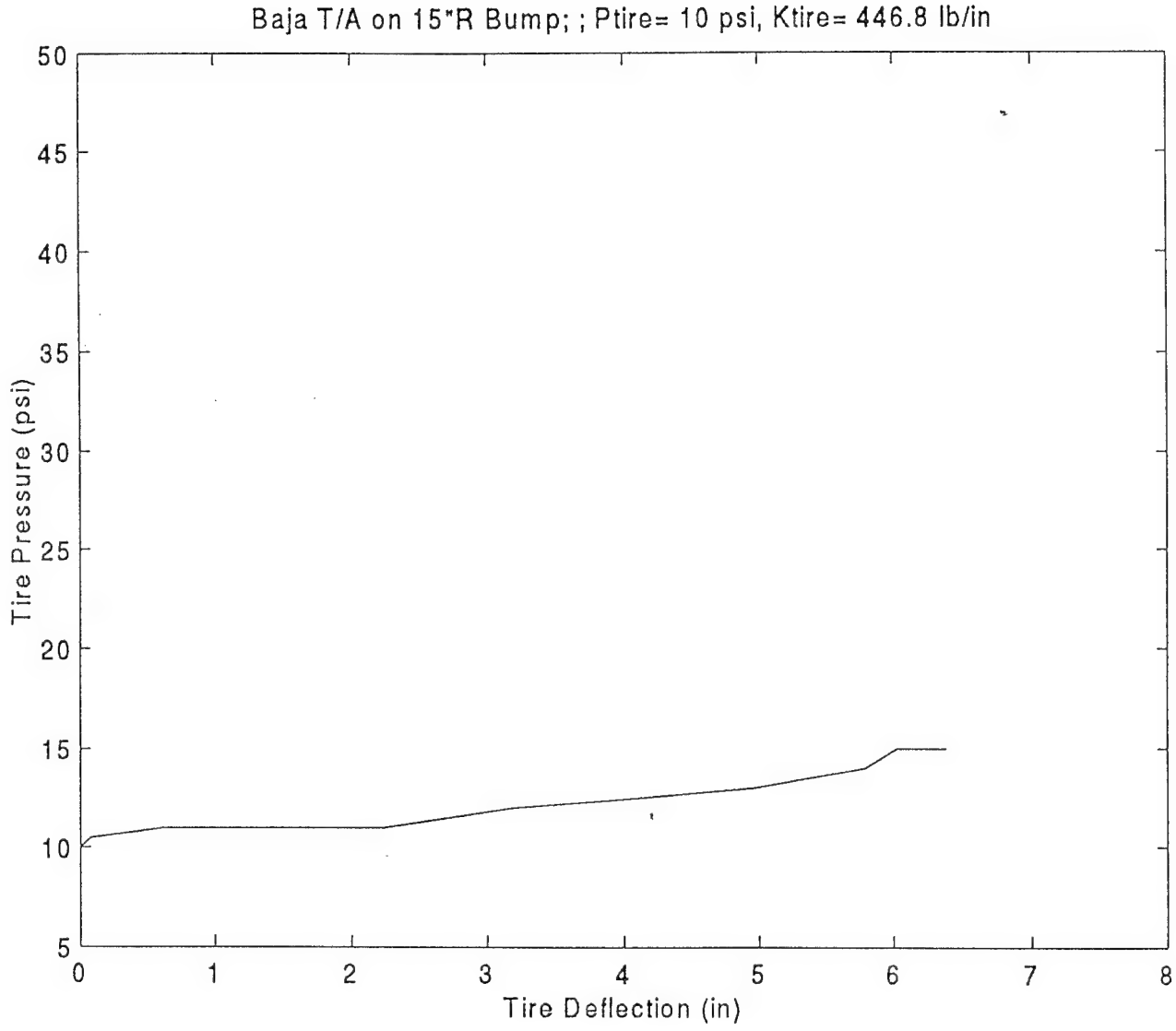
Baja T/A on 15"R Bump; ; Ptire= 10 psi, Ktire= 446.8 lb/in
Tire Pressure (psi)
Tire Deflection (in)
50
45
40
35
30
25
20
15
10
5
0
1
2
3
4
5
6
7
8

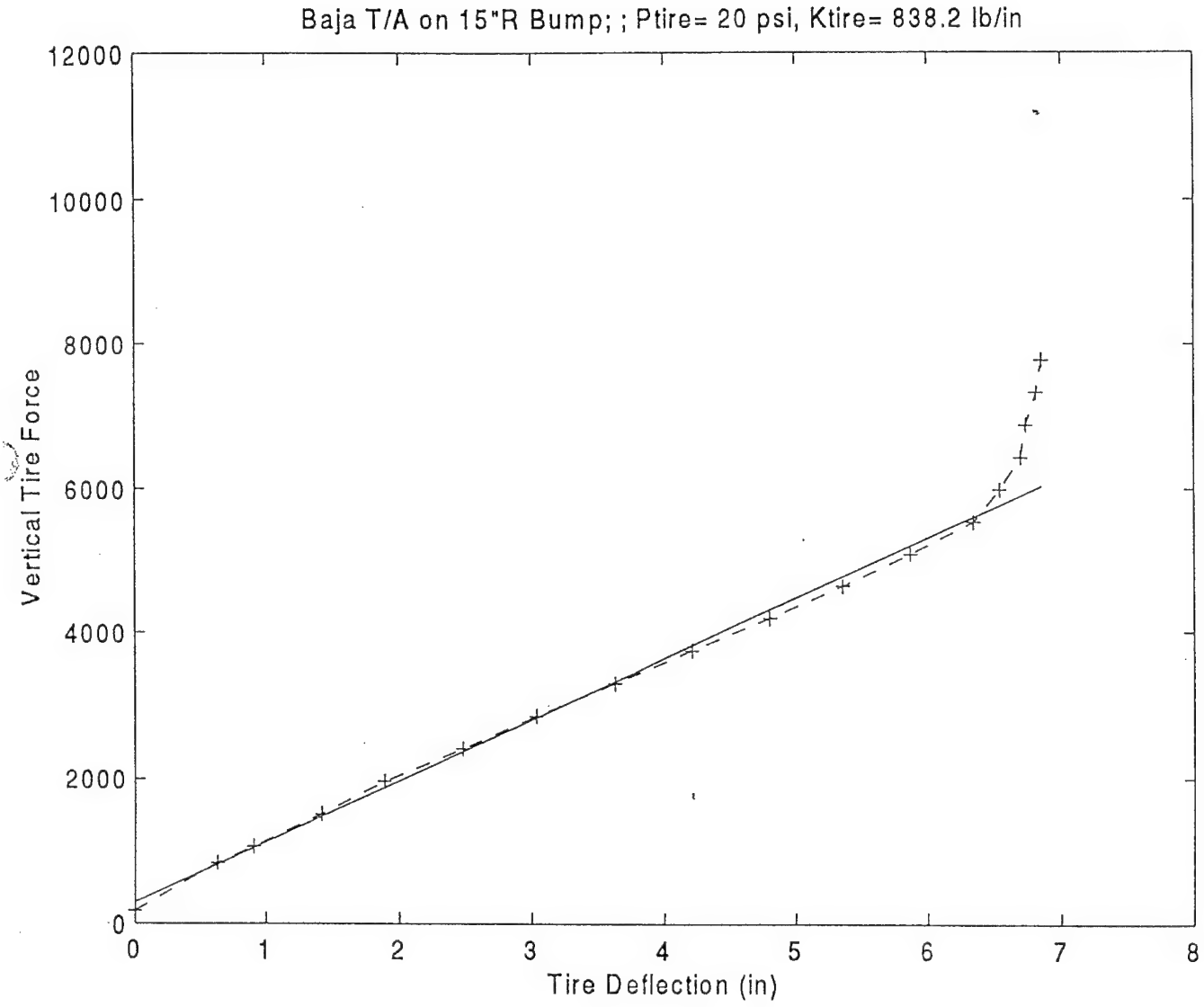
Baja T/A on 15"R Bump; ; Ptire= 20 psi, Ktire= 838.2 lb/in
Vertical Tire Force
Tire Deflection (in)
12000
10000
8000
6000
4000
2000
0
0
1
2
3
4
5
6
7
8

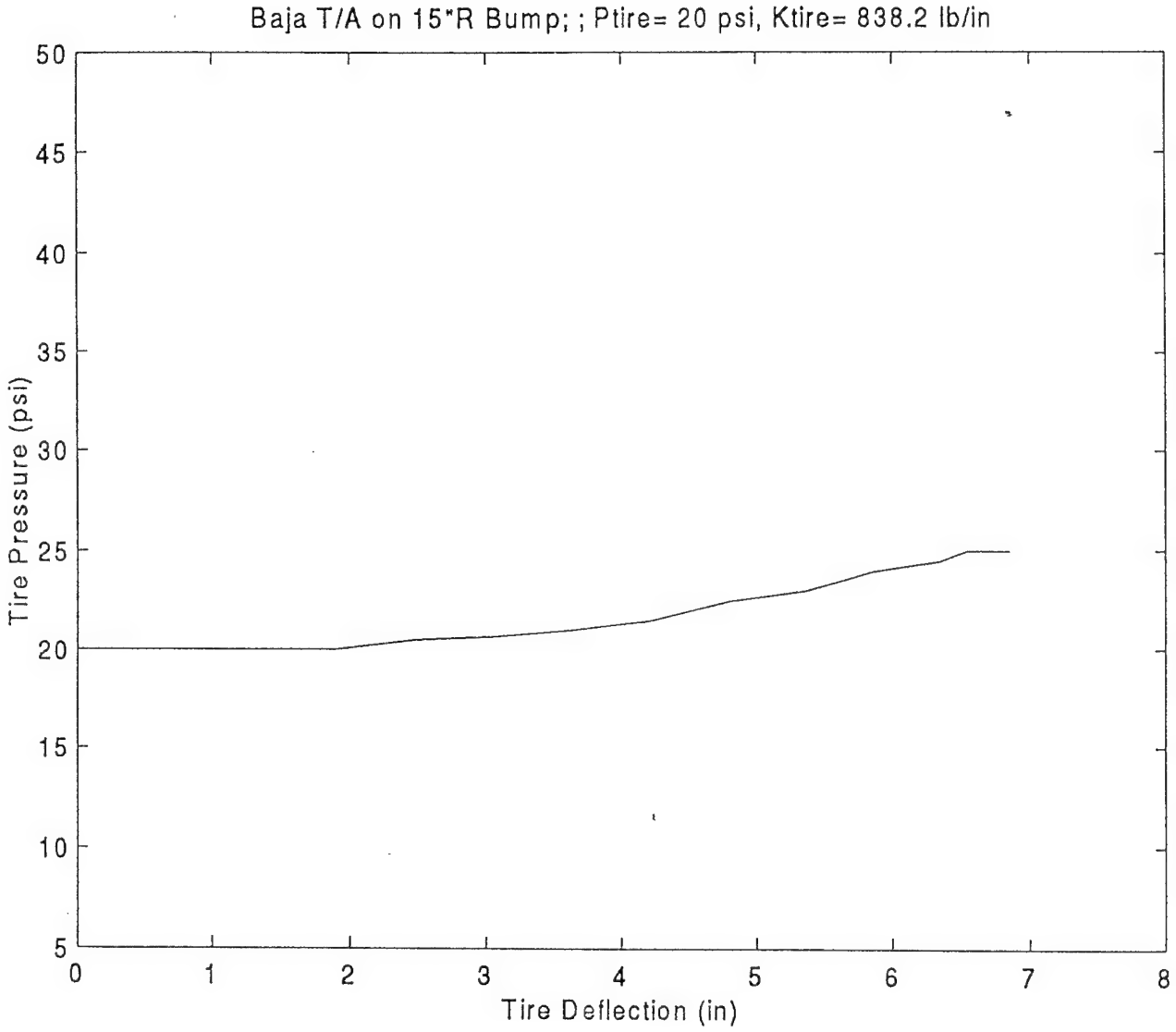
Baja T/A on 15"R Bump; ; Ptire= 20 psi, Ktire= 838.2 lb/in
Tire Pressure (psi)
Tire Deflection (in)
50
45
40
35
30
25
20
15
10
5
0
1
2
3
4
5
6
7
8

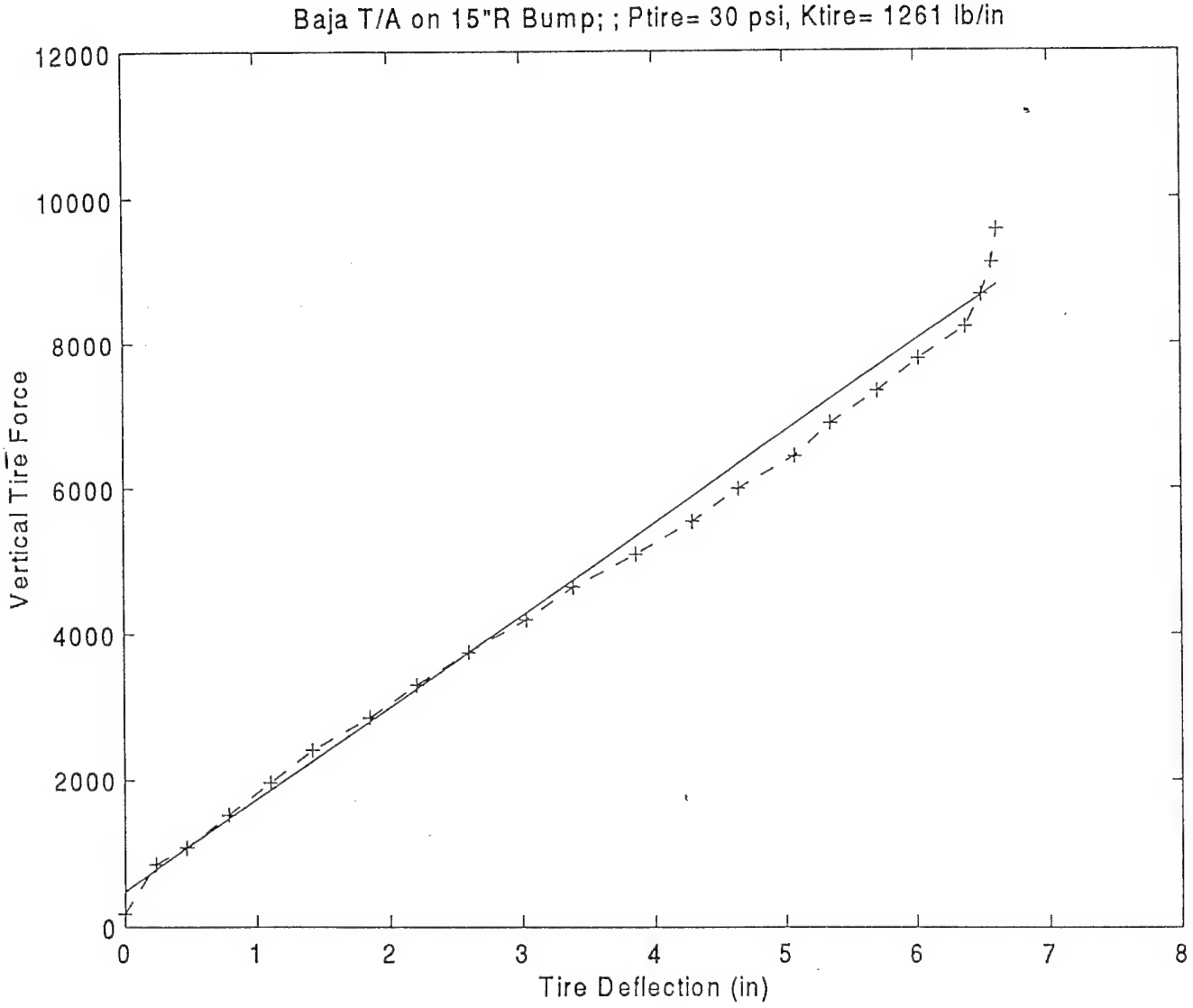
Baja T/A on 15"R Bump; ; Ptire= 30 psi, Ktire= 1261 lb/in
Vertical Tire Force
Tire Deflection (in)
12000
10000
8000
6000
4000
2000
0
0
1
2
3
4
5
6
7
8

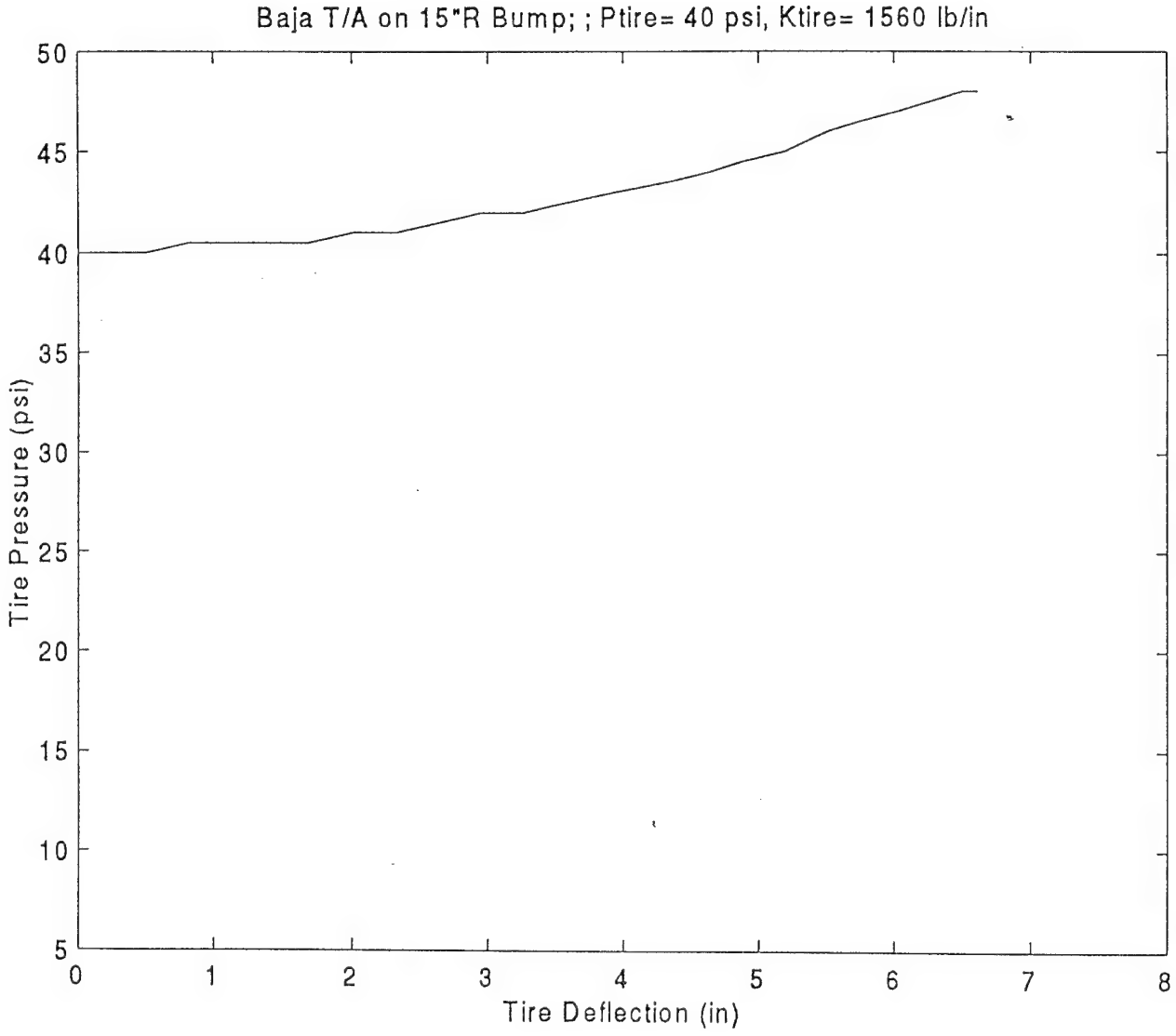
Baja T/A on 15"R Bump; ; Ptire= 40 psi, Ktire= 1560 lb/in
Tire Pressure (psi)
Tire Deflection (in)
50
45
40
35
30
25
20
15
10
5
0
1
2
3
4
5
6
7
8

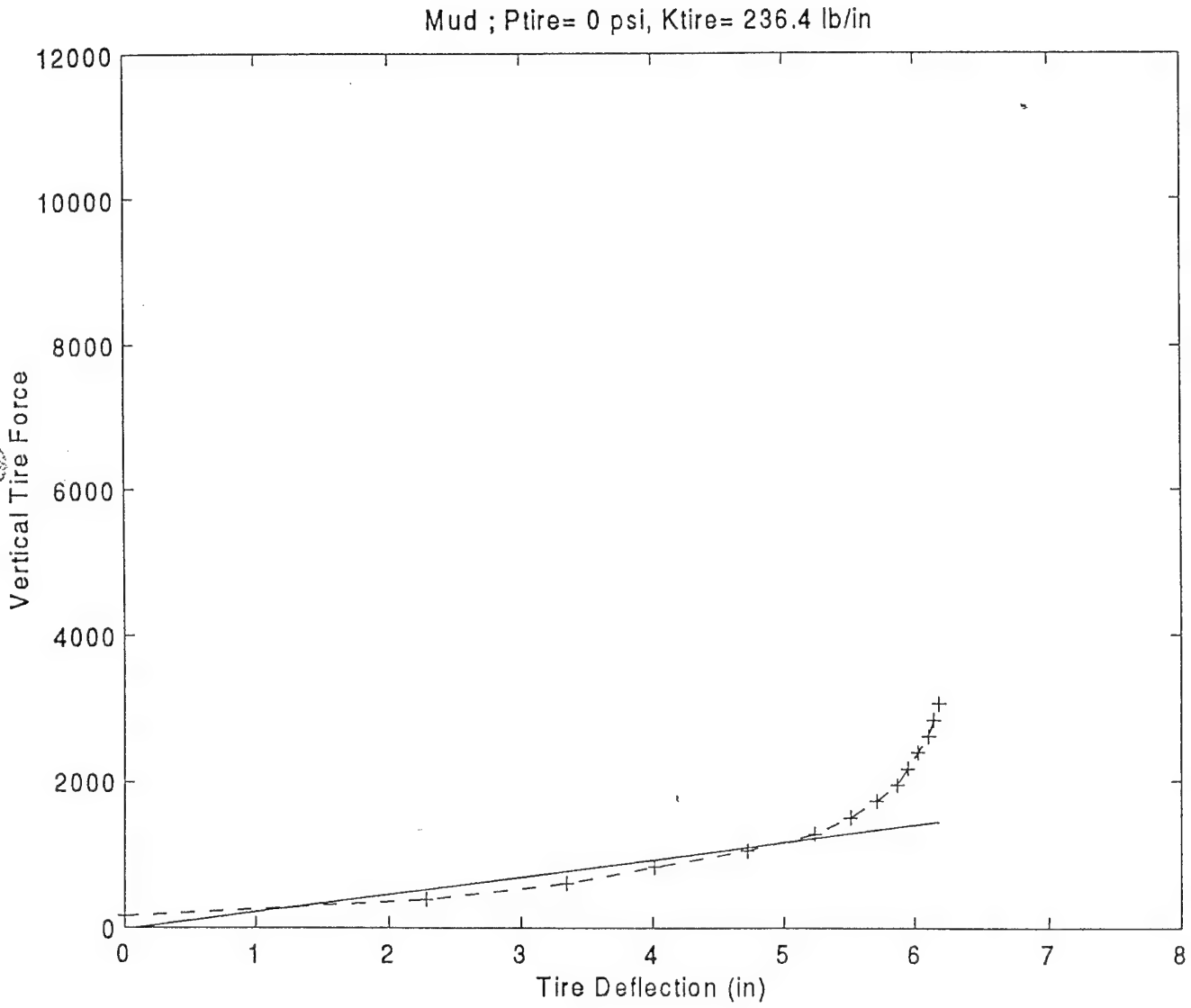
Mud ; Ptire= 0 psi, Ktire= 236.4 lb/in
Vertical Tire Force
Tire Deflection (in)
12000
10000
8000
6000
4000
2000
0
0
1
2
3
4
5
6
7
8

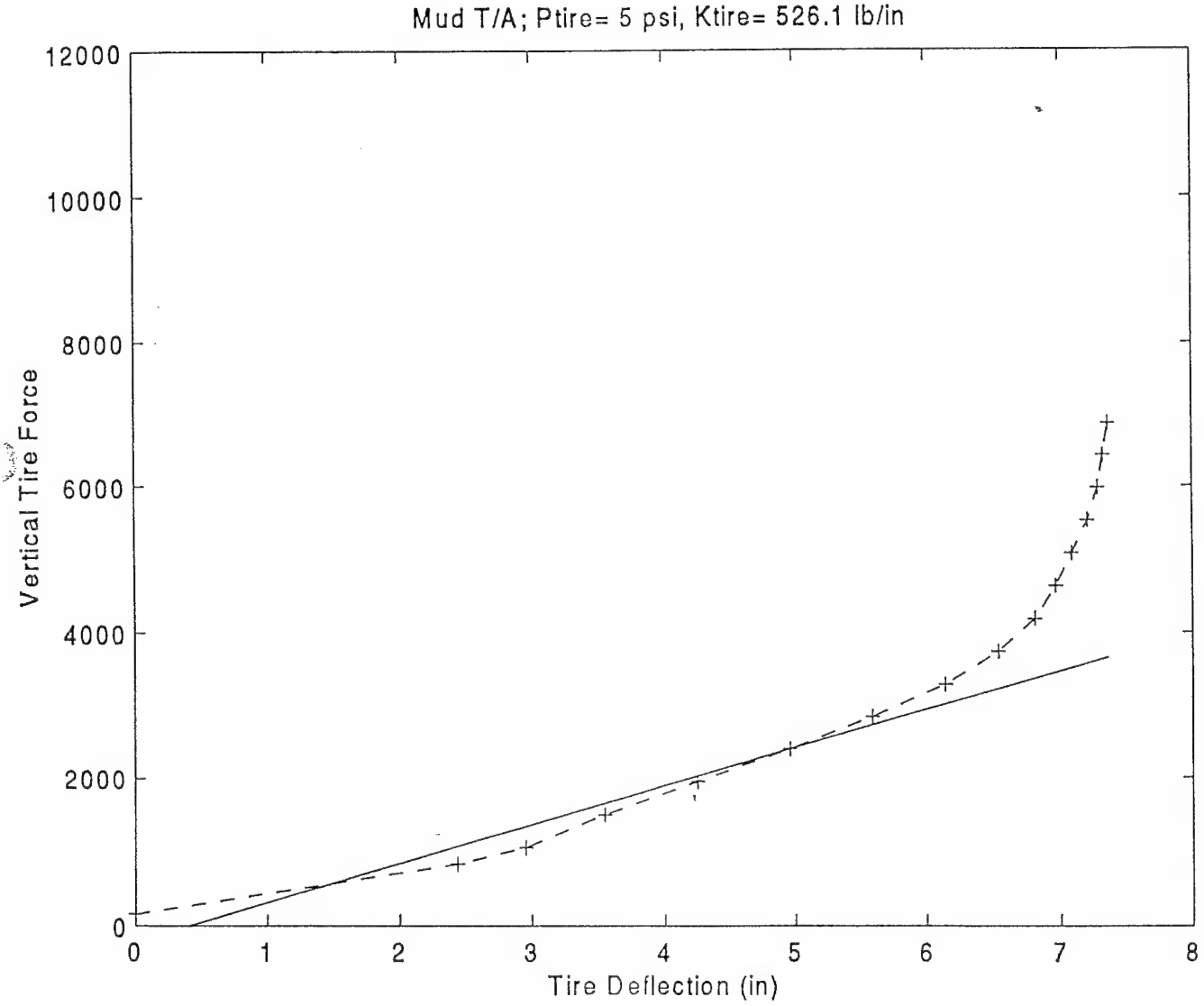
Mud T/A; Ptire= 5 psi, Ktire= 526.1 lb/in
Vertical Tire Force
Tire Deflection (in)
12000
10000
8000
6000
4000
2000
0
0
1
2
3
4
5
6
7
8

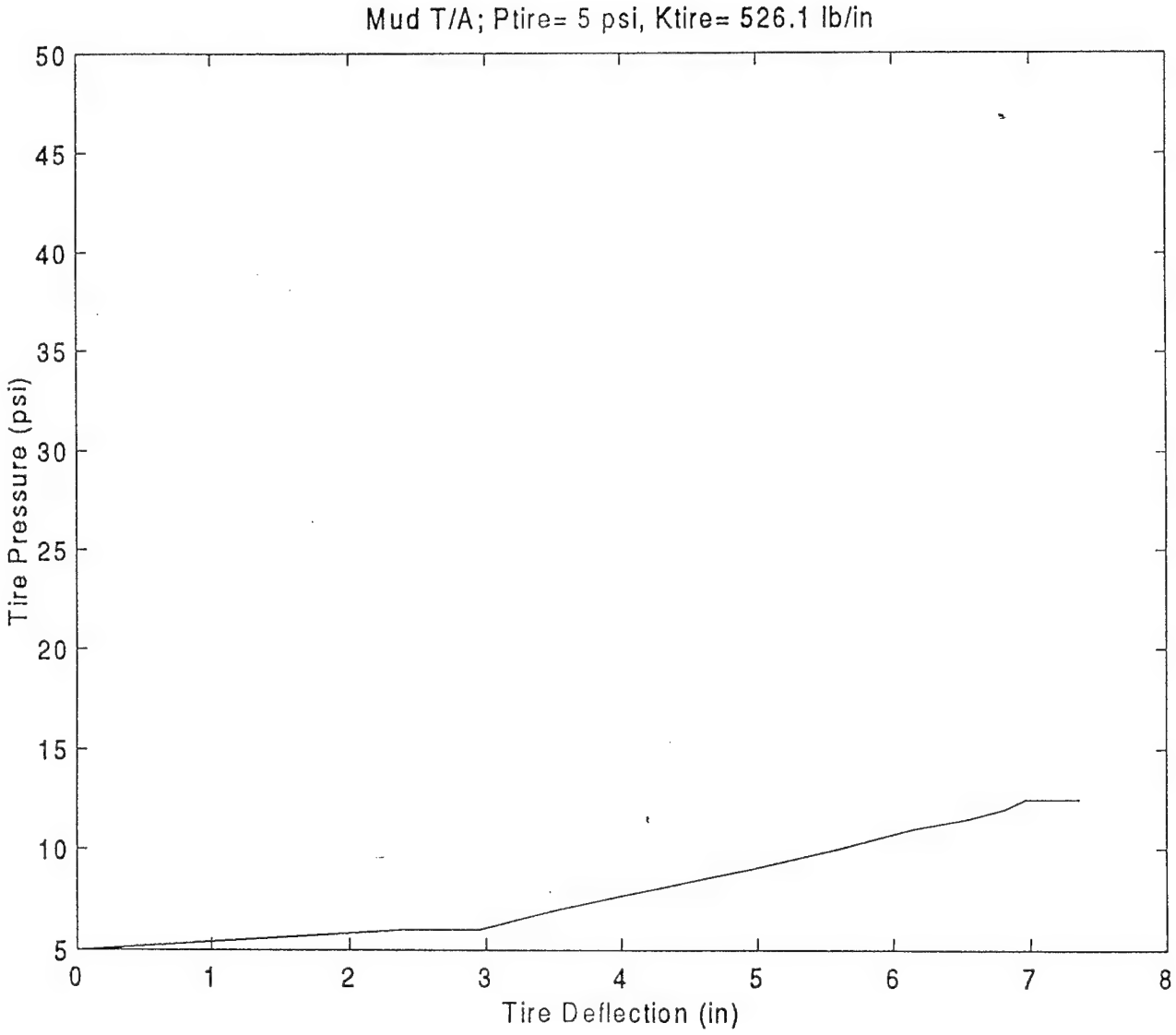
Mud T/A; Ptire= 5 psi, Ktire= 526.1 lb/in
Tire Pressure (psi)
Tire Deflection (in)
50
45
40
35
30
25
20
15
10
5
0
1
2
3
4
5
6
7
8

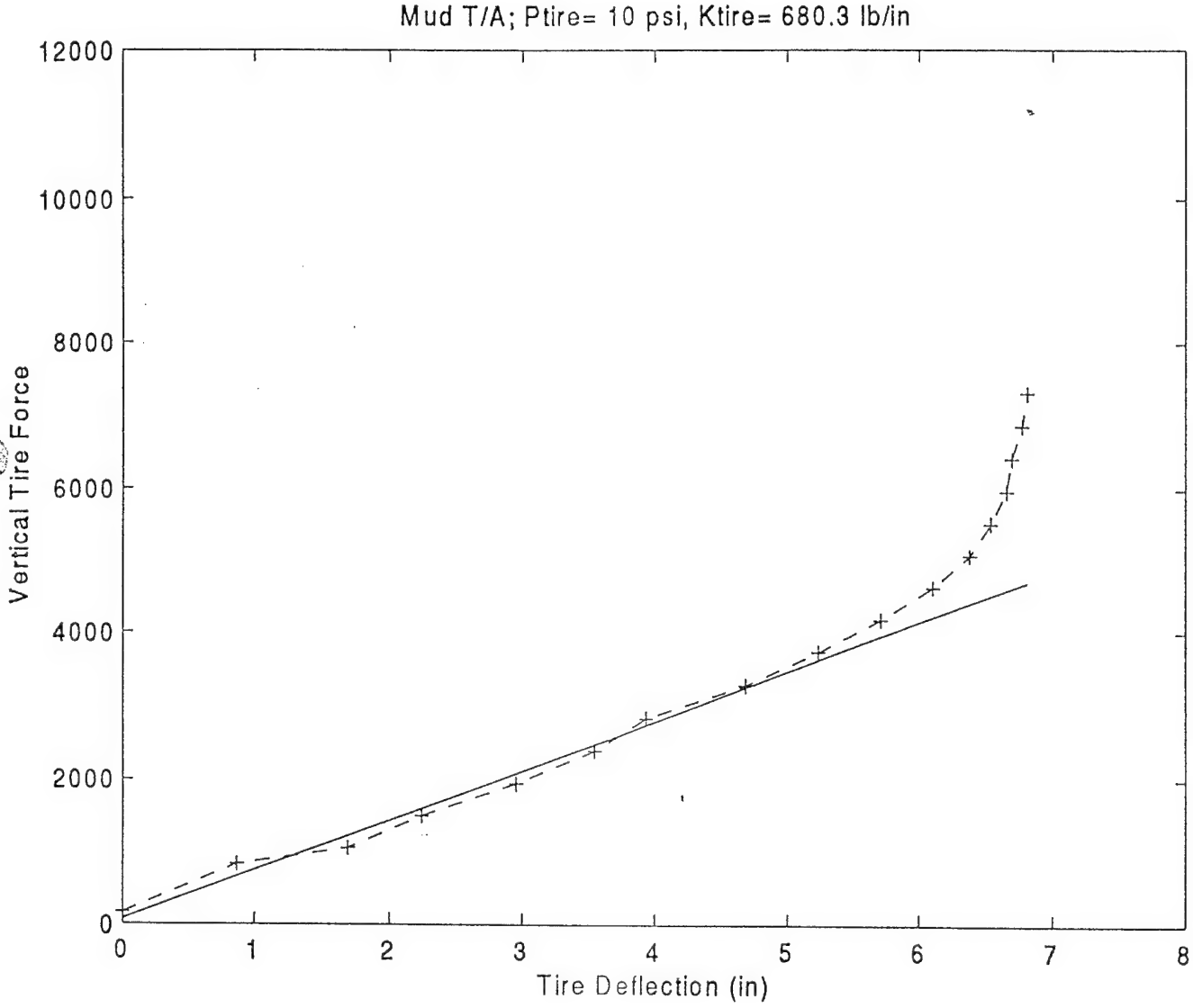
Mud T/A; Ptire= 10 psi, Ktire= 680.3 lb/in
Vertical Tire Force
Tire Deflection (in)
12000
10000
8000
6000
4000
2000
0
0
1
2
3
4
5
6
7
8

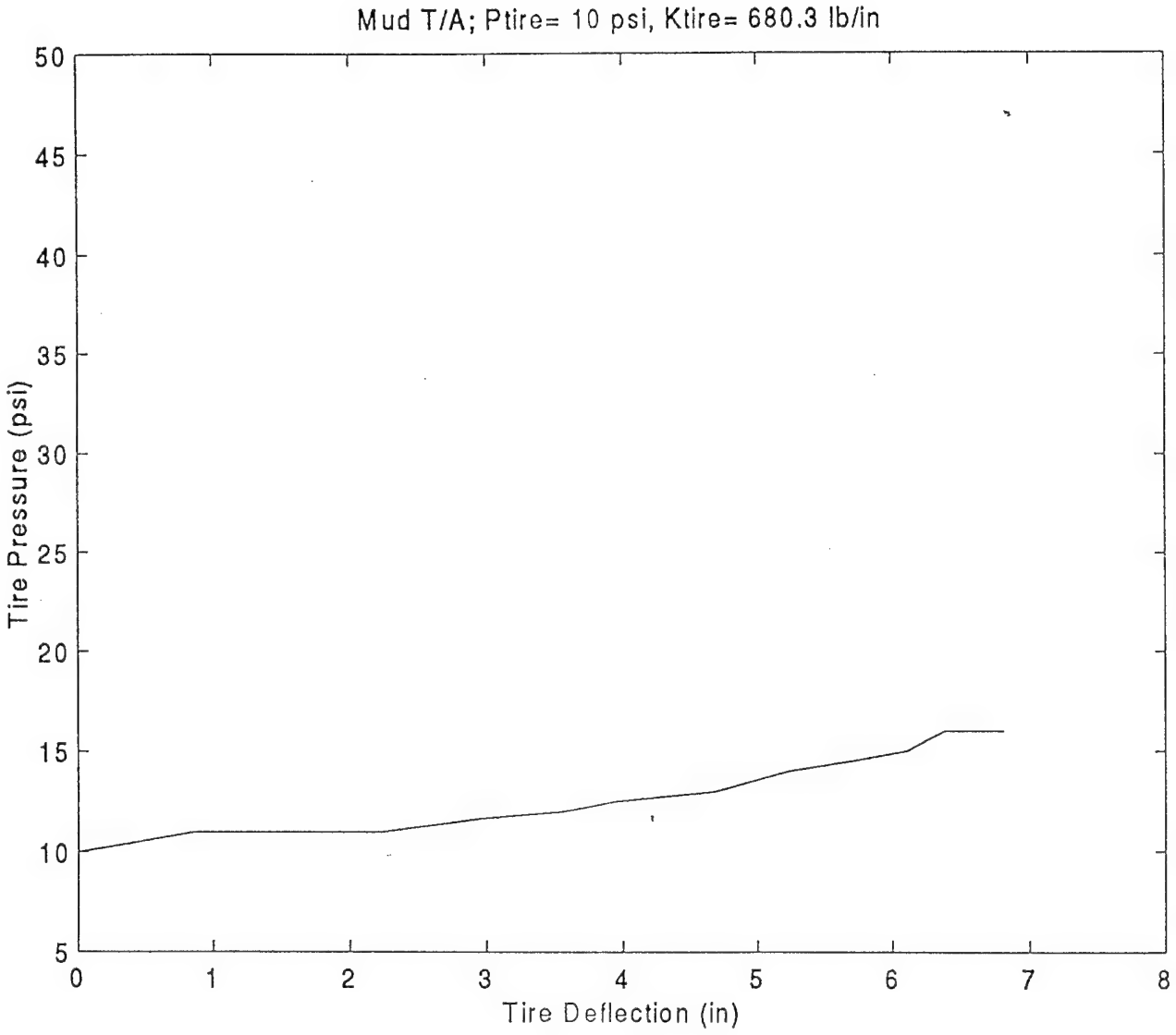
Mud T/A; Ptire= 10 psi, Ktire= 680.3 lb/in
Tire Pressure (psi)
Tire Deflection (in)
50
45
40
35
30
25
20
15
10
5
0
1
2
3
4
5
6
7
8

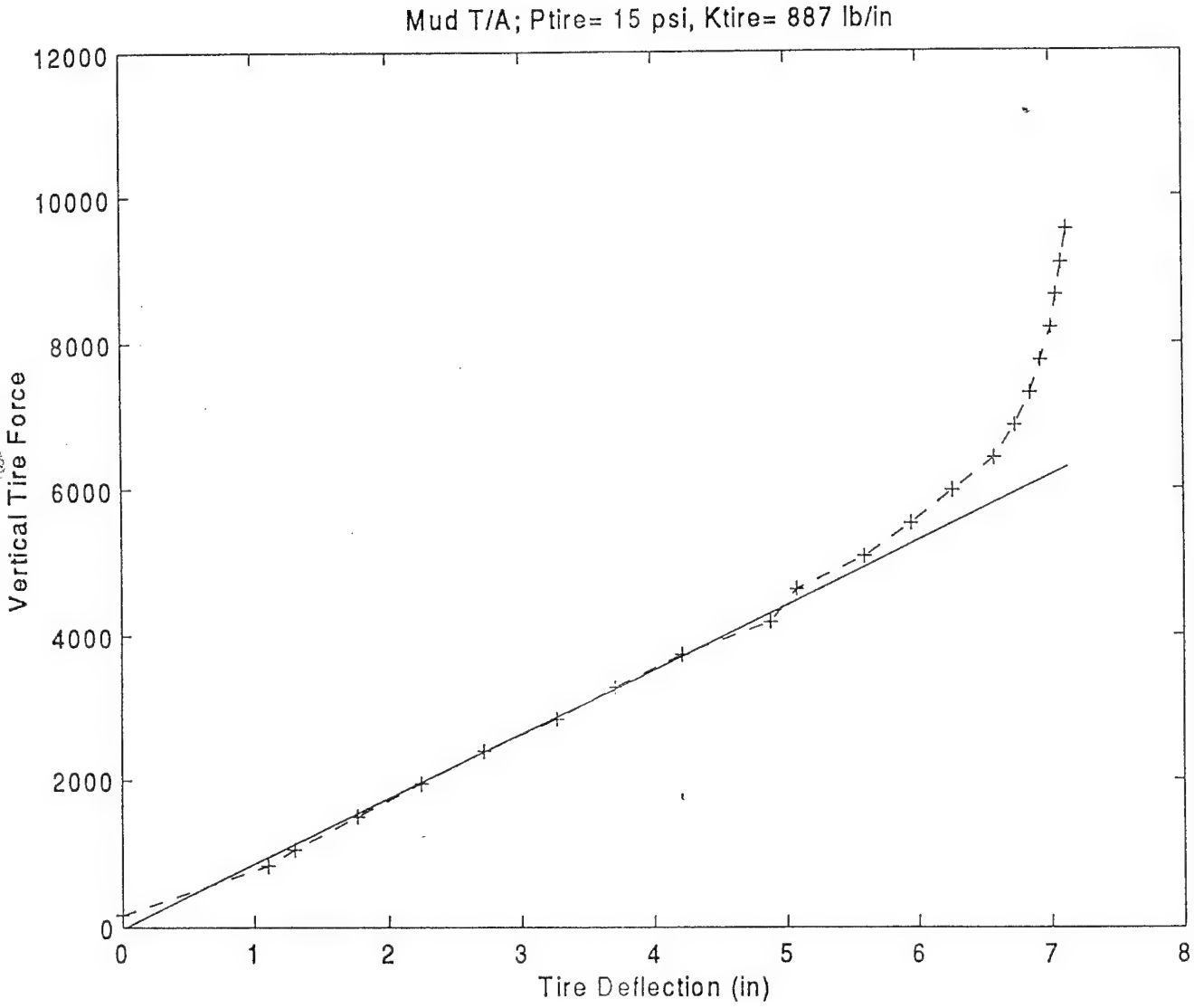
Mud T/A; Ptire= 15 psi, Ktire= 887 lb/in
Vertical Tire Force
Tire Deflection (in)
12000
10000
8000
6000
4000
2000
0
0
1
2
3
4
5
6
7
8

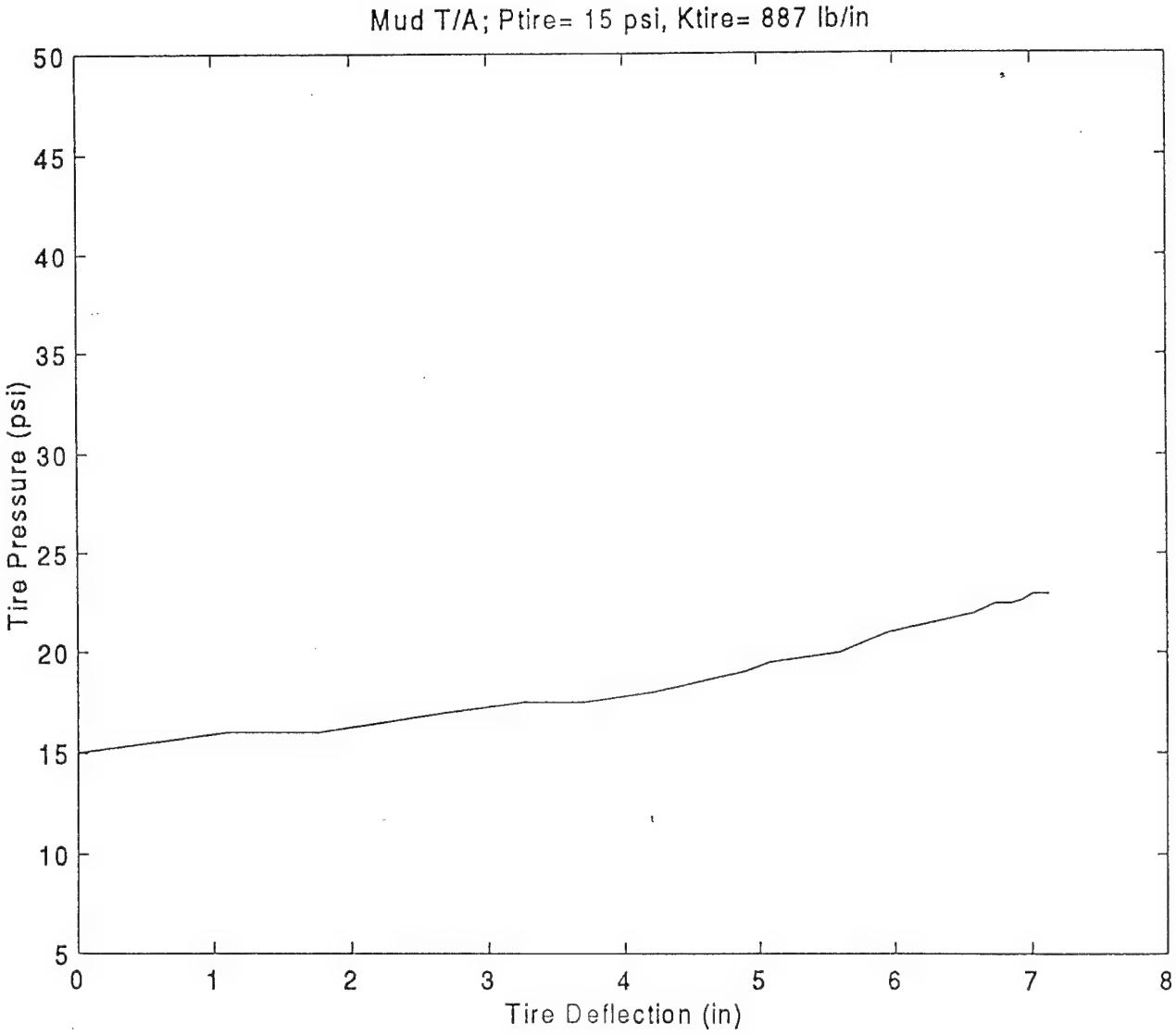
Mud T/A; Ptire= 15 psi, Ktire= 887 lb/in
Tire Pressure (psi)
Tire Deflection (in)
50
45
40
35
30
25
20
15
10
5
0
1
2
3
4
5
6
7
8

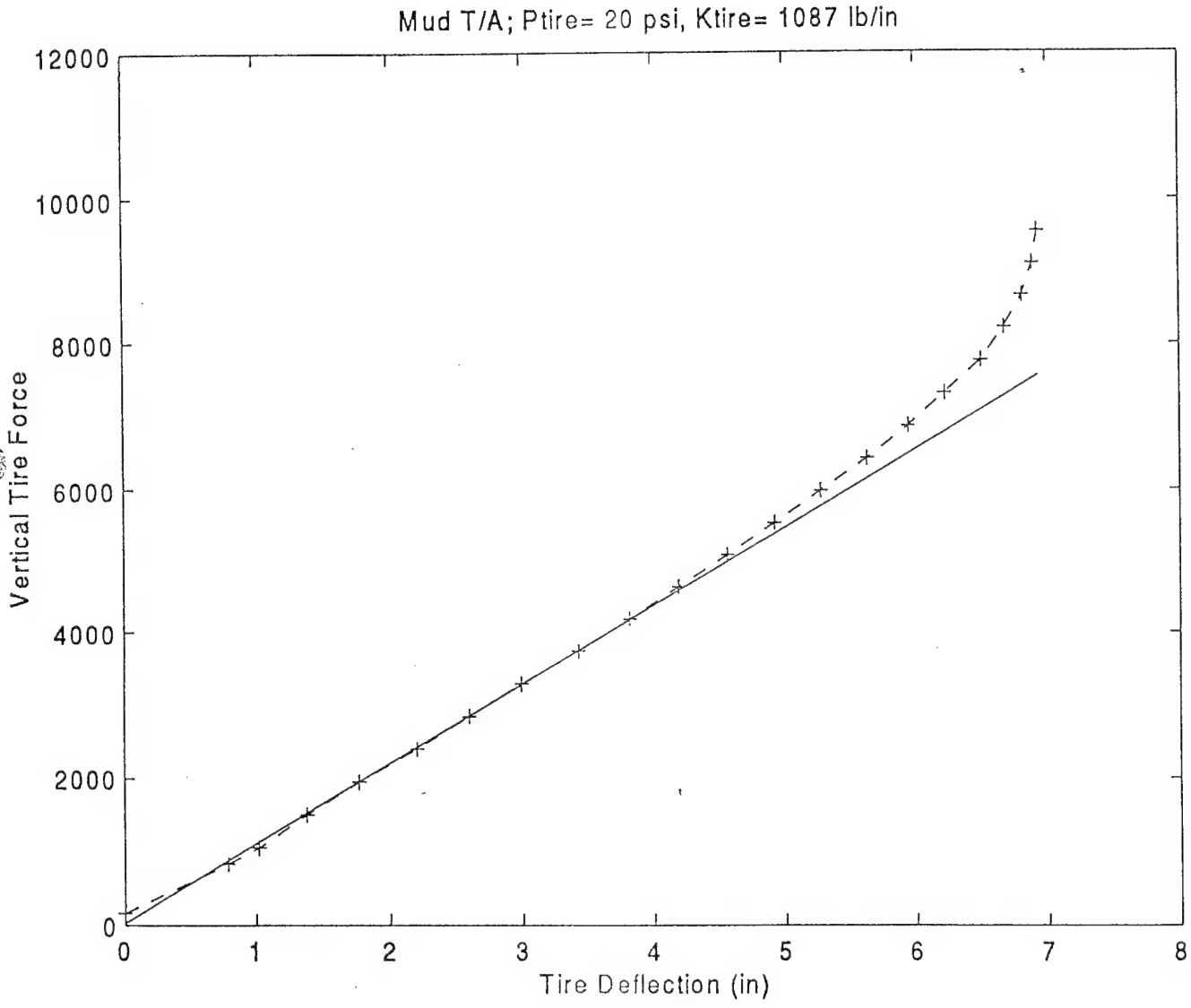
Mud T/A; Ptire= 20 psi, Ktire= 1087 lb/in
Vertical Tire Force
Tire Deflection (in)
12000
10000
8000
6000
4000
2000
0
0
1
2
3
4
5
6
7
8

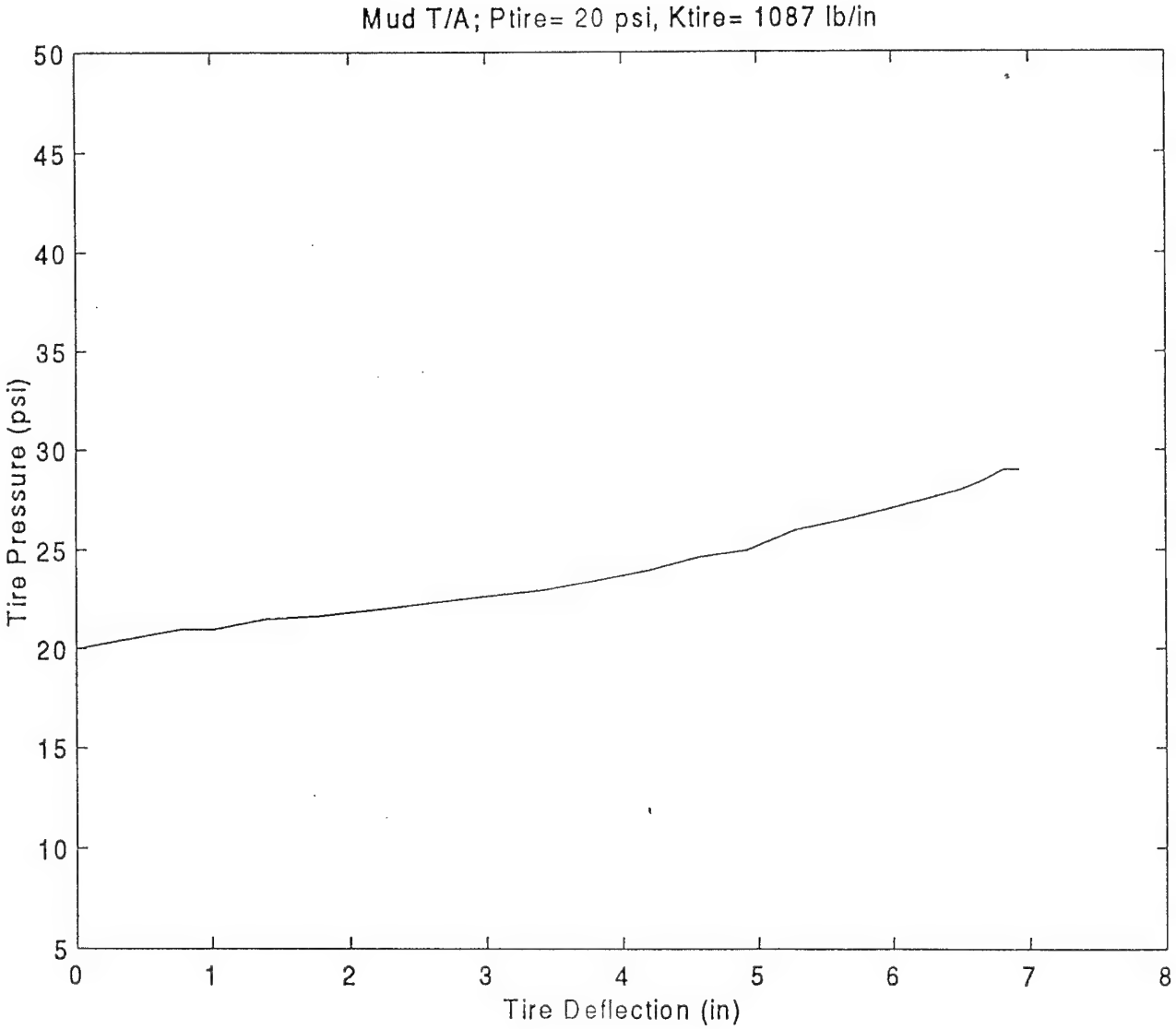
Mud T/A; Ptire= 20 psi, Ktire= 1087 lb/in
Tire Pressure (psi)
Tire Deflection (in)
50
45
40
35
30
25
20
15
10
5
0
1
2
3
4
5
6
7
8

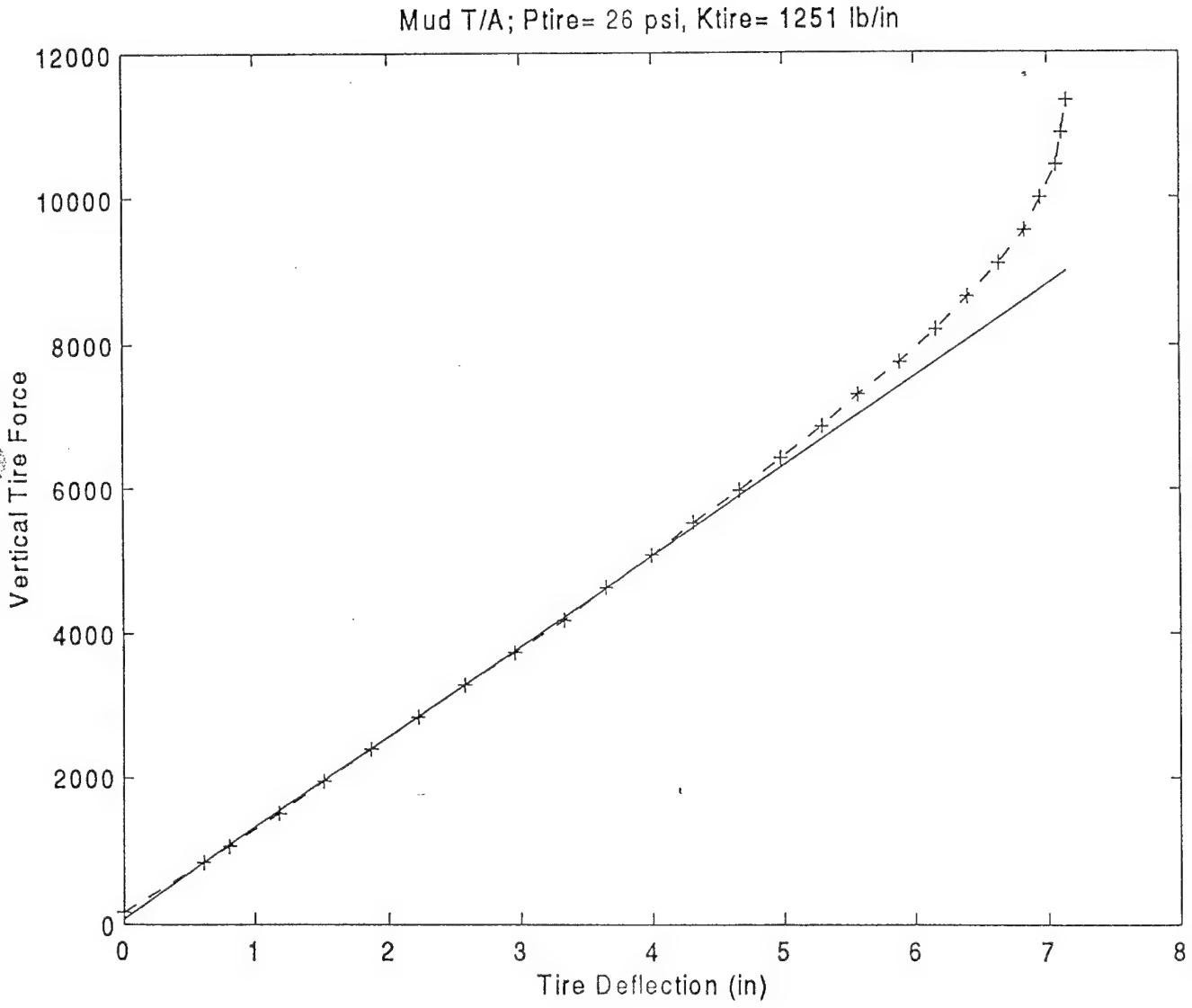
Mud T/A; Ptire= 26 psi, Ktire= 1251 lb/in
Vertical Tire Force
Tire Deflection (in)
12000
10000
8000
6000
4000
2000
0
0
1
2
3
4
5
6
7
8

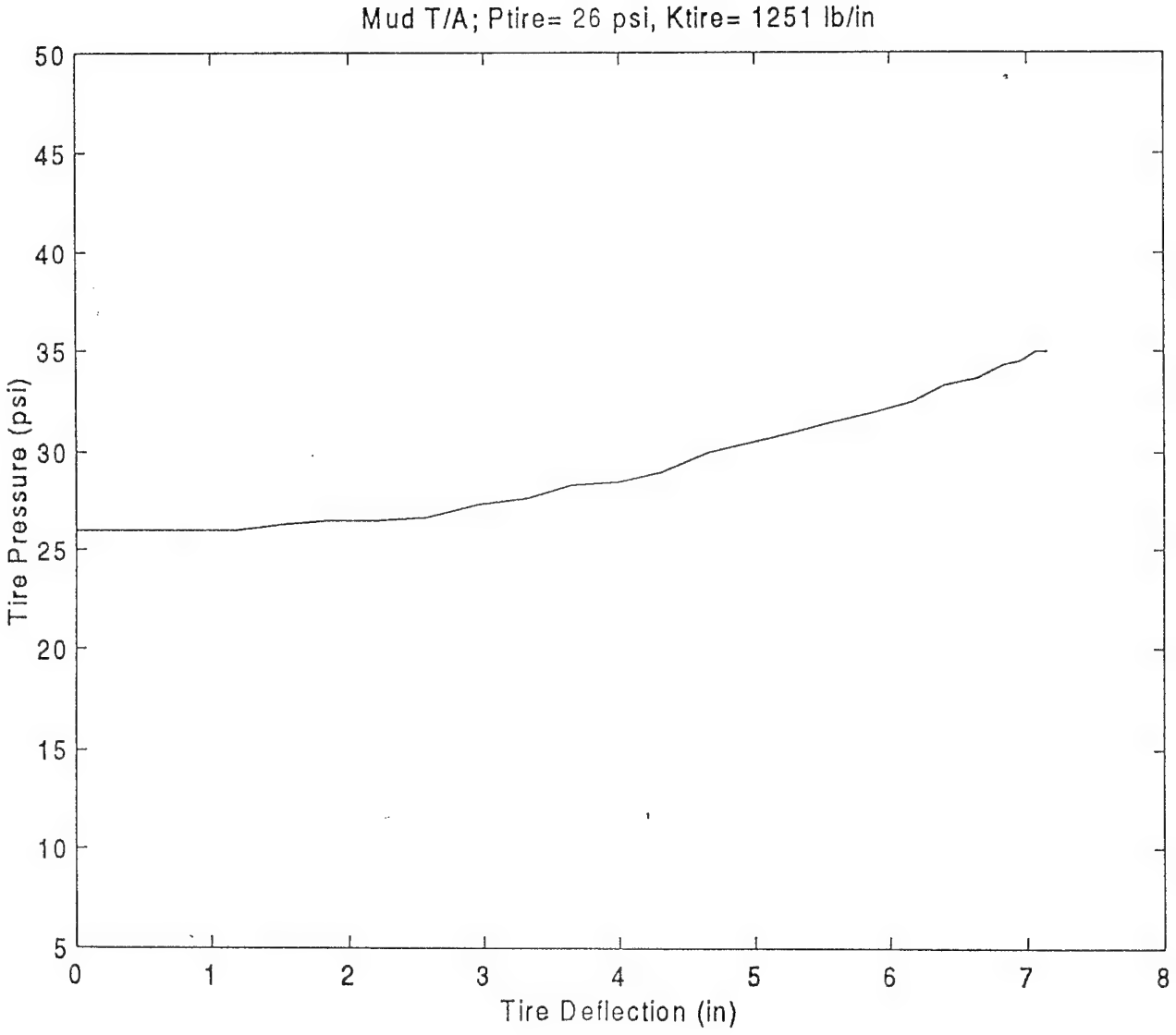
Mud T/A; Ptire= 26 psi, Ktire= 1251 lb/in
Tire Pressure (psi)
Tire Deflection (in)
50
45
40
35
30
25
20
15
10
5
0
1
2
3
4
5
6
7
8

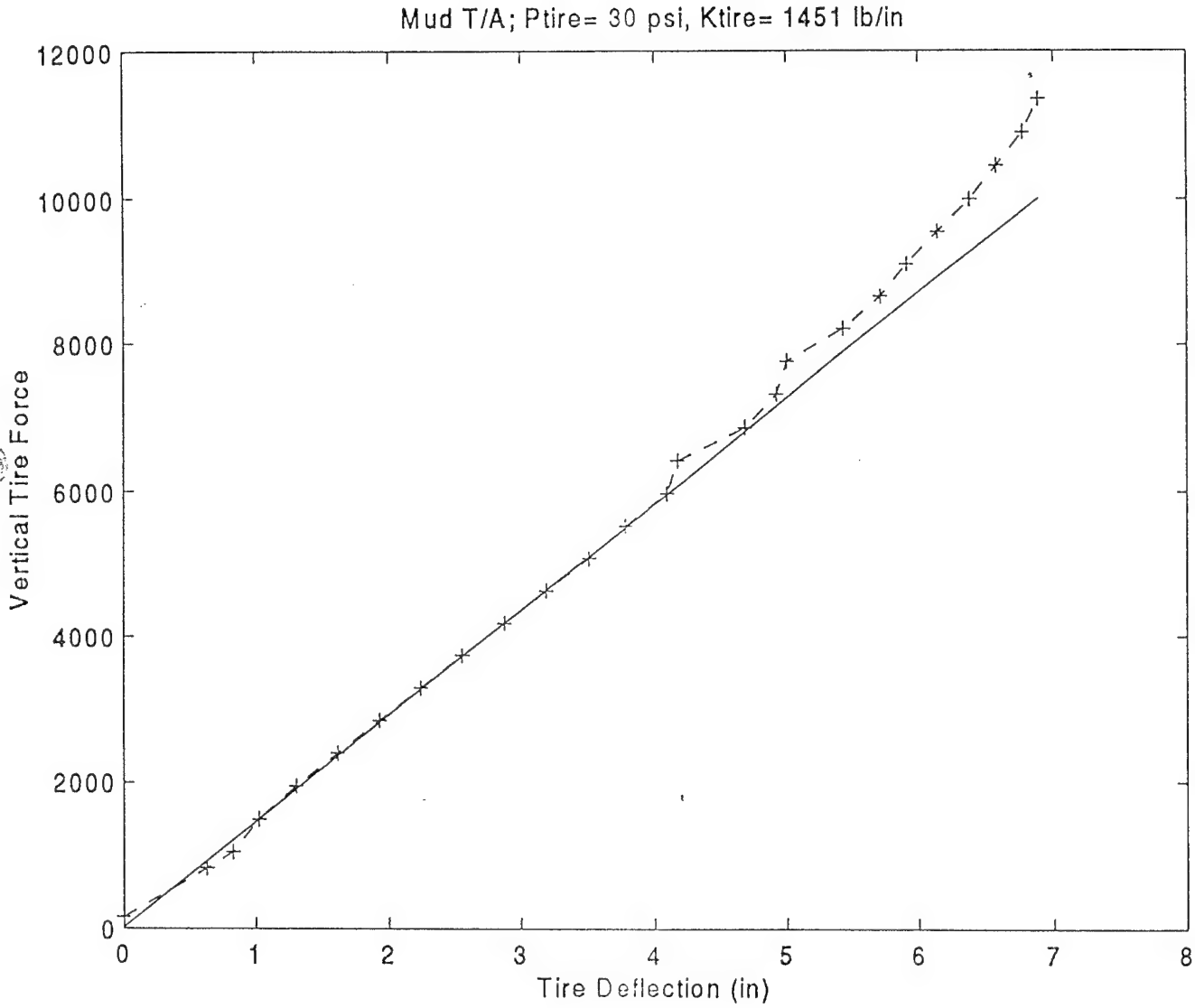
Mud T/A; Ptire= 30 psi, Ktire= 1451 lb/in
Vertical Tire Force
Tire Deflection (in)
0
2000
4000
6000
8000
10000
12000
0
1
2
3
4
5
6
7
8

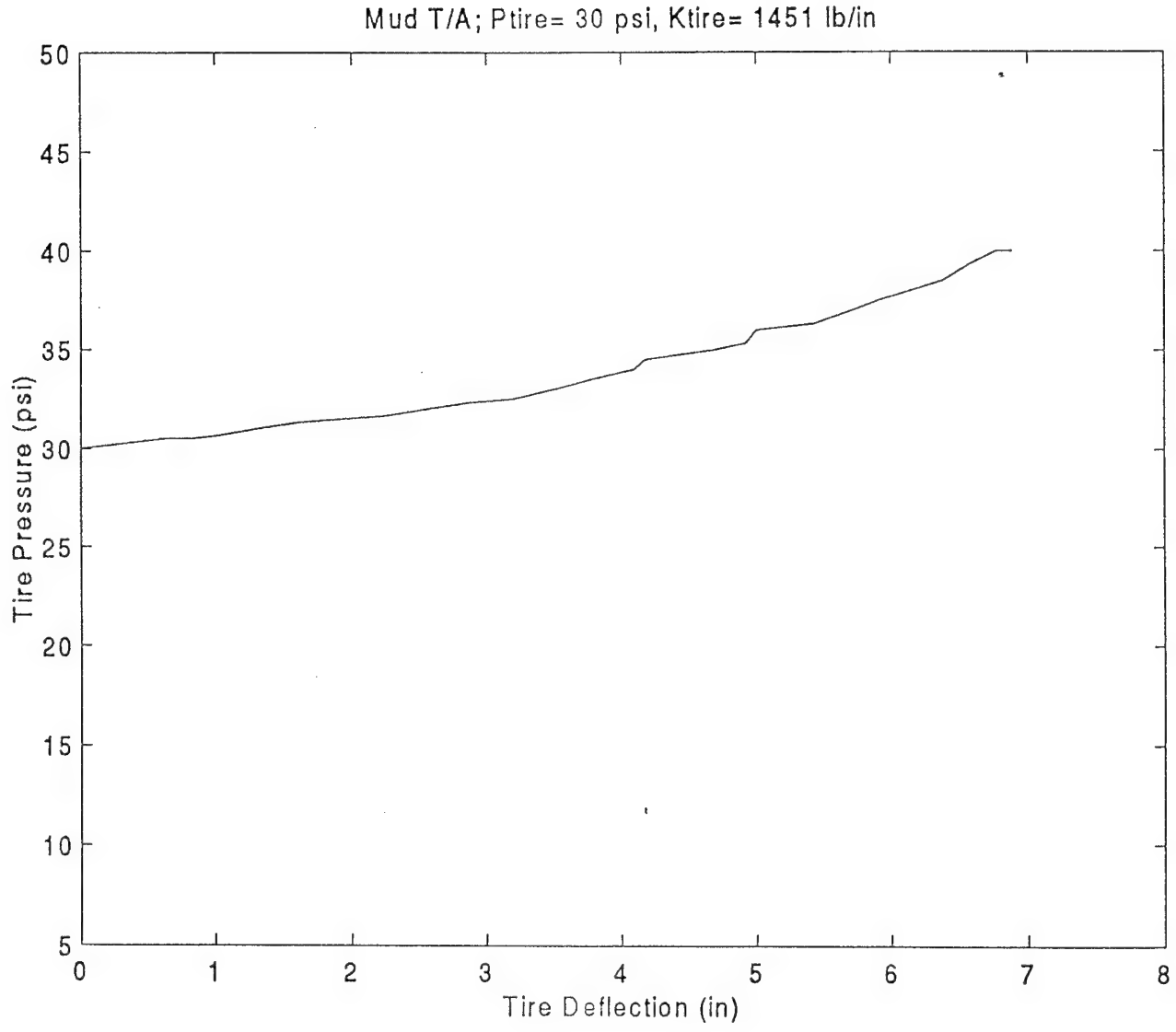
Mud T/A; Ptire= 30 psi, Ktire= 1451 lb/in
Tire Pressure (psi)
Tire Deflection (in)
50
45
40
35
30
25
20
15
10
5
0
1
2
3
4
5
6
7
8

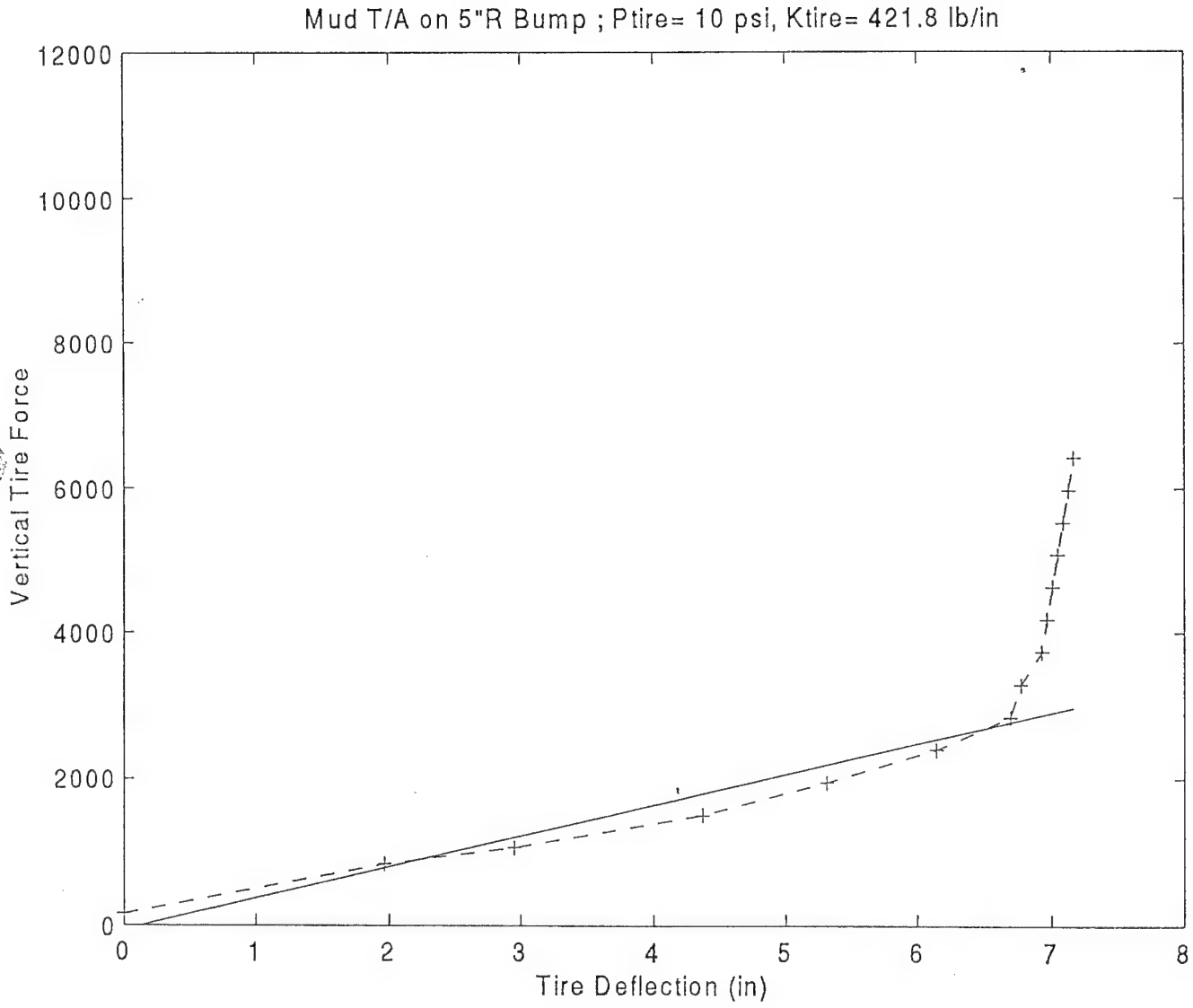
Mud T/A on 5"R Bump ; Ptire= 10 psi, Ktire= 421.8 lb/in
Vertical Tire Force
Tire Deflection (in)
12000
10000
8000
6000
4000
2000
0
0
1
2
3
4
5
6
7
8

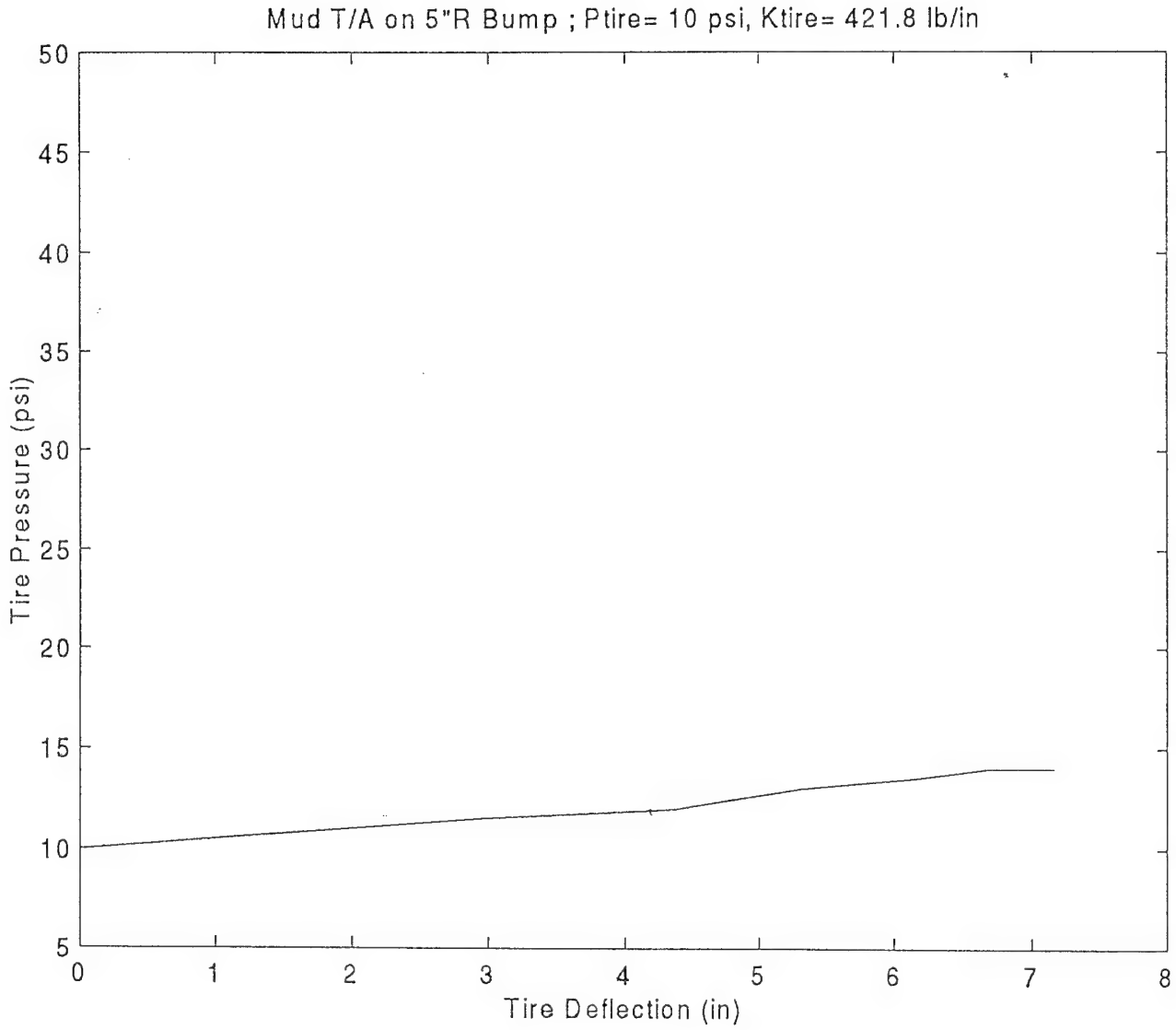
Mud T/A on 5"R Bump ; Ptire= 10 psi, Ktire= 421.8 lb/in
Tire Pressure (psi)
Tire Deflection (in)
50
45
40
35
30
25
20
15
10
5
0
1
2
3
4
5
6
7
8

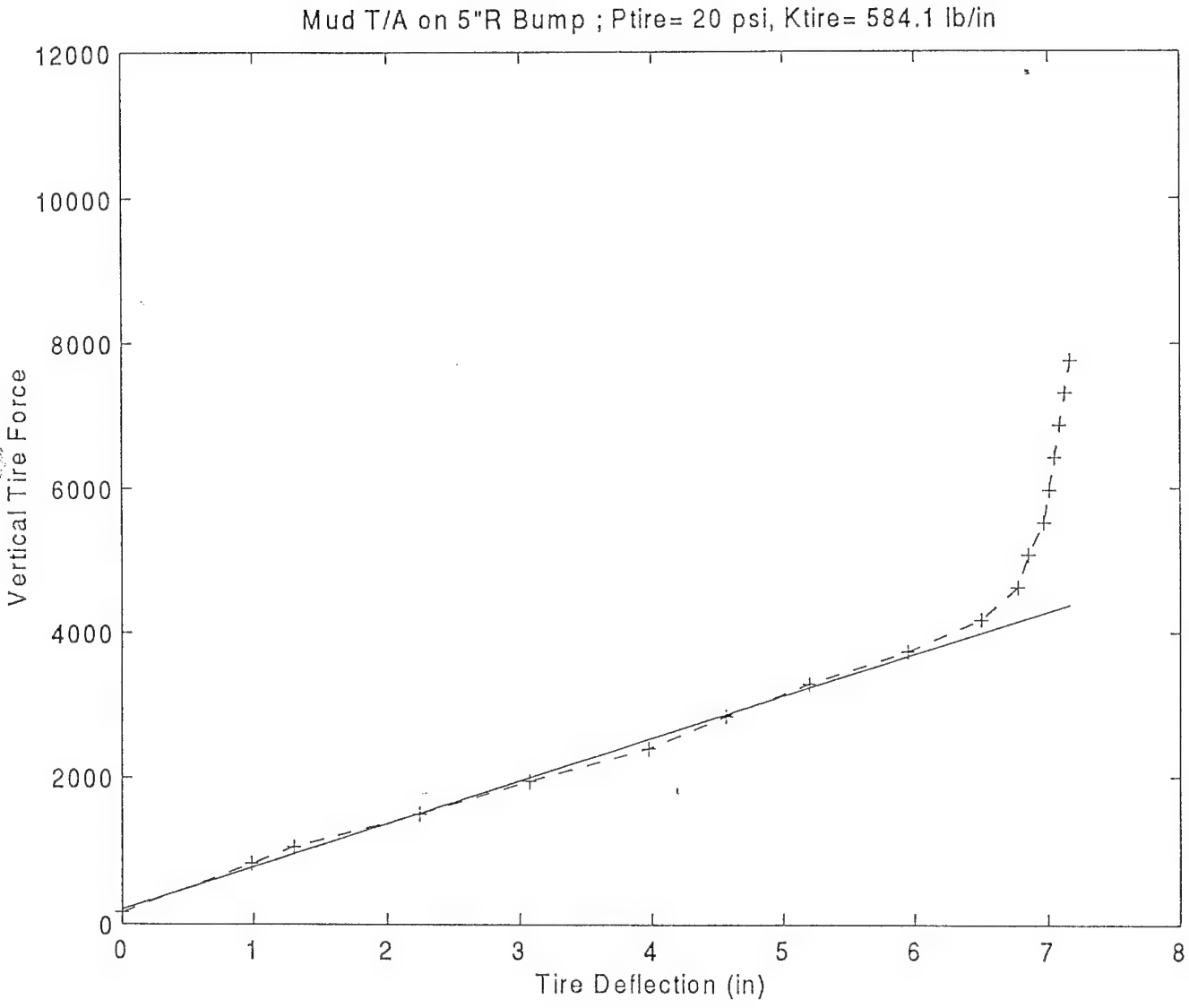
Mud T/A on 5"R Bump ; Ptire= 20 psi, Ktire= 584.1 lb/in
Vertical Tire Force
Tire Deflection (in)
12000
10000
8000
6000
4000
2000
0
0
1
2
3
4
5
6
7
8

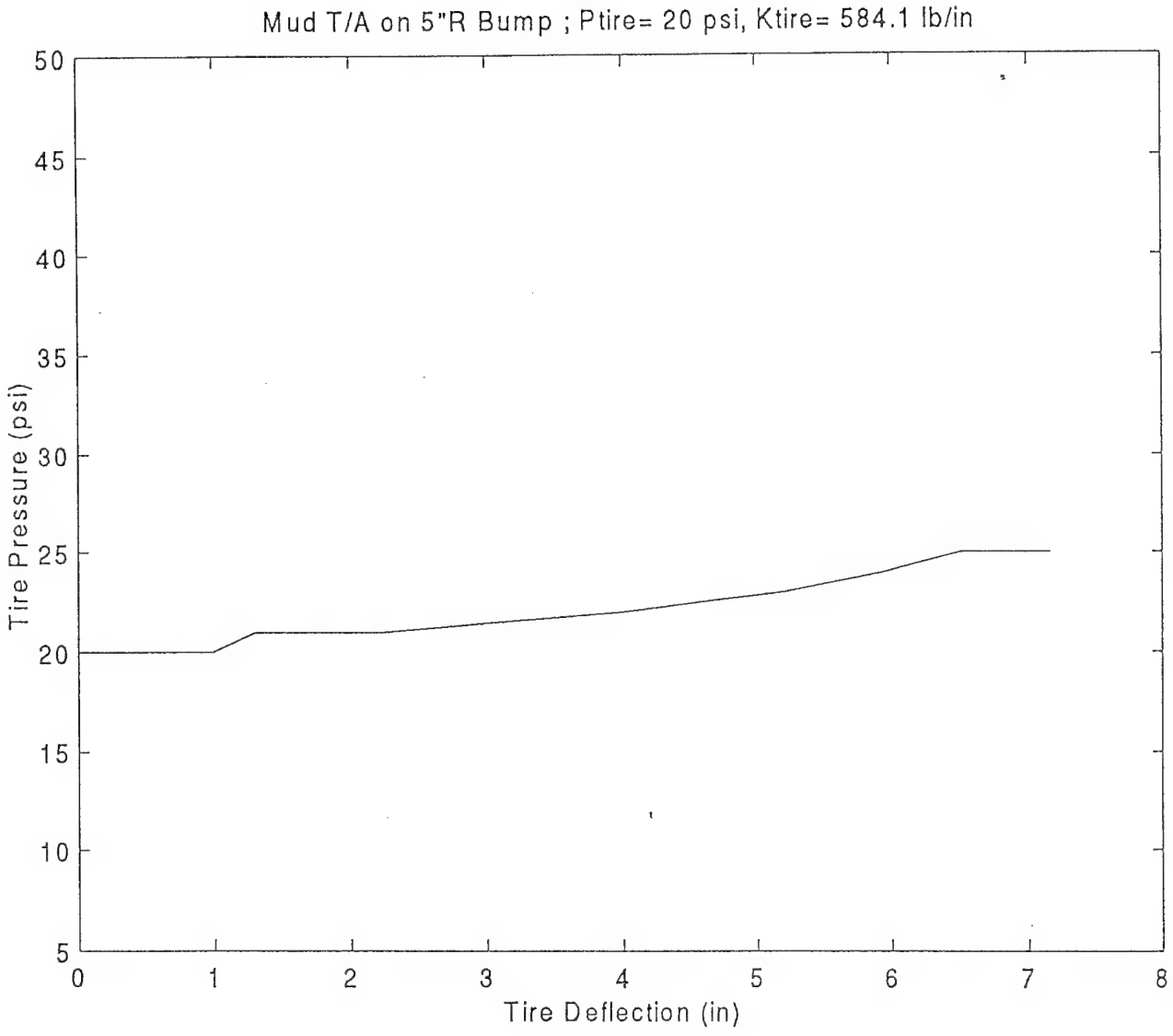
Mud T/A on 5"R Bump ; Ptire= 20 psi, Ktire= 584.1 lb/in
Tire Pressure (psi)
Tire Deflection (in)
50
45
40
35
30
25
20
15
10
5
0
1
2
3
4
5
6
7
8

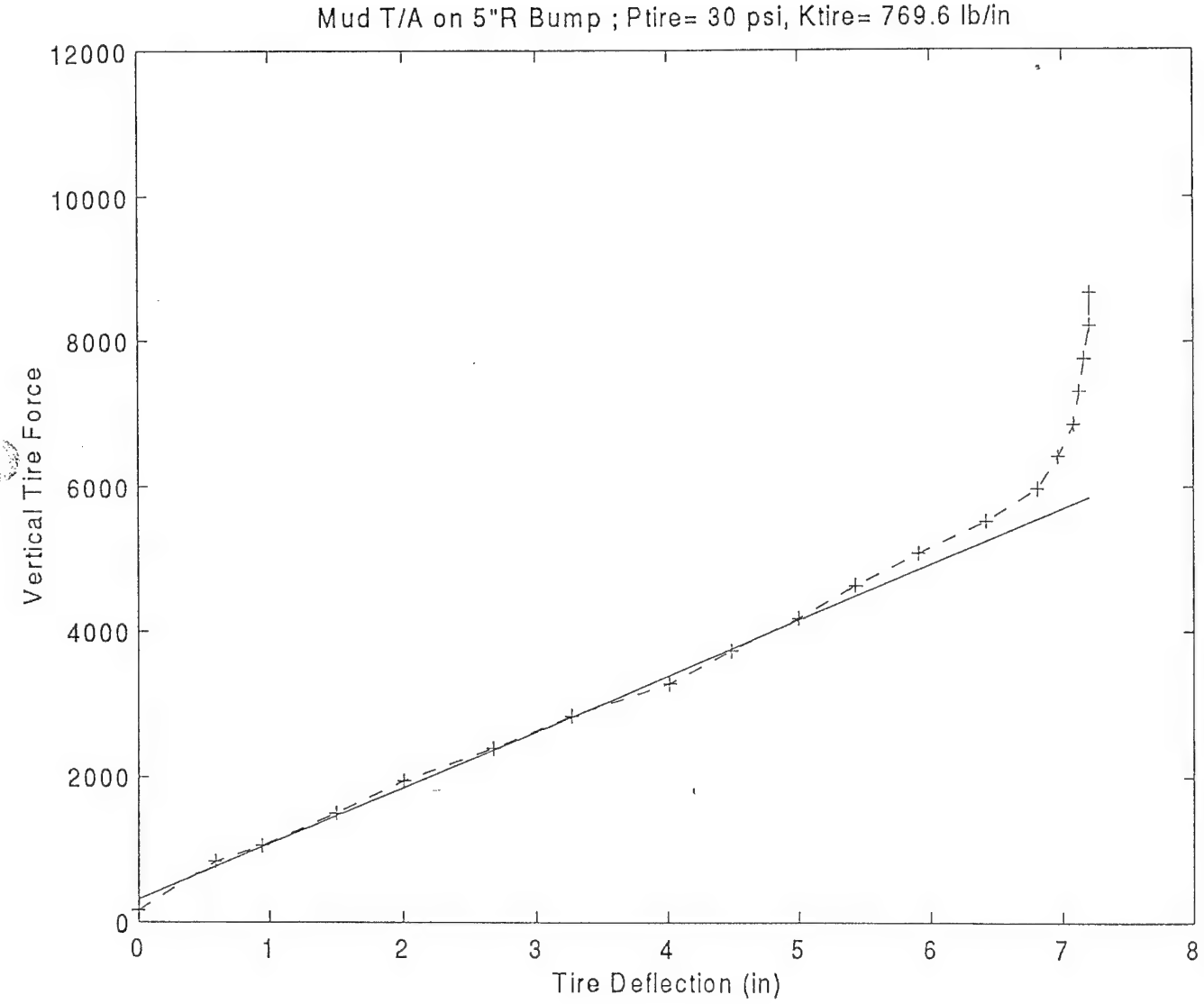
Mud T/A on 5"R Bump ; Ptire= 30 psi, Ktire= 769.6 lb/in
Vertical Tire Force
Tire Deflection (in)
0
2000
4000
6000
8000
10000
12000
0
1
2
3
4
5
6
7
8

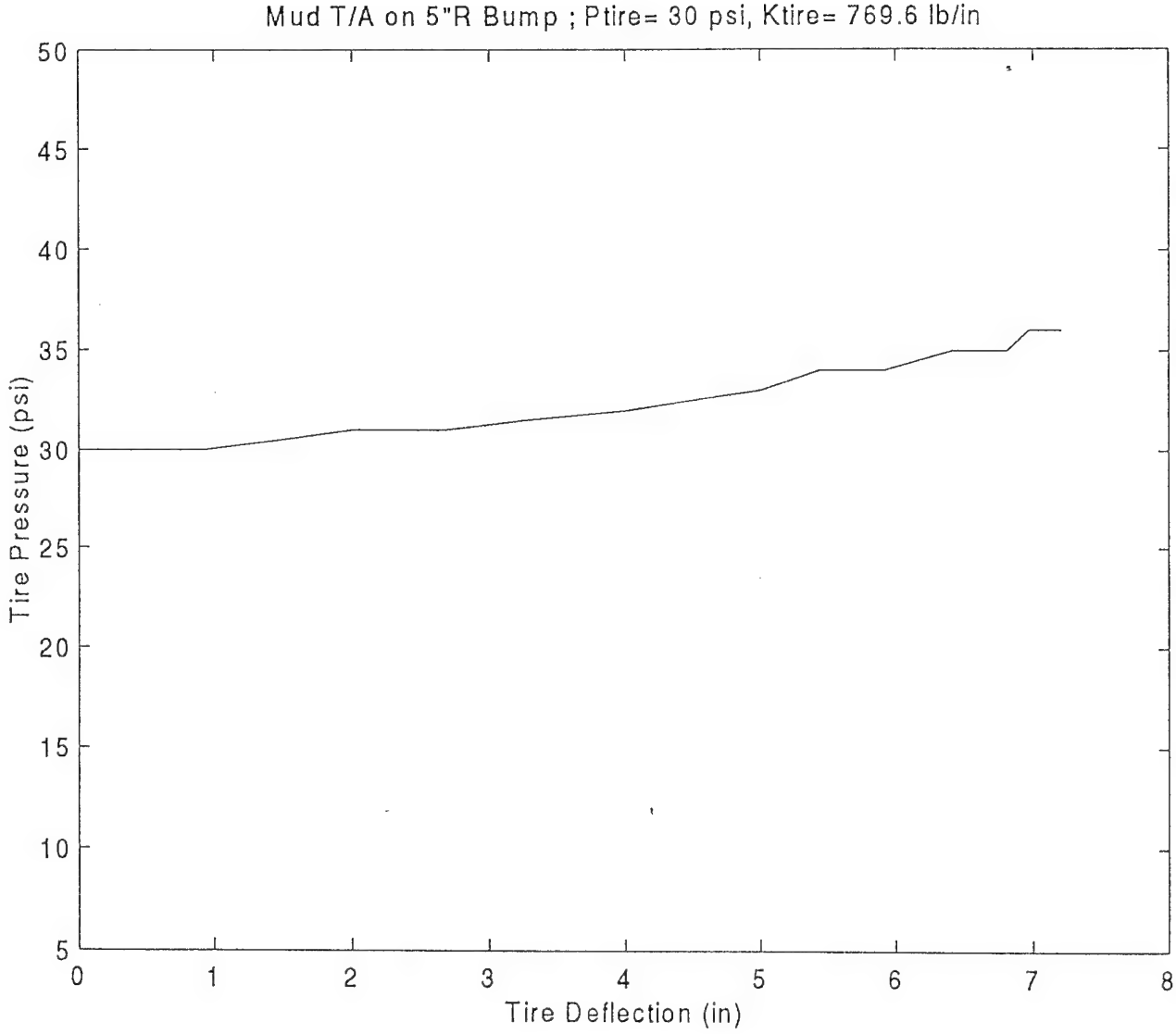
Mud T/A on 5"R Bump ; Ptire= 30 psi, Ktire= 769.6 lb/in
Tire Pressure (psi)
Tire Deflection (in)
50
45
40
35
30
25
20
15
10
5
0
1
2
3
4
5
6
7
8

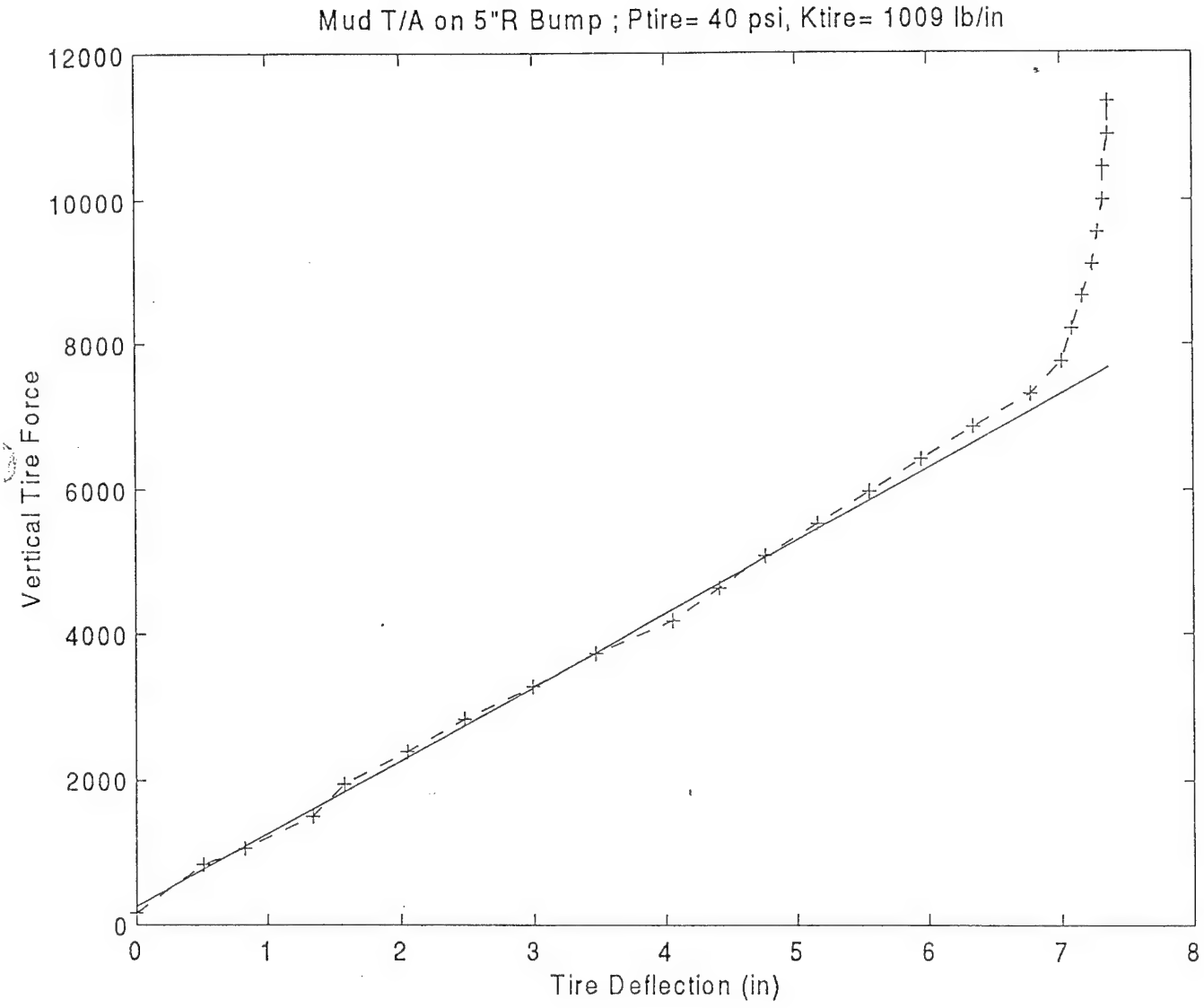
Mud T/A on 5"R Bump ; Ptire= 40 psi, Ktire= 1009 lb/in
Vertical Tire Force
Tire Deflection (in)
12000
10000
8000
6000
4000
2000
0
0
1
2
3
4
5
6
7
8

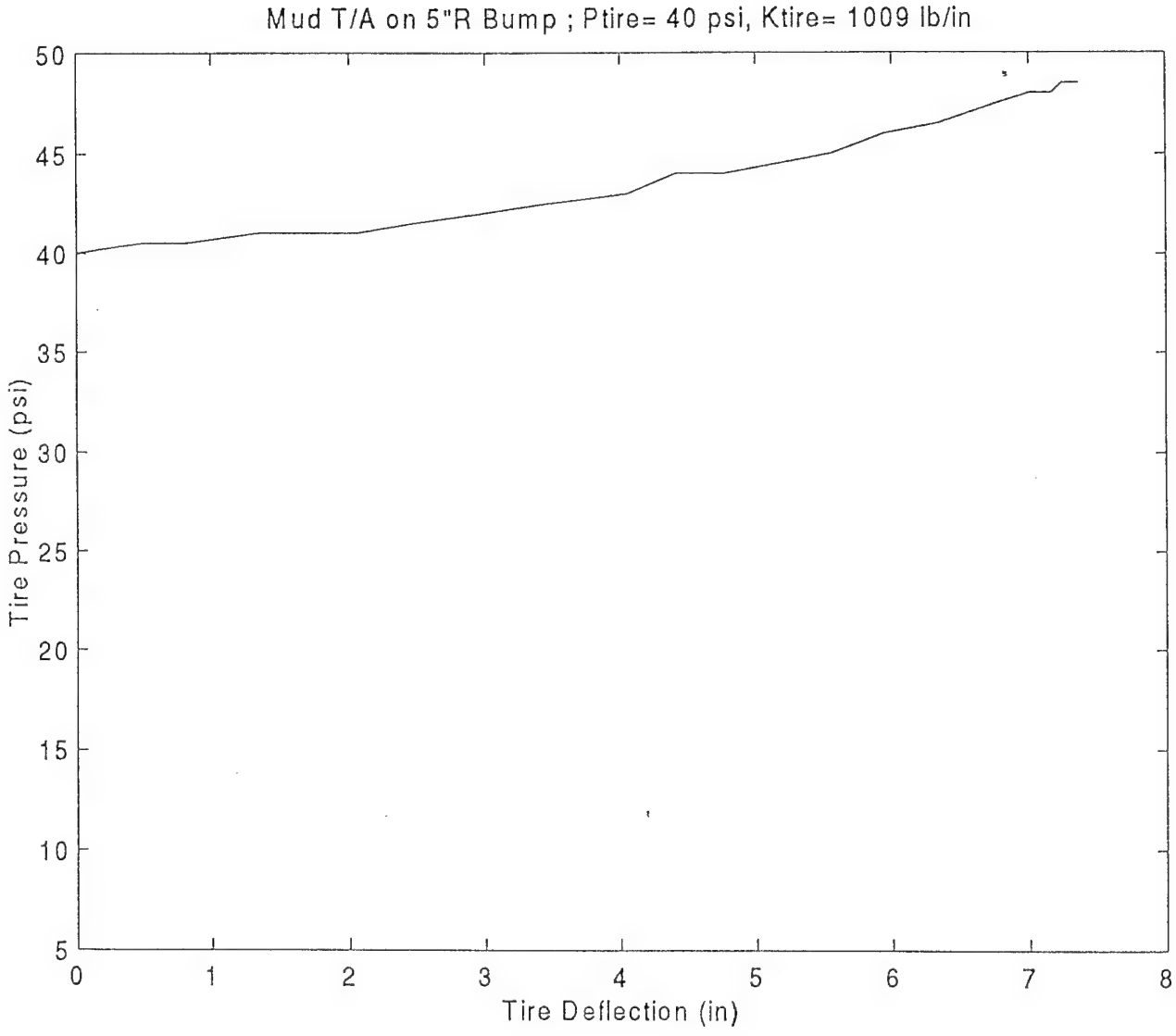
Mud T/A on 5"R Bump ; Ptire= 40 psi, Ktire= 1009 lb/in
Tire Pressure (psi)
Tire Deflection (in)
50
45
40
35
30
25
20
15
10
5
0
1
2
3
4
5
6
7
8

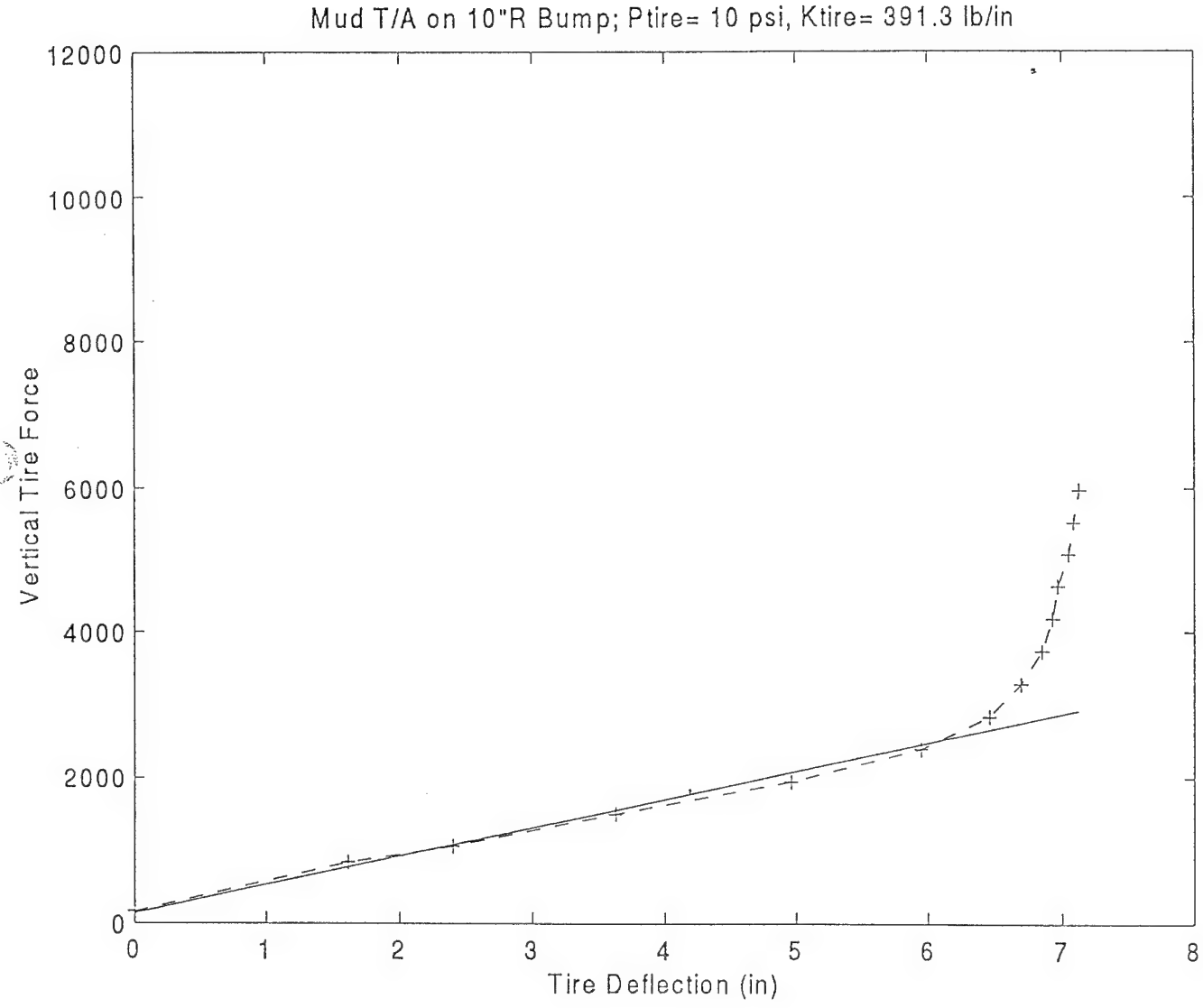
Mud T/A on 10"R Bump; Ptire= 10 psi, Ktire= 391.3 lb/in
Vertical Tire Force
Tire Deflection (in)
12000
10000
8000
6000
4000
2000
0
0
1
2
3
4
5
6
7
8

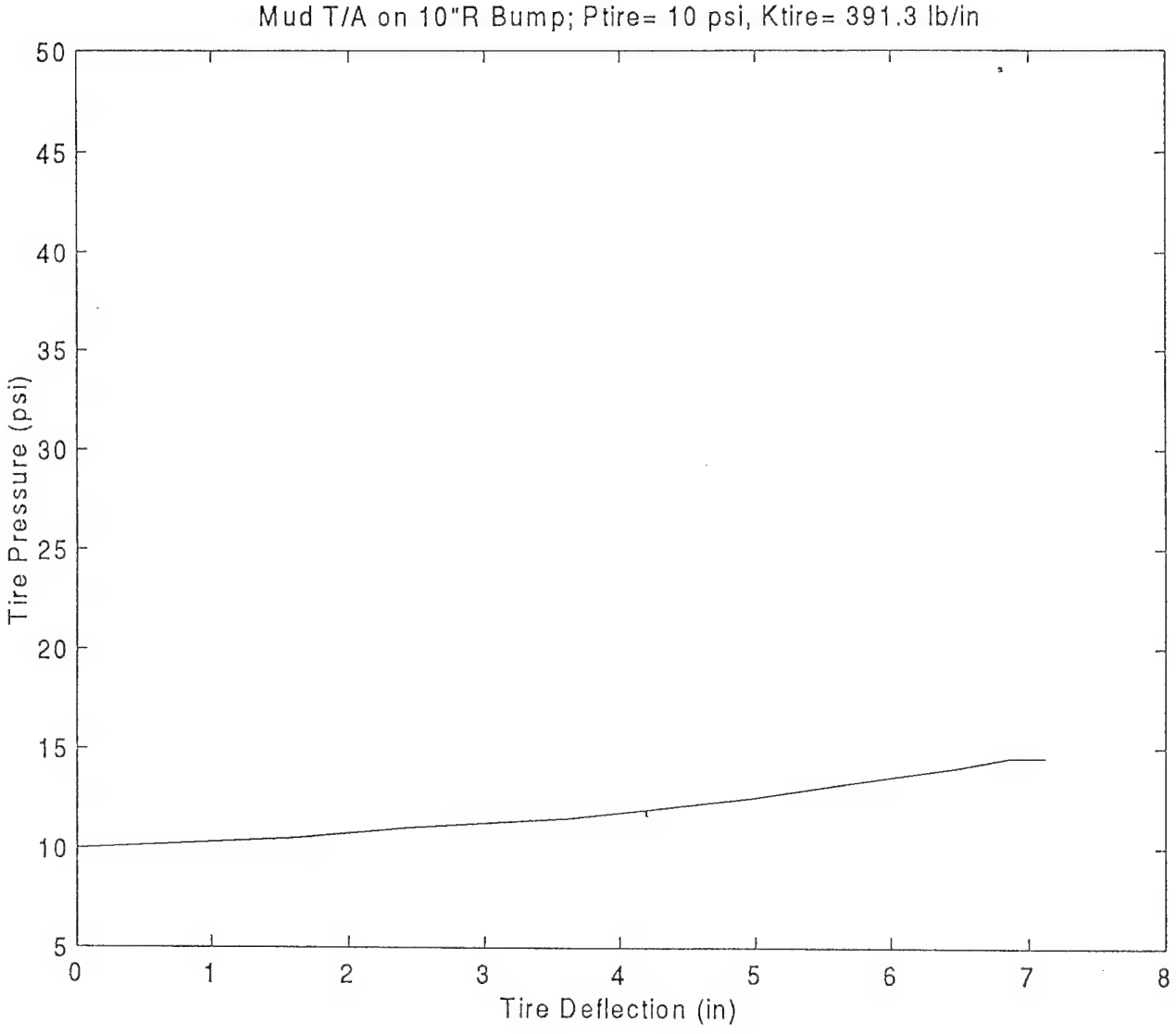
Mud T/A on 10"R Bump; Ptire= 10 psi, Ktire= 391.3 lb/in
Tire Pressure (psi)
50
45
40
35
30
25
20
15
10
5
0
1
2
3
4
5
6
7
8
Tire Deflection (in)

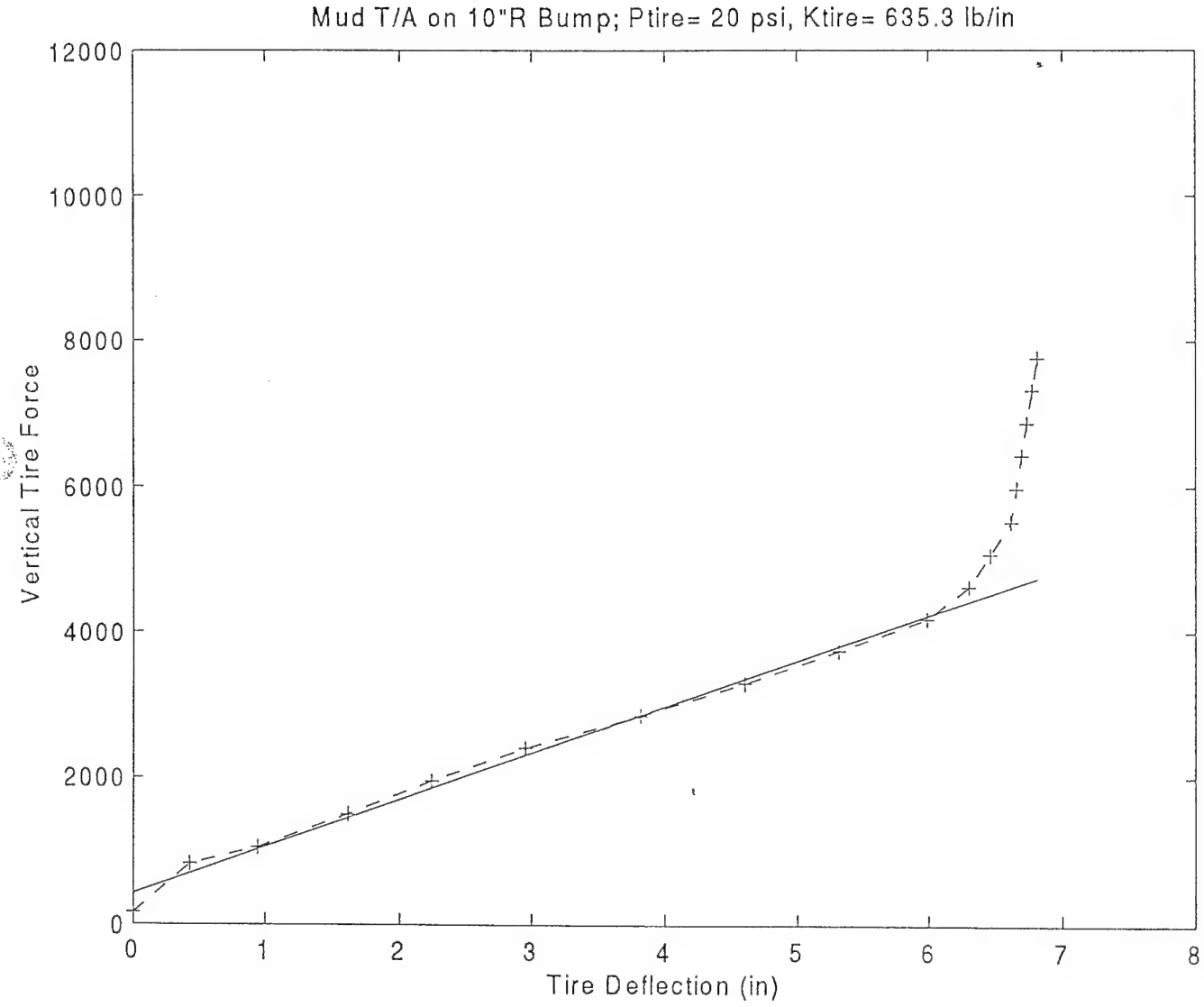
Mud T/A on 10"R Bump; Ptire= 20 psi, Ktire= 635.3 lb/in
Vertical Tire Force
Tire Deflection (in)
0
2000
4000
6000
8000
10000
12000
0
1
2
3
4
5
6
7
8

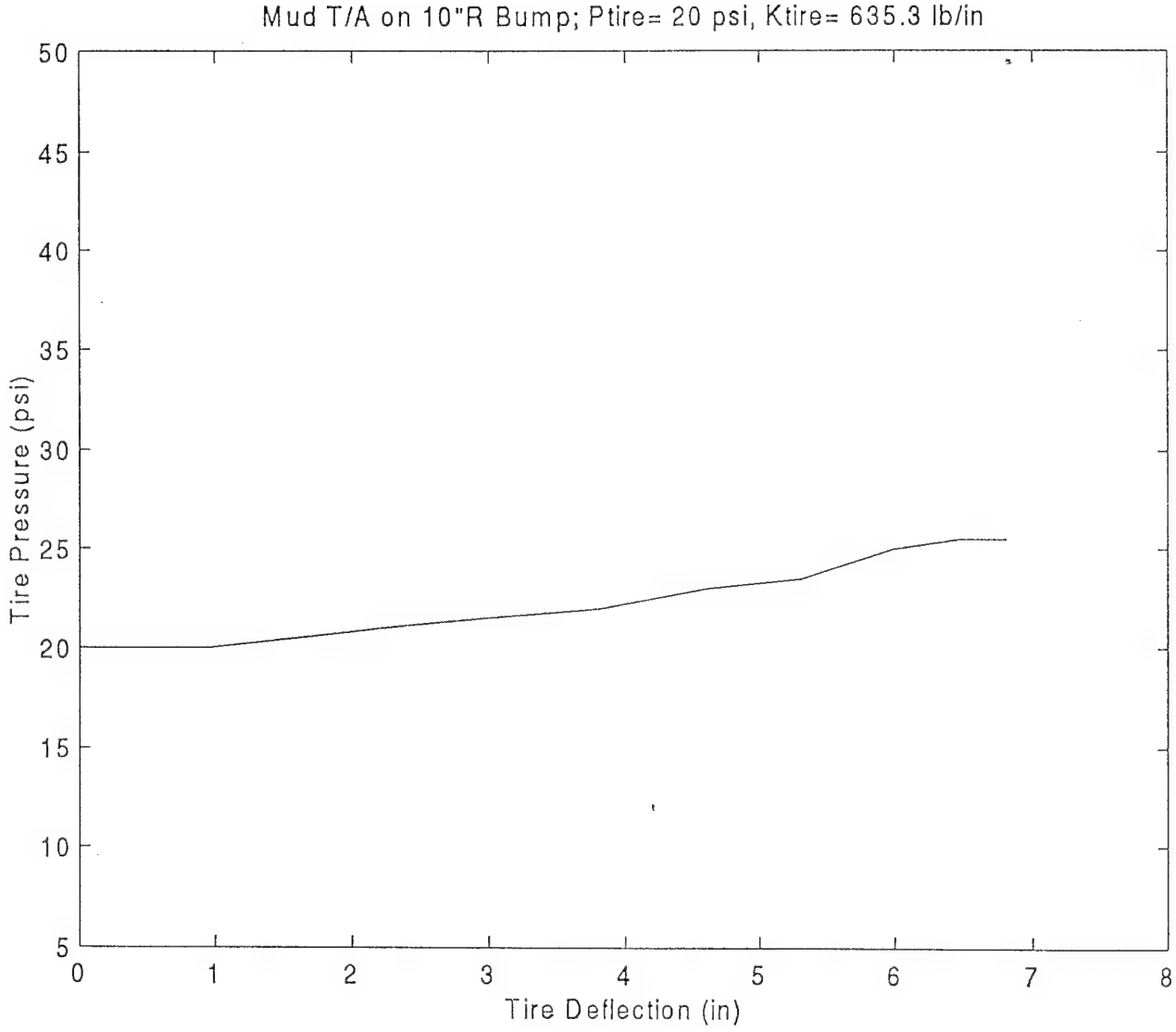
Mud T/A on 10"R Bump; Ptire= 20 psi, Ktire= 635.3 lb/in
Tire Pressure (psi)
Tire Deflection (in)
50
45
40
35
30
25
20
15
10
5
0
1
2
3
4
5
6
7
8

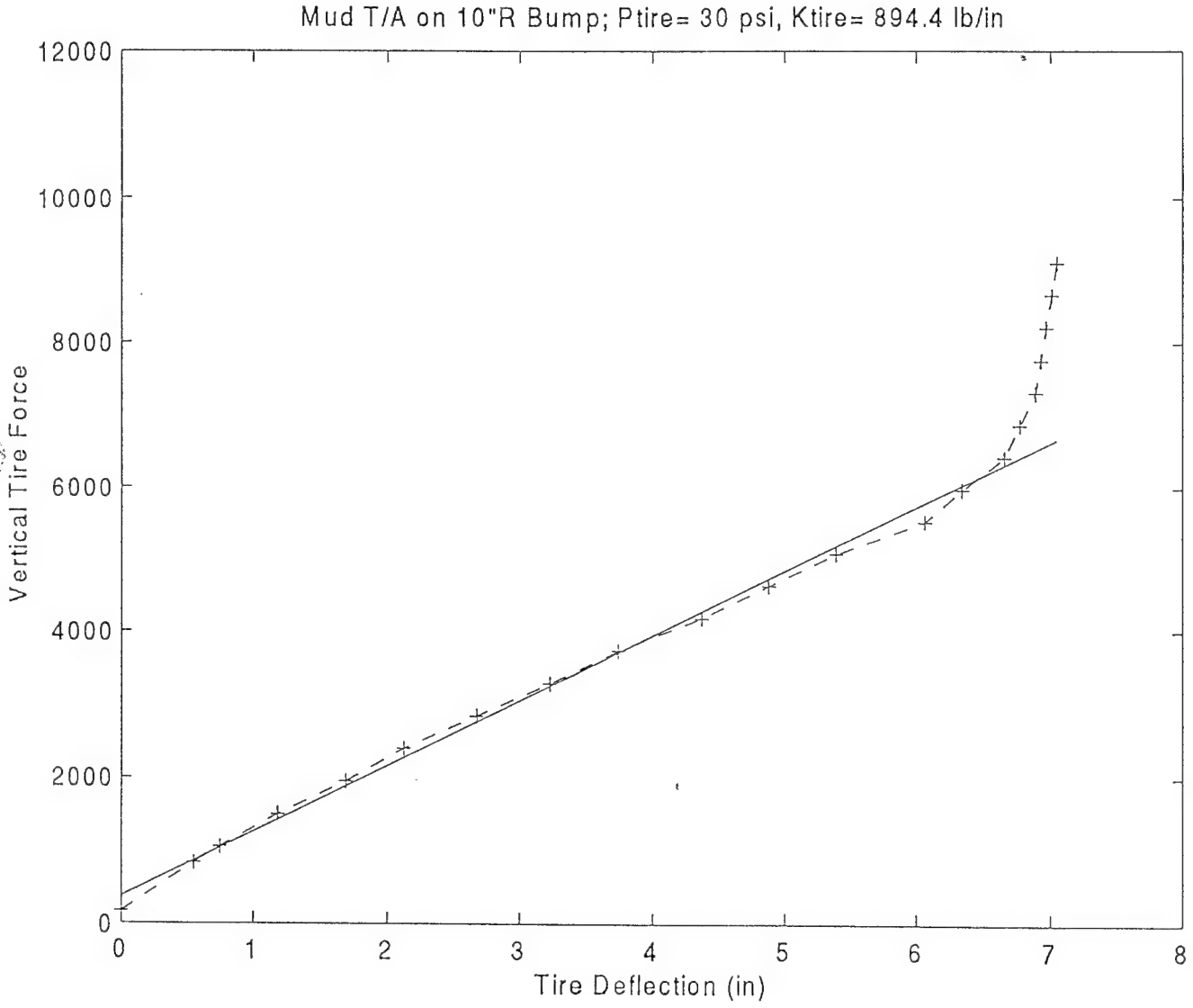
Mud T/A on 10"R Bump; Ptire= 30 psi, Ktire= 894.4 lb/in
Vertical Tire Force
Tire Deflection (in)
12000
10000
8000
6000
4000
2000
0
0
1
2
3
4
5
6
7
8

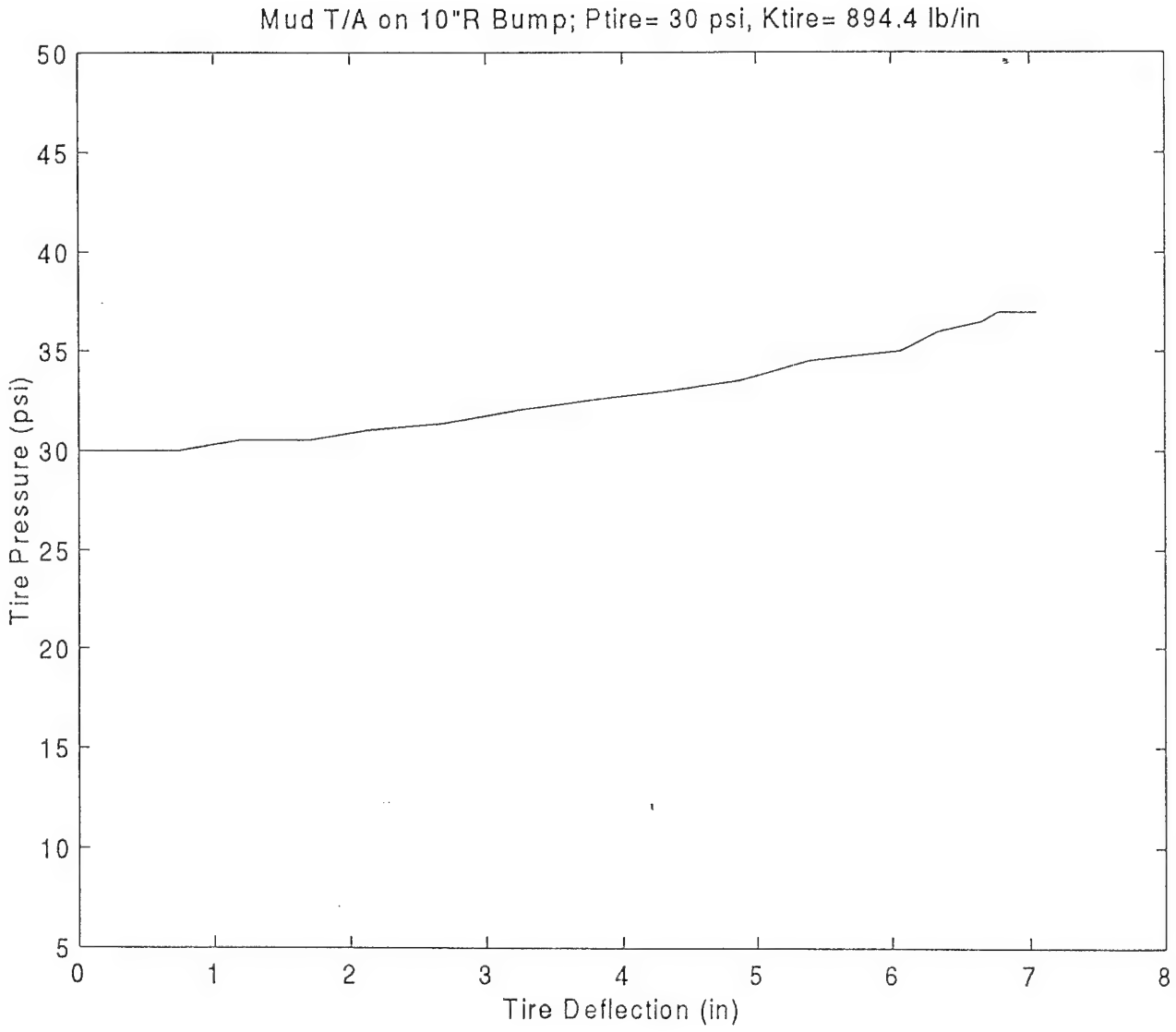
Mud T/A on 10"R Bump; Ptire= 30 psi, Ktire= 894.4 lb/in
Tire Pressure (psi)
Tire Deflection (in)
50
45
40
35
30
25
20
15
10
5
0
1
2
3
4
5
6
7
8

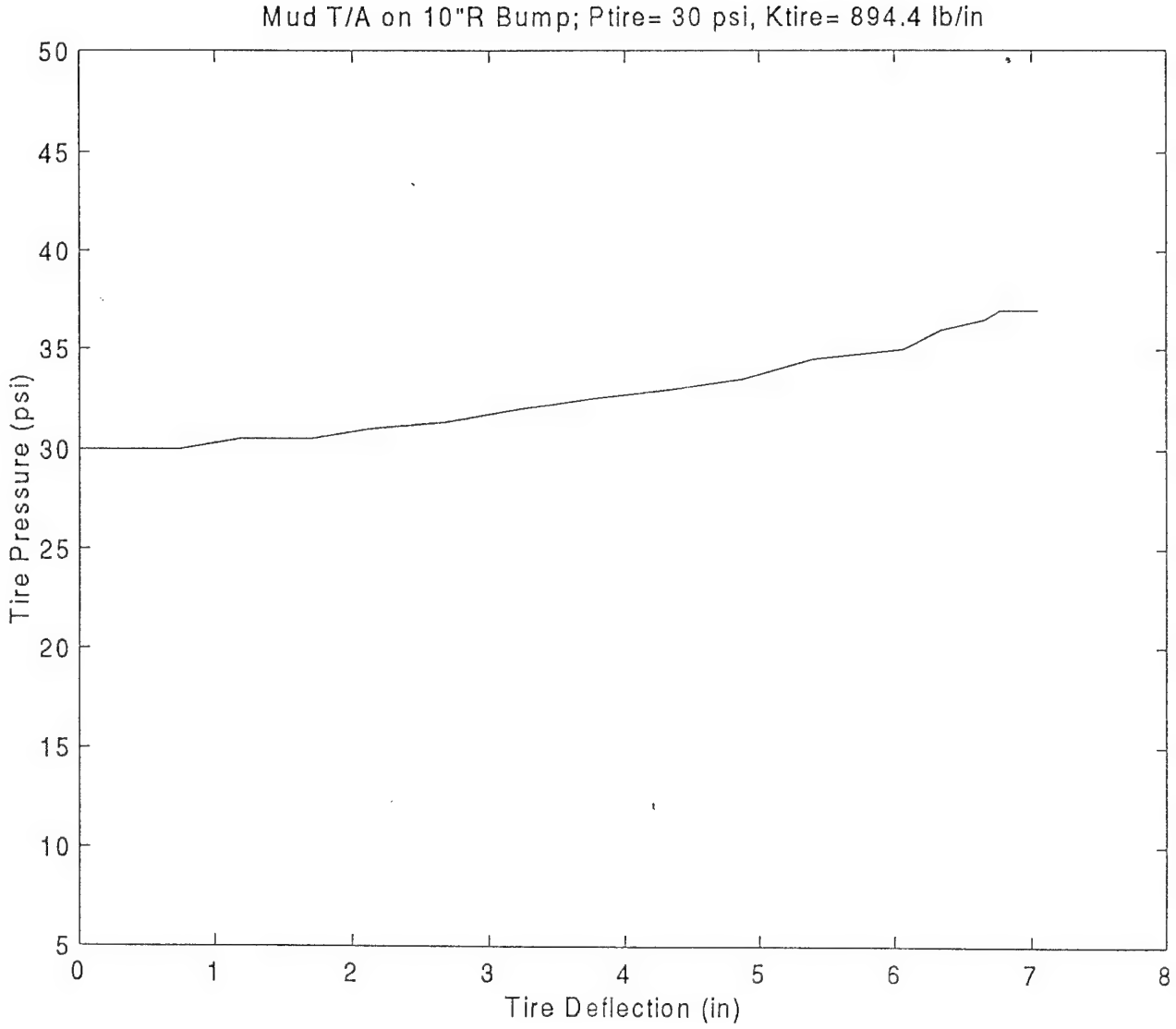
Mud T/A on 10"R Bump; Ptire= 30 psi, Ktire= 894.4 lb/in
Tire Pressure (psi)
Tire Deflection (in)
50
45
40
35
30
25
20
15
10
5
0
1
2
3
4
5
6
7
8

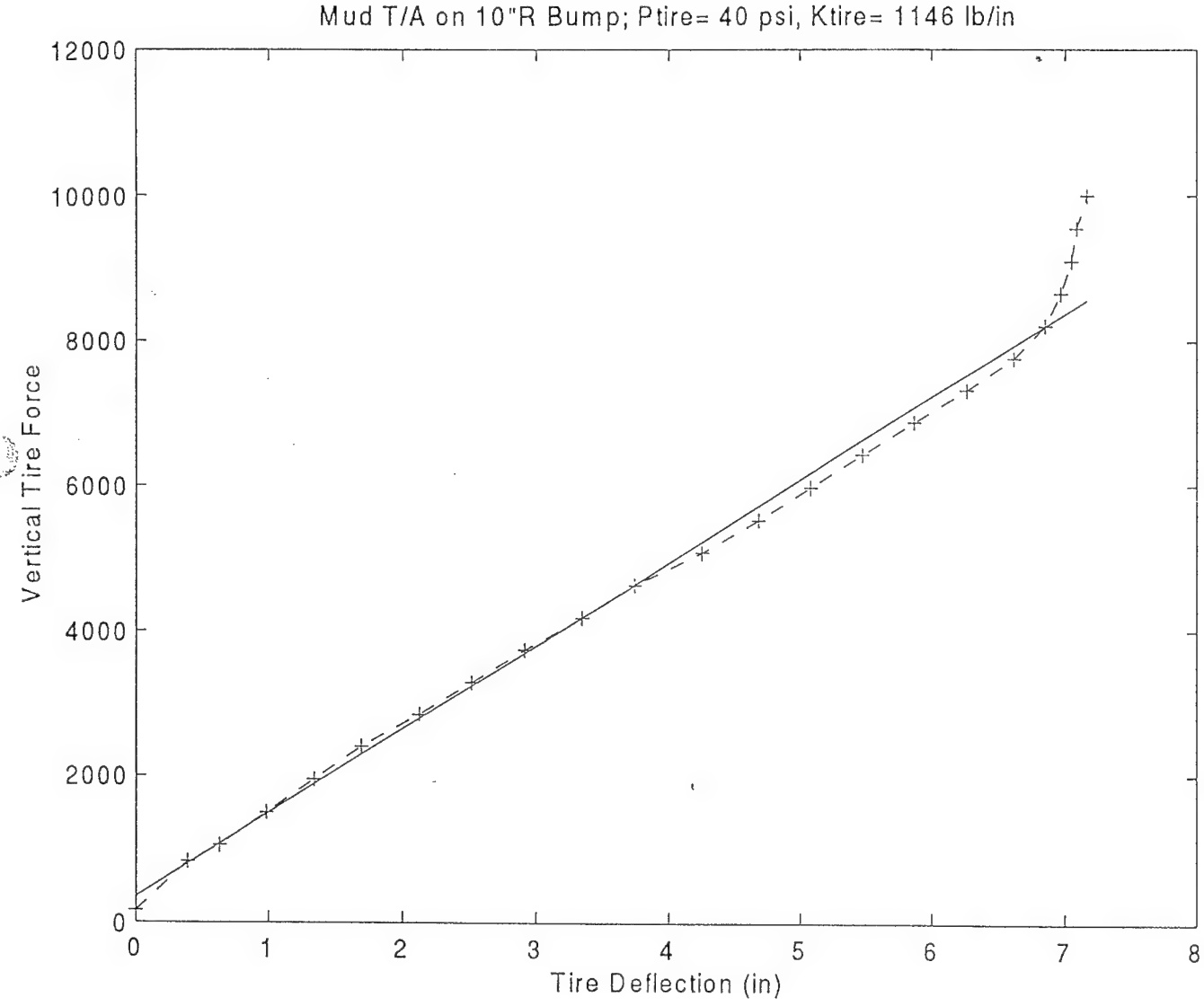
Mud T/A on 10"R Bump; Ptire= 40 psi, Ktire= 1146 lb/in
Vertical Tire Force
Tire Deflection (in)
12000
10000
8000
6000
4000
2000
0
0
1
2
3
4
5
6
7
8

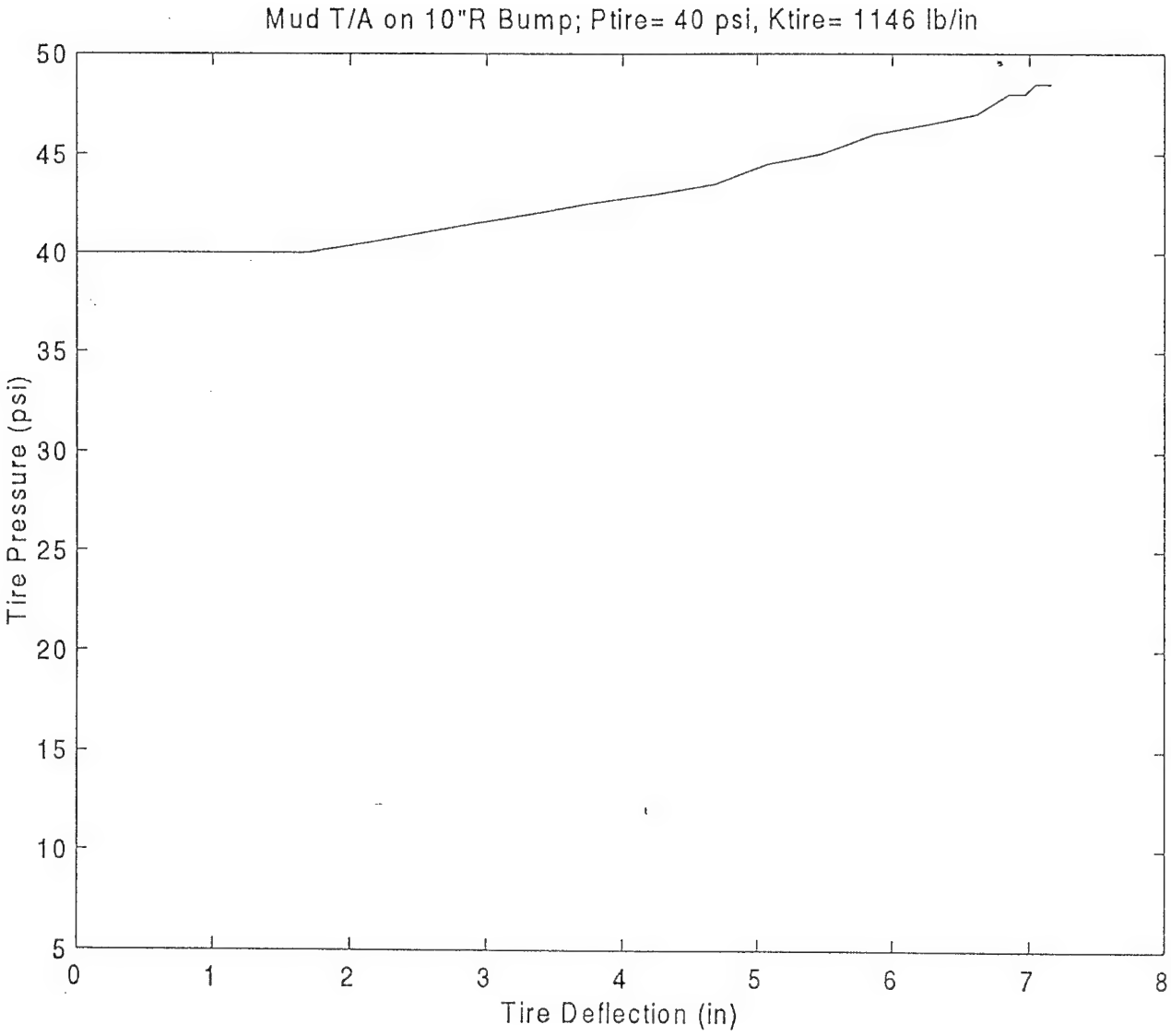
Mud T/A on 10"R Bump; Ptire= 40 psi, Ktire= 1146 lb/in
Tire Pressure (psi)
Tire Deflection (in)
50
45
40
35
30
25
20
15
10
5
0
1
2
3
4
5
6
7
8

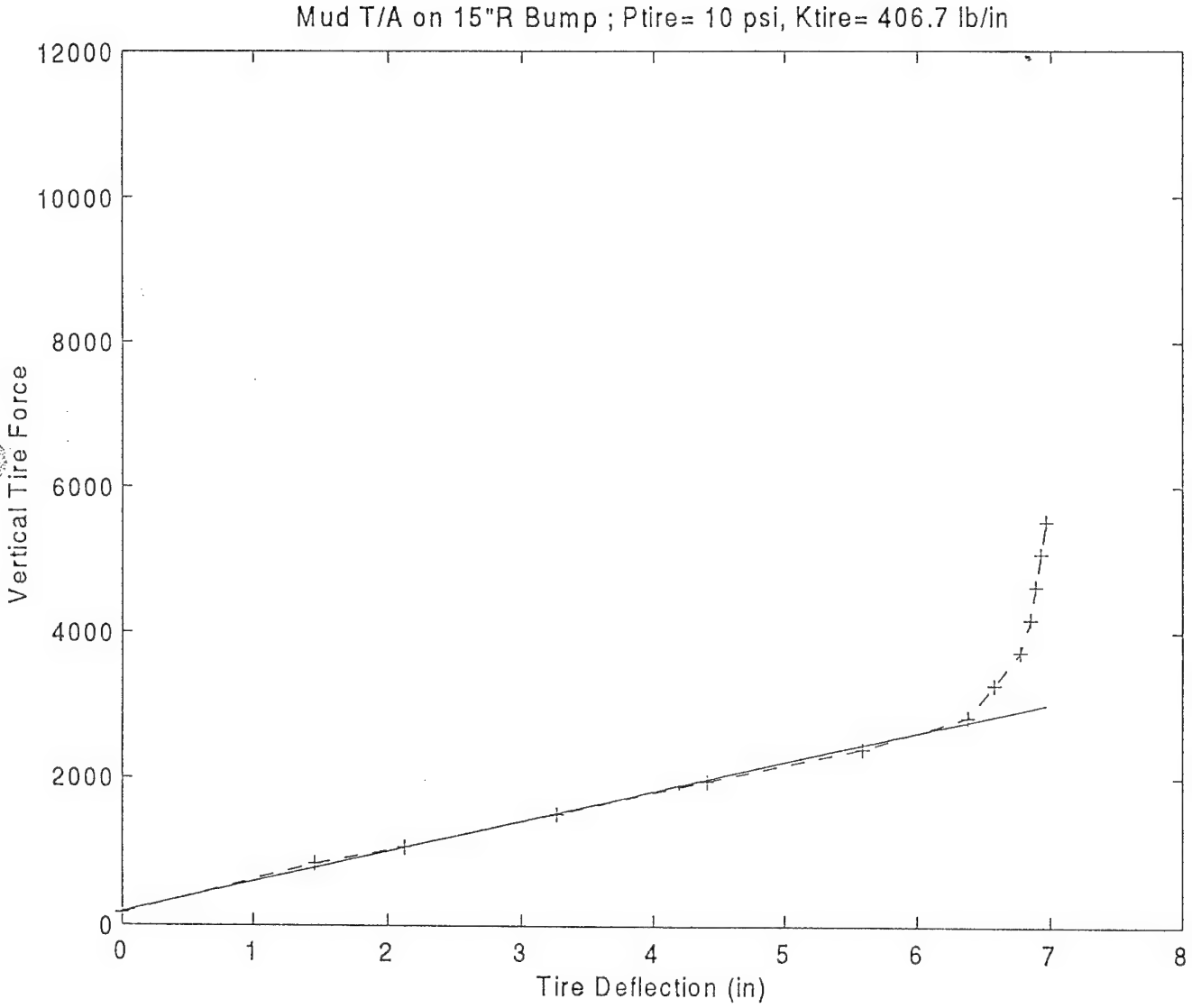
Mud T/A on 15"R Bump ; Ptire= 10 psi, Ktire= 406.7 lb/in
Vertical Tire Force
Tire Deflection (in)
12000
10000
8000
6000
4000
2000
0
0
1
2
3
4
5
6
7
8

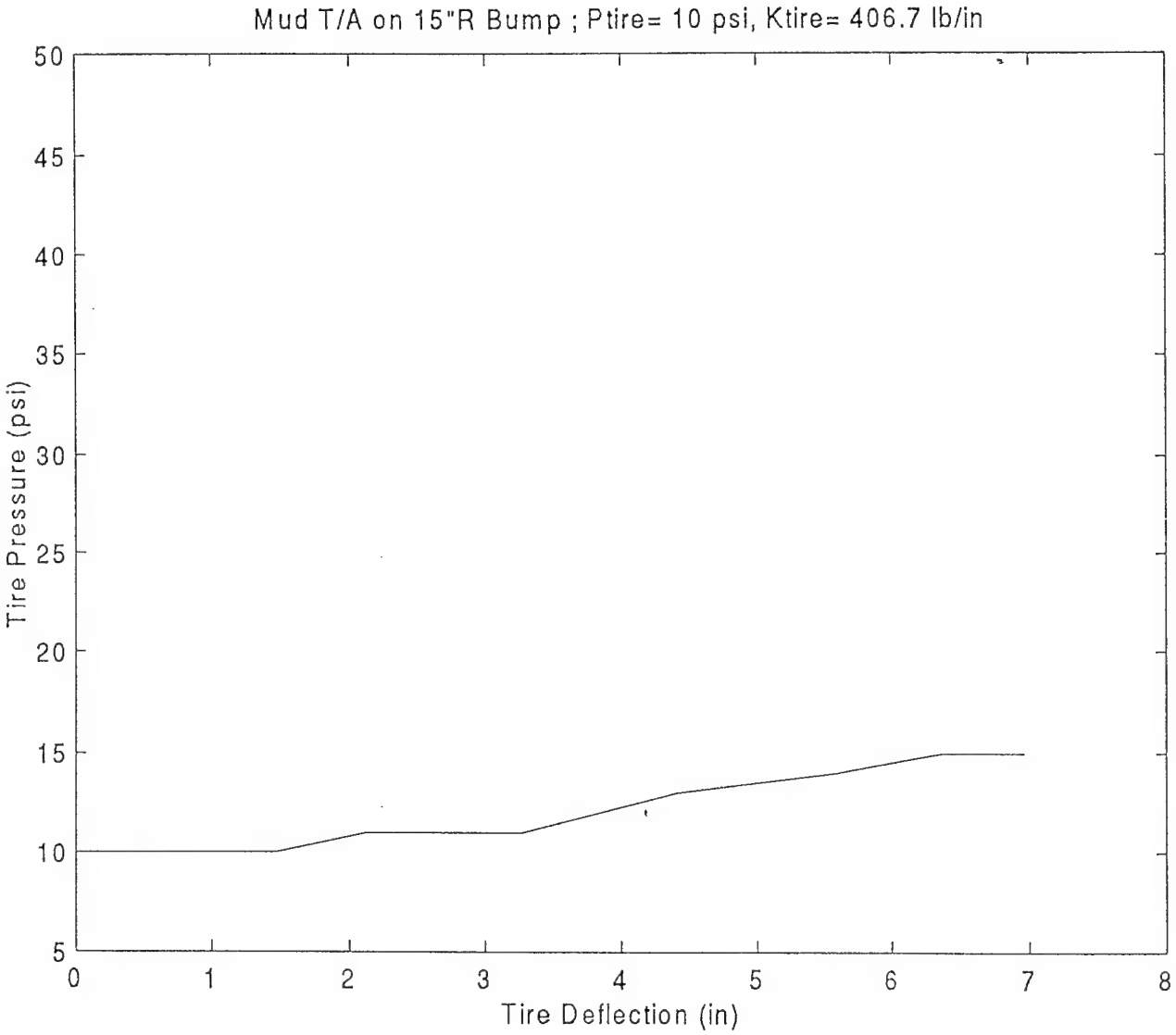
Mud T/A on 15"R Bump ; Ptire= 10 psi, Ktire= 406.7 lb/in
Tire Pressure (psi)
Tire Deflection (in)
50
45
40
35
30
25
20
15
10
5
0
1
2
3
4
5
6
7
8

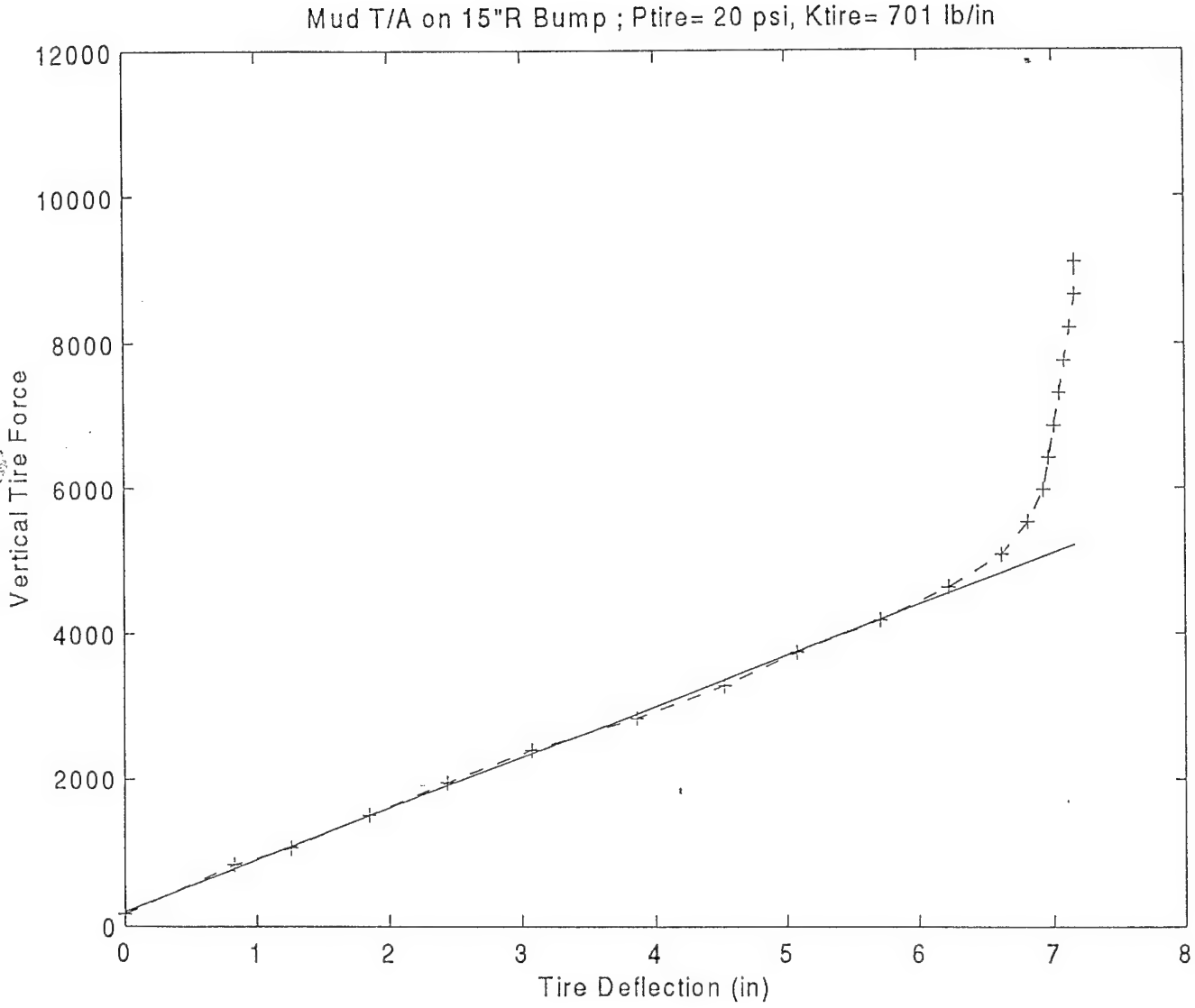
Mud T/A on 15"R Bump ; Ptire= 20 psi, Ktire= 701 lb/in
Vertical Tire Force
Tire Deflection (in)
12000
10000
8000
6000
4000
2000
0
0
1
2
3
4
5
6
7
8

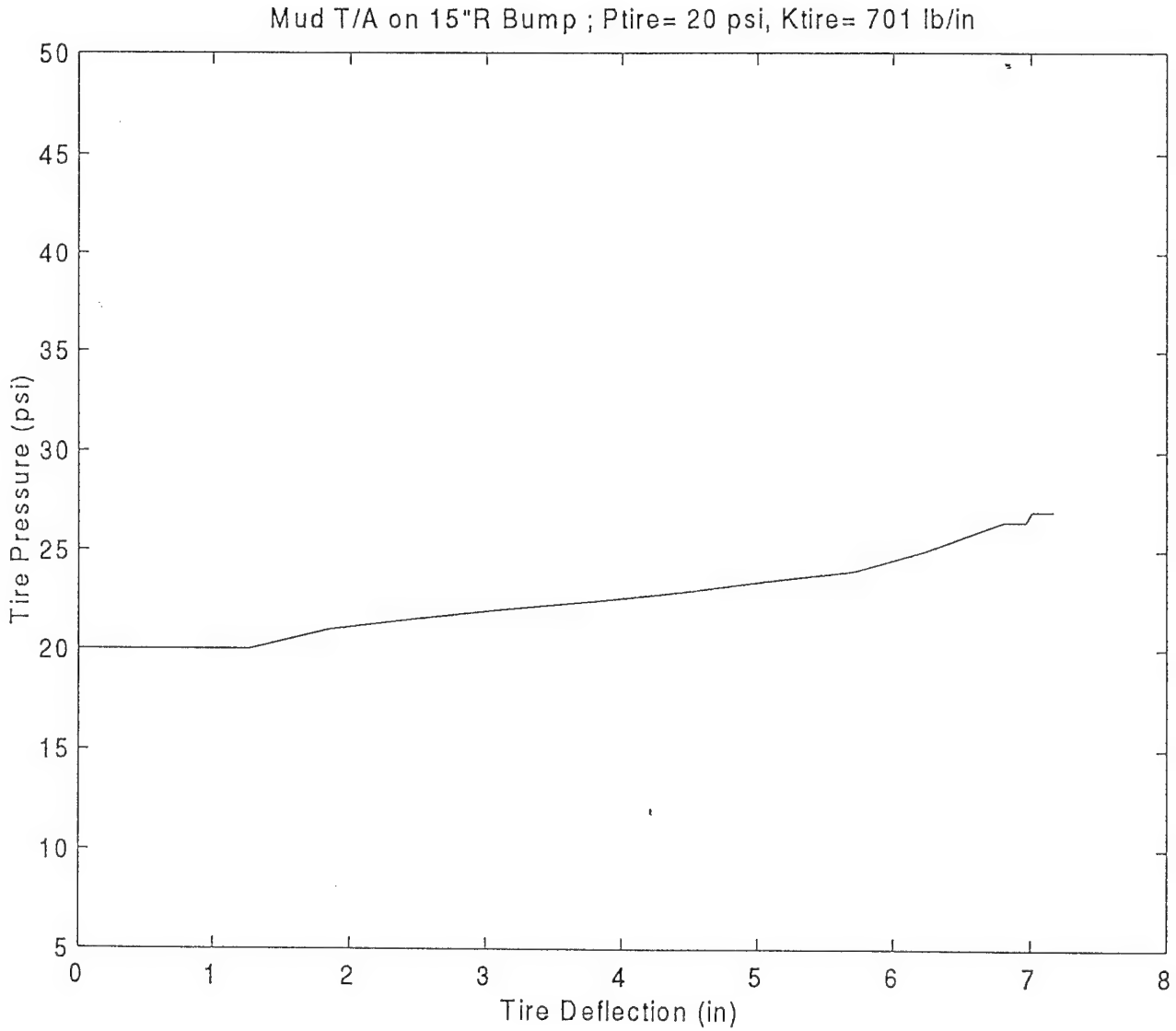
Mud T/A on 15"R Bump ; Ptire= 20 psi, Ktire= 701 lb/in
Tire Pressure (psi)
Tire Deflection (in)
50
45
40
35
30
25
20
15
10
5
0
1
2
3
4
5
6
7
8

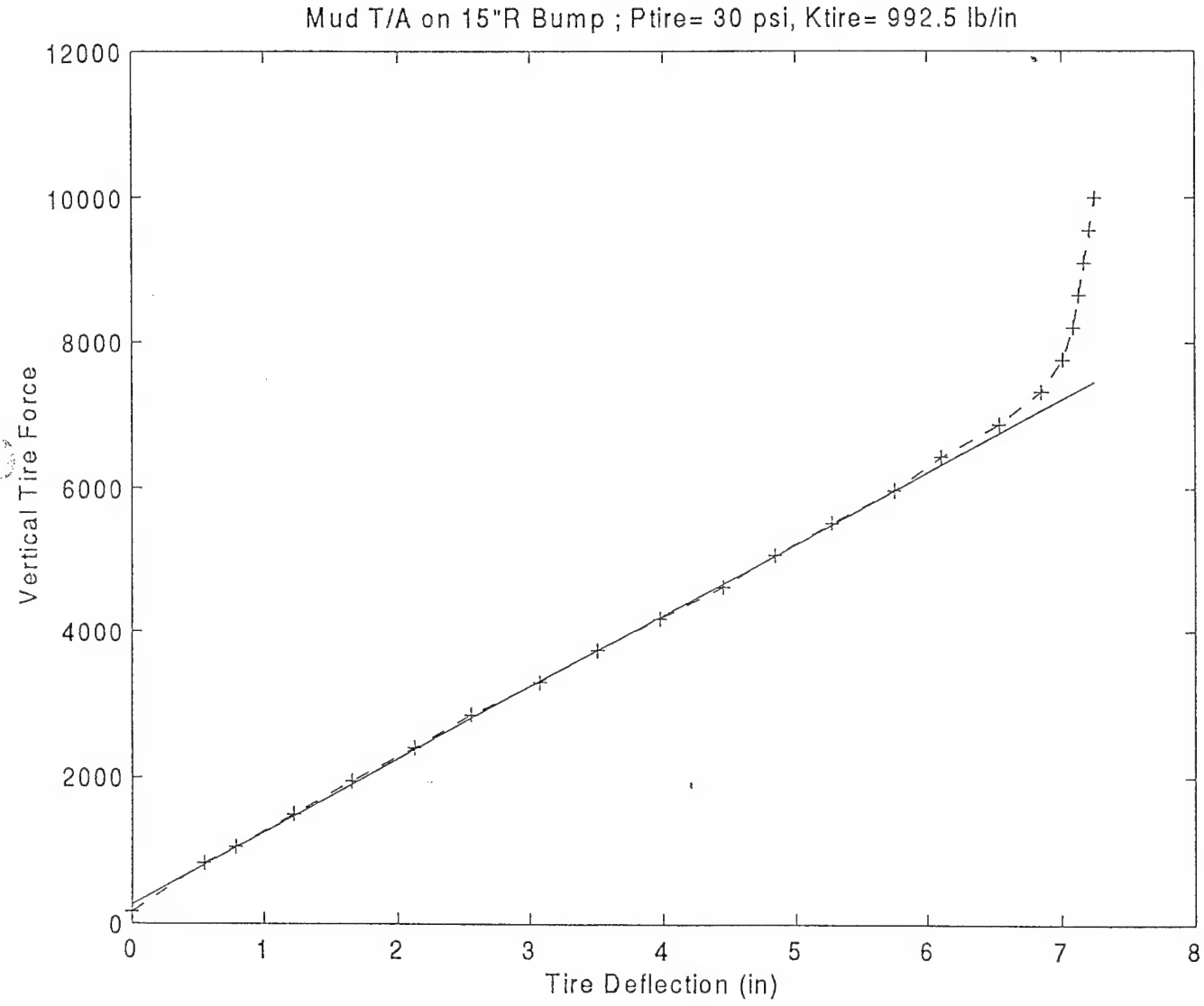
Mud T/A on 15"R Bump ; Ptire= 30 psi, Ktire= 992.5 lb/in
Vertical Tire Force
Tire Deflection (in)
12000
10000
8000
6000
4000
2000
0
0
1
2
3
4
5
6
7
8

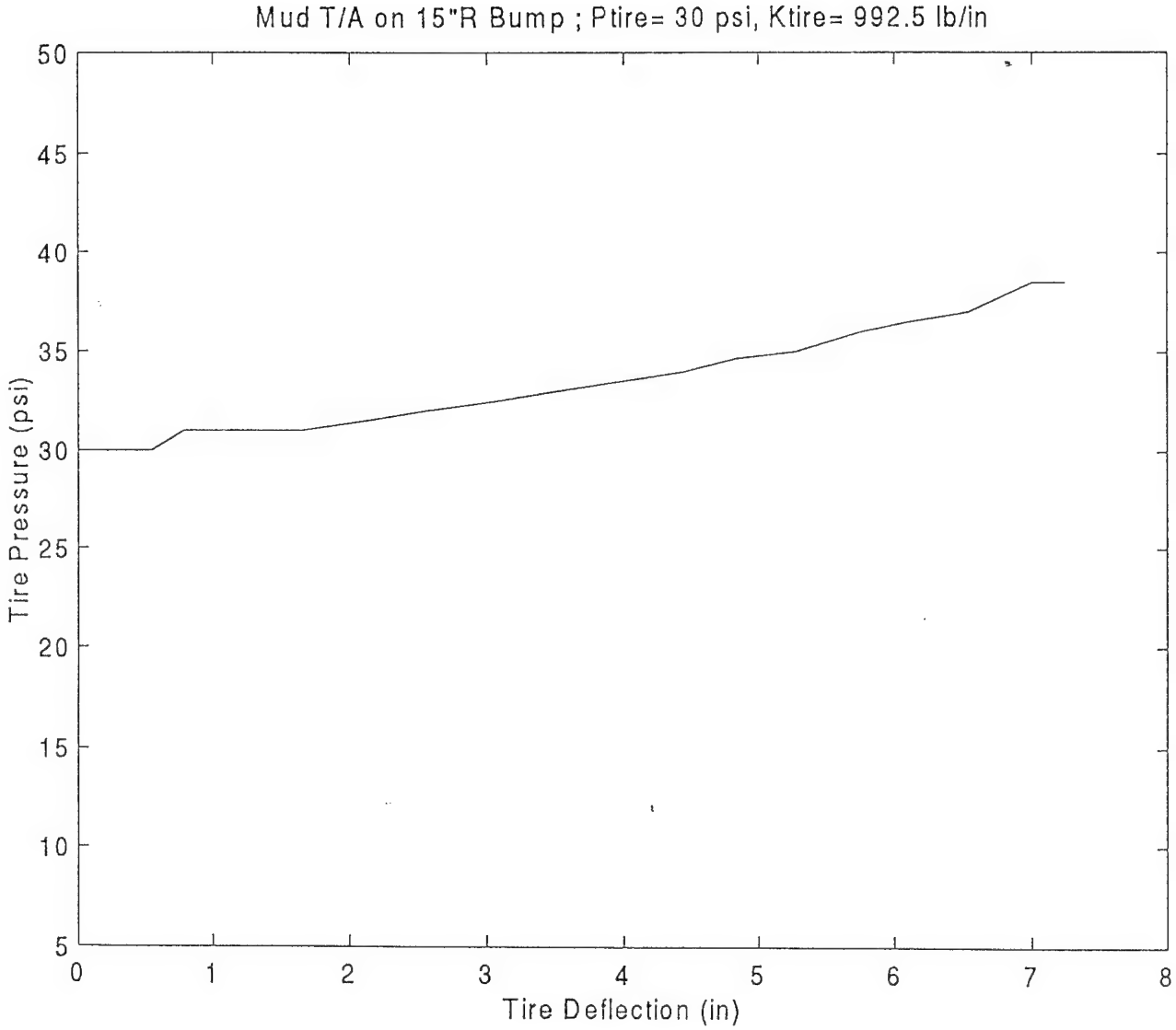
Mud T/A on 15"R Bump ; Ptire= 30 psi, Ktire= 992.5 lb/in
Tire Pressure (psi)
Tire Deflection (in)
50
45
40
35
30
25
20
15
10
5
0
1
2
3
4
5
6
7
8

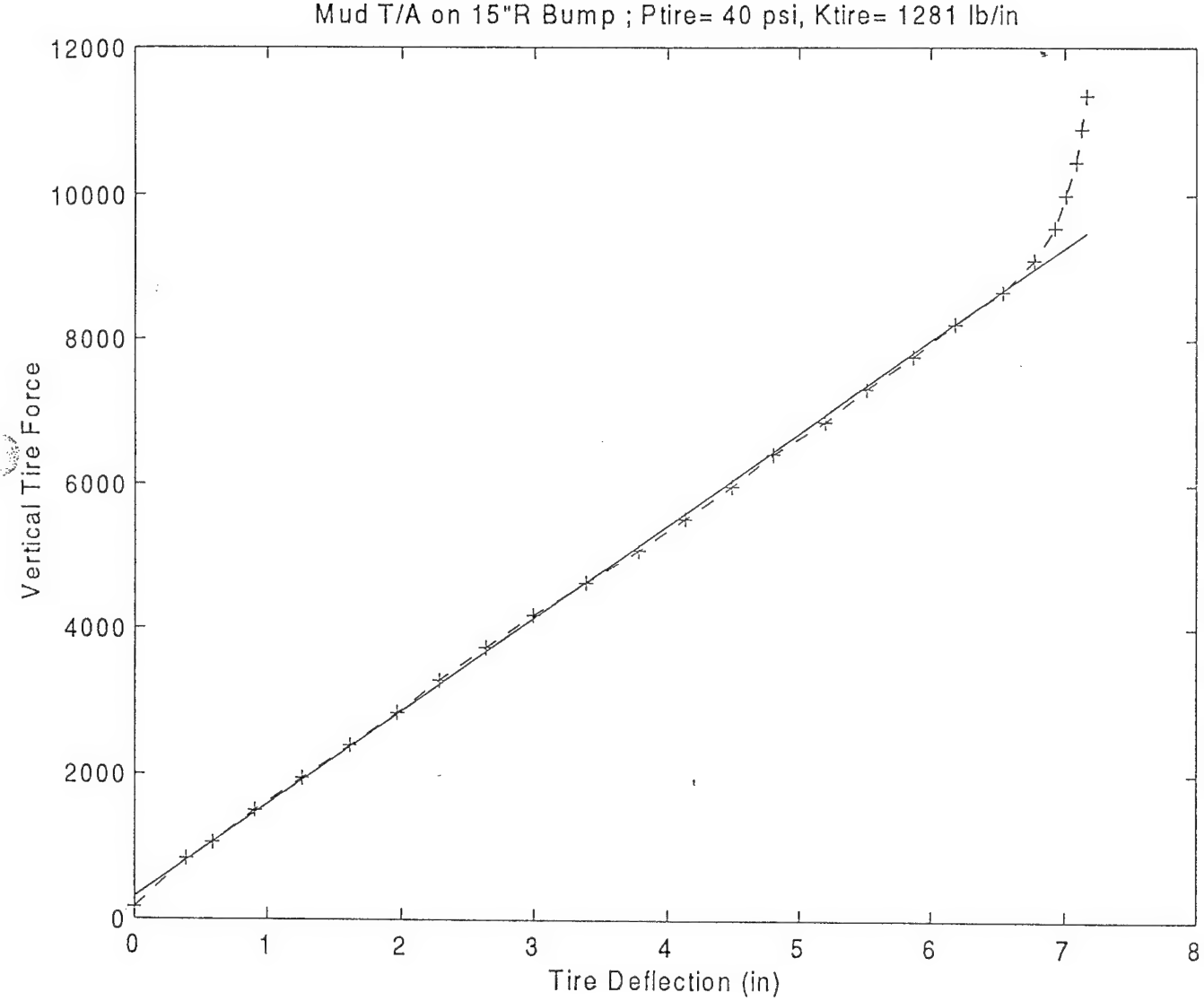
Mud T/A on 15"R Bump ; Ptire= 40 psi, Ktire= 1281 lb/in
Vertical Tire Force
Tire Deflection (in)
12000
10000
8000
6000
4000
2000
0
0
1
2
3
4
5
6
7
8

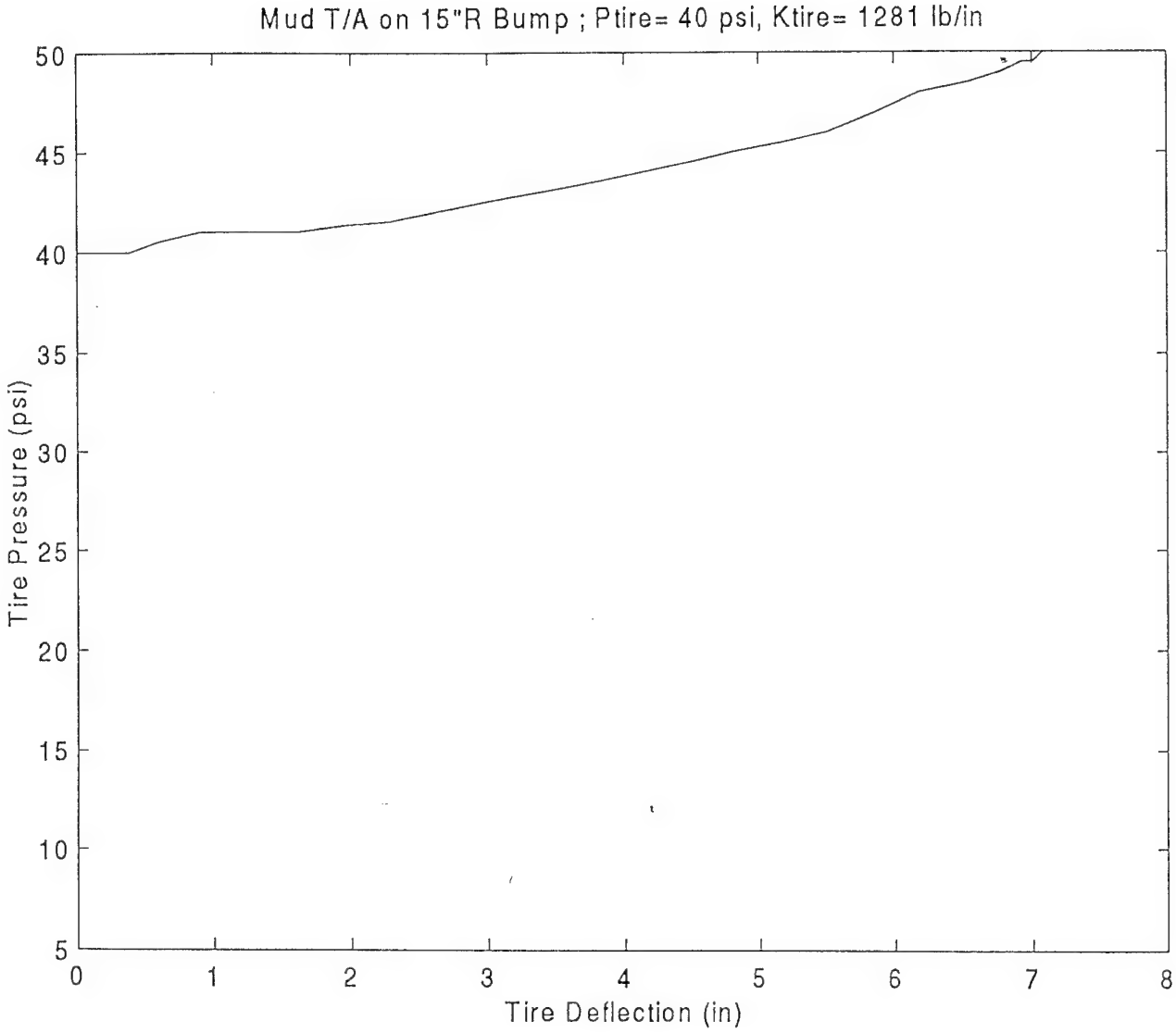
Mud T/A on 15"R Bump ; Ptire= 40 psi, Ktire= 1281 lb/in
Tire Pressure (psi)
Tire Deflection (in)
50
45
40
35
30
25
20
15
10
5
0
1
2
3
4
5
6
7
8

# Appendix III

## Shock Dynamometer Data

Test series: mg# 2 ½" Bore Damper with orifice and Blow-off passive valves
Controllable valve open
Reservoir on cylinder side of damper

Test series: mgc# 2 ½" Bore Damper with orifice and Blow-off passive valves
Controllable valve closed
Reservoir on cylinder side of damper

Test series: mo# 2 ½" Bore Damper with orifice and Blow-off passive valves
Controllable valve open
Reservoir on rod side of damper

Test series: moc# 2 ½" Bore Damper with orifice and Blow-off passive valves
Controllable valve closed
Reservoir on rod side of damper

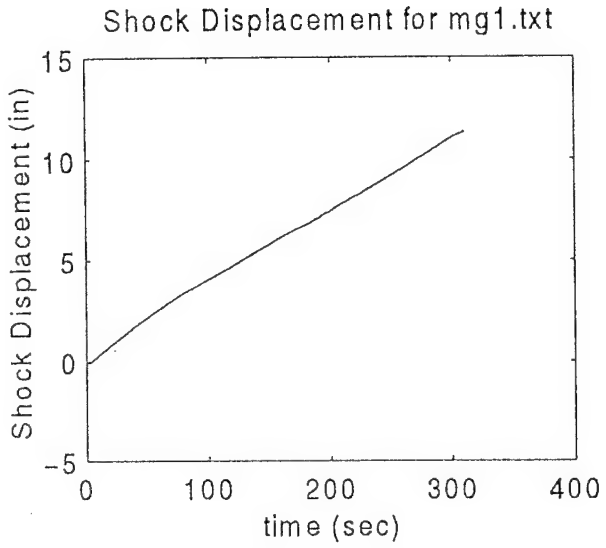
Shock Displacement for mg1.txt
Shock Displacement (in)
15
10
5
0
-5
0
100
200
300
400
time (sec)

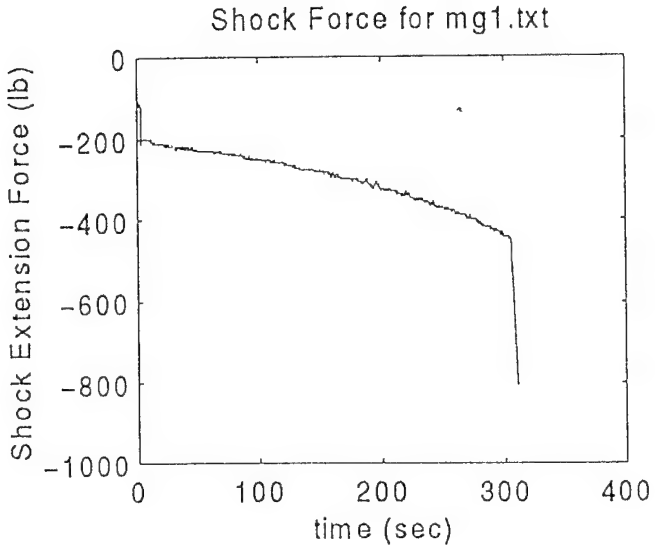
Shock Force for mg1.txt
Shock Extension Force (lb)
0
-200
-400
-600
-800
-1000
0
100
200
300
400
time (sec)

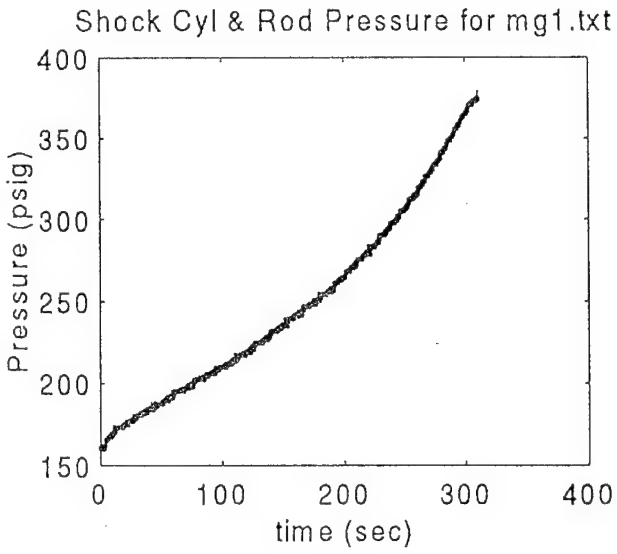
Shock Cyl & Rod Pressure for mg1.txt
Pressure (psig)
400
350
300
250
200
150
0
100
200
300
400
time (sec)

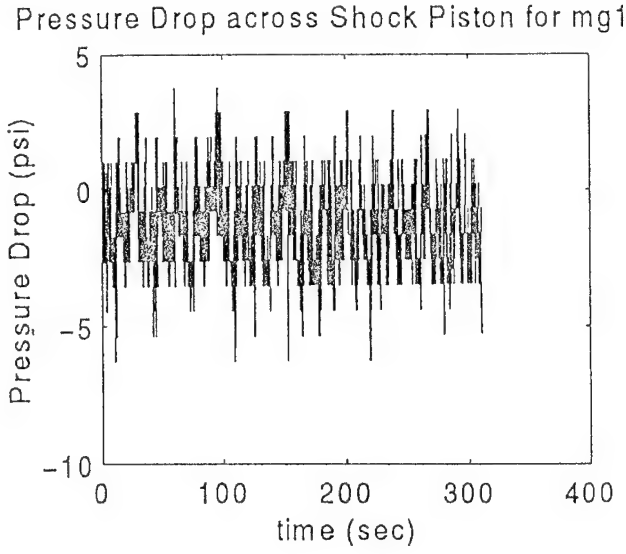
Pressure Drop across Shock Piston for mg1.txt
Pressure Drop (psi)
5
0
-5
-10
0
100
200
300
400
time (sec)

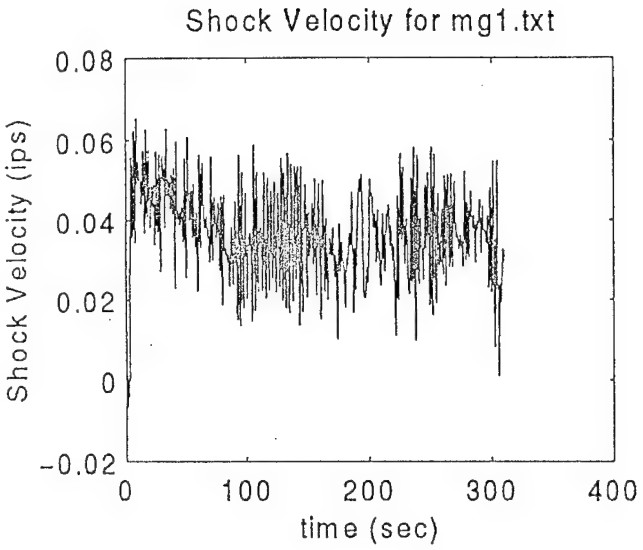
Shock Velocity for mg1.txt
Shock Velocity (ips)
0.08
0.06
0.04
0.02
0
-0.02
0
100
200
300
400
time (sec)

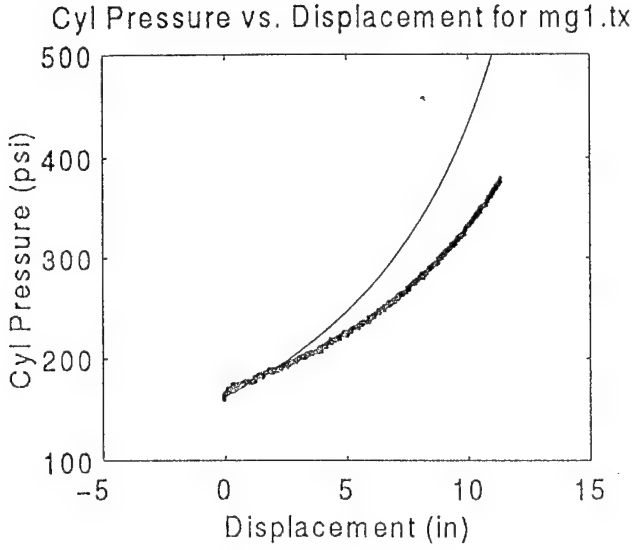
Cyl Pressure vs. Displacement for mg1.txt
Cyl Pressure (psi)
500
400
300
200
100
-5
0
5
10
15
Displacement (in)

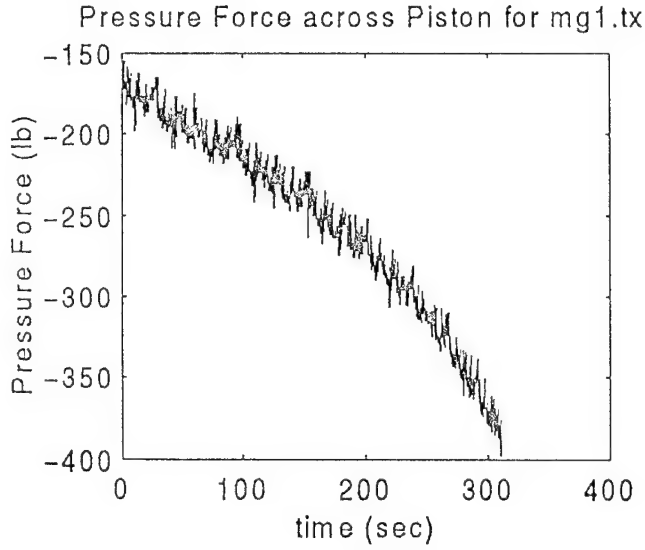
Pressure Force across Piston for mg1.txt
Pressure Force (lb)
-150
-200
-250
-300
-350
-400
0
100
200
300
400
time (sec)

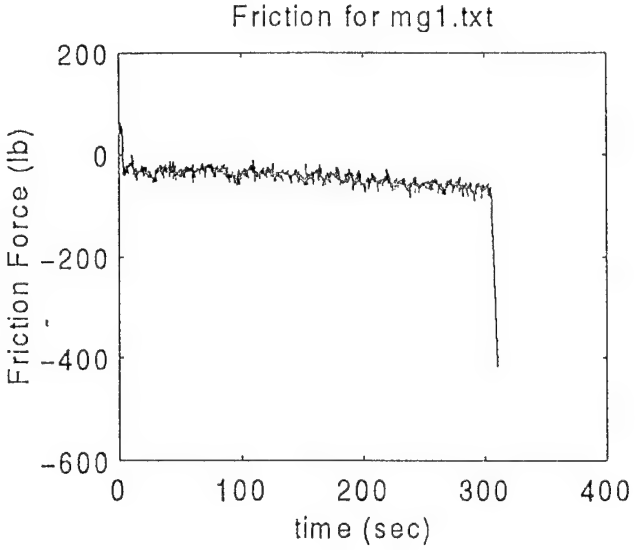
Friction for mg1.txt
Friction Force (lb)
200
0
-200
-400
-600
0
100
200
300
400
time (sec)

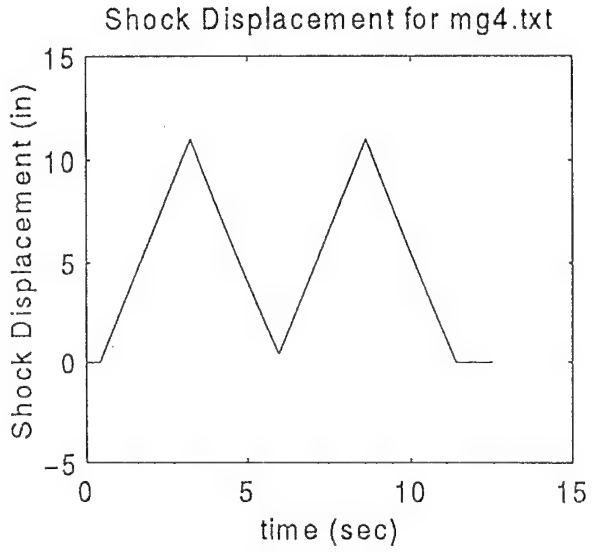
Shock Displacement for mg4.txt
Shock Displacement (in)
15
10
5
0
−5
0
5
10
15
time (sec)

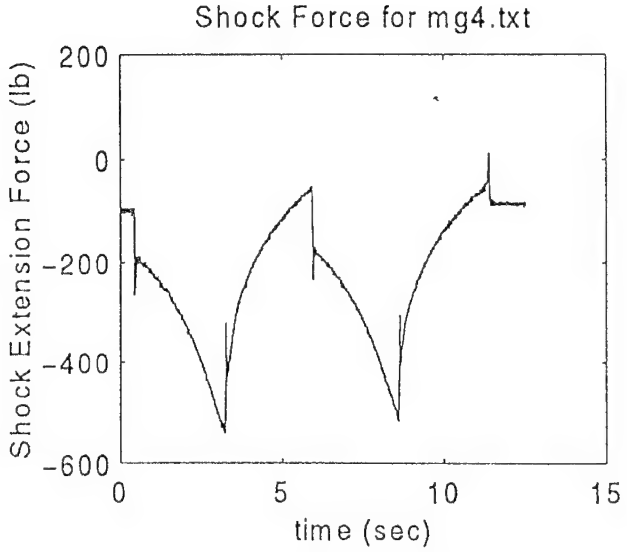
Shock Force for mg4.txt
Shock Extension Force (lb)
200
0
−200
−400
−600
0
5
10
15
time (sec)

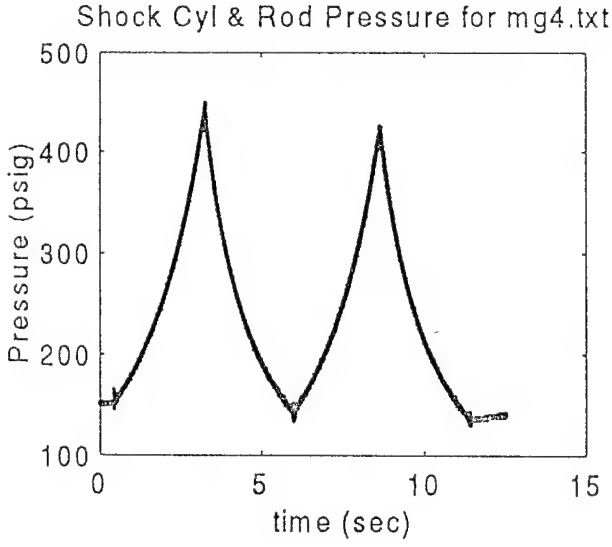
Shock Cyl & Rod Pressure for mg4.txt
Pressure (psig)
500
400
300
200
100
0
5
10
15
time (sec)

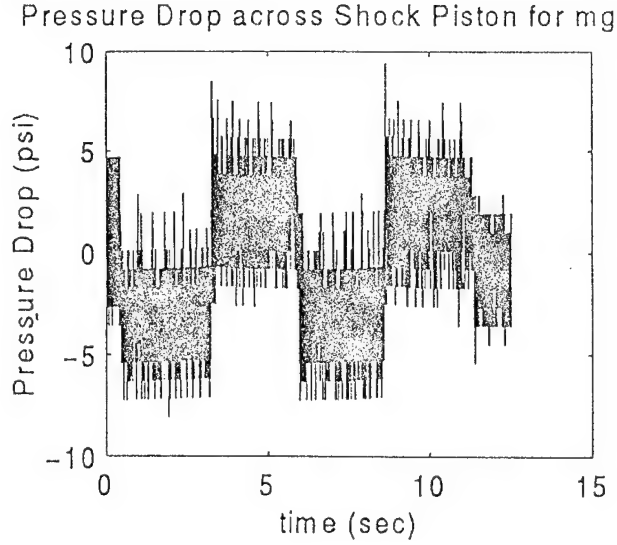
Pressure Drop across Shock Piston for mg4.txt
Pressure Drop (psi)
10
5
0
−5
−10
0
5
10
15
time (sec)

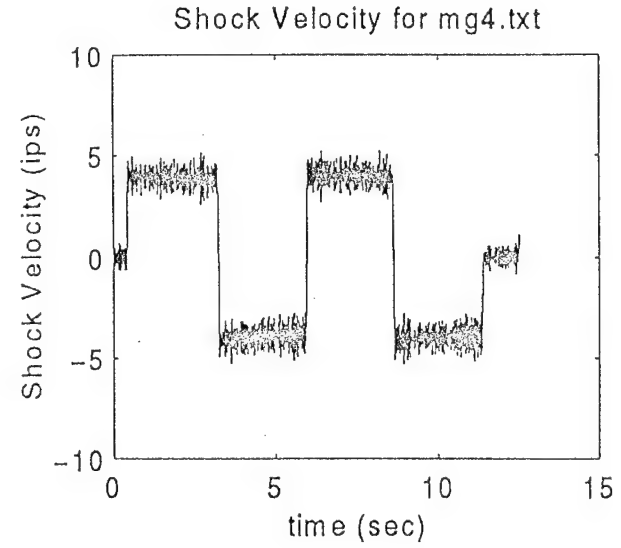
Shock Velocity for mg4.txt
Shock Velocity (ips)
time (sec)
10
5
0
-5
-10
0
5
10
15

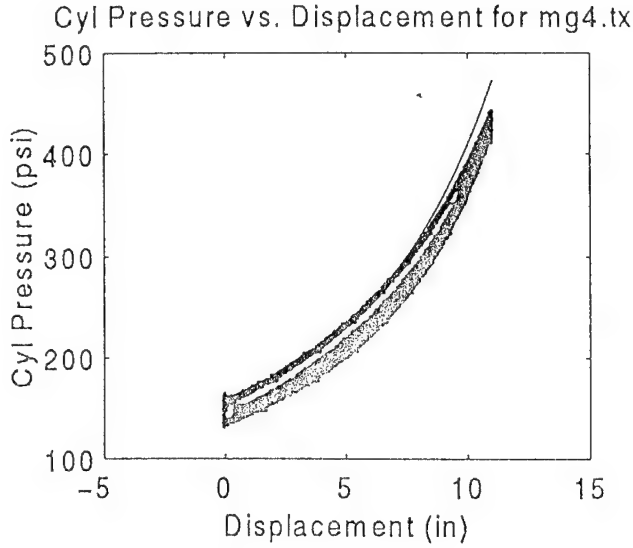
Cyl Pressure vs. Displacement for mg4.txt
Cyl Pressure (psi)
Displacement (in)
500
400
300
200
100
-5
0
5
10
15

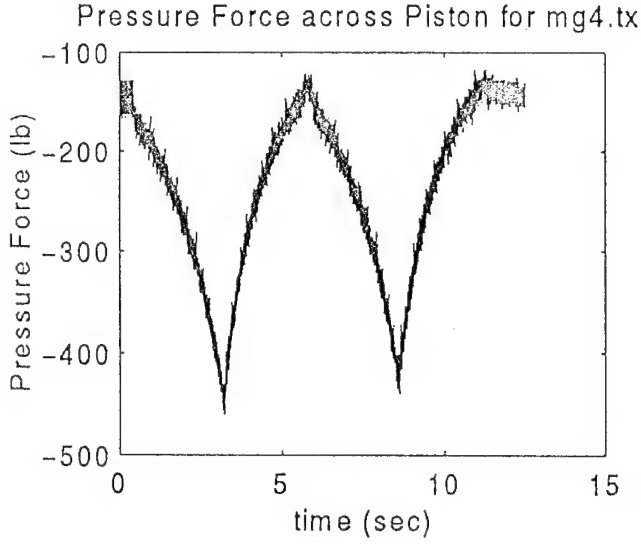
Pressure Force across Piston for mg4.txt
Pressure Force (lb)
time (sec)
-100
-200
-300
-400
-500
0
5
10
15

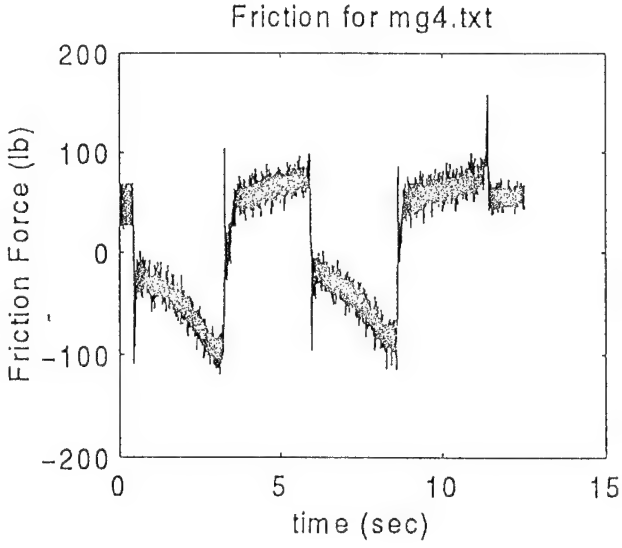
Friction for mg4.txt
Friction Force (lb)
time (sec)
200
100
0
-100
-200
0
5
10
15

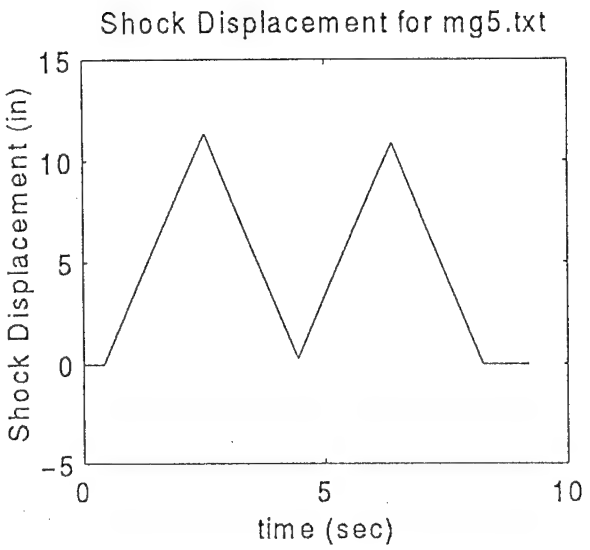
Shock Displacement for mg5.txt
Shock Displacement (in)
15
10
5
0
-5
0
5
10
time (sec)

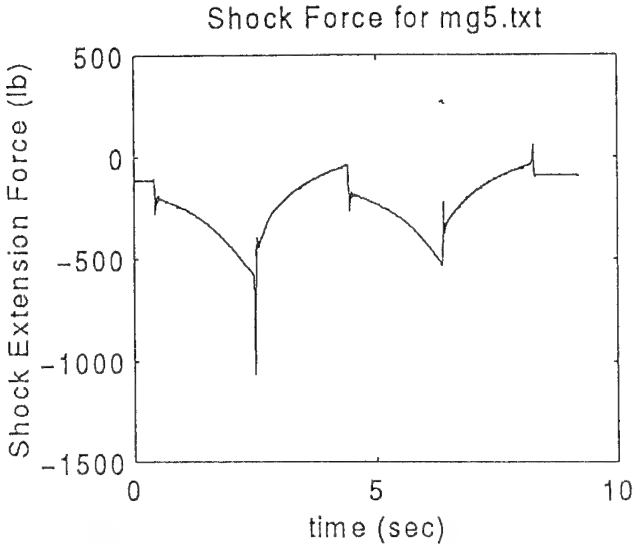
Shock Force for mg5.txt
Shock Extension Force (lb)
500
0
-500
-1000
-1500
0
5
10
time (sec)

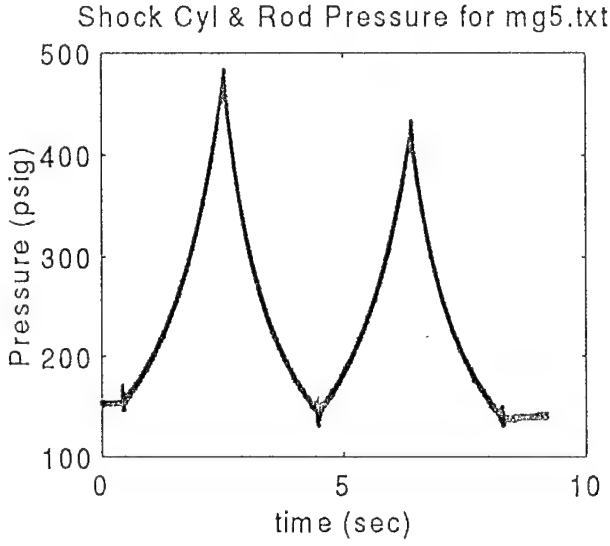
Shock Cyl & Rod Pressure for mg5.txt
Pressure (psig)
500
400
300
200
100
0
5
10
time (sec)

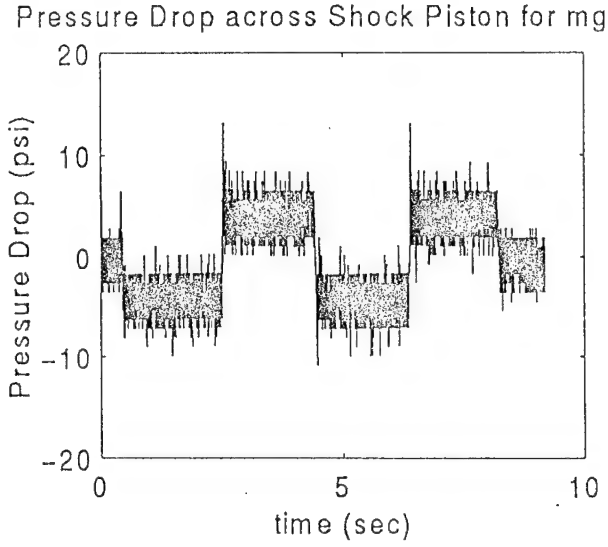
Pressure Drop across Shock Piston for mg5.txt
Pressure Drop (psi)
20
10
0
-10
-20
0
5
10
time (sec)

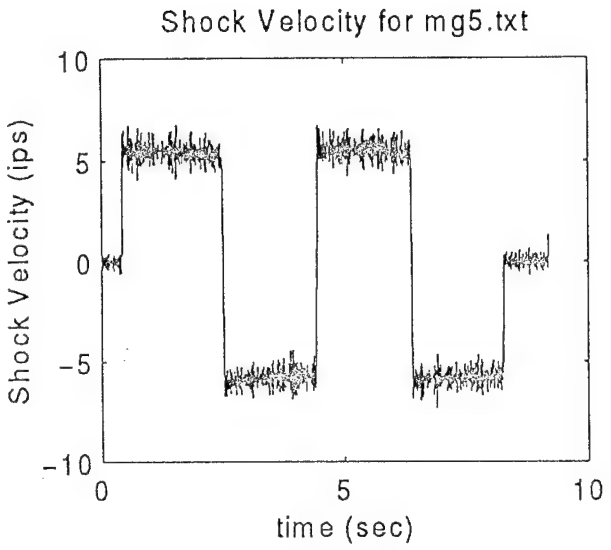
Shock Velocity for mg5.txt
Shock Velocity (ips)
time (sec)
10
5
0
-5
-10
0
5
10

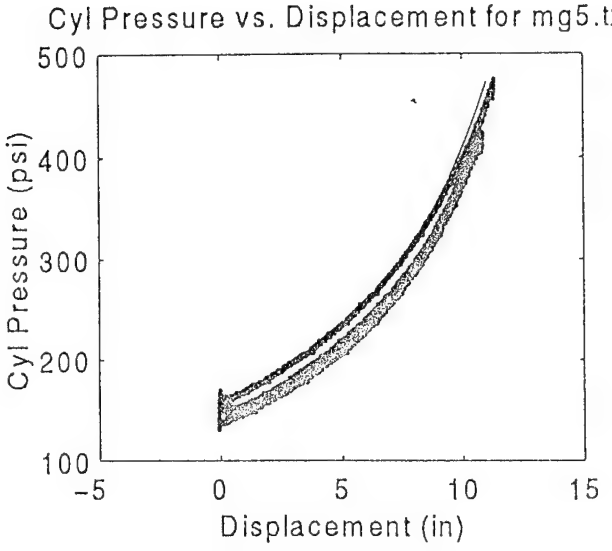
Cyl Pressure vs. Displacement for mg5.txt
Cyl Pressure (psi)
Displacement (in)
500
400
300
200
100
-5
0
5
10
15

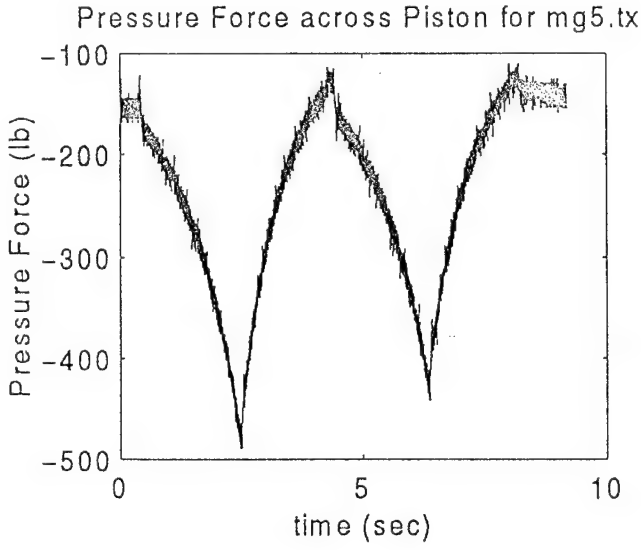
Pressure Force across Piston for mg5.txt
Pressure Force (lb)
time (sec)
-100
-200
-300
-400
-500
0
5
10

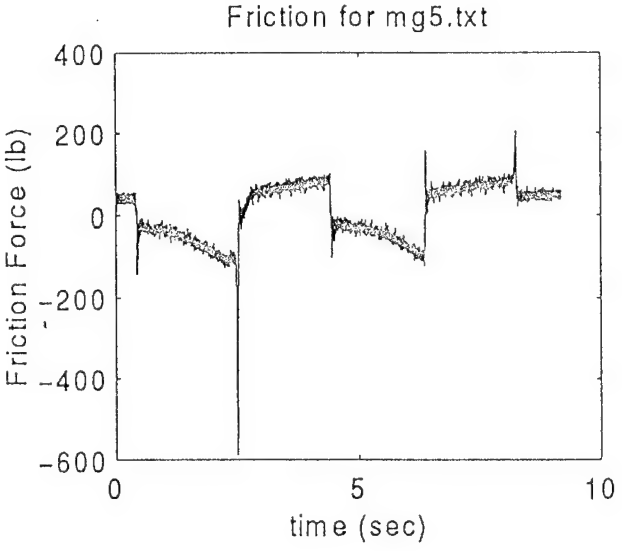
Friction for mg5.txt
Friction Force (lb)
time (sec)
400
200
0
-200
-400
-600
0
5
10

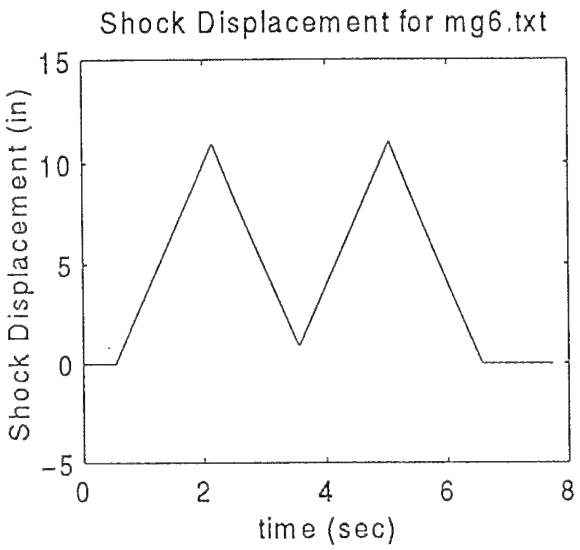
Shock Displacement for mg6.txt
Shock Displacement (in)
15
10
5
0
−5
0
2
4
6
8
time (sec)

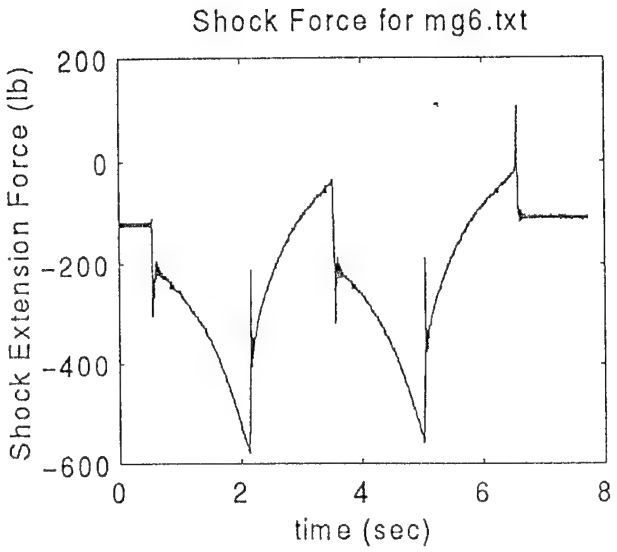
Shock Force for mg6.txt
Shock Extension Force (lb)
200
0
−200
−400
−600
0
2
4
6
8
time (sec)

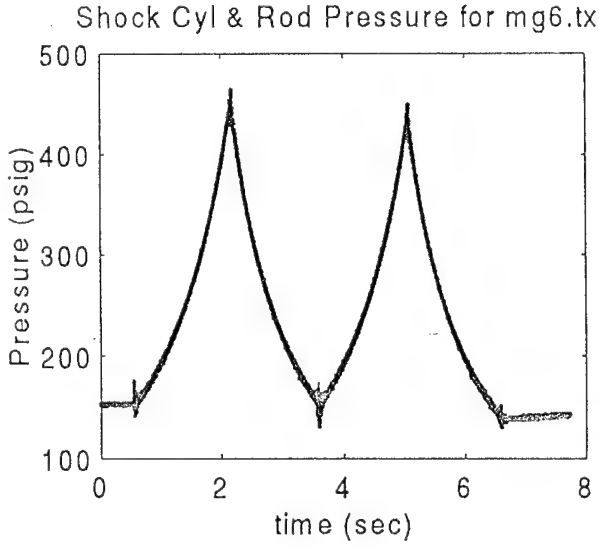
Shock Cyl & Rod Pressure for mg6.txt
Pressure (psig)
500
400
300
200
100
0
2
4
6
8
time (sec)

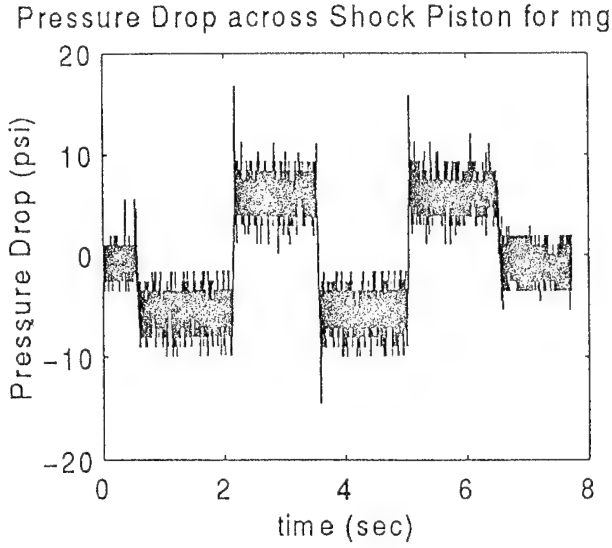
Pressure Drop across Shock Piston for mg6.txt
Pressure Drop (psi)
20
10
0
−10
−20
0
2
4
6
8
time (sec)

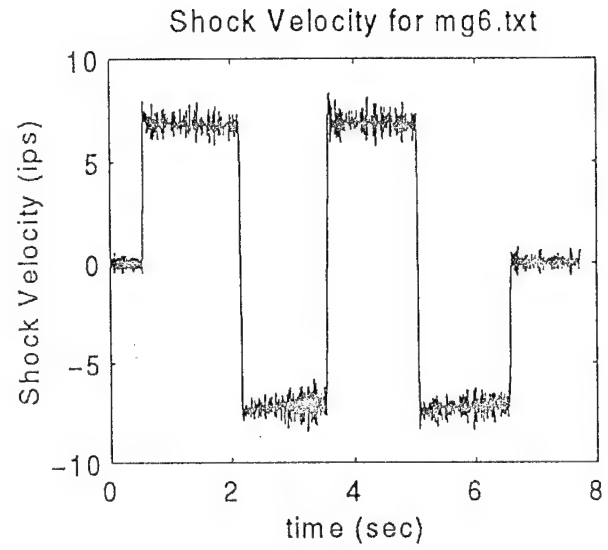
Shock Velocity for mg6.txt
Shock Velocity (ips)
time (sec)
10
5
0
-5
-10
0
2
4
6
8

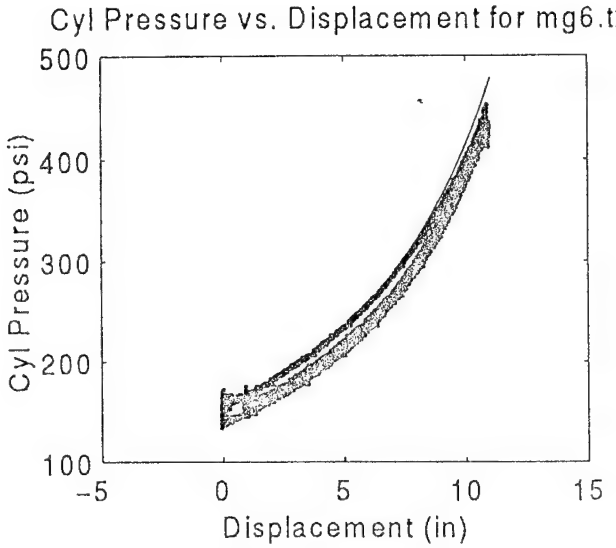
Cyl Pressure vs. Displacement for mg6.txt
Cyl Pressure (psi)
Displacement (in)
500
400
300
200
100
-5
0
5
10
15

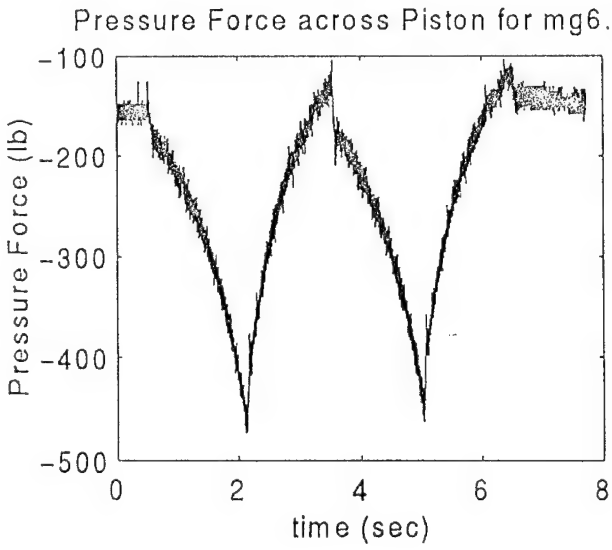
Pressure Force across Piston for mg6.txt
Pressure Force (lb)
time (sec)
-100
-200
-300
-400
-500
0
2
4
6
8

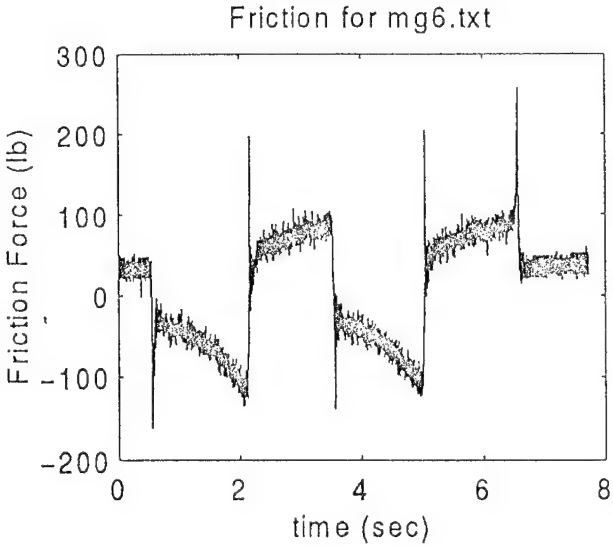
Friction for mg6.txt
Friction Force (lb)
time (sec)
300
200
100
0
-100
-200
0
2
4
6
8

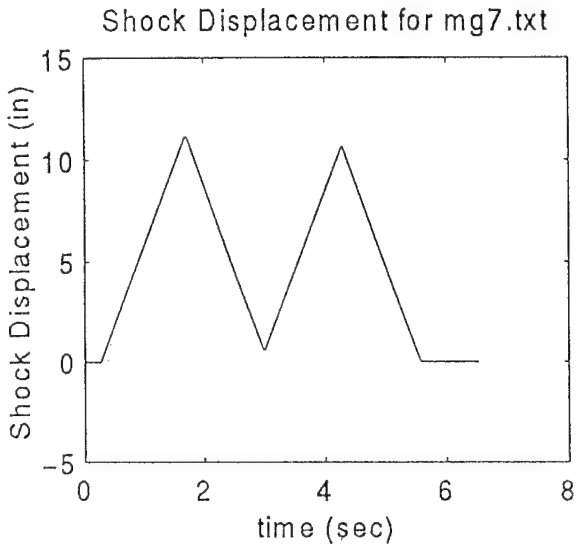
Shock Displacement for mg7.txt
Shock Displacement (in)
15
10
5
0
−5
0
2
4
6
8
time (sec)

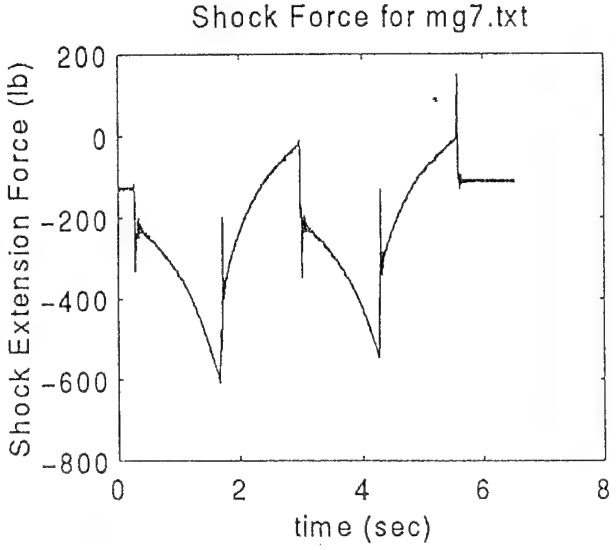
Shock Force for mg7.txt
Shock Extension Force (lb)
200
0
−200
−400
−600
−800
0
2
4
6
8
time (sec)

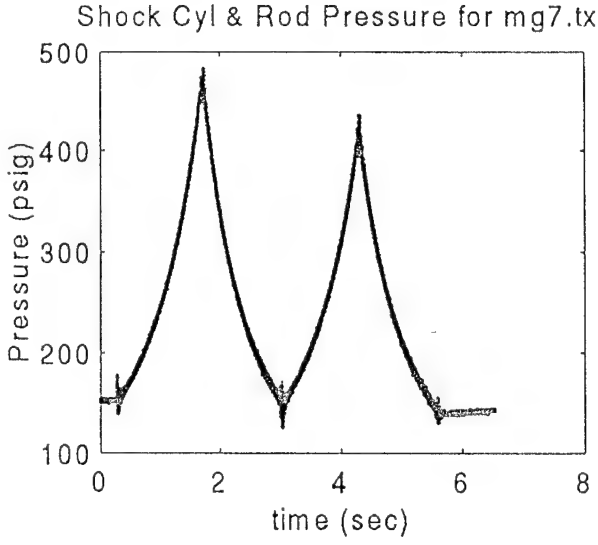
Shock Cyl & Rod Pressure for mg7.txt
Pressure (psig)
500
400
300
200
100
0
2
4
6
8
time (sec)

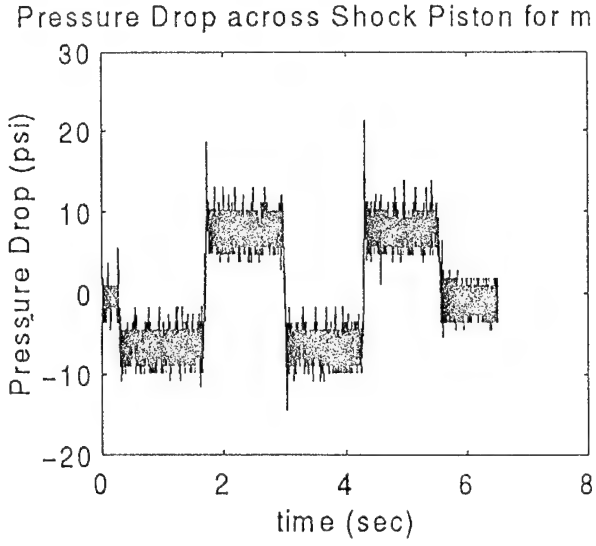
Pressure Drop across Shock Piston for mg7.txt
Pressure Drop (psi)
30
20
10
0
−10
−20
0
2
4
6
8
time (sec)

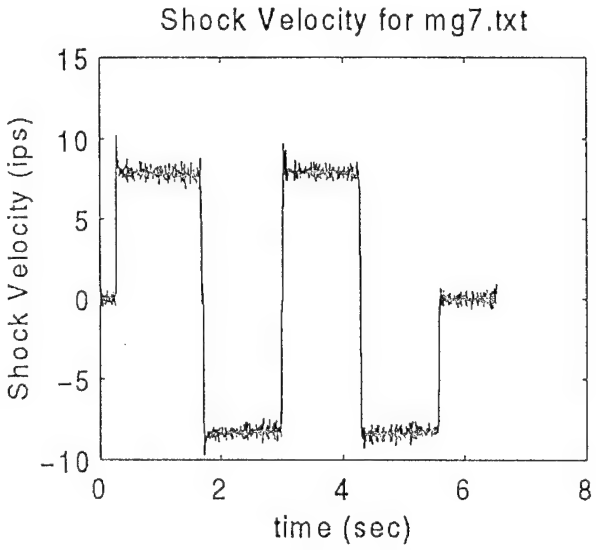
Shock Velocity for mg7.txt
Shock Velocity (ips)
time (sec)
15
10
5
0
-5
-10
0
2
4
6
8

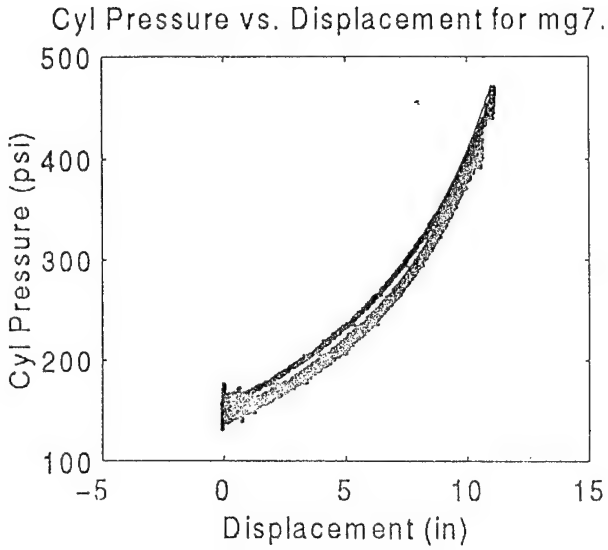
Cyl Pressure vs. Displacement for mg7.txt
Cyl Pressure (psi)
Displacement (in)
500
400
300
200
100
-5
0
5
10
15

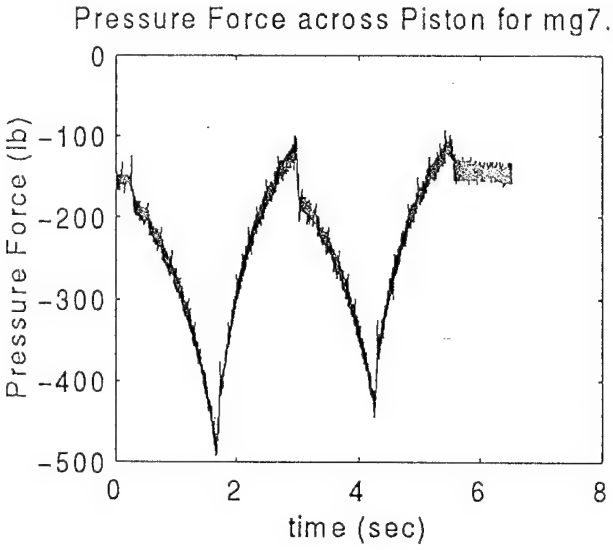
Pressure Force across Piston for mg7.txt
Pressure Force (lb)
time (sec)
0
-100
-200
-300
-400
-500
0
2
4
6
8

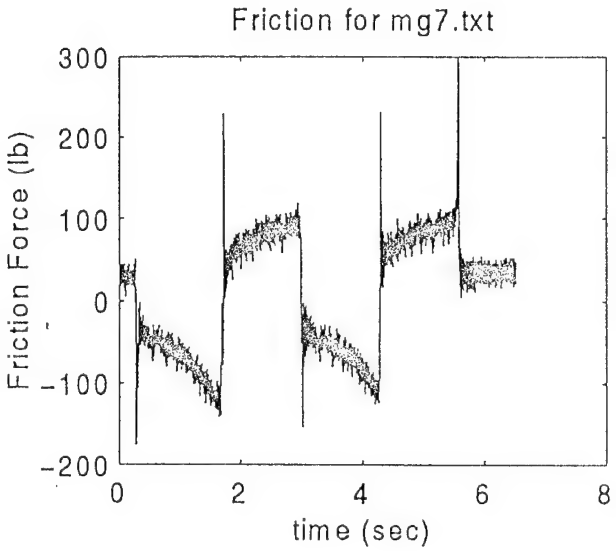
Friction for mg7.txt
Friction Force (lb)
time (sec)
300
200
100
0
-100
-200
0
2
4
6
8

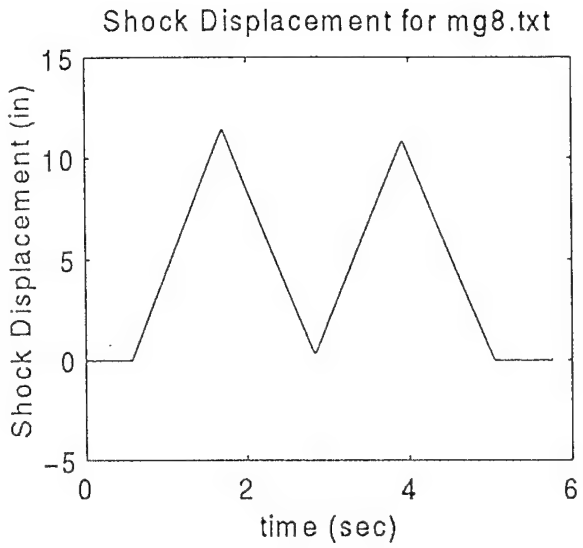
Shock Displacement for mg8.txt
Shock Displacement (in)
15
10
5
0
-5
0
2
4
6
time (sec)

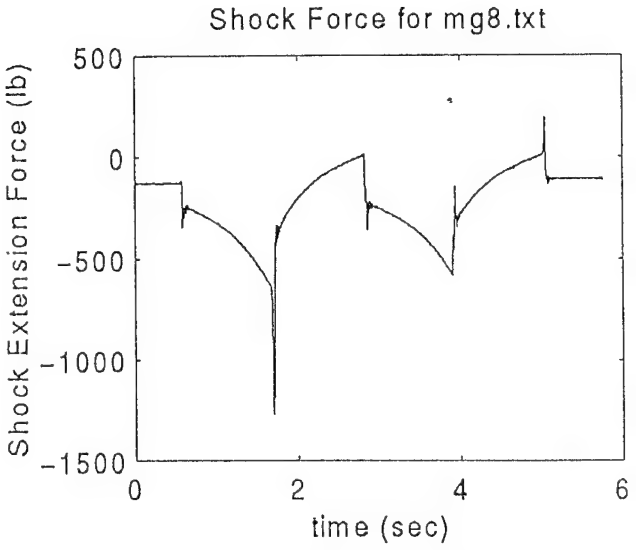
Shock Force for mg8.txt
Shock Extension Force (lb)
500
0
-500
-1000
-1500
0
2
4
6
time (sec)

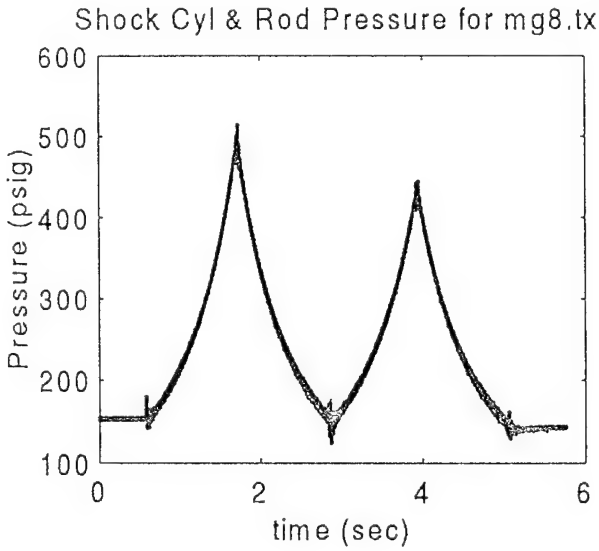
Shock Cyl & Rod Pressure for mg8.txt
Pressure (psig)
600
500
400
300
200
100
0
2
4
6
time (sec)

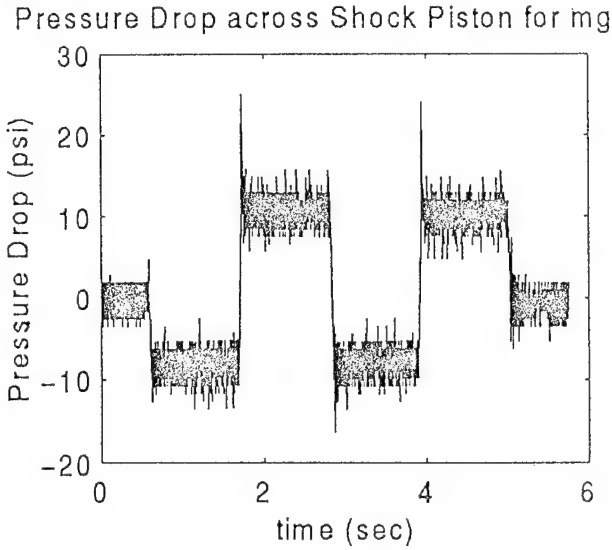
Pressure Drop across Shock Piston for mg8.txt
Pressure Drop (psi)
30
20
10
0
-10
-20
0
2
4
6
time (sec)

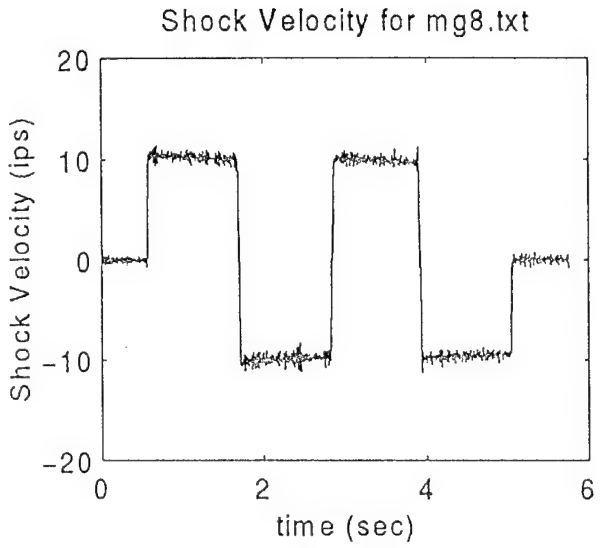
Shock Velocity for mg8.txt
Shock Velocity (ips)
time (sec)
20
10
0
-10
-20
0
2
4
6

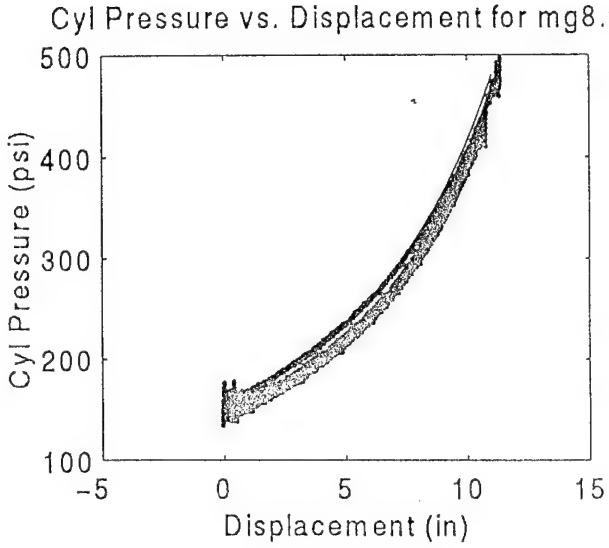
Cyl Pressure vs. Displacement for mg8.txt
Cyl Pressure (psi)
Displacement (in)
500
400
300
200
100
-5
0
5
10
15

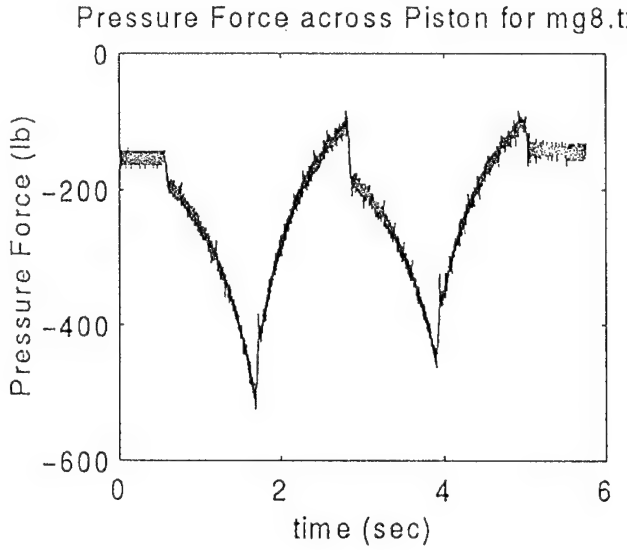
Pressure Force across Piston for mg8.txt
Pressure Force (lb)
time (sec)
0
-200
-400
-600
0
2
4
6

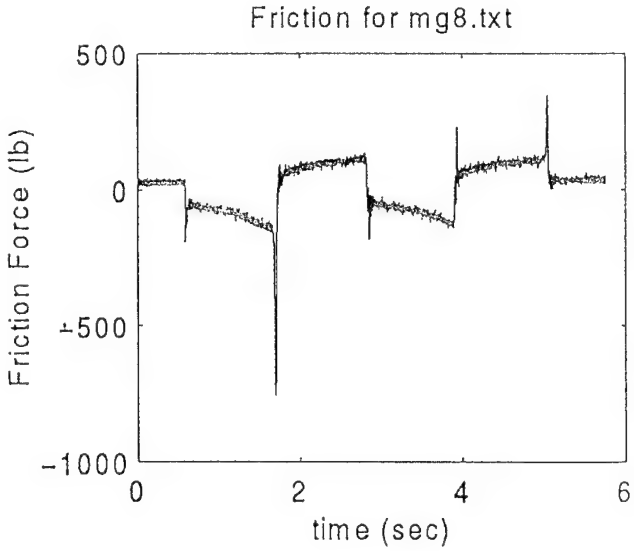
Friction for mg8.txt
Friction Force (lb)
time (sec)
500
0
-500
-1000
0
2
4
6

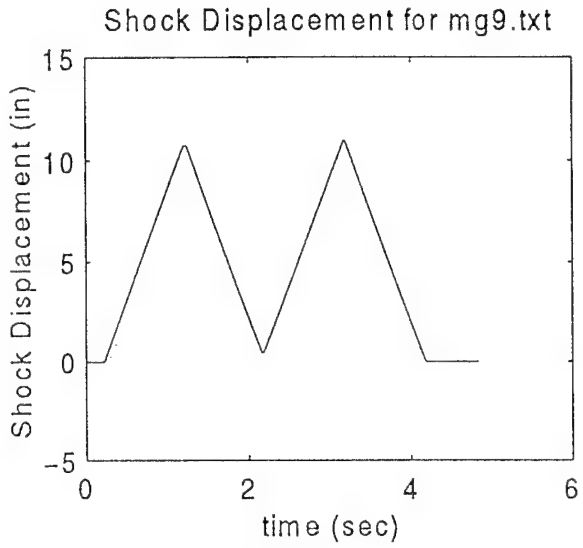
Shock Displacement for mg9.txt
Shock Displacement (in)
time (sec)
15
10
5
0
−5
0
2
4
6

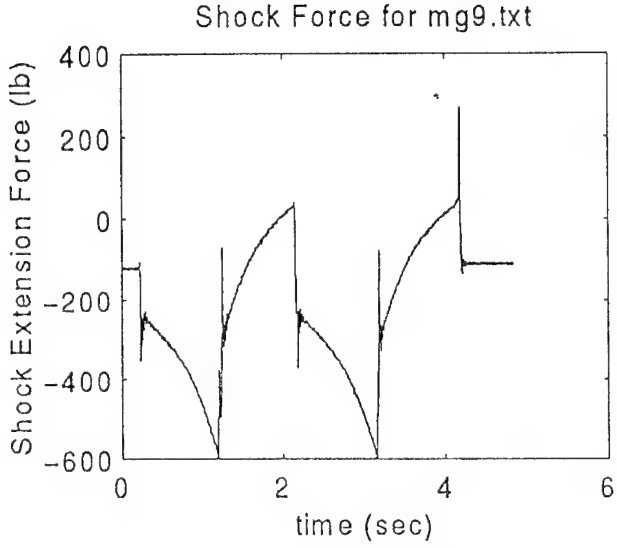
Shock Force for mg9.txt
Shock Extension Force (lb)
time (sec)
400
200
0
−200
−400
−600
0
2
4
6

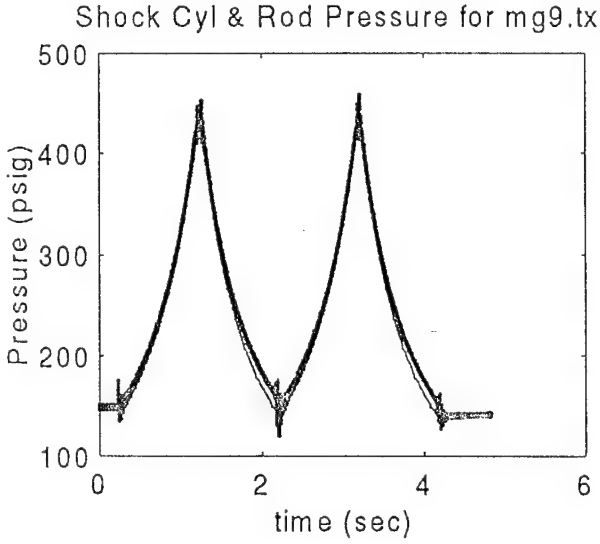
Shock Cyl & Rod Pressure for mg9.txt
Pressure (psig)
time (sec)
500
400
300
200
100
0
2
4
6

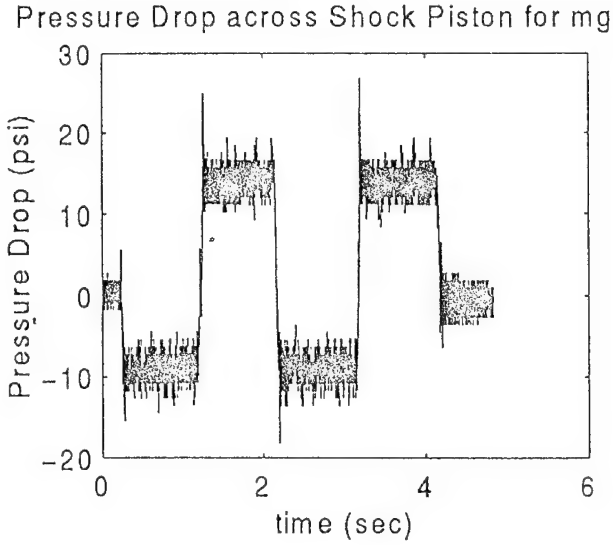
Pressure Drop across Shock Piston for mg9.txt
Pressure Drop (psi)
time (sec)
30
20
10
0
−10
−20
0
2
4
6

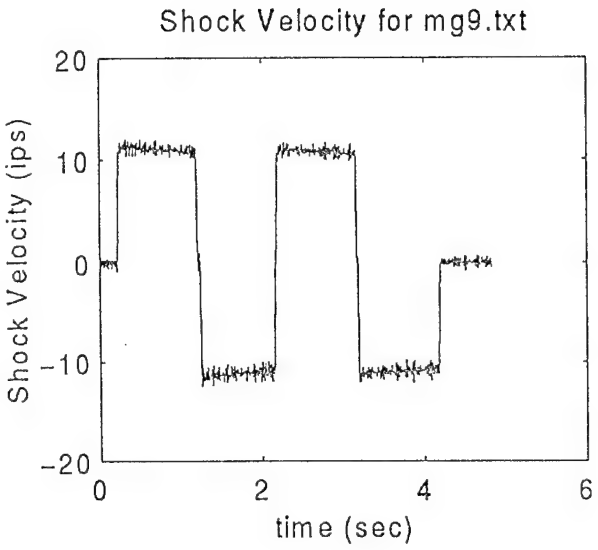
Shock Velocity for mg9.txt
Shock Velocity (ips)
time (sec)
20
10
0
-10
-20
0
2
4
6

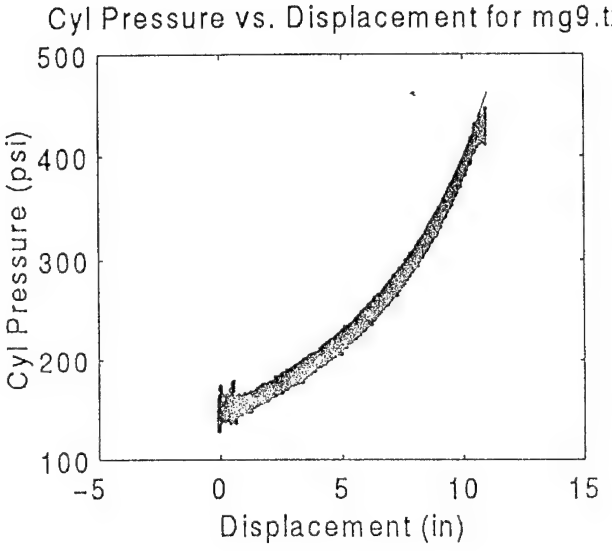
Cyl Pressure vs. Displacement for mg9.txt
Cyl Pressure (psi)
Displacement (in)
500
400
300
200
100
-5
0
5
10
15

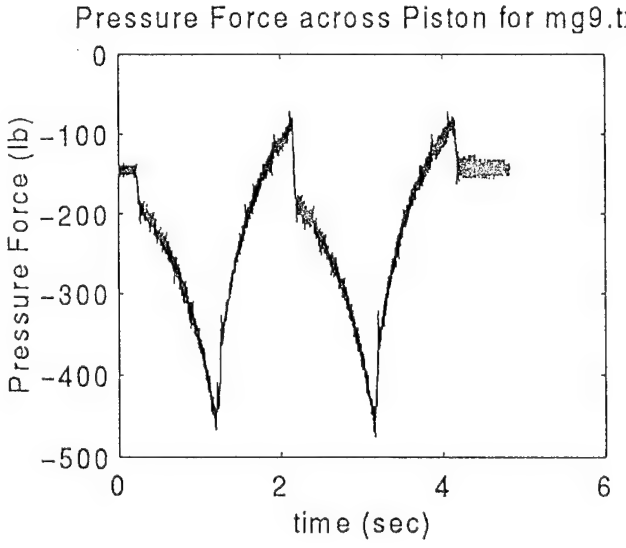
Pressure Force across Piston for mg9.txt
Pressure Force (lb)
time (sec)
0
-100
-200
-300
-400
-500
0
2
4
6

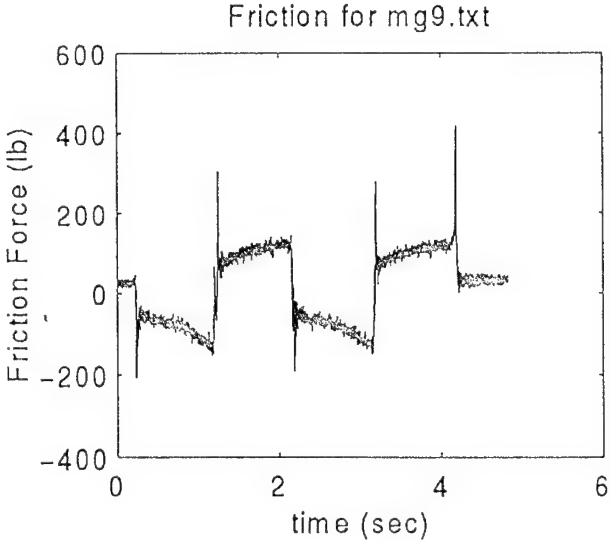
Friction for mg9.txt
Friction Force (lb)
time (sec)
600
400
200
0
-200
-400
0
2
4
6

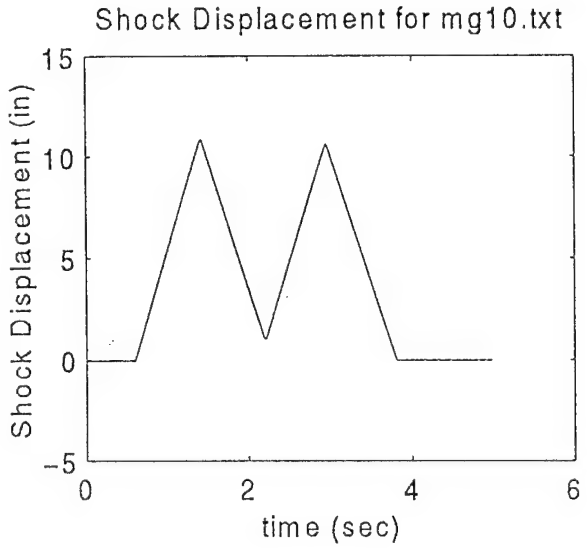
Shock Displacement for mg10.txt
Shock Displacement (in)
15
10
5
0
−5
0
2
4
6
time (sec)

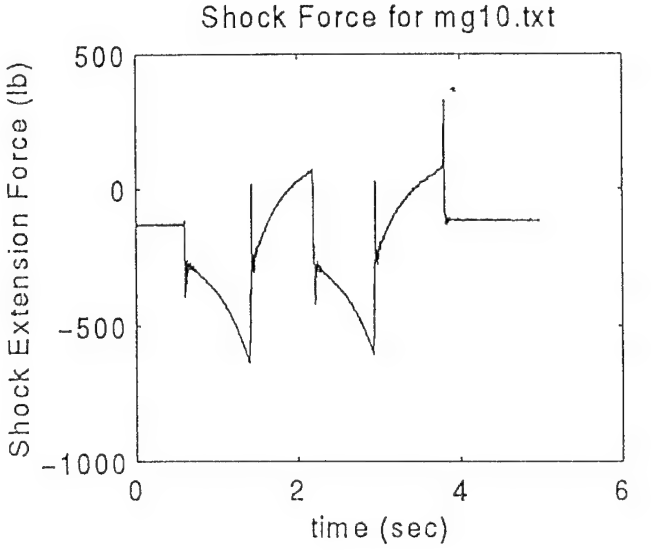
Shock Force for mg10.txt
Shock Extension Force (lb)
500
0
−500
−1000
0
2
4
6
time (sec)

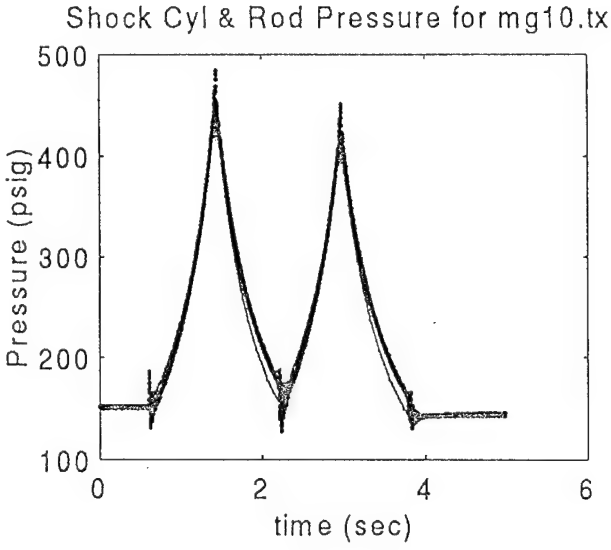
Shock Cyl & Rod Pressure for mg10.txt
Pressure (psig)
500
400
300
200
100
0
2
4
6
time (sec)

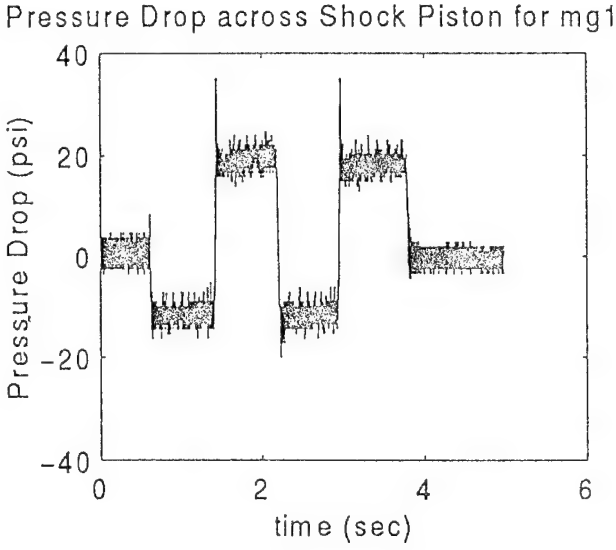
Pressure Drop across Shock Piston for mg10.txt
Pressure Drop (psi)
40
20
0
−20
−40
0
2
4
6
time (sec)

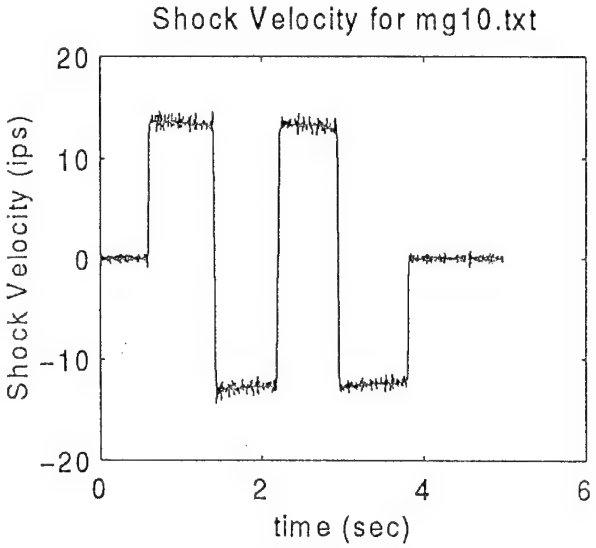
Shock Velocity for mg10.txt
Shock Velocity (ips)
time (sec)
20
10
0
-10
-20
0
2
4
6

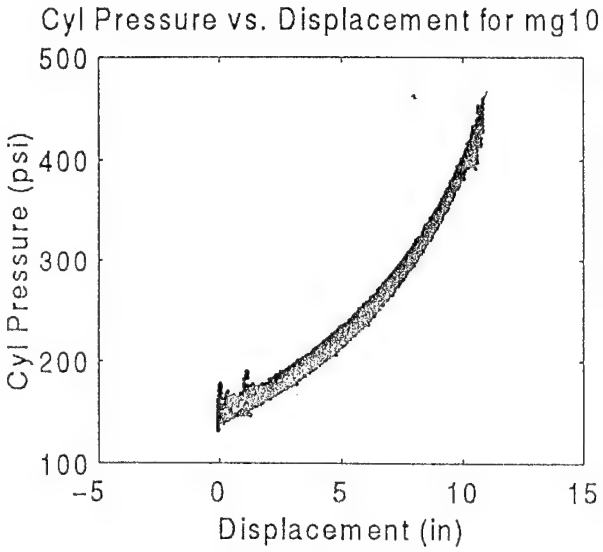
Cyl Pressure vs. Displacement for mg10.txt
Cyl Pressure (psi)
Displacement (in)
500
400
300
200
100
-5
0
5
10
15

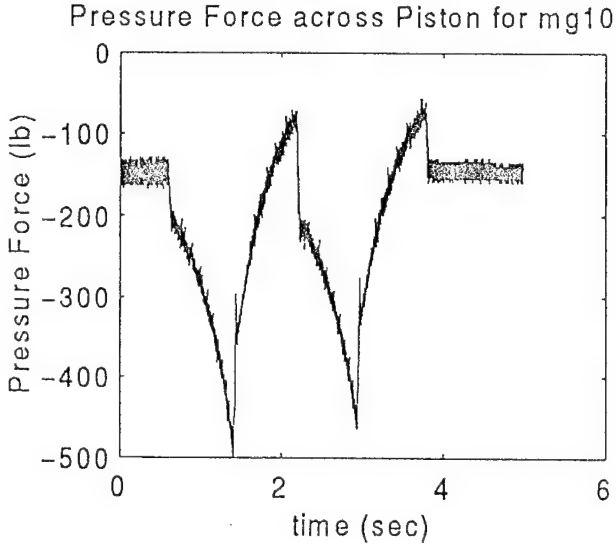
Pressure Force across Piston for mg10.txt
Pressure Force (lb)
time (sec)
0
-100
-200
-300
-400
-500
0
2
4
6

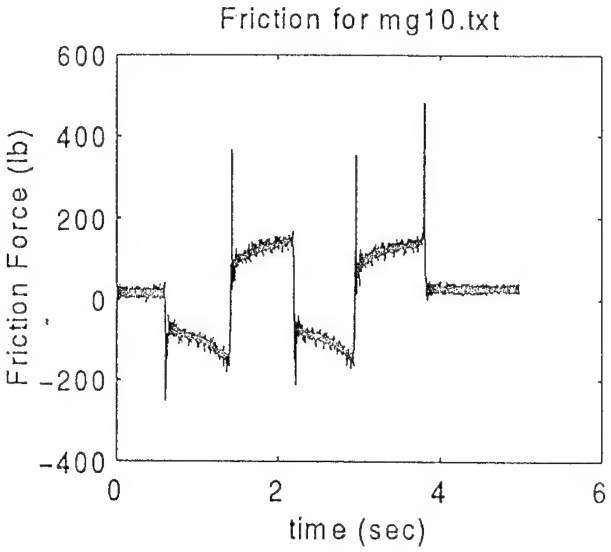
Friction for mg10.txt
Friction Force (lb)
time (sec)
600
400
200
0
-200
-400
0
2
4
6

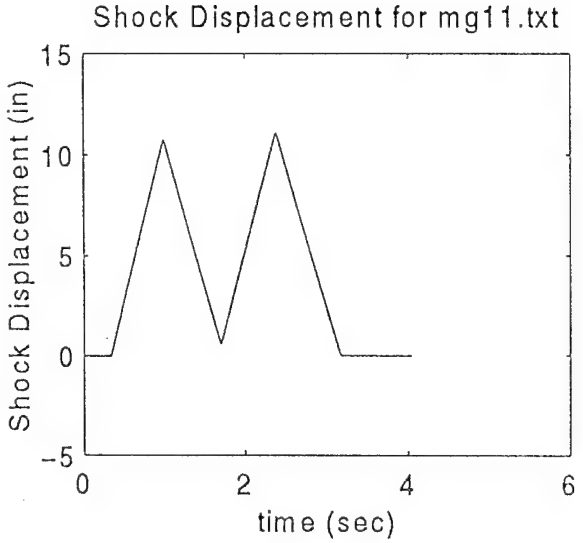
Shock Displacement for mg11.txt
Shock Displacement (in)
15
10
5
0
−5
0
2
4
6
time (sec)

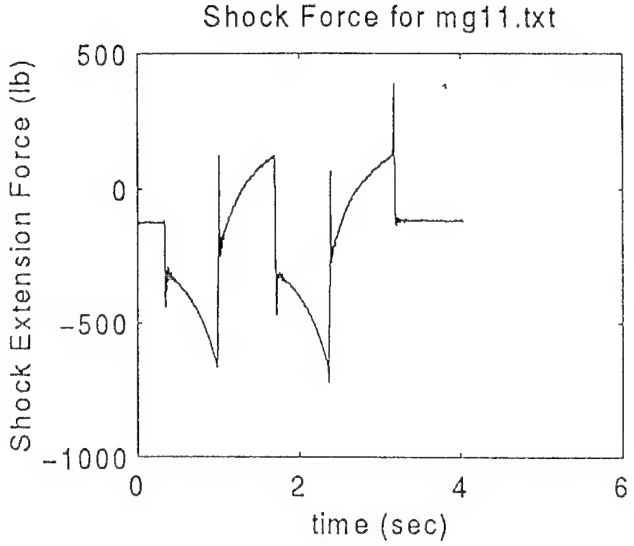
Shock Force for mg11.txt
Shock Extension Force (lb)
500
0
−500
−1000
0
2
4
6
time (sec)

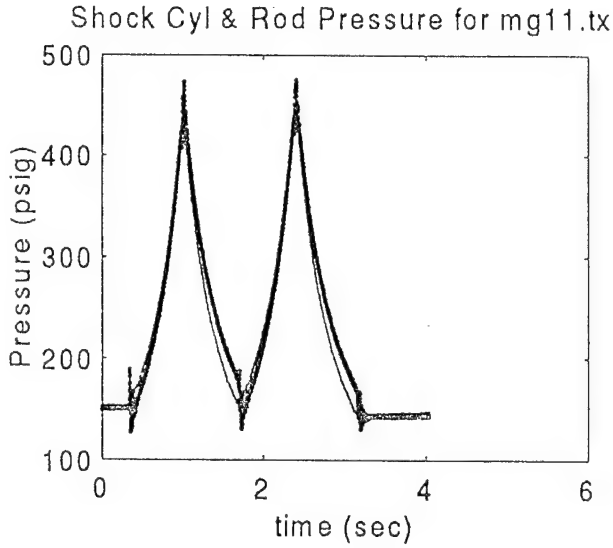
Shock Cyl & Rod Pressure for mg11.txt
Pressure (psig)
500
400
300
200
100
0
2
4
6
time (sec)

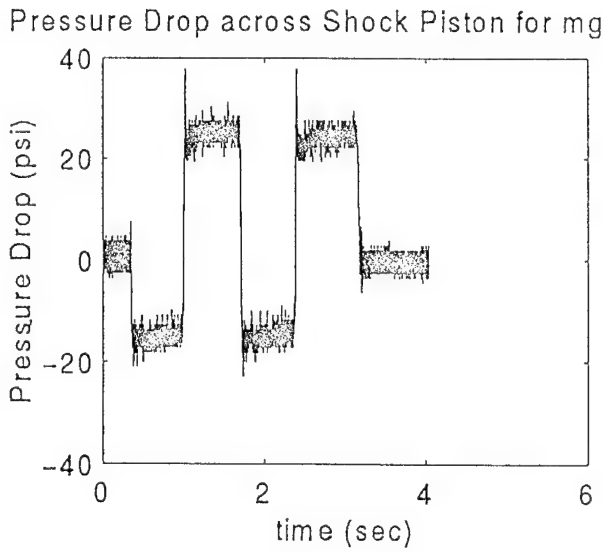
Pressure Drop across Shock Piston for mg11.txt
Pressure Drop (psi)
40
20
0
−20
−40
0
2
4
6
time (sec)

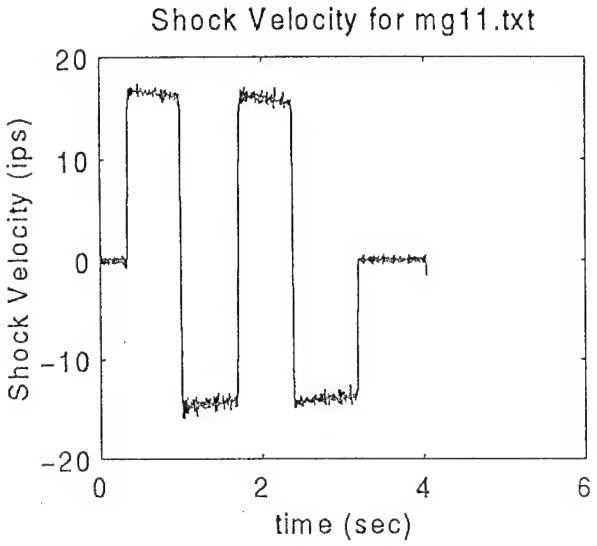
Shock Velocity for mg11.txt
Shock Velocity (ips)
time (sec)
20
10
0
-10
-20
0
2
4
6

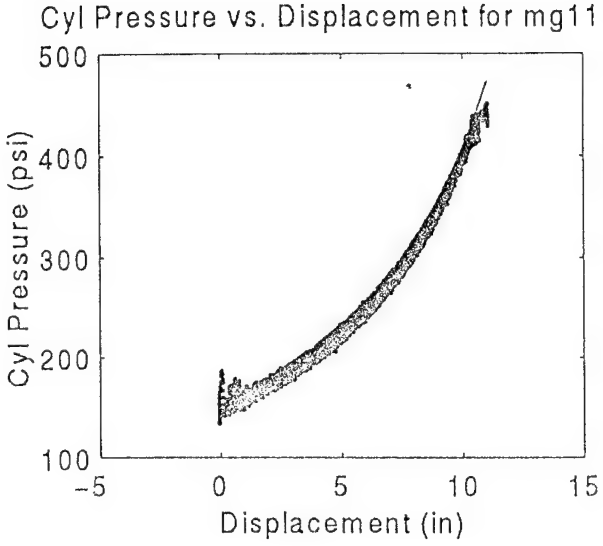
Cyl Pressure vs. Displacement for mg11.txt
Cyl Pressure (psi)
Displacement (in)
500
400
300
200
100
-5
0
5
10
15

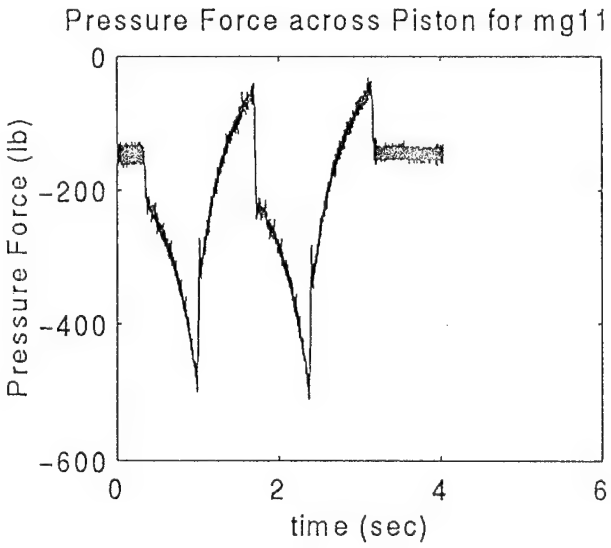
Pressure Force across Piston for mg11.txt
Pressure Force (lb)
time (sec)
0
-200
-400
-600
0
2
4
6

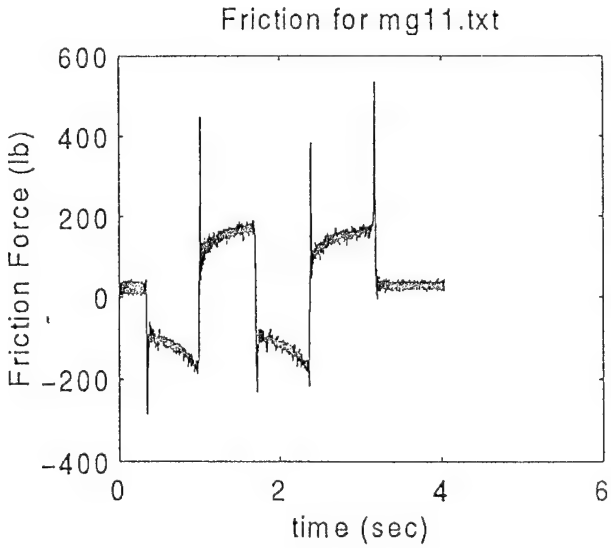
Friction for mg11.txt
Friction Force (lb)
time (sec)
600
400
200
0
-200
-400
0
2
4
6

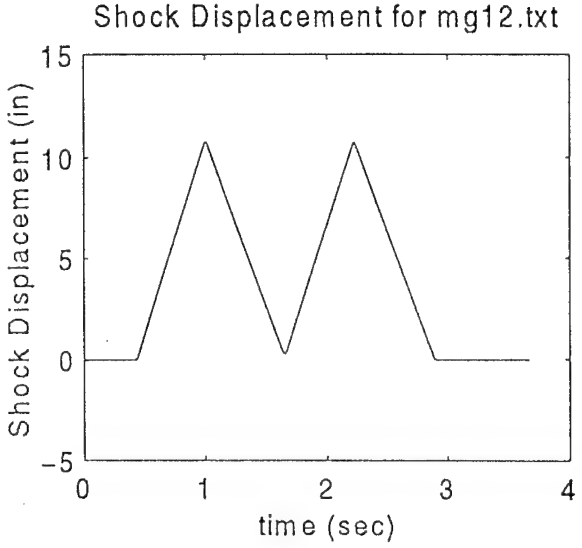
Shock Displacement for mg12.txt
Shock Displacement (in)
15
10
5
0
−5
0
1
2
3
4
time (sec)

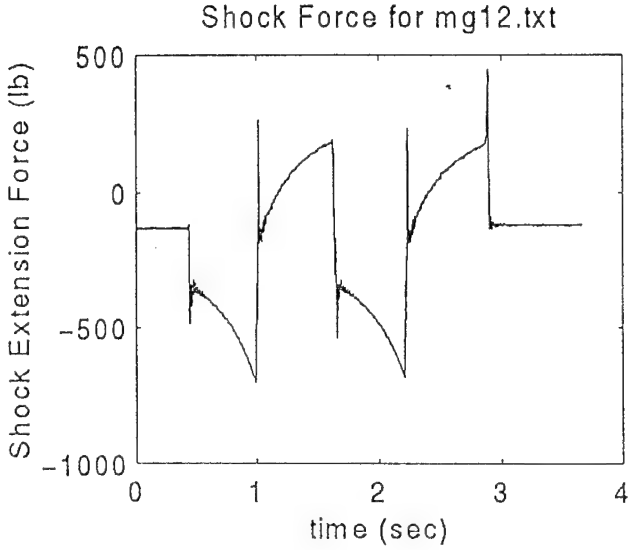
Shock Force for mg12.txt
Shock Extension Force (lb)
500
0
−500
−1000
0
1
2
3
4
time (sec)

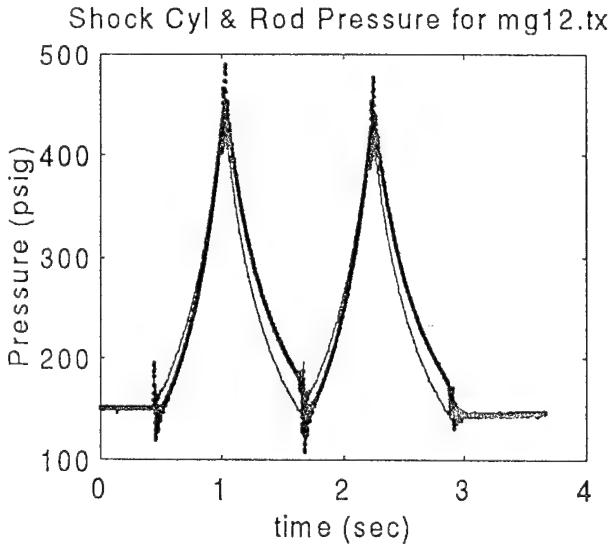
Shock Cyl & Rod Pressure for mg12.txt
Pressure (psig)
500
400
300
200
100
0
1
2
3
4
time (sec)

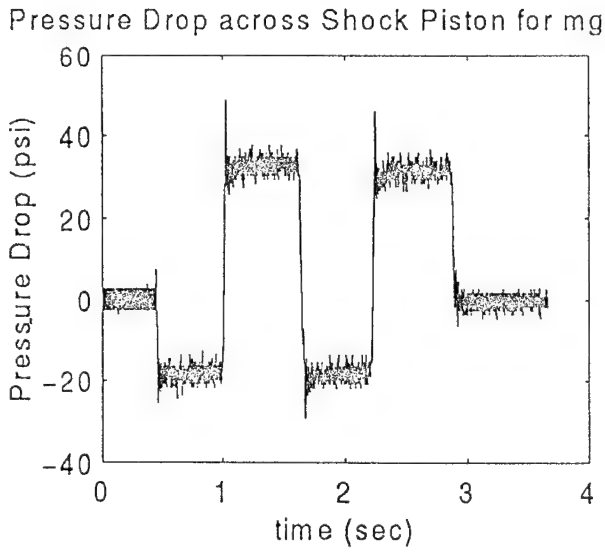
Pressure Drop across Shock Piston for mg12.txt
Pressure Drop (psi)
60
40
20
0
−20
−40
0
1
2
3
4
time (sec)

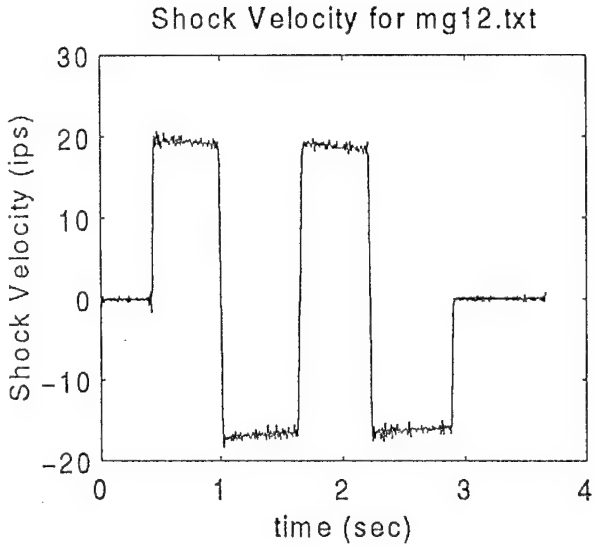
Shock Velocity for mg12.txt
Shock Velocity (ips)
time (sec)
30
20
10
0
-10
-20
0
1
2
3
4

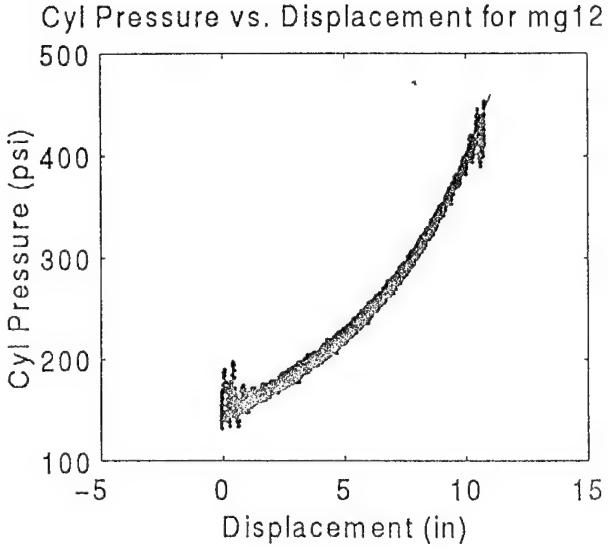
Cyl Pressure vs. Displacement for mg12.txt
Cyl Pressure (psi)
Displacement (in)
500
400
300
200
100
-5
0
5
10
15

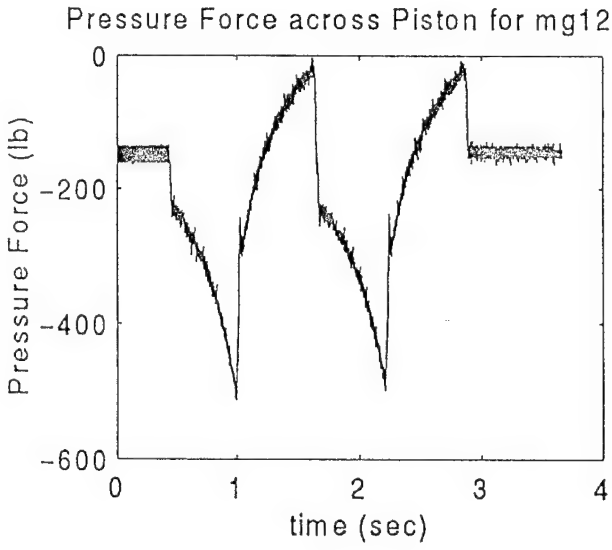
Pressure Force across Piston for mg12.txt
Pressure Force (lb)
time (sec)
0
-200
-400
-600
0
1
2
3
4

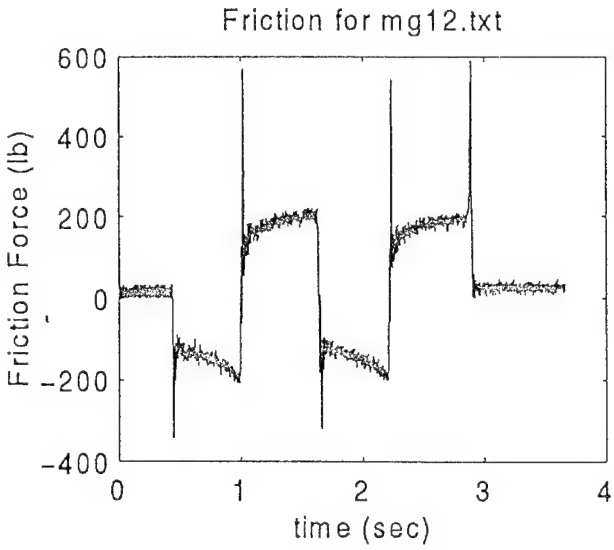
Friction for mg12.txt
Friction Force (lb)
time (sec)
600
400
200
0
-200
-400
0
1
2
3
4

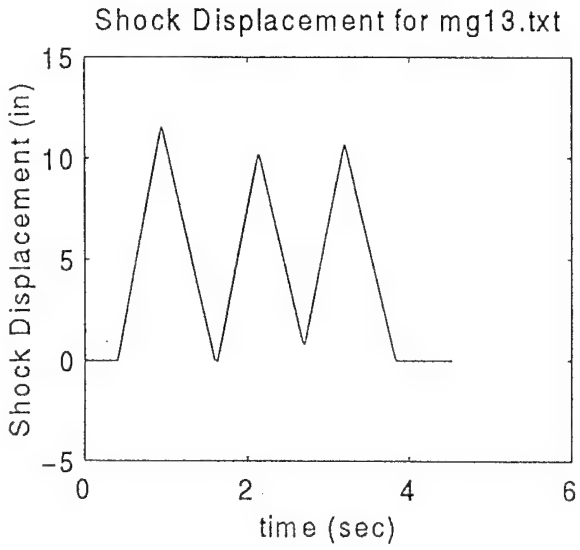
Shock Displacement for mg13.txt
Shock Displacement (in)
15
10
5
0
−5
0
2
4
6
time (sec)

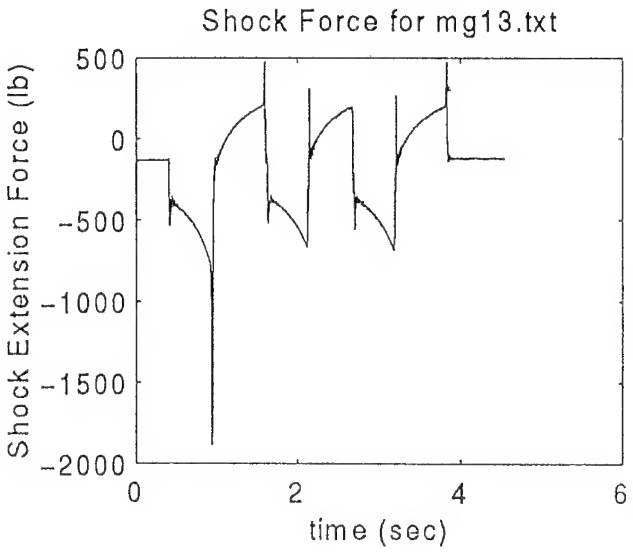
Shock Force for mg13.txt
Shock Extension Force (lb)
500
0
−500
−1000
−1500
−2000
0
2
4
6
time (sec)

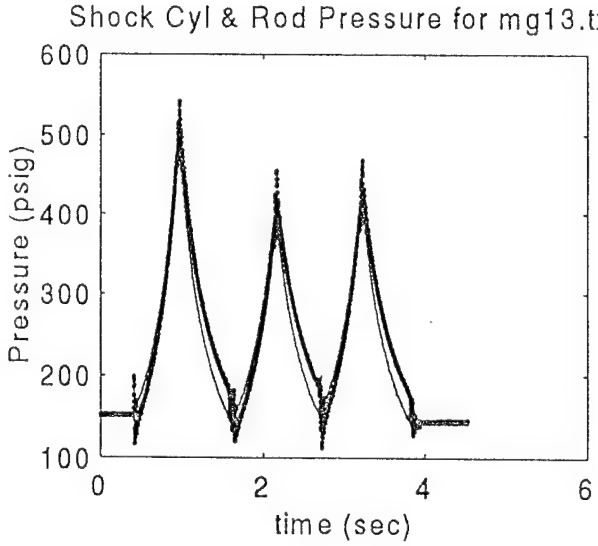
Shock Cyl & Rod Pressure for mg13.txt
Pressure (psig)
600
500
400
300
200
100
0
2
4
6
time (sec)

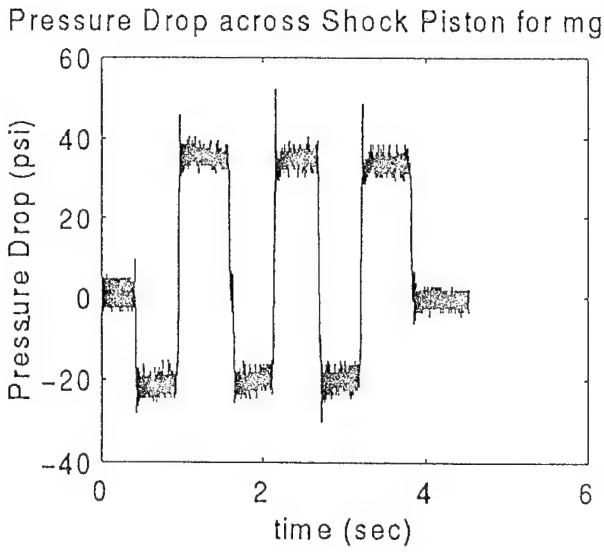
Pressure Drop across Shock Piston for mg13.txt
Pressure Drop (psi)
60
40
20
0
−20
−40
0
2
4
6
time (sec)

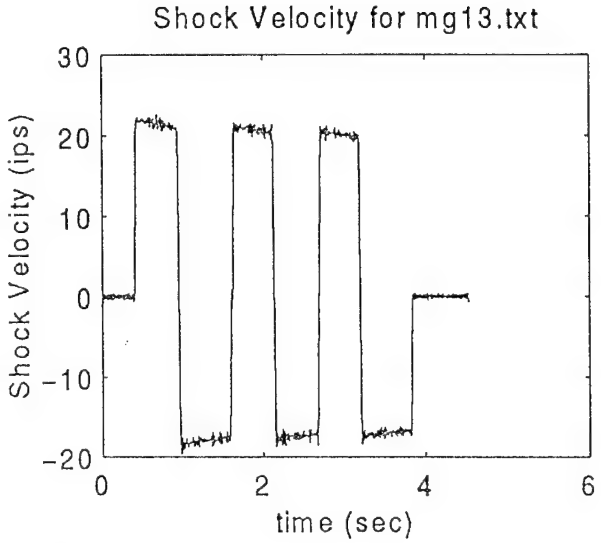
Shock Velocity for mg13.txt
Shock Velocity (ips)
time (sec)
30
20
10
0
-10
-20
0
2
4
6

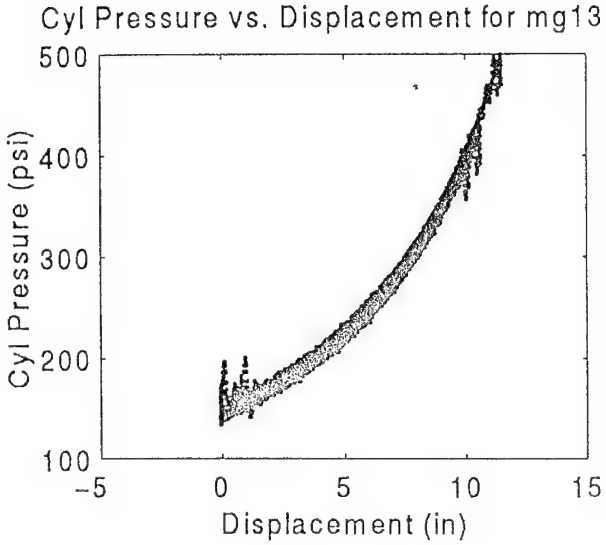
Cyl Pressure vs. Displacement for mg13.txt
Cyl Pressure (psi)
Displacement (in)
500
400
300
200
100
-5
0
5
10
15

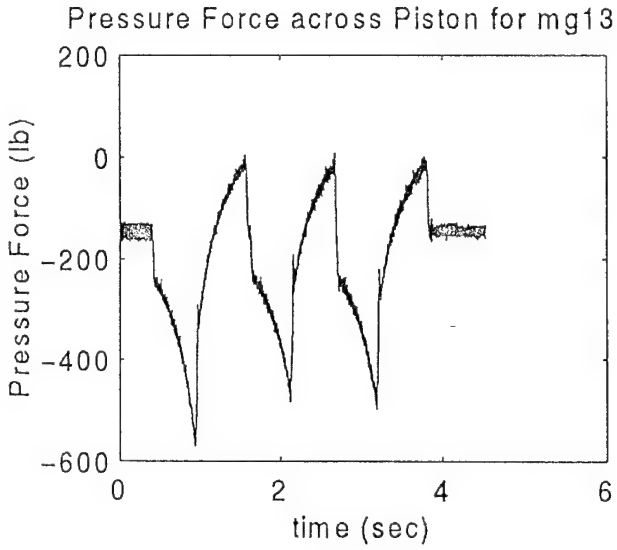
Pressure Force across Piston for mg13.txt
Pressure Force (lb)
time (sec)
200
0
-200
-400
-600
0
2
4
6

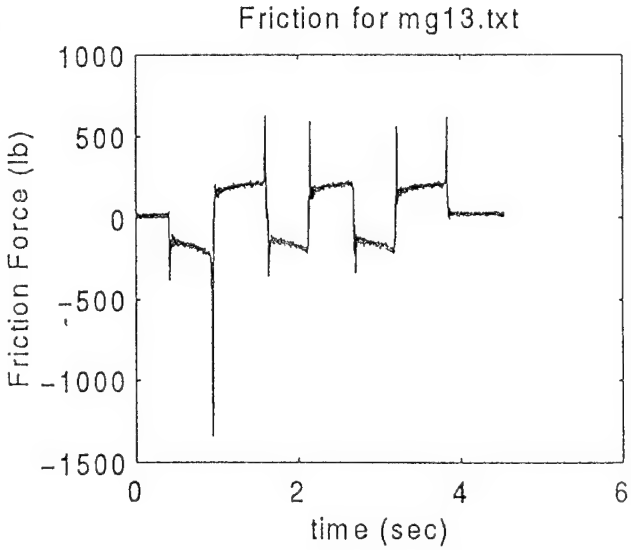
Friction for mg13.txt
Friction Force (lb)
time (sec)
1000
500
0
-500
-1000
-1500
0
2
4
6

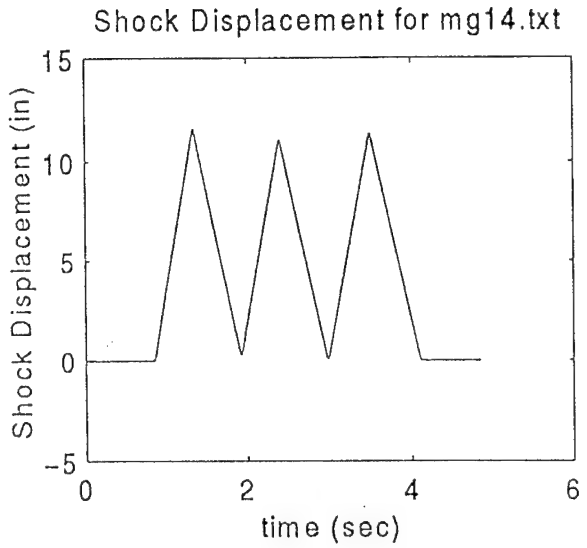
Shock Displacement for mg14.txt
Shock Displacement (in)
15
10
5
0
−5
0
2
4
6
time (sec)

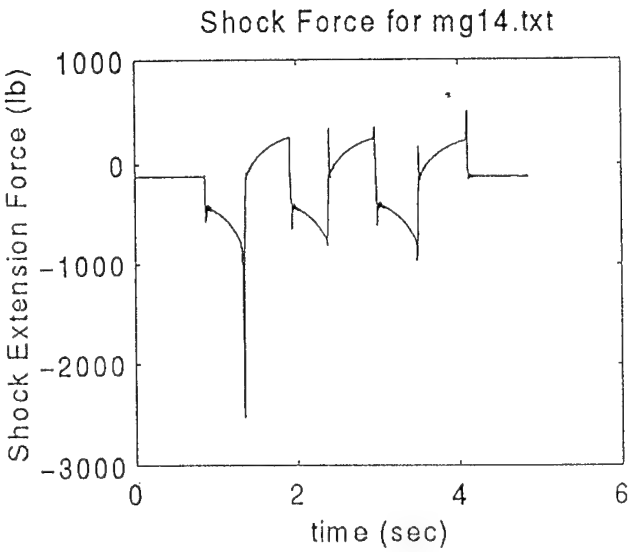
Shock Force for mg14.txt
Shock Extension Force (lb)
1000
0
−1000
−2000
−3000
0
2
4
6
time (sec)

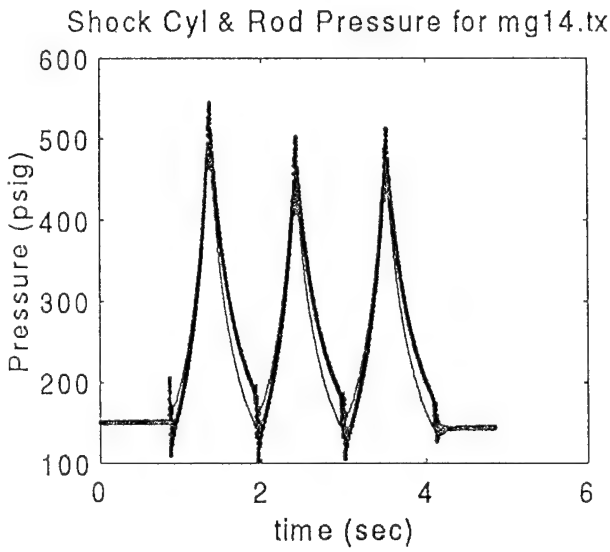
Shock Cyl & Rod Pressure for mg14.txt
Pressure (psig)
600
500
400
300
200
100
0
2
4
6
time (sec)

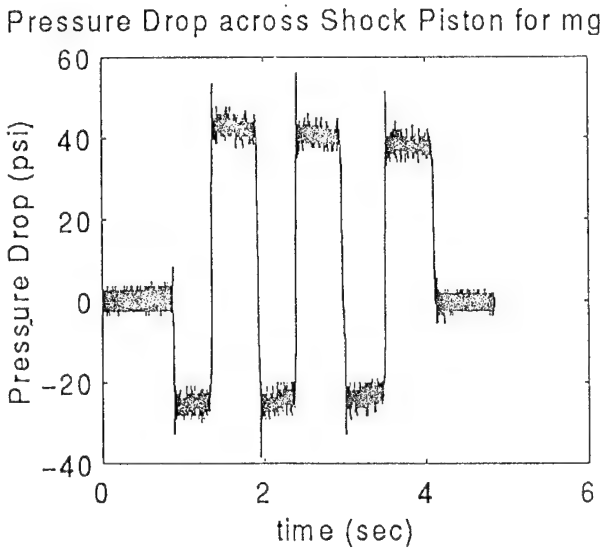
Pressure Drop across Shock Piston for mg14.txt
Pressure Drop (psi)
60
40
20
0
−20
−40
0
2
4
6
time (sec)

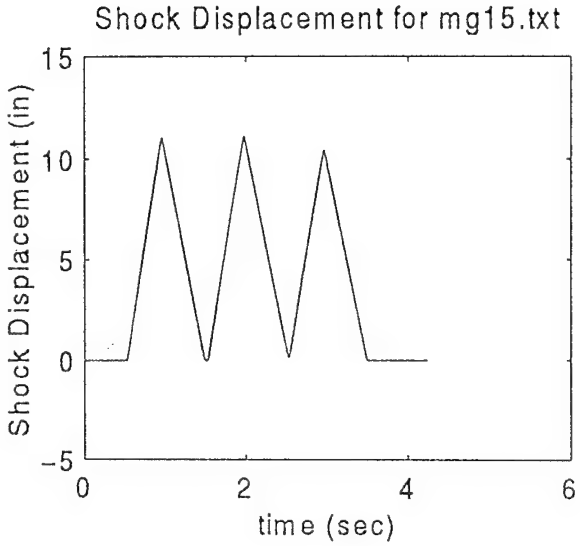
Shock Displacement for mg15.txt
Shock Displacement (in)
15
10
5
0
−5
0
2
4
6
time (sec)

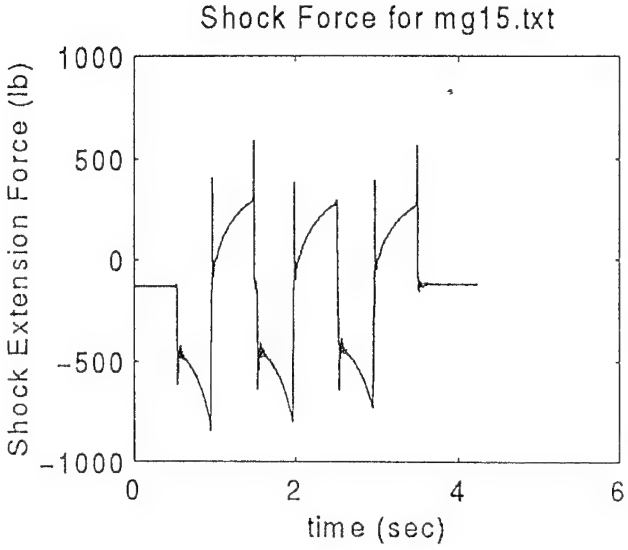
Shock Force for mg15.txt
Shock Extension Force (lb)
1000
500
0
−500
−1000
0
2
4
6
time (sec)

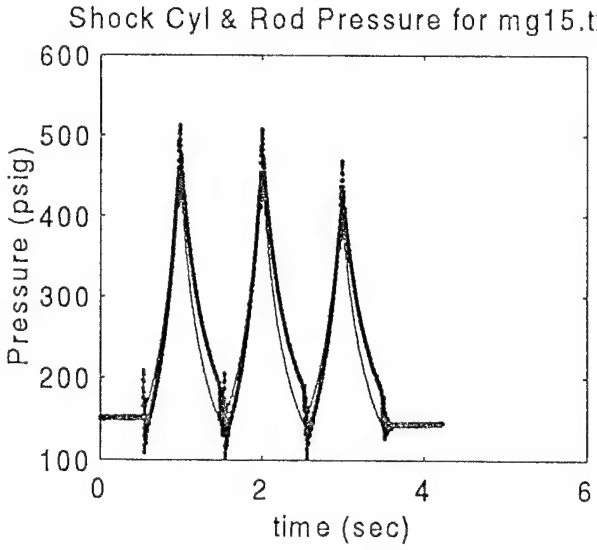
Shock Cyl & Rod Pressure for mg15.txt
Pressure (psig)
600
500
400
300
200
100
0
2
4
6
time (sec)

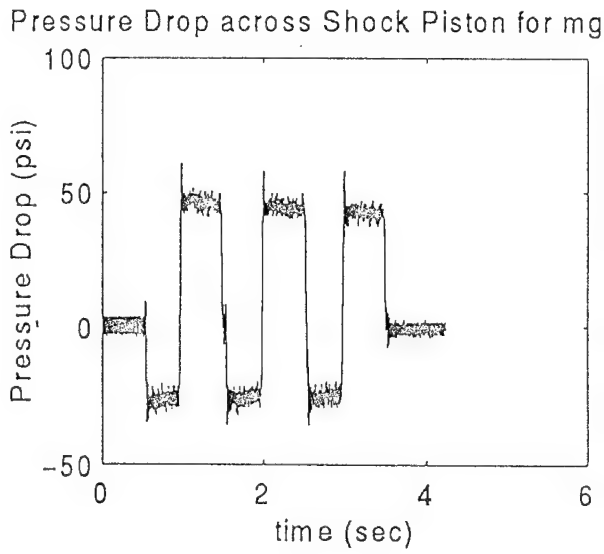
Pressure Drop across Shock Piston for mg15.txt
Pressure Drop (psi)
100
50
0
−50
0
2
4
6
time (sec)

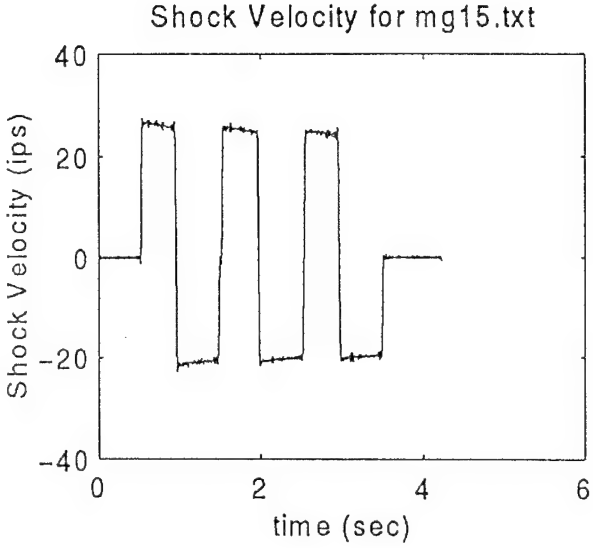
Shock Velocity for mg15.txt
Shock Velocity (ips)
time (sec)
40
20
0
-20
-40
0
2
4
6

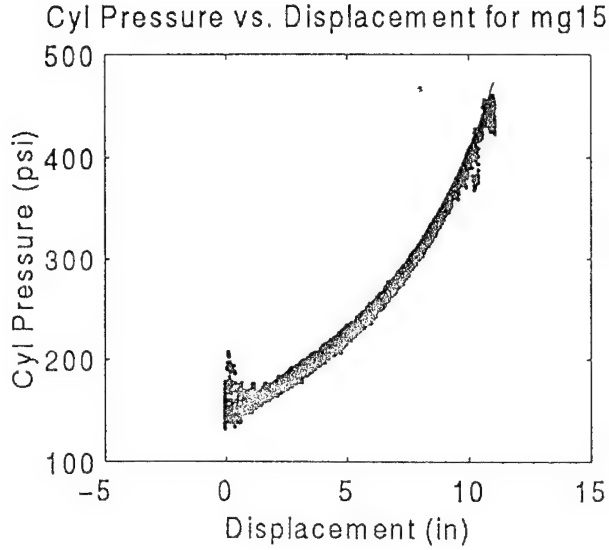
Cyl Pressure vs. Displacement for mg15.txt
Cyl Pressure (psi)
Displacement (in)
500
400
300
200
100
-5
0
5
10
15

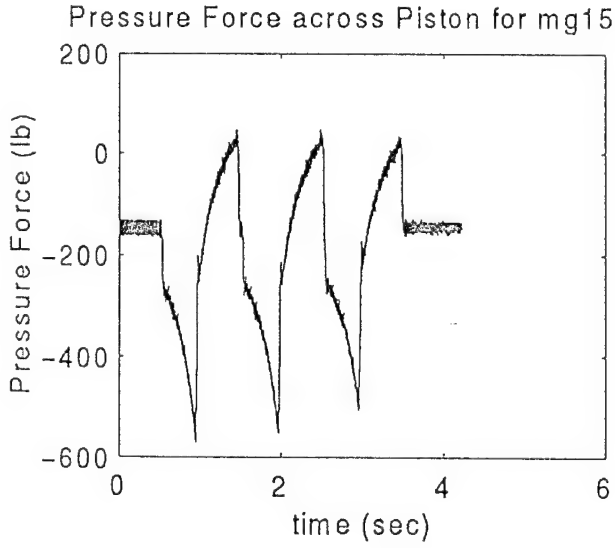
Pressure Force across Piston for mg15.txt
Pressure Force (lb)
time (sec)
200
0
-200
-400
-600
0
2
4
6

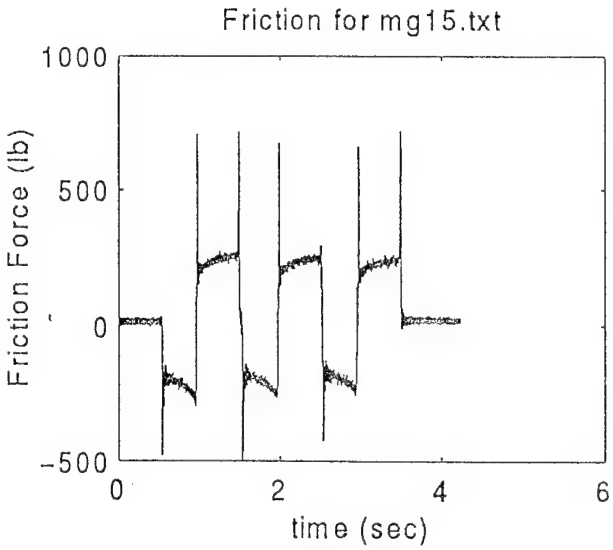
Friction for mg15.txt
Friction Force (lb)
time (sec)
1000
500
0
-500
0
2
4
6

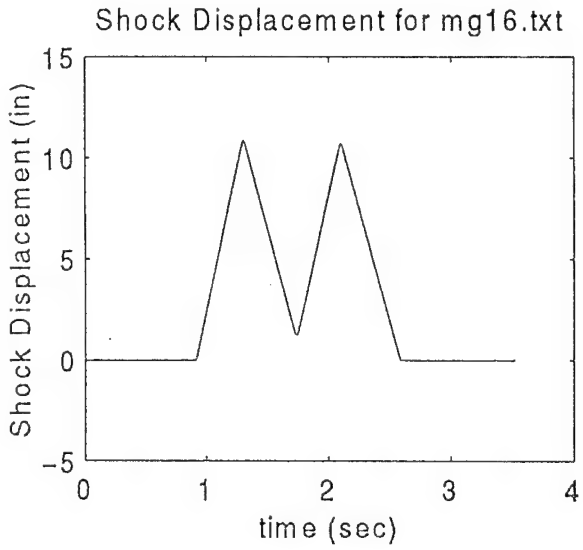
Shock Displacement for mg16.txt
Shock Displacement (in)
15
10
5
0
−5
0
1
2
3
4
time (sec)

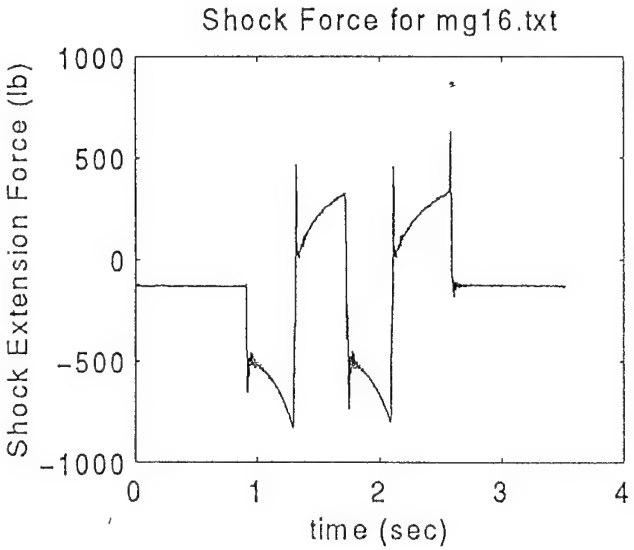
Shock Force for mg16.txt
Shock Extension Force (lb)
1000
500
0
−500
−1000
0
1
2
3
4
time (sec)

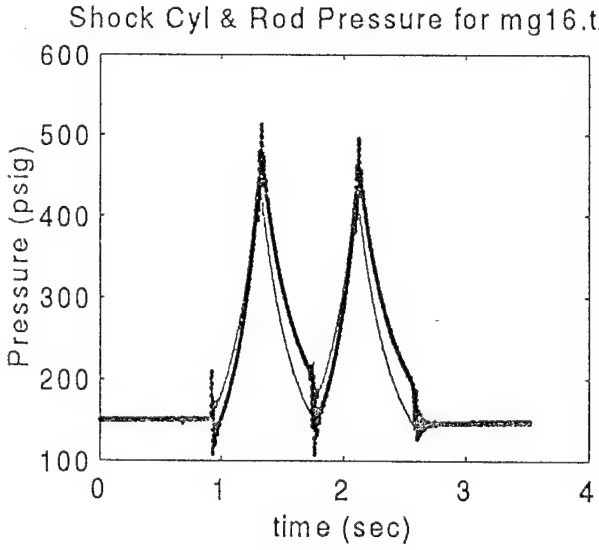
Shock Cyl & Rod Pressure for mg16.txt
Pressure (psig)
600
500
400
300
200
100
0
1
2
3
4
time (sec)

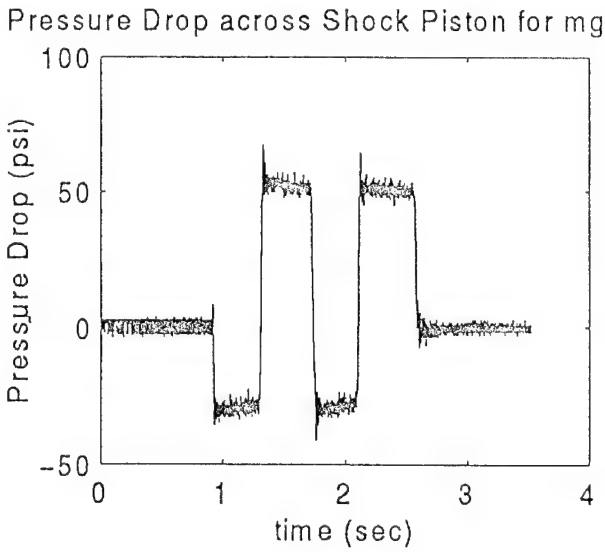
Pressure Drop across Shock Piston for mg16.txt
Pressure Drop (psi)
100
50
0
−50
0
1
2
3
4
time (sec)

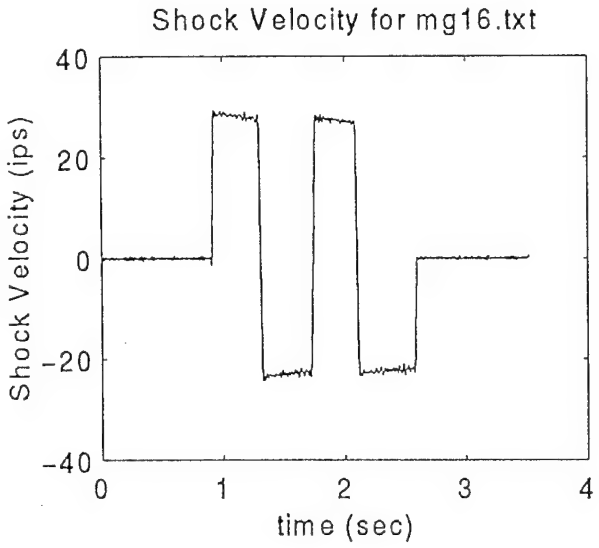
Shock Velocity for mg16.txt
Shock Velocity (ips)
time (sec)
40
20
0
-20
-40
0
1
2
3
4

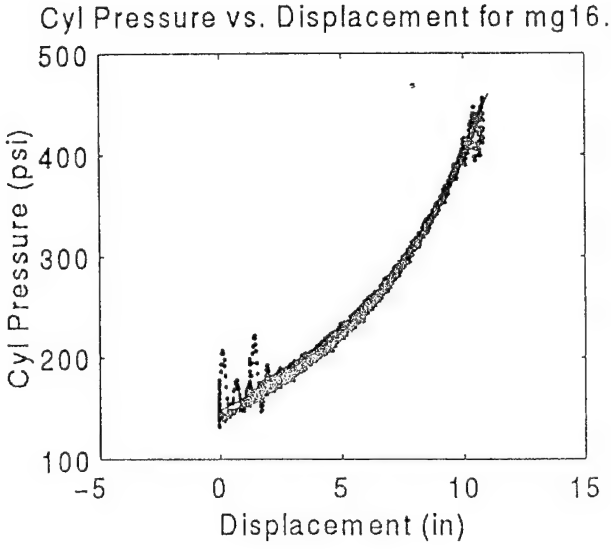
Cyl Pressure vs. Displacement for mg16.txt
Cyl Pressure (psi)
Displacement (in)
500
400
300
200
100
-5
0
5
10
15

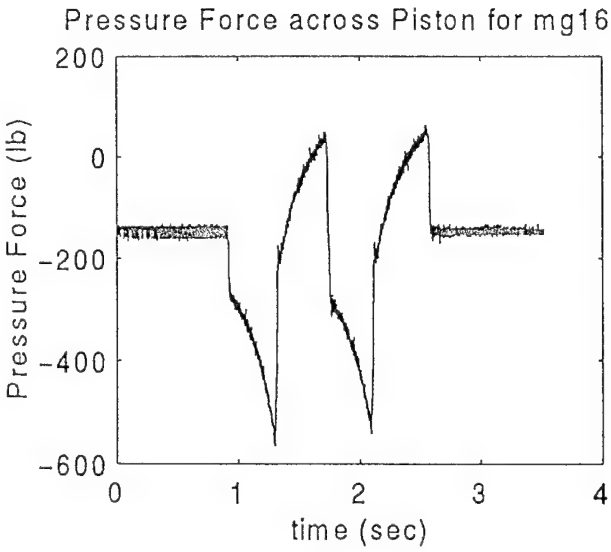
Pressure Force across Piston for mg16.txt
Pressure Force (lb)
time (sec)
200
0
-200
-400
-600
0
1
2
3
4

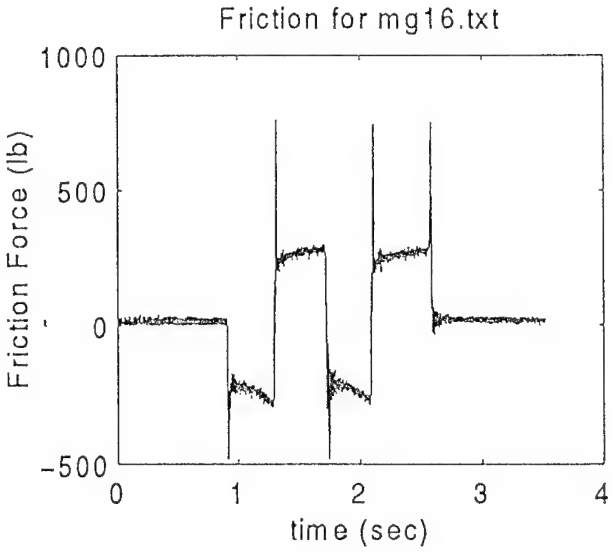
Friction for mg16.txt
Friction Force (lb)
time (sec)
1000
500
0
-500
0
1
2
3
4

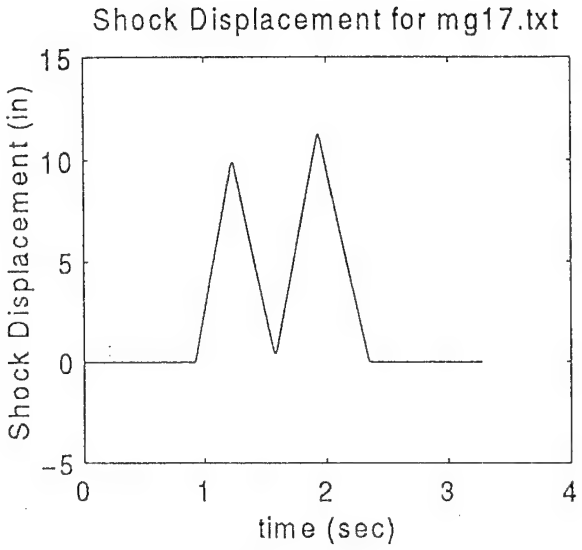
Shock Displacement for mg17.txt
Shock Displacement (in)
15
10
5
0
-5
0
1
2
3
4
time (sec)

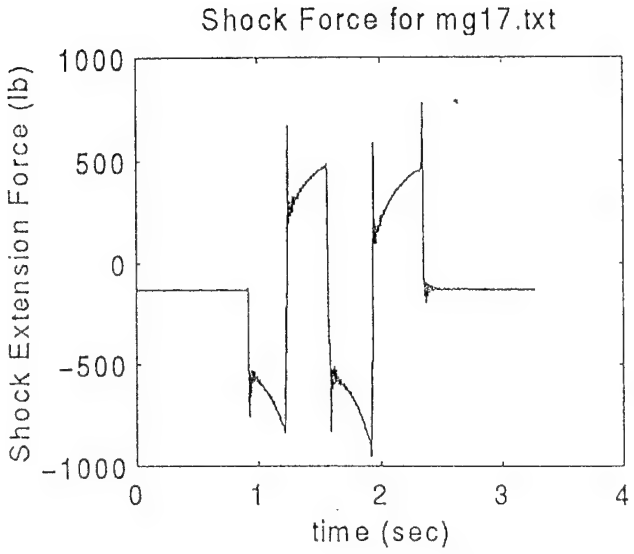
Shock Force for mg17.txt
Shock Extension Force (lb)
1000
500
0
-500
-1000
0
1
2
3
4
time (sec)

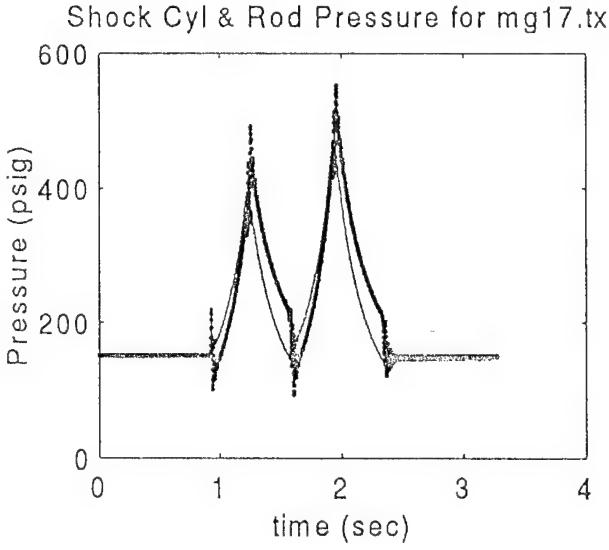
Shock Cyl & Rod Pressure for mg17.txt
Pressure (psig)
600
400
200
0
0
1
2
3
4
time (sec)

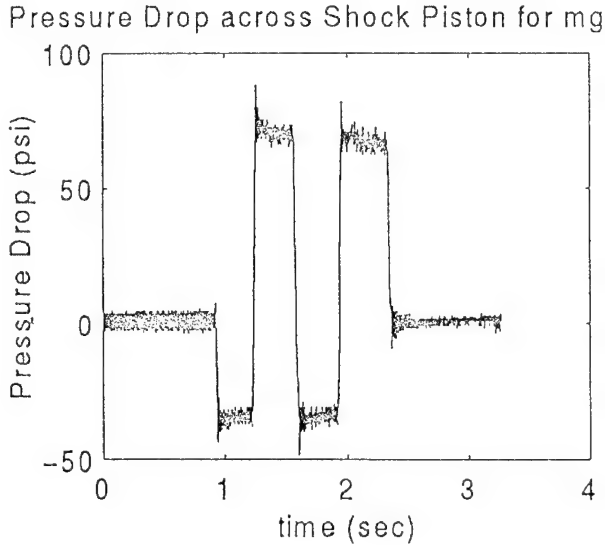
Pressure Drop across Shock Piston for mg17.txt
Pressure Drop (psi)
100
50
0
-50
0
1
2
3
4
time (sec)

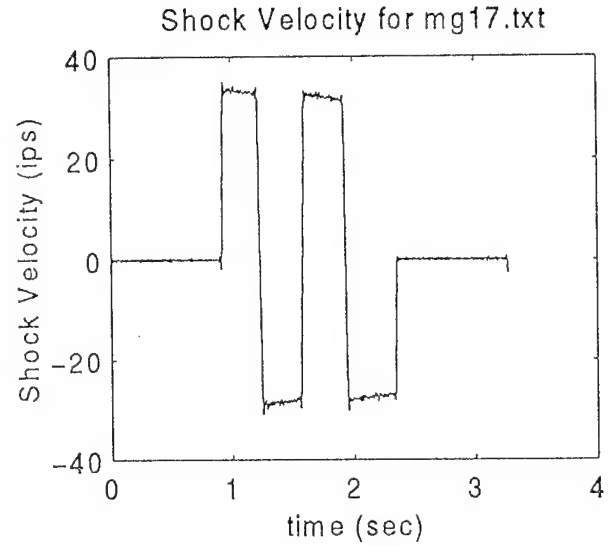
Shock Velocity for mg17.txt
Shock Velocity (ips)
time (sec)
40
20
0
-20
-40
0
1
2
3
4

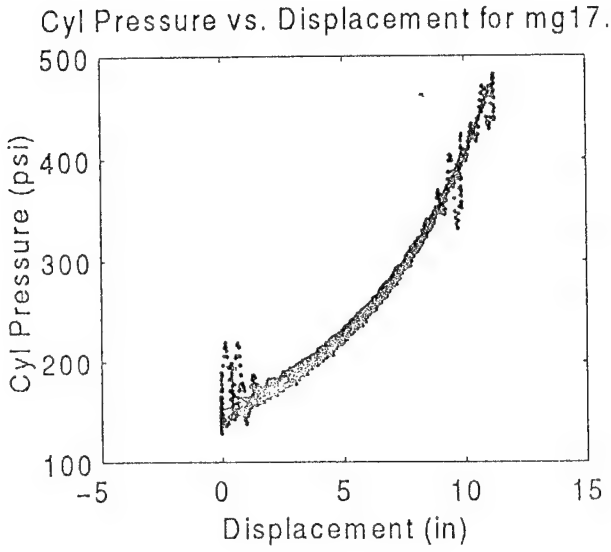
Cyl Pressure vs. Displacement for mg17.txt
Cyl Pressure (psi)
Displacement (in)
500
400
300
200
100
-5
0
5
10
15

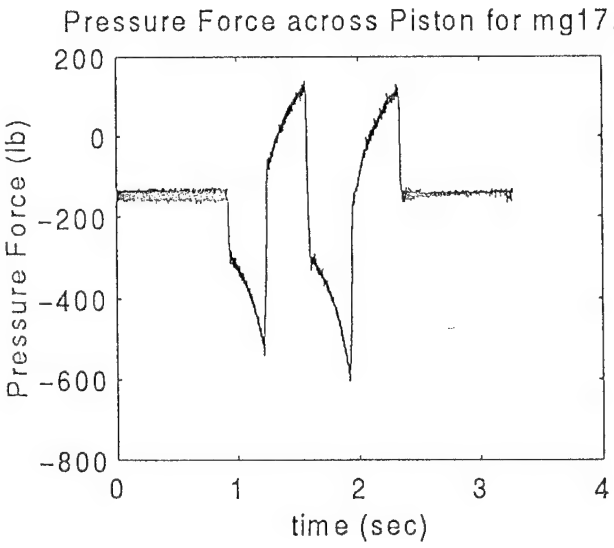
Pressure Force across Piston for mg17.txt
Pressure Force (lb)
time (sec)
200
0
-200
-400
-600
-800
0
1
2
3
4

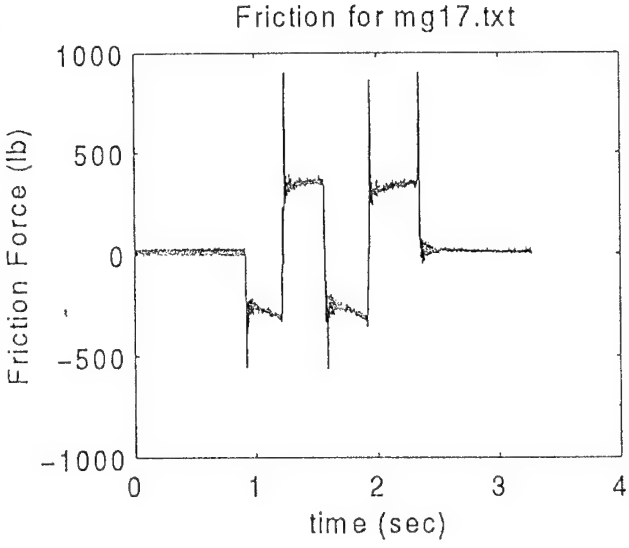
Friction for mg17.txt
Friction Force (lb)
time (sec)
1000
500
0
-500
-1000
0
1
2
3
4

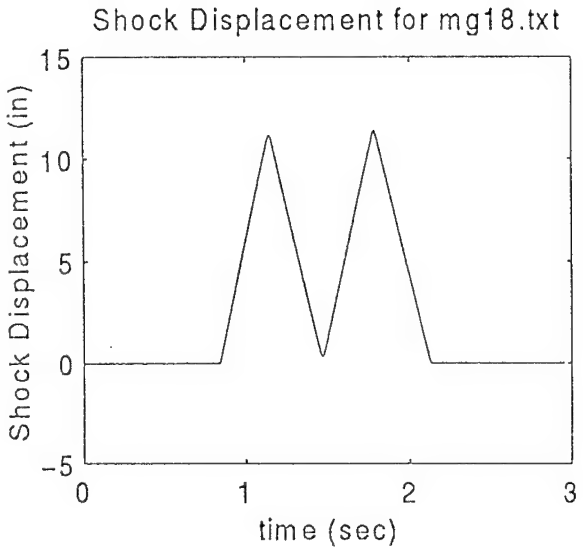
Shock Displacement for mg18.txt
Shock Displacement (in)
15
10
5
0
-5
0
1
2
3
time (sec)

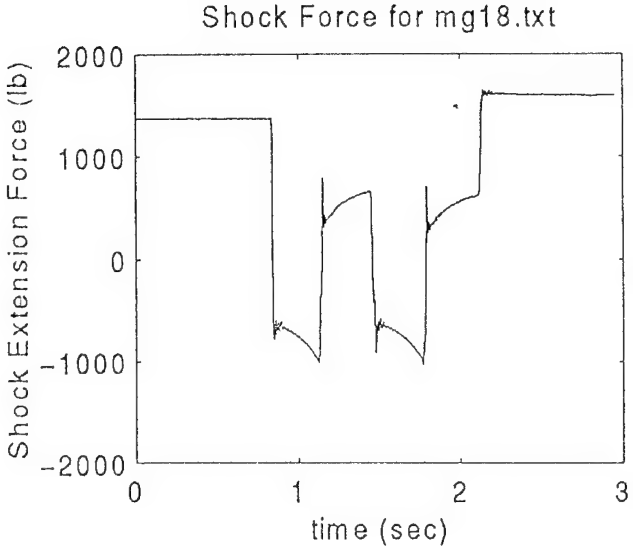
Shock Force for mg18.txt
Shock Extension Force (lb)
2000
1000
0
-1000
-2000
0
1
2
3
time (sec)

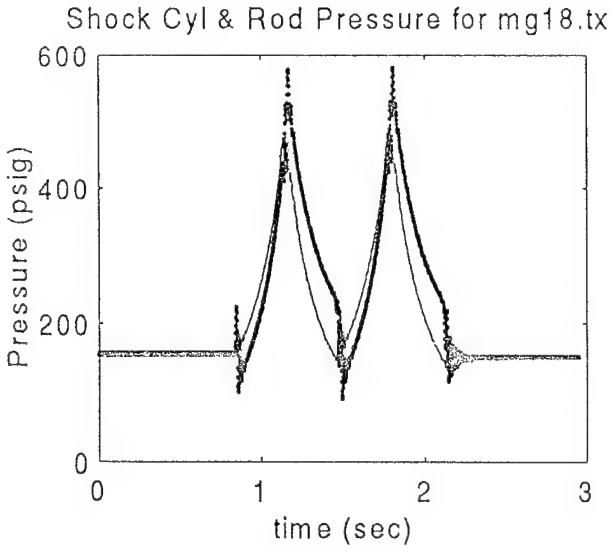
Shock Cyl & Rod Pressure for mg18.txt
Pressure (psig)
600
400
200
0
0
1
2
3
time (sec)

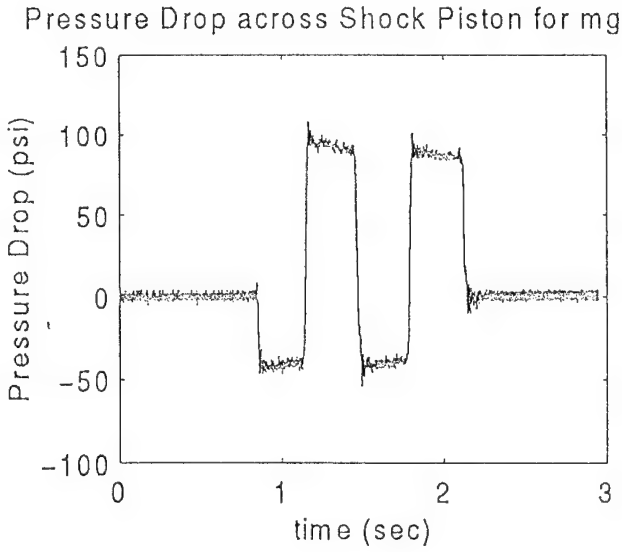
Pressure Drop across Shock Piston for mg18.txt
Pressure Drop (psi)
150
100
50
0
-50
-100
0
1
2
3
time (sec)

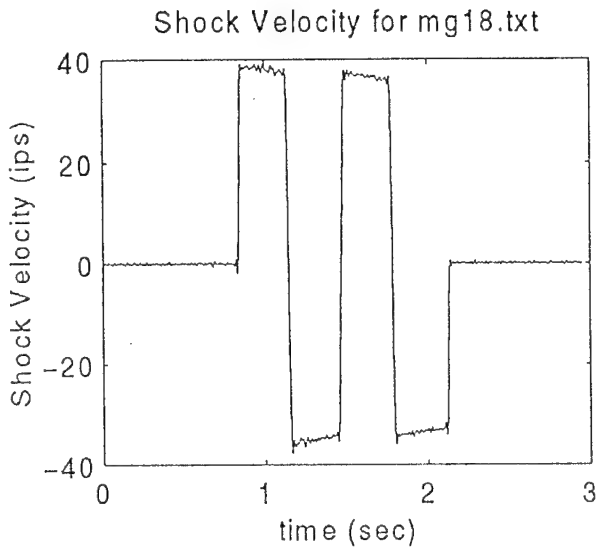
Shock Velocity for mg18.txt
Shock Velocity (ips)
time (sec)
40
20
0
-20
-40
0
1
2
3

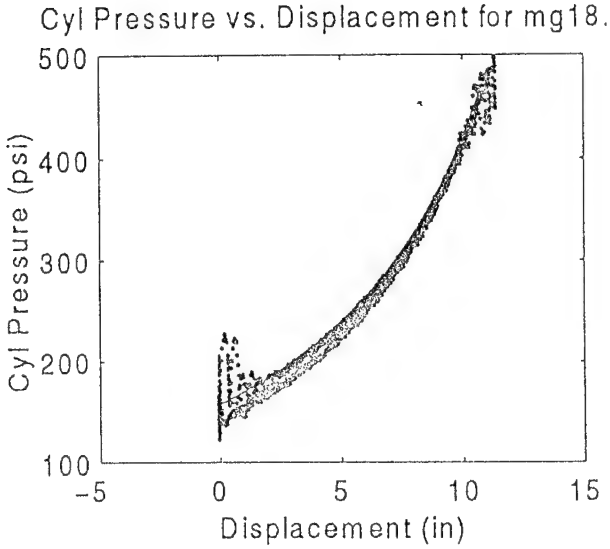
Cyl Pressure vs. Displacement for mg18.txt
Cyl Pressure (psi)
Displacement (in)
500
400
300
200
100
-5
0
5
10
15

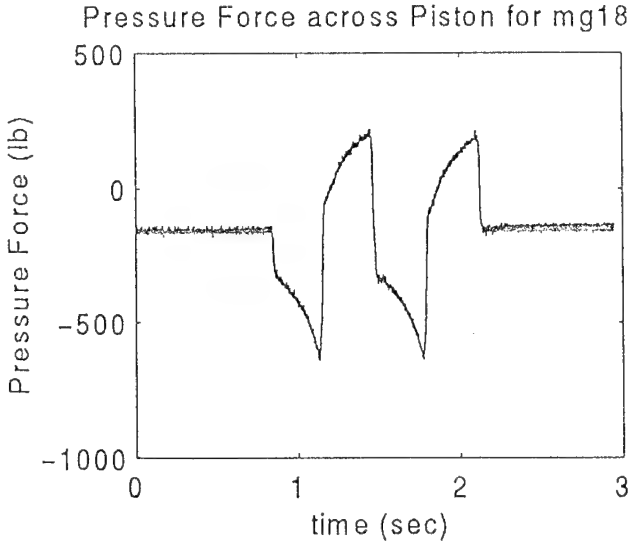
Pressure Force across Piston for mg18.txt
Pressure Force (lb)
time (sec)
500
0
-500
-1000
0
1
2
3

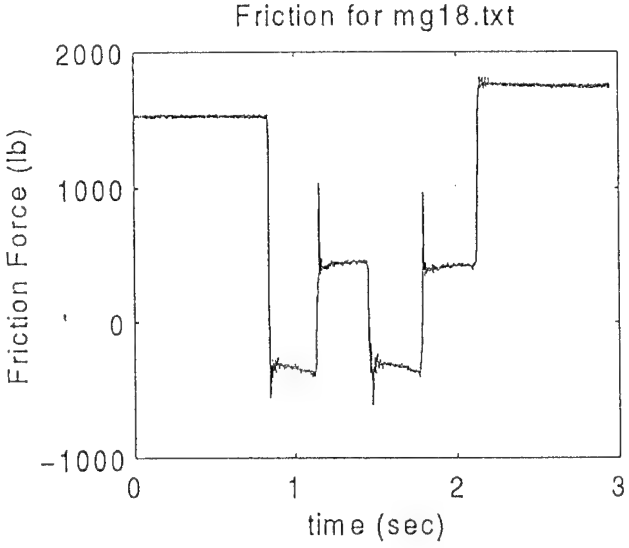
Friction for mg18.txt
Friction Force (lb)
time (sec)
2000
1000
0
-1000
0
1
2
3

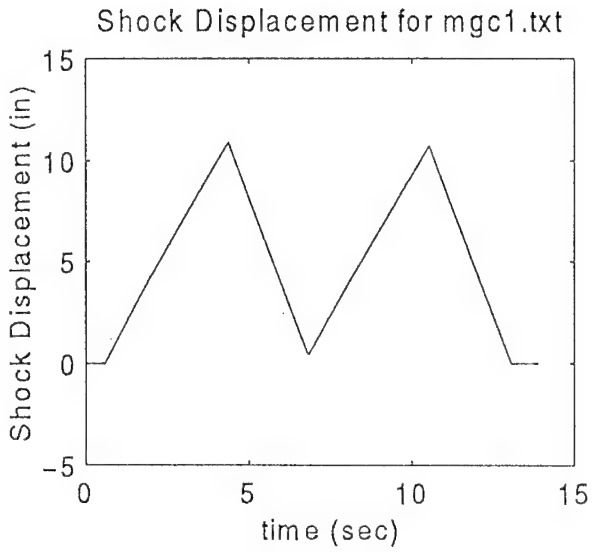
Shock Displacement for mgc1.txt
Shock Displacement (in)
15
10
5
0
-5
0
5
10
15
time (sec)

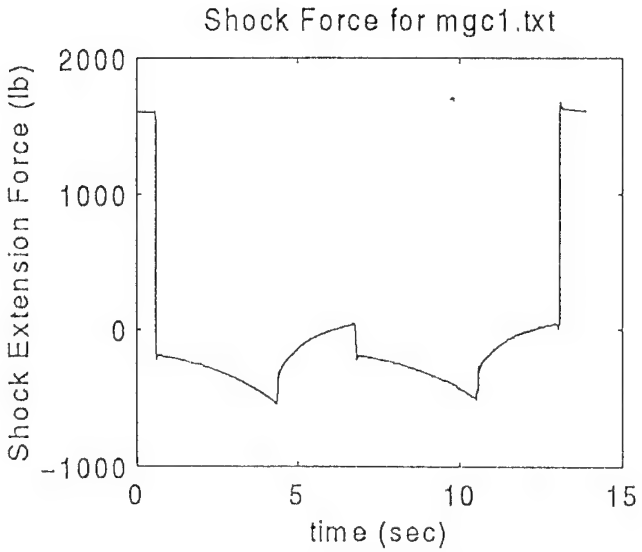
Shock Force for mgc1.txt
Shock Extension Force (lb)
2000
1000
0
-1000
0
5
10
15
time (sec)

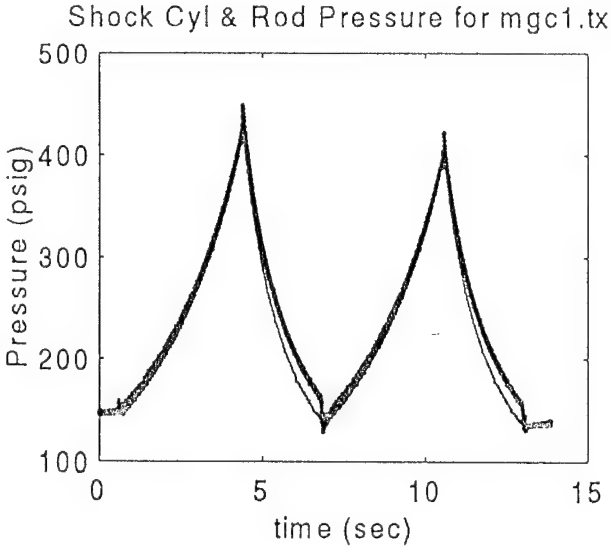
Shock Cyl & Rod Pressure for mgc1.txt
Pressure (psig)
500
400
300
200
100
0
5
10
15
time (sec)

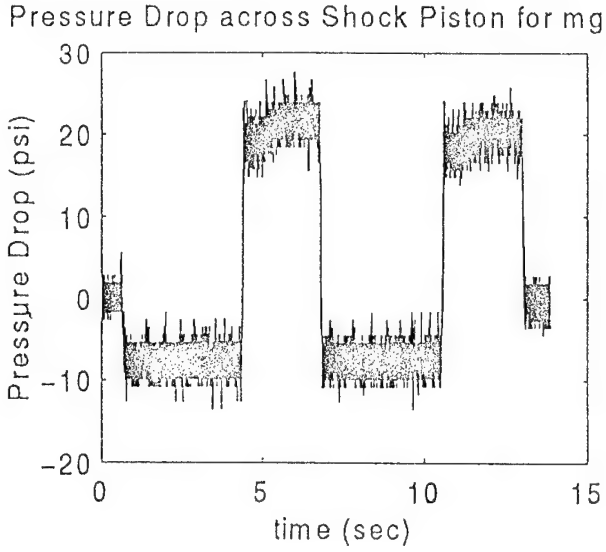
Pressure Drop across Shock Piston for mgc1.txt
Pressure Drop (psi)
30
20
10
0
-10
-20
0
5
10
15
time (sec)

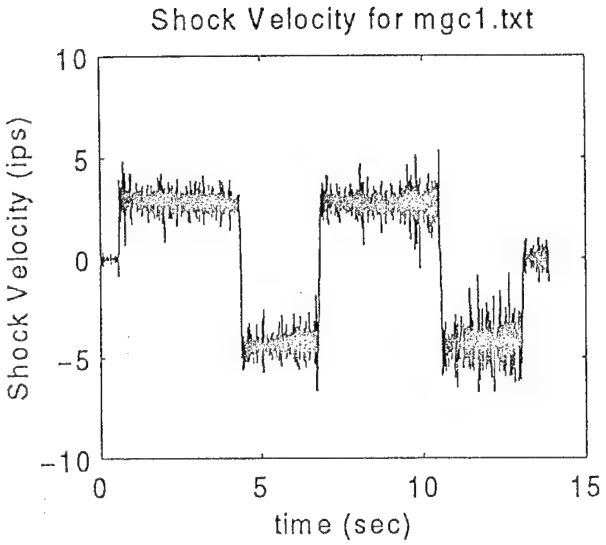
Shock Velocity for mgc1.txt
Shock Velocity (ips)
time (sec)
10
5
0
-5
-10
0
5
10
15

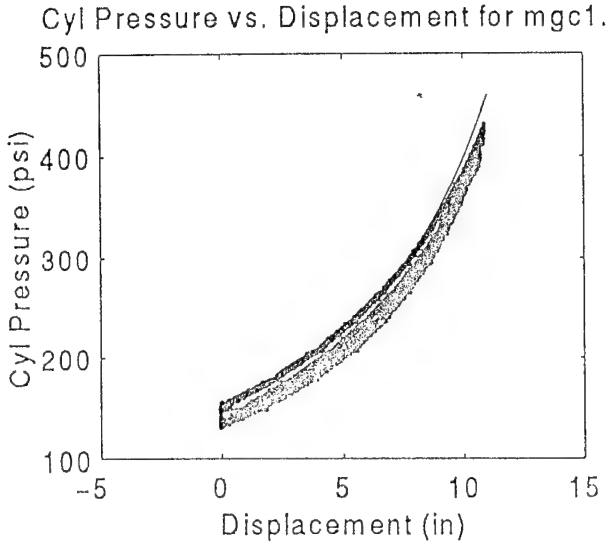
Cyl Pressure vs. Displacement for mgc1.txt
Cyl Pressure (psi)
Displacement (in)
500
400
300
200
100
-5
0
5
10
15

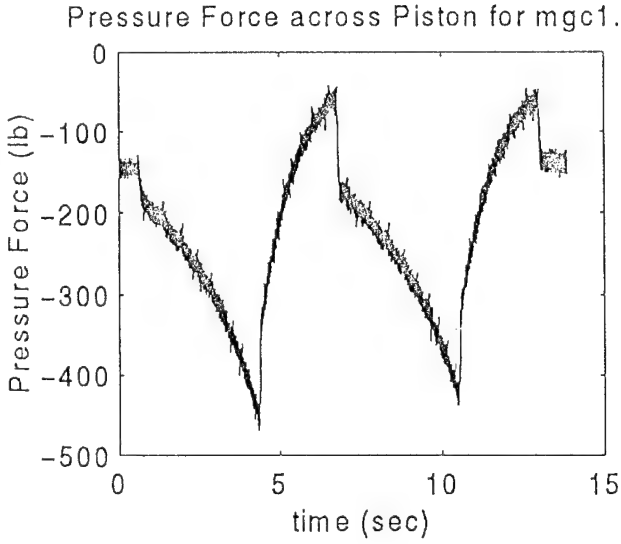
Pressure Force across Piston for mgc1.txt
Pressure Force (lb)
time (sec)
0
-100
-200
-300
-400
-500
0
5
10
15

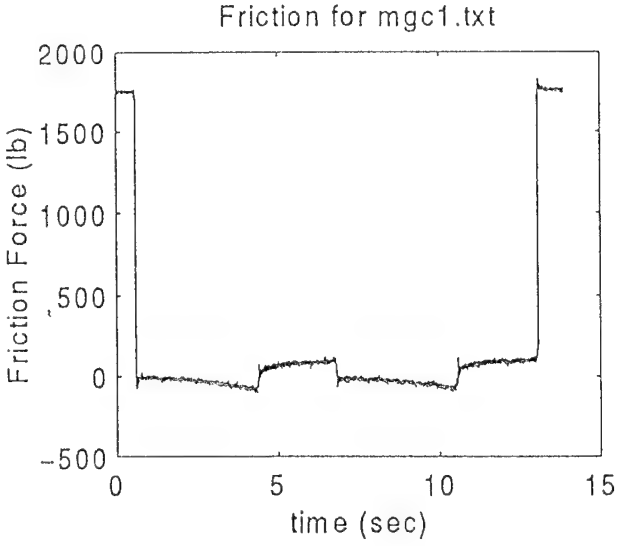
Friction for mgc1.txt
Friction Force (lb)
time (sec)
2000
1500
1000
500
0
-500
0
5
10
15

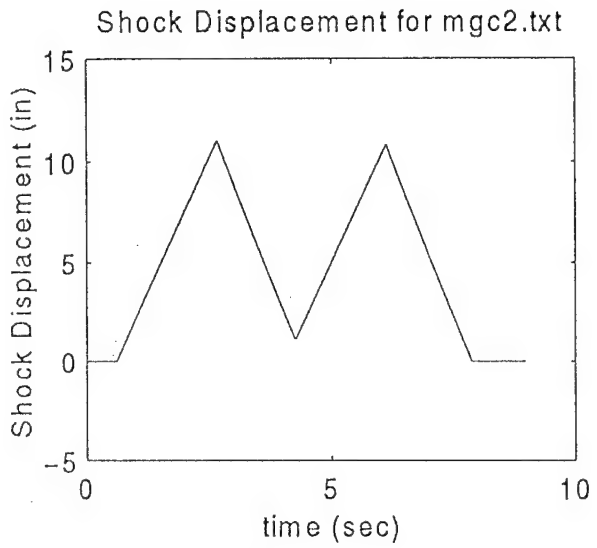
Shock Displacement for mgc2.txt
Shock Displacement (in)
15
10
5
0
-5
0
5
10
time (sec)

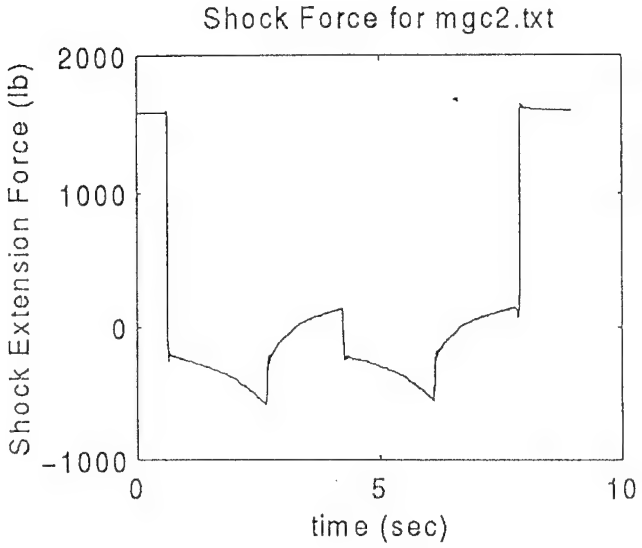
Shock Force for mgc2.txt
Shock Extension Force (lb)
2000
1000
0
-1000
0
5
10
time (sec)

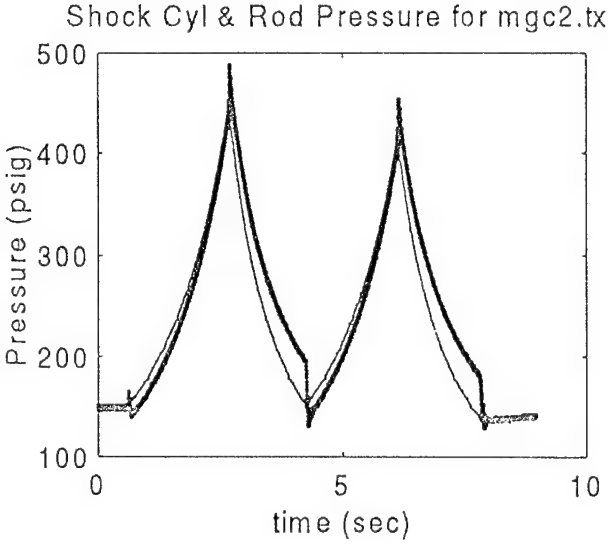
Shock Cyl & Rod Pressure for mgc2.txt
Pressure (psig)
500
400
300
200
100
0
5
10
time (sec)

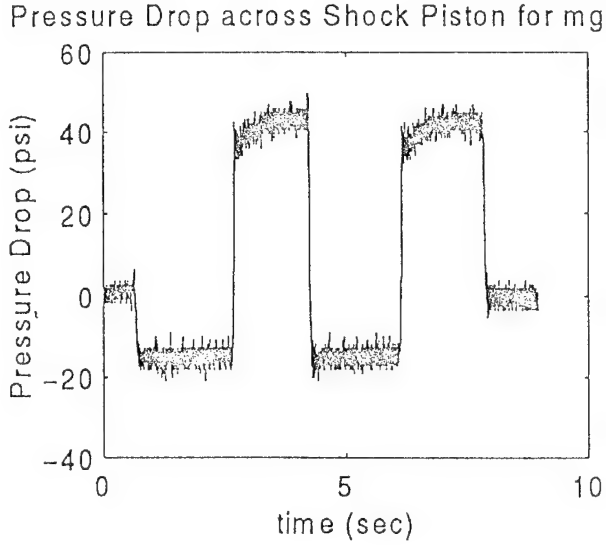
Pressure Drop across Shock Piston for mgc2.txt
Pressure Drop (psi)
60
40
20
0
-20
-40
0
5
10
time (sec)

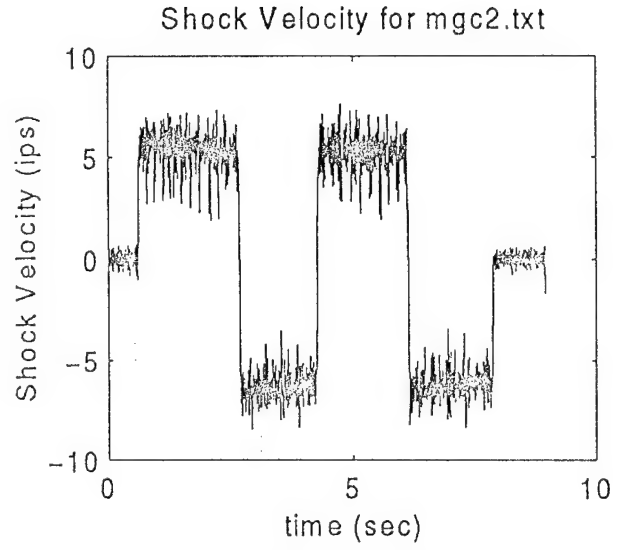
Shock Velocity for mgc2.txt
Shock Velocity (ips)
time (sec)
10
5
0
-5
-10
0
5
10

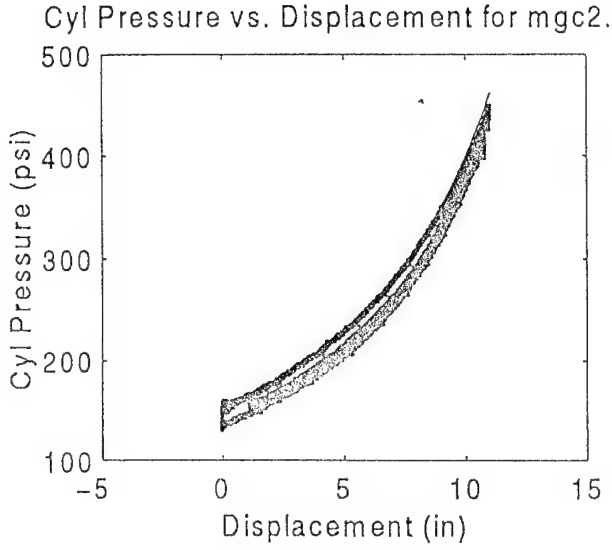
Cyl Pressure vs. Displacement for mgc2.txt
Cyl Pressure (psi)
Displacement (in)
500
400
300
200
100
-5
0
5
10
15

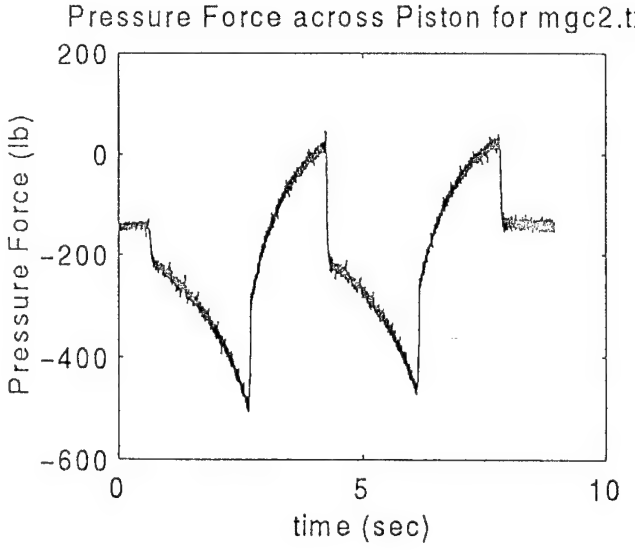
Pressure Force across Piston for mgc2.txt
Pressure Force (lb)
time (sec)
200
0
-200
-400
-600
0
5
10

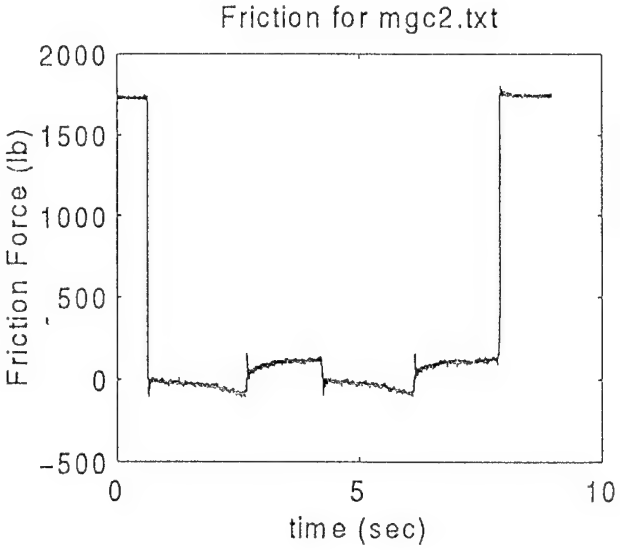
Friction for mgc2.txt
Friction Force (lb)
time (sec)
2000
1500
1000
500
0
-500
0
5
10

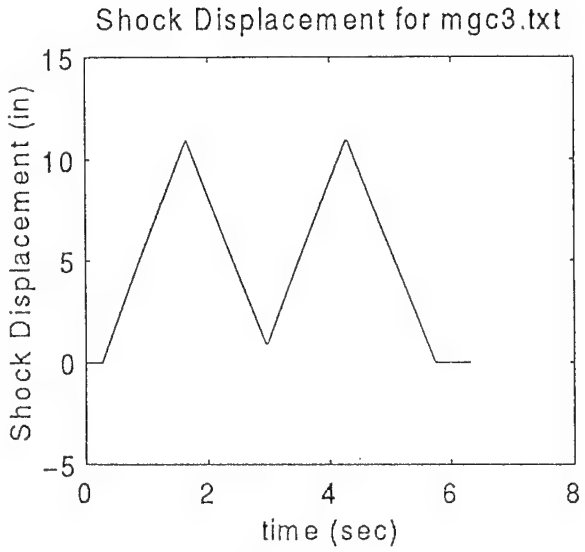
Shock Displacement for mgc3.txt
Shock Displacement (in)
15
10
5
0
−5
0
2
4
6
8
time (sec)

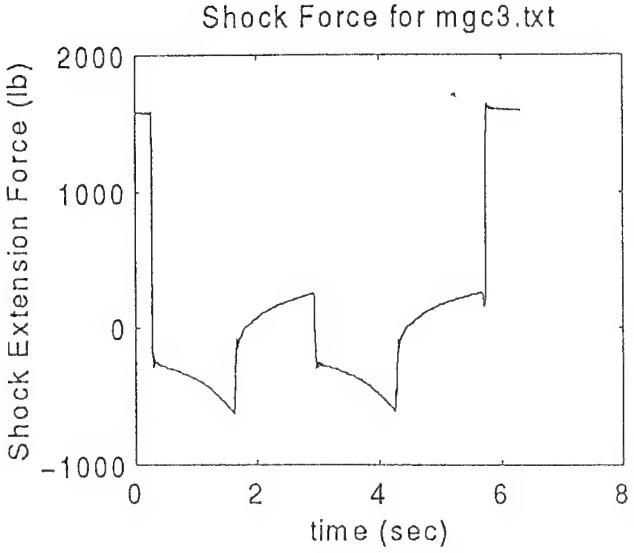
Shock Force for mgc3.txt
Shock Extension Force (lb)
2000
1000
0
−1000
0
2
4
6
8
time (sec)

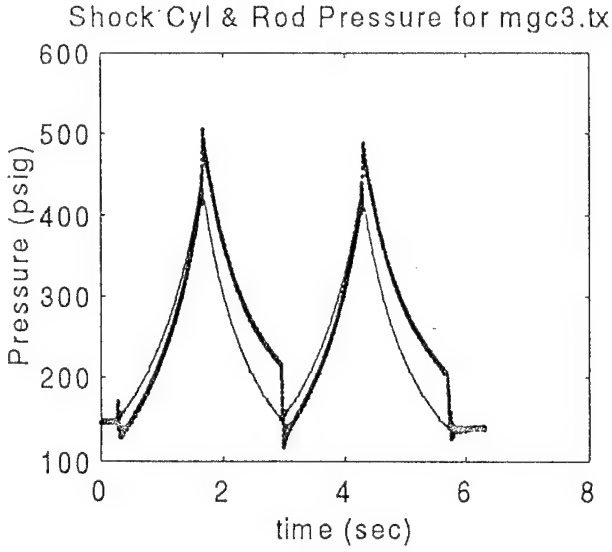
Shock Cyl & Rod Pressure for mgc3.txt
Pressure (psig)
600
500
400
300
200
100
0
2
4
6
8
time (sec)

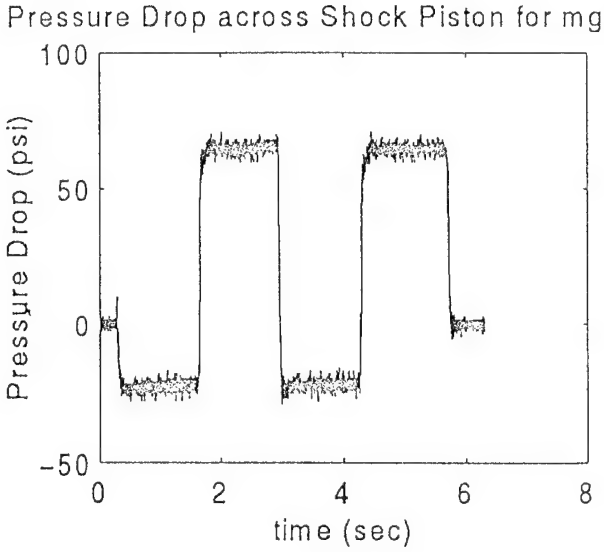
Pressure Drop across Shock Piston for mgc3.txt
Pressure Drop (psi)
100
50
0
−50
0
2
4
6
8
time (sec)

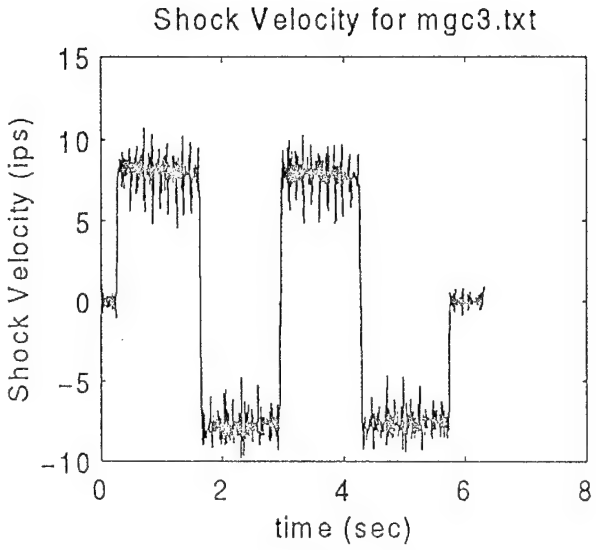
Shock Velocity for mgc3.txt
Shock Velocity (ips)
time (sec)
15
10
5
0
-5
-10
0
2
4
6
8

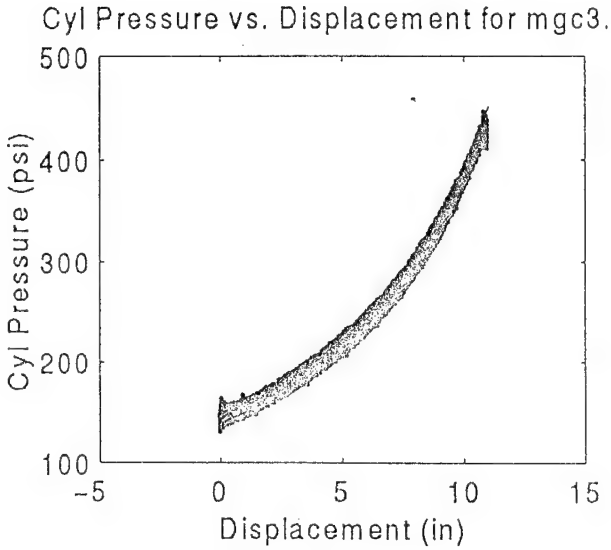
Cyl Pressure vs. Displacement for mgc3.txt
Cyl Pressure (psi)
Displacement (in)
500
400
300
200
100
-5
0
5
10
15

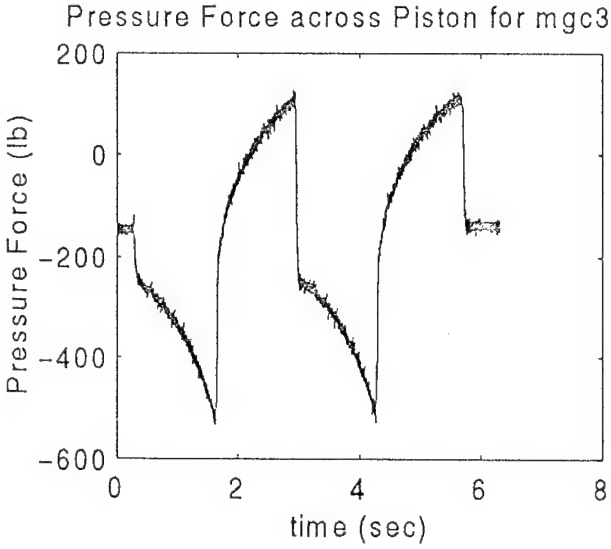
Pressure Force across Piston for mgc3.txt
Pressure Force (lb)
time (sec)
200
0
-200
-400
-600
0
2
4
6
8

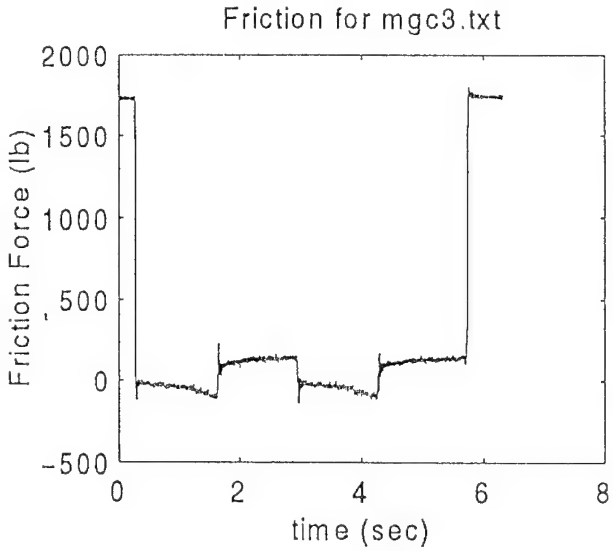
Friction for mgc3.txt
Friction Force (lb)
time (sec)
2000
1500
1000
500
0
-500
0
2
4
6
8

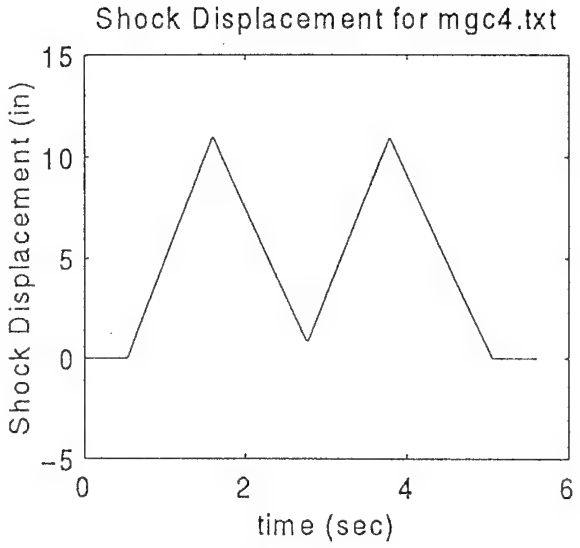
Shock Displacement for mgc4.txt
Shock Displacement (in)
15
10
5
0
-5
0
2
4
6
time (sec)

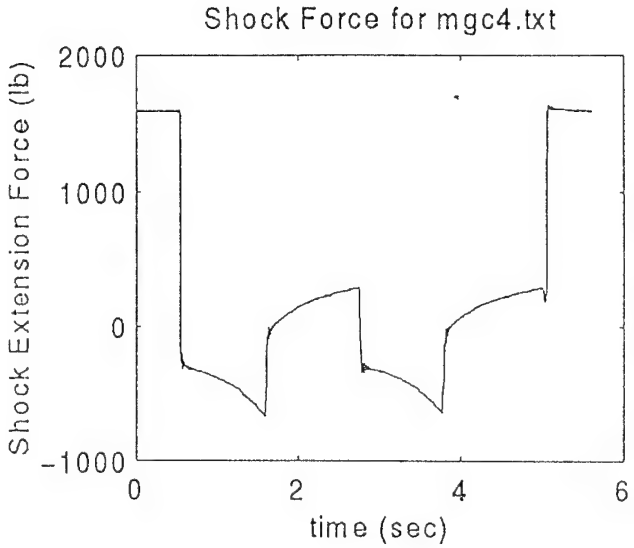
Shock Force for mgc4.txt
Shock Extension Force (lb)
2000
1000
0
-1000
0
2
4
6
time (sec)

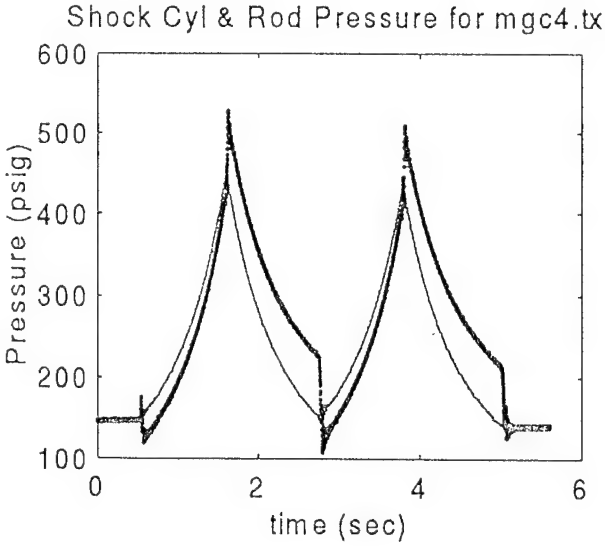
Shock Cyl & Rod Pressure for mgc4.txt
Pressure (psig)
600
500
400
300
200
100
0
2
4
6
time (sec)

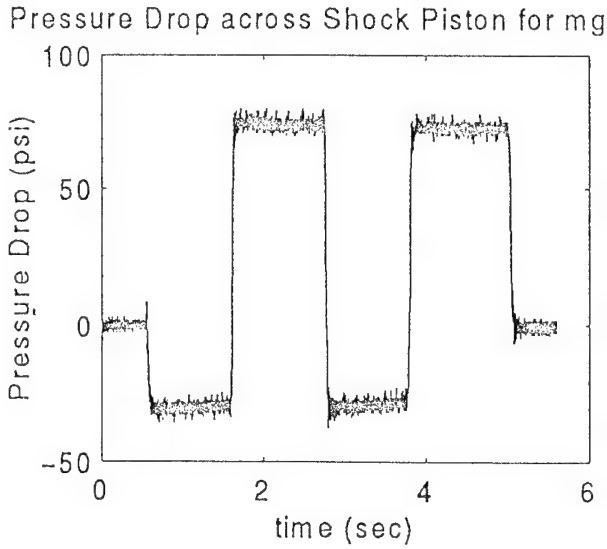
Pressure Drop across Shock Piston for mgc4.txt
Pressure Drop (psi)
100
50
0
-50
0
2
4
6
time (sec)

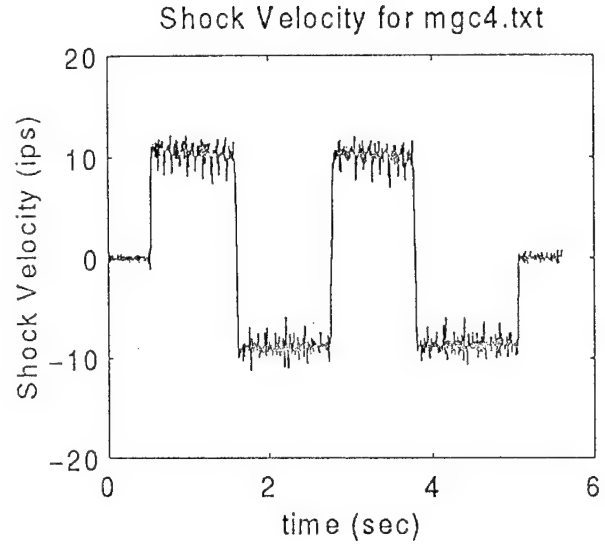
Shock Velocity for mgc4.txt
Shock Velocity (ips)
time (sec)
20
10
0
-10
-20
0
2
4
6

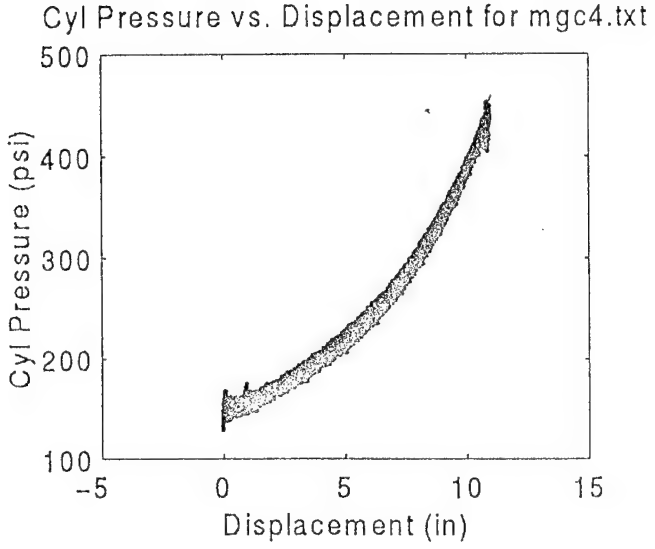
Cyl Pressure vs. Displacement for mgc4.txt
Cyl Pressure (psi)
Displacement (in)
500
400
300
200
100
-5
0
5
10
15

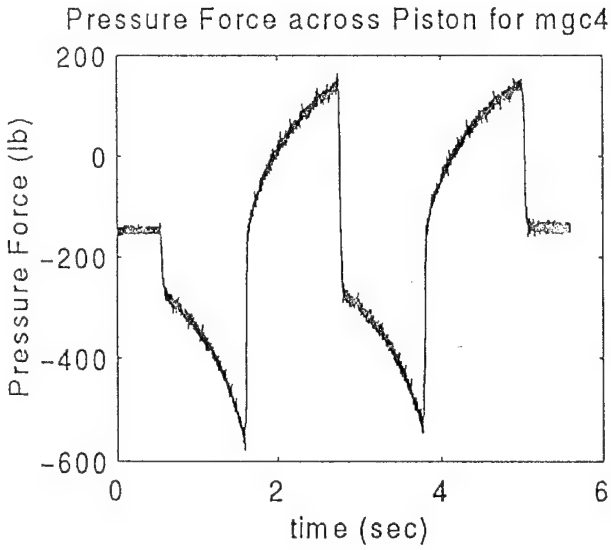
Pressure Force across Piston for mgc4.txt
Pressure Force (lb)
time (sec)
200
0
-200
-400
-600
0
2
4
6

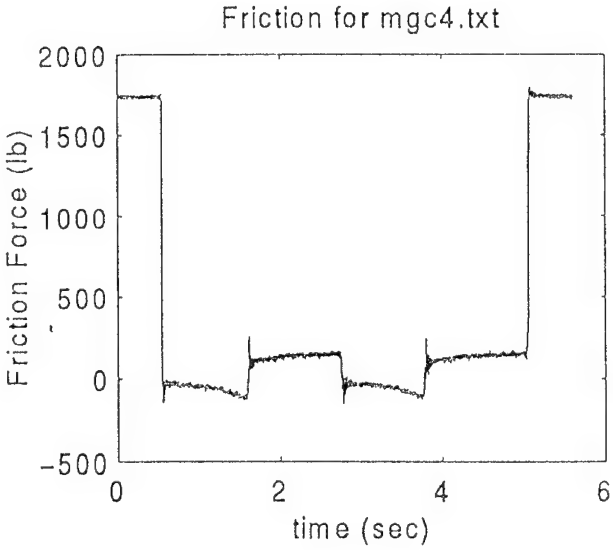
Friction for mgc4.txt
Friction Force (lb)
time (sec)
2000
1500
1000
500
0
-500
0
2
4
6

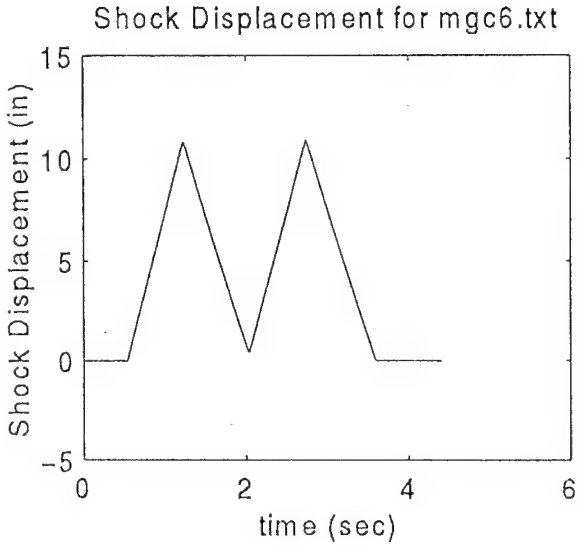
Shock Displacement for mgc6.txt
Shock Displacement (in)
15
10
5
0
-5
0
2
4
6
time (sec)

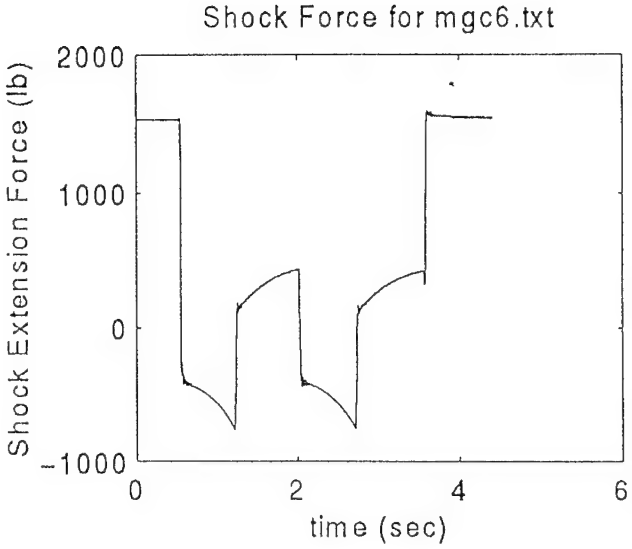
Shock Force for mgc6.txt
Shock Extension Force (lb)
2000
1000
0
-1000
0
2
4
6
time (sec)

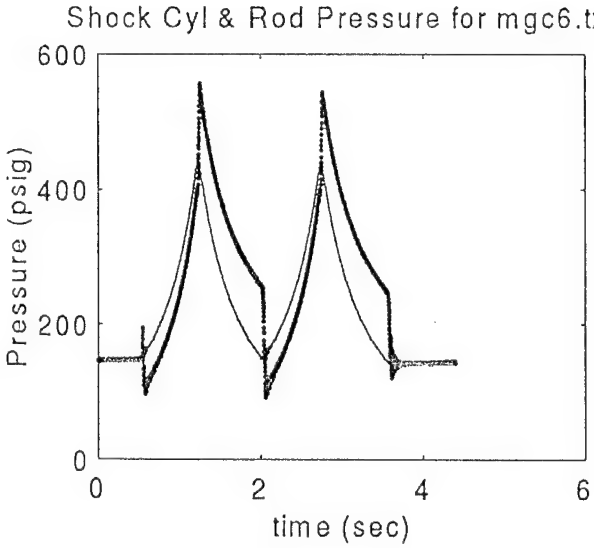
Shock Cyl & Rod Pressure for mgc6.txt
Pressure (psig)
600
400
200
0
0
2
4
6
time (sec)

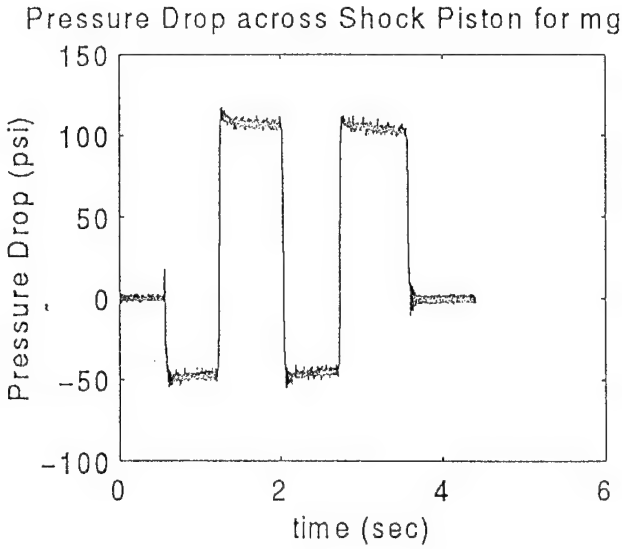
Pressure Drop across Shock Piston for mgc6.txt
Pressure Drop (psi)
150
100
50
0
-50
-100
0
2
4
6
time (sec)

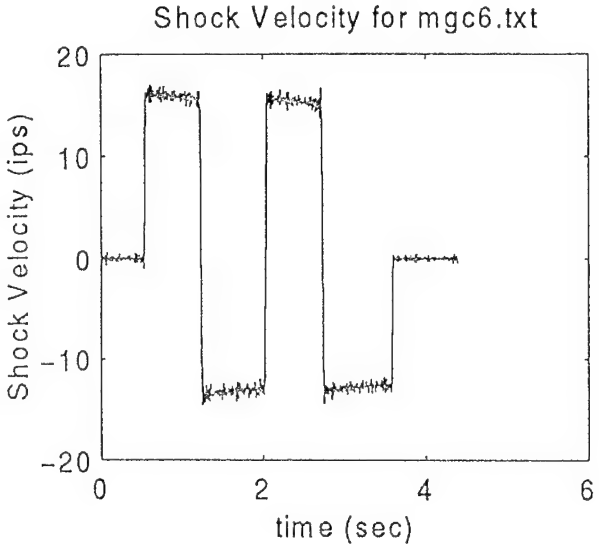
Shock Velocity for mgc6.txt
Shock Velocity (ips)
time (sec)
20
10
0
-10
-20
0
2
4
6

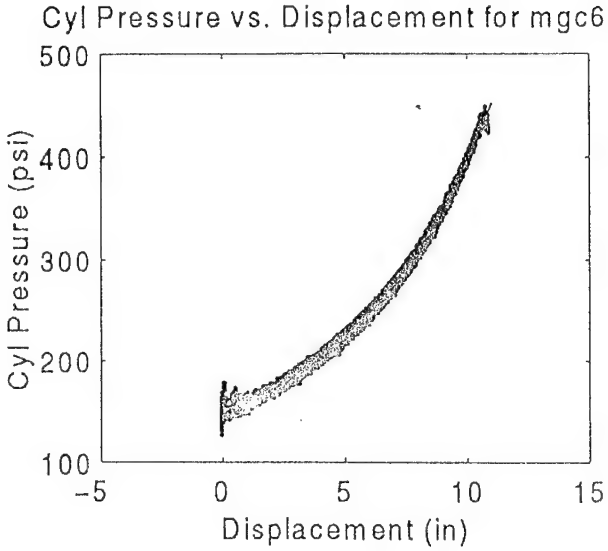
Cyl Pressure vs. Displacement for mgc6.txt
Cyl Pressure (psi)
Displacement (in)
500
400
300
200
100
-5
0
5
10
15

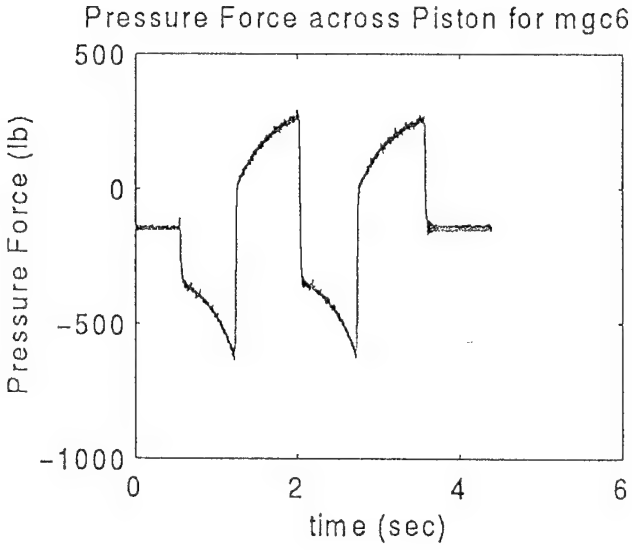
Pressure Force across Piston for mgc6.txt
Pressure Force (lb)
time (sec)
500
0
-500
-1000
0
2
4
6

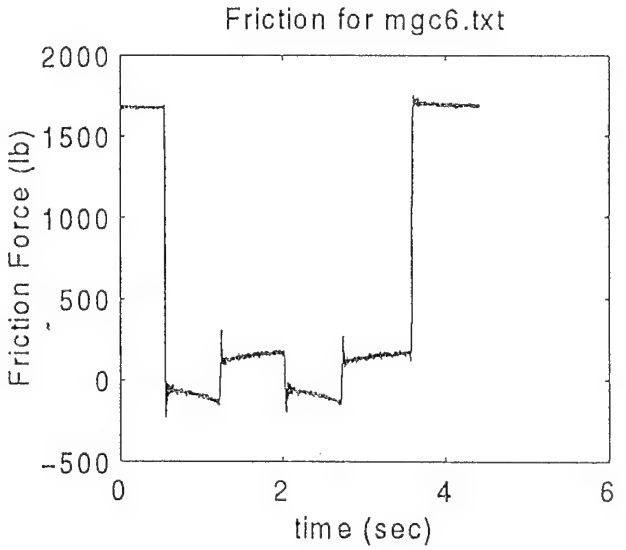
Friction for mgc6.txt
Friction Force (lb)
time (sec)
2000
1500
1000
500
0
-500
0
2
4
6

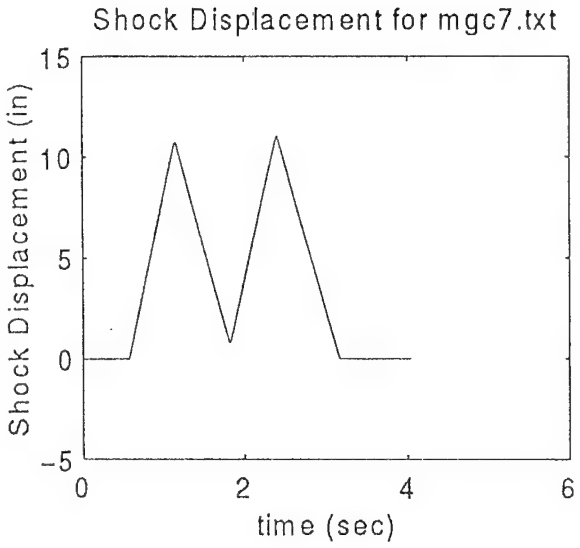
Shock Displacement for mgc7.txt
Shock Displacement (in)
15
10
5
0
−5
0
2
4
6
time (sec)

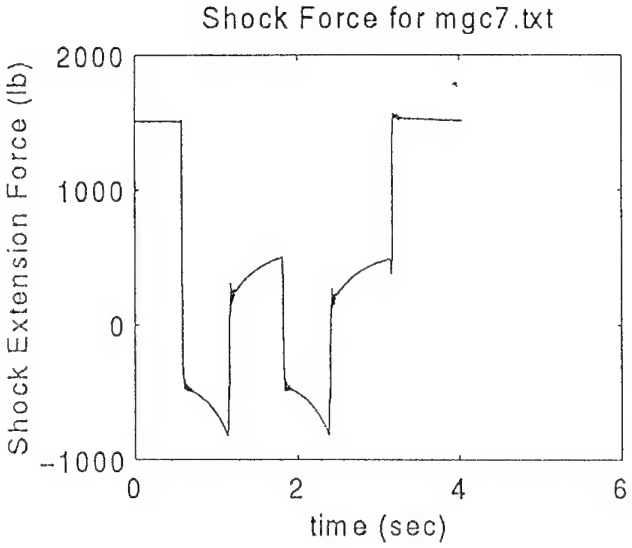
Shock Force for mgc7.txt
Shock Extension Force (lb)
2000
1000
0
−1000
0
2
4
6
time (sec)

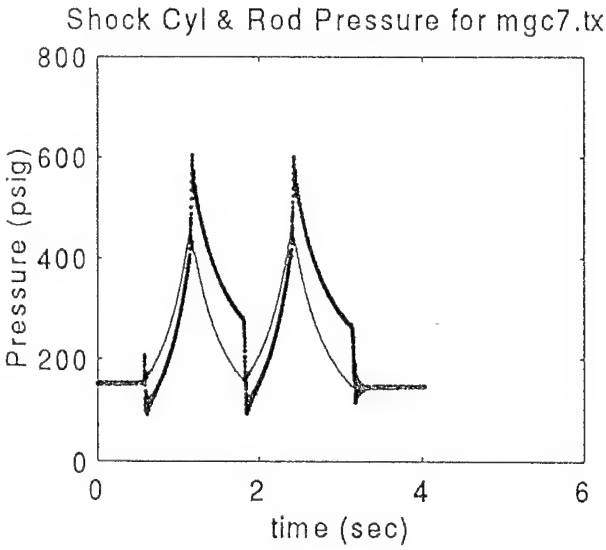
Shock Cyl & Rod Pressure for mgc7.txt
Pressure (psig)
800
600
400
200
0
0
2
4
6
time (sec)

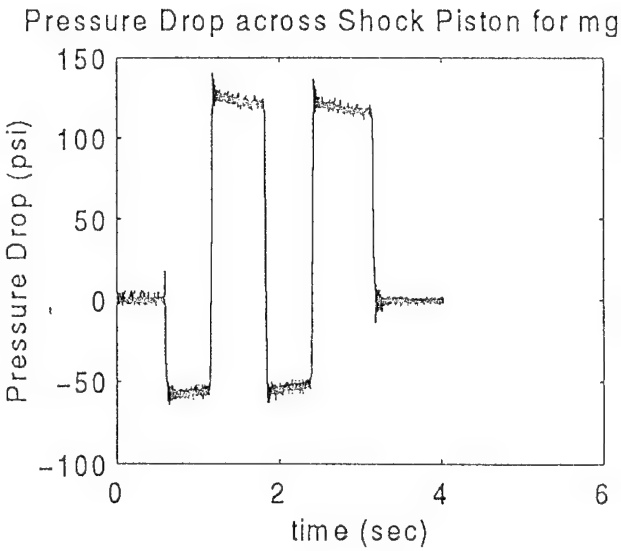
Pressure Drop across Shock Piston for mgc7.txt
Pressure Drop (psi)
150
100
50
0
−50
−100
0
2
4
6
time (sec)

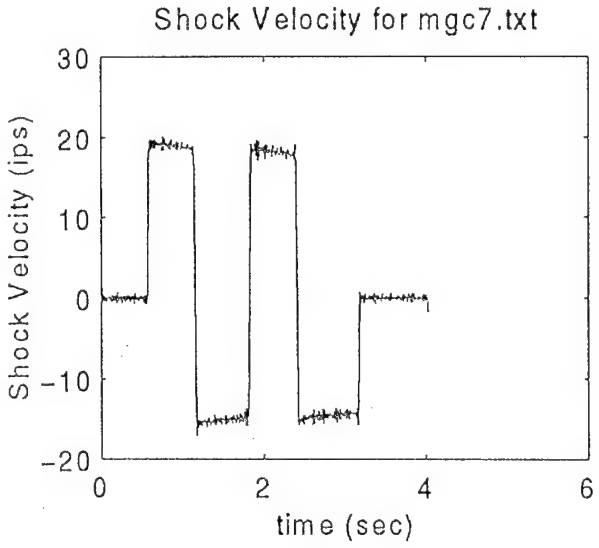
Shock Velocity for mgc7.txt
Shock Velocity (ips)
time (sec)
30
20
10
0
-10
-20
0
2
4
6

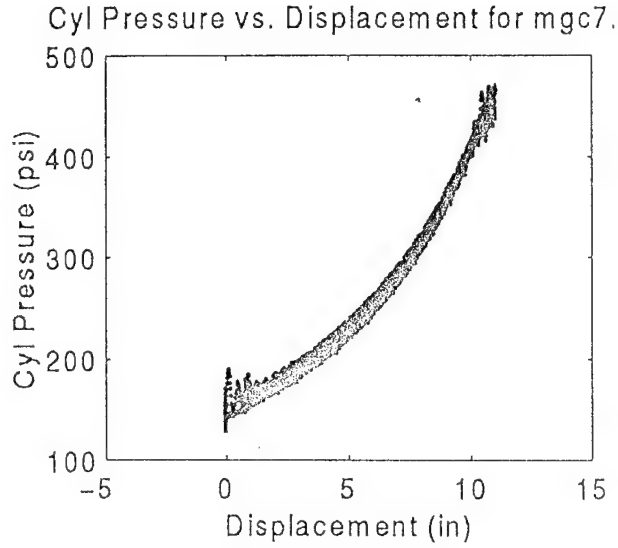
Cyl Pressure vs. Displacement for mgc7.txt
Cyl Pressure (psi)
Displacement (in)
500
400
300
200
100
-5
0
5
10
15

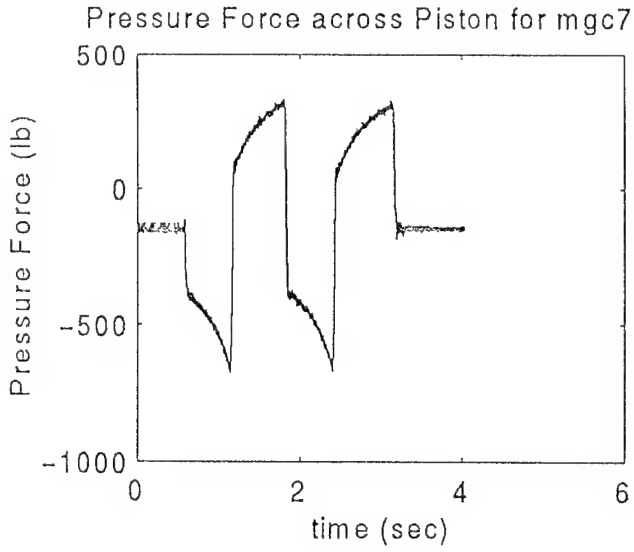
Pressure Force across Piston for mgc7.txt
Pressure Force (lb)
time (sec)
500
0
-500
-1000
0
2
4
6

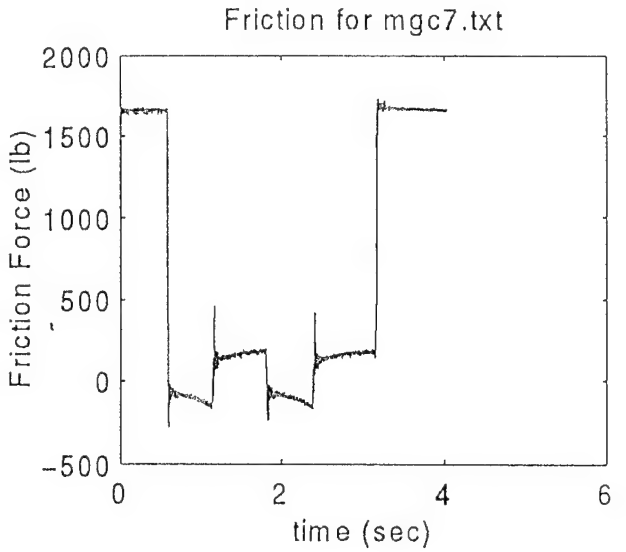
Friction for mgc7.txt
Friction Force (lb)
time (sec)
2000
1500
1000
500
0
-500
0
2
4
6

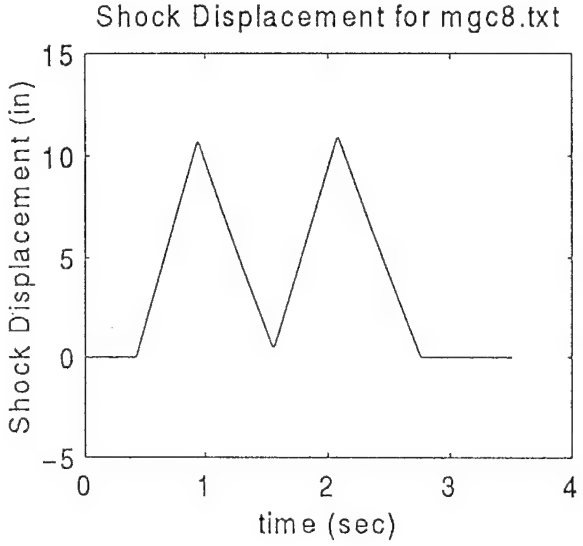
Shock Displacement for mgc8.txt
Shock Displacement (in)
15
10
5
0
−5
0
1
2
3
4
time (sec)

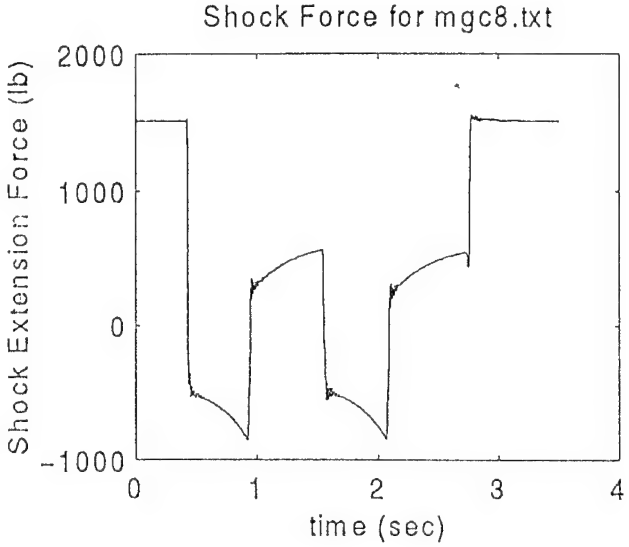
Shock Force for mgc8.txt
Shock Extension Force (lb)
2000
1000
0
−1000
0
1
2
3
4
time (sec)

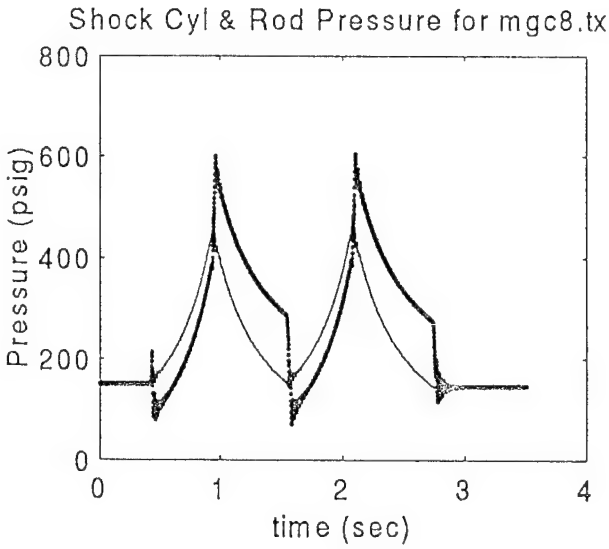
Shock Cyl & Rod Pressure for mgc8.txt
Pressure (psig)
800
600
400
200
0
0
1
2
3
4
time (sec)

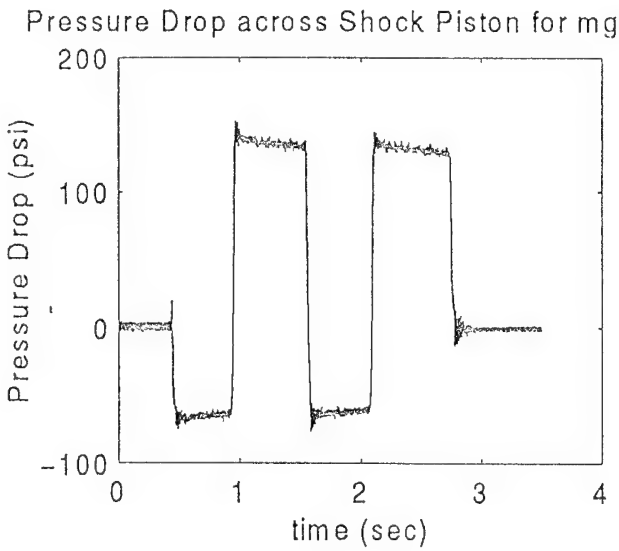
Pressure Drop across Shock Piston for mgc8.txt
Pressure Drop (psi)
200
100
0
−100
0
1
2
3
4
time (sec)

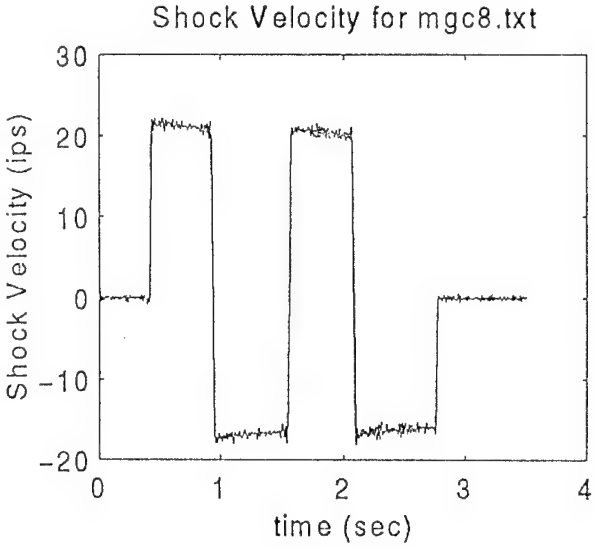
Shock Velocity for mgc8.txt
Shock Velocity (ips)
time (sec)
30
20
10
0
-10
-20
0
1
2
3
4

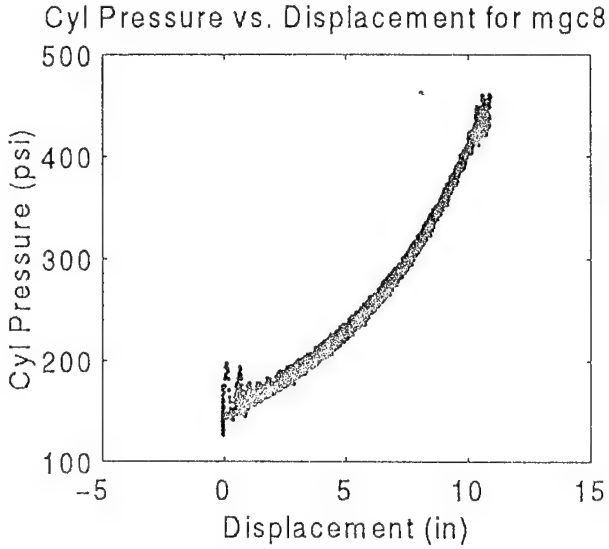
Cyl Pressure vs. Displacement for mgc8.txt
Cyl Pressure (psi)
Displacement (in)
500
400
300
200
100
-5
0
5
10
15

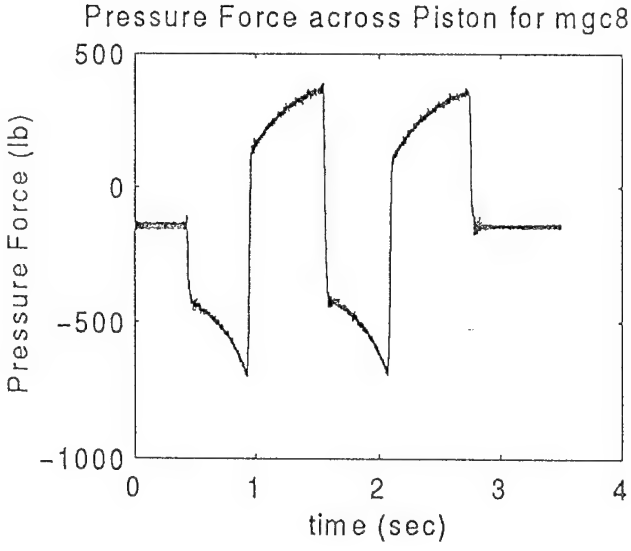
Pressure Force across Piston for mgc8.txt
Pressure Force (lb)
time (sec)
500
0
-500
-1000
0
1
2
3
4

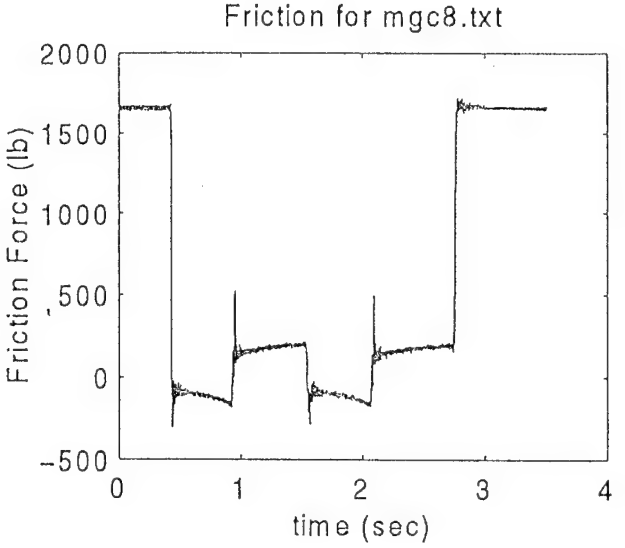
Friction for mgc8.txt
Friction Force (lb)
time (sec)
2000
1500
1000
500
0
-500
0
1
2
3
4

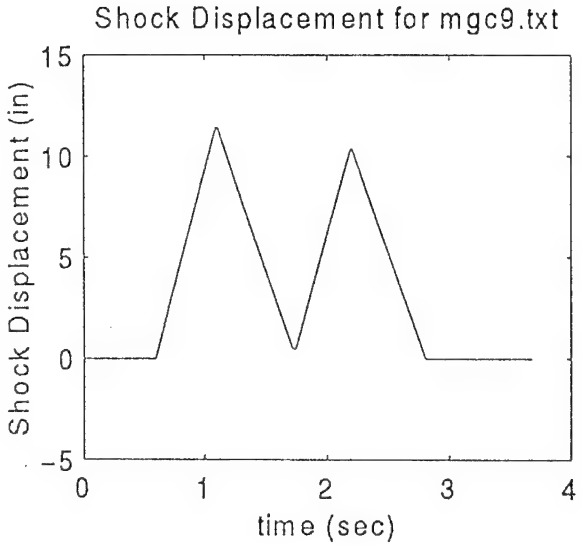
Shock Displacement for mgc9.txt
Shock Displacement (in)
15
10
5
0
−5
0
1
2
3
4
time (sec)

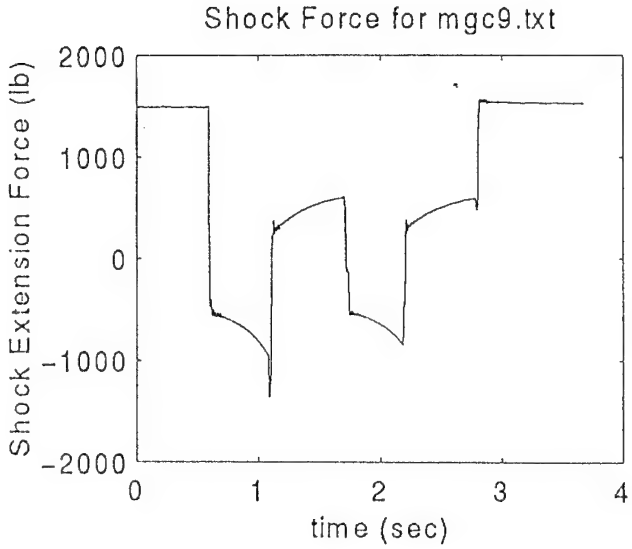
Shock Force for mgc9.txt
Shock Extension Force (lb)
2000
1000
0
−1000
−2000
0
1
2
3
4
time (sec)

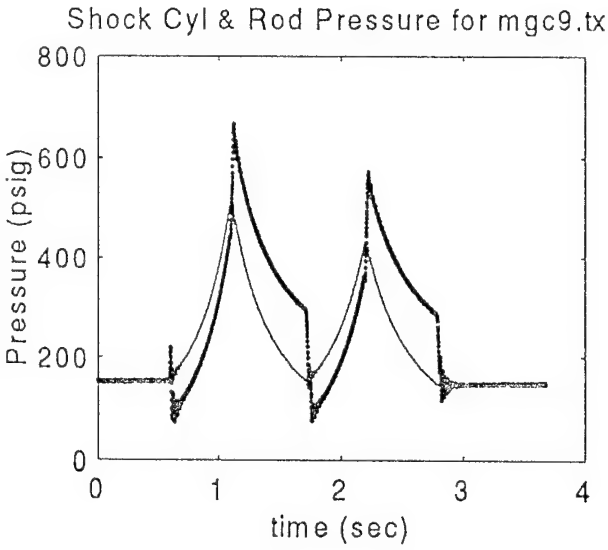
Shock Cyl & Rod Pressure for mgc9.txt
Pressure (psig)
800
600
400
200
0
0
1
2
3
4
time (sec)

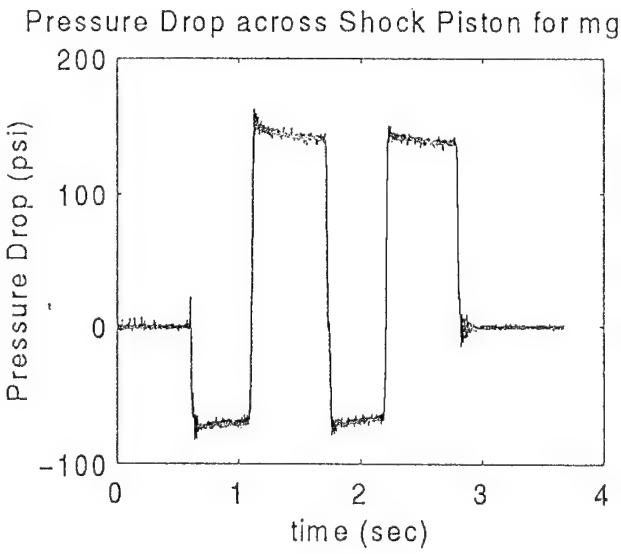
Pressure Drop across Shock Piston for mgc9.txt
Pressure Drop (psi)
200
100
0
−100
0
1
2
3
4
time (sec)

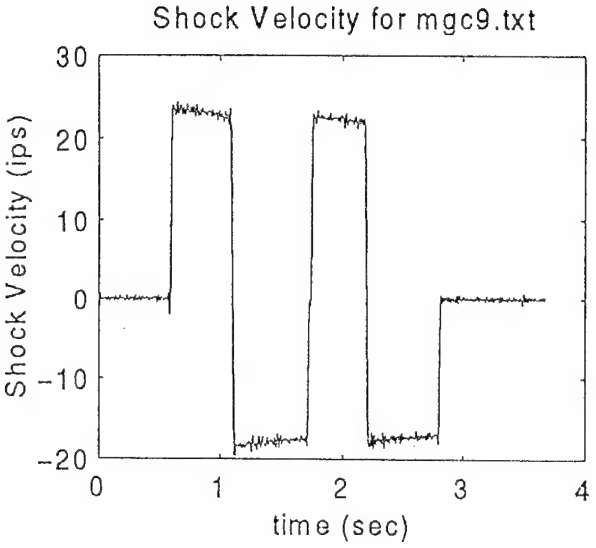
Shock Velocity for mgc9.txt
Shock Velocity (ips)
time (sec)
30
20
10
0
-10
-20
0
1
2
3
4

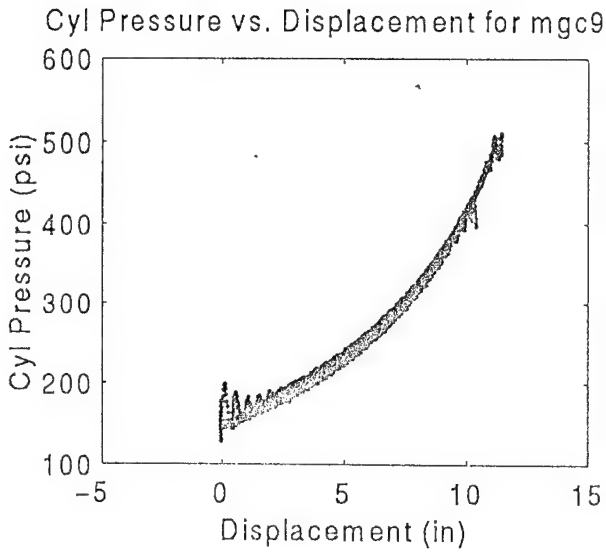
Cyl Pressure vs. Displacement for mgc9.txt
Cyl Pressure (psi)
Displacement (in)
600
500
400
300
200
100
-5
0
5
10
15

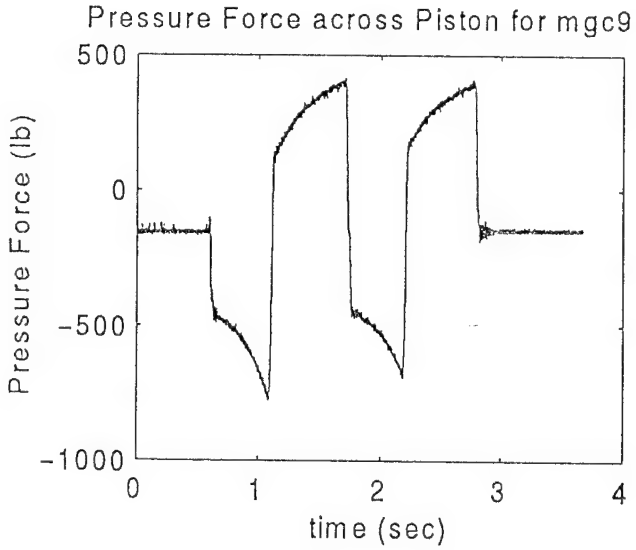
Pressure Force across Piston for mgc9.txt
Pressure Force (lb)
time (sec)
500
0
-500
-1000
0
1
2
3
4

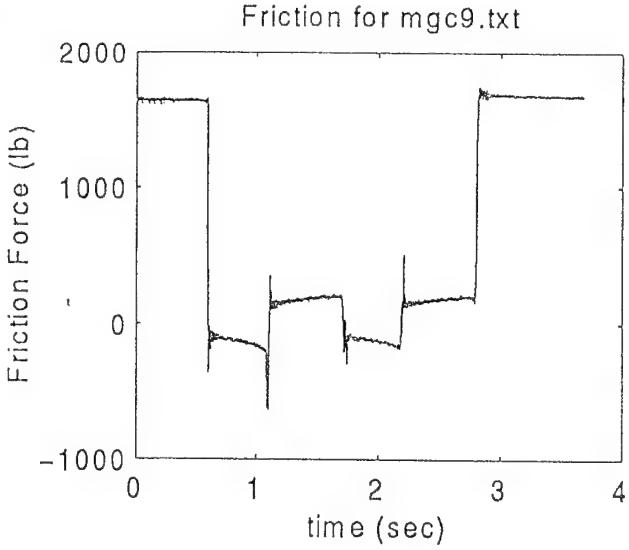
Friction for mgc9.txt
Friction Force (lb)
time (sec)
2000
1000
0
-1000
0
1
2
3
4

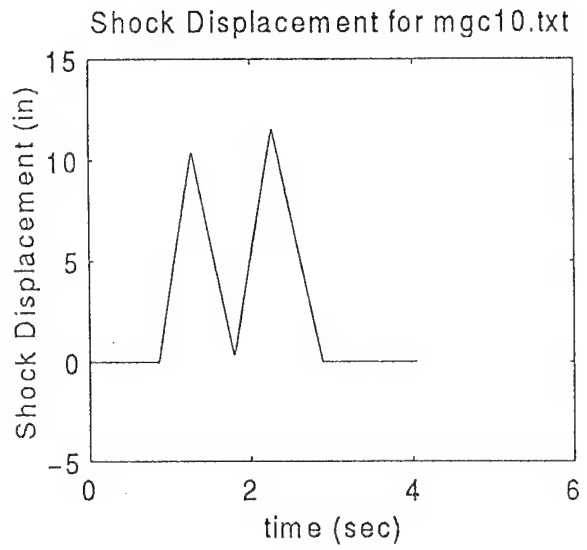
Shock Displacement for mgc10.txt
Shock Displacement (in)
15
10
5
0
-5
0
2
4
6
time (sec)

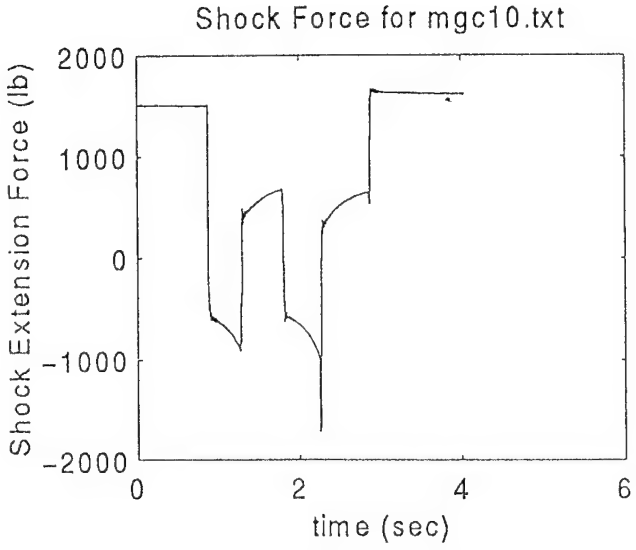
Shock Force for mgc10.txt
Shock Extension Force (lb)
2000
1000
0
-1000
-2000
0
2
4
6
time (sec)

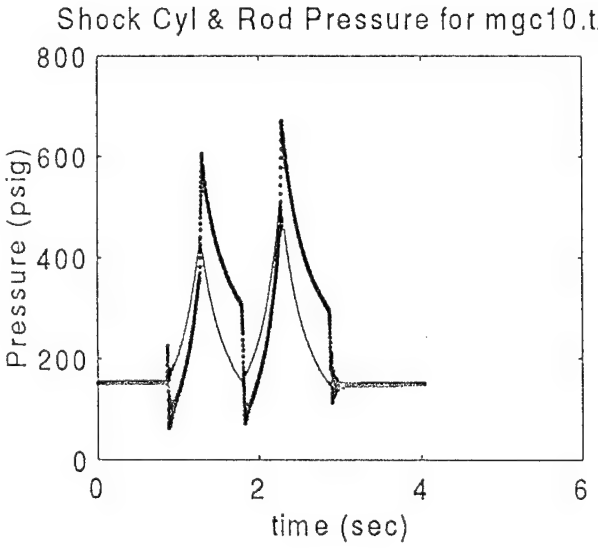
Shock Cyl & Rod Pressure for mgc10.txt
Pressure (psig)
800
600
400
200
0
0
2
4
6
time (sec)

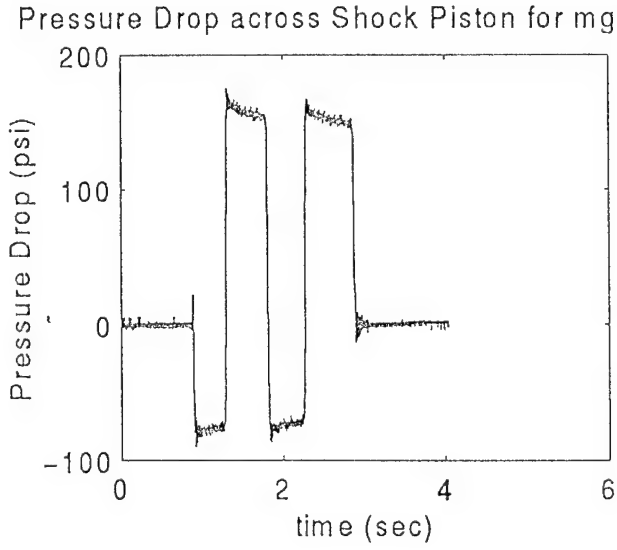
Pressure Drop across Shock Piston for mgc10.txt
Pressure Drop (psi)
200
100
0
-100
0
2
4
6
time (sec)

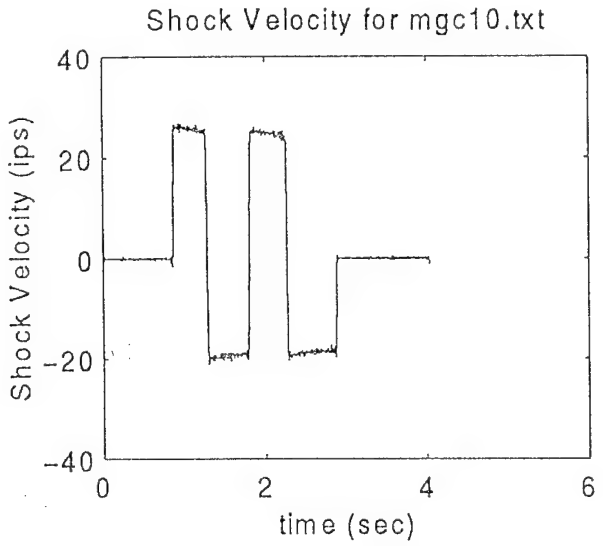
Shock Velocity for mgc10.txt
Shock Velocity (ips)
time (sec)
40
20
0
-20
-40
0
2
4
6

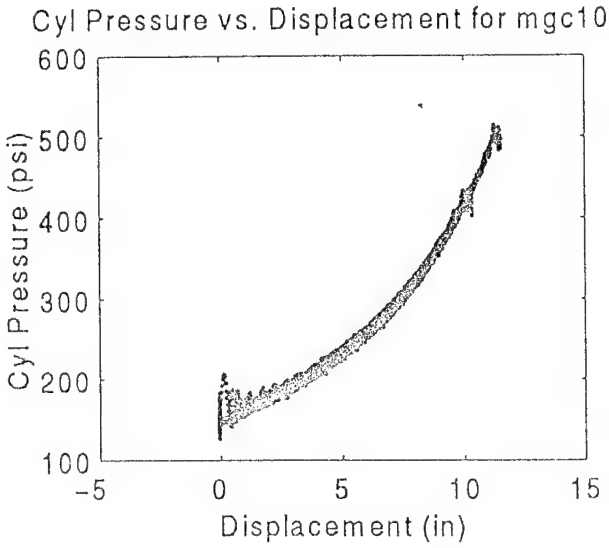
Cyl Pressure vs. Displacement for mgc10.txt
Cyl Pressure (psi)
Displacement (in)
600
500
400
300
200
100
-5
0
5
10
15

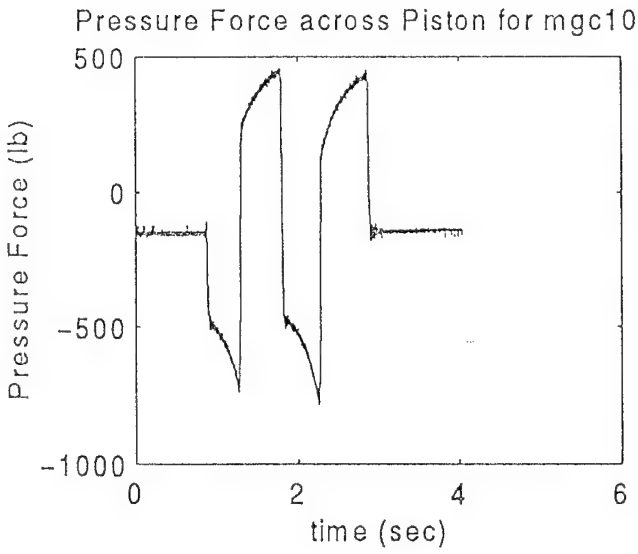
Pressure Force across Piston for mgc10.txt
Pressure Force (lb)
time (sec)
500
0
-500
-1000
0
2
4
6

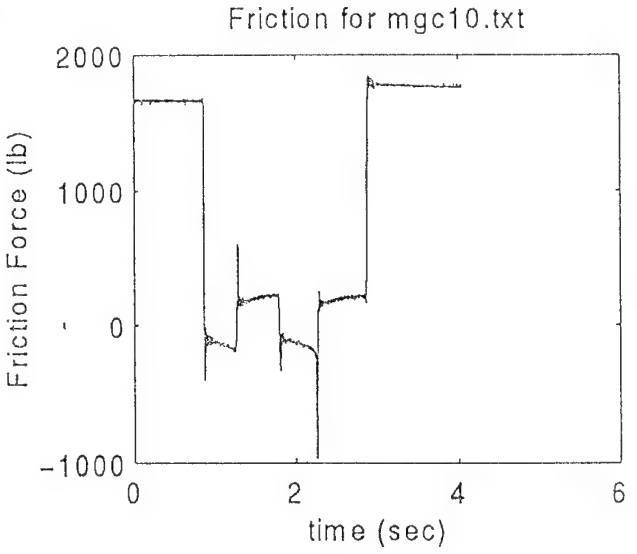
Friction for mgc10.txt
Friction Force (lb)
time (sec)
2000
1000
0
-1000
0
2
4
6

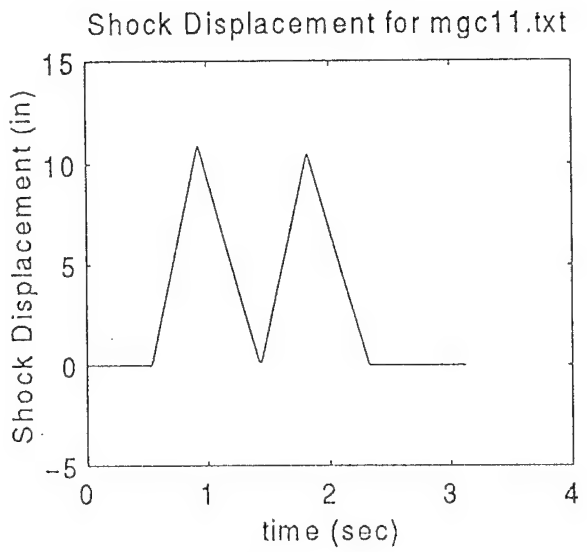
Shock Displacement for mgc11.txt
Shock Displacement (in)
15
10
5
0
-5
0
1
2
3
4
time (sec)

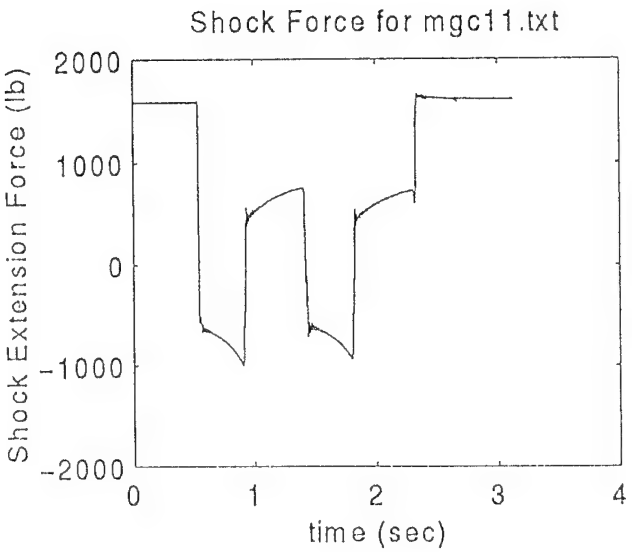
Shock Force for mgc11.txt
Shock Extension Force (lb)
2000
1000
0
-1000
-2000
0
1
2
3
4
time (sec)

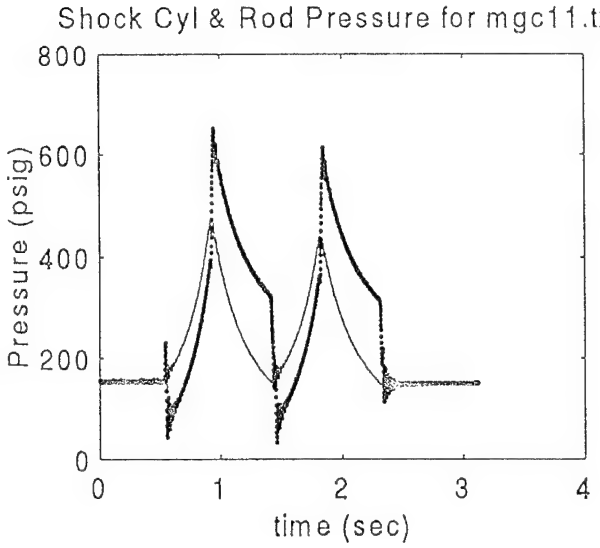
Shock Cyl & Rod Pressure for mgc11.txt
Pressure (psig)
800
600
400
200
0
0
1
2
3
4
time (sec)

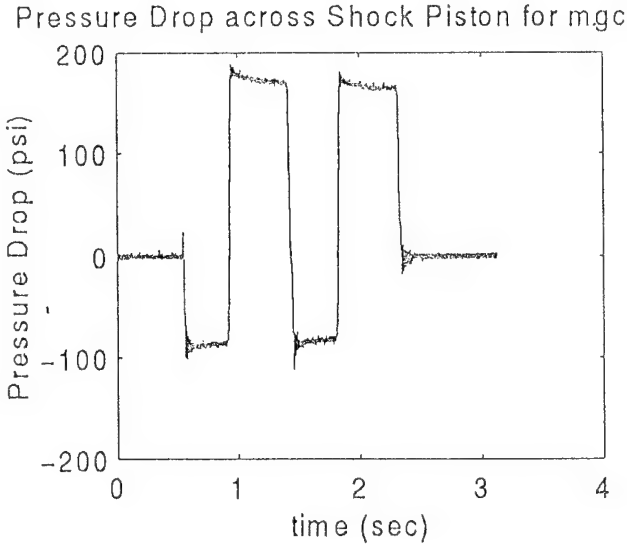
Pressure Drop across Shock Piston for mgc11.txt
Pressure Drop (psi)
200
100
0
-100
-200
0
1
2
3
4
time (sec)

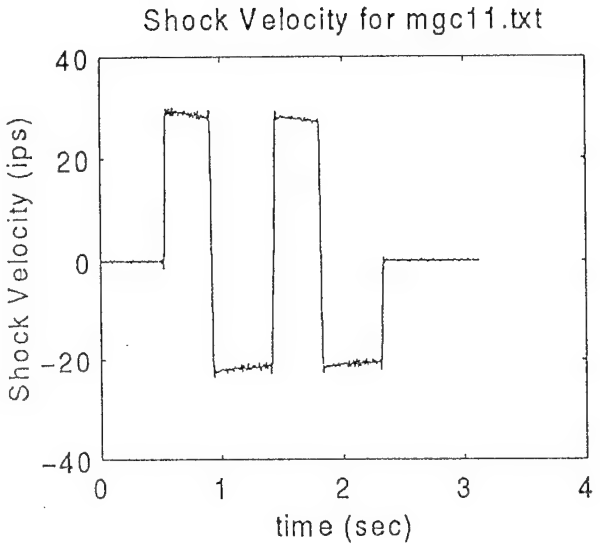
Shock Velocity for mgc11.txt
Shock Velocity (ips)
time (sec)
40
20
0
-20
-40
0
1
2
3
4

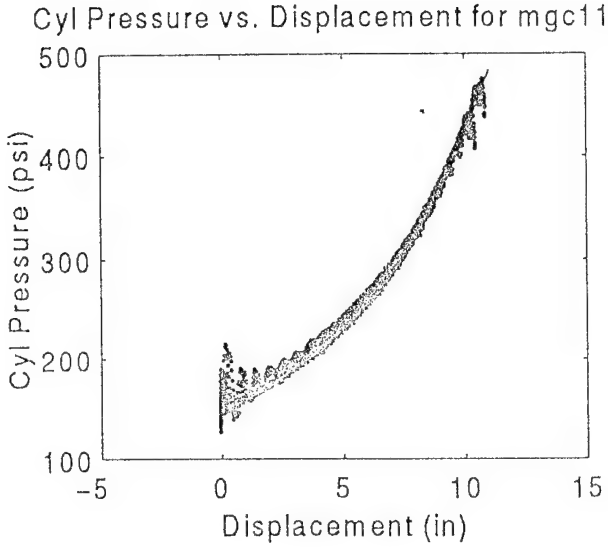
Cyl Pressure vs. Displacement for mgc11.txt
Cyl Pressure (psi)
Displacement (in)
500
400
300
200
100
-5
0
5
10
15

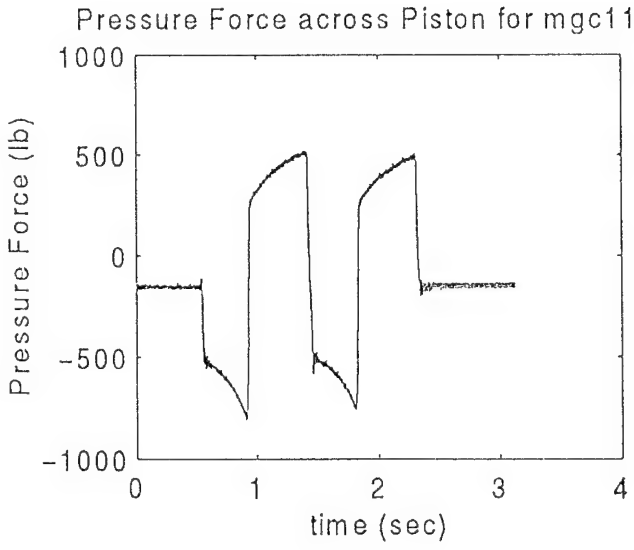
Pressure Force across Piston for mgc11.txt
Pressure Force (lb)
time (sec)
1000
500
0
-500
-1000
0
1
2
3
4

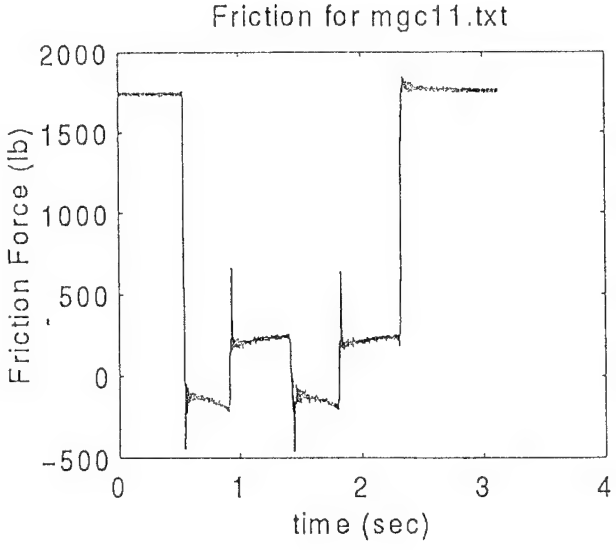
Friction for mgc11.txt
Friction Force (lb)
time (sec)
2000
1500
1000
500
0
-500
0
1
2
3
4

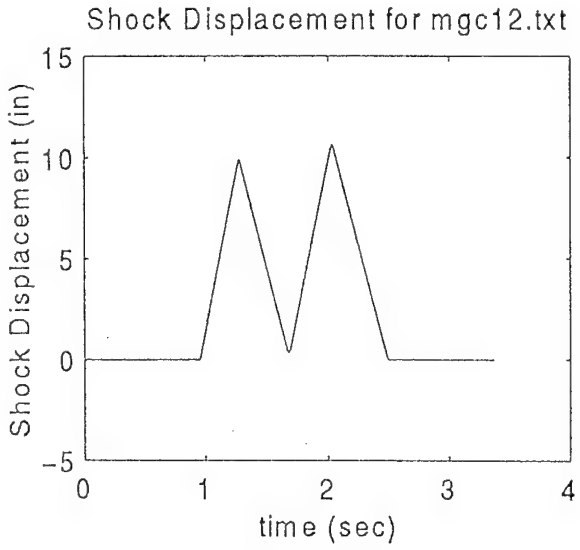
Shock Displacement for mgc12.txt
Shock Displacement (in)
15
10
5
0
-5
0
1
2
3
4
time (sec)

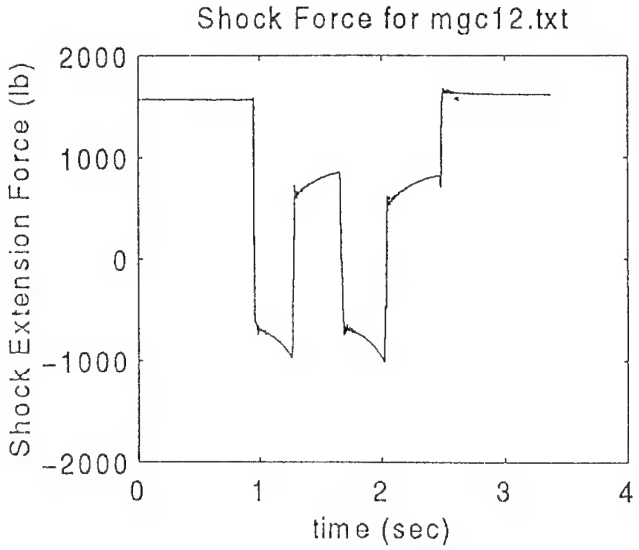
Shock Force for mgc12.txt
Shock Extension Force (lb)
2000
1000
0
-1000
-2000
0
1
2
3
4
time (sec)

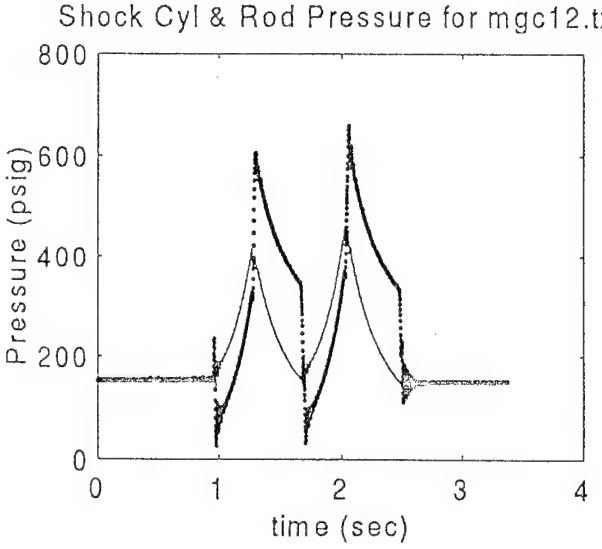
Shock Cyl & Rod Pressure for mgc12.txt
Pressure (psig)
800
600
400
200
0
0
1
2
3
4
time (sec)

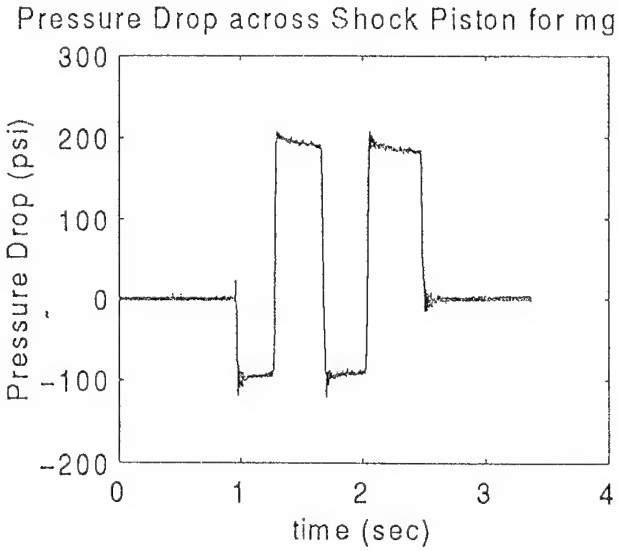
Pressure Drop across Shock Piston for mgc12.txt
Pressure Drop (psi)
300
200
100
0
-100
-200
0
1
2
3
4
time (sec)

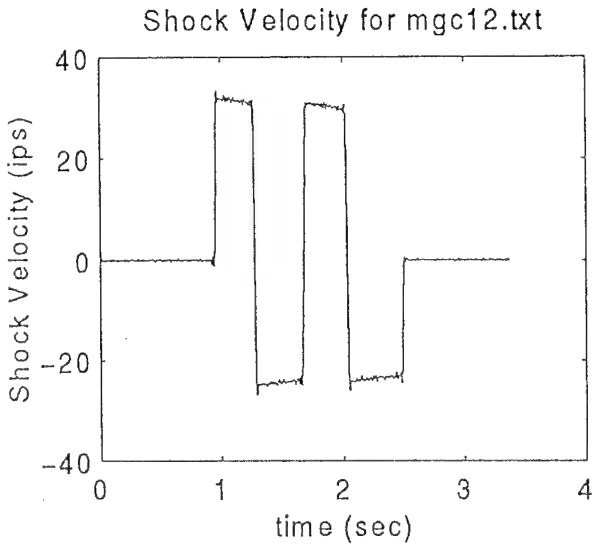
Shock Velocity for mgc12.txt
Shock Velocity (ips)
time (sec)
40
20
0
-20
-40
0
1
2
3
4

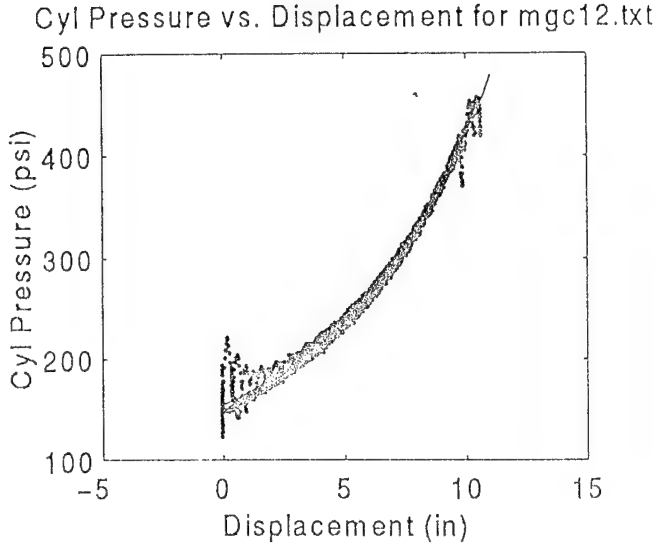
Cyl Pressure vs. Displacement for mgc12.txt
Cyl Pressure (psi)
Displacement (in)
500
400
300
200
100
-5
0
5
10
15

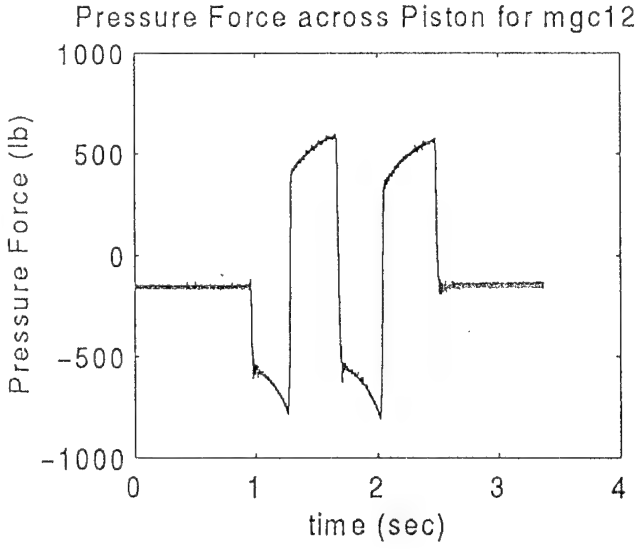
Pressure Force across Piston for mgc12.txt
Pressure Force (lb)
time (sec)
1000
500
0
-500
-1000
0
1
2
3
4

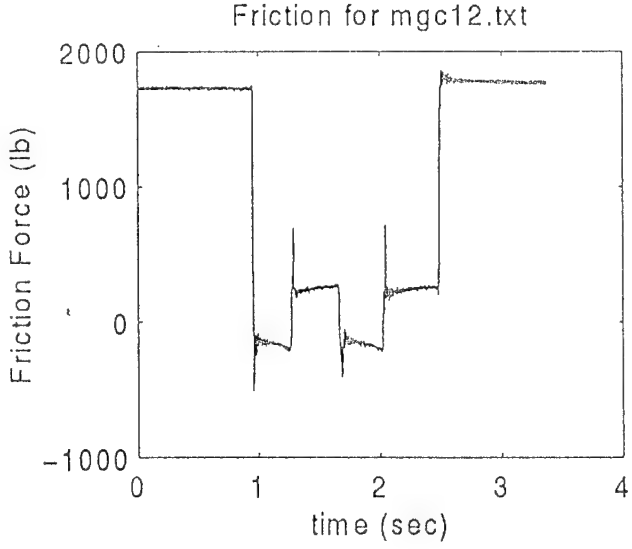
Friction for mgc12.txt
Friction Force (lb)
time (sec)
2000
1000
0
-1000
0
1
2
3
4

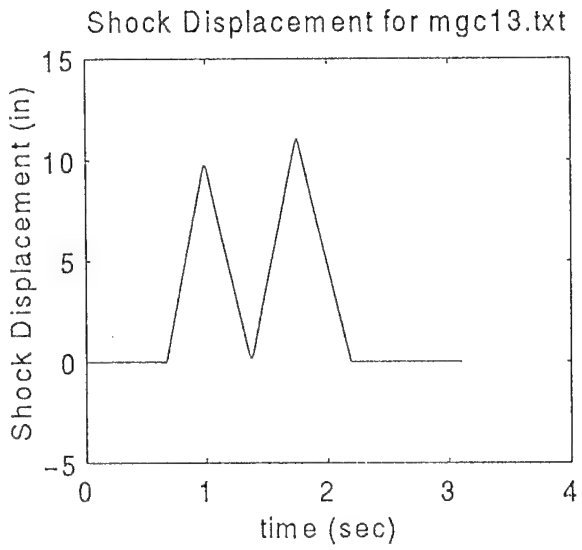
Shock Displacement for mgc13.txt
Shock Displacement (in)
15
10
5
0
-5
0
1
2
3
4
time (sec)

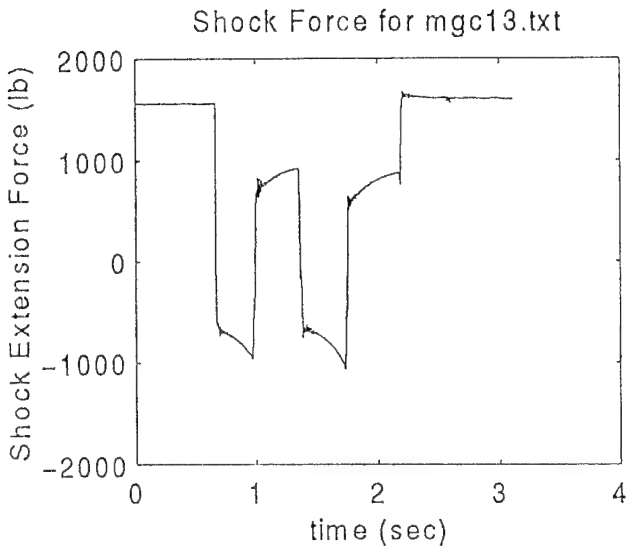
Shock Force for mgc13.txt
Shock Extension Force (lb)
2000
1000
0
-1000
-2000
0
1
2
3
4
time (sec)

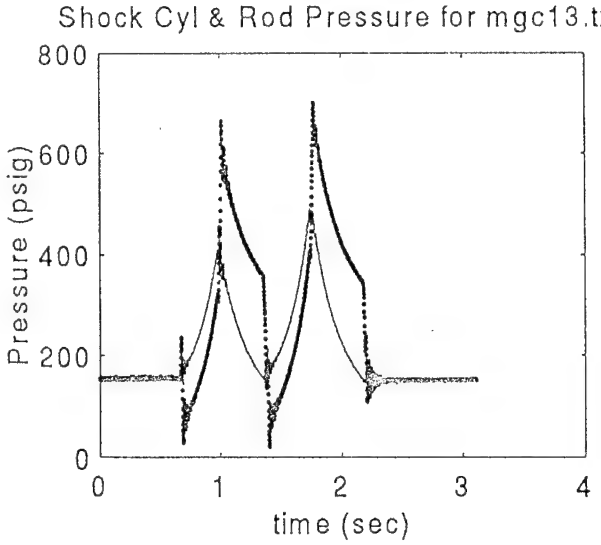
Shock Cyl & Rod Pressure for mgc13.txt
Pressure (psig)
800
600
400
200
0
0
1
2
3
4
time (sec)

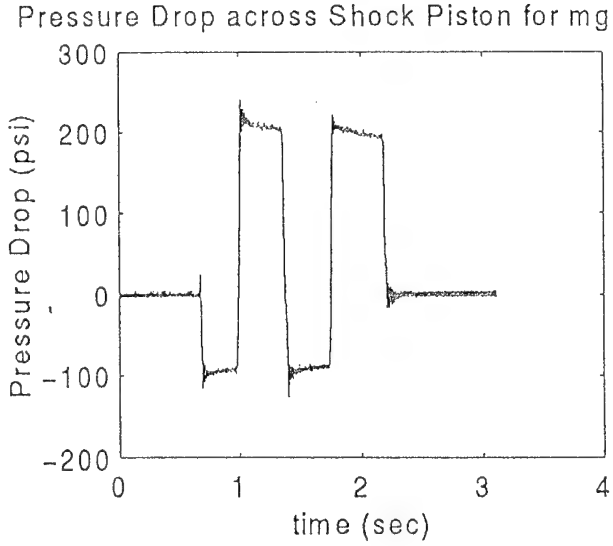
Pressure Drop across Shock Piston for mgc13.txt
Pressure Drop (psi)
300
200
100
0
-100
-200
0
1
2
3
4
time (sec)

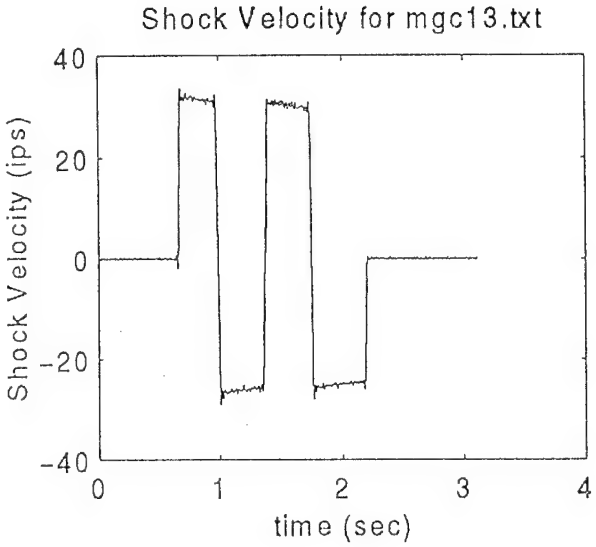
Shock Velocity for mgc13.txt
Shock Velocity (ips)
time (sec)
40
20
0
-20
-40
0
1
2
3
4

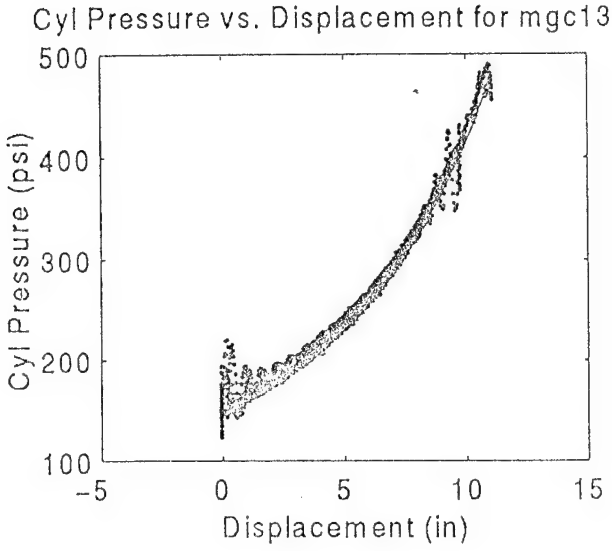
Cyl Pressure vs. Displacement for mgc13.txt
Cyl Pressure (psi)
Displacement (in)
500
400
300
200
100
-5
0
5
10
15

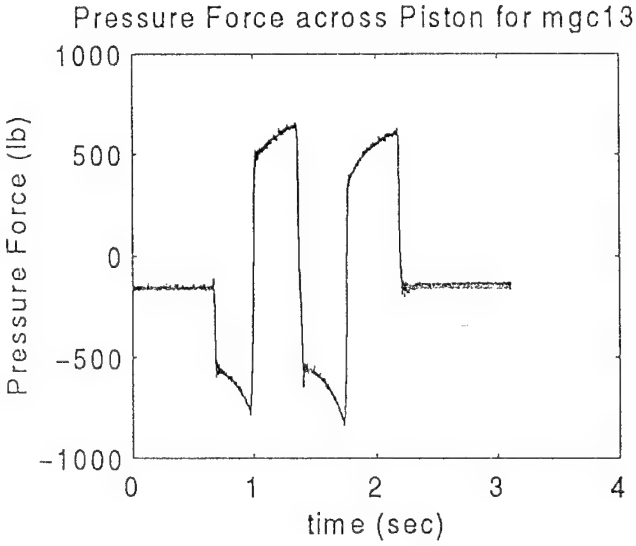
Pressure Force across Piston for mgc13.txt
Pressure Force (lb)
time (sec)
1000
500
0
-500
-1000
0
1
2
3
4

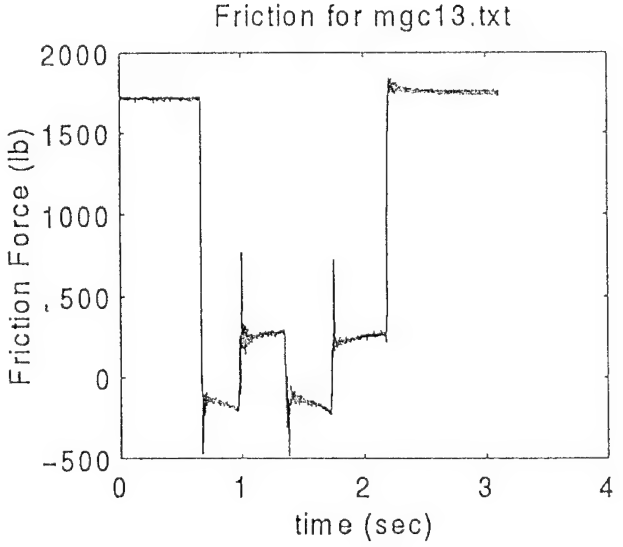
Friction for mgc13.txt
Friction Force (lb)
time (sec)
2000
1500
1000
500
0
-500
0
1
2
3
4

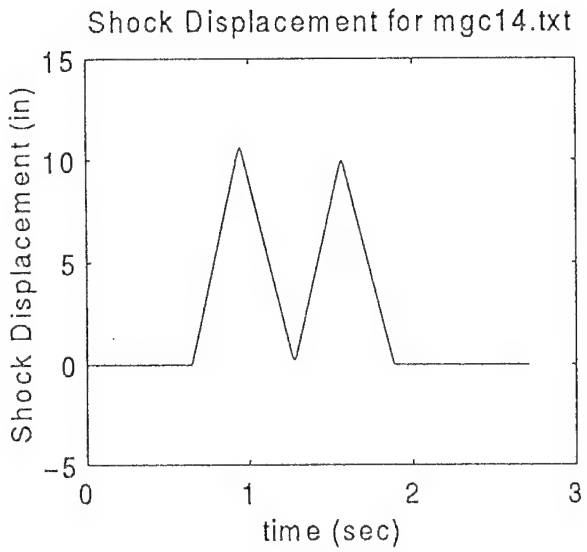
Shock Displacement for mgc14.txt
Shock Displacement (in)
15
10
5
0
−5
0
1
2
3
time (sec)

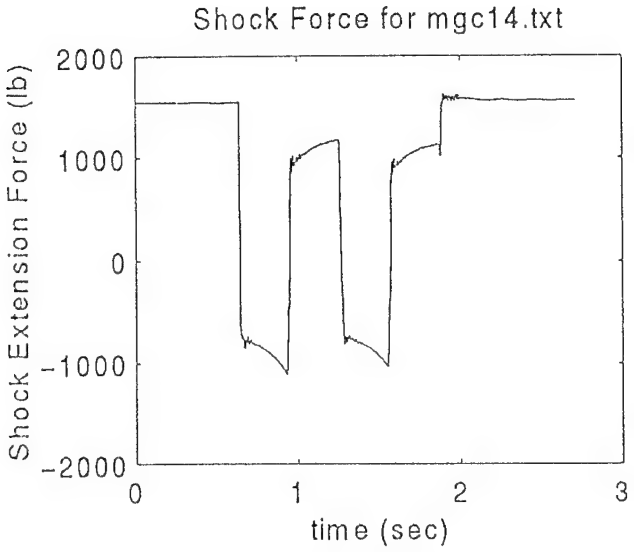
Shock Force for mgc14.txt
Shock Extension Force (lb)
2000
1000
0
−1000
−2000
0
1
2
3
time (sec)

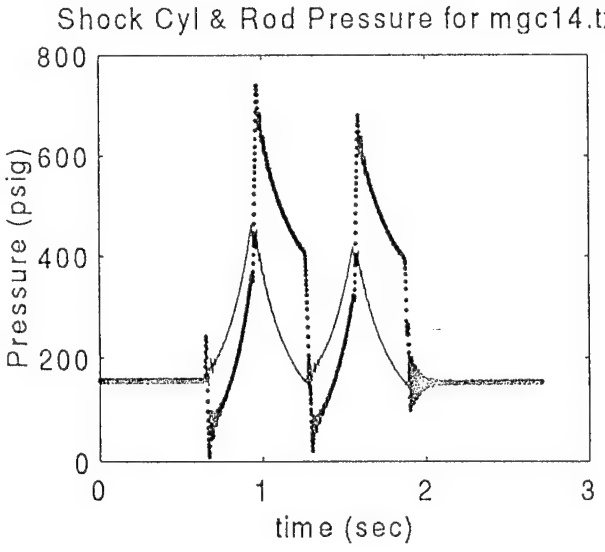
Shock Cyl & Rod Pressure for mgc14.txt
Pressure (psig)
800
600
400
200
0
0
1
2
3
time (sec)

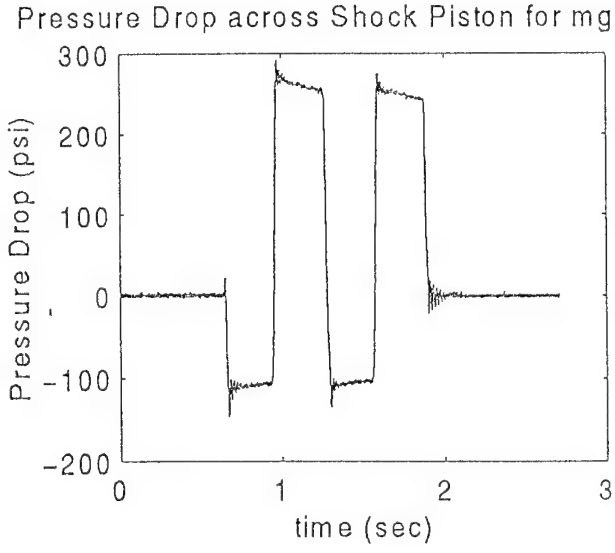
Pressure Drop across Shock Piston for mgc14.txt
Pressure Drop (psi)
300
200
100
0
−100
−200
0
1
2
3
time (sec)

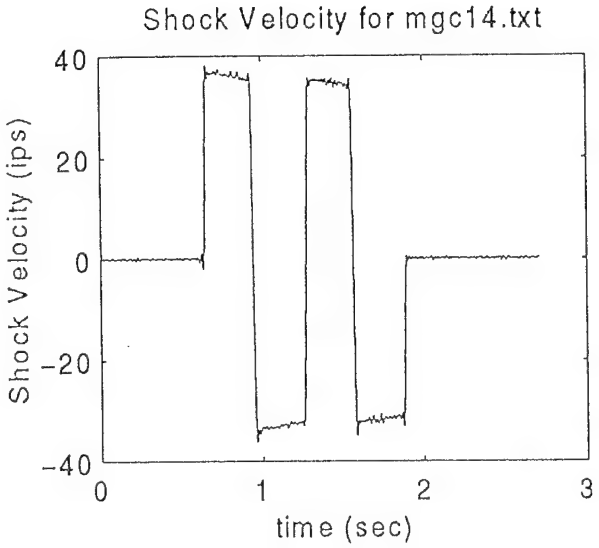
Shock Velocity for mgc14.txt
Shock Velocity (ips)
time (sec)
40
20
0
-20
-40
0
1
2
3

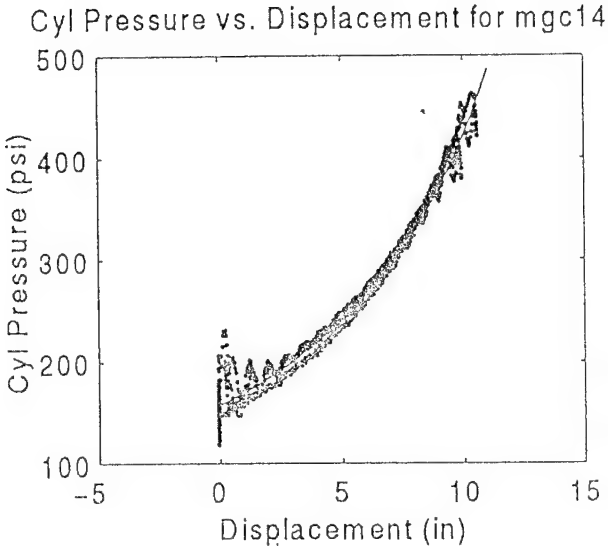
Cyl Pressure vs. Displacement for mgc14.txt
Cyl Pressure (psi)
Displacement (in)
500
400
300
200
100
-5
0
5
10
15

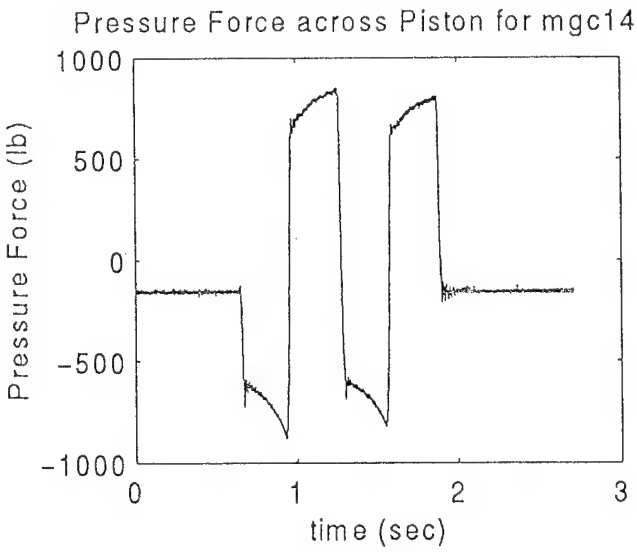
Pressure Force across Piston for mgc14.txt
Pressure Force (lb)
time (sec)
1000
500
0
-500
-1000
0
1
2
3

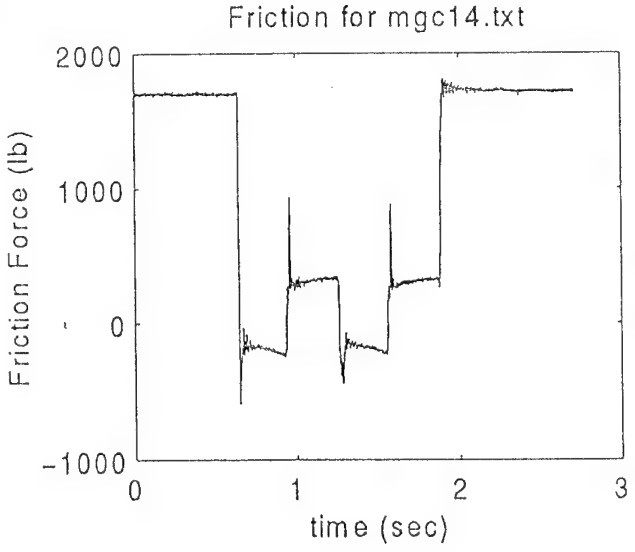
Friction for mgc14.txt
Friction Force (lb)
time (sec)
2000
1000
0
-1000
0
1
2
3

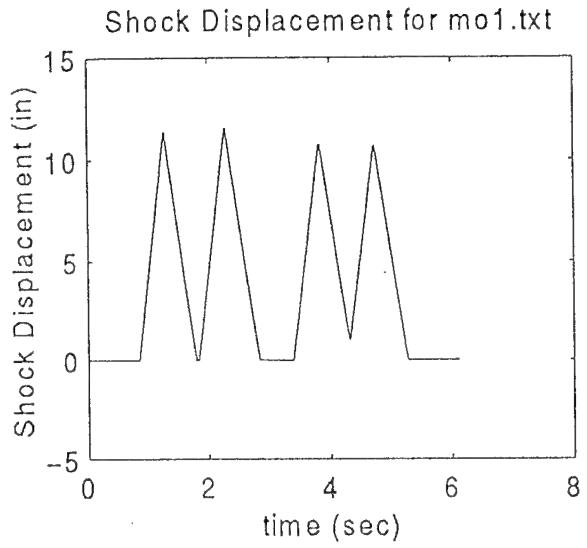
Shock Displacement for mo1.txt
Shock Displacement (in)
15
10
5
0
-5
0
2
4
6
8
time (sec)

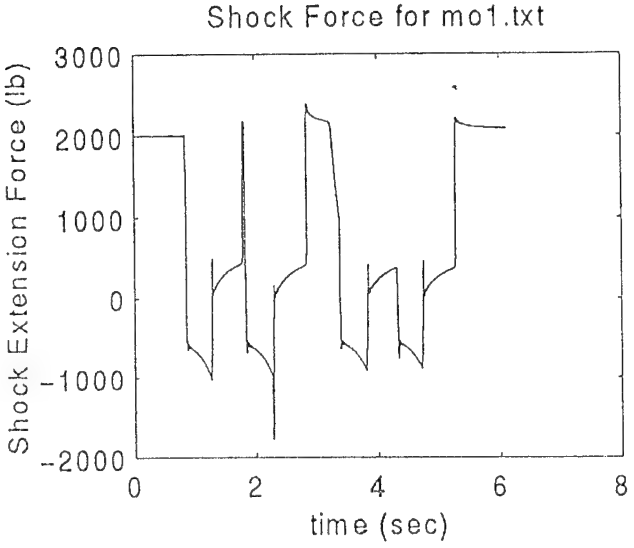
Shock Force for mo1.txt
Shock Extension Force (lb)
3000
2000
1000
0
-1000
-2000
0
2
4
6
8
time (sec)

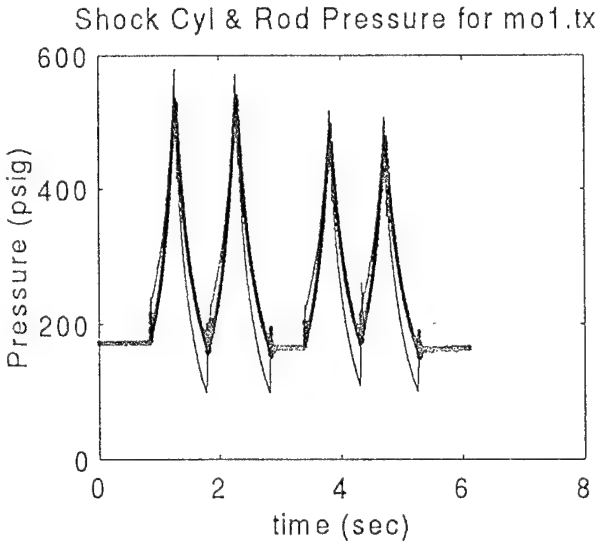
Shock Cyl & Rod Pressure for mo1.txt
Pressure (psig)
600
400
200
0
0
2
4
6
8
time (sec)

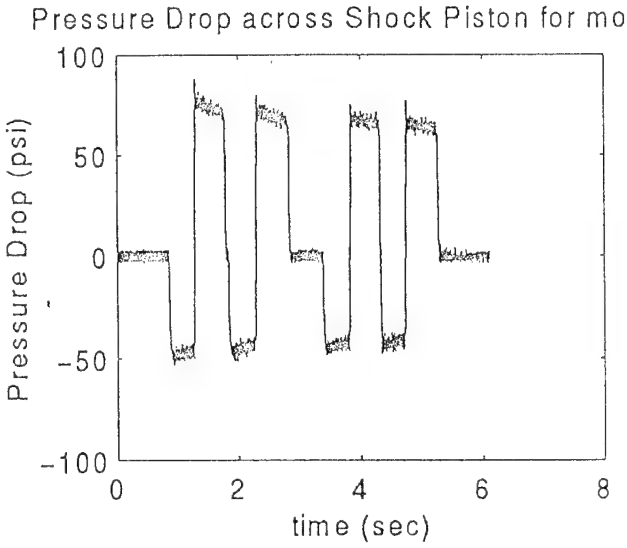
Pressure Drop across Shock Piston for mo1.txt
Pressure Drop (psi)
100
50
0
-50
-100
0
2
4
6
8
time (sec)

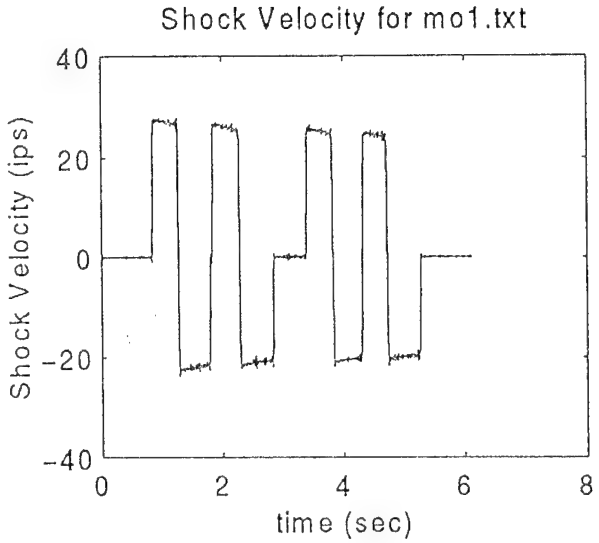
Shock Velocity for mo1.txt
Shock Velocity (ips)
time (sec)
40
20
0
-20
-40
0
2
4
6
8

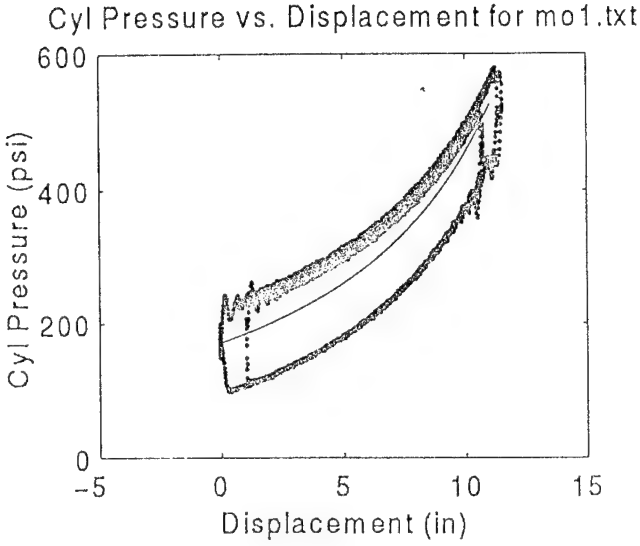
Cyl Pressure vs. Displacement for mo1.txt
Cyl Pressure (psi)
Displacement (in)
600
400
200
0
-5
0
5
10
15

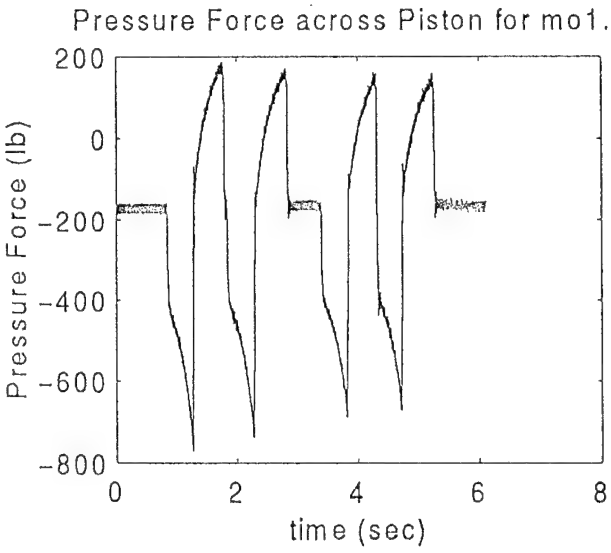
Pressure Force across Piston for mo1.txt
Pressure Force (lb)
time (sec)
200
0
-200
-400
-600
-800
0
2
4
6
8

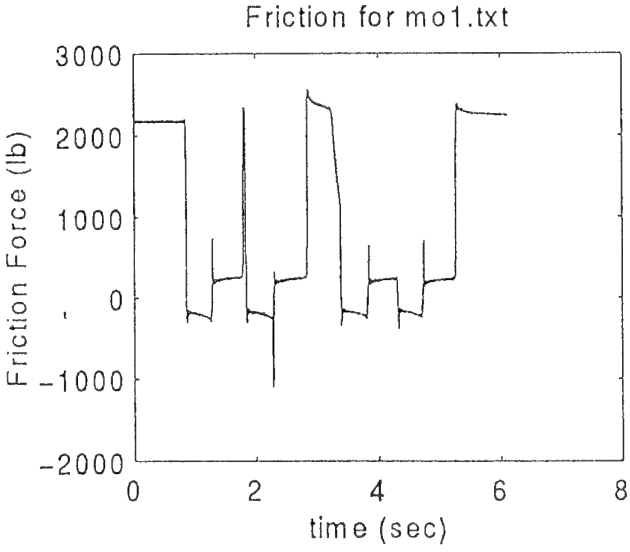
Friction for mo1.txt
Friction Force (lb)
time (sec)
3000
2000
1000
0
-1000
-2000
0
2
4
6
8

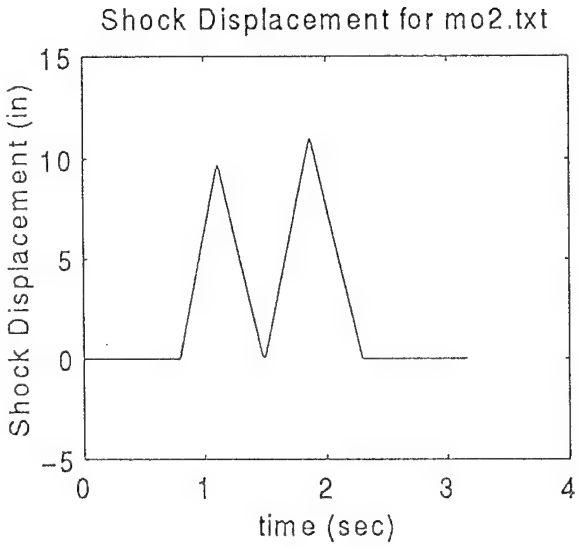
Shock Displacement for mo2.txt
Shock Displacement (in)
15
10
5
0
−5
0
1
2
3
4
time (sec)

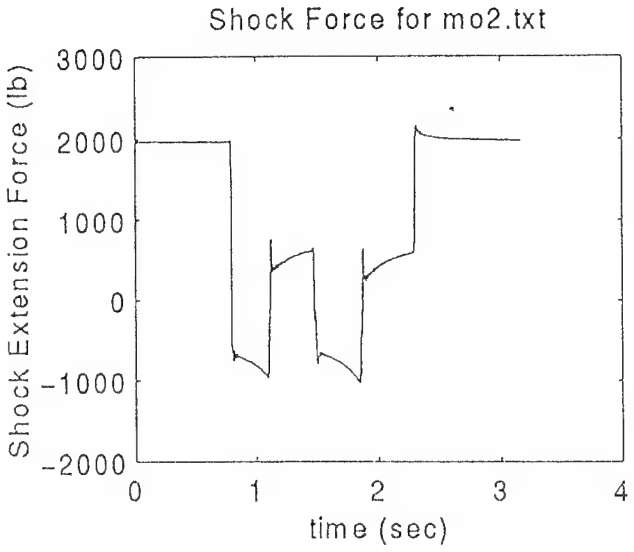
Shock Force for mo2.txt
Shock Extension Force (lb)
3000
2000
1000
0
−1000
−2000
0
1
2
3
4
time (sec)

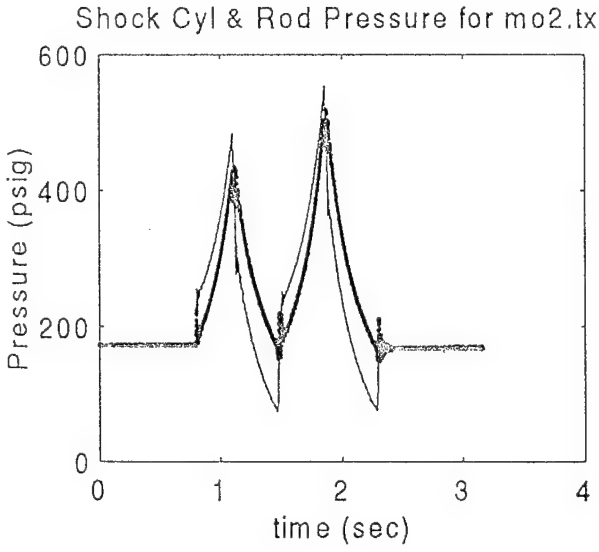
Shock Cyl & Rod Pressure for mo2.txt
Pressure (psig)
600
400
200
0
0
1
2
3
4
time (sec)

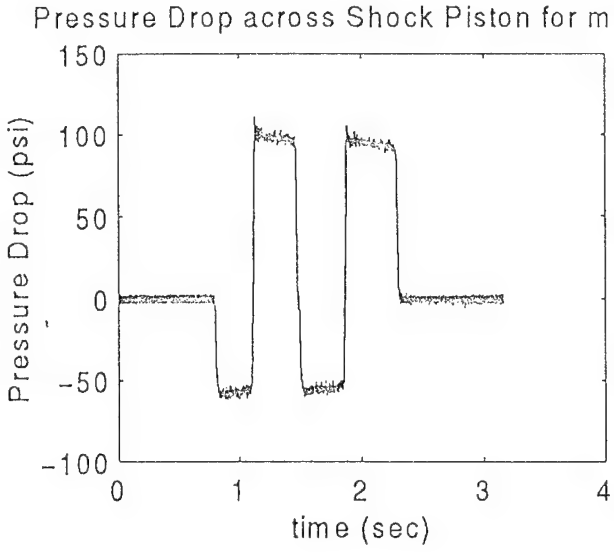
Pressure Drop across Shock Piston for mo2.txt
Pressure Drop (psi)
150
100
50
0
−50
−100
0
1
2
3
4
time (sec)

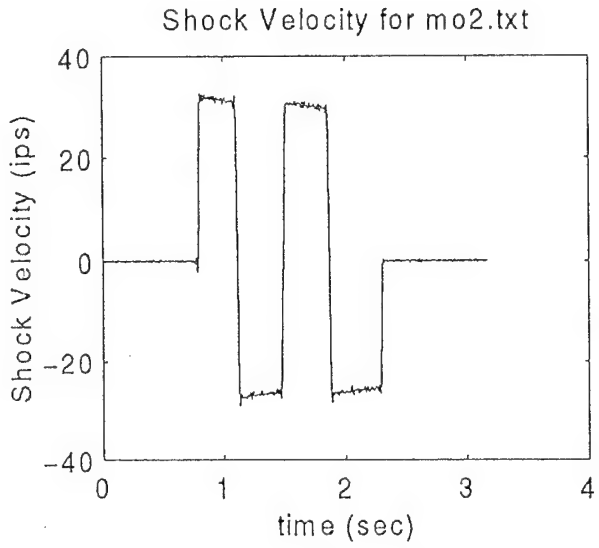
Shock Velocity for mo2.txt
Shock Velocity (ips)
time (sec)
40
20
0
-20
-40
0
1
2
3
4

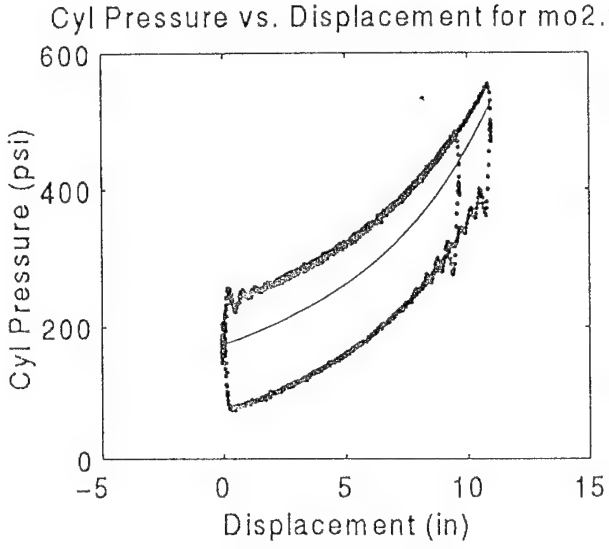
Cyl Pressure vs. Displacement for mo2.txt
Cyl Pressure (psi)
Displacement (in)
600
400
200
0
-5
0
5
10
15

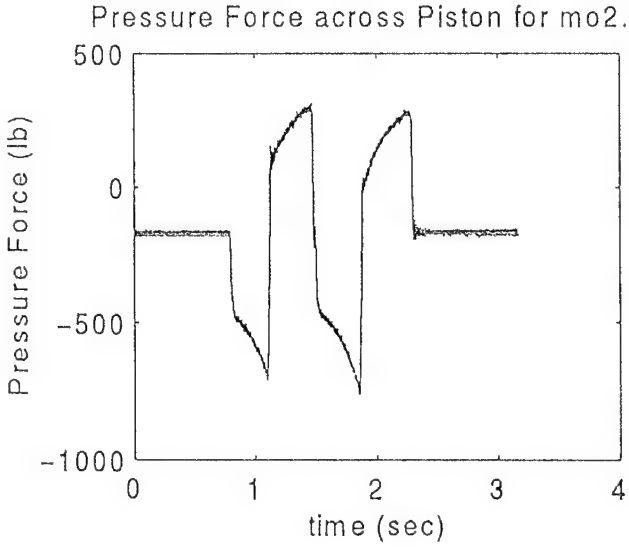
Pressure Force across Piston for mo2.txt
Pressure Force (lb)
time (sec)
500
0
-500
-1000
0
1
2
3
4

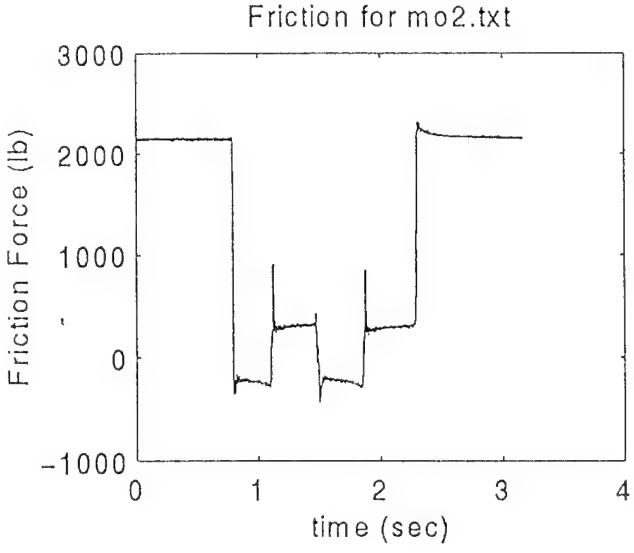
Friction for mo2.txt
Friction Force (lb)
time (sec)
3000
2000
1000
0
-1000
0
1
2
3
4

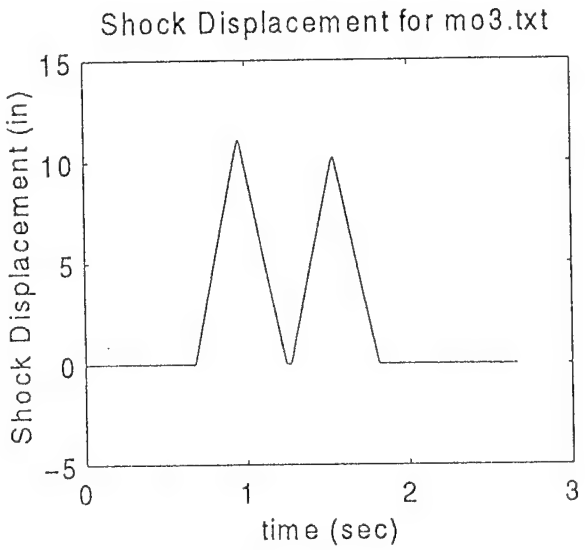
Shock Displacement for mo3.txt
Shock Displacement (in)
15
10
5
0
-5
0
1
2
3
time (sec)

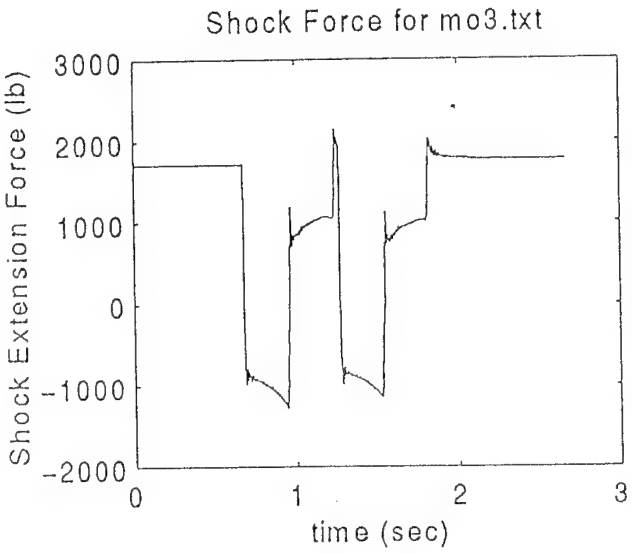
Shock Force for mo3.txt
Shock Extension Force (lb)
3000
2000
1000
0
-1000
-2000
0
1
2
3
time (sec)

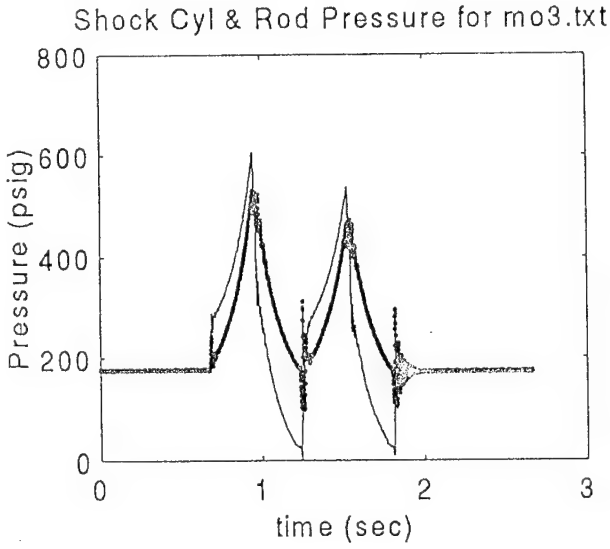
Shock Cyl & Rod Pressure for mo3.txt
Pressure (psig)
800
600
400
200
0
0
1
2
3
time (sec)

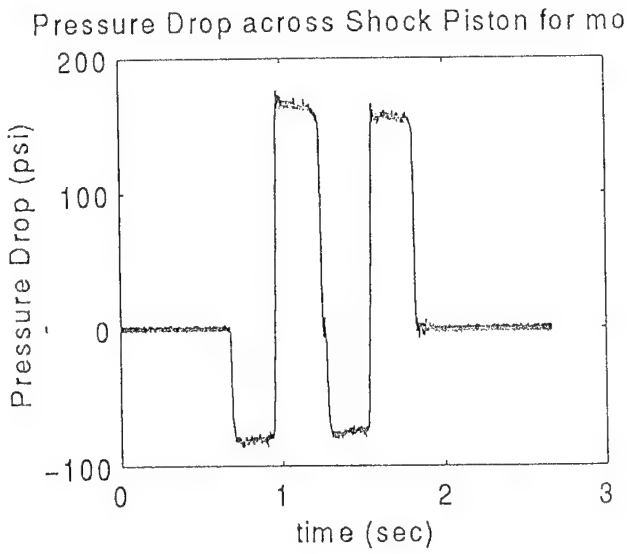
Pressure Drop across Shock Piston for mo3.txt
Pressure Drop (psi)
200
100
0
-100
0
1
2
3
time (sec)

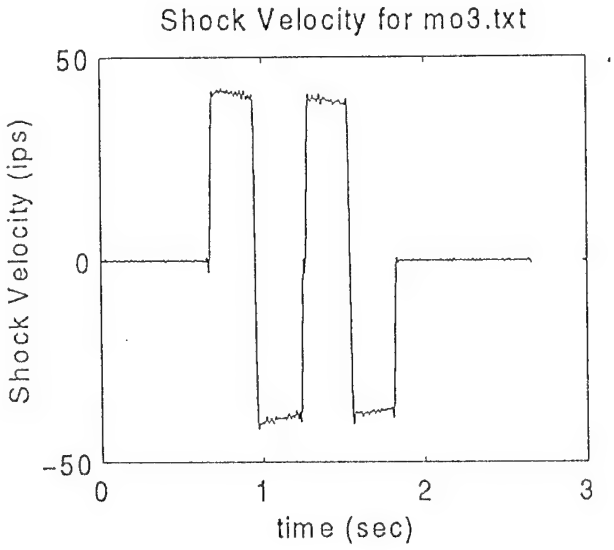
Shock Velocity for mo3.txt
Shock Velocity (ips)
time (sec)
50
0
-50
0
1
2
3

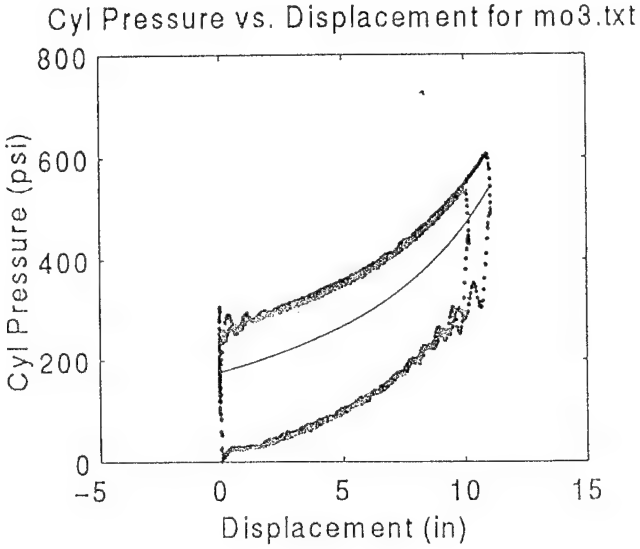
Cyl Pressure vs. Displacement for mo3.txt
Cyl Pressure (psi)
Displacement (in)
800
600
400
200
0
-5
0
5
10
15

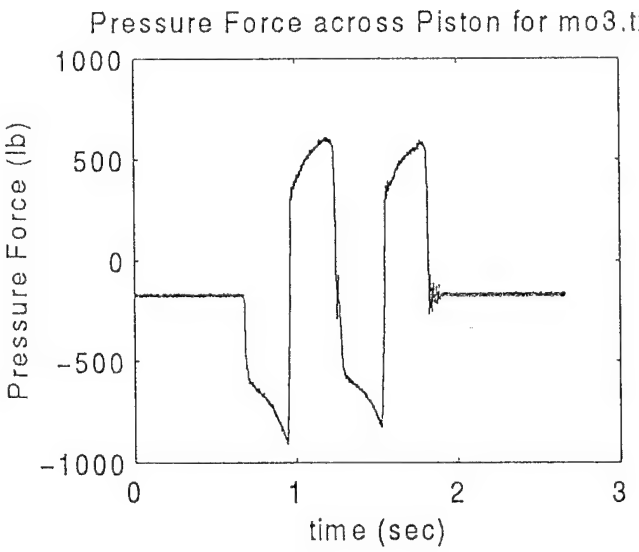
Pressure Force across Piston for mo3.txt
Pressure Force (lb)
time (sec)
1000
500
0
-500
-1000
0
1
2
3

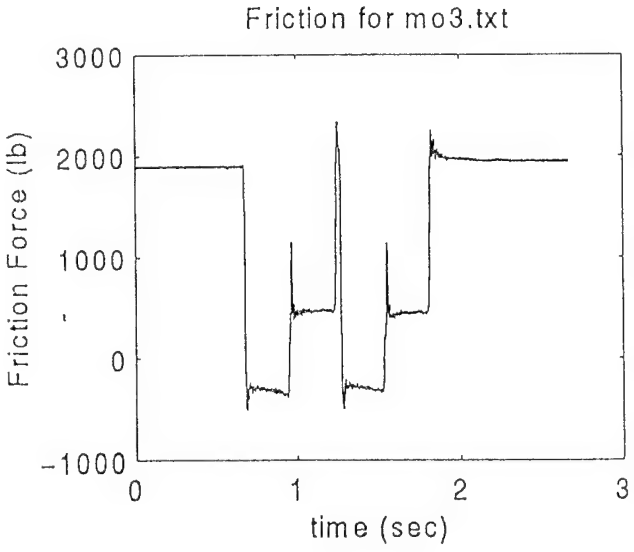
Friction for mo3.txt
Friction Force (lb)
time (sec)
3000
2000
1000
0
-1000
0
1
2
3

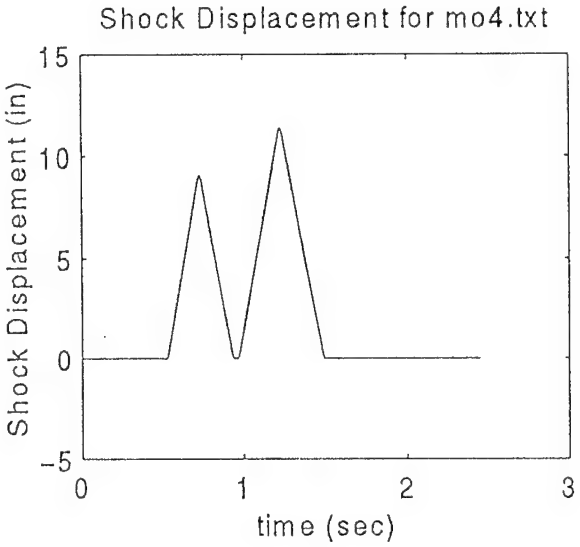
Shock Displacement for mo4.txt
Shock Displacement (in)
15
10
5
0
-5
0
1
2
3
time (sec)

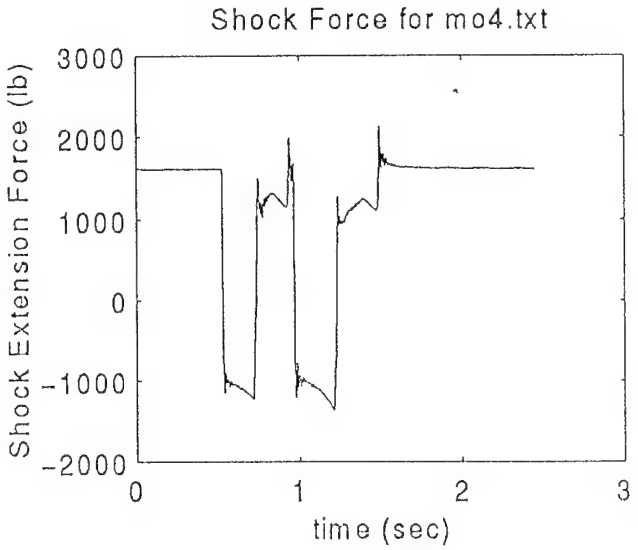
Shock Force for mo4.txt
Shock Extension Force (lb)
3000
2000
1000
0
-1000
-2000
0
1
2
3
time (sec)

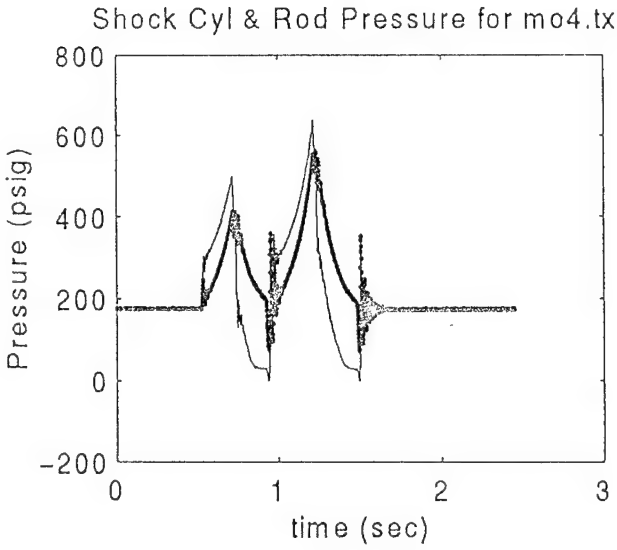
Shock Cyl & Rod Pressure for mo4.txt
Pressure (psig)
800
600
400
200
0
-200
0
1
2
3
time (sec)

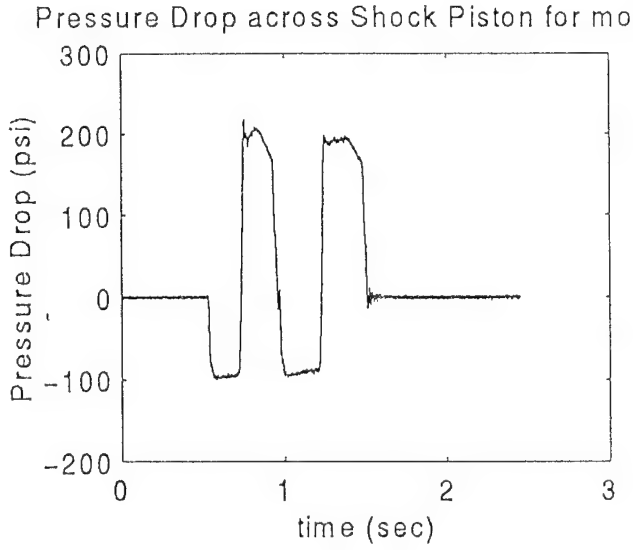
Pressure Drop across Shock Piston for mo4.txt
Pressure Drop (psi)
300
200
100
0
-100
-200
0
1
2
3
time (sec)

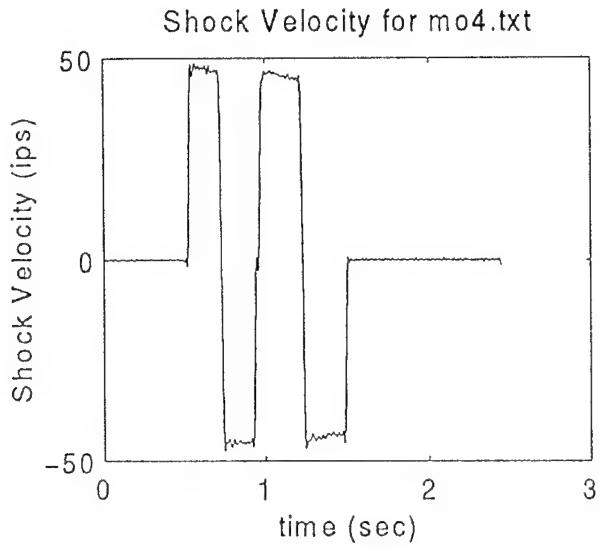
Shock Velocity for mo4.txt
Shock Velocity (ips)
time (sec)
50
0
-50
0
1
2
3

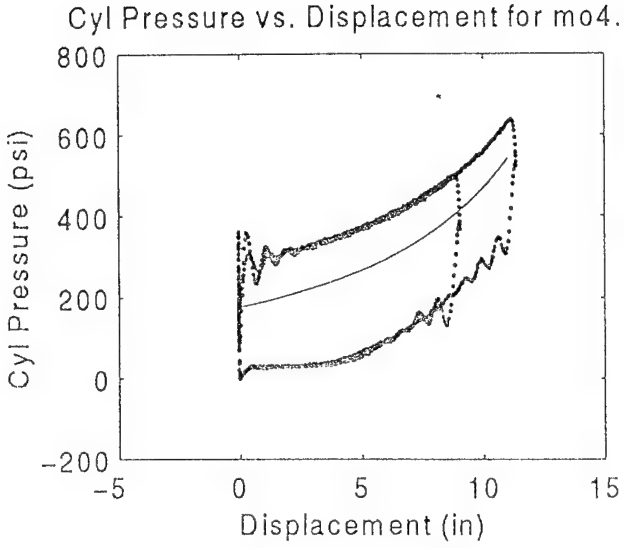
Cyl Pressure vs. Displacement for mo4.txt
Cyl Pressure (psi)
Displacement (in)
800
600
400
200
0
-200
-5
0
5
10
15

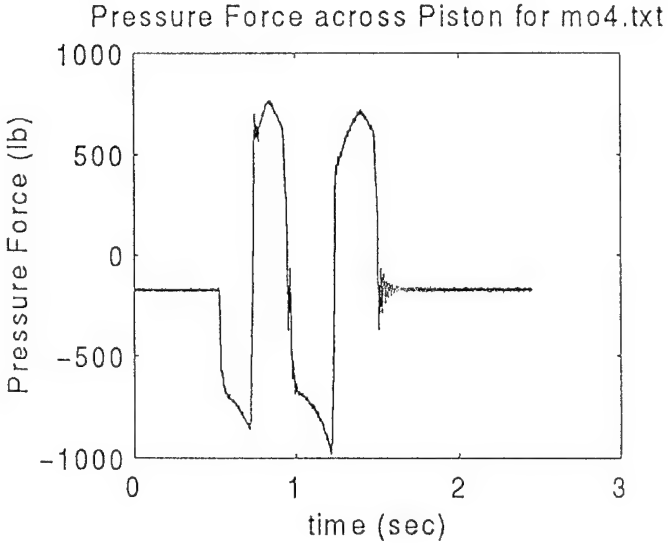
Pressure Force across Piston for mo4.txt
Pressure Force (lb)
time (sec)
1000
500
0
-500
-1000
0
1
2
3

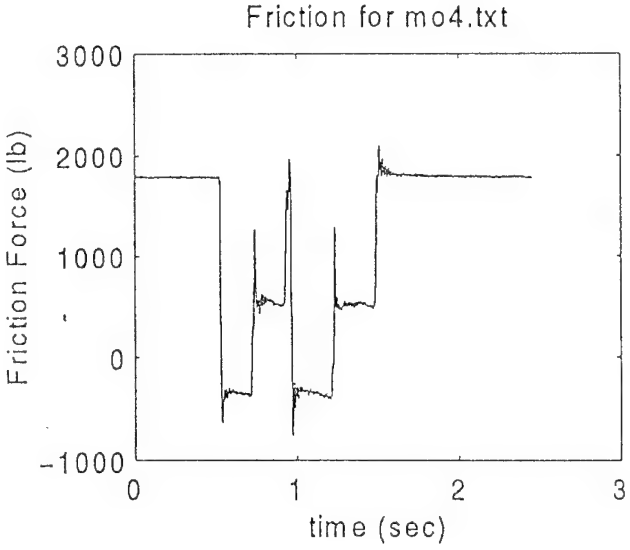
Friction for mo4.txt
Friction Force (lb)
time (sec)
3000
2000
1000
0
-1000
0
1
2
3

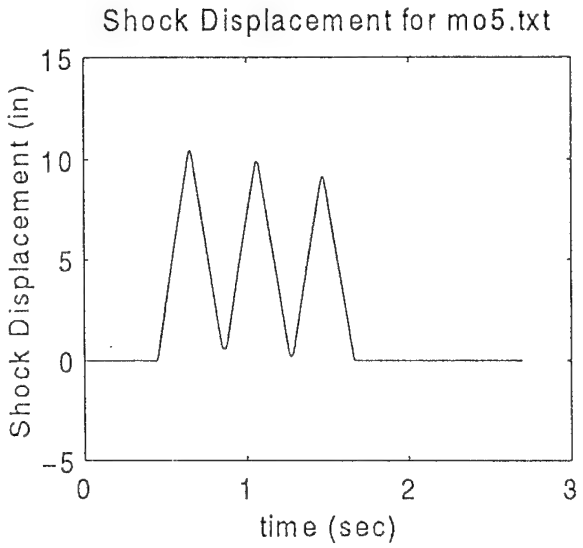
Shock Displacement for mo5.txt
Shock Displacement (in)
15
10
5
0
-5
0
1
2
3
time (sec)

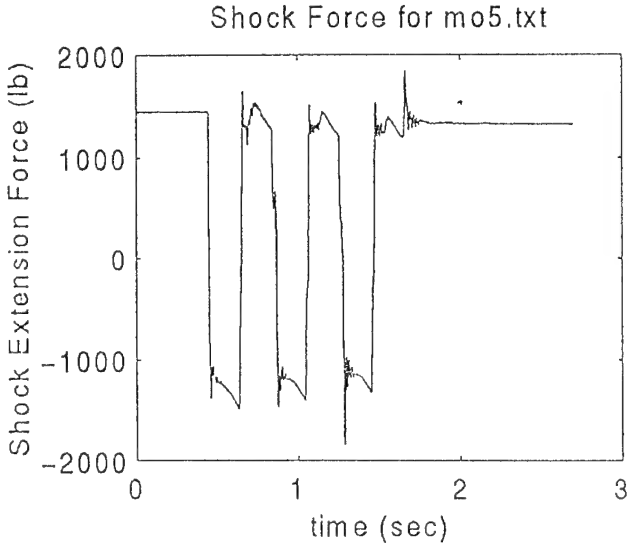
Shock Force for mo5.txt
Shock Extension Force (lb)
2000
1000
0
-1000
-2000
0
1
2
3
time (sec)

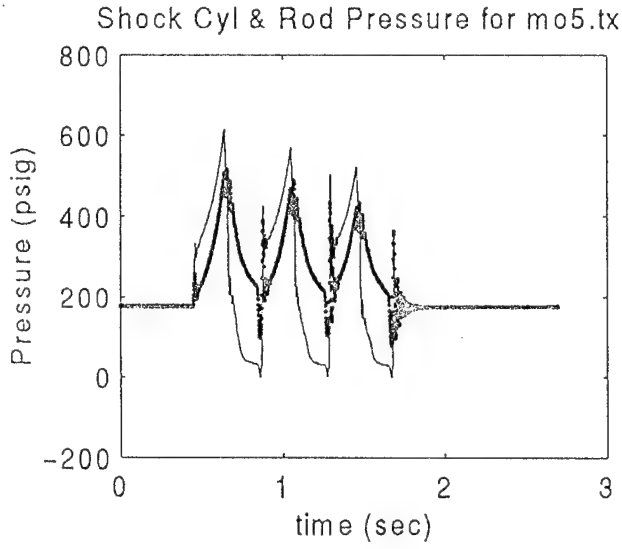
Shock Cyl & Rod Pressure for mo5.txt
Pressure (psig)
800
600
400
200
0
-200
0
1
2
3
time (sec)

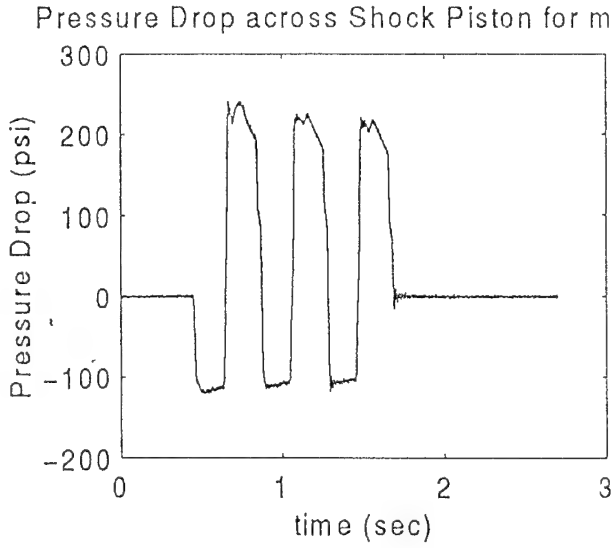
Pressure Drop across Shock Piston for mo5.txt
Pressure Drop (psi)
300
200
100
0
-100
-200
0
1
2
3
time (sec)

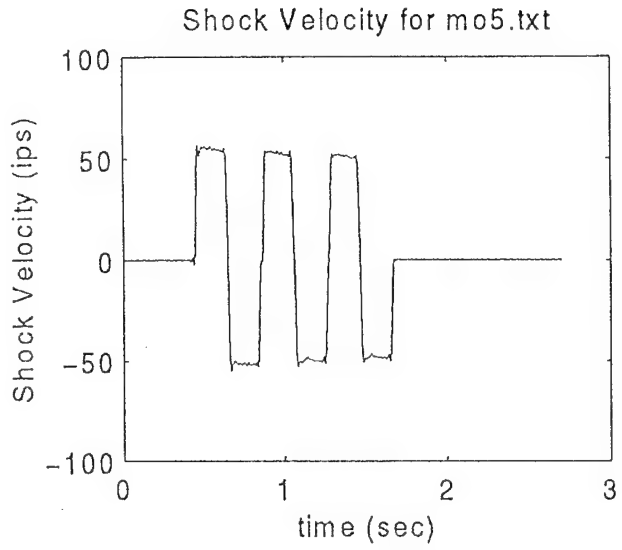
Shock Velocity for mo5.txt
Shock Velocity (ips)
100
50
0
-50
-100
0
1
2
3
time (sec)

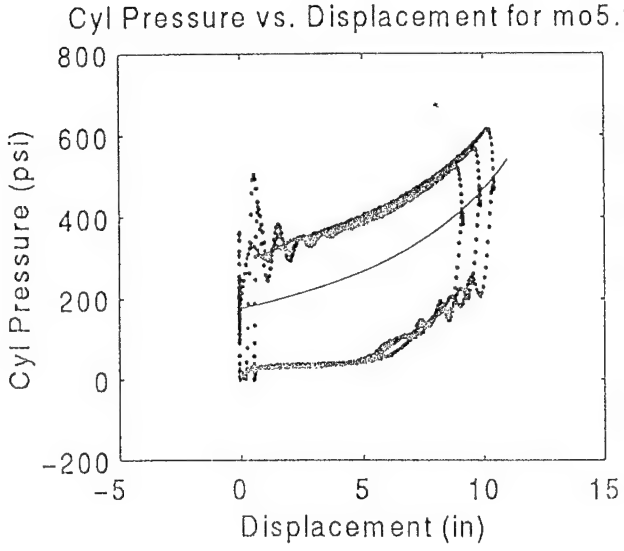
Cyl Pressure vs. Displacement for mo5.txt
Cyl Pressure (psi)
800
600
400
200
0
-200
-5
0
5
10
15
Displacement (in)

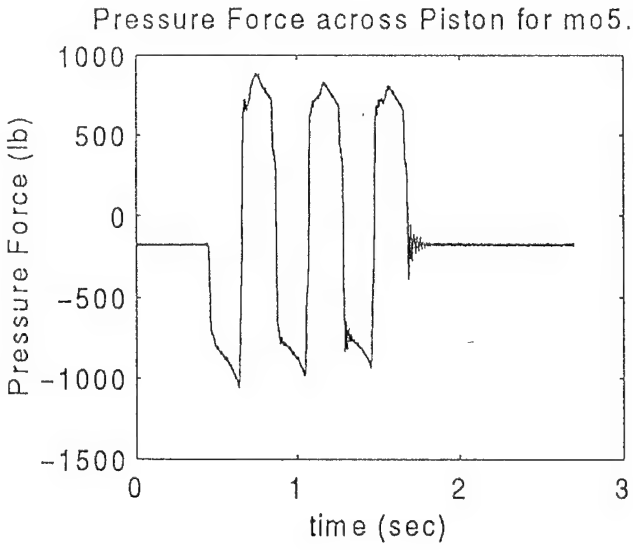
Pressure Force across Piston for mo5.txt
Pressure Force (lb)
1000
500
0
-500
-1000
-1500
0
1
2
3
time (sec)

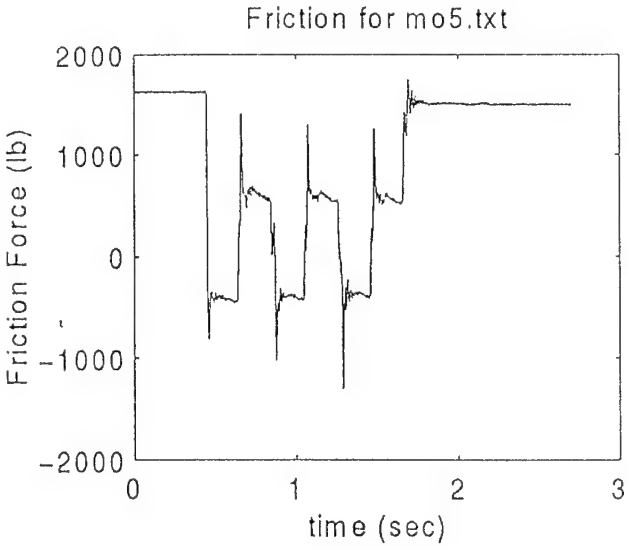
Friction for mo5.txt
Friction Force (lb)
2000
1000
0
-1000
-2000
0
1
2
3
time (sec)

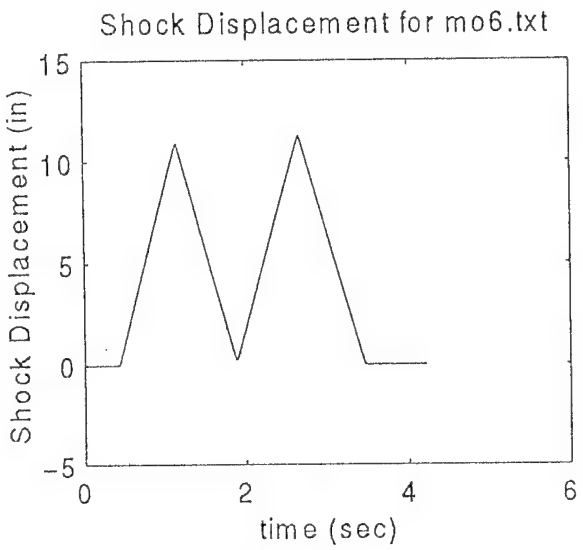
Shock Displacement for mo6.txt
Shock Displacement (in)
15
10
5
0
−5
0
2
4
6
time (sec)

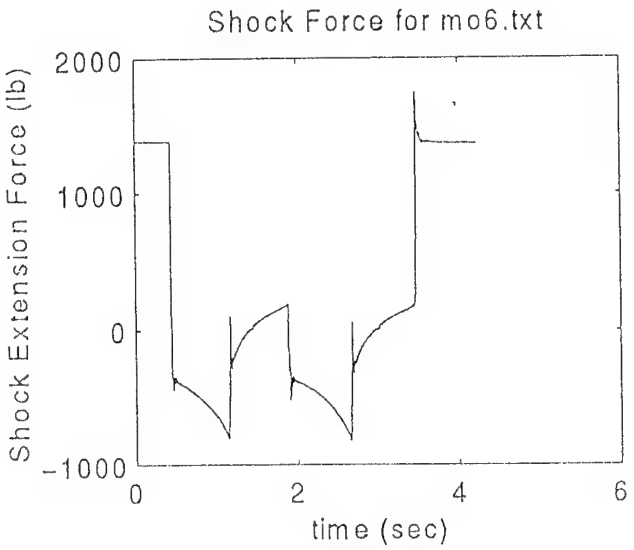
Shock Force for mo6.txt
Shock Extension Force (lb)
2000
1000
0
−1000
0
2
4
6
time (sec)

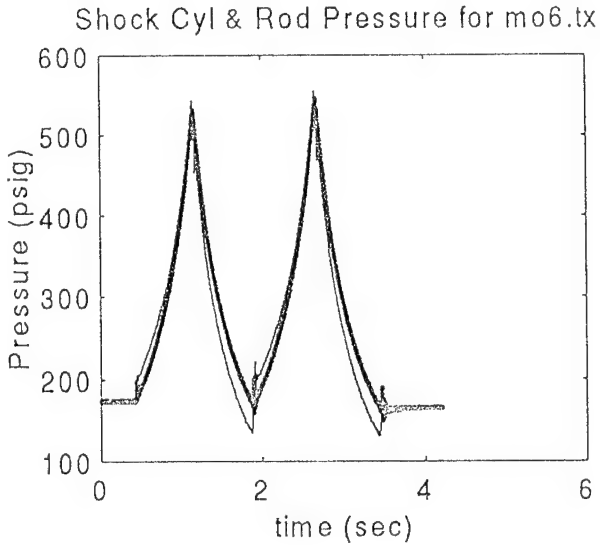
Shock Cyl & Rod Pressure for mo6.txt
Pressure (psig)
600
500
400
300
200
100
0
2
4
6
time (sec)

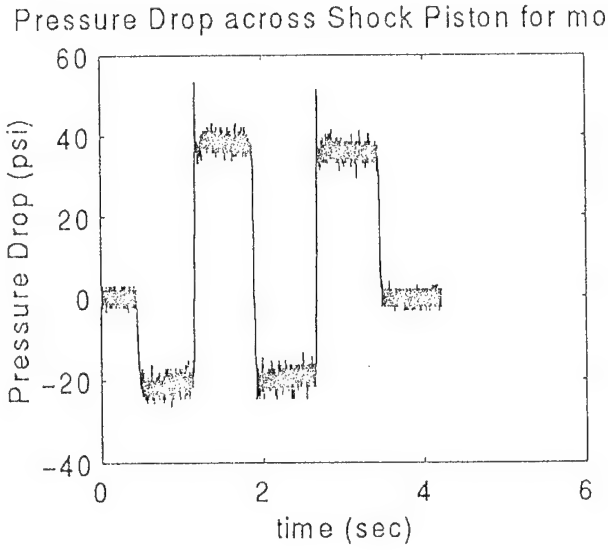
Pressure Drop across Shock Piston for mo6.txt
Pressure Drop (psi)
60
40
20
0
−20
−40
0
2
4
6
time (sec)

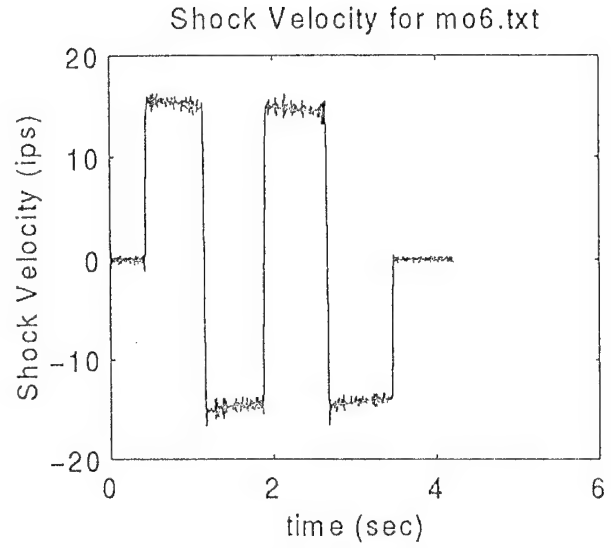
Shock Velocity for mo6.txt
Shock Velocity (ips)
time (sec)
20
10
0
-10
-20
0
2
4
6

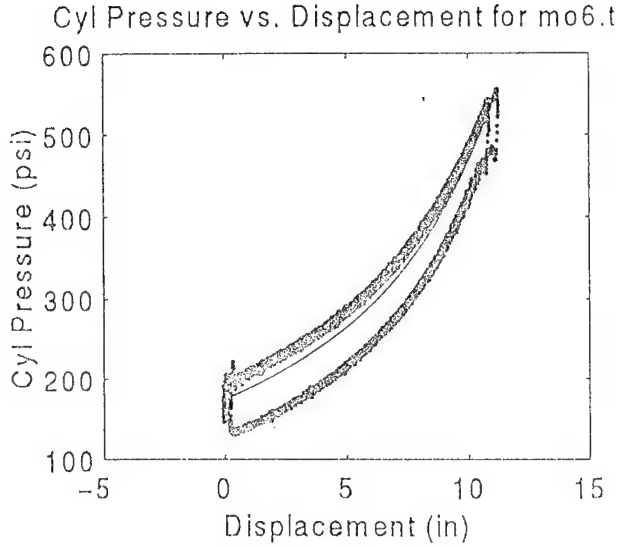
Cyl Pressure vs. Displacement for mo6.txt
Cyl Pressure (psi)
Displacement (in)
600
500
400
300
200
100
-5
0
5
10
15

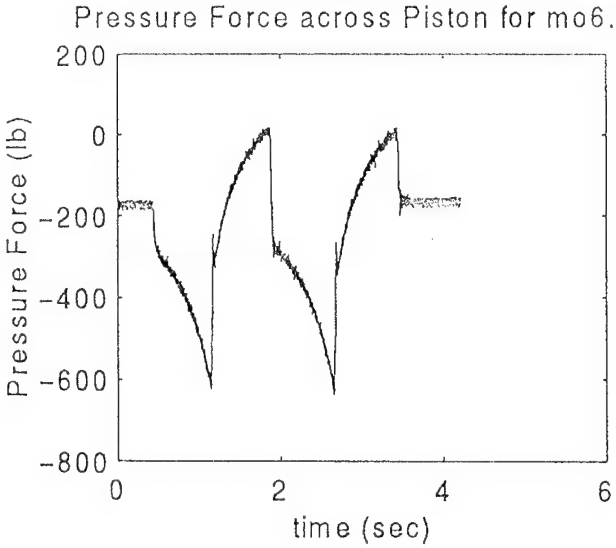
Pressure Force across Piston for mo6.txt
Pressure Force (lb)
time (sec)
200
0
-200
-400
-600
-800
0
2
4
6

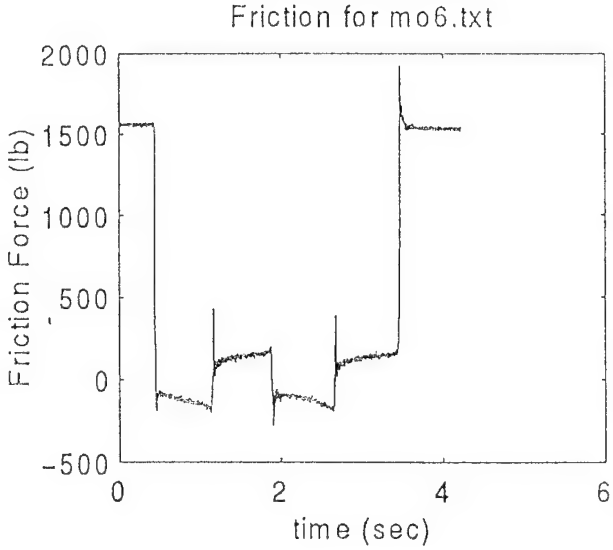
Friction for mo6.txt
Friction Force (lb)
time (sec)
2000
1500
1000
500
0
-500
0
2
4
6

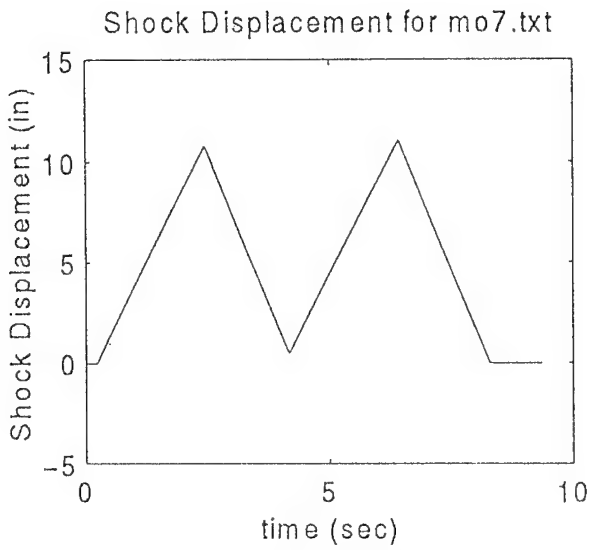
Shock Displacement for mo7.txt
Shock Displacement (in)
15
10
5
0
-5
0
5
10
time (sec)

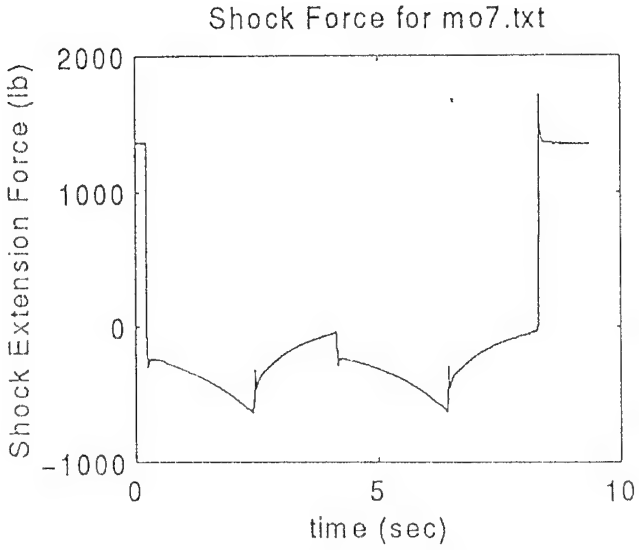
Shock Force for mo7.txt
Shock Extension Force (lb)
2000
1000
0
-1000
0
5
10
time (sec)

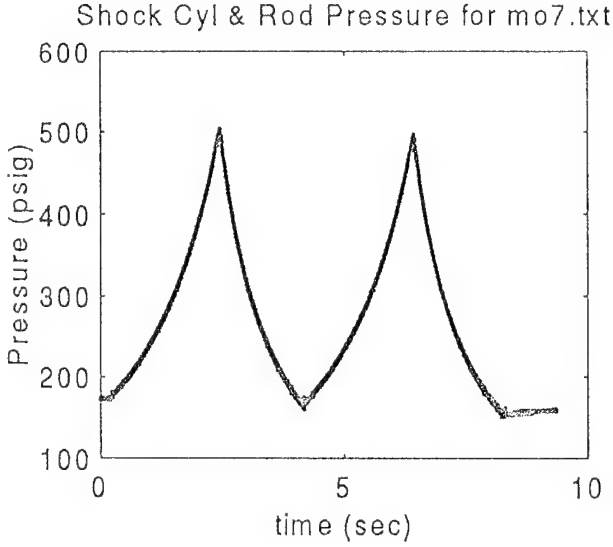
Shock Cyl & Rod Pressure for mo7.txt
Pressure (psig)
600
500
400
300
200
100
0
5
10
time (sec)

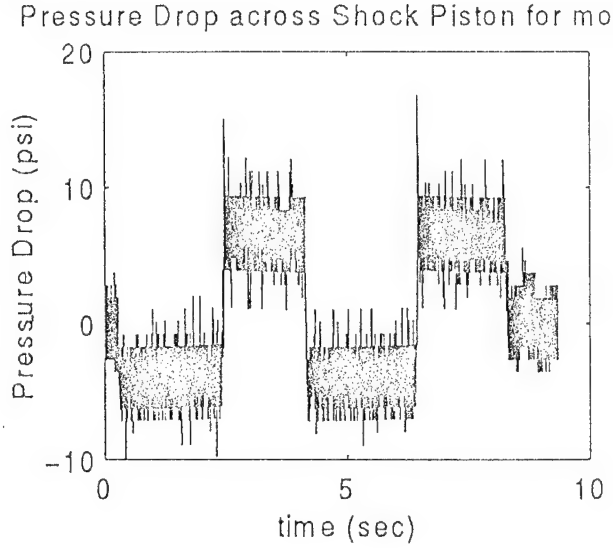
Pressure Drop across Shock Piston for mo7.txt
Pressure Drop (psi)
20
10
0
-10
0
5
10
time (sec)

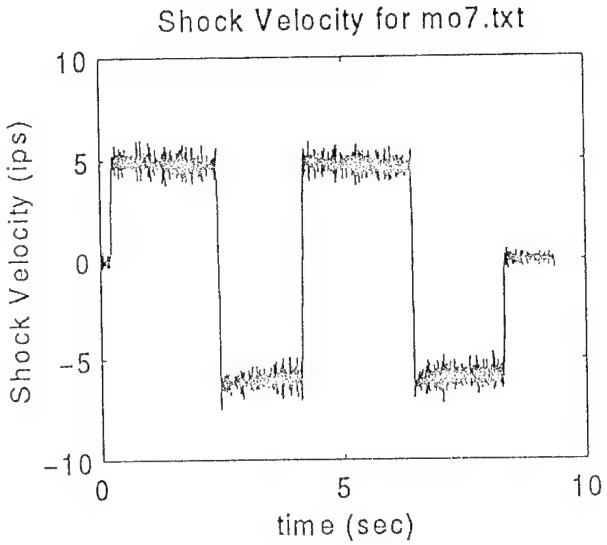
Shock Velocity for mo7.txt
Shock Velocity (ips)
time (sec)
10
5
0
-5
-10
0
5
10

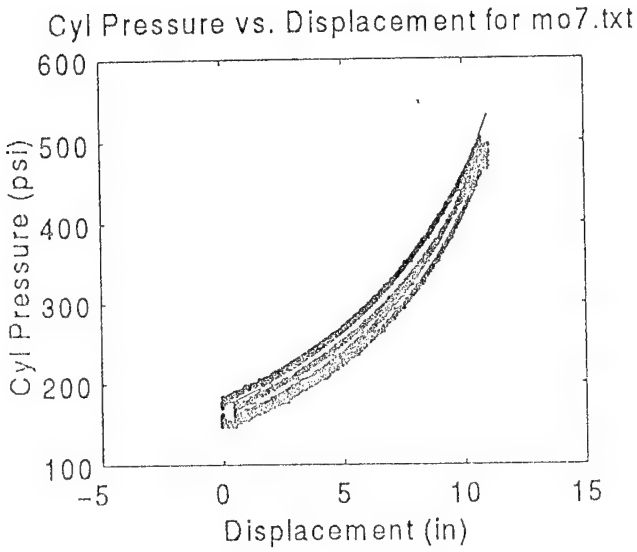
Cyl Pressure vs. Displacement for mo7.txt
Cyl Pressure (psi)
Displacement (in)
600
500
400
300
200
100
-5
0
5
10
15

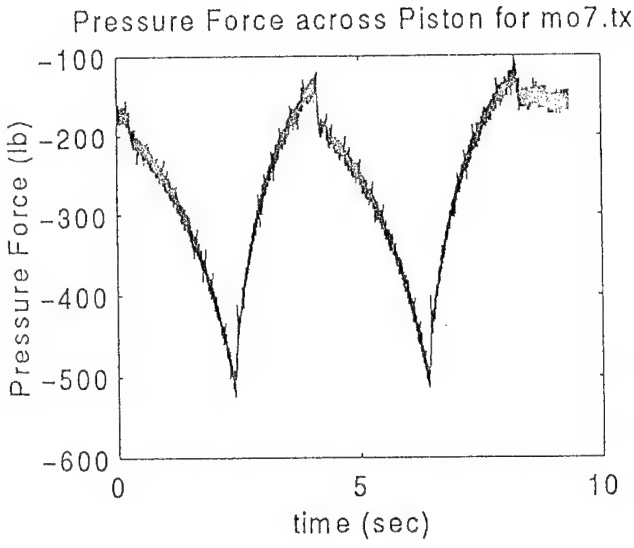
Pressure Force across Piston for mo7.txt
Pressure Force (lb)
time (sec)
-100
-200
-300
-400
-500
-600
0
5
10

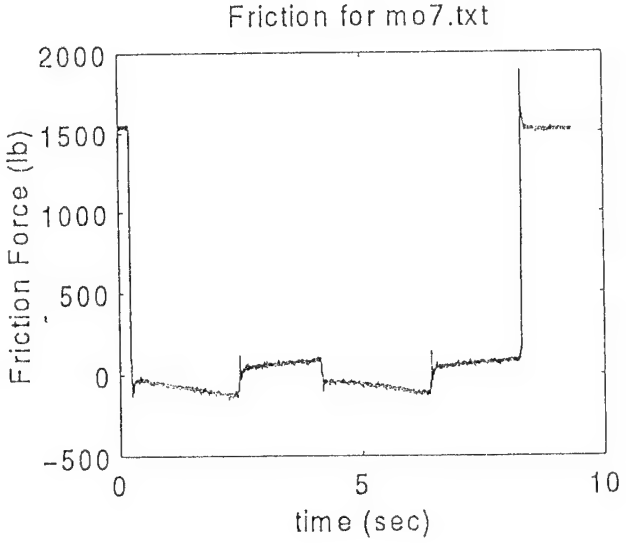
Friction for mo7.txt
Friction Force (lb)
time (sec)
2000
1500
1000
500
0
-500
0
5
10

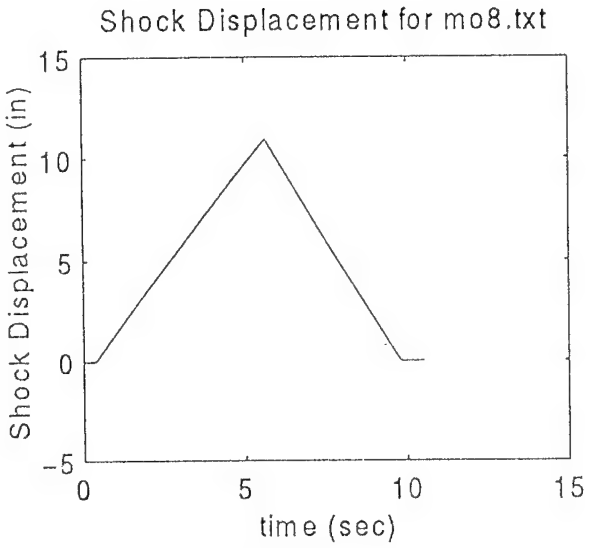
Shock Displacement for mo8.txt
Shock Displacement (in)
15
10
5
0
−5
0
5
10
15
time (sec)

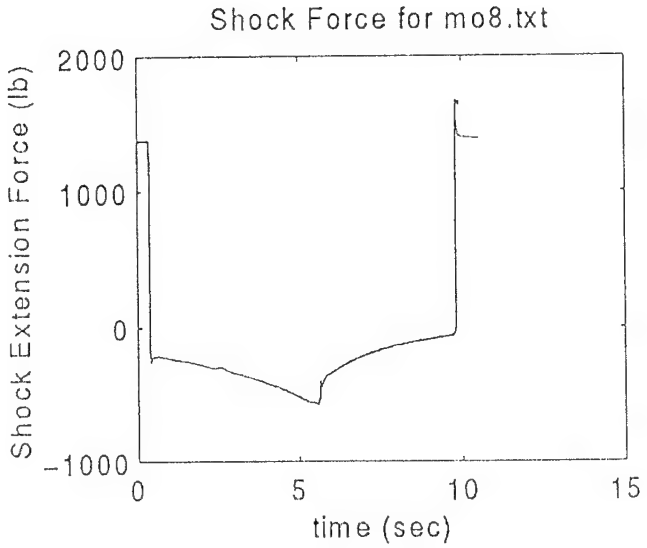
Shock Force for mo8.txt
Shock Extension Force (lb)
2000
1000
0
−1000
0
5
10
15
time (sec)

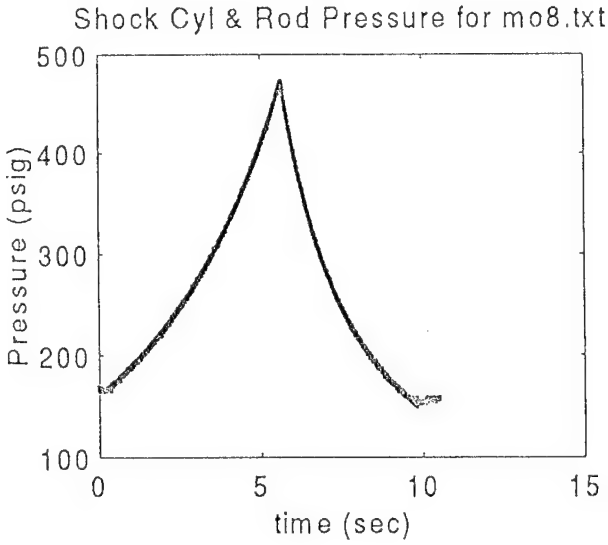
Shock Cyl & Rod Pressure for mo8.txt
Pressure (psig)
500
400
300
200
100
0
5
10
15
time (sec)

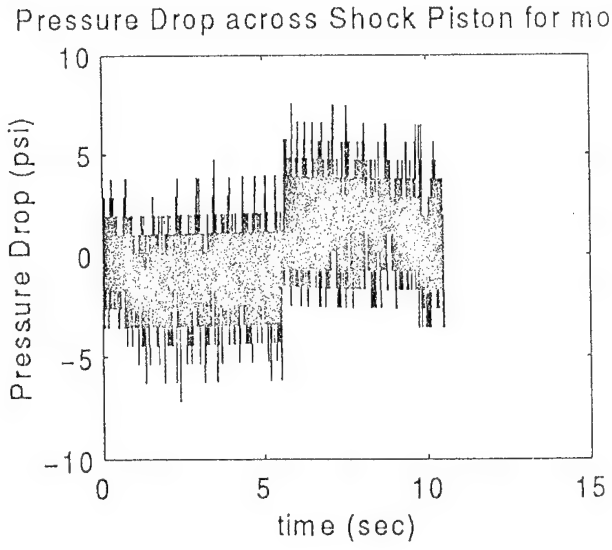
Pressure Drop across Shock Piston for mo8.txt
Pressure Drop (psi)
10
5
0
−5
−10
0
5
10
15
time (sec)

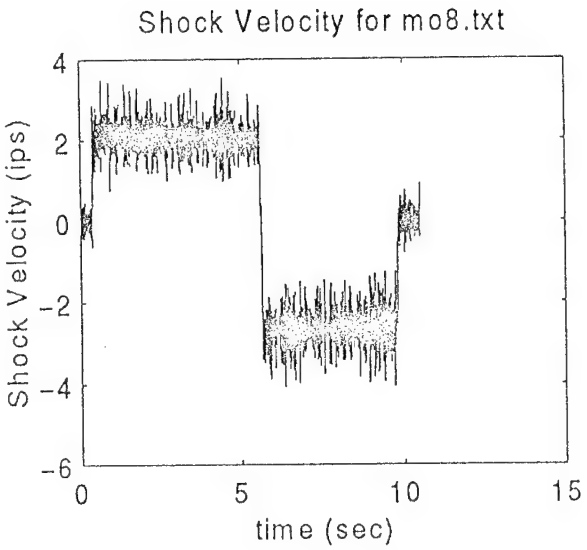
Shock Velocity for mo8.txt
Shock Velocity (ips)
time (sec)
4
2
0
-2
-4
-6
0
5
10
15

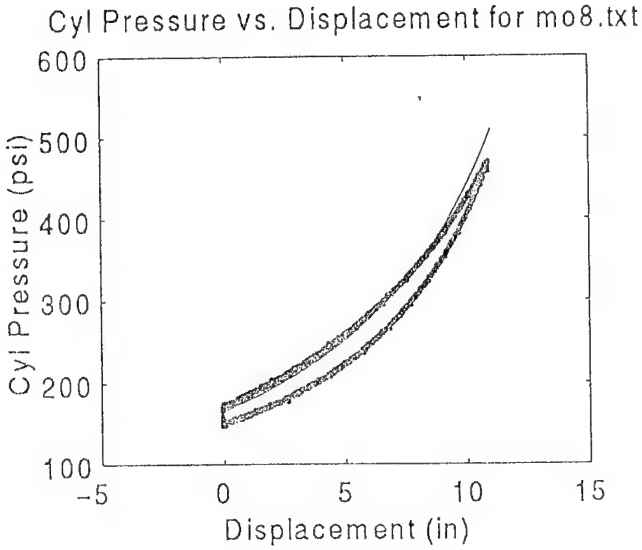
Cyl Pressure vs. Displacement for mo8.txt
Cyl Pressure (psi)
Displacement (in)
600
500
400
300
200
100
-5
0
5
10
15

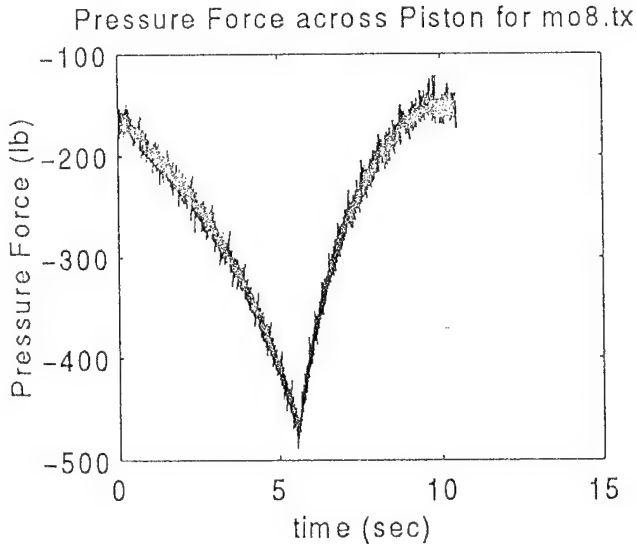
Pressure Force across Piston for mo8.txt
Pressure Force (lb)
time (sec)
-100
-200
-300
-400
-500
0
5
10
15

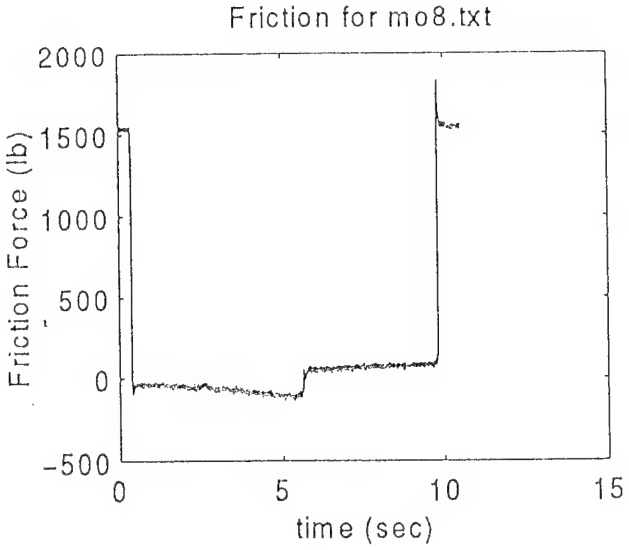
Friction for mo8.txt
Friction Force (lb)
time (sec)
2000
1500
1000
500
0
-500
0
5
10
15

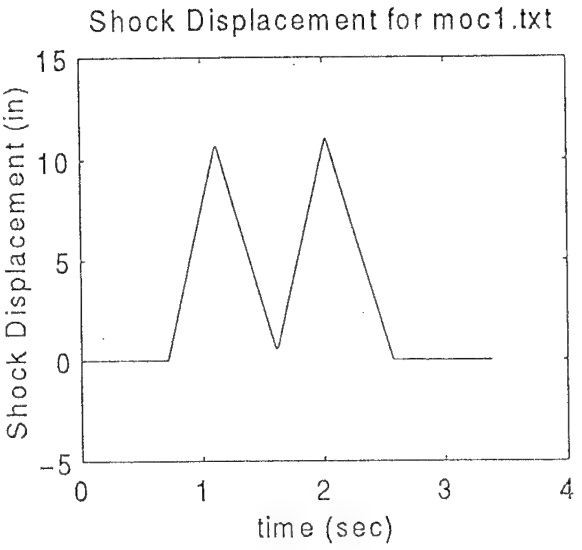
Shock Displacement for moc1.txt
Shock Displacement (in)
15
10
5
0
-5
0
1
2
3
4
time (sec)

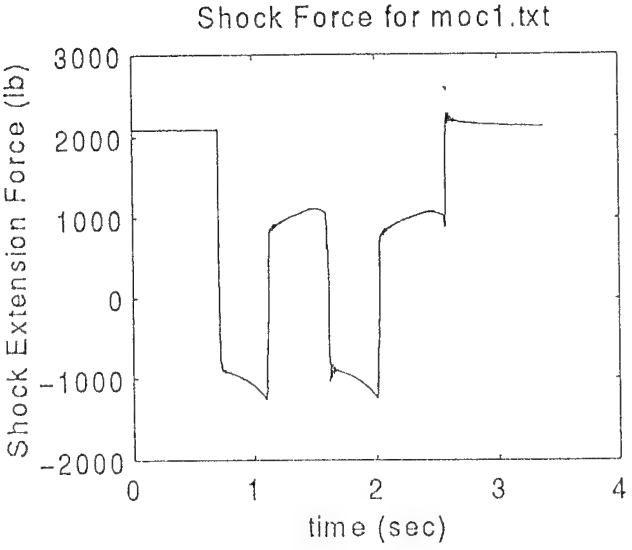
Shock Force for moc1.txt
Shock Extension Force (lb)
3000
2000
1000
0
-1000
-2000
0
1
2
3
4
time (sec)

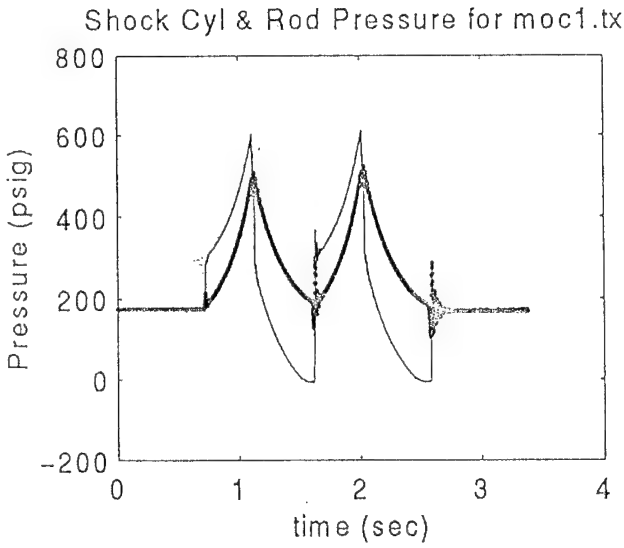
Shock Cyl & Rod Pressure for moc1.txt
Pressure (psig)
800
600
400
200
0
-200
0
1
2
3
4
time (sec)

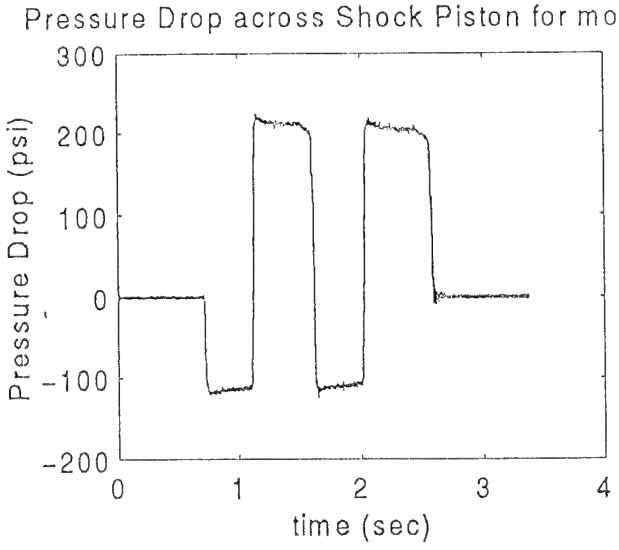
Pressure Drop across Shock Piston for moc1.txt
Pressure Drop (psi)
300
200
100
0
-100
-200
0
1
2
3
4
time (sec)

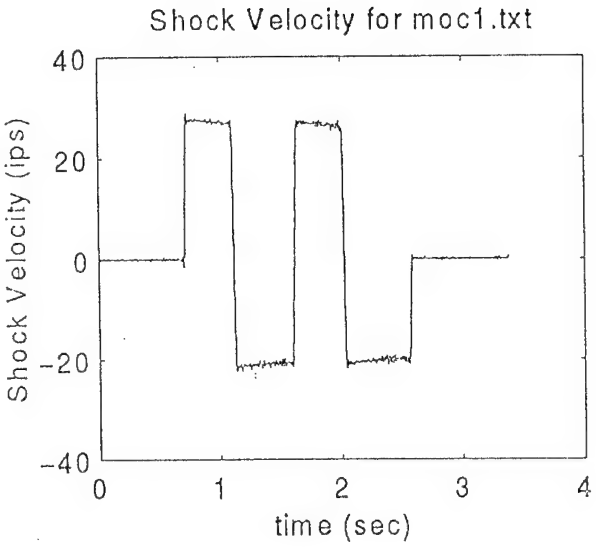
Shock Velocity for moc1.txt
Shock Velocity (ips)
time (sec)
40
20
0
-20
-40
0
1
2
3
4

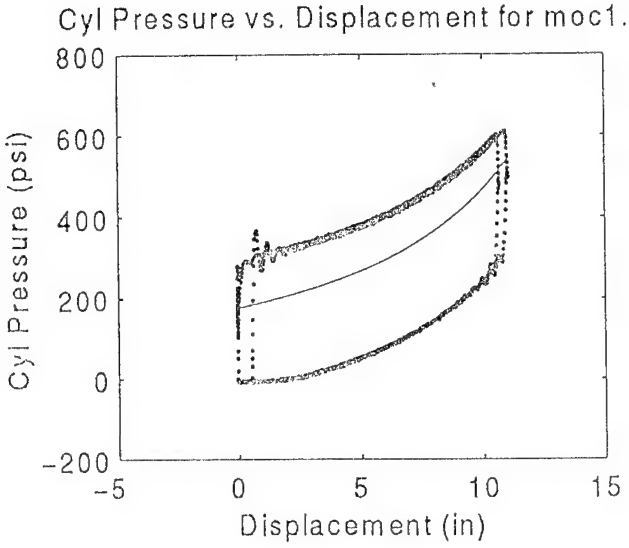
Cyl Pressure vs. Displacement for moc1.txt
Cyl Pressure (psi)
Displacement (in)
800
600
400
200
0
-200
-5
0
5
10
15

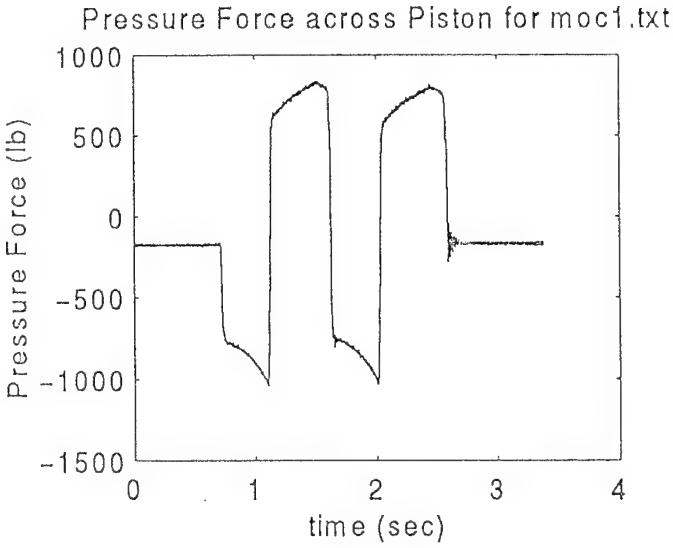
Pressure Force across Piston for moc1.txt
Pressure Force (lb)
time (sec)
1000
500
0
-500
-1000
-1500
0
1
2
3
4

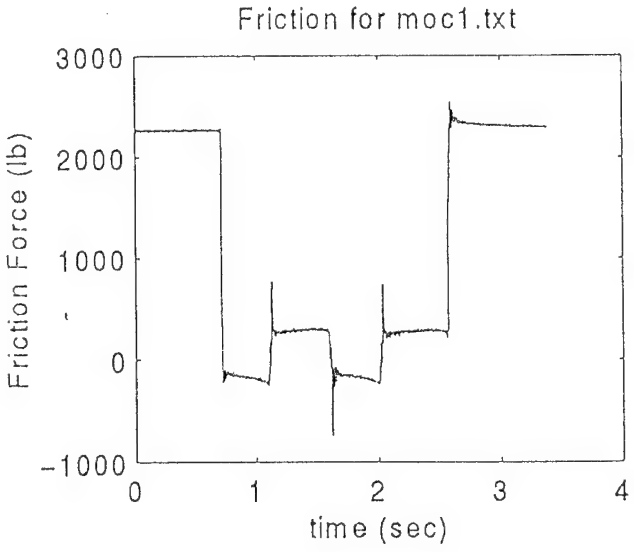
Friction for moc1.txt
Friction Force (lb)
time (sec)
3000
2000
1000
0
-1000
0
1
2
3
4

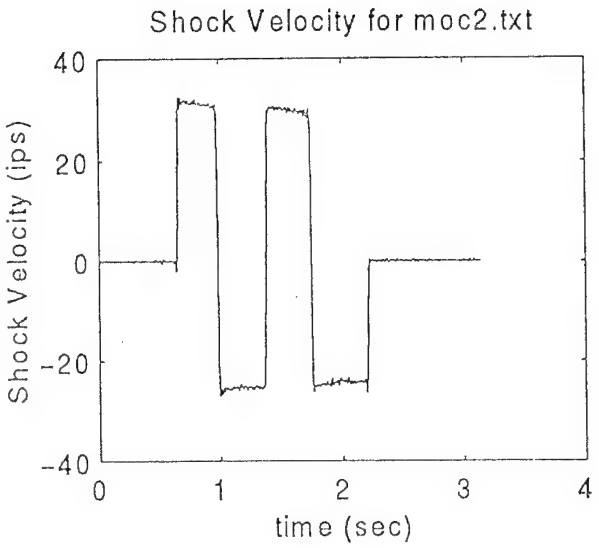
Shock Velocity for moc2.txt
Shock Velocity (ips)
time (sec)
40
20
0
-20
-40
0
1
2
3
4

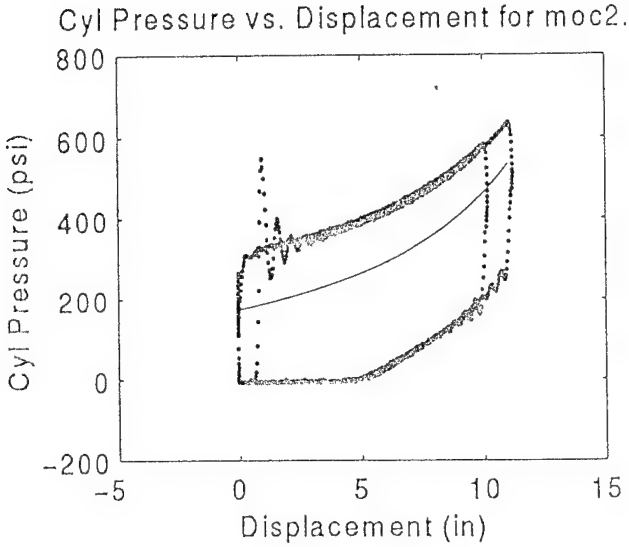
Cyl Pressure vs. Displacement for moc2.txt
Cyl Pressure (psi)
Displacement (in)
800
600
400
200
0
-200
-5
0
5
10
15

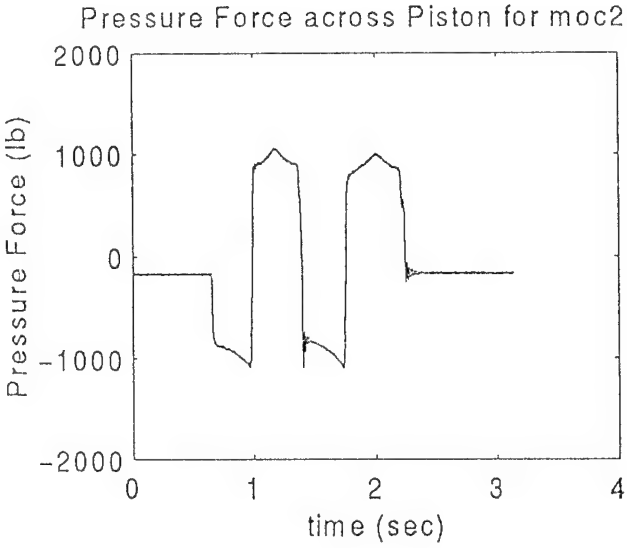
Pressure Force across Piston for moc2.txt
Pressure Force (lb)
time (sec)
2000
1000
0
-1000
-2000
0
1
2
3
4

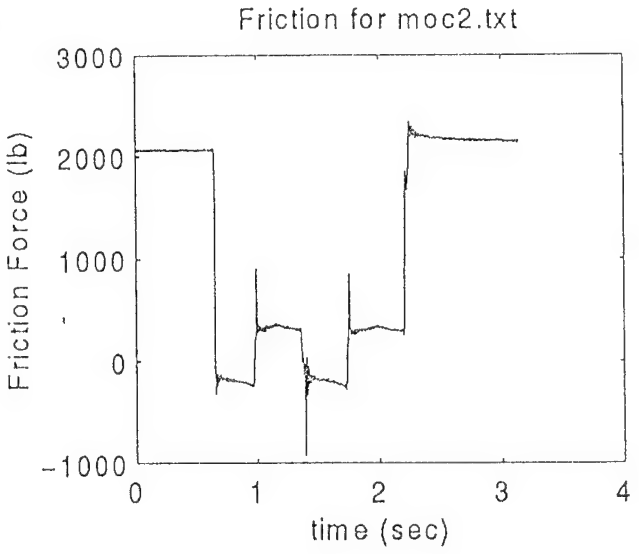
Friction for moc2.txt
Friction Force (lb)
time (sec)
3000
2000
1000
0
-1000
0
1
2
3
4

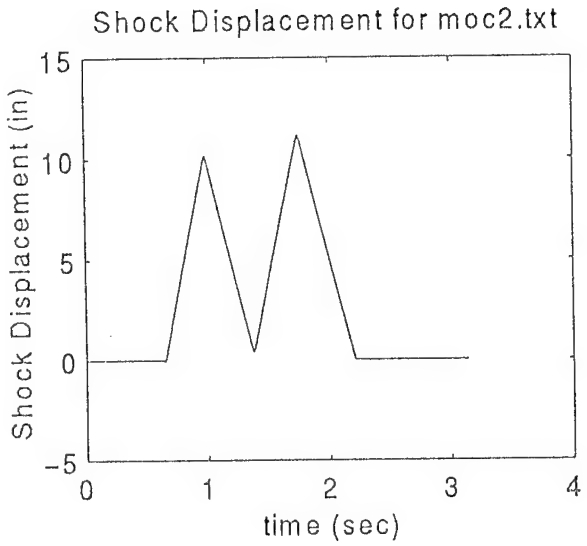
Shock Displacement for moc2.txt
Shock Displacement (in)
15
10
5
0
-5
0
1
2
3
4
time (sec)

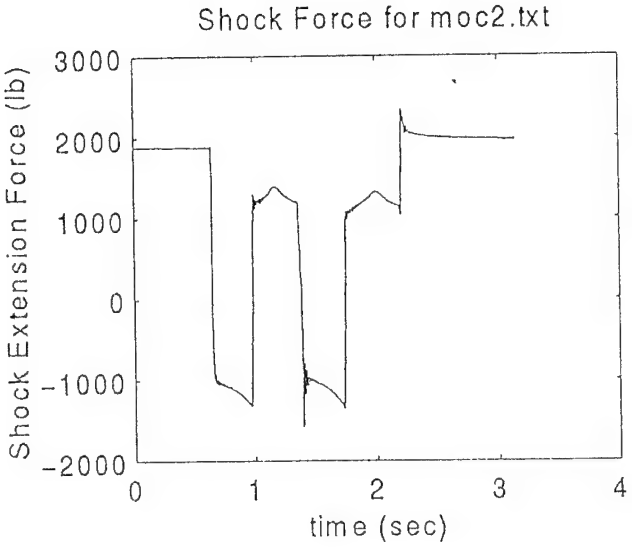
Shock Force for moc2.txt
Shock Extension Force (lb)
3000
2000
1000
0
-1000
-2000
0
1
2
3
4
time (sec)

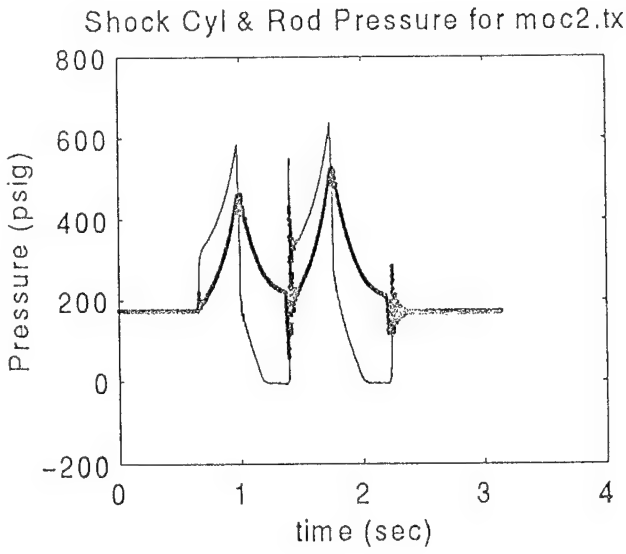
Shock Cyl & Rod Pressure for moc2.txt
Pressure (psig)
800
600
400
200
0
-200
0
1
2
3
4
time (sec)

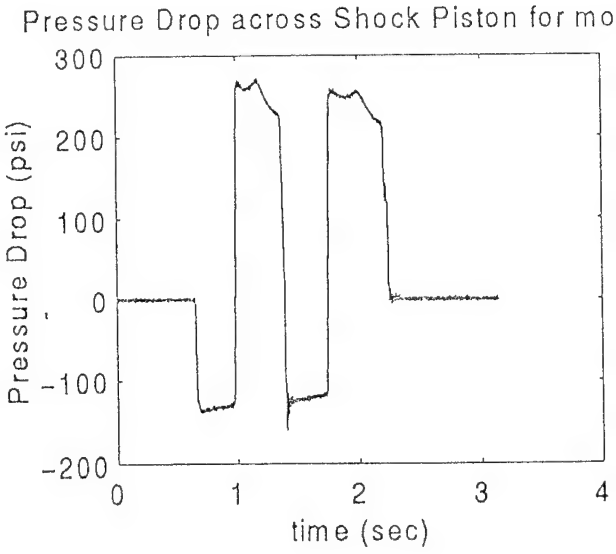
Pressure Drop across Shock Piston for moc2.txt
Pressure Drop (psi)
300
200
100
0
-100
-200
0
1
2
3
4
time (sec)

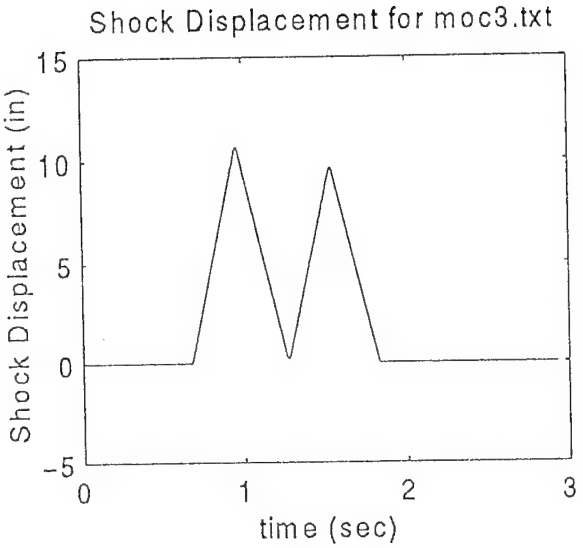
Shock Displacement for moc3.txt
Shock Displacement (in)
15
10
5
0
-5
0
1
2
3
time (sec)

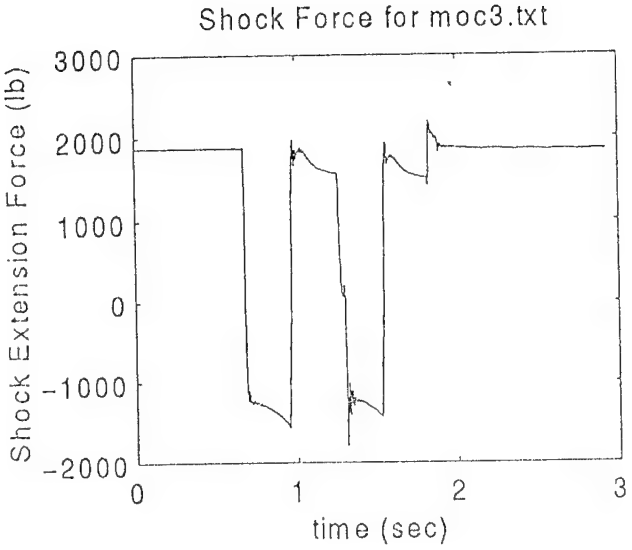
Shock Force for moc3.txt
Shock Extension Force (lb)
3000
2000
1000
0
-1000
-2000
0
1
2
3
time (sec)

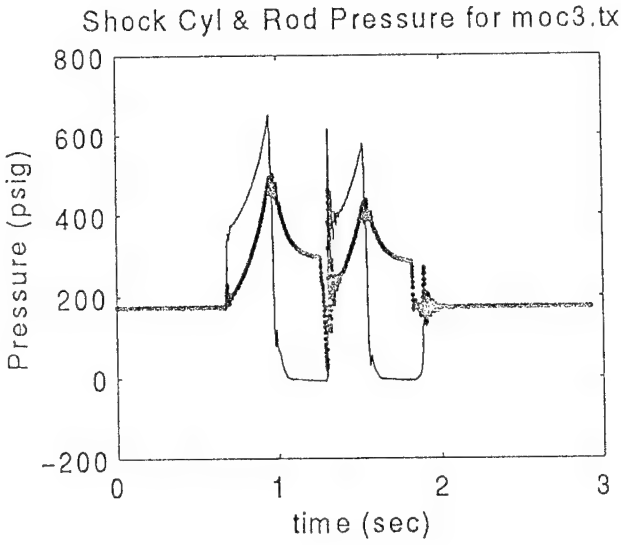
Shock Cyl & Rod Pressure for moc3.txt
Pressure (psig)
800
600
400
200
0
-200
0
1
2
3
time (sec)

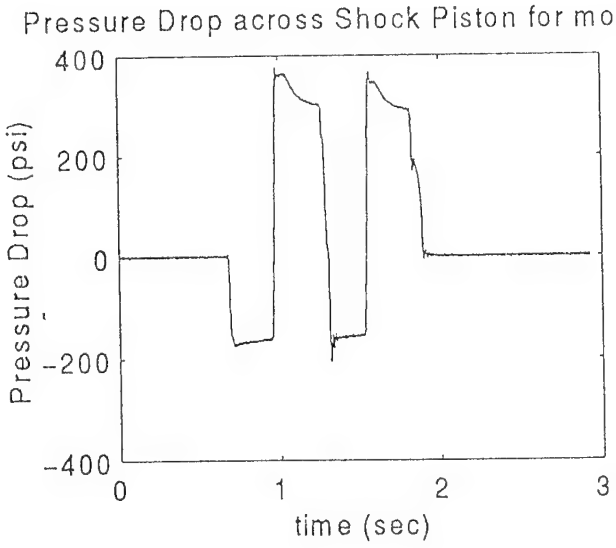
Pressure Drop across Shock Piston for moc3.txt
Pressure Drop (psi)
400
200
0
-200
-400
0
1
2
3
time (sec)

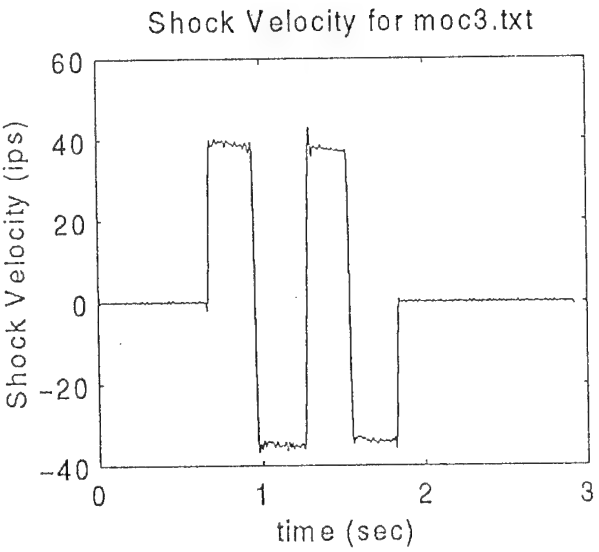
Shock Velocity for moc3.txt
Shock Velocity (ips)
60
40
20
0
-20
-40
0
1
2
3
time (sec)

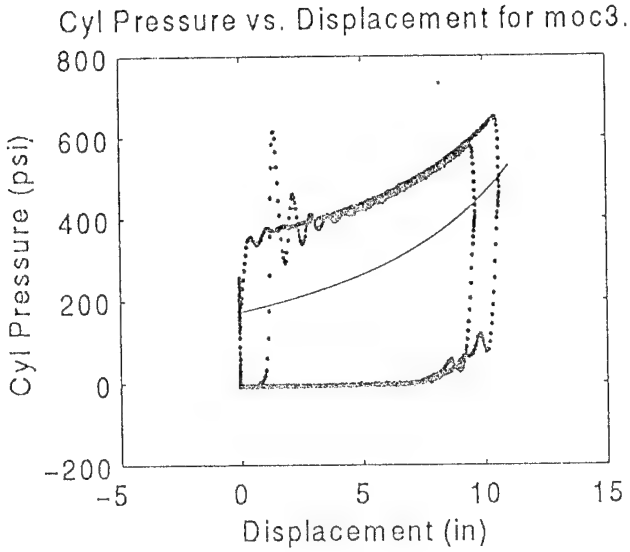
Cyl Pressure vs. Displacement for moc3.txt
Cyl Pressure (psi)
800
600
400
200
0
-200
-5
0
5
10
15
Displacement (in)

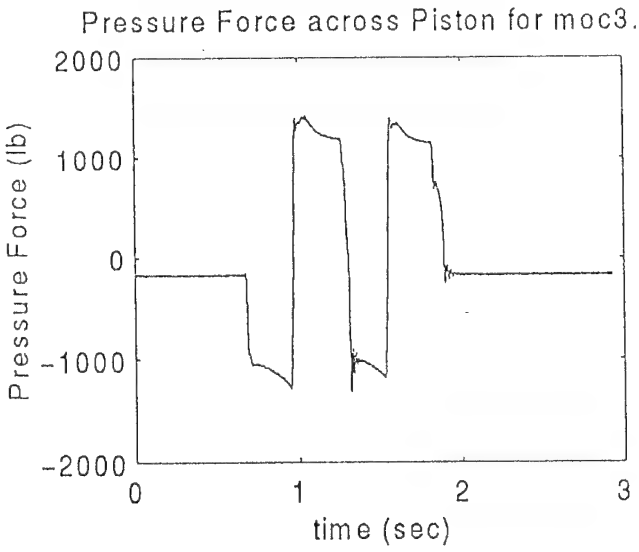
Pressure Force across Piston for moc3.txt
Pressure Force (lb)
2000
1000
0
-1000
-2000
0
1
2
3
time (sec)

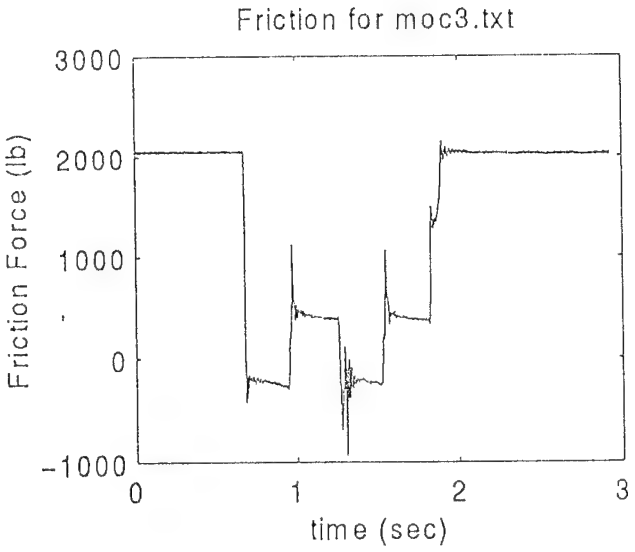
Friction for moc3.txt
Friction Force (lb)
3000
2000
1000
0
-1000
0
1
2
3
time (sec)

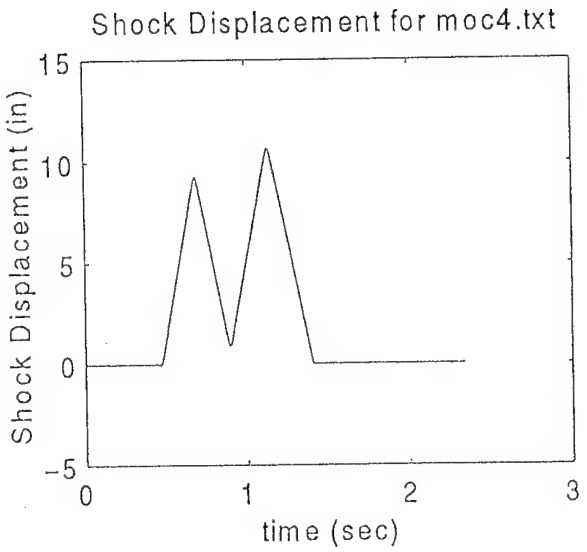
Shock Displacement for moc4.txt
Shock Displacement (in)
15
10
5
0
-5
0
1
2
3
time (sec)

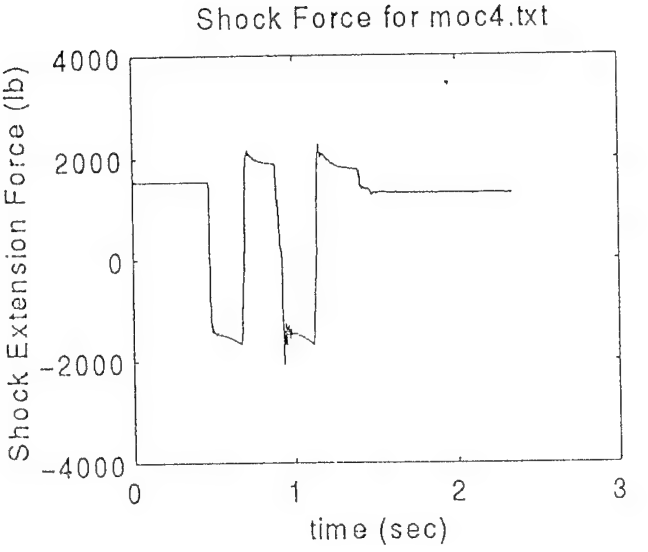
Shock Force for moc4.txt
Shock Extension Force (lb)
4000
2000
0
-2000
-4000
0
1
2
3
time (sec)

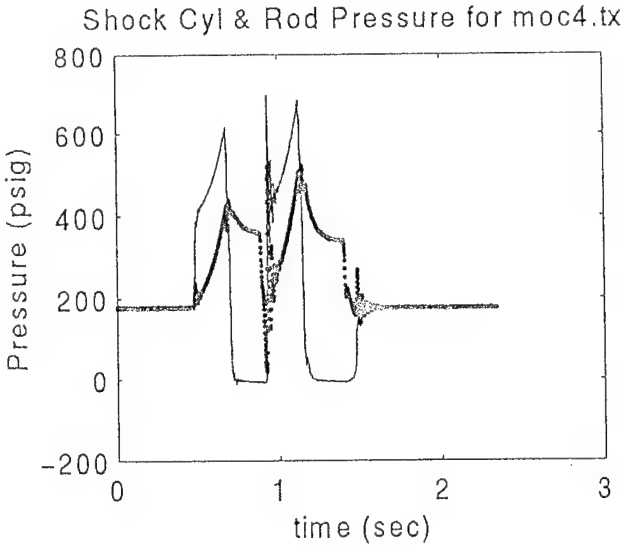
Shock Cyl & Rod Pressure for moc4.txt
Pressure (psig)
800
600
400
200
0
-200
0
1
2
3
time (sec)

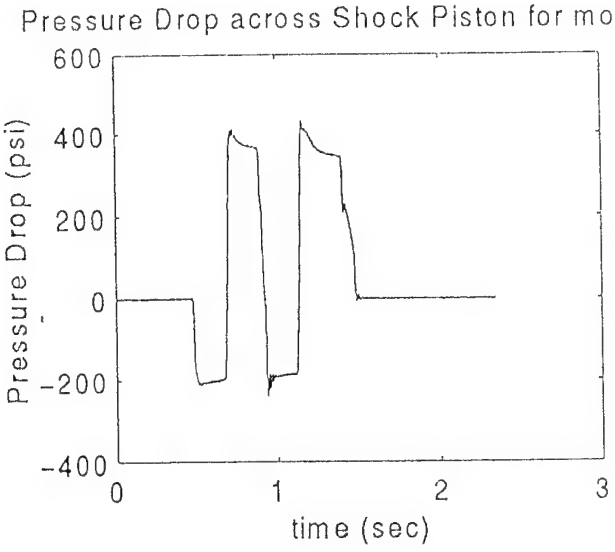
Pressure Drop across Shock Piston for moc4.txt
Pressure Drop (psi)
600
400
200
0
-200
-400
0
1
2
3
time (sec)

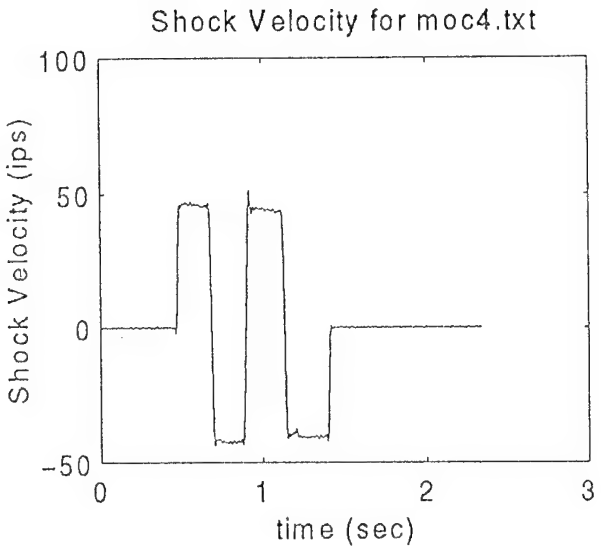
Shock Velocity for moc4.txt
Shock Velocity (ips)
time (sec)
100
50
0
-50
0
1
2
3

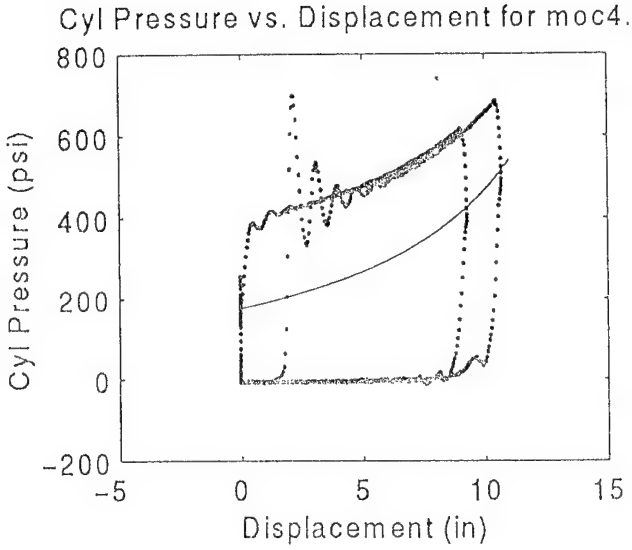
Cyl Pressure vs. Displacement for moc4.txt
Cyl Pressure (psi)
Displacement (in)
800
600
400
200
0
-200
-5
0
5
10
15

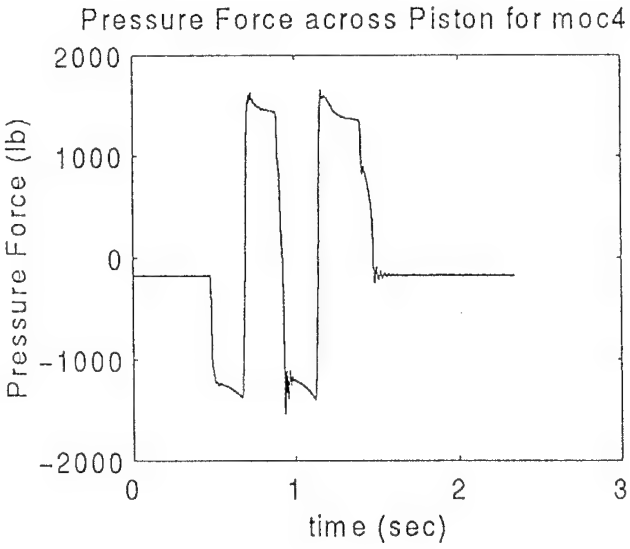
Pressure Force across Piston for moc4.txt
Pressure Force (lb)
time (sec)
2000
1000
0
-1000
-2000
0
1
2
3

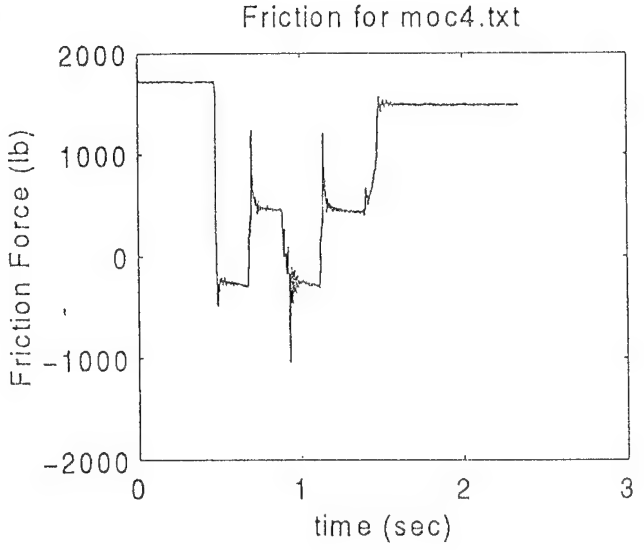
Friction for moc4.txt
Friction Force (lb)
time (sec)
2000
1000
0
-1000
-2000
0
1
2
3

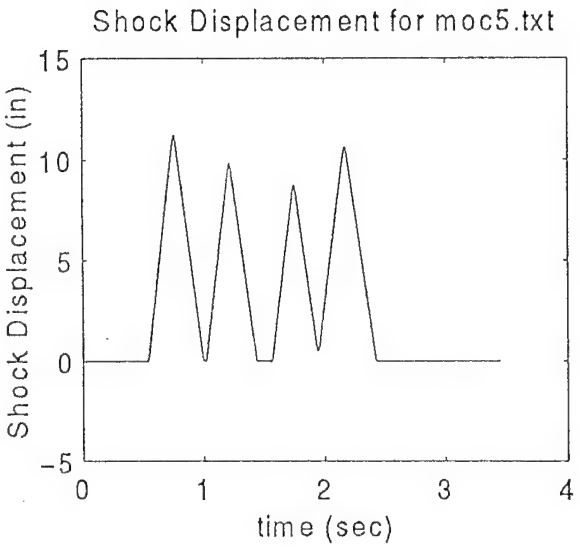
Shock Displacement for moc5.txt
Shock Displacement (in)
15
10
5
0
-5
0
1
2
3
4
time (sec)

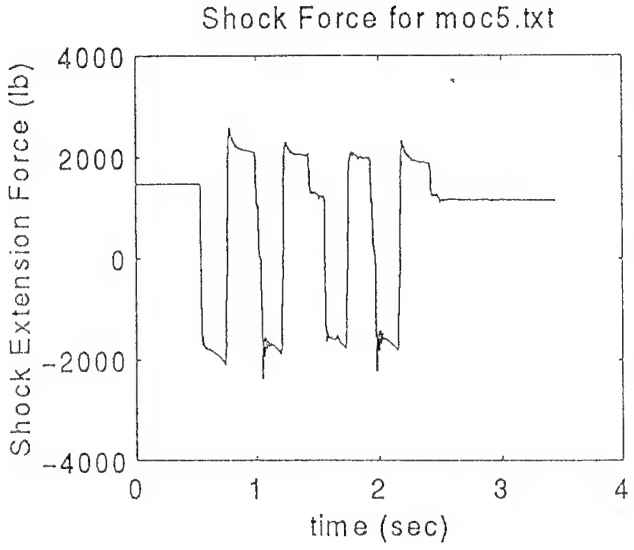
Shock Force for moc5.txt
Shock Extension Force (lb)
4000
2000
0
-2000
-4000
0
1
2
3
4
time (sec)

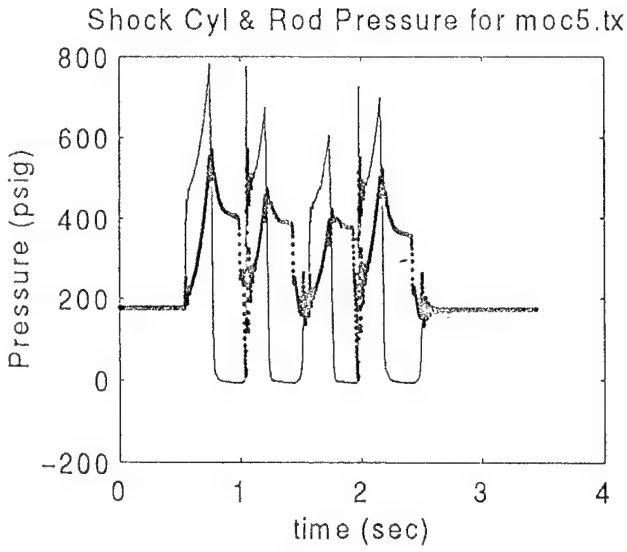
Shock Cyl & Rod Pressure for moc5.txt
Pressure (psig)
800
600
400
200
0
-200
0
1
2
3
4
time (sec)

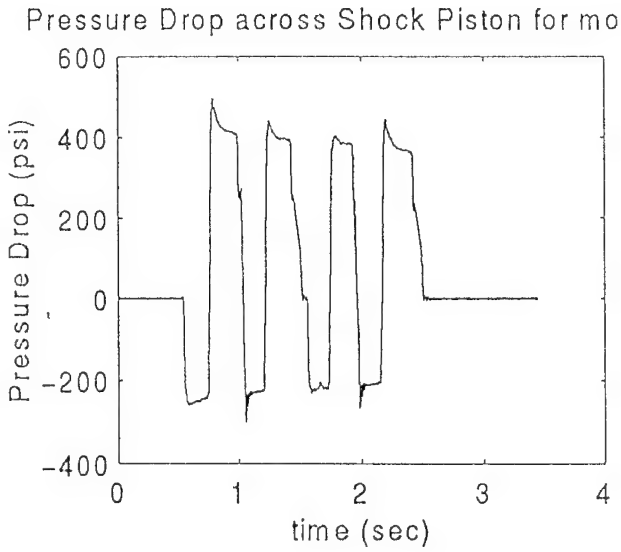
Pressure Drop across Shock Piston for moc5.txt
Pressure Drop (psi)
600
400
200
0
-200
-400
0
1
2
3
4
time (sec)

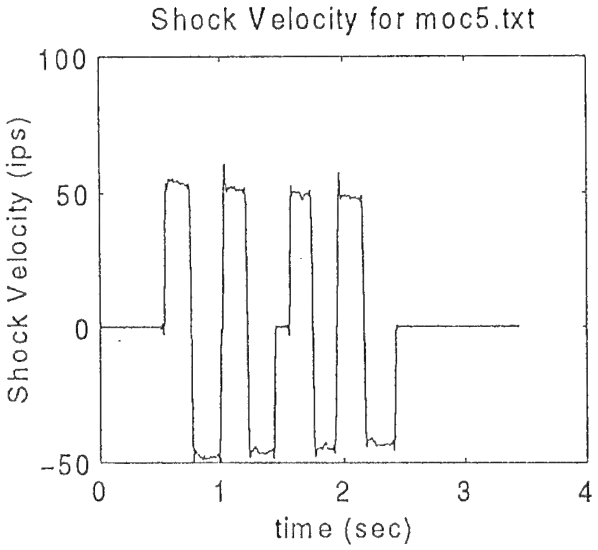
Shock Velocity for moc5.txt
Shock Velocity (ips)
100
50
0
-50
0
1
2
3
4
time (sec)

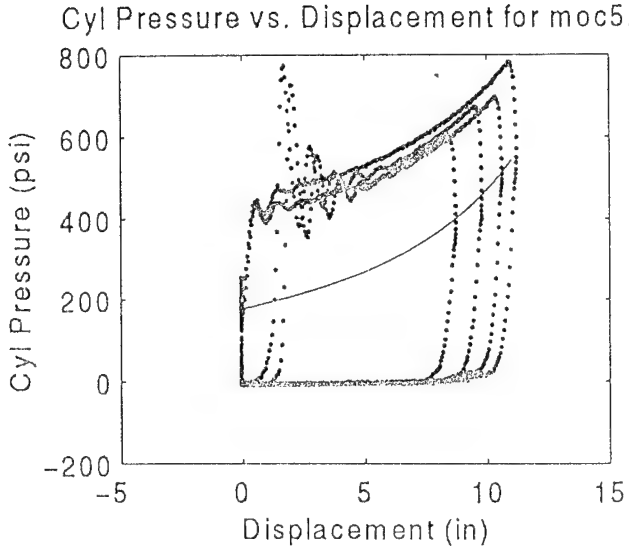
Cyl Pressure vs. Displacement for moc5.txt
Cyl Pressure (psi)
800
600
400
200
0
-200
-5
0
5
10
15
Displacement (in)

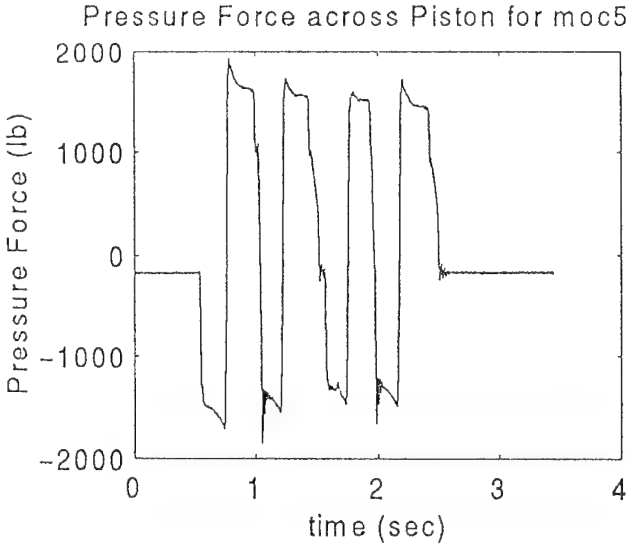
Pressure Force across Piston for moc5.txt
Pressure Force (lb)
2000
1000
0
-1000
-2000
0
1
2
3
4
time (sec)

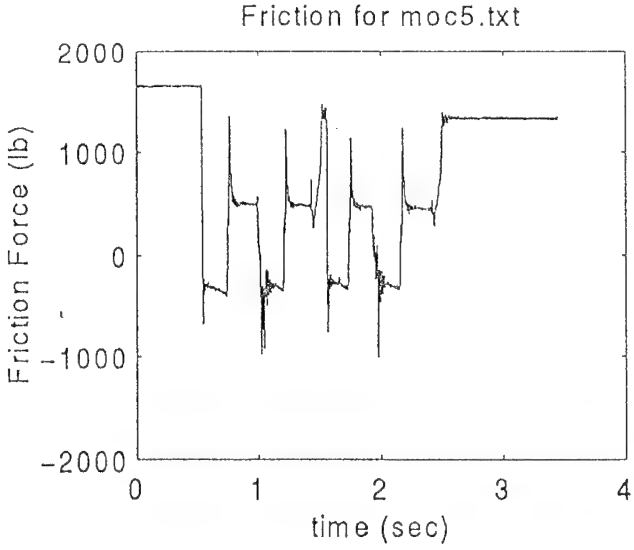
Friction for moc5.txt
Friction Force (lb)
2000
1000
0
-1000
-2000
0
1
2
3
4
time (sec)

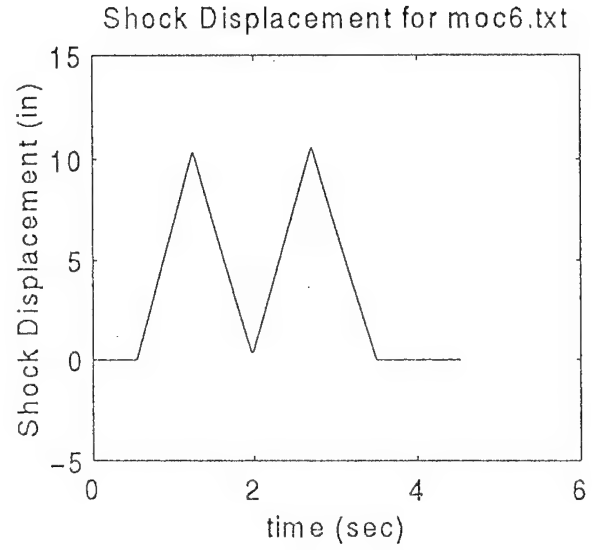
Shock Displacement for moc6.txt
Shock Displacement (in)
15
10
5
0
−5
0
2
4
6
time (sec)

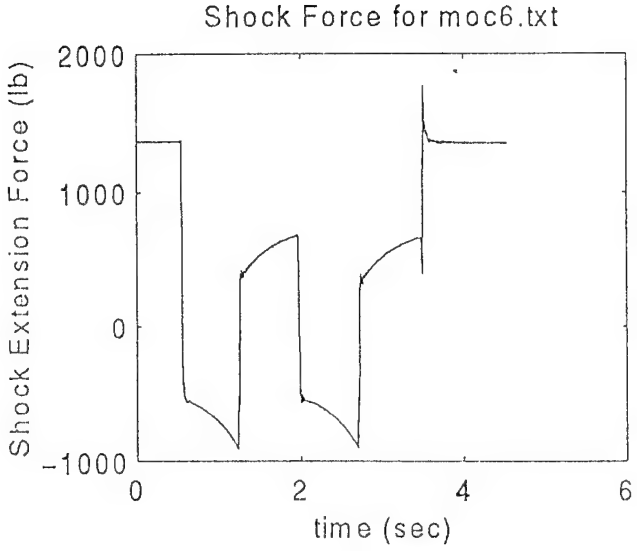
Shock Force for moc6.txt
Shock Extension Force (lb)
2000
1000
0
−1000
0
2
4
6
time (sec)

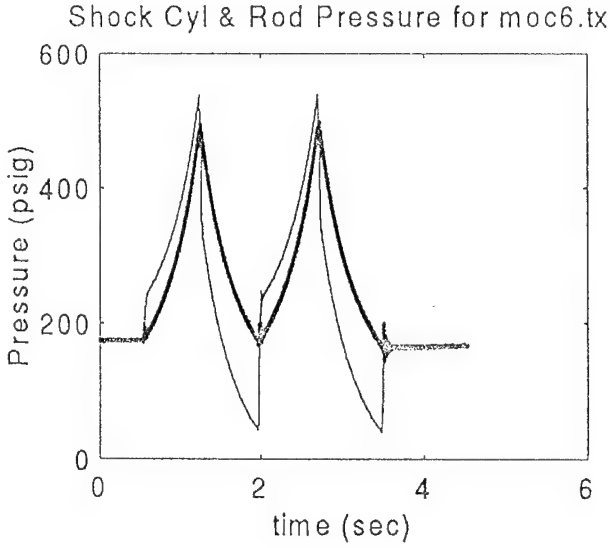
Shock Cyl & Rod Pressure for moc6.txt
Pressure (psig)
600
400
200
0
0
2
4
6
time (sec)

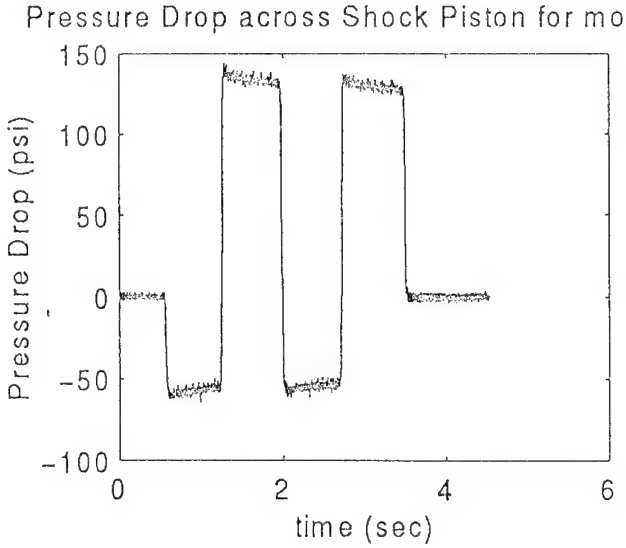
Pressure Drop across Shock Piston for moc6.txt
Pressure Drop (psi)
150
100
50
0
−50
−100
0
2
4
6
time (sec)

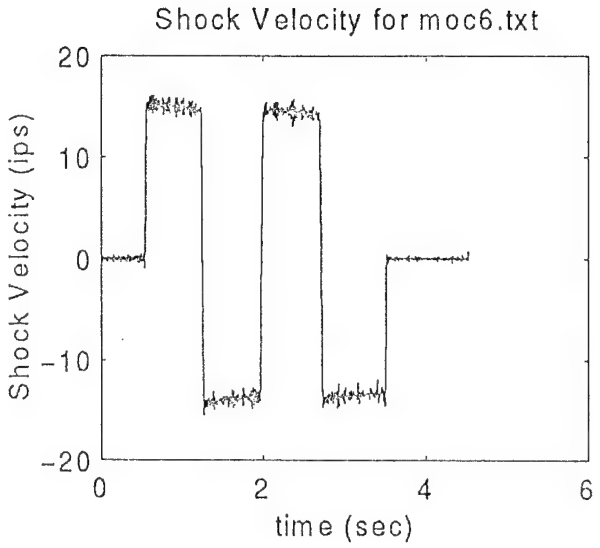
Shock Velocity for moc6.txt
Shock Velocity (ips)
time (sec)
20
10
0
-10
-20
0
2
4
6

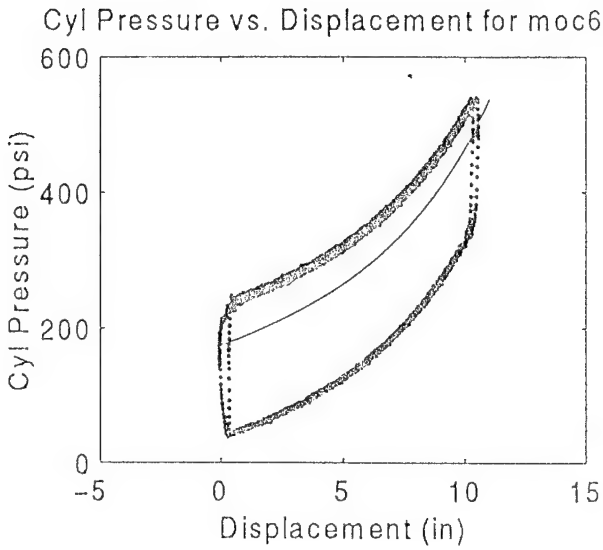
Cyl Pressure vs. Displacement for moc6.txt
Cyl Pressure (psi)
Displacement (in)
600
400
200
0
-5
0
5
10
15

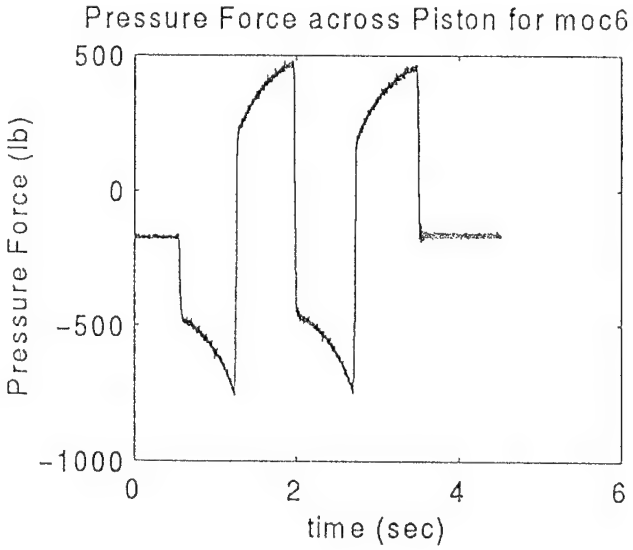
Pressure Force across Piston for moc6.txt
Pressure Force (lb)
time (sec)
500
0
-500
-1000
0
2
4
6

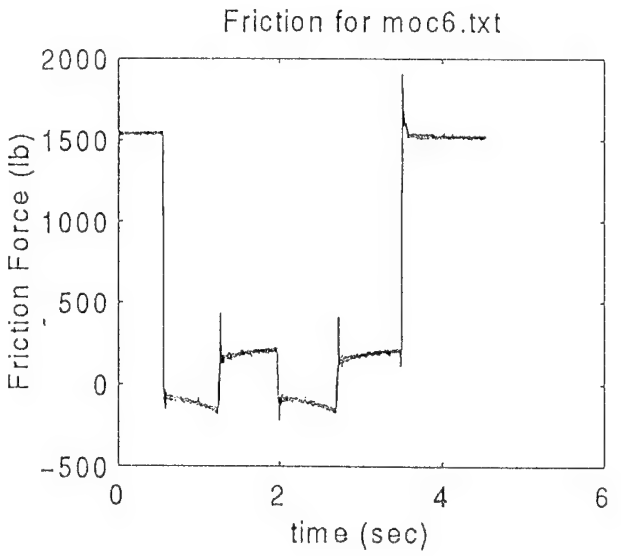
Friction for moc6.txt
Friction Force (lb)
time (sec)
2000
1500
1000
500
0
-500
0
2
4
6

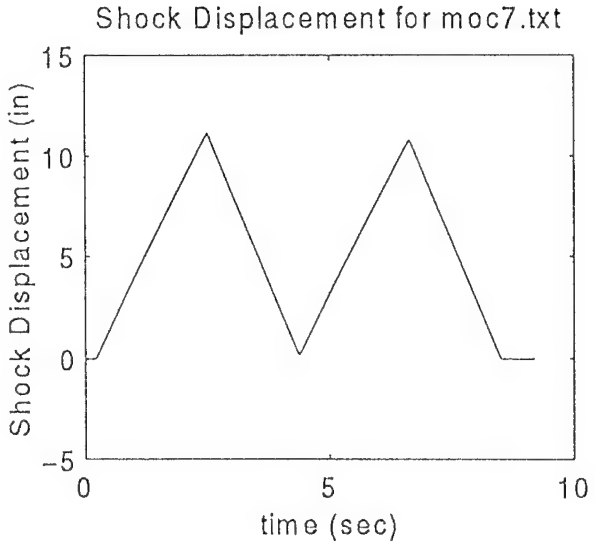
Shock Displacement for moc7.txt
Shock Displacement (in)
15
10
5
0
−5
0
5
10
time (sec)

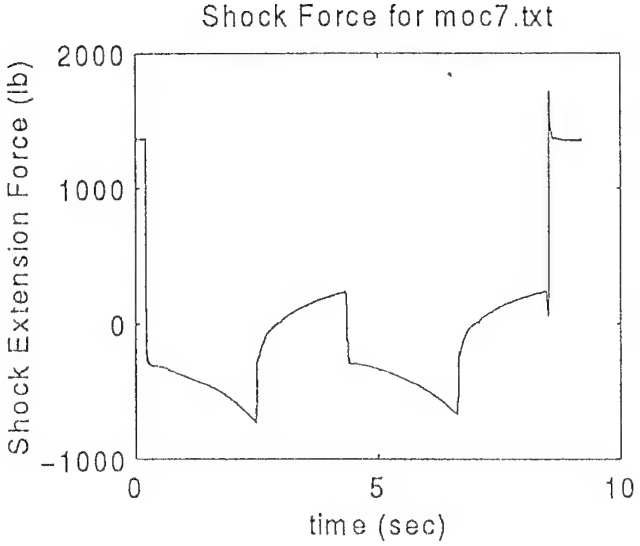
Shock Force for moc7.txt
Shock Extension Force (lb)
2000
1000
0
−1000
0
5
10
time (sec)

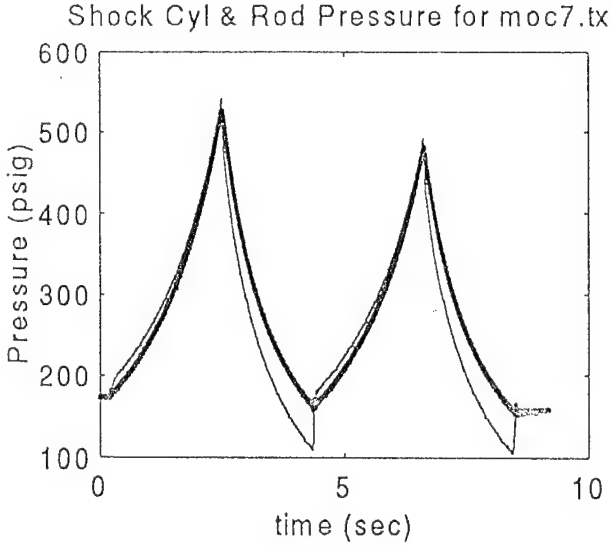
Shock Cyl & Rod Pressure for moc7.txt
Pressure (psig)
600
500
400
300
200
100
0
5
10
time (sec)

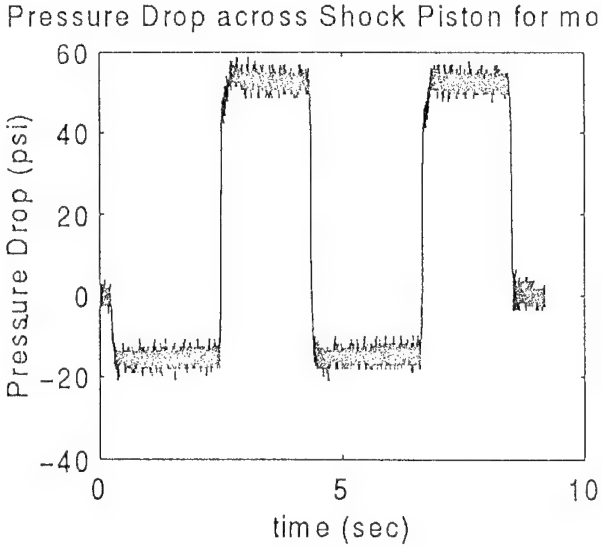
Pressure Drop across Shock Piston for moc7.txt
Pressure Drop (psi)
60
40
20
0
−20
−40
0
5
10
time (sec)

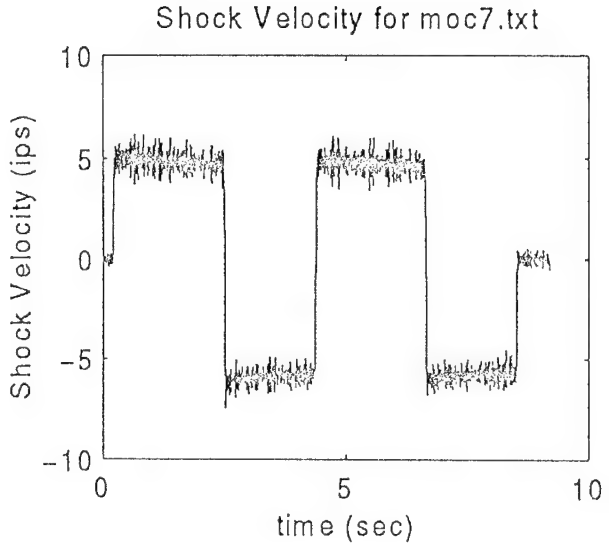
Shock Velocity for moc7.txt
Shock Velocity (ips)
time (sec)
10
5
0
-5
-10
0
5
10

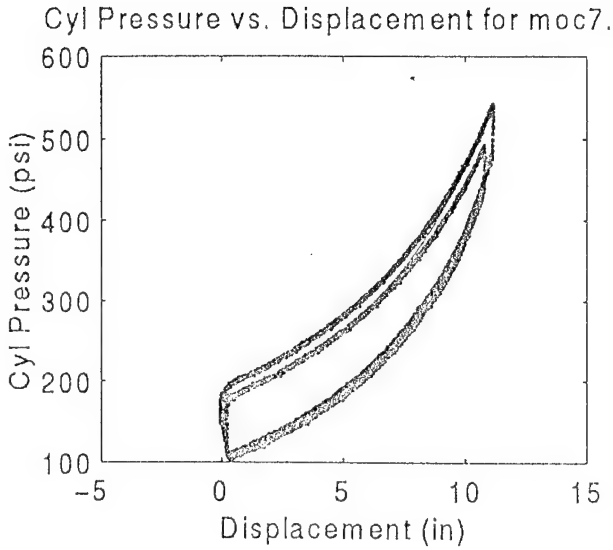
Cyl Pressure vs. Displacement for moc7.txt
Cyl Pressure (psi)
Displacement (in)
600
500
400
300
200
100
-5
0
5
10
15

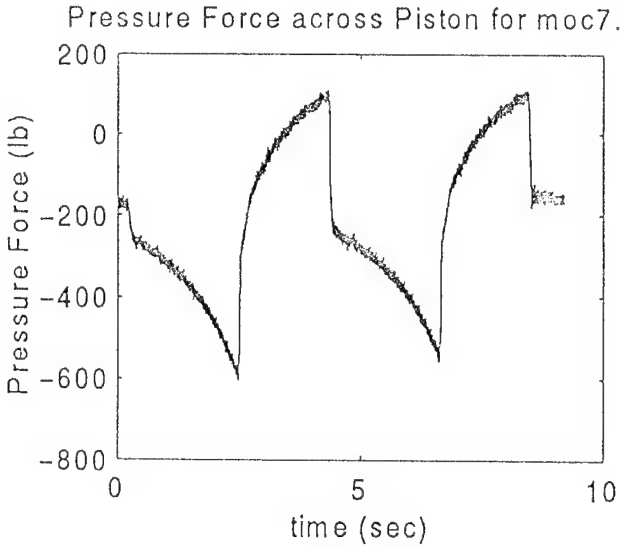
Pressure Force across Piston for moc7.txt
Pressure Force (lb)
time (sec)
200
0
-200
-400
-600
-800
0
5
10

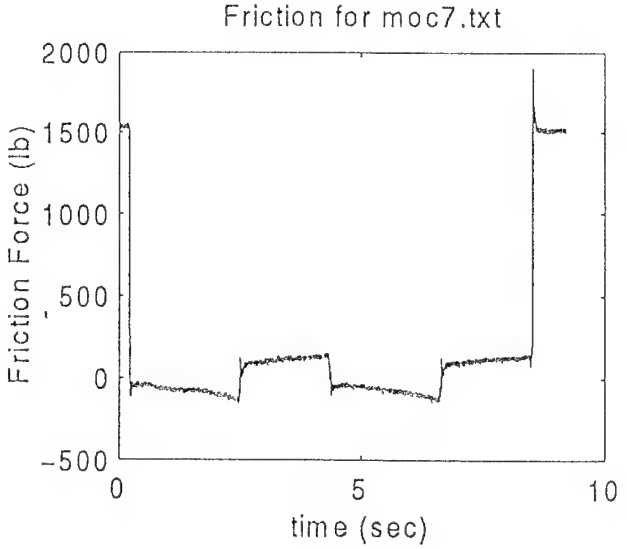
Friction for moc7.txt
Friction Force (lb)
time (sec)
2000
1500
1000
500
0
-500
0
5
10

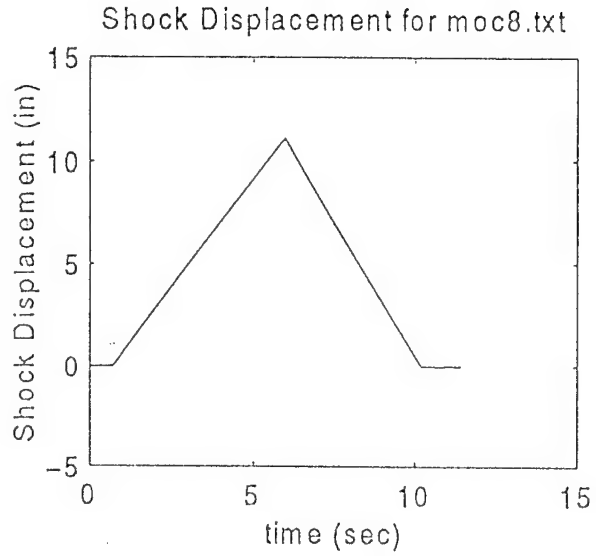
Shock Displacement for moc8.txt
Shock Displacement (in)
15
10
5
0
−5
0
5
10
15
time (sec)

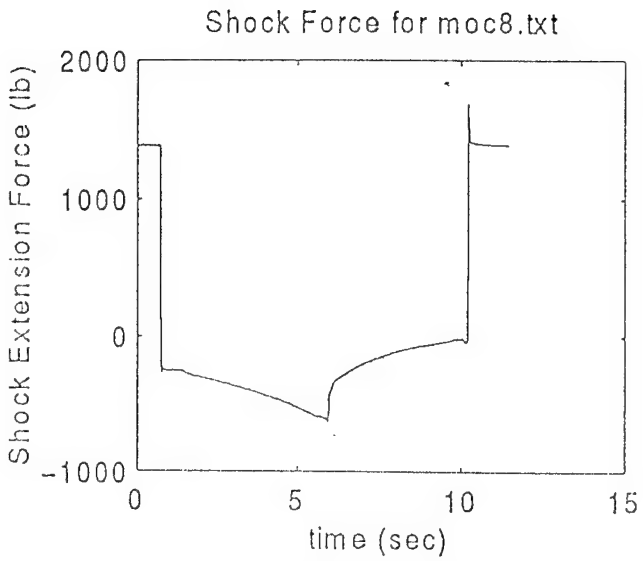
Shock Force for moc8.txt
Shock Extension Force (lb)
2000
1000
0
−1000
0
5
10
15
time (sec)

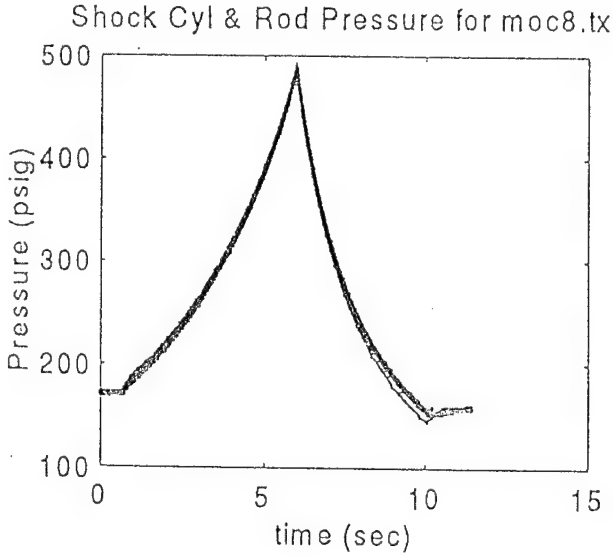
Shock Cyl & Rod Pressure for moc8.txt
Pressure (psig)
500
400
300
200
100
0
5
10
15
time (sec)

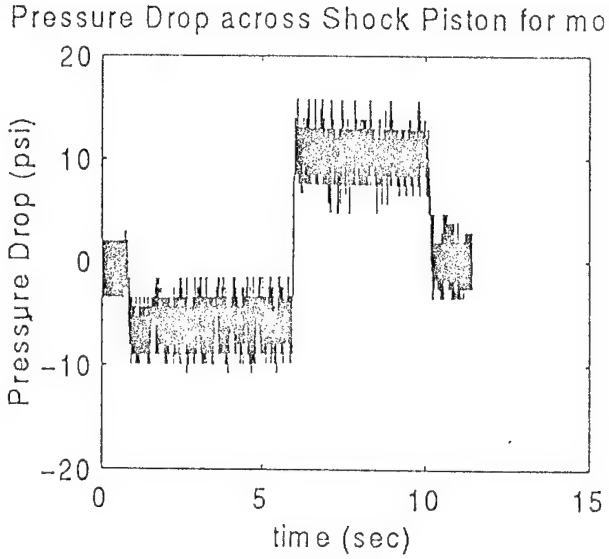
Pressure Drop across Shock Piston for moc8.txt
Pressure Drop (psi)
20
10
0
−10
−20
0
5
10
15
time (sec)

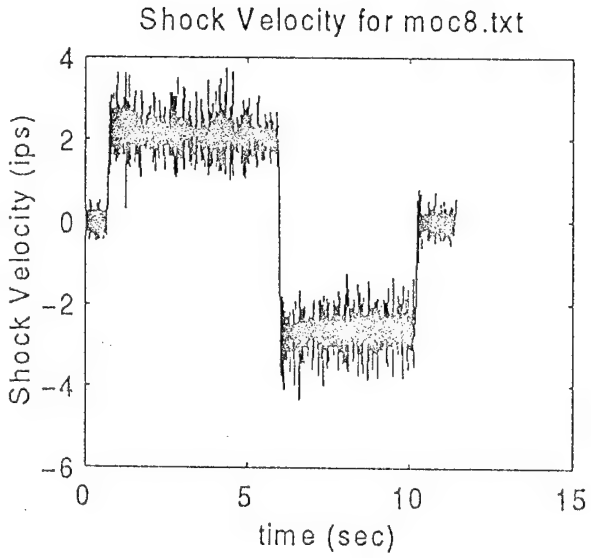
Shock Velocity for moc8.txt
Shock Velocity (ips)
time (sec)
4
2
0
-2
-4
-6
0
5
10
15

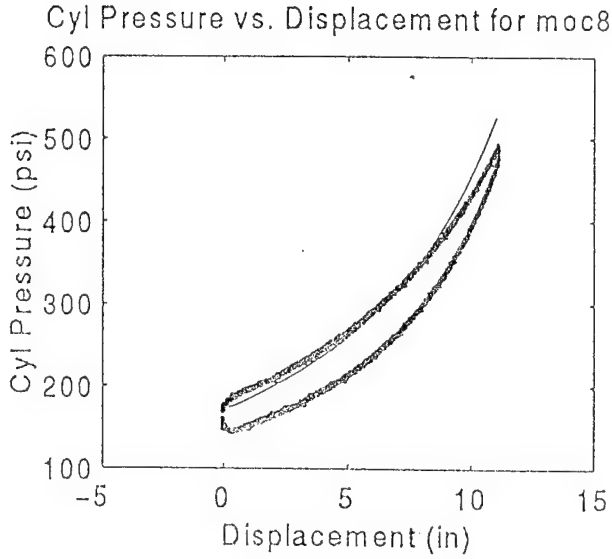
Cyl Pressure vs. Displacement for moc8.txt
Cyl Pressure (psi)
Displacement (in)
600
500
400
300
200
100
-5
0
5
10
15

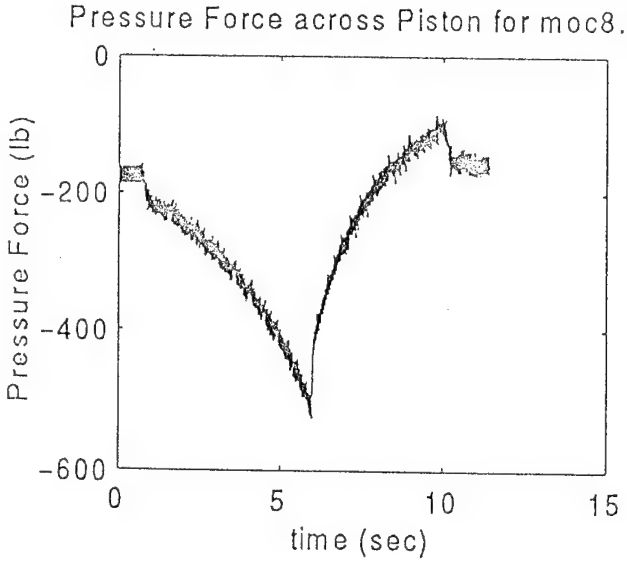
Pressure Force across Piston for moc8.txt
Pressure Force (lb)
time (sec)
0
-200
-400
-600
0
5
10
15

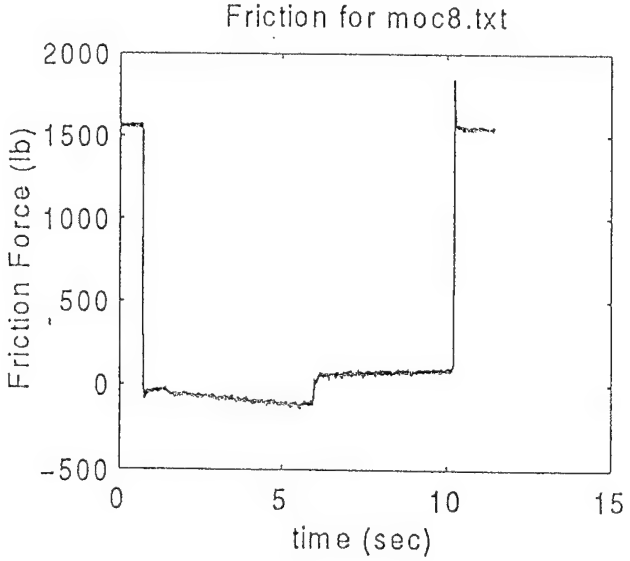
Friction for moc8.txt
Friction Force (lb)
time (sec)
2000
1500
1000
500
0
-500
0
5
10
15

# Appendix IV

# Hydraulic Damper Model

# shcksim1.m

Shock model with table look up for piston resistance
x dot + in compression

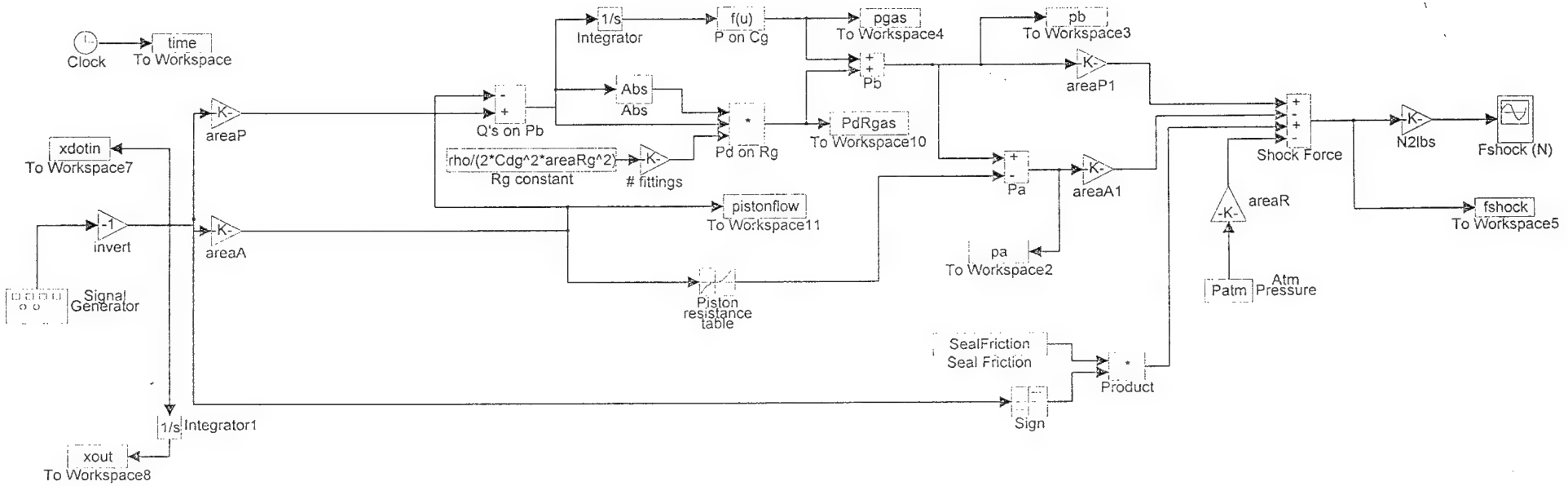

```
% shcksm1d.m
% defines shock model with simple orifice in piston

% general parameters
rho=900;

% conversion factors
pa2psi=1/6894.759;
psi2pa=6894.759;
n2lb=1/4.448222;
lb2n=4.448222;
m2in=1/0.0254;
in2m=0.0254;
gpm2m3s=231*(0.0254^3)*(1/60);

% areas
areaP=(pi/4)*2.5^2 *(0.0254)^2;
areaR=(pi/4)*1.125^2 *(0.0254)^2;
areaA=areaP-areaR;

% valve loss coefs
Cdg=0.4;
Cdp=0.4;

% valve areas
% resistance between cylinder and gas reservoir
% assume that it is just an orifice with no line resistance or dynamics
% dash 10 fitting ID = 0.480"
areaRg=(pi/4)*0.480^2*(0.0254)^2;

% resistance in shock piston
% the test pistons have four holes of equal diameter
holeDia=0.0995 *(0.0254);
areaRp=4*(pi/4)*holeDia^2;

qpmax=200*(0.0254)*areaP;
qptable=[-qpmax:(2*qpmax)/99:qpmax];
presspTable=rho/(2*Cdp^2*areaRp^2)*abs(qptable).*qptable;


% general parameters
rho=900;

SealFriction=(190/2)*4.448222;

% Gas reservoir
Patm=14.7*6894.759;
P0=(450 +14.7)*6894.759;
resdia=1.825*(0.0254);
reslength0=0.565*(11 - 2*0.530 - 0.850/3)*(0.0254);
Vol0=1 * (pi/4)*resdia^2*reslength0;
```

```
% hose and fitting resistances
% for hose
% dp=72 psi at 25 gpm for 10 ft
% resistance = dp/q^2
% Reshose10ft=72*psi2pa/(25*gpm2m3s)^2

% for fitting
% restfitting=rho/(2*Cdg^2*areaRg^2)
% for a given flow of areaR*1 m/s
% flowq=areaR*4;
% dPhose=Reshose10ft*flowq^2*pa2psi
% dPfitting=restfitting*flowq^2*pa2psi
% 10 ft of hose appx. equal to one fitting
```

# shcksim2.m

Test shock with simple orifice and controlled orifice
x dot + in compression

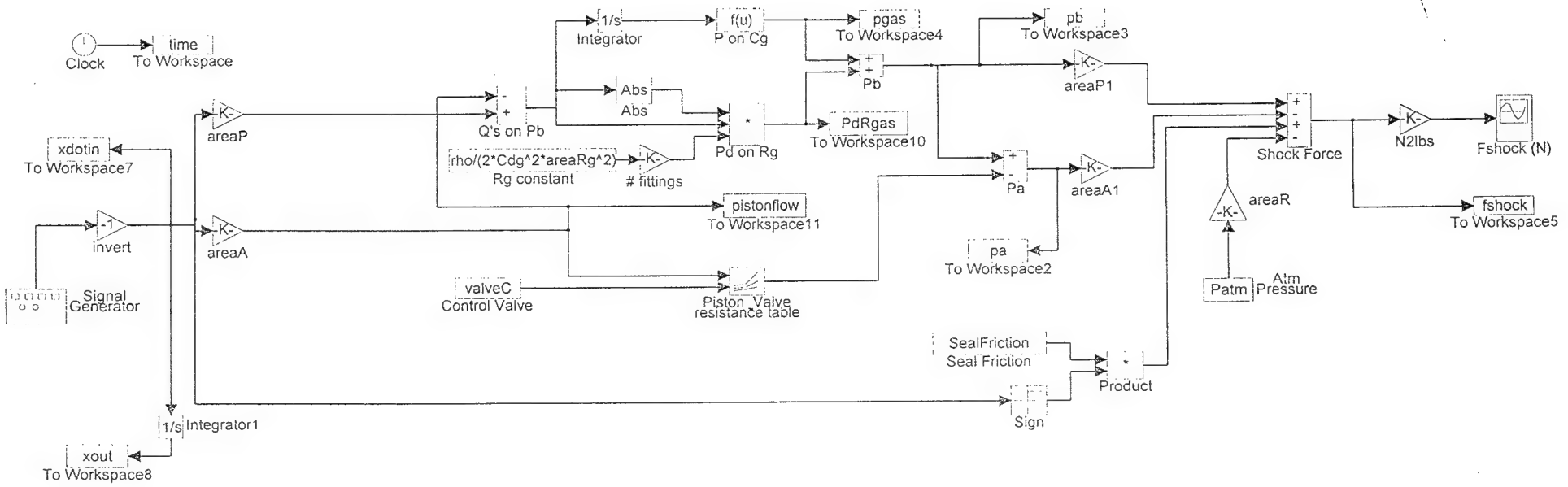

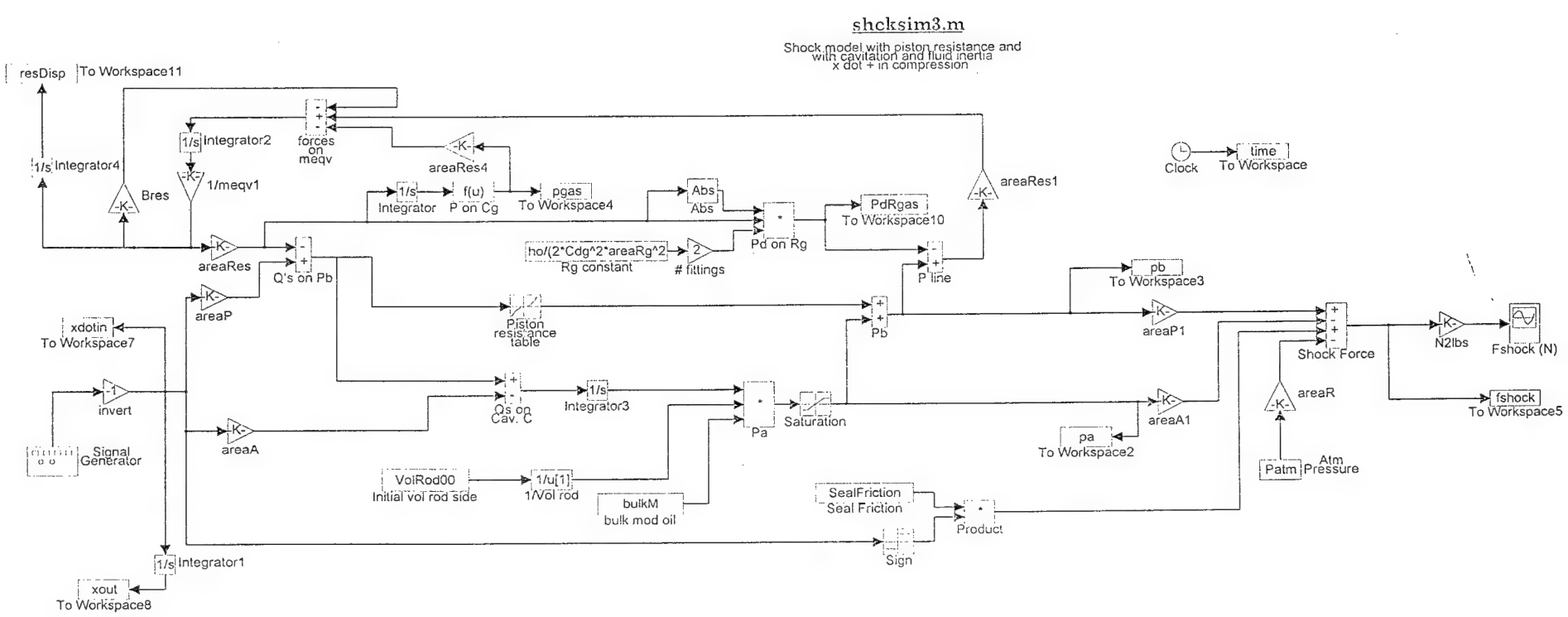
shcksim3.m
Shock model with piston resistance and with cavitation and fluid inertia
x dot + in compression
resDisp
To Workspace11
1/s
Integrator4
Bres
1/s
Integrator2
forces on meqv
areaRes4
1/meqv1
areaRes
Q's on Pb
areaP
xdotin
To Workspace7
invert
Signal Generator
areaA
1/s
Integrator1
xout
To Workspace8
1/s
Integrator
f(u)
P on Cg
pgas
To Workspace4
Abs
Abs
Pd on Rg
PdRgas
To Workspace10
areaRes1
ho/(2*Cdg^2*areaRg^2
Rg constant
2
# fittings
P line
Piston resistance table
Pb
pb
To Workspace3
areaP1
Qs on Cav. C
1/s
Integrator3
Pa
Saturation
areaA1
pa
To Workspace2
VolRod00
Initial vol rod side
1/u[1]
1/Vol rod
bulkM
bulk mod oil
SealFriction
Seal Friction
Product
Sign
Clock
time
To Workspace
Shock Force
areaR
Patm
Atm Pressure
N2lbs
Fshock (N)
fshock
To Workspace5

# Appendix V

# Quarter Car Model

qrtcar0.m

Quarter Car Nonlinear Model

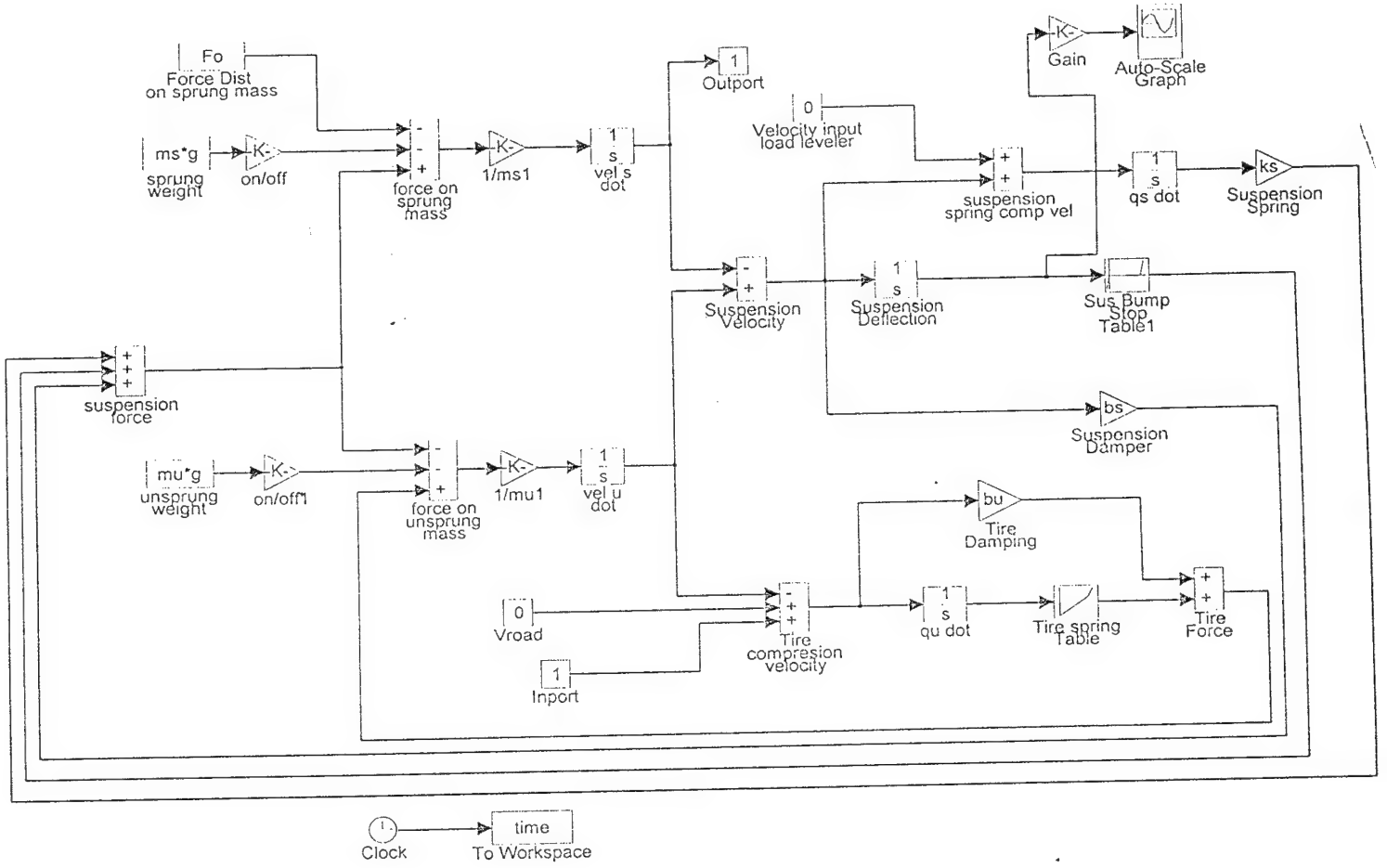

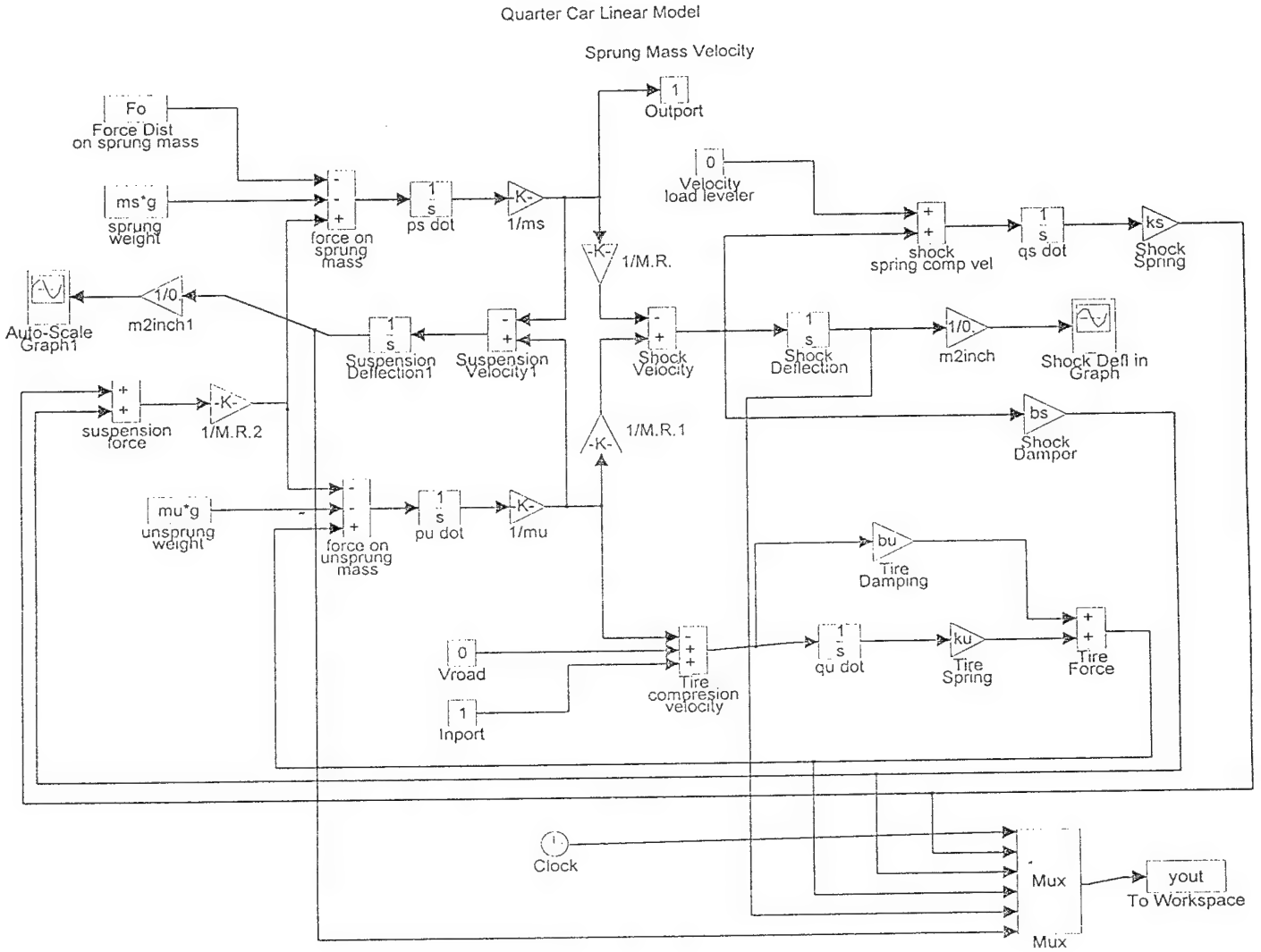
Quarter Car Linear Model
Sprung Mass Velocity
Fo
Force Dist on sprung mass
ms*g
sprung weight
force on sprung mass
1/s
ps dot
1/ms
1
Outport
0
Velocity load leveler
shock spring comp vel
qs dot
ks
Shock Spring
1/M.R.
Auto-Scale Graph1
1/0
m2inch1
Suspension Deflection1
Suspension Velocity1
Shock Velocity
Shock Deflection
m2inch
Shock Defl in Graph
suspension force
1/M.R.2
1/M.R.1
bs
Shock Damper
mu*g
unsprung weight
force on unsprung mass
pu dot
1/mu
bu
Tire Damping
0
Vroad
1
Inport
Tire compresion velocity
qu dot
ku
Tire Spring
Tire Force
Clock
Mux
Mux
yout
To Workspace

```
% qrtcar2d.m
% Defining Parameters for Quarter Car Nonlinear Suspension Model
%
g=9.81;
motionratio=1.6;
ms=(5665-4*140)/4*(1/2.204);
mu=140*(1/2.204);
ks=700*(4.448222)*(1/0.0254);
kseq=ks/motionratio^2;
bs=2*(0.4)*sqrt(kseq/ms)*ms*motionratio^2;
bseq=2*(0.4)*sqrt(kseq/ms)*ms;
bu=0;
Fo=0;

% motion ratio=wheelTravel/suspTravel=suspForce/wheelForce
% assume constant

% 1 dim look-up Table for nonlinear tire
% Baja T/A on flat at 20 psi
tireDeflection=(0.0254)*[-1,0,5.2953,5.5906,5.8661,6.1417,6.3386,6.5354
,6.6535,6.7323,6.7913];
tireForce=(4.448222)*[    0,0,   6883,   7330,   7777,   8224,   8672,   9141
,   9678,  10237,  10684];
ku=(4.448222/0.0254)*6883/5.2953;          % for steady state conditions

% 2 dim look-up table for semi-active shock
% linear shock to compare to linear model
% semishockDisp=[-1,1];      % for x axis (rows) of table
% semishockVel=[-1,0,1];     % for y axis (columns) of table
% semishockTable=[-bs,0,bs;-bs,0,bs];

% 2 dim look-up table for semi-active shock based on wheel values
wheelDisp=[-1,1]/0.0254;   % input in meters converted to wheel Disp in
 inches
semishockDisp=(1/motionratio)*(0.0254)*wheelDisp;   % for x axis (rows)
 of table
wheelVel=[-1,0,1]/0.0254;  % wheel Vel in ips
semishockVel=(1/motionratio)*(0.0254)*wheelVel;    % for y axis (column
s) of table
wheelTable=[-bseq,0,bseq;-bseq,0,bseq]/(4.448222);  % in lbs.
semishockTable=motionratio*(4.448222)*wheelTable;

% John L's passive shock from notes
%wheelDisp=[-5,-3,-1,3,7,9,11];                          % wheel Disp in
 inches
%semishockDisp=(1/motionratio)*(0.0254)*wheelDisp;   % for x axis (rows
) of table
%wheelVel=[-150,-75,-50,-25,-5,-1,1,5,25,50,75,150];    % wheel Velocit
y in ips
%semishockVel=(1/motionratio)*(0.0254)*wheelVel;      % for y axis (col
umns) of table
%wheelTable=[-7700,-3800,-2500,-1300,-250,-50,10,20,400,1000,1500,3000;
```

```
%             -7700,-3800,-2500,-1300,-250,-50,10,20,400,1000,1500,3000;
%             -7700,-3800,-2500,-1300,-250,-50,10,20,400,1000,1500,3000;
%             -7700,-3800,-2500,-1300,-250,-50,30,60,600,1400,2000,4000;
%             -7700,-3800,-2500,-1300,-250,-50,50,300,800,1800,2500,5000
;
%             -7700,-3800,-2500,-1300,-250,-50,50,300,800,1800,2500,5000
;
%             -7700,-3800,-2500,-1300,-250,-50,50,300,800,1800,2500,5000
];
% semishockTable=motionratio*(4.448222)*wheelTable;

% John L's ideal shock from notes (compression only, made rebound symet
ric)
%wheelDisp=[-5,-3,-1,1,3,5,7,9,11];
%semishockDisp=(1/motionratio)*(0.0254)*wheelDisp;     % for x axis (ro
ws) of table
%wheelVel=[-150,-100,-75,-50,-25,-5,-1,1,5,25,50,75,100,150];
%semishockVel=(1/motionratio)*(0.0254)*wheelVel;      % for y axis (col
umns) of table
%wheelTable=[-7700,-5100,-3800,-2500,-1300,-250, -50, 50,150,250,1000,2
000,5000,10000;
%             -7700,-5100,-3800,-2500,-1300,-250, -50, 50,150,250, 750,2
000,5000,10000;
%             -7700,-5100,-3800,-2500,-1300,-250, -50, 50,150,160, 500,2
000,5000,10000;
%             -7700,-5100,-3800,-2500,-1300,-250, -50, 50,150,160, 500,2
000,7500,10000;
%             -7700,-5100,-3800,-2500,-1300,-250, -50, 50,150,160, 500,3
000,10000,10000;
%             -7700,-5100,-3800,-2500,-1300,-250, -50, 50,150,250,1000,5
000,10000,10000;
%             -7700,-5100,-3800,-2500,-1300,-250, -50, 50,250,500,5000,1
0000,10000,10000;
%             -7700,-5100,-3800,-2500,-1300,-250, -50,100,500,2500,10000
,10000,10000,10000;
%             -7700,-5100,-3800,-2500,-1300,-250, -50,1000,5000,7500,100
00,10000,10000,10000];
%semishockTable=motionratio*(4.448222)*wheelTable;

% 2 dim look-up table for bump-stop
wheelBSDisp=[-1,0,1];  % in inches of wheel travel  (rows of table)
bumpstopDisp=(1/motionratio)*(0.0254)*wheelBSDisp;
wheelBSVel=[-1,1];     % in ips of wheel velocity  (columns of table)
bumpstopVel=(1/motionratio)*(0.0254)*wheelBSVel;
wheelBSTable=[0 0;0 0;0,0];  % in lbs. at wheel travel/velocity
bumpstopTable=motionratio*(4.448222)*wheelBSTable;


figure(1)
mesh(wheelVel,wheelDisp,wheelTable,0*wheelTable)

%plot(wheelVel,wheelTable(1,:), ...
```

```
%       wheelVel,wheelTable(2,:), ...
%       wheelVel,wheelTable(3,:), ...
%       wheelVel,wheelTable(4,:), ...
%       wheelVel,wheelTable(5,:), ...
%       wheelVel,wheelTable(6,:), ...
%       wheelVel,wheelTable(7,:))
```

# Appendix VII

# Full Car Model

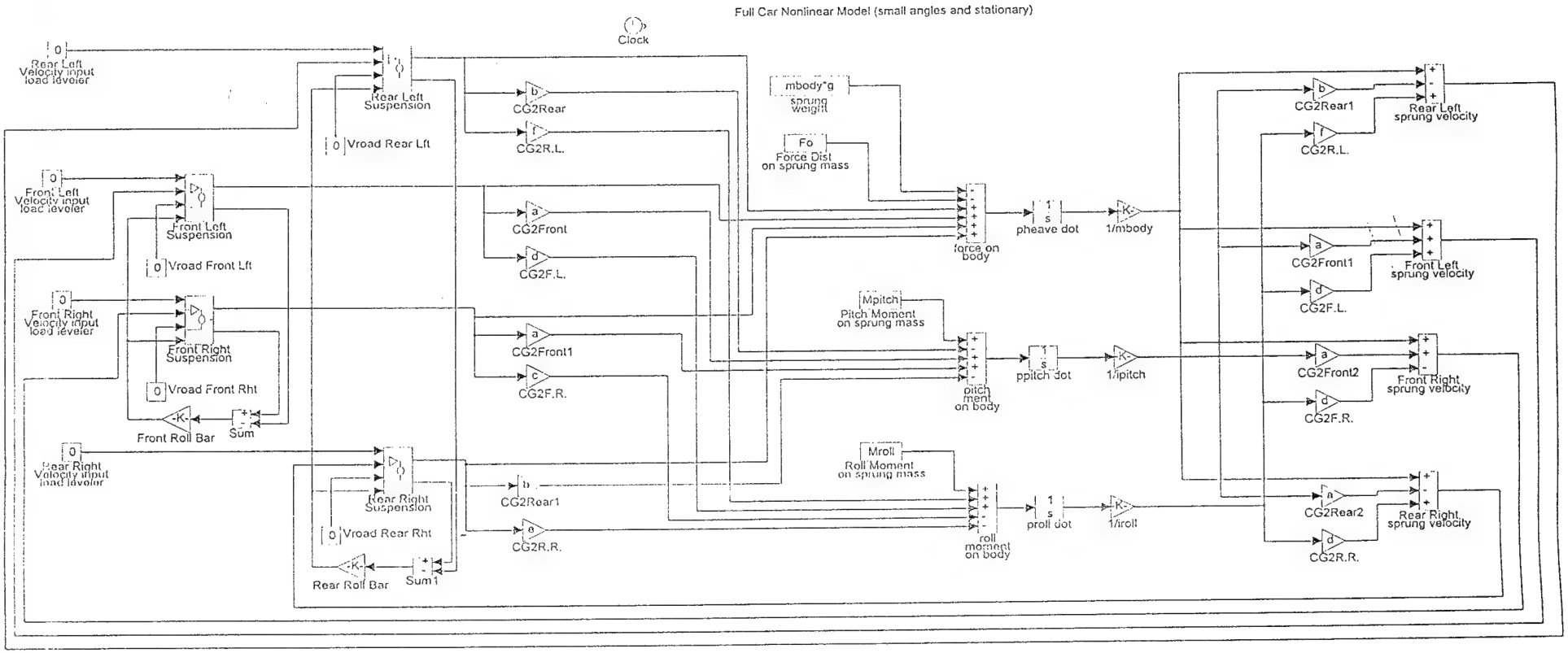
Full Car Nonlinear Model (small angles and stationary)
Clock
Rear Left Velocity input load leveler
Rear Left Suspension
Vroad Rear Lft
CG2Rear
CG2R.L.
mbody*g
sprung weight
Fo
Force Dist on sprung mass
Front Left Velocity input load leveler
Front Left Suspension
Vroad Front Lft
CG2Front
CG2F.L.
Front Right Velocity input load leveler
Front Right Suspension
Vroad Front Rht
Front Roll Bar
Sum
CG2Front1
CG2F.R.
Mpitch
Pitch Moment on sprung mass
Rear Right Velocity input load leveler
Rear Right Suspension
Vroad Rear Rht
Rear Roll Bar
Sum1
CG2Rear1
CG2R.R.
Mroll
Roll Moment on sprung mass
force on body
pheave dot
1/mbody
pitch ment on body
ppitch dot
1/ipitch
roll moment on body
proll dot
1/iroll
CG2Rear1
CG2R.L.
Rear Left sprung velocity
CG2Front1
CG2F.L.
Front Left sprung velocity
CG2Front2
CG2F.R.
Front Right sprung velocity
CG2Rear2
CG2R.R.
Rear Right sprung velocity

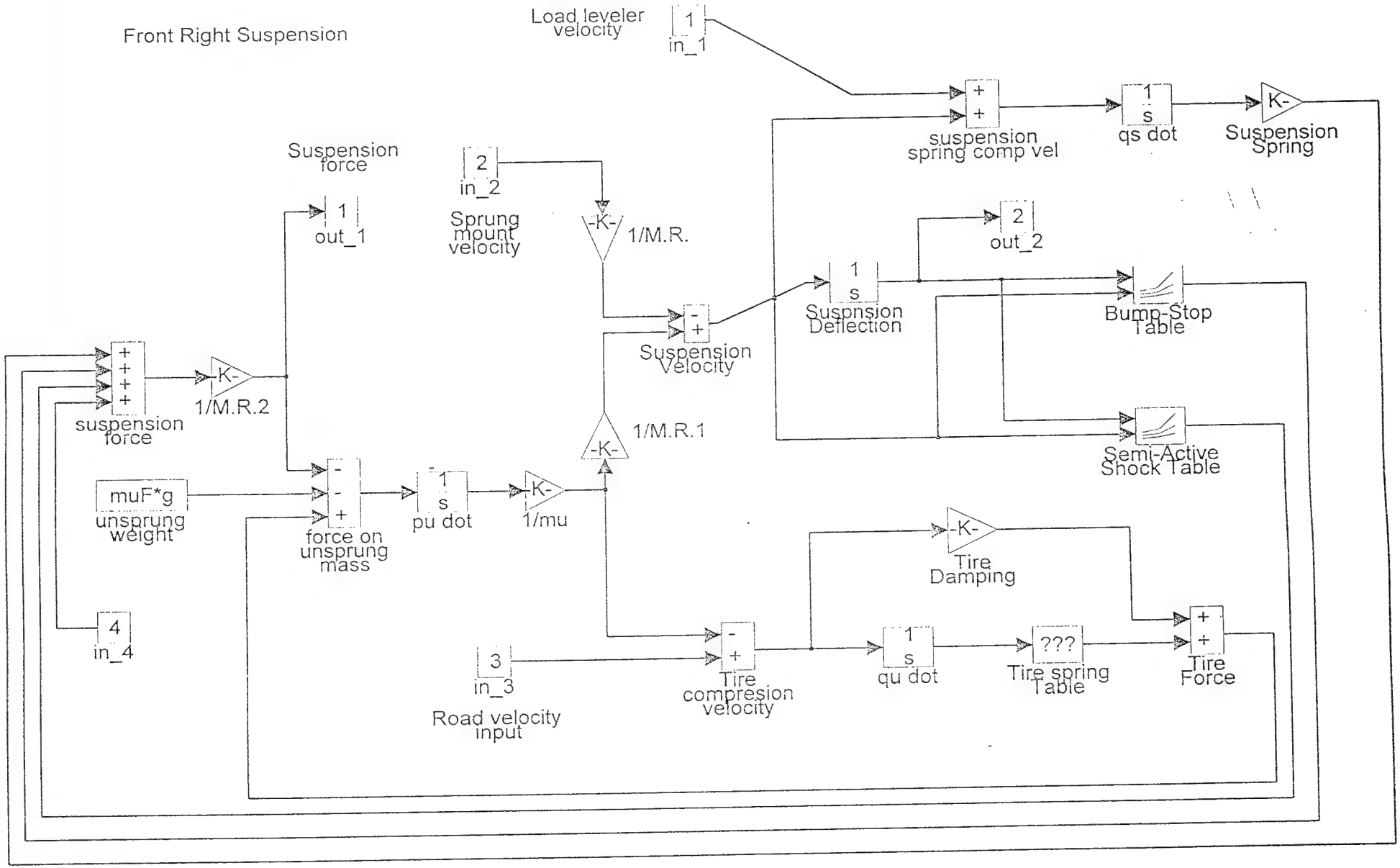
Front Right Suspension
Load leveler velocity
1
in_1
suspension spring comp vel
1
s
qs dot
K-
Suspension Spring
Suspension force
2
in_2
Sprung mount velocity
-K-
1/M.R.
1
out_1
2
out_2
1
s
Suspnsion Deflection
Bump-Stop Table
Suspension Velocity
suspension force
K-
1/M.R.2
-K-
1/M.R.1
Semi-Active Shock Table
muF*g
unsprung weight
force on unsprung mass
1
s
pu dot
K-
1/mu
K-
Tire Damping
4
in_4
3
in_3
Road velocity input
Tire compresion velocity
1
s
qu dot
???
Tire spring Table
Tire Force

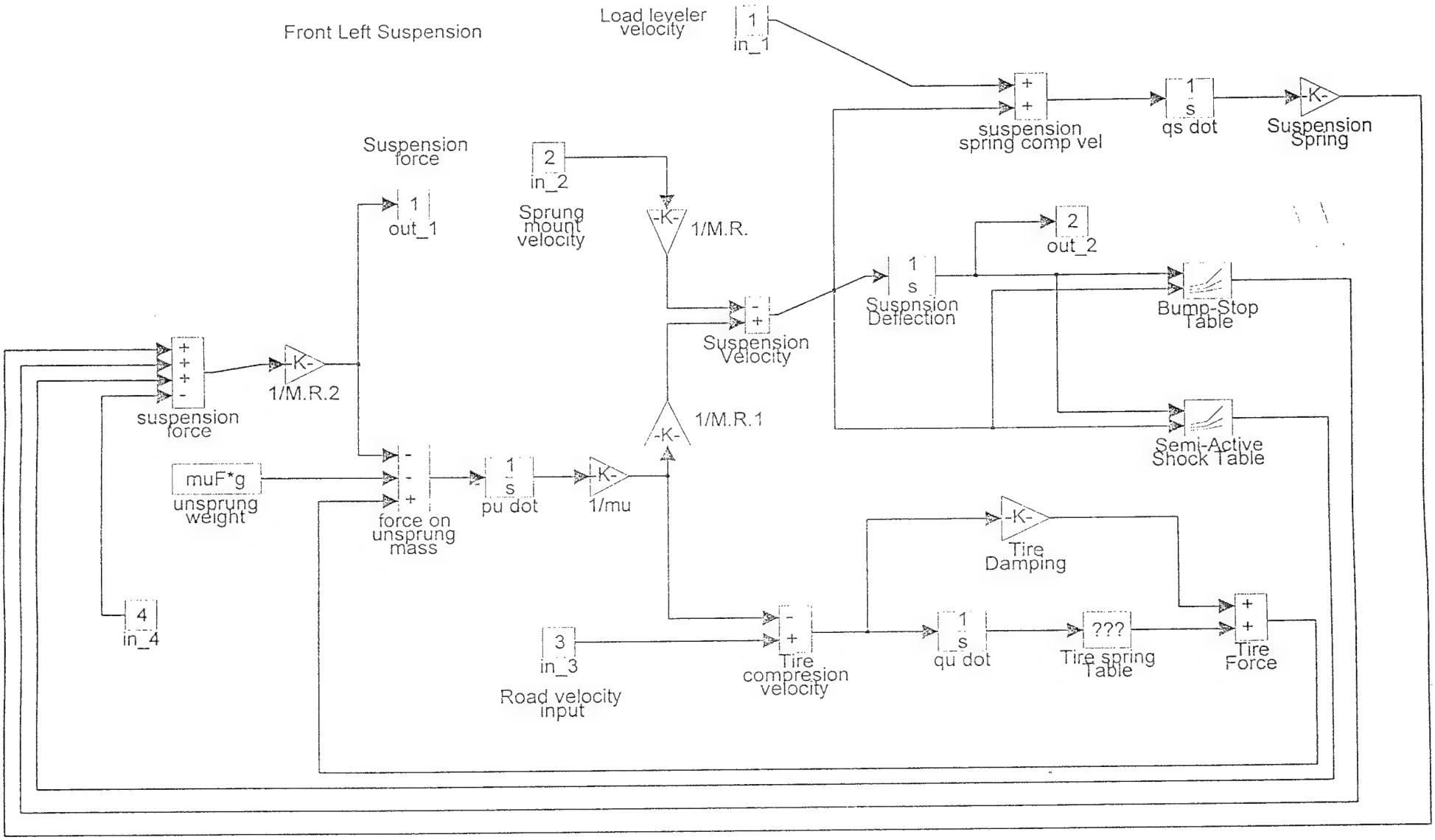
Front Left Suspension
Load leveler velocity
1
in_1
suspension spring comp vel
1
s
qs dot
-K-
Suspension Spring
Suspension force
1
out_1
2
in_2
Sprung mount velocity
-K-
1/M.R.
2
out_2
1
s
Suspnsion Deflection
Bump-Stop Table
Suspension Velocity
suspension force
-K-
1/M.R.2
-K-
1/M.R.1
Semi-Active Shock Table
muF*g
unsprung weight
1
s
pu dot
-K-
1/mu
force on unsprung mass
-K-
Tire Damping
4
in_4
3
in_3
Road velocity input
Tire compresion velocity
1
s
qu dot
???
Tire spring Table
Tire Force

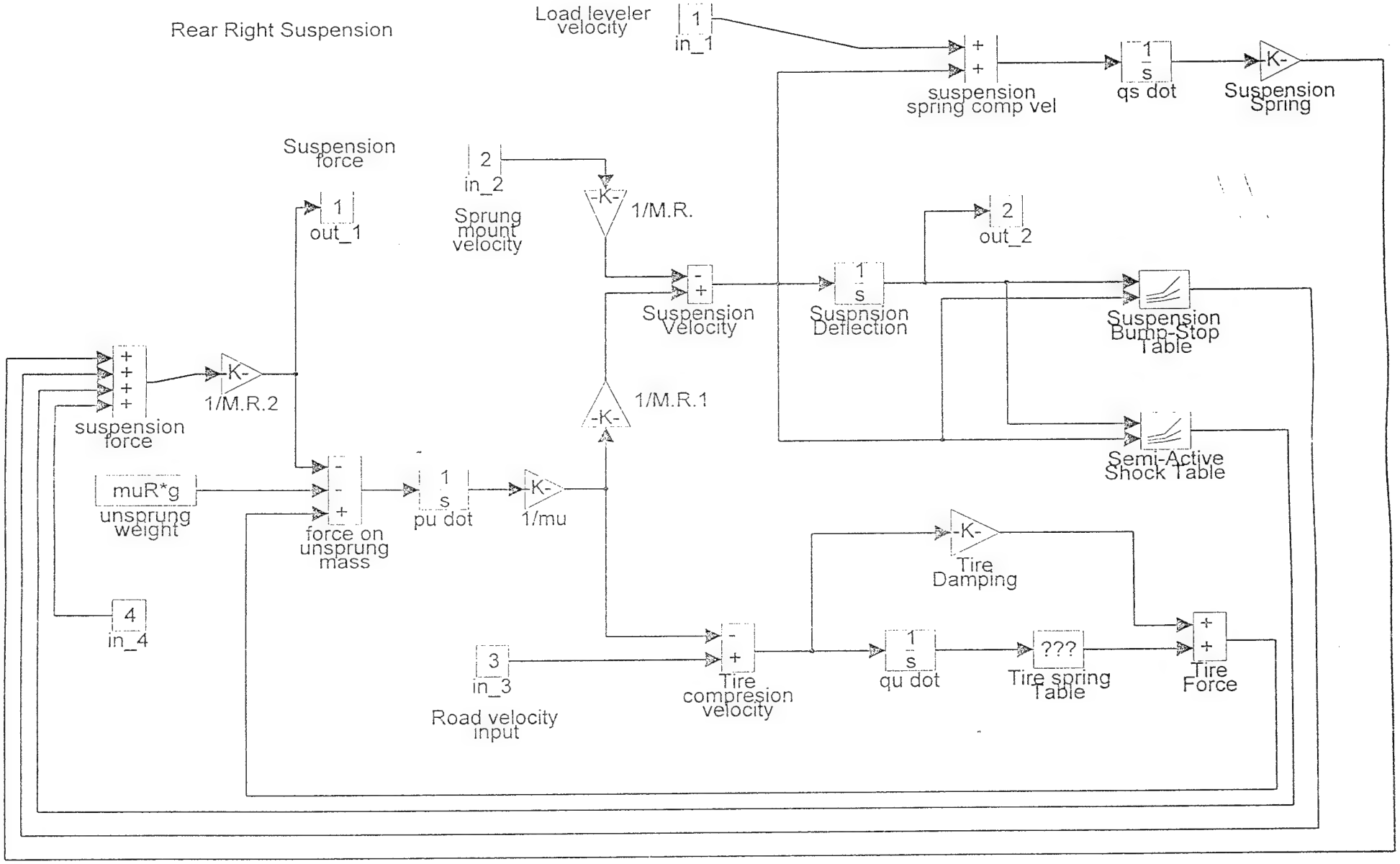
Rear Right Suspension
Load leveler velocity
1
in_1
suspension spring comp vel
1/s
qs dot
K-
Suspension Spring
Suspension force
1
out_1
2
in_2
Sprung mount velocity
-K-
1/M.R.
2
out_2
Suspension Velocity
1/s
Suspnsion Deflection
Suspension Bump-Stop Table
suspension force
K-
1/M.R.2
-K-
1/M.R.1
Semi-Active Shock Table
muR*g
unsprung weight
force on unsprung mass
1/s
pu dot
K-
1/mu
-K-
Tire Damping
4
in_4
3
in_3
Road velocity input
Tire compresion velocity
1/s
qu dot
???
Tire spring Table
Tire Force

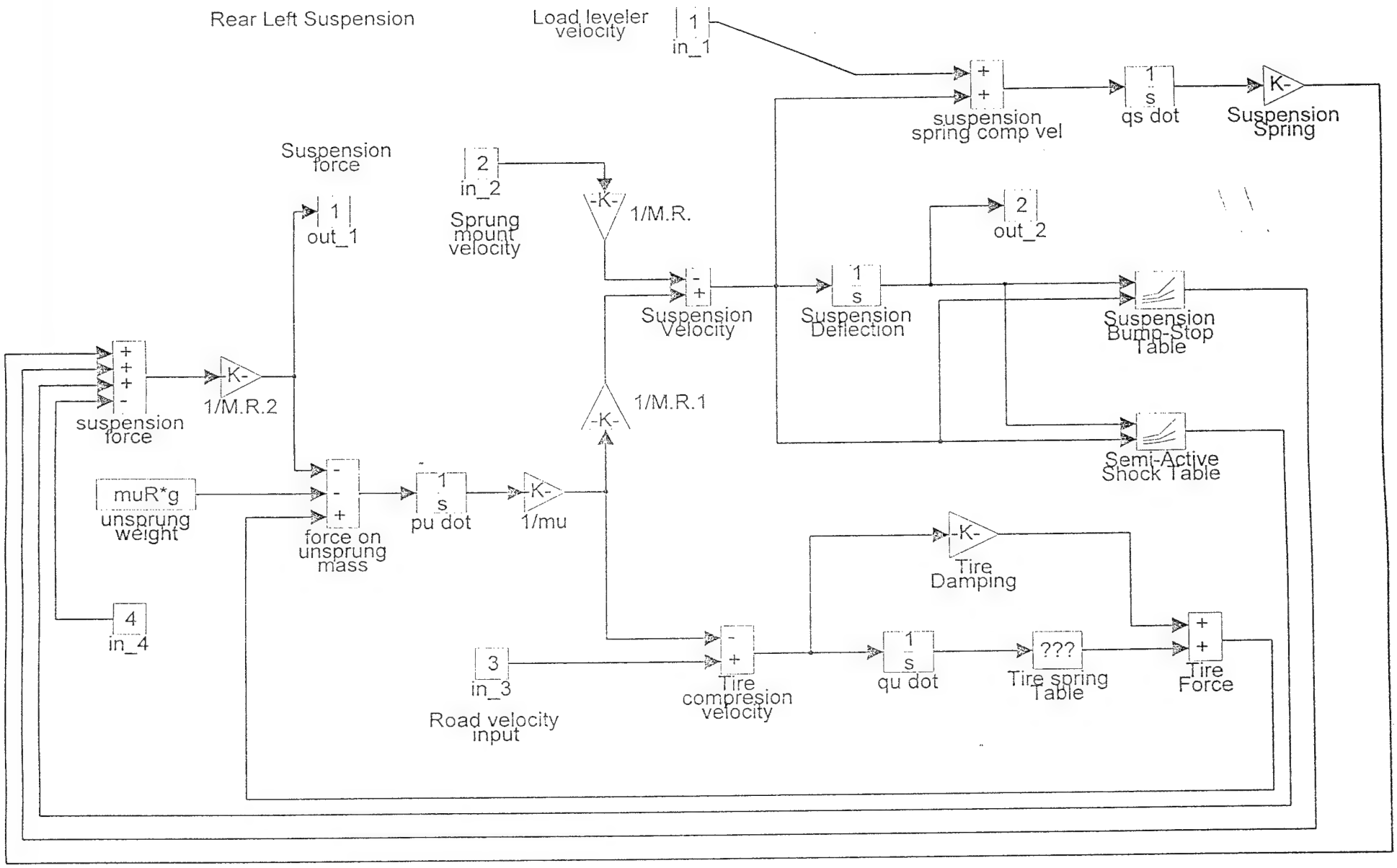
Rear Left Suspension
Load leveler velocity
1
in_1
suspension spring comp vel
1/s
qs dot
K-
Suspension Spring
Suspension force
1
out_1
2
in_2
Sprung mount velocity
-K-
1/M.R.
2
out_2
Suspension Velocity
1/s
Suspension Deflection
Suspension Bump-Stop Table
Semi-Active Shock Table
+
+
+
-
suspension force
K-
1/M.R.2
-K-
1/M.R.1
muR*g
unsprung weight
force on unsprung mass
1/s
pu dot
K-
1/mu
K-
Tire Damping
4
in_4
3
in_3
Road velocity input
Tire compresion velocity
1/s
qu dot
???
Tire spring Table
Tire Force

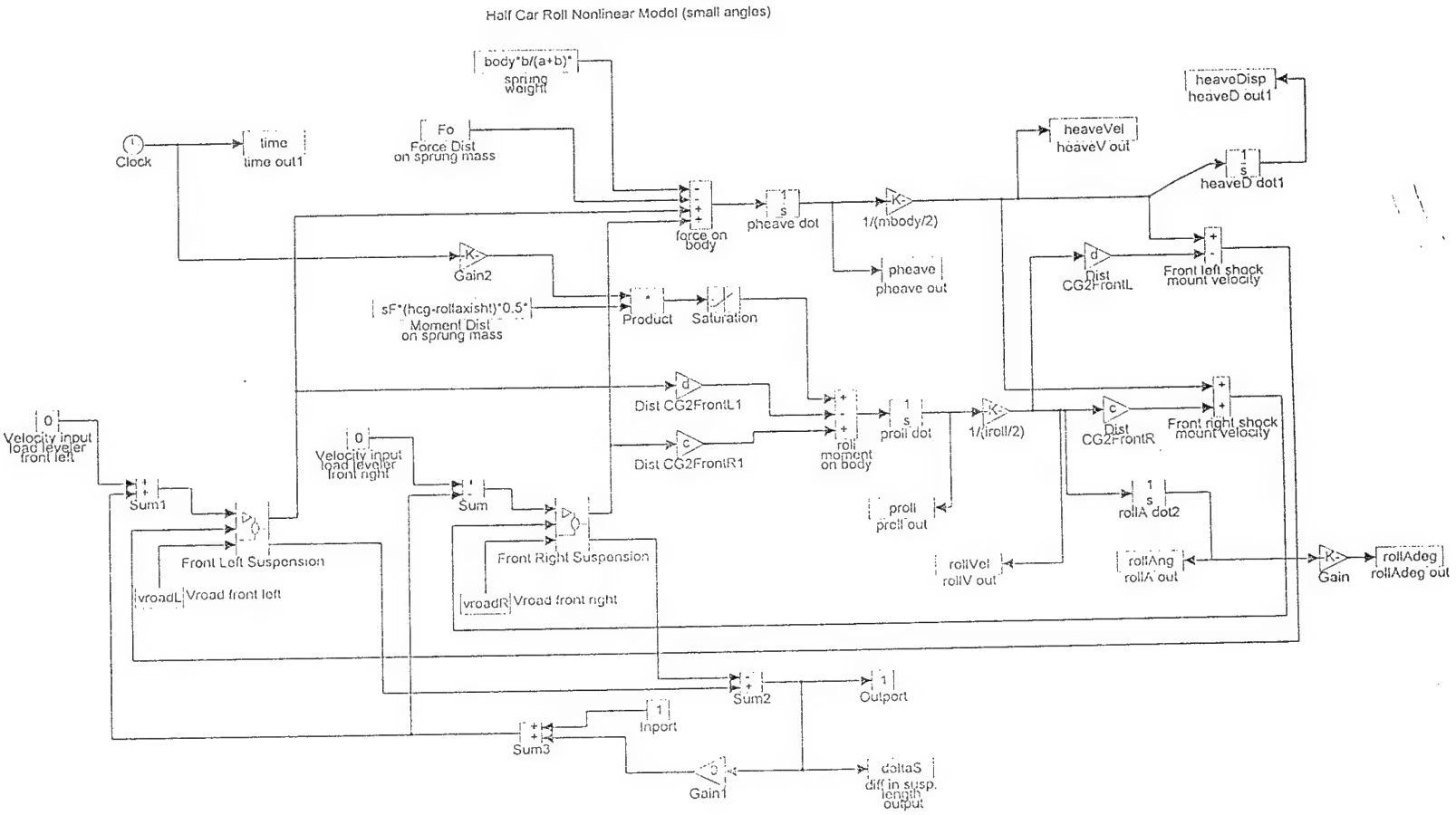
Half Car Roll Nonlinear Model (small angles)
body*b/(a+b)*
sprung
weight
heaveDisp
heaveD out1
Clock
time
time out1
Fo
Force Dist
on sprung mass
heaveVel
heaveV out
1
s
heaveD dot1
force on
body
1
s
pheave dot
1/(mbody/2)
Gain2
pheave
pheave out
d
Dist
CG2FrontL
Front left shock
mount velocity
sF*(hcg-rollaxisht)*0.5*
Moment Dist
on sprung mass
Product
Saturation
Dist CG2FrontL1
0
Velocity input
load leveler
front left
roll
moment
on body
1
s
proll dot
1/(Iroll/2)
c
Dist
CG2FrontR
Front right shock
mount velocity
0
Velocity input
load leveler
front right
Dist CG2FrontR1
Sum1
Sum
proll
proll out
1
s
rollA dot2
Front Left Suspension
Front Right Suspension
rollVel
rollV out
rollAng
rollA out
Gain
rollAdeg
rollAdeg out
vroadL
Vroad front left
vroadR
Vroad front right
Sum2
1
Outport
1
Inport
Sum3
Gain1
deltaS
diff in susp.
length
output

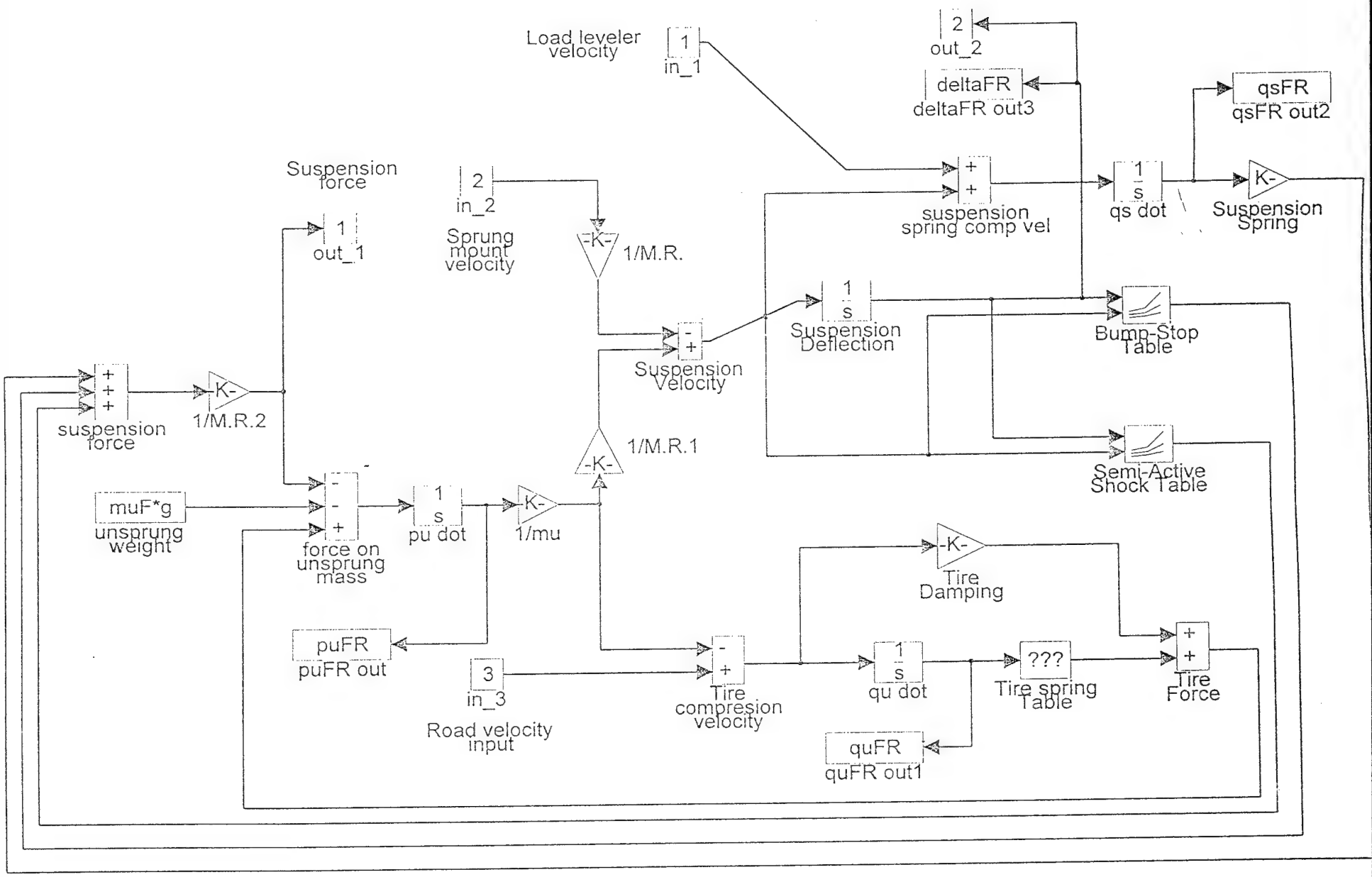
Load leveler velocity
1
in_1
2
out_2
deltaFR
deltaFR out3
qsFR
qsFR out2
Suspension force
1
out_1
2
in_2
Sprung mount velocity
-K-
1/M.R.
+
+
suspension spring comp vel
1
s
qs dot
K-
Suspension Spring
1
s
Suspension Deflection
Bump-Stop Table
-
+
Suspension Velocity
+
+
+
suspension force
K-
1/M.R.2
-K-
1/M.R.1
Semi-Active Shock Table
muF*g
unsprung weight
-
-
+
force on unsprung mass
1
s
pu dot
K-
1/mu
-K-
Tire Damping
puFR
puFR out
3
in_3
Road velocity input
-
+
Tire compresion velocity
1
s
qu dot
???
Tire spring Table
+
+
Tire Force
quFR
quFR out1

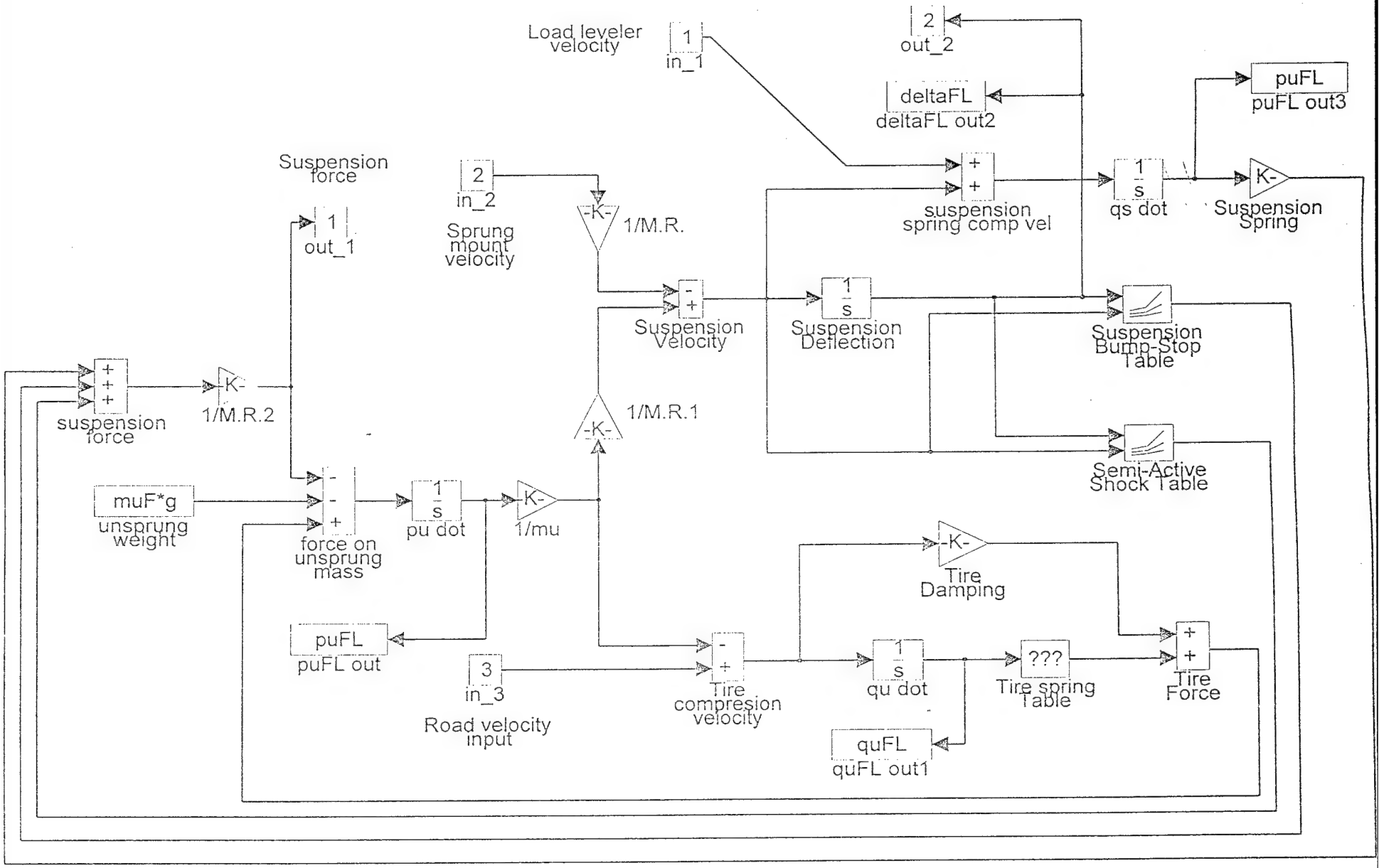
Load leveler velocity
1
in_1
2
out_2
deltaFL
deltaFL out2
puFL
puFL out3
Suspension force
1
out_1
2
in_2
Sprung mount velocity
-K-
1/M.R.
+
+
suspension spring comp vel
1
s
qs dot
K-
Suspension Spring
-
+
Suspension Velocity
1
s
Suspension Deflection
Suspension Bump-Stop Table
+
+
+
suspension force
K-
1/M.R.2
-K-
1/M.R.1
Semi-Active Shock Table
muF*g
unsprung weight
-
-
+
force on unsprung mass
1
s
pu dot
K-
1/mu
K-
Tire Damping
puFL
puFL out
3
in_3
Road velocity input
-
+
Tire compresion velocity
1
s
qu dot
???
Tire spring Table
+
+
Tire Force
quFL
quFL out1

```
% hlfrolld.m
% Defining Parameters for Half Car Nonlinear Suspension Model
%
Gcroll=5000;
rollcontrolnum=Gcroll*conv([1,5],[1,7]);
rollcontrolden=conv(conv([1,100],[1,200]),[1,2000]);
rollcontrolnum=5;
rollcontrolden=1;

g=9.81;
hcg=26*(0.0254);
rollaxisht=4.149*(0.0254);
a=58.22*(0.0254);  % to front
b=60.78*(0.0254);  % to rear
trackwidth=52.5*(0.0254);
c=trackwidth/2; % to right side
d=trackwidth/2; % to left side
mbody=(5665-4*140)*(1/2.204);
msF=mbody*b/(a+b);
muF=140*(1/2.204);
muR=140*(1/2.204);
ipitch=3000;
iroll=400;
ksF=700*(4.448222)*(1/0.0254);
ksR=300*(4.448222)*(1/0.0254);
motionratioF=1.6;
motionratioR=1.53;

kseqF=ksF/motionratioF^2;
zetaPF=0.2;
zetaAF=0.5;
bpF=2*(zetaPF)*sqrt(kseqF/msF)*msF*motionratioF^2;
bpeqF=2*(zetaPF)*sqrt(kseqF/msF)*msF;
bpeqR=bpeqF;

baF=2*(zetaAF)*sqrt(kseqF/msF)*msF*motionratioF;
baeqF=2*(zetaAF)*sqrt(kseqF/msF)*msF;

buF=0;
buR=0;
Fo=0;
Mo=0;


% Front tire
% 1 dim look-up Table for nonlinear tire
% Baja T/A on flat at 20 psi
tireDeflectionF=(0.0254)*[-1,0,5.2953,5.5906,5.8661,6.1417,6.3386,6.535
4,6.6535,6.7323,6.7913];
tireForceF=(4.448222)*[    0,0,  6883,  7330,  7777,  8224,  8672,  914
1,  9678, 10237, 10684];
kuF=tireForceF(3)/tireDeflectionF(3);         % for steady state condit
```

```
ions

% Rear tire
% Baja T/A on flat at 20 psi
tireDeflectionR=(0.0254)*[-1,0,5.2953,5.5906,5.8661,6.1417,6.3386,6.535
4,6.6535,6.7323,6.7913];
tireForceR=(4.448222)*[    0,0,  6883,  7330,  7777,  8224,  8672,  914
1,  9678, 10237, 10684];
kuR=tireForceR(3)/tireDeflectionR(3);          % for steady state condit
ions

% Front
% 2 dim look-up table for semi-active shock
% linear shock to compare to linear model
%semishockDispF=[-1,1];      % for x axis (rows) of table
%semishockVelF=[-1,0,1];     % for y axis (columns) of table
%semishockTableF=[-bs,0,bs;-bs,0,bs];

% 2 dim look-up table for semi-active shock based on wheel values
wheelDispF=[-1,1]/0.0254;   % wheel Disp in inches
semishockDispF=(1/motionratioF)*(0.0254)*wheelDispF;   % for x axis (ro
ws) of table
wheelVelF=[-1,0,1]/0.0254;  % wheel Vel in ips
semishockVelF=(1/motionratioF)*(0.0254)*wheelVelF;    % for y axis (col
umns) of table
wheelTableF=[-bpeqF,0,bpeqF;-bpeqF,0,bpeqF]/(4.448222);  % in lbs.
semishockTableF=motionratioF*(4.448222)*wheelTableF;

% John L's passive shock from notes (compression only, made rebound sym
etric)
wheelDispF=[-5,-3,-1,3,7,9,11];                          % wheel Disp in
 inches
semishockDispF=(1/motionratioF)*(0.0254)*wheelDispF;   % for x axis (ro
ws) of table
wheelVelF=[-150,-75,-50,-25,-5,-1,1,5,25,50,75,150];     % wheel Velocit
y in ips
semishockVelF=(1/motionratioF)*(0.0254)*wheelVelF;       % for y axis (c
olumns) of table
wheelTableF=[-7700,-3800,-2500,-1300,-250,-50,10,20,400,1000,1500,3000;
             -7700,-3800,-2500,-1300,-250,-50,10,20,400,1000,1500,3000;
             -7700,-3800,-2500,-1300,-250,-50,10,20,400,1000,1500,3000;
             -7700,-3800,-2500,-1300,-250,-50,30,60,600,1400,2000,4000;
             -7700,-3800,-2500,-1300,-250,-50,50,300,800,1800,2500,5000;
             -7700,-3800,-2500,-1300,-250,-50,50,300,800,1800,2500,5000;
             -7700,-3800,-2500,-1300,-250,-50,50,300,800,1800,2500,5000]
;
 semishockTableF=motionratioF*(4.448222)*wheelTableF;

% John L's ideal shock from notes (compression only, made rebound symet
ric)
%wheelDispF=[-5,-3,-1,1,3,5,7,9,11];
%semishockDispF=(1/motionratioF)*(0.0254)*wheelDispF;     % for x axis
```

```
(rows) of table
%wheelVelF=[-150,-100,-75,-50,-25,-5,-1,1,5,25,50,75,100,150];
%semishockVelF=(1/motionratioF)*(0.0254)*wheelVelF;      % for y axis (
columns) of table
%wheelTableF=[-7700,-5100,-3800,-2500,-1300,-250, -50, 50,150,250,1000,
2000,5000,10000;
%             -7700,-5100,-3800,-2500,-1300,-250, -50, 50,150,250, 750,2
000,5000,10000;
%             -7700,-5100,-3800,-2500,-1300,-250, -50, 50,150,160, 500,2
000,5000,10000;
%             -7700,-5100,-3800,-2500,-1300,-250, -50, 50,150,160, 500,2
000,7500,10000;
%             -7700,-5100,-3800,-2500,-1300,-250, -50, 50,150,160, 500,3
000,10000,10000;
%             -7700,-5100,-3800,-2500,-1300,-250, -50, 50,150,250,1000,5
000,10000,10000;
%             -7700,-5100,-3800,-2500,-1300,-250, -50, 50,250,500,5000,1
0000,10000,10000;
%             -7700,-5100,-3800,-2500,-1300,-250, -50,100,500,2500,10000
,10000,10000,10000;
%             -7700,-5100,-3800,-2500,-1300,-250, -50,1000,5000,7500,100
00,10000,10000,10000];
%semishockTableF=motionratioF*(4.448222)*wheelTableF;


% Rear
% 2 dim look-up table for semi-active shock
% linear shock to compare to linear model
%semishockDispR=[-1,1];     % for x axis (rows) of table
%semishockVelR=[-1,0,1];    % for y axis (columns) of table
%semishockTableR=[-bs,0,bs;-bs,0,bs];

% 2 dim look-up table for semi-active shock based on wheel values
wheelDispR=[-1,1]/0.0254;   % wheel Disp in inches
semishockDispR=(1/motionratioR)*(0.0254)*wheelDispR;   % for x axis (ro
ws) of table
wheelVelR=[-1,0,1]/0.0254;  % wheel Vel in ips
semishockVelR=(1/motionratioR)*(0.0254)*wheelVelR;    % for y axis (col
umns) of table
wheelTableR=[-bpeqR,0,bpeqR;-bpeqR,0,bpeqR]/(4.448222);  % in lbs.
semishockTableR=motionratioR*(4.448222)*wheelTableR;

% John L's passive shock from notes
wheelDispR=[-5,-3,-1,3,7,9,11];                          % wheel Disp in
 inches
semishockDispR=(1/motionratioR)*(0.0254)*wheelDispR;   % for x axis (ro
ws) of table
wheelVelR=[-150,-75,-50,-25,-5,-1,1,5,25,50,75,150];    % wheel Velocit
y in ips
semishockVelR=(1/motionratioR)*(0.0254)*wheelVelR;      % for y axis (c
olumns) of table
wheelTableR=[-7700,-3800,-2500,-1300,-250,-50,10,20,400,1000,1500,3000;
```

```
            -7700,-3800,-2500,-1300,-250,-50,10,20,400,1000,1500,3000;
            -7700,-3800,-2500,-1300,-250,-50,10,20,400,1000,1500,3000;
            -7700,-3800,-2500,-1300,-250,-50,30,60,600,1400,2000,4000;
            -7700,-3800,-2500,-1300,-250,-50,50,300,800,1800,2500,5000;
            -7700,-3800,-2500,-1300,-250,-50,50,300,800,1800,2500,5000;
            -7700,-3800,-2500,-1300,-250,-50,50,300,800,1800,2500,5000]
;
 semishockTableR=motionratioR*(4.448222)*wheelTableR;

% John L's ideal shock from notes
%wheelDispR=[-5,-3,-1,1,3,5,7,9,11];
%semishockDispR=(1/motionratioR)*(0.0254)*wheelDispR;      % for x axis
(rows) of table
%wheelVelR=[-150,-100,-75,-50,-25,-5,-1,1,5,25,50,75,100,150];
%semishockVelR=(1/motionratioR)*(0.0254)*wheelVelR;       % for y axis (
columns) of table
%wheelTableR=[-7700,-5100,-3800,-2500,-1300,-250, -50, 50,150,250,1000,
2000,5000,10000;
%            -7700,-5100,-3800,-2500,-1300,-250, -50, 50,150,250, 750,2
000,5000,10000;
%            -7700,-5100,-3800,-2500,-1300,-250, -50, 50,150,160, 500,2
000,5000,10000;
%            -7700,-5100,-3800,-2500,-1300,-250, -50, 50,150,160, 500,2
000,7500,10000;
%            -7700,-5100,-3800,-2500,-1300,-250, -50, 50,150,160, 500,3
000,10000,10000;
%            -7700,-5100,-3800,-2500,-1300,-250, -50, 50,150,250,1000,5
000,10000,10000;
%            -7700,-5100,-3800,-2500,-1300,-250, -50, 50,250,500,5000,1
0000,10000,10000;
%            -7700,-5100,-3800,-2500,-1300,-250, -50,100,500,2500,10000
,10000,10000,10000;
%            -7700,-5100,-3800,-2500,-1300,-250, -50,1000,5000,7500,100
00,10000,10000,10000];
%semishockTableR=motionratioR*(4.448222)*wheelTableR;



% 2 dim look-up table for bump-stop
% Front
wheelBSDispF=[-1,0,1];  % in inches of wheel travel  (rows of table)
bumpstopDispF=(1/motionratioF)*(0.0254)*wheelBSDispF;
wheelBSVelF=[-1,1];     % in ips of wheel velocity  (columns of table)
bumpstopVelF=(1/motionratioF)*(0.0254)*wheelBSVelF;
wheelBSTableF=[0 0;0 0;0,0];  % in lbs. at wheel travel/velocity
bumpstopTableF=motionratioF*(4.448222)*wheelBSTableF;

% Rear
wheelBSDispR=[-1,0,1];  % in inches of wheel travel  (rows of table)
bumpstopDispR=(1/motionratioR)*(0.0254)*wheelBSDispR;
wheelBSVelR=[-1,1];     % in ips of wheel velocity  (columns of table)
bumpstopVelR=(1/motionratioR)*(0.0254)*wheelBSVelR;
```

```
wheelBSTableR=[0 0;0 0;0,0];  % in lbs. at wheel travel/velocity
bumpstopTableR=motionratioR*(4.448222)*wheelBSTableR;


% Initial conditions
RtireOF=16*(0.0254);
RtireOR=16*(0.0254);     % tire diameter unloaded is 16 in
loada=(mbody/2)*b*g/(a+b);
loadb=(mbody/2)*a*g/(a+b);
qsF0=loada*motionratioF/ksF;
qsR0=loadb*motionratioR/ksR;
ShDefl0F=0;
ShDefl0R=0;
loadtF=loada+muF*g;
loadtR=loadb+muR*g;
quF0=loadtF/kuF;
quR0=loadtR/kuR;
RtireEqF=RtireOF-quF0;
RtireEqR=RtireOR-quR0;
```

# Appendix VI

## Half Car Models

### Pitch Model

### Roll Model

Half Car Nonlinear Model – Pitch

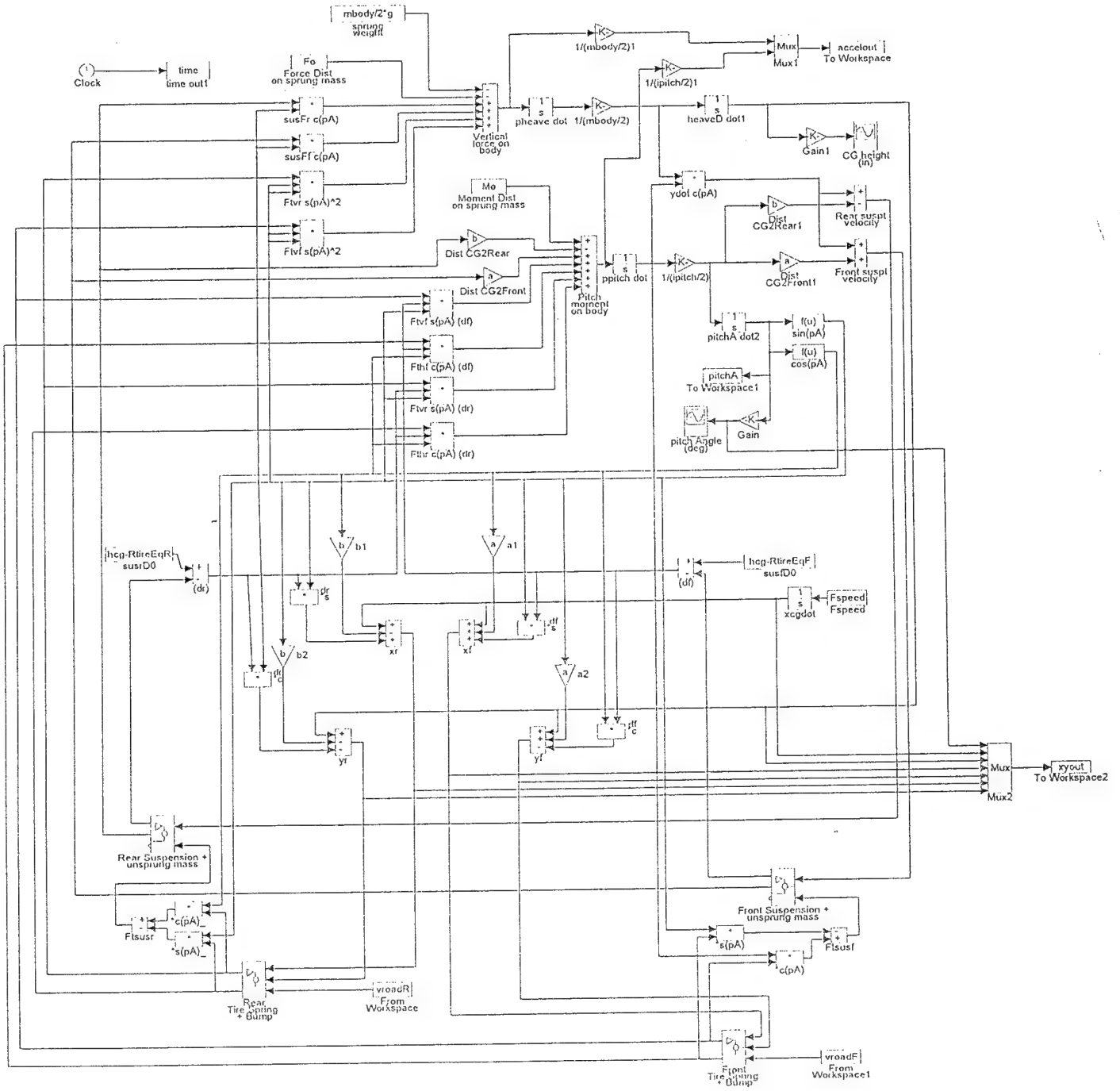

Front suspension and Unsprung Mass

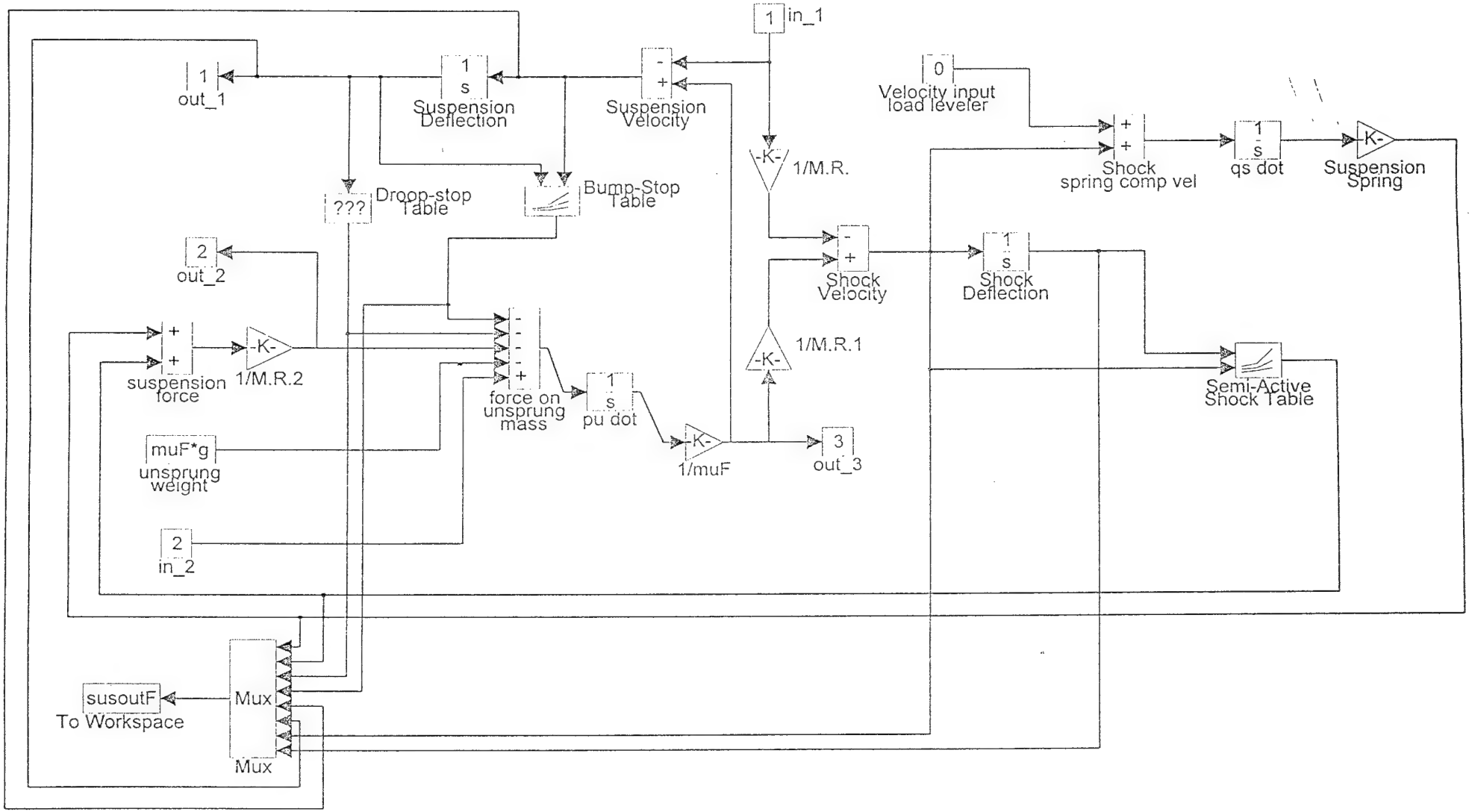

Rear Suspension plus Unspring Mass

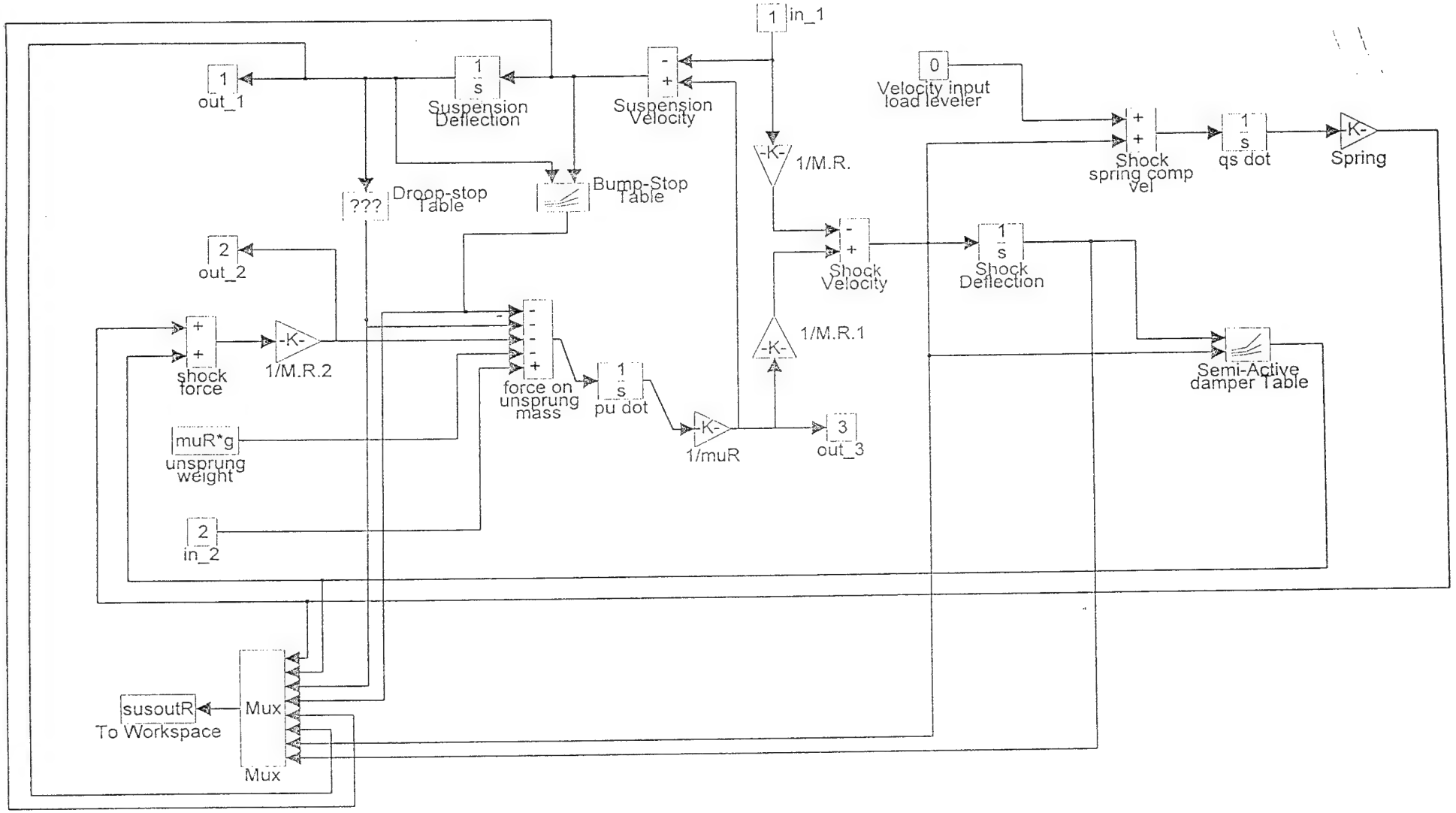

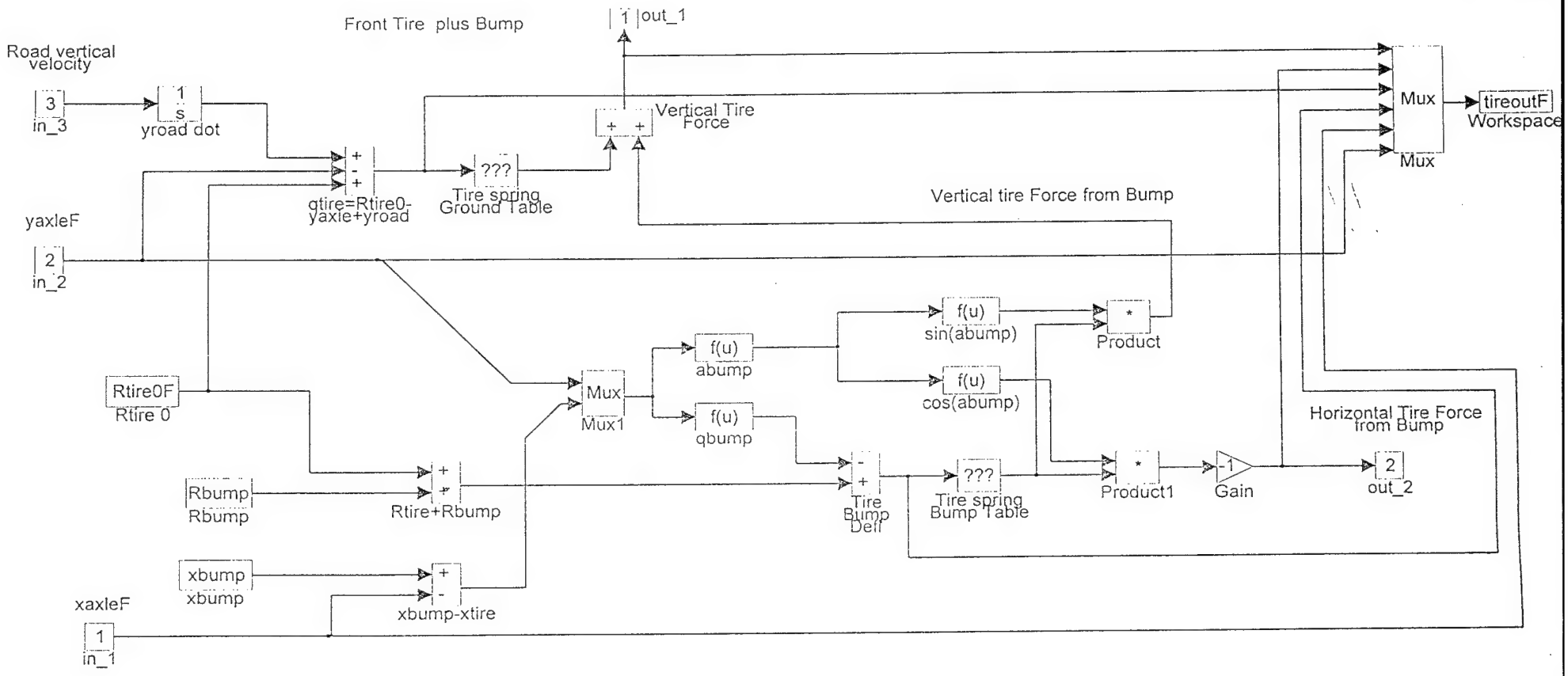
Front Tire plus Bump
1
out_1
Road vertical velocity
3
in_3
1
s
yroad dot
Vertical Tire Force
Mux
tireoutF
Workspace
Mux
qtire=Rtire0-yaxle+yroad
???
Tire spring Ground Table
Vertical tire Force from Bump
yaxleF
2
in_2
f(u)
sin(abump)
*
Product
f(u)
abump
Rtire0F
Rtire 0
Mux
Mux1
f(u)
cos(abump)
f(u)
qbump
Horizontal Tire Force from Bump
Rbump
Rbump
Rtire+Rbump
Tire Bump Defl
???
Tire spring Bump Table
*
Product1
-1
Gain
2
out_2
xbump
xbump
xbump-xtire
xaxleF
1
in_1

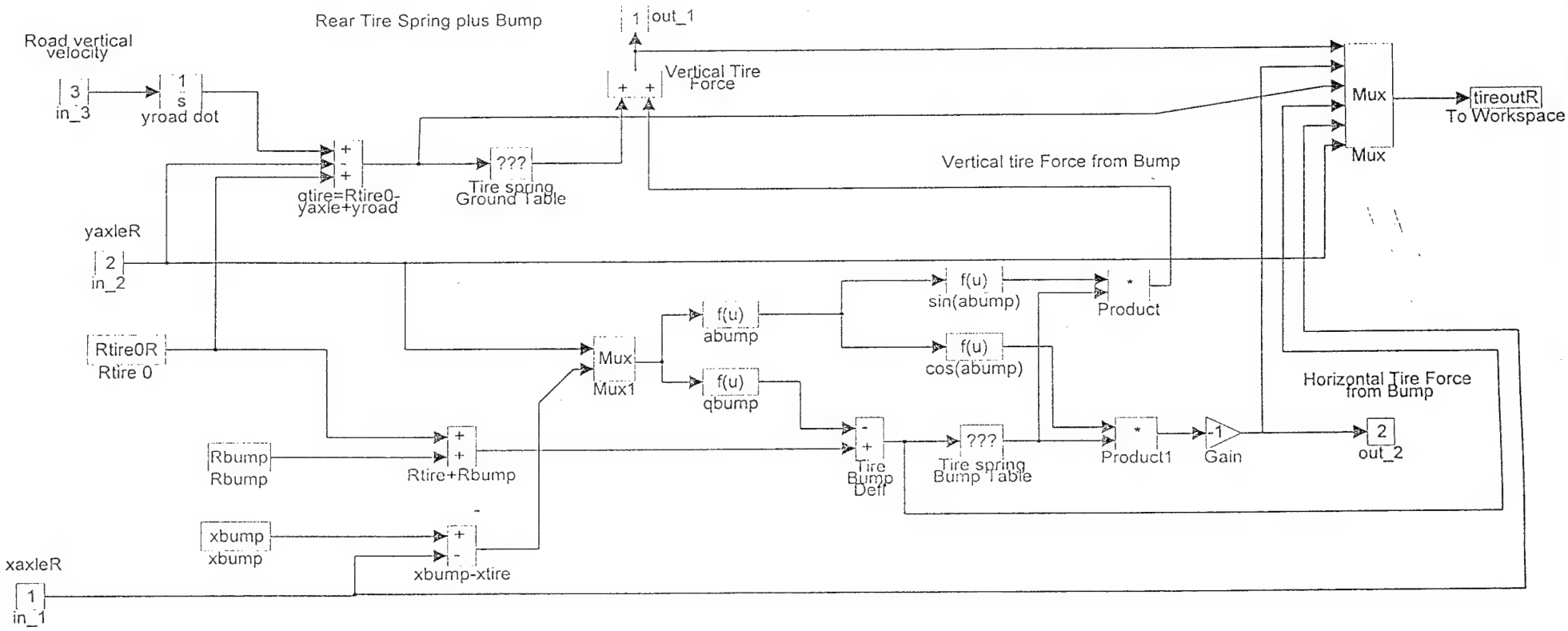
Rear Tire Spring plus Bump
1
out_1
Road vertical velocity
3
in_3
1
s
yroad dot
Vertical Tire Force
Mux
tireoutR
To Workspace
Mux
Vertical tire Force from Bump
???
Tire spring Ground Table
qtire=Rtire0-yaxle+yroad
yaxleR
2
in_2
f(u)
sin(abump)
Product
f(u)
abump
Rtire0R
Rtire 0
Mux
Mux1
f(u)
cos(abump)
f(u)
qbump
Horizontal Tire Force from Bump
Rbump
Rbump
Rtire+Rbump
Tire Bump Deff
???
Tire spring Bump Table
Product1
-1
Gain
2
out_2
xbump
xbump
xbump-xtire
xaxleR
1
in_1

```
% hlfcar2d.m
% Defining Parameters for Half Car Pitch Nonlinear Suspension Model
%
g=9.81;
a=119*0.52*(0.0254);
b=119*0.48*(0.0254);;
mbody=(5665-4*140)*(1/2.204);
muF=140*(1/2.204);
muR=140*(1/2.204);
ipitch=2500;
ksF=700*(4.448222)*(1/0.0254);
ksR=300*(4.448222)*(1/0.0254);
motionratioF=1.6;
motionratioR=1.53;
buF=0;
buR=0;
Fo=0;
Mo=0;

% Front tire
% 1 dim look-up Table for nonlinear tire
% Baja T/A on flat at 20 psi
tireDeflectionF=(0.0254)*[-1,0,5.2953,5.5906,5.8661,6.1417,6.3386,6.535
4,6.6535,6.7323,6.7913];
tireForceF=(4.448222)*[    0,0,   6883,   7330,   7777,   8224,   8672,   914
1,   9678,  10237,  10684];
kuF=(4.448222/0.0254)*6883/5.2953;          % for steady state condition
s

% Rear tire
% Baja T/A on flat at 20 psi
tireDeflectionR=(0.0254)*[-1,0,5.2953,5.5906,5.8661,6.1417,6.3386,6.535
4,6.6535,6.7323,6.7913];
tireForceR=(4.448222)*[    0,0,   6883,   7330,   7777,   8224,   8672,   914
1,   9678,  10237,  10684];
kuR=(4.448222/0.0254)*6883/5.2953;          % for steady state condition
s

% Front
% 2 dim look-up table for semi-active shock
% linear shock to compare to linear model
%semishockDispF=[-1,1];      % for x axis (rows) of table
%semishockVelF=[-1,0,1];     % for y axis (columns) of table
%semishockTableF=[-bs,0,bs;-bs,0,bs];

% 2 dim look-up table for semi-active shock based on wheel values
wheelDispF=[-1,1]/0.0254;   % wheel Disp in inches
semishockDispF=(1/motionratioF)*(0.0254)*wheelDispF;   % for x axis (ro
ws) of table
wheelVelF=[-1,0,1]/0.0254;  % wheel Vel in ips
semishockVelF=(1/motionratioF)*(0.0254)*wheelVelF;     % for y axis (col
umns) of table
```

```
wheelTableF=[-bseq,0,bseq;-bseq,0,bseq]/(4.448222);  % in lbs.
semishockTableF=motionratioF*(4.448222)*wheelTableF;

% John L's passive shock from notes (compression only, made rebound sym
etric)
wheelDispF=[-5,-3,-1,3,7,9,11];                          % wheel Disp in
 inches
semishockDispF=(1/motionratioF)*(0.0254)*wheelDispF;    % for x axis (ro
ws) of table
wheelVelF=[-150,-75,-50,-25,-5,-1,1,5,25,50,75,150];     % wheel Velocit
y in ips
semishockVelF=(1/motionratioF)*(0.0254)*wheelVelF;       % for y axis (c
olumns) of table
wheelTableF=[-7700,-3800,-2500,-1300,-250,-50,10,20,400,1000,1500,3000;
             -7700,-3800,-2500,-1300,-250,-50,10,20,400,1000,1500,3000;
             -7700,-3800,-2500,-1300,-250,-50,10,20,400,1000,1500,3000;
             -7700,-3800,-2500,-1300,-250,-50,30,60,600,1400,2000,4000;
             -7700,-3800,-2500,-1300,-250,-50,50,300,800,1800,2500,5000;
             -7700,-3800,-2500,-1300,-250,-50,50,300,800,1800,2500,5000;
             -7700,-3800,-2500,-1300,-250,-50,50,300,800,1800,2500,5000]
;
 semishockTableF=motionratioF*(4.448222)*wheelTableF;

% John L's ideal shock from notes (compression only, made rebound symet
ric)
%wheelDispF=[-5,-3,-1,1,3,5,7,9,11];
%semishockDispF=(1/motionratioF)*(0.0254)*wheelDispF;      % for x axis
(rows) of table
%wheelVelF=[-150,-100,-75,-50,-25,-5,-1,1,5,25,50,75,100,150];
%semishockVelF=(1/motionratioF)*(0.0254)*wheelVelF;       % for y axis (
columns) of table
%wheelTableF=[-7700,-5100,-3800,-2500,-1300,-250, -50, 50,150,250,1000,
2000,5000,10000;
%             -7700,-5100,-3800,-2500,-1300,-250, -50, 50,150,250, 750,2
000,5000,10000;
%             -7700,-5100,-3800,-2500,-1300,-250, -50, 50,150,160, 500,2
000,5000,10000;
%             -7700,-5100,-3800,-2500,-1300,-250, -50, 50,150,160, 500,2
000,7500,10000;
%             -7700,-5100,-3800,-2500,-1300,-250, -50, 50,150,160, 500,3
000,10000,10000;
%             -7700,-5100,-3800,-2500,-1300,-250, -50, 50,150,250,1000,5
000,10000,10000;
%             -7700,-5100,-3800,-2500,-1300,-250, -50, 50,250,500,5000,1
0000,10000,10000;
%             -7700,-5100,-3800,-2500,-1300,-250, -50,100,500,2500,10000
,10000,10000,10000;
%             -7700,-5100,-3800,-2500,-1300,-250, -50,1000,5000,7500,100
00,10000,10000,10000];
%semishockTableF=motionratioF*(4.448222)*wheelTableF;
```

```
% Rear
% 2 dim look-up table for semi-active shock
% linear shock to compare to linear model
%semishockDispR=[-1,1];      % for x axis (rows) of table
%semishockVelR=[-1,0,1];     % for y axis (columns) of table
%semishockTableR=[-bs,0,bs;-bs,0,bs];

% 2 dim look-up table for semi-active shock based on wheel values
wheelDispR=[-1,1]/0.0254;   % wheel Disp in inches
semishockDispR=(1/motionratioR)*(0.0254)*wheelDispR;   % for x axis (ro
ws) of table
wheelVelR=[-1,0,1]/0.0254;  % wheel Vel in ips
semishockVelR=(1/motionratioR)*(0.0254)*wheelVelR;    % for y axis (col
umns) of table
wheelTableR=[-bseq,0,bseq;-bseq,0,bseq]/(4.448222);  % in lbs.
semishockTableR=motionratioR*(4.448222)*wheelTableR;

% John L's passive shock from notes
wheelDispR=[-5,-3,-1,3,7,9,11];                          % wheel Disp in
 inches
semishockDispR=(1/motionratioR)*(0.0254)*wheelDispR;   % for x axis (ro
ws) of table
wheelVelR=[-150,-75,-50,-25,-5,-1,1,5,25,50,75,150];    % wheel Velocit
y in ips
semishockVelR=(1/motionratioR)*(0.0254)*wheelVelR;      % for y axis (c
olumns) of table
wheelTableR=[-7700,-3800,-2500,-1300,-250,-50,10,20,400,1000,1500,3000;
             -7700,-3800,-2500,-1300,-250,-50,10,20,400,1000,1500,3000;
             -7700,-3800,-2500,-1300,-250,-50,10,20,400,1000,1500,3000;
             -7700,-3800,-2500,-1300,-250,-50,30,60,600,1400,2000,4000;
             -7700,-3800,-2500,-1300,-250,-50,50,300,800,1800,2500,5000;
             -7700,-3800,-2500,-1300,-250,-50,50,300,800,1800,2500,5000;
             -7700,-3800,-2500,-1300,-250,-50,50,300,800,1800,2500,5000]
;
 semishockTableR=motionratioR*(4.448222)*wheelTableR;

% John L's ideal shock from notes
%wheelDispR=[-5,-3,-1,1,3,5,7,9,11];
%semishockDispR=(1/motionratioR)*(0.0254)*wheelDispR;     % for x axis
(rows) of table
%wheelVelR=[-150,-100,-75,-50,-25,-5,-1,1,5,25,50,75,100,150];
%semishockVelR=(1/motionratioR)*(0.0254)*wheelVelR;      % for y axis (
columns) of table
%wheelTableR=[-7700,-5100,-3800,-2500,-1300,-250, -50, 50,150,250,1000,
2000,5000,10000;
%            -7700,-5100,-3800,-2500,-1300,-250, -50, 50,150,250, 750,2
000,5000,10000;
%            -7700,-5100,-3800,-2500,-1300,-250, -50, 50,150,160, 500,2
000,5000,10000;
%            -7700,-5100,-3800,-2500,-1300,-250, -50, 50,150,160, 500,2
000,7500,10000;
%            -7700,-5100,-3800,-2500,-1300,-250, -50, 50,150,160, 500,3
```

```
000,10000,10000;
%            -7700,-5100,-3800,-2500,-1300,-250, -50, 50,150,250,1000,5
000,10000,10000;
%            -7700,-5100,-3800,-2500,-1300,-250, -50, 50,250,500,5000,1
0000,10000,10000;
%            -7700,-5100,-3800,-2500,-1300,-250, -50,100,500,2500,10000
,10000,10000,10000;
%            -7700,-5100,-3800,-2500,-1300,-250, -50,1000,5000,7500,100
00,10000,10000,10000];
%semishockTableR=motionratioR*(4.448222)*wheelTableR;



% 2 dim look-up table for bump-stop
% Front
wheelBSDispF=[-1,0,1];  % in inches of wheel travel  (rows of table)
bumpstopDispF=(1/motionratioF)*(0.0254)*wheelBSDispF;
wheelBSVelF=[-1,1];     % in ips of wheel velocity  (columns of table)
bumpstopVelF=(1/motionratioF)*(0.0254)*wheelBSVelF;
wheelBSTableF=[0 0;0 0;0,0];  % in lbs. at wheel travel/velocity
bumpstopTableF=motionratioF*(4.448222)*wheelBSTableF;

% Rear
wheelBSDispR=[-1,0,1];  % in inches of wheel travel  (rows of table)
bumpstopDispR=(1/motionratioR)*(0.0254)*wheelBSDispR;
wheelBSVelR=[-1,1];     % in ips of wheel velocity  (columns of table)
bumpstopVelR=(1/motionratioR)*(0.0254)*wheelBSVelR;
wheelBSTableR=[0 0;0 0;0,0];  % in lbs. at wheel travel/velocity
bumpstopTableR=motionratioR*(4.448222)*wheelBSTableR;
```